NON-DESTRUCTIVE TESTING OF MASONRY ARCH BRIDGES

by
CAMILLA COLLA
Dott. Arch.

Thesis submitted for the Degree of Doctor of Philosophy

The University of Edinburgh
Department of Civil and Environmental Engineering
1997

To my family

Declaration

This thesis, the work discussed and results reported were carried out solely by myself unless otherwise stated within the text.

Camilla Colla
Edinburgh, September 1997

ABSTRACT

Stone masonry arch bridges form a critical part of the transportation system. Present methods of assessment are sometimes too conservative and a number of bridges fail the assessment even though they appear in good condition. Non-Destructive Testing can play a key role and three Non-Destructive techniques - radar, sonics and conductivity measurements- are proposed for bridge testing with the aim of obtaining structural dimensions, material characteristics and integrity information which would lead to a more accurate assessment of the structural conditions being made.

After discussing problems and limitations with current analytical and load testing methods of assessment, a review of archetypal forms of bridge construction methods employed along the centuries is made, showing that a greater variety of bridges than commonly believed, exists. The review also enables an Engineer to have some indication of construction type relating to the area, era and designer.

The work then includes site work on two masonry bridges and laboratory experiments. On site, the three Non-Destructive Techniques mentioned were used for testing two Scottish stone masonry bridges (one with a brick arch ring) with the aim of obtaining information about the condition and nature of the materials in the fill, the internal configuration of the structure and the geometrical dimensions of the elements. Data from each technique were plotted in the form of cross-sectional tomographic maps and the results interpreted and compared. Limitations are also discussed.

In the laboratory, experiments with radar were undertaken to calibrate the technique in controlled conditions and also, and more importantly, to obtain information about phenomena of signal behaviour and material properties as would be found in a masonry arch bridge. The findings served the purpose of aiding a better planning of radar surveys to be made and an improved understanding and interpretation of the radar data to be obtained.

ACKNOWLEDGEMENTS

The time spent in Edinburgh has been an experience which was to broaden my horizons and to give a different perspective to my personal and professional life.

There is a very great number of people who have helped me or contributed to my education and my achievements in many ways. I am conscious that I owe a lot to them.

The University of Edinburgh
I am firstly indebted to Prof. Michael C. Forde, for his role as adviser and supervisor and for the support and guidance. Also for invaluable discussions which unveiled visions and, as Head of Department, for making the University facilities available.

Acknowledgements are also due to Prof. Dave McCann, who, in his role as second supervisor, found the time to come and visit me in Edinburgh regularly, and contributed to the work with expert advice during all phases of the research.

Mr Kevin Broughton's unfailing enthusiasm and professional technical expertise are also gratefully acknowledged.

Among my friends and colleagues in the Department, mentions and thanks go to Ivo Padaratz for reciprocal consultations, long expert conversations and friendship. To David Prentice for availability in giving me access to his double-span bridge model for radar testing; I am indebted and grateful to him. To Barbara Lane and Anu Mathew for sisterly reciprocal support and encouragement at critical times during laboratory testing.

Highways Agency
The Highways Agency provided industrial sponsorship for the EPSRC Case award and their financial assistance is gratefully acknowledged.

Friends and Family
To all the incredible persons I have met and later became my friends in Edinburgh: you have made me feel at home.

To my family, the greatest thanks for always being with me from far and for tireless support and encouragement.

LIST OF CONTENTS

LIST OF FIGURES

LIST OF TABLES

NOTATIONS

A	attenuation factor
c	electromagnetic wave velocity in free space (m s^{-1})
d	depth (m)
f	centre frequency of the transmitted signal (Hz)
j	$\sqrt{-1}$
R	reflection coefficient
S	(Siemen) unit of conductivity
T	transmission coefficient
t	time variable (s)
tanδ	loss tangent or dissipator factor
v	wave velocity
Z_r	impedance of material r
α	attenuation (Np m^{-1})
ε	dielectric permittivity (F m^{-1})
ε_c	complex permittivity
ε_o	permittivity of free space
ε_r	relative permittivity of material r or dielectric constant
ε'	real part of complex permittivity
ε"	imaginary part of complex permittivity (loss factor)
λ	wavelength
μ	magnetic permeability (H m^{-1})
μ_0	magnetic permeability of free space
μ_r	magnetic permeability of material r
σ	conductivity (mS/m)
ω	$2\pi f$ angular frequency (rad s^{-1})
Ωm	(ohm-meter) unit of resistivity

CHAPTER 1

INTRODUCTION

1.1 Masonry arch bridges in perspective

Stone masonry arch bridges form a critical part of the transportation system in Britain, comprising over half the bridges in some areas and 40% of the bridge stock in the UK (Page, 1989). In total there are over 40,000 arch highway bridges and 33,000 railway arch span in the UK (Mair, 1994).

In other European countries the situation is similar. In France, masonry arch bridges constitute the 25% of the stock (Fig. 1.1), on a total number of 20,500 bridges (Binet, 1996). Similarly in Spain, from the summary of bridges and service passes - viaducts, foot bridges, small scale drainage bridges - in the National Highways Network appears that 30% of such bridges (Fig. 1.2) are masonry structures (classification in number of bridges by deck material). (Yanez and Alonso, 1996)

Most if not all of these bridges were designed for horse drawn traffic and are therefore carrying loads greatly in excess of those for which they were designed, yet they are showing no sign of distress.

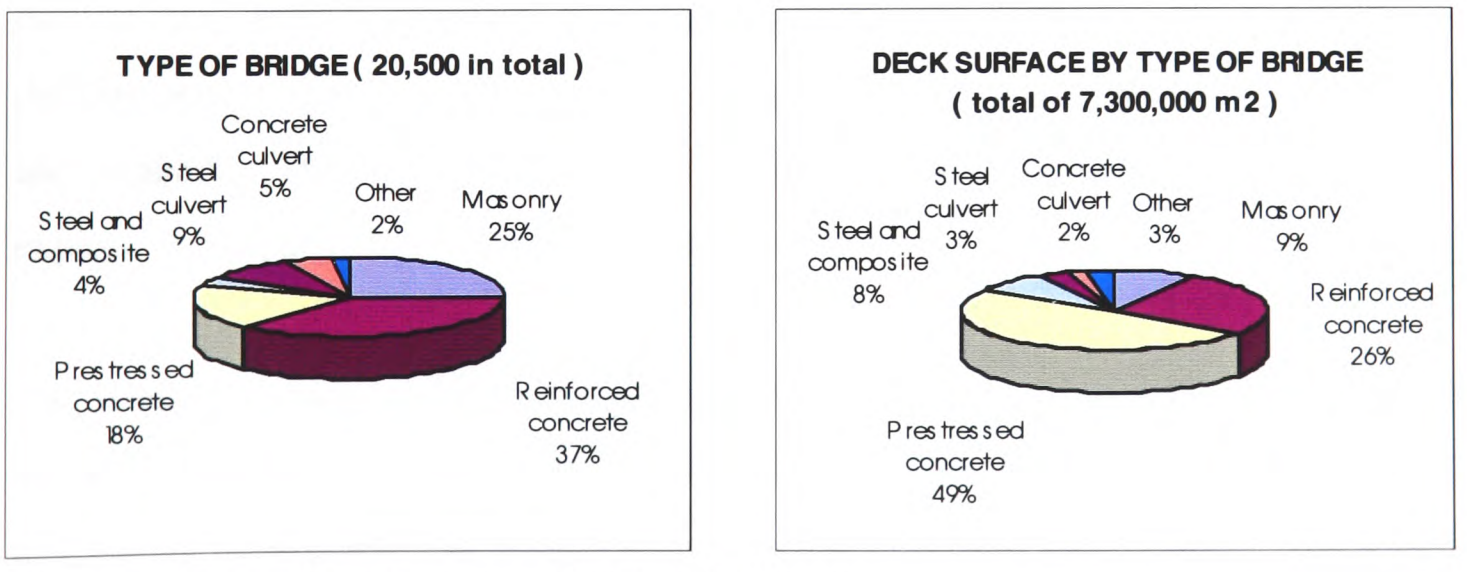

Fig. 1.1 - Proportion of masonry bridges in France.

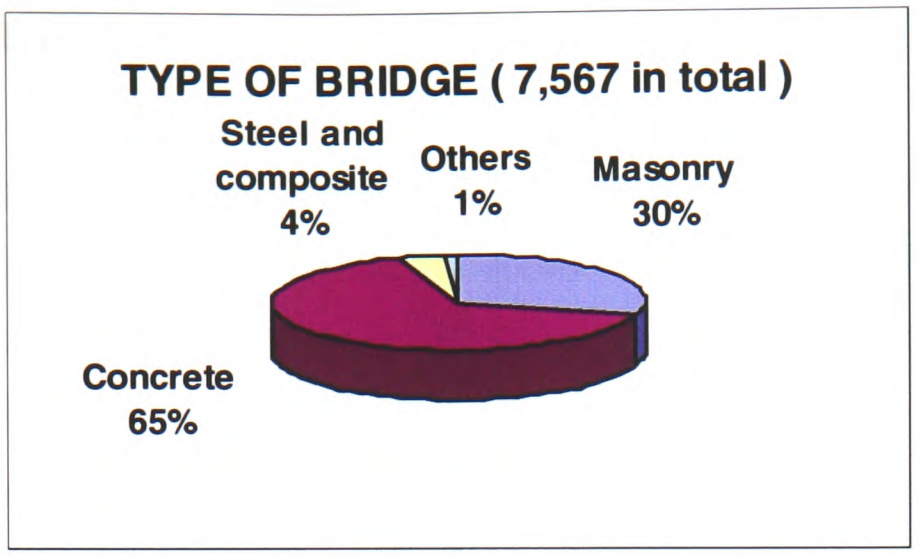

Fig. 1.2 - Proportion of masonry bridges in Spain.

The proven durability of arch bridges (compared similar concrete structures) and their pleasing appearance has resulted in a renaissance of arch construction, with several new structures being built in recent years (Anon, 1994). The resurgence of un-reinforced arch bridges, with their clear economic advantages in terms of whole life costs (Harvey *et al.*, 1988), has prompted research work on arch bridges. The Highways Agency has consequently published a Design Standard and Advice Note covering design and construction of arch bridges (Department of Transport, 1994) and specific advice on the appearance of bridges (Highways Agency, 1996).

1.2 Reasons for concern

However, most bridges were designed and built in the last century for traffic which was very different from today. The increased traffic loading since original design is one of the main causes of concern, together with material deterioration and development of structural faults due to inadequate original specifications of materials and methods. The assessment and maintenance of these structures is a difficult and expensive task, especially whilst the bridge is in service.

The strength of many of these bridges must be reassessed to determine whether heavy modern loads can be permitted to cross them safely and the Highways Agency assessment programme has been driving research work into arch bridges. The motive for much of the work that has been carried out was the difficulty experienced in

assessing arch structures for the new higher loads imposed as a result of the UK joining the EU (Harvey, 1995).

By July 1990 the UK was the only part of the EC not to allow 40 tonne vehicles on its highways. The DoT has promised the European Commission that by Jan 1999 40t lorries will be acceptable on UK roads. However, strengthening over 100,000 small span highway bridges to accommodate European legislation is a very costly proposition. There is no accurate official estimate of how much the work will cost, although unofficial estimates have put the figure at £1400M. The DoT's own financial estimates are obtained from the 1987's bridge census sample survey of $695M (Alexander, 1990).

The long term aim of the Department of Transport's sponsored research was to improve the ability to analyse the behaviour and strength of arch bridges. Masonry arch bridges are complex structures and their strength depends on the geometry and integrity of the arch, the fill content behind it, and the interaction between the soil fill and the masonry structure.

Some of the bridges deemed to be at risk may not necessarily have developed any significant or noticeable signs of distress at the time of inspection. This is because the extreme load conditions and the worst circumstances may not yet have occurred for these bridges (Das, 1996). Bridges may be at risk due to factors other than increased load, for example scour risk, and these aspects also require attention.

For this reason it is not sufficient for the bridge authorities to repair or strengthen only those bridges which have shown deterioration. A minor fault in an important part of the bridge may signify a greater risk than a more extended fault in a less critical area. It is essential to identify the bridges which are at risk, or likely to reach a state of risk, so that preventative actions can be taken in time. So inspections, including non-destructive testing and monitoring, are a prerequisite for all assessment and strengthening activities.

1.3 Bridge management and reliability strategy

Any effective management strategy therefore has to forecast the work by taking account of the overall risks faced by the bridges rather than considering deterioration alone. The required remedial work for inadequate bridges needs to be determined on the basis of risk related options, but the present rules do not have any of these flexible options.

The inherent safety levels are of considerable real strategic and financial importance for bridge authorities. Not only does the cost of new bridges depend on them, but the number of bridges to be replaced or strengthened, and the extent of strengthening required, are also essentially determined by these calculated levels (Das, 1994).

To take a considered decision it is necessary to have a better knowledge of the damage process and of the structural behaviour of deteriorated bridges. This would lead to the assessment of the bridge conditions in terms of a single and unique parameter, that is the probability of failure. Changes in the element properties would immediately reflect in variations of the probability of failure and therefore on the list of priorities. The probability of failure describes the border between safe and failure domains, with respect to the properties of the elements forming the bridge (Mancino and Pardi, 1994).

Fig. 1.3 shows the reduction of reliability (ß) as a result of loss of material resistance or rise in load effects. The purpose of strengthening work is to reverse the trend and stop this drop. The one-off type of strengthening will result in a sudden rise of type (a). Regular steady state maintenance activities have smaller but more frequent improvement steps in type (b).

Non-Destructive Testing (NDT) techniques can play a relevant role both in the inspection process and at the stage of checking the outcome of strengthening interventions.

Future bridge management systems will probably be based on simple models for predicting the residual strength of structural elements. Improved modelling of the deterioration is needed to be able to formulate optimal strategies for inspection and maintenance. However such strategies will only be useful if they are also combined with expert knowledge. It is not possible to formulate all expert experience in mathematical terms. Therefore it is believed that future management systems will be expert systems or knowledge-based systems (Thoft-Christensen, 1996).

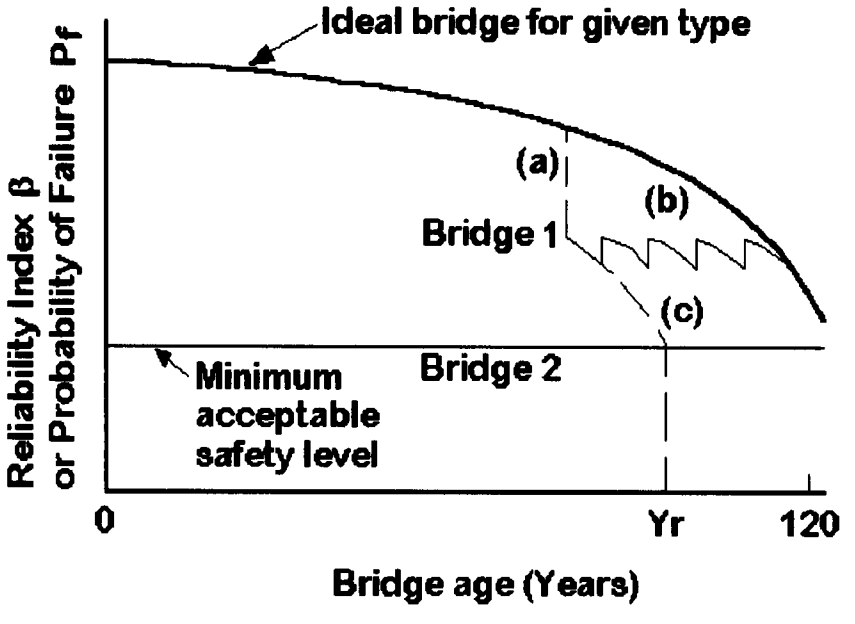

Bridge 2 must be replaced/strengthened
Bridge 1 options:
(a) strengthen now
(b) minor repairs /monitor
(c) do minimum and replace at reduced life

Fig. 1.3 - Life performance related assessment rules (after Das, 1996).

1.4. The United States scene

Whilst periodical visual inspections occupy a great part of the in-situ structural assessment in the UK, in the United States the situation is slightly dissimilar.

Due to extensive use, the infrastructure - buildings, sewers, highways pavements, water networks - is simultaneously ageing and the bridge system is also deteriorating.

The emphasis has shifted towards their preservation through repair, rehabilitation and replacement activities. This requires a rapid collection and processing of a large amount of data to select and prioritise the preservation strategies. Thus, Non-destructive Testing methods are vital to the collection of condition assessment information.

State highways agencies use a bridge maintenance programme which provides inspection, repair and rehabilitation of existing bridges to preserve both their load capacity and service performance (Frangopol and Hearn 1996). The National Bridge Inventory (NBI) stores data records and coding of bridge conditions. During an inspection, the state of deck, superstructure and substructure of the bridge is recorded, but the NBI condition ratings are qualitative and not specific to structural form or material type; the NBI scale does not identify specific types of deterioration and do not specify the load capacity of the bridge. They do not contain the quantitative information that might be used to estimate load capacity. A bridge management system (BMS) needs more detailed bridge condition information and that is where Non-destructive evaluation comes to play a decisive role. In US, NDT is widely used for the inspection of structures and relied upon for condition assessment.

1.5 Role of inspection

Diagnosis of bridges showing signs of deterioration is the first step that has to be taken before making any decision regarding maintenance or repair; and this is true for bridges as for any other structure (Colla *et al.*, 1993). It is necessary to define clearly what the damage problems are. The reason for concern usually identifies a direction for investigation. However, it is very time and money consuming to start diagnosis without knowing all information relating to the structure. The choice of inspection method is thus very important and the method procedures need to be known accurately. A plan of the work to do must be drawn before going on site, in order to collect complete information and avoid repeat visits to the site. Diagnostic work is usually disruptive for the normal functioning of the bridge and must be limited as much as possible in time and space.

It is impossible for visual inspections to identify all serious defects because these may be hidden below the road surface and waterproofing, or otherwise not accessible for inspection. Hence more accurate inspection methods, possibly non invasive, non destructive techniques would be more appropriate and could facilitate the job of the inspecting engineer. These can be selected and applied so that goals for assurance of structural condition are met.

There are requirements of high accuracy for the inspections of critical defects and some of the techniques available have the potential to be successful. However their performance in particular site situations still needs to be validated. Measurements of performance are much needed and can make possible the rational design of inspection programmes. Methods' limitations need to be clearly stated as they can produce uncertainties in the condition assessment of the bridge.

1.6 The assessment and analysis of arch bridges

To solve the problem of bridge management it is necessary to establish the load bearing capacity of each and every masonry bridge in the network. To achieve this, there is great necessity of in-depth evaluation of the condition of the single elements and of the whole bridge.

Information about the bridge (project data, code of practice when it was built, inspection data, repairs undergone, load tests, etc.) is not always available: often vital information is lost or otherwise unavailable. This is becoming increasingly true with the inspection of structures often being put out to tender and loss of the continuity provided by the traditional inspection and maintenance by the government agency.

Assessment of arches is necessarily a matter both of analysis and judgement. Fifteen years ago the only approach to assessment in common use was the MEXE's (Military Engineering Experimental Establishment) modified method. Whilst still in use and mathematically sound, MEXE bears no relation to the actual behaviour of the

structure. It is an empirical analysis which relates capacity to leading dimensions of the bridge via carefully judged factors. Then there is the equilibrium approach which seek to find an adequate load path through the structure. Finally there are stiffness analyses (including Finite Element analyses) which attempt to relate deformation of the arch to its mechanical properties. Much of the research on arches has concentrated on modelling of the ultimate limit state and determination of the reserve of strength in the structure, with aspects investigated such as soil-structure interaction of arch rings, soil structure interaction of abutments, effect of spandrel wall stiffening on the arch ring (Mair, 1994).

However, all these methods have limitations, as it will be discussed in chapter 3, and bridge assessment is very different from bridge analysis. The data from each specific bridge that is available for inputting in the analysis is extremely limited or very expensive to obtain. Even the true shape of the arch extrados is often unknown and the conventional methods of exploration which usually involve drilling from the underside are imprecise. Similarly the content of the fill may well be unknown so ascribing properties to it is quite difficult. The result is that analytical methods of assessment are imprecise and too conservative.

Thus, arch bridge assessment remains a difficult process. Engineers are confident that the arches are sound but cannot prove that by analysis. When assessing the load carrying capacity of an existing bridge, the calculations used, even though necessarily conservative, are of a precise nature. The results also have to be fairly decisive, in that the bridge authority has to take specific actions based on the results of the assessment. In this context, there would seem to be no place for "imprecise" qualitative Non Destructive Testing methods in bridge assessment.(Das *et al.*, 1995)

In the event that a bridge fails analytical assessment, the choice is usually between enforcing a load restriction or strengthening the bridge.

In the case when a bridge fails assessment by a small margin and it would pass a visual inspection, instead of the "pass or fail" type of results, it may be more logical to allow also a "monitor" option to be used.

In fact, if a bridge is found to be inadequate using all the available information and the best evaluation methods, a particular bridge may still in reality possess the required reliability. This is because the loading (traffic or dead load) applied to the bridge may be less than that envisaged in the calculations or the bridge may have greater strength than it appears to have. Inner "hidden" structural elements may contribute with a reserve of strength, for example if a particular construction type had been adopted. Knowing that the fill of the bridge is in dry and compact conditions would also play in favour of the safety of the bridge.

In such a vision, even a qualitative form of investigation could be useful to detect structural features which are likely to lead to a reserve in strength. This new information would then be taken into account in the re-calculation of the capacity of the bridge.

Non-Destructive methods could be of great value in the evaluation process for such bridges. Furthermore some of these same methods could be used for monitoring the bridge and check whether structural deterioration is taking place.

1.7 NDT

Non-destructive testing (NDT) is a multi-disciplined field of science that is concerned with the evaluation, inspection, testing, and characterisation of materials and structures through methods that do not significantly alter the material or structure (Southwest Research Institute, 1996a). NDT is a procedure which covers the inspection and/or testing of any material, component or assembly by means which do not affect its ultimate serviceability and are appropriate to establish and/or verify structural integrity. (Gilbert, 1997)

If the definition is generic, it is also comprehensive and quite straightforward. Actually, there has been some discussion on the choice of the word "testing" instead of "evaluation" and it seems that this field of work struggles defining itself. In Great Britain the form "NDT" (Non-Destructive Testing) is generally adopted to intend both testing and evaluation. In US the form "Non-Destructive Evaluation" (NDE) is preferred, intending with "NDT" just the activities concerned with the testing itself. Also to be considered are "NDC" (Non-Destructive Characterisation) and "NDI" (Non-Destructive Inspection) along with the NDT and NDE acronyms. And even the "non-destructive" part is up to debate since the Americans spell it "nondestructive" (Jones, 1996).

The scope of NDT encompasses fields such as: a) design, safety and reliability engineering, b) quality control and product specifications, c) condition monitoring and maintenance, d) industrial standards. NDT methods are aimed to assess: deficiencies in materials and products, determinations of physical and geometric properties of materials and products, structural behaviour of materials, products and installations.

Without being exclusive, the test methods include: ultrasonic and acoustic methods, electric and magnetic methods, radiation methods, leak testing, optical methods, vibration testing, stress measurements, microwave testing and thermal testing.

1.8 Relevance of NDT

With conventional bridge testing methods often it is only possible to test parts or core samples of structures to provide improved data for incorporation in the analysis. These give information which relates only to one location, thus statistical variability of samples must be taken into account. Or, like static load testing, they give global data on the structure but can often be expensive and time consuming. Alternative approaches, such as dynamic testing, are not new but deserve appropriate research with new technology.

NDT methods (those treated here) would have the advantage of rapidly and continuously investigating the state of whole elements/ structures providing a reliable assessment, often with substantial savings in term of time, cost, remedial works and reduction in traffic disruption (Wood, 1995).

In the USA, the FHWA and State DOTs have recognised the rapid growth of non-destructive testing (NDT) and non-destructive evaluation (NDE) during recent years, and how important these techniques may be in determining internal soundness and assuring satisfactory performance of repair operations.

Use of NDT and NDE has improved the process by which irregularities are detected. These technologies also provide a more reliable method of determining which products are acceptable in strengthening operations, and may potentially result in a higher acceptance rate for new products. NDT and NDE have proven indispensable to designers, engineers, and maintenance personnel concerned with reliable testing and evaluation methods, also thanks to the low costs associated with monitoring (Northwestern University Infrastructure Technology Institute, 1996).

1.9 NDE research and materials characterisation

The development of non-destructive evaluation methods used in quality management and reliability maintenance systems focuses on developing relationships between material properties and physical measurements.

For structural integrity inspection and monitoring, investigations include defect (voids, cracks, inclusions, and lack of adhesion assessment) detection, location, sizing classification, growth monitoring, and long-term global monitoring.

For material characterisation (nature, density variations etc.), relevant parameters are velocity, scattering, thickness and magnetic properties (Southwest Research Institute, 1996 b).

Many of the NDT techniques were not developed for engineering applications and even fewer for civil engineering. Hence their reliability and applicability in this field is sometimes uncertain and researchers stress the importance of performance specifications and usage procedures of these new techniques (Bungey, 1997; Washer, 1997).

1.10 Work included in this research

From the above Bridge Management strategy there follows that a key input parameter in the assessment of masonry arch bridges is NDT.

Three powerful techniques for detecting internal dimensions and defects in the bridge structure are used in this project: ground-probing radar, sonic testing and conductivity measurements.

The research work is aimed at developing techniques for enhanced masonry bridge assessment starting from documentation of the archetypal forms of this kind of structures and their variations, and by means of site testing approach and laboratory experimental calibration.

The research work employs new techniques in the investigation of structures (conductivity measurements), also new methods of application of these techniques (radar tomography and sonic tomography applied to masonry bridges) with the main advantage being the capacity of producing cross sectional plots - either horizontal or vertical - of the structure investigated.

1.11 Objectives

The global aims of the research are:

- to carry out structural testing that can provide input information to bridge management systems predicting the remaining life of a structure. This permits the

Engineer to prioritise preservation strategies with regard to economical, social and political issues involved (availability of funding, traffic disruption, etc.).

- to directly provide input parameters to analytical methods for the calculation of the load carrying capacity of the bridge. These parameters may include geometrical information relating to the bridge elements (dimensions and/or shape of the arch barrel, the spandrels, wing walls and abutments), the fill and construction characteristics (soil filled spandrels or other).

The achievement of these objectives has been pursued by

- developing assessment techniques - both contacting and non contacting - for evaluation of the condition of the structure,
- monitoring the bridge conditions with time: seasonal variations,
- investigating the construction typology of the bridge: soil filled or hollow,
- qualifying the masonry: solid, multi-wythe or rubble core walls,
- verifying the physical condition of the fill materials: moisture content, density,
- detecting the nature of the fill material: clay, sand, etc.,
- identifying voids and defects: their size and location,
- calculating the thickness of walls: spandrels and wing walls,
- calculating the thickness of arch barrel: at crown and haunches,
- making use of cross-sectional representation of the data obtained,
- suggesting the most effective method in terms of cost, time, expertise required,
- comparing the effectiveness of the methods when in singular or parallel use.

In conjunction with the above, the applications of radar to masonry bridges have shown some limitations of the technique on this kind of structures in particular circumstances and have demonstrated the need for performance measurements. Consequently,

- a study of the performance of the radar technique has been carried out by means of laboratory experiments. The investigation has considered the effectiveness of

the testing methods on masonry structures, in function of the variation of a number of variables. These included:

* material parameters
  - electrical properties of materials: dielectric properties, conductivity values;
  - physical properties of materials: moisture content, salt content, density;
* complexity of the structure investigated
  - number of interface changes;
  - soil filled, cellular structure, hollow/partially filled.

The research into performance of non-destructive testing methods aimed at developing guidelines for the selection and application of inspection methods, to achieve a reasonable level of assurance of condition in structures and masonry bridges.

The project was funded by The Highways Agency, London, under Contract No. DPU 9/2/3 with the University of Edinburgh. The Project Officer was Dr P.C. Das. In addition the candidate (C. Colla) was in receipt of a "fees only" EPSRC Studentship.

CHAPTER 2

DEVELOPMENT OF CONSTRUCTION METHODS OF HISTORICAL MASONRY BRIDGES

2.1 Introduction

From an engineering point of view, the interest in historical masonry arch bridges has grown in the past decade or so, for a number of reasons, including their proven durability, low maintenance costs and clear economic advantages in terms of whole life costs. This has prompted the construction of several new unreinforced masonry bridges whose design has looked at the past for inspiration in appearance and construction materials. Moreover, the demand for safety evaluation and load carrying capacity calculation of these bridges, which has became urgent with the introduction of new load limits has initiated an assessment programme backed up by research work on arch bridges, sponsored by the Highways Agency.

Many aspects of the structural behaviour of masonry bridges have consequently been investigated, i.e. arch behaviour, spandrel walls, soil/structure interaction, road deck and foundation issues. This has been done by applying modern scientific knowledge to 150 and more years old structures, but still the outcome of such exercises is that there is not a certain and rapid analytical assessment method applicable to every kind of bridge, and the methods used are sometimes too conservative with consequences of strategic and financial importance.

One of the reasons for this is that analytical calculations usually use, as input information, the geometrical dimensions of visible elements (thickness of arch barrel as it appears from the prospect, span and rise of the arch, and so on) and the supposed conditions of the materials as they appear from visual inspection or from occasional,

localised, usually destructive tests performed on site or on samples cored from the structure.

So the assessment engineer generally bases the bridge calculations on the typical masonry bridge typology (fig A.1) which presents one or more spans, solid piers and soil fill inside the spandrels and wing walls. A defence of this approach is the fact that, apart from a few renowned bridges which, due to their prestige or importance, retain archive information about their construction and maintenance works performed over the years, for the majority of the bridge stock no such information is available. With the whole assessment operation more and more often put out for tender, this trend is not likely to improve.

Indeed there is a whole series of masonry arch bridge typologies which are never considered when performing the load capacity calculations, because they are not well known or believed to be not very common and not relevant. The fact that for decades, in this century, almost all the new bridges were concrete bridges and more recently steel and composite bridges, has led to forget the existing variety of types of masonry bridges which are still in use.

The aim of this review exercise into construction methods of masonry bridges and development of archetypal forms during the centuries, is to "refresh our memory" of the array of bridges that the testing and assessment Engineer can come across. It is hoped that the information collected, and summarised in section 2.17, can offer some guidance on how to recognise the different types of bridges and may suggest the internal spandrel configuration (hollow or filled) and materials used. Consequently, the final objective of the review is to look at these structures bearing in mind how different designs would affect bridge behaviour, its integrity and the load carrying capacity. Indeed inadequate original design requirements (inappropriate specifications of construction materials and/or methods), and not only increased traffic loading, may contribute to material deterioration and development of structural faults.

Masonry arch bridges from different parts of Britain will be considered, focusing on the period between 1720 and 1840 - the blooming age for these bridges - outlining the peculiarities of individual designers and specific areas. Following this classification, use and development of shapes and materials will be examined; in particular it will be seen how bolder arch shapes and span-pier ratios led builders to choose different filling materials and new solutions in spandrel walls.

2.2 Origins

Great was the contribution made by the Romans throughout Europe, who are generally accepted to be the past masters in the construction of roads, bridges and aqueducts, many of which survive to the present time (Mills, 1989; Paterson, 1989; ICE, 1989). The Romans were colonisers and needed roads, and their bridges were made to last.

One of the finest is Pont Du Gard at Nimes, dated about 19 AD. It has three tiers of arches and only the top tier uses mortar. Egyptians and others had used a gypsum mortar but the Romans developed pozzolana, a cement which can set in water and is ideal for bridges. Foundations were on firm material, but if necessary, on timber piles. Over this, concrete was poured, whereas later techniques used masonry on a timber grating. The shapes they used for the arches were usually semi-circles. A reflection in water of such an arch makes a perfect circle (see fig. A2). The coursing used in their arches and vaults varied but masonry was fairly regular (fig. 2.1).

The Romans were well aware of the lateral pressure of the soil on to the spandrels and built wine jars into the spandrels to reduce the "dead weight" and the pressure on the spandrel walls. Other of their techniques were later used in bridge construction. For example, the roof of Roman aqueducts' conduit was usually formed by a vault, but less commonly the channel had a corbelled roof, that is built out from each side, stone overlapping stone until they meet in the centre, (fig. 2.2.a) or was roofed with a

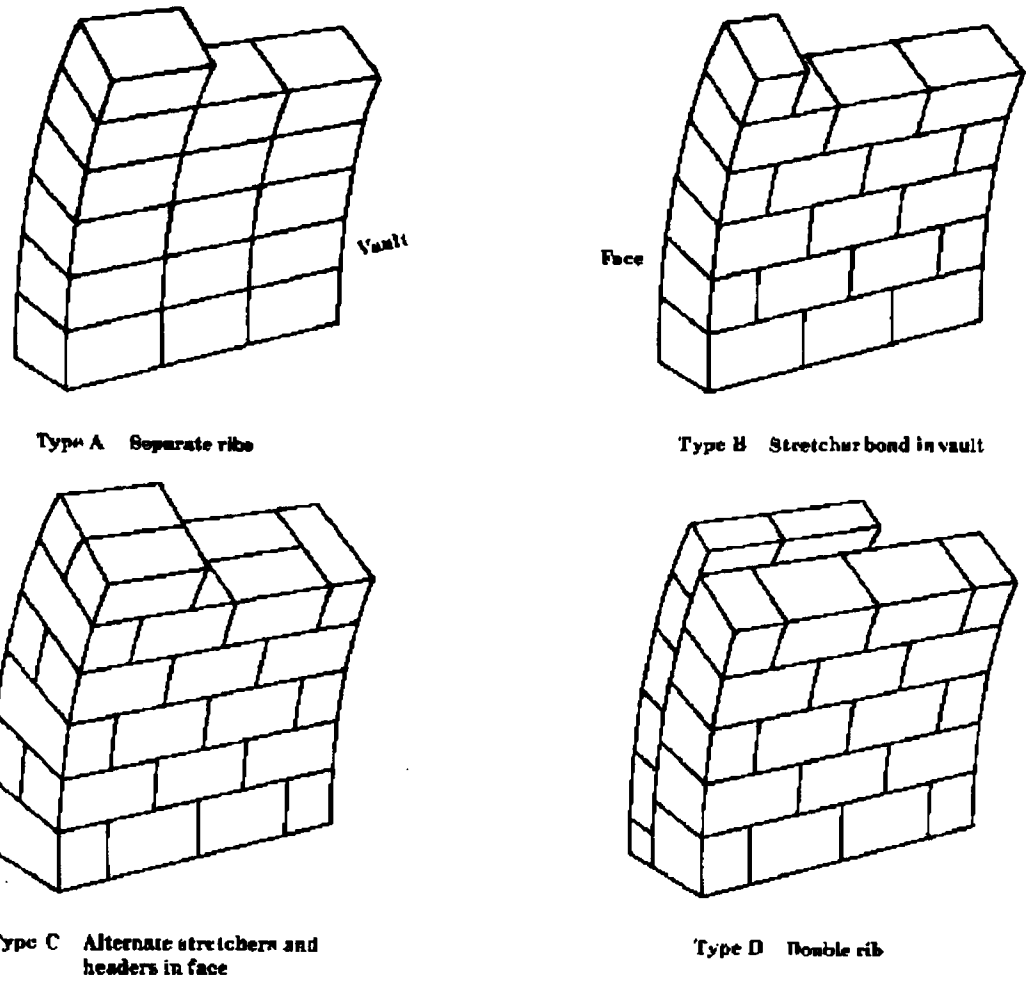

FIG. 2.1 - Coursing of Roman arches.

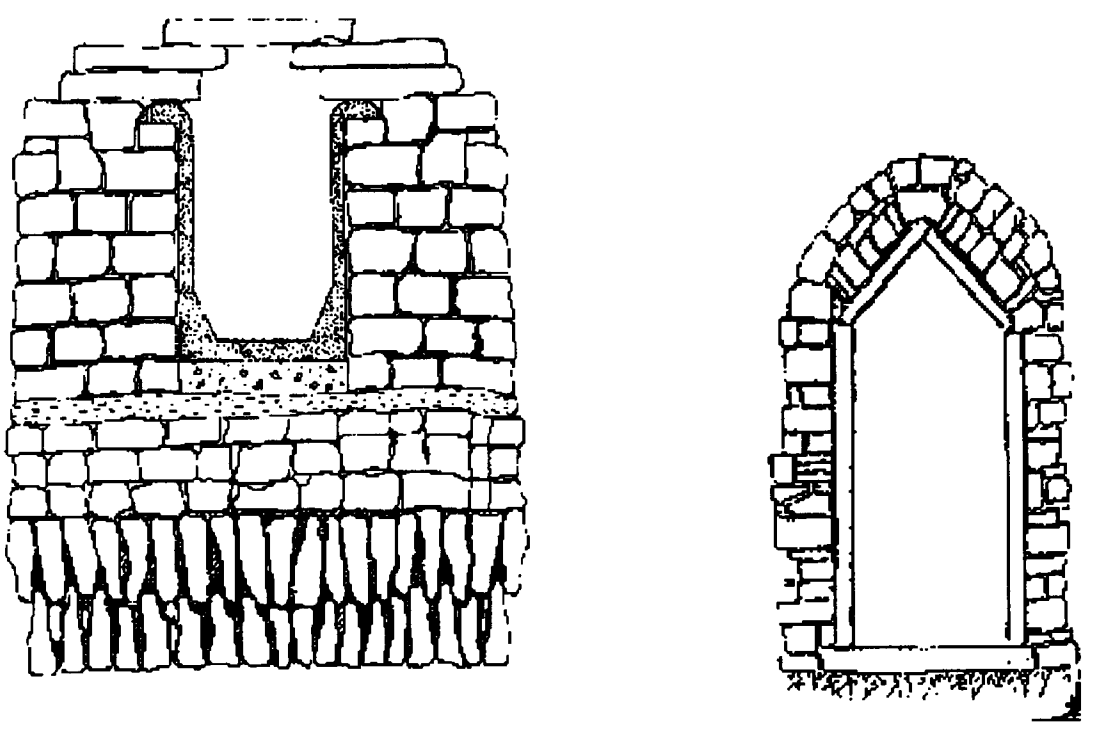

FIG. 2.2 - Cross sections of Roman aqueducts: Mont d'Or, Lyon (left); Ain Ferhat, Algeria (right).

flat stone slab or occasionally a pair of flat slabs tilted in to meet and form a pointed roof - gabled roof - (fig. 2.2.b) (Hodge, 1992). These solutions provided openings inside the spandrel walls, passing through the width of the bridge, and also inside the piers, running in the direction of the road.

At much the same period, 6th century AD, the Chinese have at Chao-hsien a masonry segmental arch bridge with relieving arches in the spandrels and with iron cramps between the stones of the 25 parallel arches of which the bridge vault is composed.

Other sophisticated bridges were built at very early ages. At Diz in Khazistan, a bridge with twenty arches may date from 350 AD. The Greeks, thought great builders, did not make much use of the arch. What they built were corbelled, but the method does not allow large spans.

Following the Norman conquest of England in 1066, local stone was used in a variety of forms and, as the work was often supervised by members of religious orders, the arches were constructed along similar lines to those which had been proven by experience in the construction of cathedrals and castles. Norman architecture adopted the familiar round arch to span openings in heavy construction. The stability of the arches was due, very largely, to their massive piers and abutments but, the amount of navigable river was much reduced. As with other buildings of the time, there was often irregularity of shape due to early foundation problems. The adoption of wide piers sometimes founded on small artificial islands formed by tipping stone into the river, induced scour especially during floods, and often resulted in settlement of the foundations during the construction period. Also inadequate centering caused deformations and collapses in bridges. Furthermore, because piers were built on the easiest place on the river, the result was uneven spans: a noticeable feature of such bridges.

The medieval bridge was often a water platform for all sort of buildings from chapels to shops and prisons. Inhabited bridges appeared in Europe around the Middle ages -

in the eleventh to twelfth centuries, depending on the country or region concerned - and enjoyed their heyday between the late Middle Ages and the end of the 16th century. They went into decline during the seventeenth century and, apart from Pulteney Bridge, in Bath, built in 1770, most were in desuetude and demolished during the course of the eighteenth century. A provisional review suggests that over a hundred inhabited bridges were built in Europe between the Middle Ages and the age of Enlightenment; only ten or so survive today (Murray and Stevens, 1996).

Many masonry bridges collapsed during construction, among the successful projects can be listed the Old London Bridge built between 1176 and 1209 under the supervision of Peter Colechurch. Elm piles were driven into the river bed and on them a platform of oak carried the free stone piers of which the lower courses were bedded in pitch. It was only 4.6 m wide and 285 m long and had twenty arches. The bridge stood for over 600 years until Rennie's new London bridge was opened in 1831. It was the longest inhabited bridge ever built in Europe. See fig. 2.3.

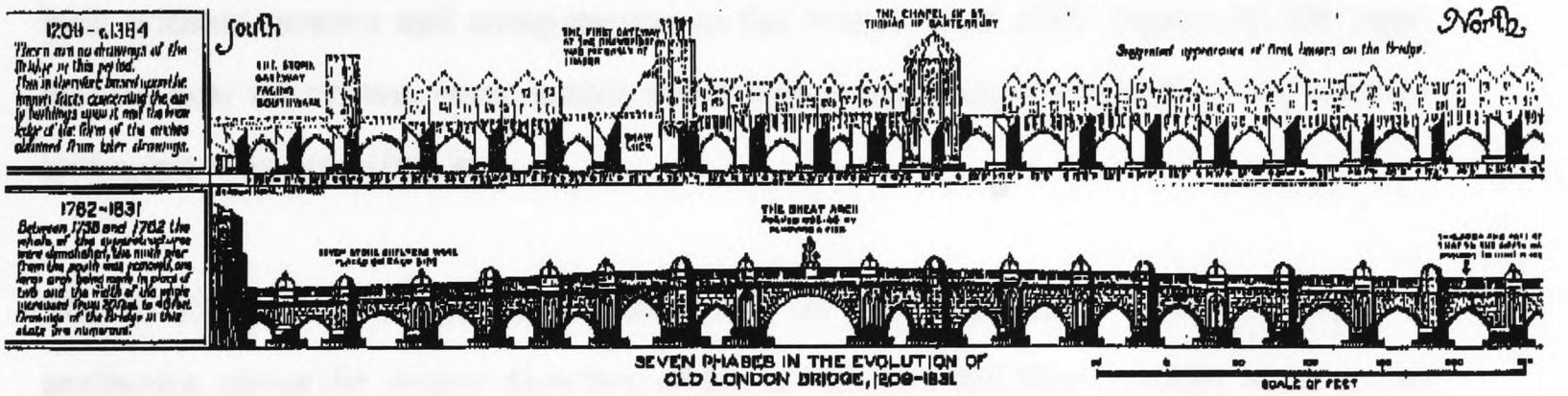

Fig. 2.3 Phases of Old London Bridge. (Museum of London).

2.3 Scotland

Most of the bridges and bridge-building in several parts of the Country were "ordinary". General Wade, in Scotland from 1724, built thirty-five bridges, of which the great part were only 3 to 6 m in span, about 3.6 m wide and had "easy" approaches. Details of either design or construction were left to the contractor but they were built of traditional forms and materials. His style continued to be used under his successors (the military road system by 1785 comprised 938 bridges) and it

has resulted in bridges all over Scotland, many in places where Wade never set foot (after the great floods of 1829, the written specifications of Thomas Telford took place).

The "style" was derived from the methods of building: the arches were built of local schistose stone ("whin"), which quarries in thin flat pieces long enough to form the thickness of an arch but with very irregular edges and surfaces. The most regular of these stones were chosen to make the faces of the arch on the elevations and others, often thinner, to make up the rest of the arch. The stones were first placed unmortared on the centring and wedged tight with thin stones or slates, then mortar was poured into the irregular voids between the stones. This is suggested by the fact that the thin voussoirs stand much nearer to vertical than to the direction radial to curve of the soffit.

However, in other bridges, the stones, for some distance up from the springings, lie at angles nearer the horizontal than radial, suggesting that these portions of arches were built without centres and using mortar as the stones were laid; higher up the same arches, near the crown, some stones stand higher than radial, suggesting that another technique was used (fig. 2.4).

The Scottish masons had clearly absorbed no inhibiting ideas from geometry or aesthetics, about the proper direction of joints. Neither did they consider semicircular arches as best and even the shortest arches are sometimes segments of no more than 90° or 100° (this would be an advantage in the tight-wedged method). All the spandrels (made of the local rubble masonry, sometimes of "whin" but equally often of granite) were filled with gravel or earth and continued without any break into the wing walls (a noticeable difference from Telford's bridges which came after them).

The common mechanism of decay for these bridges is: 1) outward bulging and spandrel collapse; 2) hole in the arches due to water percolating through the filling

material which leaches the lime out of the mortar, assisted by the ice pressure, in a progressive but slow decay.

Fig. 2.4 - Detail of spandrel wall and arch barrel of bridge near Dalwhinnie (after Ruddock, 1979).

Aberfeldy Bridge, built in 1734 as Wade's memorial, is a free stone bridge of 5 arches, about 120 m in length, the middle arch 18 m wide. The best architect in Scotland, William Adam, and master masons and carpenters from northern counties of England were employed, and the Scottish masons present, learned a lot. The bridge is entirely built of greenish-grey chlorite schist quarried locally; it has triple keystones on all the arch rings, triangular cutwaters, buttresses of trapezoidal plan and four stone obelisks at the middle arch. The most copied architectural feature is the profile of the parapet: the line is horizontal across the middle arch and then it turns vertically down and curves round to become a straight line falling at a constant gradient to the end of the bridge. The arches on each side of the middle one have to be much lower and also of much smaller span.

2.4 Wales

There are both similarities and differences between traditional Scottish bridges and those of Wales. They were similar in the sites chosen (foundation on rock), in the preference for single arches and in the form of the arches: segmental arches being as common as semicircular. The differences were in the materials used: the Welsh limestone quarries were known to give hydraulic lime as strong as any in Britain, and there was hard stone in most parts of Wales which quarried easily into oblong blocks, generally of small size but with true surfaces and with good square edges and corners. The thickness varied but were sometimes very small, as little as 5-7 cm.

As a result the Welsh masonry is very much neater than Scottish rubble and looks almost like hewn work. The arches were built with joints strictly radial to the soffit curve and with constant thickness of mortar, at least on the faces. The largest stones available were chosen for the arch rings, whilst thinner stones used for less regular courses in the rest of the arch were "flushed" with mortar of pouring consistency.

There is reason to believe that, at least in some instances, the thickness of the arch through these inner parts is less than that of the arch rings and in that case the thickness is smaller than the text-book rules of proportion demanded (on the other hand, the high strength of the lime in use, together with ignorance of the text book language could do much to explain this practice). (Barr, 1994; Jervoise, 1936; Barr, 1978)

2.5 England

The description above would apply to most of the Welsh bridges of the eighteenth century. In England, at that time, county bridges were still ribbed or pointed (marks of medievality), and even for short spans, semicircular arches were not common and the largest arches were segments between 90° and 120°. The most unsatisfactory feature however, was the narrowness of the bridges (from 3 to 4.2 m).

2.5.1 Westminster Bridge

When, in 1734, the construction of Westminster Bridge was decided, there were no guidelines, either in books or in standing bridges of such a large bridge in Britain. All the books about bridge-design and construction were from Italy (Palladio suggests span-pier ratios between 3.5 and 5.0) or France and, at the time, the semicircular shape of arches was considered the strongest. At this time Langley outlined the "scientific" curve of an inverted catenary and consequently proposed the use of cylindrical voids over the two haunches of each arch through the spandrels and directly over the middle of each pier.

Labelye, who was finally appointed engineer for the construction, offered in 1737 a design in which inside the spandrels - 13 m wide - each semicircular arch was backed with a "secondary arch" tapering from about 0.75 m. thick at the crown to a very large thickness at the springings. Over these arches, the space was divided into nine compartments by four walls of dry stone and filled with gravel (fig. 2.5). The proportion of arch span to pier thickness is about 4.5. This type of construction was so unusual that no one had experience about the appropriate rate to pay for it.

As a result of the settlement of the fourth pier, in 1748 it was decided to rebuild the two arches thinner than before with large voids roofed by segmental arches in the spandrels (see fig. 2.6). The bridge was finally opened to traffic in 1750 and its influence on British design was great: many people worked on it and the successful completion inspired new ideas.

2.6 Arch bridge design in the 1st half of the 18th century

Meanwhile, in 1729, the first book by Bernard de Belidor had been published, containing some advice on the proportions of arches and piers and on the use of various materials, but it was mostly of use to designers. It was only in 1752 in his "Architecture hydraulique" that he laid down firm rules for masonry bridge construction allowing thinner arches and piers than Gautier's rules.

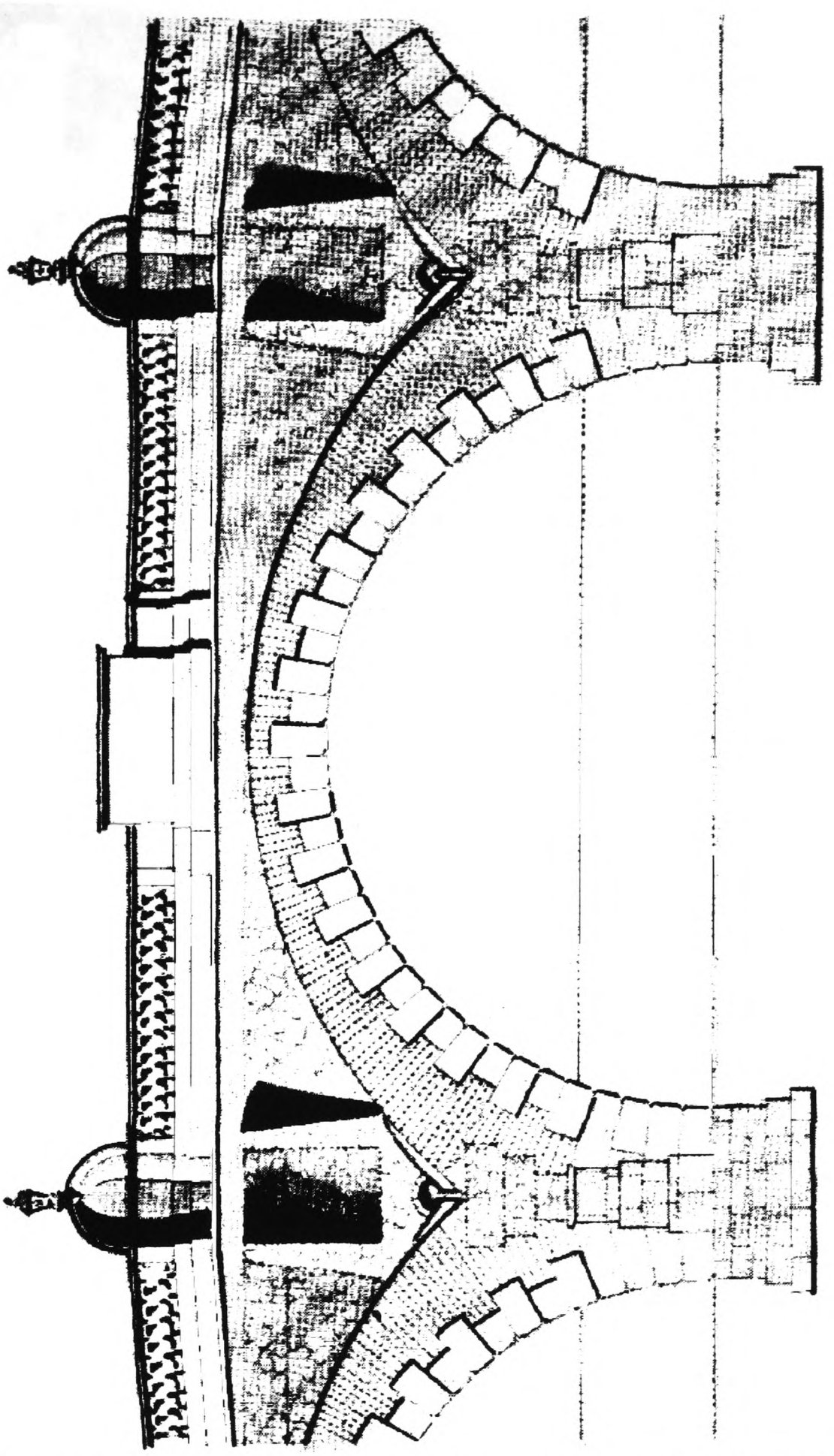

FIG 2.5- Section of Labelye's final design for Westminster Bridge (afterWalker,1979)

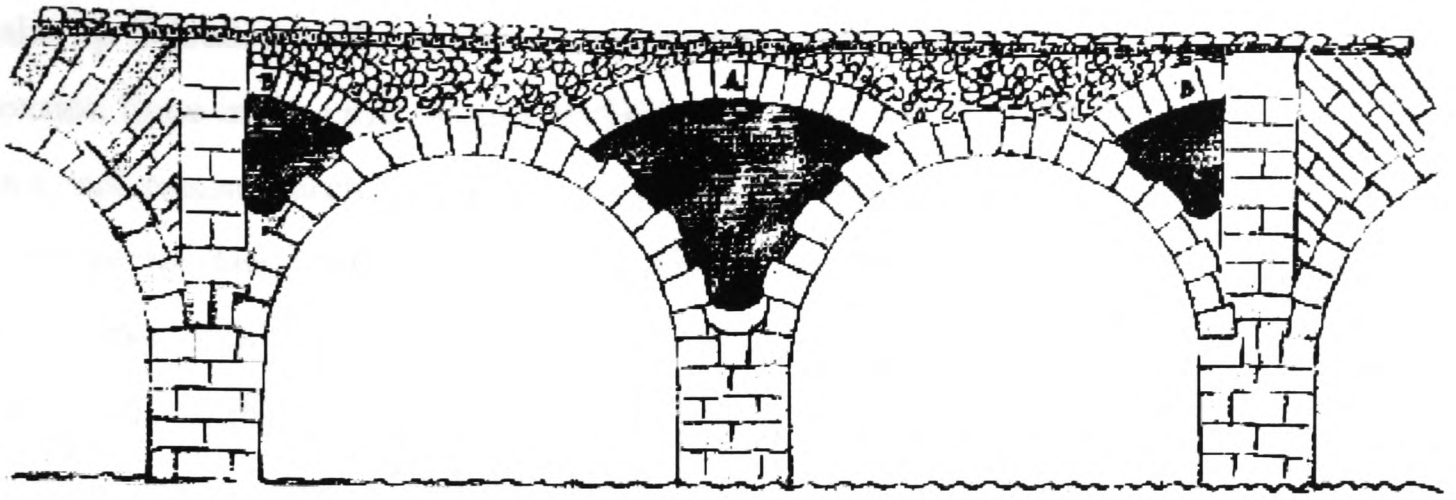

FIG. 2.6 - Westminster Bridge: William Stukeley's proposal for relieving the sinking pier, 1748 (Walker, 1979).

Gautier's Traite des Ponts which was published in Paris in 1714 was the first comprehensive treatise specifically on bridge building in any language and was used as a standard reference by British Engineers and Architects during the eighteenth century. The book provided a historical survey of bridges, practical guidance on construction and empirical design rules for dimensioning arches and piers.

Belidor's recommendations were: width between the parapets of 8.1 m., but 14.5 in a city to favour the traffic; the springings of arches at, and never below, low water, except in pointed arches; arches should be semicircles or ellipses with rise equal to one-third span; courses in the outside of the spandrels should be radial and the interior filled with masonry; thickness of arches at the keystone should be 1/24 of span for semicircular arches and 1/12 of radius at crown plus 1 ft. for elliptical arches.

Before the dawn of the eighteenth century, science twice offered guidance about the design of arches: firstly with "the catenaria", in 1676, by Robert Hooke, but the problem was that a real masonry arch is not at all flexible and not loaded only with its own weight; secondly with "the theory of equilibration" (1695, P. de la Hire) in which perspective the required weight for equilibrium increases from the keystone to the springings. This suggests either the voussoirs extend radially or voussoirs carry columns of masonry of varying heights. The curve of arch derived for a given shape of spandrels does not collapse if it is the curve, inverted, which a flexible cord would

take up if loaded with weights corresponding to the shape of the wall. The line of tension force in the cord, would be the line of compression force or thrust in the arch. In a real masonry arch, where there is frictional contact between voussoirs, there is no need for the line of thrust to be perpendicular to the joints (and therefore parallel to the soffit); it is enough that it lies within the thickness of the arch at every joint (Emerson, 1758). This theory would be relevant only for an arch bridge light enough to cause no movement of its supports, and not thin enough to cause risk of the line of thrust staying outside the thickness of the arch.

2.7 Pontypridd Bridge

Pontypridd bridge, Wales, designed by William Edward, collapsed with a wrong distribution of weight in the spandrels. With such a thin arch the weight of the spandrels would have to be close to the ideal weight. The arch collapsed upward and Edward somehow understood that the load was too great on the haunches. In 1756 he corrected the load by forming three voids through each spandrel of 2.7, 1.8 and 1.2m diameter and filling over the voids with charcoal instead of gravel (Fig. 2.7). At the time, the bridge had the longest arch span in Britain, 42 m. Even though built of so called rubble masonry and of very small stones it is, in fact, a perfect example of the traditional Welsh bridge-building, except in its long span and circular voids.

Designers reacted to the Pontypridd failure by proposing circular voids in the spandrels, especially in single-arch bridges and sometimes also between spans - mostly in South Wales and the adjacent counties of England, but there are instances of this form of construction in the North and in Scotland. Most of them would not need the voids to equilibrate their arches but the voids became part of the tradition; William Edward also began a family tradition of bridge-building: the bridges of all of the family, most built between 1760 and 1790, belong to the earlier Welsh style but with Edward's additions (used until well into the 20th century).

2.8 Blackfriars Bridge and Robert Mylne

In 1759, from over 50 designs for Blackfriars Bridge, preference was given to for Robert Mylne's design but objections were raised that elliptical arches were deficient in strength and stability (he would have had the piers as small and thin as possible). There was a striking change of architecture between the designs submitted for Westminster Bridge in the 1730s and those for Blackfriars Bridge: the source of ideas was no longer Palladio but the neo-classic by members of the Franco-Roman school in the 1740s.

Mylne sought to understand the relative strength of arches by imagining their physical behaviour: the middle part of the arch yields a lateral pressure against the haunches. These are thus secured by a counter arch, rubble work and a horizontal course of stone, so that all the structure from the haunches of the arches downward becomes a pier to support a small part of arch in the middle as a segment of a circle (fig. 2.8). The splitting of the arch at the haunches was original: the general concept was to employ a "skeleton" of stiff members of hewn stone and fill between them with rubble (Kentish rugstone); the horizontal course of stone from haunch to haunch and not the reversed arch (too deeply curved) was to carry the horizontal thrust. The design had nine arches and the parapets and the road sloped in two straight lines to an apex in midstream, with gradients of 1 to 30.

In a very short time after the acceptance of his design, Mylne had altered his proposals for the masonry of the piers (the widening of their base obtained by vertical steps at the edges of the first courses) and he replaced the reversed arch by a second horizontal course of hewn Purbeck stone similar to the higher course (Portland). The main arches were reduced in thickness to 5 ft. at mid-span and 6 ft. at the haunches. Each arch course was built of stones alternately the full thickness of the arch and half of the thickness. Blackfriars Bridge was opened to traffic in 1769 and continued to be used until 1864. The Portland stone used for all the exterior (due to its attractiveness resulting from brightness and excellent cleavage) was not resistant to atmospheric decay and especially susceptible to frost damage.

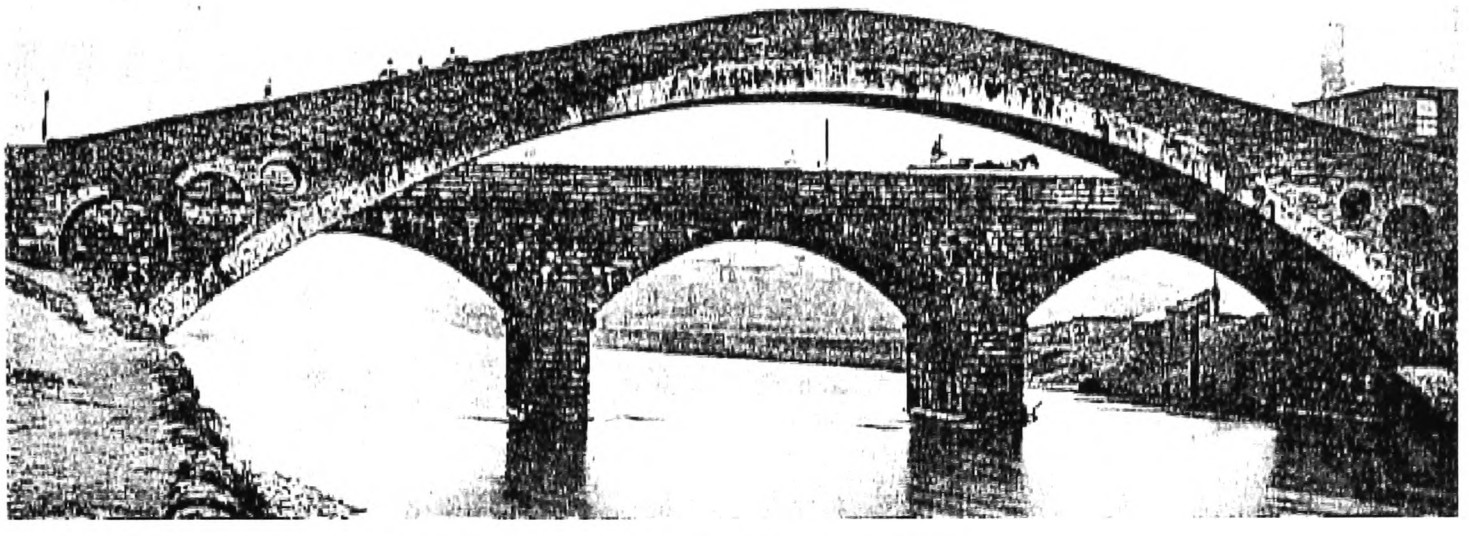

FIG. 2.7 Pontypridd Bridge (after Ruddock, 1979).

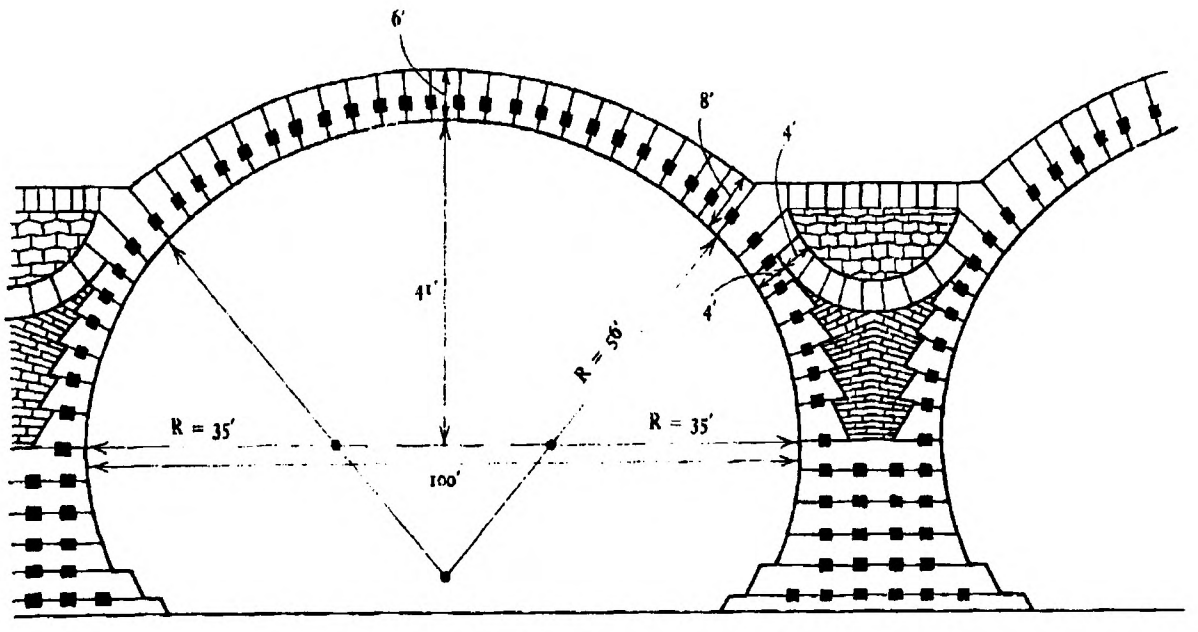

FIG. 2.8 Design by Mylne for Blackfriars Bridge (after Ruddock, 1979)

Although Robert Mylne was the first man to build elliptical arches in a large British bridge, there are no other elliptical arches in any of the bridges he is known to have designed. The arches he built after Blackfriars Bridge were segments of circles varying from 85° to 120° and therefore considerably flatter than any that Smeaton built, though they were of similar spans. They were distinctly thicker, however, even at the crowns, and in every arch of which the section thickness is known, there was an increase of thickness towards the haunch and/or springing. At Dubh Loch, the facades of the bridge showed a taper and it was not the same taper as in the section.

2.9 John Smeaton and Perth Bridge

Smeaton was a self-styled engineer and his bridges are all still standing. For the sequence of large bridges which were built, namely Coldstream, Perth, Banff and Hexham, Smeaton adapted his preference for arches of about 120° so as to make all the arches of a bridge have the same radius. The constancy of form and decoration in these four large bridges contrasts sharply with the variety shown in his earlier designs.

The early Hexam design (1756) appears to have been made with ill-judged economy, having four arches of equal span (22.8 m) and a horizontal road and parapets across the middle two arches and half of each end arch; but then a steep slope of 1 in 7½ down to the banks; the width between parapets was only 3.45 m. After that, Smeaton always adopted 5.4 m as the minimum width of road on a public bridge. The widths at Coldstream (6.6 m) and Hexam (5.4 m) were sufficient for the traffic until the early 1960s, when both were widened and the stone parapets rebuilt. The maximum gradient Smeaton allowed after 1756 was 1 in 12.

In his design for Blackfriars, though generally austere, there were two special aesthetic details. First, each cutwater up to spandrel was dressed back from its triangular plan to a trapezium not by a sloping plane, as was common, but by a curved surface with a decorative flourish at its bottom tip. Second, a course of stone with sharply curved soffit at the springing of each arch.

Though he may have drawn Blackfriars Bridge in anticipation of a prejudice against segmental arches, Smeaton clearly liked it. In the designs for Glasgow and Wentworth the arches were segments of very low profile as little as 65° of arc. These are the most original and striking designs that Smeaton made: the soffits were so long and low to look like a 20° century bridge.

All the ornament, Smeaton used first in Coldstream Bridge (comprising masonry rings on the spandrels with keystones on the ends of the vertical and horizontal diameters, triple keystones on the main arches and modiglions under a plain cornice), moreover he adopted these elements in nearly all his subsequent designs of large bridges. Smeaton recommended scrabbled masonry for the piers and the spandrels of the bridges of Perth, Banff and Hexham, with smooth-hewn arch ring mouldings and quoins. Similar finishes were used on most large Scottish bridges for a considerable time.

The line of the parapet of Coldstream was a continuous gentle curve (Mylne had done this in Blackfriars Bridge) over five arches of constant radius but varying span and height. He used elliptical arches only twice in large bridges in the end arches of Perth and Hexham bridges to lower their crowns more than he could do with circular segments, and thus reduce the height of approaches. His design for small masonry bridges show greater variety than those of large bridges.

Hollow spandrels had been proposed by Batty Langley for Westminster Bridge and by others for Bristol and Blackfriars Bridges, one had been made at Westminster over the "sunken pier", and circular voids had solved the problem of the Pontypridd arch in 1756. In his designs for bridges at Coldstream and Perth in 1763 and '64 Smeaton drew large rings on the spandrels but the circles within were to be filled with black rubble masonry (perhaps to look like a void) and the inside of the spandrels was to be filled with rubble masonry for 1.8 m above the springing of the arches and with gravel from there to the road level. Coldstream was built like that, with gravel of poor quality. At Perth all the arches were built and the rubble filling placed, before any of

the gravel was added; only two of the arches were still incomplete at the end of 1769 and Smeaton ordered that the spandrels should be hollow. Its importance is that it is a full design for the method of hollowing: the longitudinal voids shown as covered by pointed vaults of good rubble masonry and the whole structure tied from side to side over the tops of these vaults by iron chain-bars. This construction appears to have stood from then till now without serious derangement - fig. 2.9.

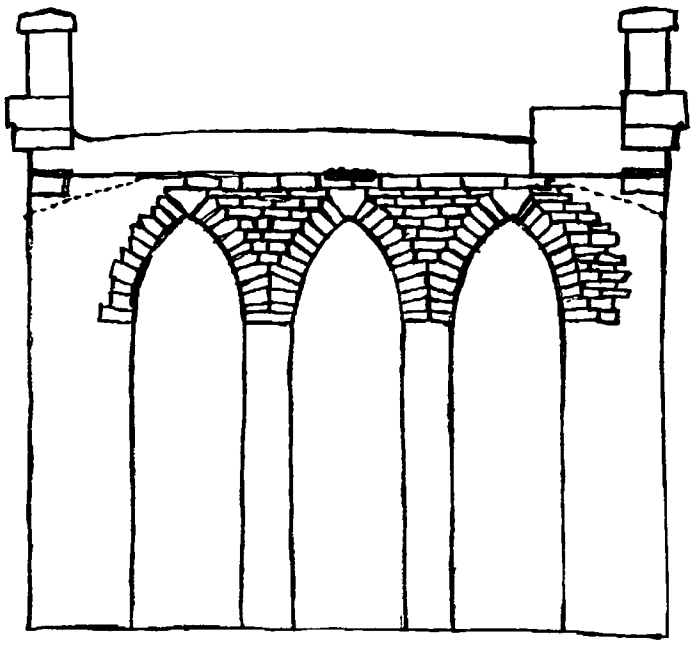

FIG. 2.9 Section of hollow spandrels of Perth Bridge.

2.10 Hollow spandrel wall construction

In August of the same year, 1769, part of North Bridge collapsed in Edinburgh. The drawing for the bridge were prepared in 1759 by William Mylne, Robert's younger brother, and he proposed three semicircular arches, each 72 ft. span, and two small abutment arches, all on tallish piers and connecting long earth-filled approaches each hollowed by three rubble vaults. The architecture was unexceptionable and all the construction conventional. However, the height of the bridge was not conventional and too heavy for conventional proportions of span to pier thickness and conventional thickness of retaining walls. William Mylne must have been aware of difficulties, for he thickened some walls and broadened the foundations during the four years he took to finish the bridge.

Within that time both Smeaton and Robert Mylne had submitted schemes for the repair of a bridge at Dumbarton. Smeaton's proposal for the tilted piers shows a plan of the spandrels over the reconstructed pier, the spandrels hollowed by longitudinal voids between walls which must run from back to back of the adjacent arches. A repair of this form had been proposed by William Halfpenny for the sinking pier of Westminster in 1748, but no practical use of it is known before 1768. In the same year, however, William Mylne made a design for a seven-arch bridge at Glasgow and he hollowed each spandrel by a large cylindrical void to reduce the weight and perhaps also the pressure of fill on the spandrel walls. This meant that he had learned the errors of his Edinburgh design but it was too late, for on August 1769 three vaults in the approach collapsed.

Smeaton, being in Scotland, was asked to report and from his experience on Perth Bridge he insisted on lightening the bridge: reduction of level of the roadway, larger voids in the approaches and new arched voids in the spandrels. For the spandrel voids Mylne or his brother Robert made cylindrical arches fully 20 ft in diameter which did not show on the outside walls.

Robert Mylne does not seem to have been convinced of a general necessity to make North Bridge spandrels hollow, though he may have made the first design for the Glasgow Bridge and he made a cylindrical void over the only pier of the Aray Bridge designed in 1773. In his part of Newcastle bridge he hollowed the spandrels to be filled with rubble and "rubbish" (probably allowing the use of stone and mortar from demolished buildings and other alternatives to clean gravel).

The smaller spandrels of Smeaton's Coldstream Bridge, which were gravel-filled, had to be taken down and rebuilt with longitudinal voids in 1828. By then, it was the accepted way of building spandrels between large arches. It accomplished at one stroke a reduction of load on the foundations, the elimination of outward pressure on the exterior walls of the bridge and a considerable mutual bracing of the adjacent arches against which the ends of the longitudinal walls were built. Whether Smeaton

derived it consciously from William Halfpenny's proposal for the repair of Westminster, invented it de novo or had knowledge of medieval bridges in Persia or elsewhere, it is impossible to say.

In England some notable bridge designs were made by James Paine engaged to design four large stone bridges across the Thames between 1774 and '84. In every spandrel of all the bridges there was a cylindrical void surrounded by an arch of brick, and brick was also used as hearting for some piers and abutments. The facing stone was from Purbeck or Swanage, after the first bridge, Richmond, where the most expensive Portland stone was used for the exterior. Chain-bars tied in the moulded architraves of long curved stones which Paine applied as the visible rings on the faces of the arches. Each arch springing was emphasised by three stepped rectangular blocks, expressing rugged strength at this point, and there were pavilions over the abutments with large cavities under them.

2.11 The Adams

A large part of the architecture of bridge design was due to the Adam brothers, John, Robert and James. The surviving collection of their bridge drawings number well over a hundred: none of them, however shows the internal construction.

The great majority of the drawings was made by Robert who was influenced by the ideas of triumphal bridges but he departed from the ideas of the Roman School in often designing segmental arches, sometimes of very low rise and in never placing columns on the spandrels as Piranesi and Mylne did. Adam's commonest spandrel decoration was apsidal niches with urns or vases; on plainer bridges he used medallions. He often drew the spandrels with radial joints and he chose moulded arch rings, cornices and balustrades with wide variety and with which he created the "Adam style". None of his very ornate bridge designs were ever built, but there are examples of his simpler designs standing in Derbyshire, in Essex and at Dalkeith House in Midlothian.

The two best bridges built in the early years of the brother's practice are of loosely classical form. The first is a three-arch bridge, in the grounds of Dumfries House at Cumnock in Ayrshire, built by John between 1760 and '62. The most unusual thing at that date is the form of arches which are ellipses, the middle one of 50 ft in span.

The second bridge was built in 1760-1 at Inveraray and is the Garden bridge or Frew's bridge. It consists of a single arch of 18 m span and again of elliptical form (form found in none of Robert's drawings), surmounted by spandrels of radial courses with masonry rings on them (both features which are found in Robert's design). The elliptical arches in these two bridges must be among the very first built in Britain, forestalling in construction, if not in design, those of Blackfriars bridge. In nearly all of Robert's design the parapets sweep down over the wing walls beyond the abutments.

At a time when old bridges with houses on them were being taken down and replaced, the Adam brothers produced several designs of these bridges. One, designed about 1785, was the South Bridge, in Edinburgh, continuing the line of North Bridge. The bridge being hidden, Robert Adam's taste was applied to the buildings but the bridge and buildings were built by others: the overall plan was not altered but the facades flanking the road were drastically simplified.

2.12 Alexander Stevens

Alexander Stevens of Prestonhall, Midlothian, from the style of his bridges must certainly be called an architect: he liked the "Aberfeldy profile" (from William Adam) and it was also his habit to build bridges with plenty of ornaments. He drew the Aberfeldy profile at Blackadder House, Berwickshire, a single arch bridge, and at Drygrange Bridge over the Tweed near Melrose. This was his most daring design (date 1778-80), of three high arches, the middle one 30 m in span, 10.2 m in rise and only 0.75 m thick at the crown, increasing 1.22 m at the springing; and the side ones 16.5 m in span and 8.1 m rise. The spandrels were hollow with two internal longitudinal walls to support the road, which was 4.8 m wide. The features show that

Stevens knew the most up-to-date structural techniques There were pavilions over the abutments with large cavities under them. He decorated the faces on the triangular buttresses which surmount the cutwaters with quatrefoil medallions and made a large circular panel on each spandrel with a classical urn of yellow sandstone standing before a black background. The rest of the bridge was mixed red and yellow sandstone and he placed conical spirelets on the ends of the parapets. The structure was strengthened in the 1920s by laying concrete 0.76 m thick over the crown of the large arch and 0.3 m thick over the spandrels voids, but little or none of the old masonry has been renewed (the bridge was closed to traffic in 1974).

In 1784 he constructed Ancrum Bridge over the Teviot: it has the Aberfeldy profile and three segmental arches of 15.3 and 16.8 m span and rather low rise, rusticated arch rings and a smooth parapet supported on corbels all in a pale pink sandstone.

The next two designs attributed to Stevens rank with Aberfeldy and Drygrange as the most decorated public bridges in Scotland. They are those of the Teviot bridge just upstream of its confluence with the Tweed at Kelso, and the bridge of Dum over the South Esk near Montrose. Stevens provided a first design for Teviot bridge in 1784 and it was still under consideration in 1792. The bridge as built by Elliot, of Kelso, about 1795, is of three high arches (the side arches are of 16.3 m span and 3.66 m rise, the middle arch 19.7 m span, 4.65 m rise and 0.74 m thick), the parapet following the Aberfeldy line with modillons under the cornice and well-detailed newels at the ends of the wingwalls; from the top of each cutwater rise two columns (first introduced by Robert Mylne in Blackfriars bridge in London, 1760-69), supporting a rectangular recess. Teviot bridge is true to the classical model, also having a horizontal entablature over the columns.

Bridge of Dum, dated 1785, is similar to the other Stevens' bridges in the structural details and the Aberfeldy shape, but he placed three stone columns each of three coupled shafts, on each cutwater to support the stone floor of a squared recess. On the spandrels are deeply carved crosses and inset panels; the faces of the long

approaches are carved with similar crosses and topped by corbels supporting the parapets. Such fulsome ornaments shows that Stevens was devoted to decorative masonry at economical costs.

In 1791 there was a powerful challenge to current ideas about bridge design: the speculative builder and architect John Nash offered a design for Newport bridge, Monmonthshire, with a single masonry arch of 85.5 m span, enormously high, being a segment of a circle of 93 m diameter. It surpassed by no less than 30 m the spans of the largest stone arches in the world. The scheme remained a project, but the dream of enormous arches had became a real project on a real site. It was time for great changes in bridge-building.

2.13 1790-1800

Until about 1790, architects (the meaning of the term was not what it is today but referred to men acting as mason contractors more often than as designers or supervising surveyors) were the majority of builders for important bridges.

In the decade 1790-1800 major bridge-builders changed from the architects to engineers. In those years John Rennie and Thomas Telford established themselves as the masters of bridge design, overtaking the older architects Mylne, Stevens, Harrison and Dance and younger aspirants like Soane and Nash.

Rennie was the youngest of all these men; in 1780-83 he attended Edinburgh University where he was instructed in the equilibration of arches but Rennie looked beyond the theory for broad design rules. One way of reducing the weiglit of the spandrels over the reins or haunches, was to make the arches elliptical, and it became Rennie's habit to make his arches elliptical unless they could be very flat segments with correspondingly low spandrels; he also made the spandrels hollow. He gave priority to durability over appearance, giving special attention to the springings of arches and the mutual abutment of adjacent arches. In 1795 he wrote: "... in flat arches the springing should commence in a gradual manner from near the

foundations". Between adjacent arches of multi-arch bridges he always made an inverted arch of hewn stone to carry the thrust from one main arch to the next. When he was designing Kelso Bridge in 1798, he made sketches with approximate lines of thrust within the masonry of the main and inverted arches. This was his first major road bridge and he explained the standards of construction advising against the use of rubble masonry. For the form of the bridge he chose a level road and parapet with a high approach embankment to have a symmetrical bridge that provided 110 m of waterway in five elliptical arches of 22 m span and 5.8 m rise. The arches were elliptical "not only because they give much more waterway, but because are better suited to the load they have to sustain". Inside the spandrels were inverted arches and longitudinal voids above them; the external masonry was to be all ashlar with Doric columns engaged to the face of the spandrels. Full repointing and some strengthening were carried out in 1921.

Thomas Telford was also a Scot and studied stone carving, drawing and architecture. His first major bridge was built at Montford on the Severn in 1790-92: it was a sandstone bridge of three elliptical arches, a form he seldom used again. He also built solid piers up to a certain height, but above that they were hollow, thus reducing the load on the foundations and placing the inside of the walls open to inspection. This became a regular practice in Telford's high bridges and also those of others who followed him.

2.14 1800-35

In the years 1800-35 there were developments in the design of masonry bridges: a lengthening of the spans of the largest arches (for practical reasons but also because of a competitive impulse to build a record span) and changes of form and architecture derived partly from France where Jean Rodolphe Perronet, first head of the school of Ingenieurs founded in 1747, developed his style characterised by three regular features and one occasional. These were: 1) pointed cutwaters, rounded at the shoulders and often from point to shoulders also, that extended up the spandrels to well above the springings of the arches and were sloped at the top. The interior of the

spandrels was normally filled solid with masonry; 2) arch curves either circular segments or ellipses and frequently of very low profile: the ratio of span to rise could be more than 12, which was quite as flat as most of the iron arches in Britain. Only the abutments were designed to resist horizontal thrust while the piers were made unusually narrow: the ratio of arch span to width of piers could be 9. It was necessary to erect centring for all the arches at once. 3) The lines of the roadway and parapets were generally horizontal or very near to so. 4) The sloping or chamfering of the edges of arches, tapering crescents on the elevations: cornes de vache (special fame in the bridge of Neuilly at Paris) which were found on older French bridges, gave a hydraulic benefit. In 1783 his methods became available to British designers.

2.14.1 John Rennie

In John Rennie's masonry bridges there are three elements which conform to the French style (arches of low profile, cutwaters with curved shoulders and horizontal or near horizontal parapet line) but in other respects they differ. The Esk bridge at Musselburgh, designed in 1803, has the profile of the road in a gentle curve, pilasters and niches and 5 low segmental arches springing from high-water, the end arches having span to rise ratio of 12 and the largest span to pier ratio of 6 1/2, which is more conservative than Perronet's (later his span to rise ratio will be about 7). The spandrels are hollowed by longitudinal voids, also unlike French methods. All his designs have pilasters on the spandrels and abutments and classical details; there is nothing at all French in their appearance, apart from the shape of the arches and parapets line.

Moreover Rennie made several designs in which there is even less French influence: in Kelso bridge there is only the horizontal road; also in Waterlow bridge, built in 1811-17, the road and parapet line were perfectly horizontal. The bridge had nine arches, each of 36 m span and most of the exterior masonry was of Cornish granite from Pernyn but a little Craigleith sandstone from Edinburgh and "Yorkshire stone" (sandstone or gritstone) were used externally and much more internally. Four flat bars of iron were set in selected joints of each arch and the voussoirs of the arches

varied in depth. The masonry inside the spandrels was laid in the form of an inverted arch and over that the spandrels were hollowed by longitudinal brick walls. The courses of stone were built up from both springings at once and the inverted arch completed as soon as the arches at each side of it were up to that level. The top of the centres was loaded to prevent distortion while the first courses near the springings were built. When the arch was keyed, the centring was eased immediately and the settlement which took place at the crowns varied from only 0.6 cm to 4.2 cm. This was the sort of behaviour Rennie had attributed to arches of equilibration when the line of thrust lies at the middle of the thickness of the arch throughout its length; this would be achieved by a correct lengthening of the voussoirs towards the haunches of a segmental arch.

2.14.2 George Rennie

George Rennie, the eldest son of John had been placed by his father at Edinburgh University in 1807, made the design for the new London bridge (Fig. 2.10) for his father in 1820 and projected 5 elliptical arches. George employed theoretical calculations in designing arches, being perhaps the first to apply theory to large structures which were actually built. For Harrison's Grosvenor bridge he proposed changes in the dimension of the voussoirs and form and dimensions of the abutments to make them conform to "the correct principles of equilibrium" and he made it a typical Rennie's structure: the arch proper was 1.2 m thick at the crown and 1.8 m at the springings but there is a large thickness of radial masonry over almost the whole of the extrados, as well as radiated courses in the abutments. The body of the arch is of Cheshire sandstone but the springing courses are granite.

2.14.3 Thomas Telford

Telford's views on bridge design were markedly different from Rennie's. He thought that there should be an odd number of arches, all springing from the same level and increasing in height and span towards midstream, so as to give a gradient on the road of about 1 in 24. He criticised columns and entablatures as improper because they were derived from Greek temples. At the start of his practice in Shropshire most of

his designs were conventional, built of hewn stone throughout, V-jointed on the faces and soffits of the arches.

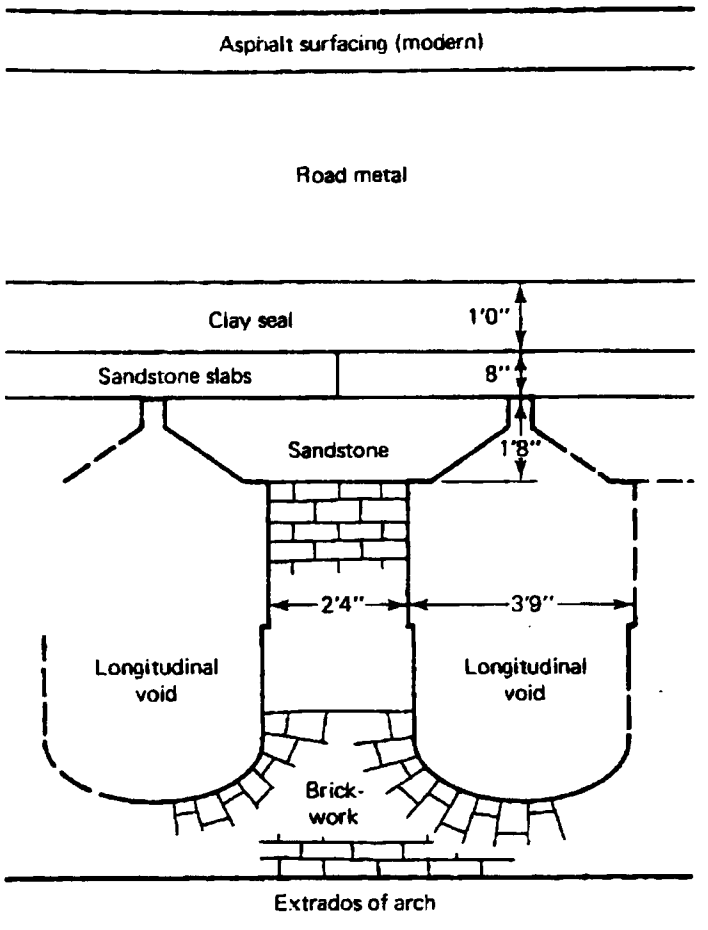

Fig. 2.10 - Cross section through spandrels of London Bridge (after Ruddock, 1979).

Moving in the next few years into Scottish landscapes, in the 1800s he built a series of quite different bridges at Scottish sites. They were all of 3 or 5 segmental arches, the road and the parapet curved in elevation, and trapezoidal buttresses or pilaster over the cutwaters providing recesses at the level of the road. They are practical structures with no added ornament. Even less pretentious are the rubble stone bridges built in hundreds for the Highlands Roads Commissioners of the same materials as the military bridges (see Wade) but with several improvements: arches of longer span, roadways wider. Telford's way of designing the many small single-span bridges was to write a standard specification for the bridges of any one road, describing the masonry of the arch, abutments, spandrels and parapets and giving the dimensions to be used in bridges of various different spans. The materials, at least for work above water level, seem to have been very similar to the older bridges; but there is one structural improvement never omitted even in the smallest bridges and which is an

almost foolproof of distinction between pre-1800 and post-1800 bridges of this type, namely the battered form of the wingwalls in the latter. The form of the vertical spandrels and battered wingwalls, became the commonest and it continued to be the standard construction for bridges in the Highlands until at least the end of the nineteenth century. In Telford's design the arches were segments but higher than Rennie's and there were no inverted arches over the piers or radiated courses in the abutments; there were always solid pilasters of considerable bulk over the cutwaters and never columns. Telford showed interest in the form of the "cornes de vaches", because it gives a great appearance of highness.

In Dean bridge in Edinburgh, Pathhead bridge in Midlothian and Stonebyres bridge in Lanarkshire, all built in the years 1827-30, he deliberately created shadows on the spandrels and an appearance of height by placing a slim projection on the faces of the tall piers and springing subsidiary arches from the projections at the points well above the springings of the main arches. Telford gave no aesthetic reason for this form but the resident engineer for Dean Bridge, Charles Atherton, wrote that the form was devised to overcome the criticism that the great mass of masonry being uppermost, the superstructure appears too massive. In Dean bridge, the forward projection of the higher arches is 1.8 m, in Pathhead bridge the projection is only 0.6 m, the arches of smaller span and the effect is rather fussy.

However, the highest tribute to his skill in the design of masonry bridges is that of Dean Bridge (Fig. 2.11), the farthest development of his architectural experiments, where he also achieved an excellence of construction and abiding strength which can seldom have been equalled. The whole interior, both of piers and spandrels, was built hollow with tie stones which connect the outer spandrels walls (0.9 m in thickness) to the inner parallel walls (0.6 m) and the interstices are covered with flat stones (Fig. 2.12), to support the roadway (the cavities are interconnected transversely by means of access holes for inspection (fig. 2.13). The whole of the masonry of this bridge consists of square sandstone, of excellent quality. The road construction itself was

novel, for in addition to the clay seal used earlier, Telford used hydraulic concrete as a base for the gravel or broken stone pavement (fig. 2.14).

The arches in the design were 18 m in span and the edifice about 32 m in height from the bed of the river to the surface of the roadway, the whole breath between the parapets 12 m and the total length 124 m. The design originally consisted of three arches, than changed into four arches. The main arches have the springing at 21 m from the foundations, and rise 9 m; at 6 m higher other arches, of 28,8 m span and 3 m rise. The subsidiary arches extended inwards over the main arches a distance of 0.95 m. To allow both sets of arches to settle freely when their centres were eased, they were built independently of each other and the centres eased before any spandrel walls could be built. The subsidiary arches, which are only 0.75 m thick, had therefore to be built and very gentle de-centred, all four spans together. The ratio of span-to-arch thickness was 38 and the ratio of span-to-pier thickness 19, which is more than double Perronet's maximum value of 9. After the first month during which the arches subsided by about 11.5 cm at each crown, the spandrels walls were built up between them and the main arches, thus providing much increased stability. The bridge was commenced in October 1829 and completed in December 1831.

Pathhead or Lothian bridge over the Tyne Water was designed by Telford in 1827, built by James Lees and opened in 1831. It consists of 5 arches, each of 15 m span and 7.5 m rise from their springings which is at about 15 m above the bed of the river. The piers are not solid masonry, the side and cross walls being 0.6 m in thickness; the width between the parapets is 7.8 m; the bridge consists of square sandstone. The design for Pathhead bridge preceded that of Dean bridge and here for the first time Telford introduced the "external" shallow arches.

2.14.4 Contemporaries

A few of the contemporaries of the two great engineers, Rennie and Telford, were Thomas Fletcher, Hugh Baird, James Walker, Robert Stevenson who built by

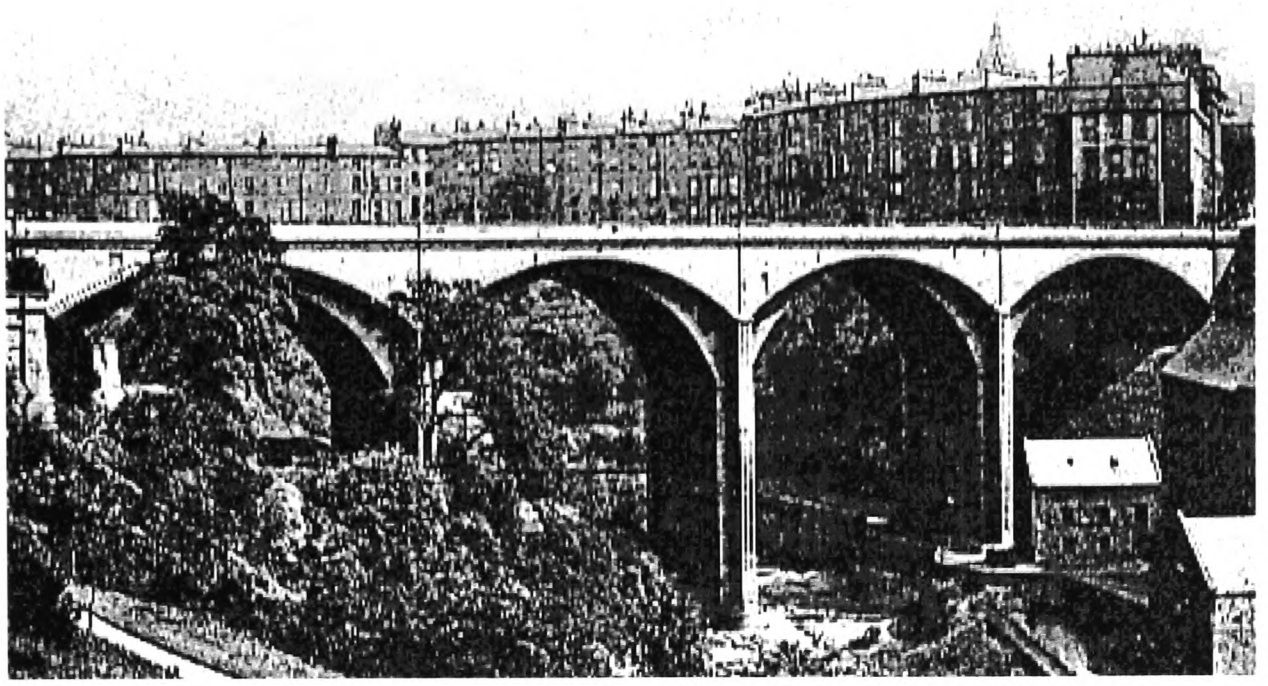

Fig. 2.11 - Dean Bridge, Edinburgh.

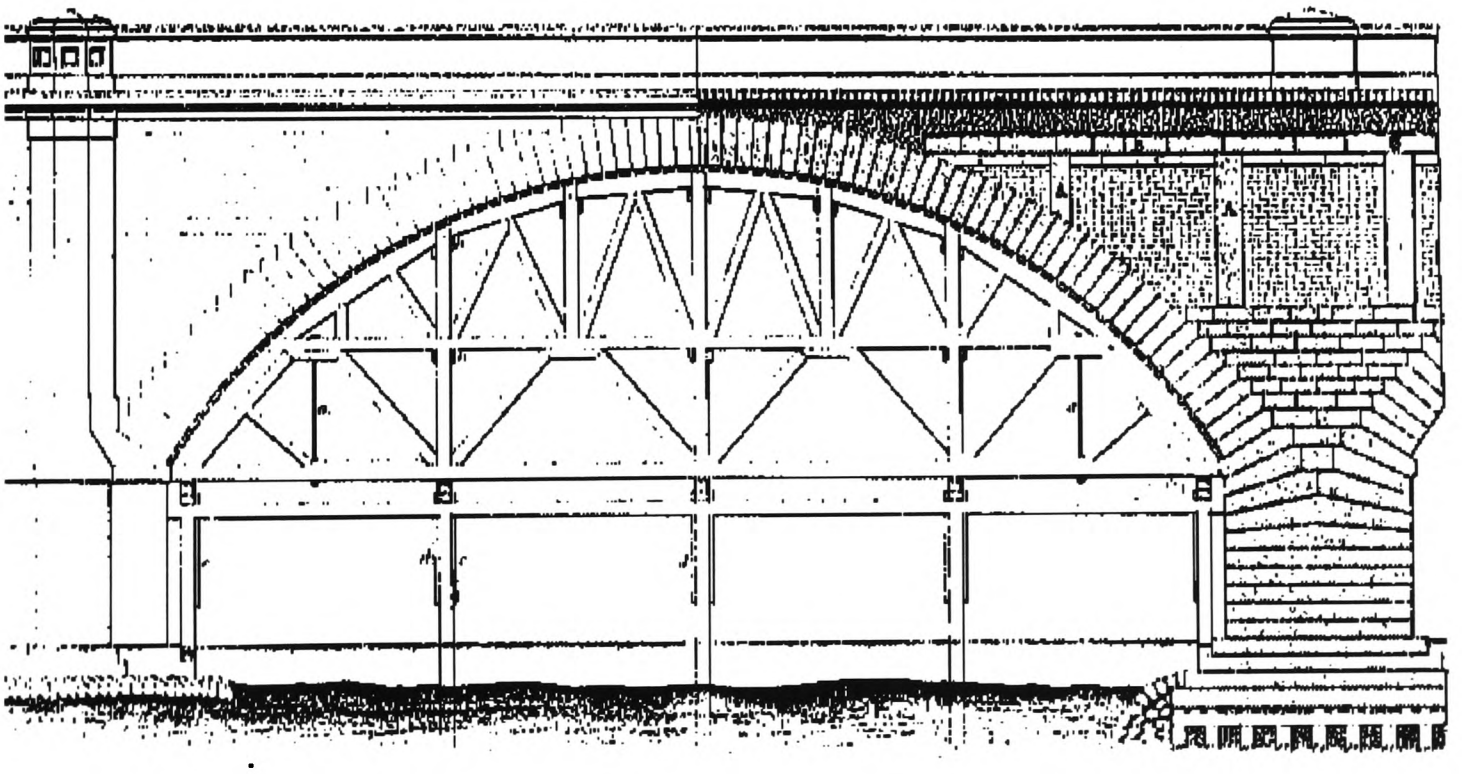

Fig. 2.12 - Prospect and section of Telford's bridge over the River Don, in Aberdeen (Nelson, 1990).

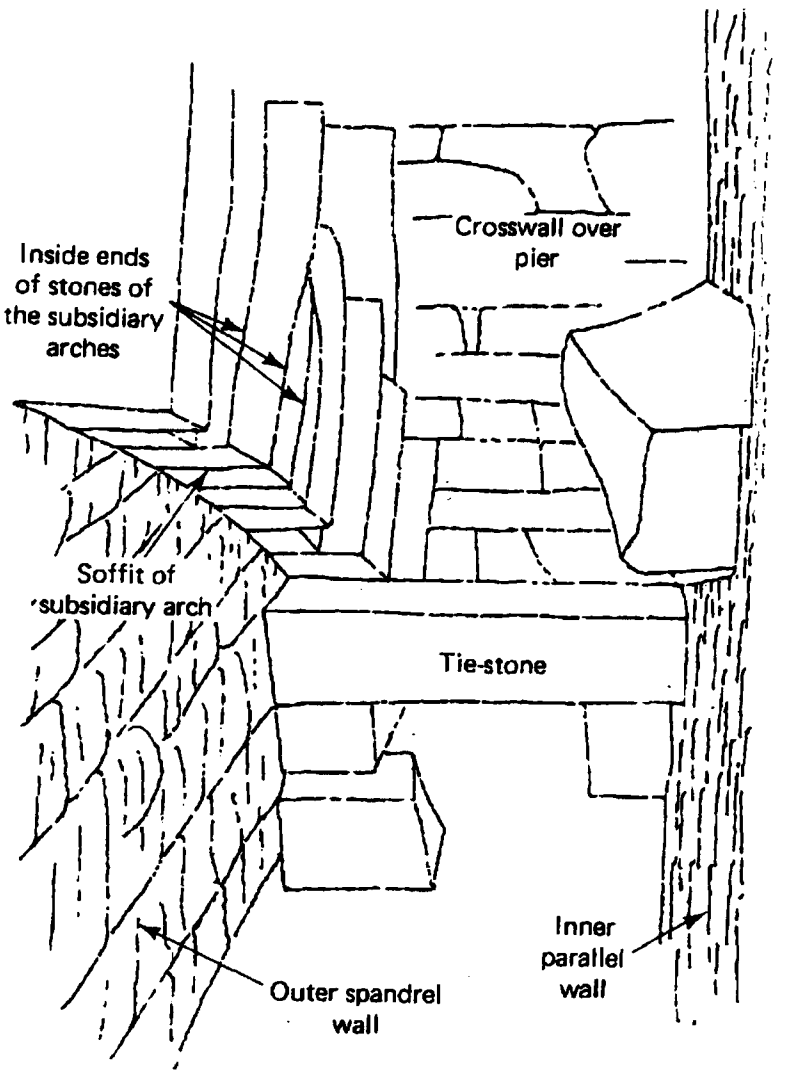

FIG. 2.13 Interior of spandrel of Dean Bridge (after Ruddock, 1979).

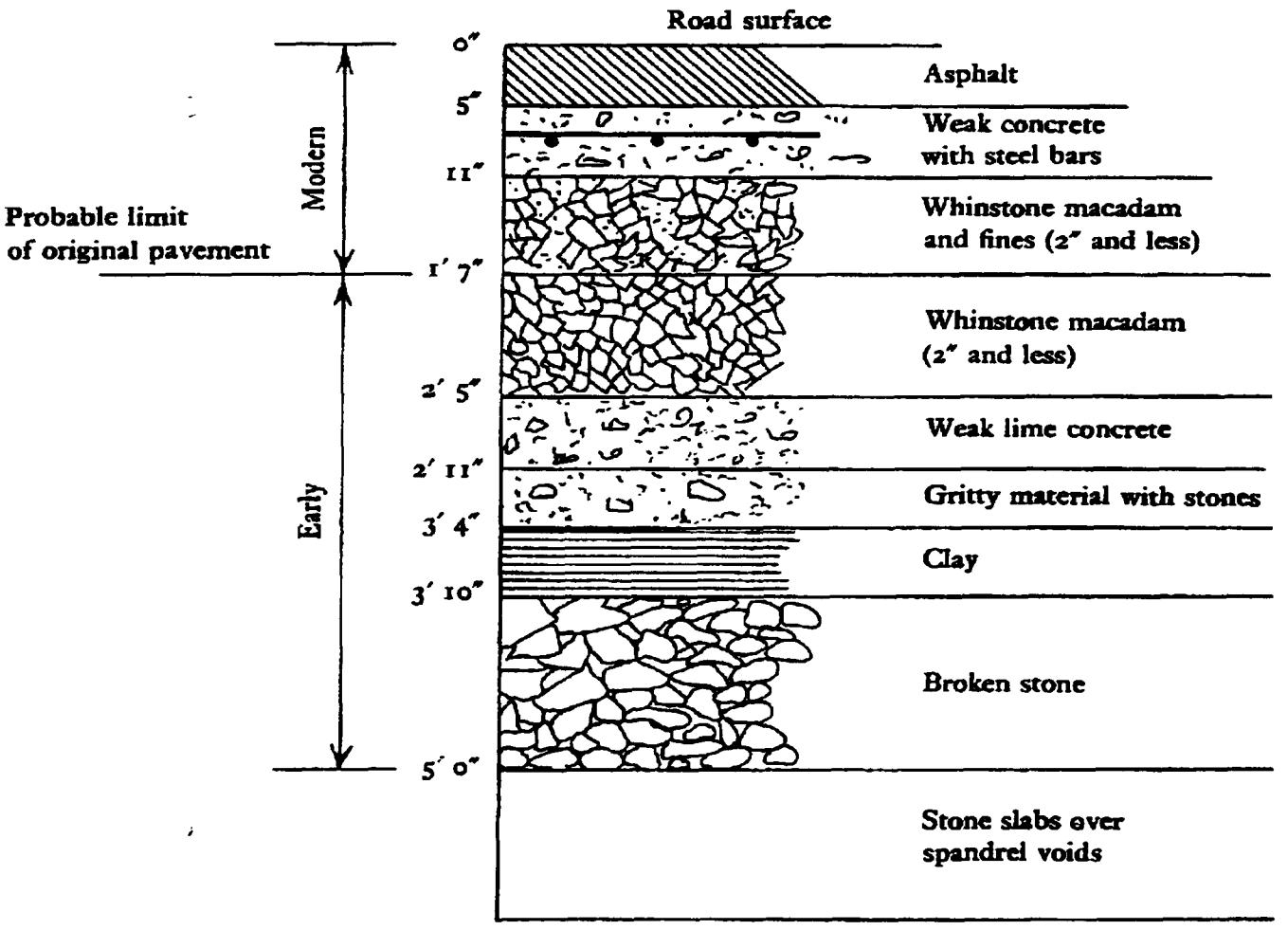

FIG. 2.14 Cross-section of roadway of Dean Bridge (after Ruddock, 1979).

methods similar to those of Rennie and Telford, using some segmental arches of low rise, but not so low as some of Rennie's.

Alexander Nimmo became a bridge designer without undergoing any training as an architect or engineer. The bridges he is known to have designed show that he was as conscious of style as Telford but there is more attention to the style of individual bridges, even when they were very small. In Wellesley bridge (1824-35) Nimmo was not content with ordinary "cornes de vache" and he curved the whole soffit. In everything except size Nimmo's bridge is the equal of any of Perronet's and in its basic form at least a little nearer perfection.

With Telford's, Rennie's, Harrison's and Potter's bridges, together these bridges represent the best of the art and skill of bridge-builders at the opening of the railway age. Bridge loadings up to the railway age were generally so light in comparison with the dead weight of the structure as not to have any material effect on the structural considerations

2.15 Other materials and 2nd half of the 19th Century

However from about 1800, cast iron, wrought iron and later steel were commercially available. This led almost immediately to the development to a great diversity of new types of bridge, even though many hundreds of masonry arch bridges of up to 12 metres span were still built in Britain during the periods of canal and railway construction in the late eighteen century (the 127 year old masonry rail bridge collapsed at Ness, Scotland in 1989, because undermined by scour, revealed its spandrels were filled with rubble masonry up to a certain height and then with soil up to the rail level). At about 1900 reinforced concrete, which combined the good quality of both stone and steel economically, was developed and became the predominant structural material.

Fuller gave his construction for the thrust line in 1875, but the masonry arch was already obsolescent by the mid-nineteenth century. Also, Sejourne' published in six

volumes early in the twentieth century a definitive catalogue of large span masonry bridges throughout the world, but the ninth edition of the Encyclopedia Britannica devotes in 1876 most of the space to wrought iron and steel, and little to masonry bridges. Indeed there seem to have been little further work on the masonry arch, until well into the twentieth century when there was a renewed interest just before the second World War, due to the activity of Pippard.

2.16 The 20th Century

At the end of the 19th Century, a number of architectural and engineering manuals reviewed construction typology of masonry bridges. Rankine gives a detailed description of a masonry bridge and terms associated with it in his 'A manual of Civil Engineering' (Rankine, 1900).

The outer or convex surface of the ring of arch-stones is described as either a curved surface or a series of steps. However the thickness of the arch ring visible on the external face of a bridge not necessarily represents the thickness of the barrel. In fact, behind the surface voussoirs the masonry is less well cut and may have only half the thickness. This deceit is not practised in larger spans. (Heyman, 1982) Recent restoration work on a multi-span railway viaduct (Fig. 2.15) and a road bridge - Nasmyth bridge, near Edinburgh - both revealed examples of very uneven voussoir thickness in the arch (Paxton, 1996 b; Ruddock, 1996).

The description of masonry used for arches is either ashlar or block-in-course, the beds being perpendicular or nearly perpendicular to the direction of the thrust through the arch ring, and the side joints perpendicular to the beds and to the soffit. Ashlar is generally built like regular coursed rubble but the height of the courses of stone is regular (fig. 2.16.3). Ashlar is the best type of masonry and was the most expensive (McMillan, 1987).

Rankine describes how to build a stone arch and points out that some engineers have placed sheets of lead in the bed-joints, to distribute the pressure between the stones.

This practice of using lead seems less common than what initially thought (Howe, 1897; Melbourne *et al.*, 1997).

Rankine again continues: "The backing of an arch consists of block-in-course, coursed rubble or random rubble (see fig. 2.16.1), and sometime of concrete. When the backs of the arch-stones are cut into steps, the backing is built in courses of the same depth with those steps, and thus bonded with them. Sometimes the backing is built in radiating courses, whose beds are prolongations of the bed-joints of the voussoirs. Both these methods are favourable to strength and stability."

Page's description of the backing material is, instead, of 'cemented material', often rubble loosely cemented together, and almost as stiff as properly placed masonry and which was free draining. With brick arches the backing is usually brick which may be laid almost to the crown and laid to a slope away from the crown. (Page, 1993).

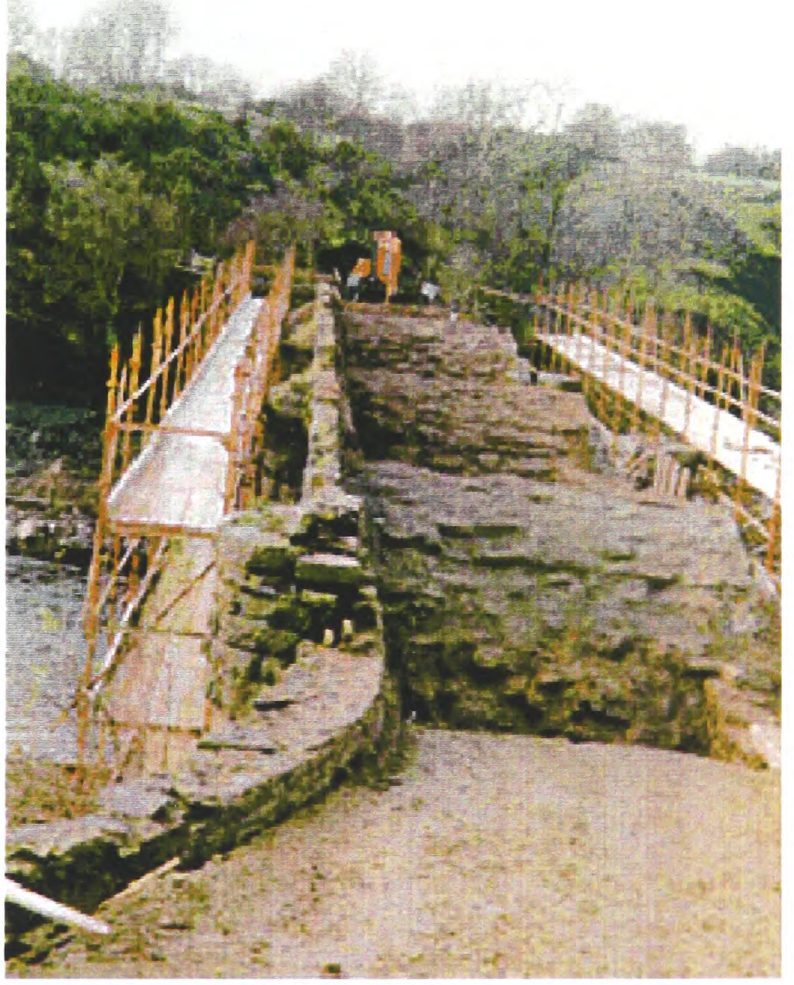

FIG. 2.15 - Laigh Milton railway viaduct, Ayrshire, after removal of the clay infill from the spandrels (Paxton, 1996 a).

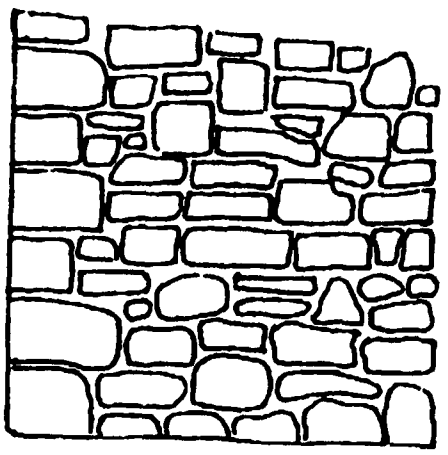

a) Uncoursed

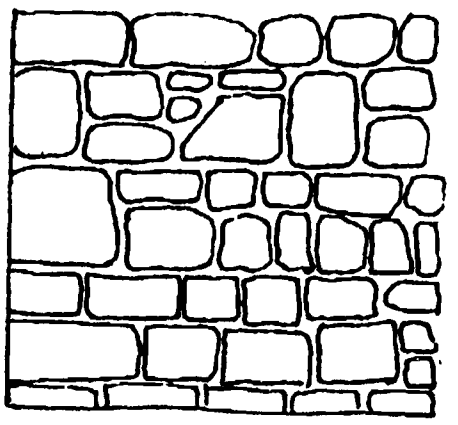

b) Coursed

FIG. 2.16.1 Random rubble masonry: a) uncoursed, b) coursed.

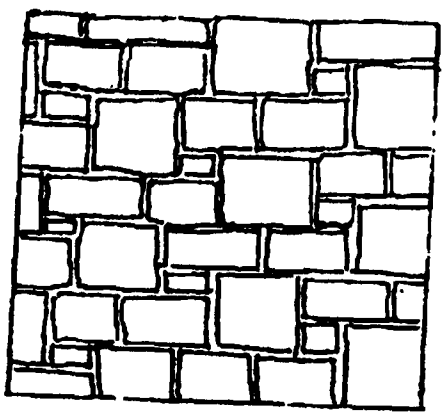

c) Uncoursed

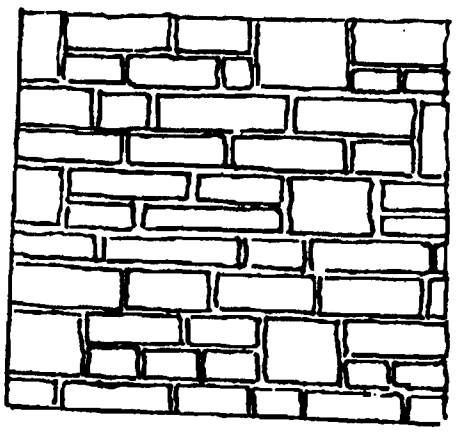

d) Coursed

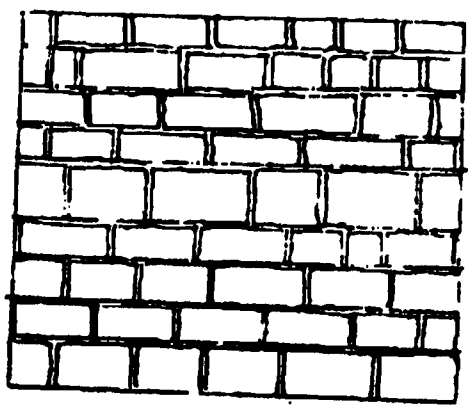

e) Regular-coursed squared rubble

FIG. 2.16.2 Squared rubble masonry: c) uncoursed; d) coursed; e) regular-coursed.

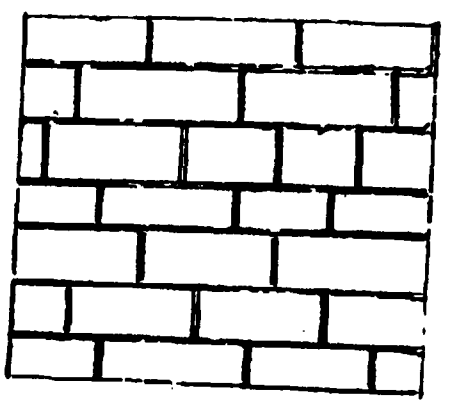

FIG. 2.16.3 Ashlar masonry. (McMillan, 1987)

Backing also constitutes an increase in the overall lateral stability of a multi-span bridge, as confirmed by studies of experimental load testing on bridge models: an average increase in the collapse load of 19% occurs when a wedge is in place between two spans to simulate backing between the arches (Prentice and Ponniah, 1994). Rankine continues: "The upper surface of the backing and of that part of the arch, if any, near the crown, which is without backing, is coated with a layer of waterproof material, such as clay puddle, (refer to Appendix A) mixed cement or bituminous concrete."

With respect to spandrel walls, the space between them is filled up to a certain level with solid masonry, and above that level it is sometimes filled with earth or rubbish". So the larger part of the total weight of a masonry arch lies in the non-structural fill. In a small arch the fill may be composed of rubble, of earth, or of gravel or hoggin, built up to the desired height to carry the road surface; the fill cover at the crown is often less than 2 ft.

Other times the internal of the spandrel is occupied by a series of internal spandrel walls parallel to the external ones and having vacant spaces between them. In order to form a continuous platform for the roadway, the space between the internal spandrels are sometimes covered with flags of some strong stone, such as slate (Fig. 2.17), and sometimes arched over with small transverse arches. The external spandrel walls are the abutments of those arches, and must have stability sufficient to sustain their thrust. Mitchell (Mitchell and Chettoe, 1925) reports that stresses in such a bridge are more or less indeterminate" but not necessarily worse than in soil filled bridges. Sometimes tie-walls in the hollow spandrels of arches are present. These are transverse walls at right angles to the spandrel walls. The distance from centre to centre of the tie-walls may be from three to five times the distance from centre to centre of the spandrel walls.

Abutments for reasons of stability and economy can also be built with hollows in them, or with narrow archways passing through them, perpendicular to the main

archways which the abutment support. These archways should have inverted arches at the bottom, to distribute the load over as large a base as possible. The hollows or archways may occupy about one-third of the whole volume of the abutment. Piers, like abutments, are advantageously lightened, especially when very lofty, as in viaducts, by being built hollow or by having archways transversing them, with inverted arches at the base. Arches and their abutments and piers may be made light and stiff by building them in parallel deep ribs, with thinner portions of masonry between them; but this of course involves additional workmanship and so it was not commonly done.

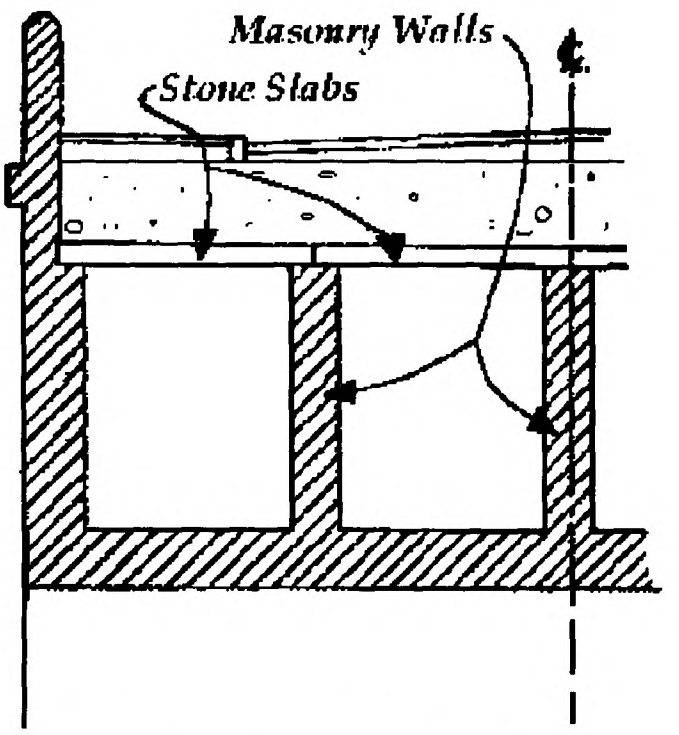

FIG. 2.17 - Vertical cross section, through the arch, of bridge with parallel spandrel walls.

Familiarity with types of masonry arch bridges was soon forgotten and from the 2nd WW onwards, various tests carried out by the Building Research Station "demonstrated" the complexity of the masonry arch and surveys highlighted the constructional variations which occurred between masonry bridges and which could not be fully determined without demolishing the structure. Variations included: 1) fill which could be clay, rubble or a mixture of each. 2) the barrel varying in thickness between arches but also having a different thickness for the interior, to that indicated on the elevation. 3) stepped arch barrels lying between the spandrel walls. 4) concrete

saddles placed over the arch in earlier strengthening schemes and not recorded. 5) quality of foundations to abutments. 6) quality of masonry or brickwork, which can vary considerably throughout the arch.

Table 2.1 reports material and geometrical information regarding a number of bridges on which load tests or strengthening work have been performed.

2.17 Conclusion

A-priori information about the materials and complexity of the structure under investigation, is often very valuable when a survey has to be carried out on site; this knowledge is sometimes essential in the NDT field. The information is equally important for the purpose of load capacity assessment. This section tries to summarise the main findings extensively described in the chapter, and where possible, it attempts to give advice on how to recognise types of bridges and/or their designers. From the age of construction, the area, the designer name or influence, it is often possible to forecast what were the materials used in the bridge, the internal spandrel configuration and the inner arch barrel shape.

Medieval bridges are heavy constructions with round or more often pointed arches and massive piers and abutments. Made of local stone, they are often of irregular shape and have uneven spans.

In Scotland, and Highlands especially, between 1724 and 1829, bridges have spans between 3 and 6 m and, in the forms and materials, they continue the pre-1724 tradition: the masonry of the arch is irregular schistose stone with voussoirs not radial to the curve of the soffit. The shapes are segments of no more than 90° or 100°. All the spandrels were made of the local rubble stone, either granite or schist, and filled with gravel or earth; they continued without break into the wingwalls (a difference with later bridges).

In 18th Century Wales, the materials are hard stone and hydraulic mortar. Spandrels are of neater masonry, almost hewn work. The arches, segmental or semicircles,

Bridge	Reference	Arch Ring			Fill			Haunching	Spandrel Walls	
		Span (m)	Thickness (mm)	Material	Material	Bulk Density (kg/m^3)	Moisture Content (%)	Description	Material	Thickness (mm)
Bridgemill	Hendry et al, 1985	18.30	711	Sandstone	Gravelly sand/clay	1890	nr	nr	Sandstone	nr
Bargower	Hendry et al, 1986	10.00	558	Sandstone	Silty gravel/sand	nr	nr	Boulder/sand, no sign of mortar	Sandstone (ext.) rubble (int.)	1400
Preston Upon the Wealdmoors	Page, 1987	4.95	360	Sandstone	Sandy clay	2000	18	Large coursed sandstone, probably cemented	Brick	600
Prestwood	Page, 1987	6.55	220	Brick	Reddish brown sand-little gravel	nr	nr	None	Brick	340
Torksey	Page, 1988	4.90	343	Brick	Non-cohesive sand, some gravel	nr	nr	Brickwork, 1.05 m below surface	Brick	380
Shinafoot	Page, 1988	6.16	390-770	Stone (random rubble)	Silty sand with some gravel and clay	nr	15	Loosely laid random stone	Random rubble	365
Strathmashie	Page, 1989	9.42	600	Stone (random rubble)	Cobbles downward	nr	nr	None	Random stone	Varies
Barlae	Page, 1989	8.53	450	Sandstone	Gravel/sand/silt/12% clay	nr	nr	Large random stones in mortared layers	Sandstone (internal spandrel walls)	400
Croft Breadsall	Davey, 1953	6,45	356	Sandstone	nr	nr	nr	nr	nr	nr
Yardley Wood Road	Davey, 1953	6.50	343	Brick	nr	nr	nr	nr	nr	nr
Alcester Road	Davey, 1953	6.45	356	Brick	nr	nr	nr	nr	nr	nr
Laigh Milton	Paxton, 1996	12.2	600	Freestone	Stiff clay	nr	nr	flat stones up to 1.5 m above springings and set in lime mortar	Coursed rubble	300-1100
Rotherham Road	Page, 1994	8.9	430	Brick	Packed stone rubble overlain by 60 cm crushed rock	2000	High	Not excluded	Brick + unreinforced concrete	215+900

TABLE 2.1 - Geometrical and material information from a number of bridges

nr = not recorded

have strictly radial joints and the thickness may be less in the inner of the barrel than on the ring faces. At the same time in England, county bridges are very narrow (3 to 4.2 m), still ribbed or pointed (semicircular arches are not common) with max. segments of 90° - 120°.

The construction of Westminster Bridge, from 1734, introduces a number of innovations which will be rapidly spread over the Country: 1)higher span/pier ratios (about 4.5); 2) semicircular arch shape; 3) arch backed with a tapering secondary arch; 4) spandrel space divided into 9 compartments by 4 perpendicular walls of dry stone and filled with gravel; 5) hollow segmental arches resting on the thinner semicircular arches of a sunken pier (1748).

In 1756, Pontypridd Bridge introduces the concept of a lighter fill above a thin arch, with voids through each rubble masonry spandrel and charcoal infilling. The innovative features were extensively copied after 1760 in South Wales and adjacent counties of England, with examples in North England and Scotland.

Blackfriars Bridge (1759) introduces thin elliptical arches with counter arches in between, filled with rubble work and topped by a horizontal course of stone from haunch to haunch. Thus, the middle portion of the arch acts as a segment of arch supported by stiff piers filled with rubble. Each arch course was built of stones alternatively the full thickness of the arch and half the thickness. Instead, all other bridges by the same designer, Robert Mylne, have segmental arches, between 85° and 120° and present a taper (thicker sections at the haunches and springings), and thinner sections in the inside of the barrel.

John Smeaton's large bridges present segmental arches (about 120°) with triple keystones and ornaments on the spandrels (masonry rings with keystones at the end of vertical and horizontal diameters). Scrabbled masonry is used for piers and spandrels, and rubble masonry infill for 1.8 m above the springings and gravel - of poor quality - from there to the road. These features were copied on most large Scottish bridges,

whilst small bridges show variety of design. Instead, Perth Bridge (1769) presents a full design for the method of hollowing: longitudinal voids covered by pointed vaults of good rubble masonry and tied by iron chain-bars.

So, from 1768-69, there are two ways of building large bridges:
a) longitudinal voids between walls, which run from back to back of adjacent arches;
b) large cylindrical voids running from spandrel to spandrel and which do not show on the outside.
By 1828 this is the accepted way of building spandrels between large arches both in Scotland and England.

Bridges presenting the "Adam style" appear from 1760 and are recognisable because very ornate, of classical form, with spandrels of radial courses and masonry rings on them. They have elliptical arches and there is no information about their internal construction. Bridges by Alexander Stevens are very ornate because they follow the Adam style, but they present tapered arches and hollow spandrels with 2 longitudinal walls supporting the road. They are made of red and yellow sandstone.

Between 1790 and 1800, John Rennie introduces more elliptical arches and inverted arches of hewn stone between spans, and longitudinal voids above them. Against rubble masonry, he used ashlar masonry. Telford, instead, seldom uses elliptical arches. His bridges have solid piers up to a certain height and hollow above (for inspection): a feature which became copied by others.

With the 19th Century, 1)spans lengthen, 2)cutwaters are pointed with round shoulders and extend up above the springings, 3)arches, either segments of circles or ellipses, have very low profile, 4) piers are narrow (span to pier ratios up to 9), 5) edges of arches may present "cornes de vache" profile. Bridges by Rennie have tapered arches of large thickness and spandrels hollowed by longitudinal voids. Inner spandrels may be made of brickwall. Instead, bridges by Telford in the Highlands are rubble stone, as the previous in the area, but with longer single spans, wider roadways

and characteristic buttered form of wingwalls. They have no ornaments, no inverted arches over the piers and no radiated courses in the abutments; always solid pilasters of considerable bulk. His large bridges have slim projecting piers with subsidiary arches springing from the piers; hollow interiors with inner walls 0.6 m thick, covered with flat stones, and outer walls 0.9 m thick of excellent sandstone masonry; the walls are connected with crosswalls and tie-stones; the road material presents clay seal and hydraulic concrete.

By mid-1800 masonry bridges are obsolete but still hundreds are built following the consolidated methods. In the 20th Century many such bridges are widened and strengthened by laying concrete over arches and spandrel voids; many of these operations are unrecorded.

The reader will be here only briefly reminded that collecting archive or bibliographic information pertinent to single bridges is not easy and not much is available either. Perhaps it would be worth creating a library of bridges where to collect the information available when the arch ring is exposed.

Finally, for the purpose of NDT: some of the materials present in masonry bridges (specifically clay materials) and some types of bridges (hollow cellular bridges) may affect the performance of the NDT techniques and even compromise the survey results. These problems will be returned to in chapter 4, 5 and 6.

CHAPTER 3

ASSESSMENT AND INSPECTION TECHNIQUES OF MASONRY ARCH BRIDGES

3.1 Introduction

Although there has been relatively little loss of life recorded in bridge failures throughout the world, there is a natural concern for safety, and failure can result in high financial loss and major disruption. Increased axle loads or change of use call for an engineering assessment and there is no method of analysis which enables the strength of single or multi-span masonry arches to be accurately determined.

Consequently, demolition is often proposed because of the high estimated cost of repairs and maintenance, without undertaking a detailed study. This is generally due to the failure to appreciate the value of the structure, or adopting inappropriate and excessive remedial measures (Mills, 1989). The need for preservation requires a study to determine whether there are any reserves of strength which may not be apparent in an analytical approach. Factors of safety could possibly be reduced. Simple well tried methods can be more appropriate and cheaper. Also it may be feasible to accept the possible failure of an isolated structural element in order to avoid a total disruption of the bridge. Problems are complicated by the lack of knowledge of traditional materials and construction techniques, as it was argued in the previous chapter.

The Bridge Engineer is faced with great problems in making an accurate assessment of masonry structures such as arch bridges and viaducts due to the absence of design criteria and the role played by many variables in the construction which can only be determined by the destruction of the structure. The hidden strength within the structure must be considered in addition to any inadequacies which may be apparent, and Non-Destructive methods can be of help in providing information about construction and materials.

In this chapter attention is drawn to consideration of interaction between bridge masonry elements other than the arch: these are equally important in the assessment process of the bridge. Fill, abutment, spandrel and wing walls, all interact with each other and the arch, and react to the load applied. Subsequently, assessment methods for arch bridges are reviewed critically and their limitations outlined with respect to consideration for the bridge materials and bridge type.

3.2 The assessment of arch bridges

It was seen from Chapter 2 how masonry bridge design was originally based upon experience which was supplemented gradually by empirical rules, generally as a result of partial or total bridge failures. These empirical rules usually related the thickness of the arch barrel to the span and/or rise. From the beginning of the present century, as knowledge of theory of structures and strength of materials improved, assessment has been approached on a more analytical basis in which the stresses induced in the structure have been estimated by considering the portion of live load likely to fall on a unit width strip of slab.

The basic process was to determine the moment, thrust and shear at the crown of the arch barrel by considering the elastic properties based upon the assumption of a fixed arch (encastre at the springings) having abutments which neither rotated nor suffered horizontal or vertical displacement. Spandrel fill was assumed to behave only as a dead load and did not contribute to the strength of the bridge, except in so far as it helped to distribute the load laterally and horizontally. The load required to produce tension in the intrados of the arch ring was taken as the ultimate load which was then divided by a factor of safety in order to determine the safe load.

Experience showed, however, that vehicles very much in excess of the estimated weight could cross the bridge without apparent ill-effects to the structure (Hume, 1989). These tests which included the study of such factors as load dispersion through the fill, the transverse strength of the arch, slab action, the effect of abutment movements, the contribution of the fill, spandrel walls and parapet walls to the strength

of the arch, demonstrated that the methods of assessment used in determining the load carrying capacity of the bridges were conservative.

Assessing the strength of historical structures is much more of an art and less of a science than is the case when dealing with new buildings. There are a number of reasons for this: a) analysis can be difficult in the extreme; b) structural members can be clearly shown by calculation to be seriously over-stressed and yet still be doing their jobs satisfactorily after many years; c) there can be clearly visible deficiencies as we understand it but the structure still behaves satisfactorily; d) vital members can be missing due to decay or careless removal but again the building still stands (Anon, 1976).

In 1942 the problem became more urgent as the Ministry of Supply wanted to classify all bridges according to their military load carrying capacity, particularly cast iron girders and masonry arches. The various tests carried out by the Building Research Station (Pippard and Chitty, 1951; Davey, 1953; Mitchell, 1954) demonstrated the complexity of the masonry arch structural behaviour even though the bridge structure itself is relatively simple. The bridge masonry elements interact with each other, with the fill and the load applied (Page, 1993). Interaction between the different parts of the structure are often difficult to quantify and can result in large errors in analysis procedures, which do not adequately allow for them.

Studies highlighted the stiffening effect of the filling which over the course of the years had become consolidated so much as to behave almost as an integral part of the arch barrel. So actual loadings may not be as severe as design loadings and the properties of the material may well be far better than those assumed in calculations. Load tests showed that there was a very considerable distribution of load to such an extent that only a small fraction of the load applied was transferred through to the portion of the arch immediately beneath the load .

Tests on dynamic loading showed that dynamic effects on the bridge due to traffic were in a smaller range than previously assumed and this reduction could also be due to the plasticity and creep within the masonry and fill.

An arch subjected to a load, undergoes substantial displacements before the collapse takes place, with large downward deflection of the arch ring at the point of load and general upward movement of the arch on the unloaded part of the span (Fig. 3.1 and 3.2).

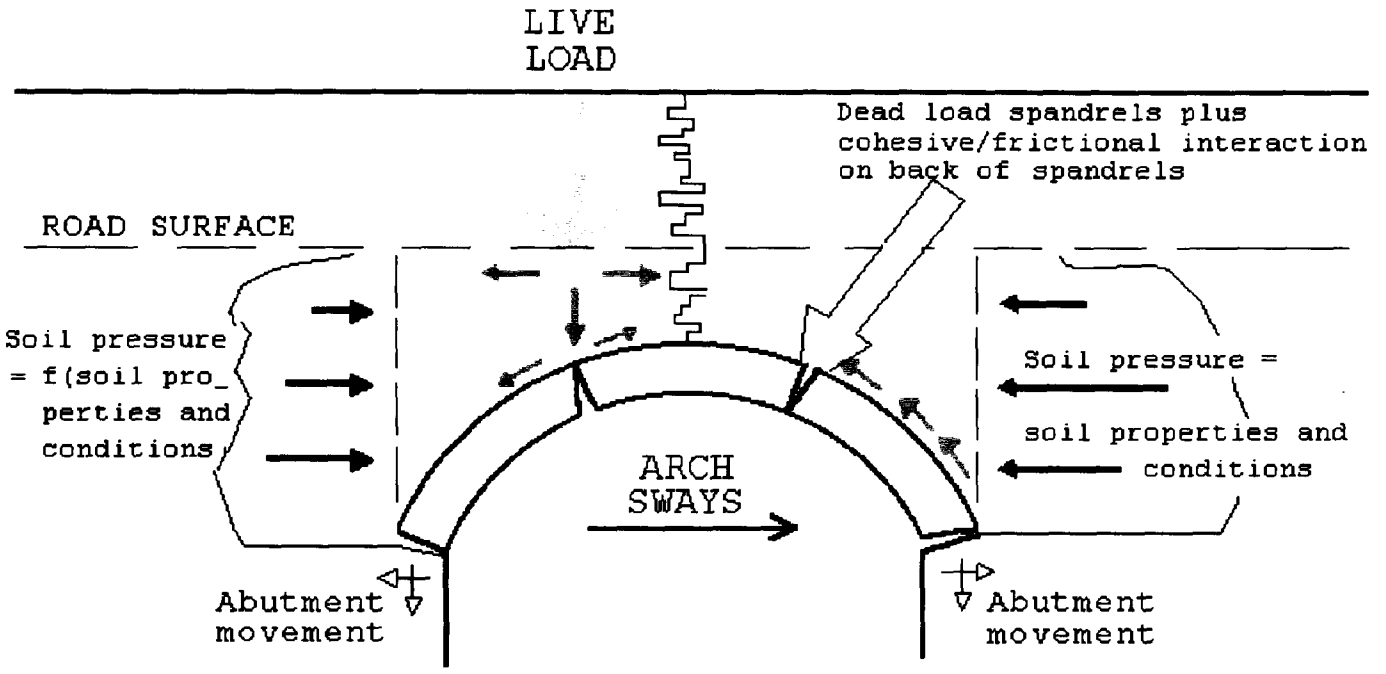

FIG. 3.1 Response of arch bridge to applied load (after Page, 1993)

However elements such as the fill, the abutments, the spandrel and wing walls, all come into action. In fact the fill spreads the load onto the arch ring and both the fill and the spandrel walls introduce horizontal forces on the unloaded side of the arch. These have the effect of stabilising the arch, in some cases to a substantial degree, depending on the geometrical dimensions of the masonry elements and the properties and conditions of the "soil" constituting the fill. To ignore the 3-dimensional effect of the spandrel wall can lead to discrepancies in the calculated behaviour, however the geotechnical aspects of the soil-structure interaction are considered to be the largest sources of error in the analyses. It has been shown (Fairfield, 1994) that these effects can significantly increase the load carrying capacity of an arch bridge.

A similar reasoning goes for the abutments and wing walls. Their stiffness contribute to reduce any movement at the springing of the arch ring, and this effect is a function

of the dimensions and characteristics of the walls. The contribution of the spandrel and wing walls to the stiffness and load capacity of the structure are generally ignored in the calculations and analytical programmes for assessing the capacity of the bridges. This is because often thickness and internal configuration of the spandrels and other masonry elements, or their construction typology, are unknown parameters and there is also the possibility of spandrel wall separation, although it has been shown that even with this defect there can be significant interaction between barrel and the walls through the fill.

Current analytical programs do not take into account the transverse behaviour of the bridge, either due to containment forces acting horizontally and transversely or to load not applied uniformly across the full width of the bridge. Analysis methods developed so far, model a two-dimensional behaviour, as can be seen in figure 3.1. It is believed that this omission is due to unknown parameters and an obvious complication of the problem in the case of a three-dimensional bridge behaviour study - a complication which would be reflected in increased time and computer power required for the calculations -. However, with the continued development of computing, complex analytical techniques can now be applied with little effort.

The fact remains that the analysis of arch bridges is not an exact science as many uncertainties are still retained about the factors which affect the load capacity, and complex analytical techniques are justified only if they provide a more accurate or greater calculated load capacity than simpler techniques or if they provide an insight into structural behaviour which would help to explain deterioration or permit more efficient strengthening systems to be applied. Expansions of analytical programs to take into account three-dimensional effects and lateral transverse loading still has not happened extensively because of lack of readily obtainable information about the bridge hidden geometrical dimensions, the bridge materials and their conditions - especially important if no other historical record about the bridge is available.

In the case of both 2 and 3-D methods of calculation, accurate input parameters are necessary and needed because their value can greatly affect the final load carrying

capacity of the bridge. This in turn, influences the total cost for strengthening and rehabilitating the bridge stock of the country.

In view of these problems NDT methods have acquired an important role in supplying information regarding material properties, conditions and geometry of the structure that can be loaded into analytical assessment methods for a more accurate calculation of the bridge load capacity.

Surveys carried out post-war by Building Research bodies highlighted the constructional variations which occurred between masonry bridges. In addition, assessment of masonry arches is complicated by the presence of gas and water mains, broken voussoirs, perished or eroded mortar. With so many variables, the only accurate way to determine the load carrying capacity of an arch seemed to undertake a load test and some confidence in the calculated values of load capacity can then be obtained by studying the pattern of behaviour prior to collapse. However load testing can be expensive and very careful monitoring is required during the load test, and account should be taken of the higher stresses which occur due to creep under sustained loading. Furthermore, the modality in which these load tests to failure are carried out and in particular the positions and the structural elements the load is applied to, may be significantly different by the loading conditions due to traffic. Thus, to transfer the outcome of such tests into an analytical method of assessment is not a straightforward operation. Another aspect to consider is that the tests are 3D procedures whilst the analyses are 2D so, to compare the results obtained by the two methods is not correct or rather, if they produce the same answer, it "proves" that the analyses are wrong (Harvey, 1997).

The assessment of multi-span masonry arches such as viaducts is even more difficult than for single span arches. Studies carried out on brickwork masonry arch bridge models with different spandrel fills have confirmed that an increase in density increases the load carrying capacity. The same study showed that, under load, the arch responds locally first, then it engages the support of the backfill and spandrel walls. The nature and extent of that support depended upon the relative stiffness of the elements. If the

arch was detached from the spandrel walls then the behaviour would be determined by the longitudinal soil pressure contribution, the resultant transverse induced stress on the back of the spandrel walls and the interaction between them (Melbourne, 1990).

The research undertaken on arch bridges in the recent years has attracted great interest which has resulted in specialised symposia (Barr *et al.*, 1994; Melbourne, 1995), and seminars (ICE, 1993; ICE, 1997a; ICE, 1997b) whilst a number of other conferences host sections on arch bridges (Forde, 1993; Forde, 1995; Forde, 1997).

3.3 Analytical methods of assessment

3.3.1 Elastic method of analysis and MEXE

The idea of an elastic method of analysis was first studied at the end of the seventeenth century and is concerned with the concept of a line of trust through the barrel. The original idea was to calculate the arch thrust in order to design the abutments against overturning.

Around the middle of this century, Pippard (Pippard, 1948) calculated abutment thrust and bending moment at the crown of the arch, which, combined with the self-weight of the arch, were used to estimate the safe value of live load for an arch of any shape. He assumed that the fill has no structural strength or contribution other than to the dead load, so that it imposes purely vertical loads on the arch. Furthermore that the fill has the same unit weight as the arch ring (Heyman, 1982). His results were obtained using an elastic method of analysis, for a two hinge arch, with a rib of parabolic shape, and for a cross-section which varies. Further Pippard confined his analysis to that of a single point load at mid-span. He constructed tables where the value of axle load for a vehicle of normal track could be read for various values of span, ring depth and crown cover.

Partly as a result of the tests conducted, guidance for the assessment of arch bridges was set out in the MEXE method based on Pippard's work (MEXE, 1963). The Military Engineering Experimental Establishment found that the maximum load as

calculated by Pippard, could be fitted quite well, for given values of unit weight of the arch and limiting compressive strength, by a nomogragh involving only the arch span and the total depth (fill + arch) at the crown. MEXE is intended for single span arches not exceeding 18 metres. In it, the assessment for the idealised bridge was modified to include factors which allowed for the way in which the actual bridge differed from the ideal in terms of the quality of the material for both the arch barrel and the fill, as well as other factors. This idea was incorporated in the Ministry of Transport memorandum of 1967 (Ministry of Transport, 1967) and updated in the Department of Transport Standards BA 16/84 and BD /84. The short span bridges (loaded length less than 50m, which cover the vast proportion of the bridges) are today assessed by using the bridge assessment criteria given in BD 21/93 (Department of Transport, 1993a). The basic information is very similar to the earlier publication but more guidance is given to assist in determining the condition factor and an amendment is added advising users that the method can produce conservative results for spans over 12 metres.

Thus for an arch of given dimensions the provisional axle loading can be read off immediately, then operated on by a series of modifying factors to allow for: (a) different span/rise ratios, (b) for a profile other than the standard parabolic, (c) for the quality of the material in the arch and fill, (d) for the mortar condition, (e) for the condition of the bridge. As can be seen from table 3.1, the variety of fill materials considered in historical bridge construction, is quite limited and there is no real diversification between materials or their properties.

In the case of multi-span arches the situation is made more complicated by the possibility of pier instability and consequent interaction between adjacent spans, which can cause a total collapse mechanism. This identifies parameters which are not overtly identified in the MEXE method.

The essential features of this approach are that 1) there is a considerable emphasis on the geometrical properties of the bridge, 2) the arch is evaluated using elastic techniques, 3) the final criterion for the load carrying capacity of the arch is based upon the attainment of a limiting value of compressive strength, 4) there is a subjective

factor included in the method, the condition factor, based on the assessment engineer's perception of the condition of the structure as a whole.

Filling	Fill factor
Concrete	1.0
Grouted material (other than those with a clay content)	0.9
Well compacted material	0.7
Weak material evidenced by tracking of the carriageway surface	0.5

TABLE 3.1 Fill factors used in the MEXE method (Page, 1993)

3.3.2 Plastic method

It was in the early 1980s that masonry arch analysis was examined securely with plastic theory (Heyman, 1982). This method assumes that the masonry has no tensile strength but infinite compressive strength and there is no sliding between voussoirs. Limit analysis equates the eccentricity of the thrust line to a bending moment, the upper limit of which occurs when the thrust line is just inside the arch barrel and is equated to the "plastic" moment. At this point a "hinge" is assumed to form. Thus the plastic theory may be applied to the masonry arch. The lower bound theorem of the plastic theory states: "If the thrust line can be found, for the complete arch, which is in equilibrium with the external loading (including self weight), and which lies everywhere within the masonry of the arch ring, then the arch is safe".

A single span masonry arch bridge will fail by the formation of four hinges, thus transforming the arch barrel into a mechanism. Studies have drawn attention to the contribution by the soil and spandrel walls to the stability of the arch barrel (Melbourne and Wagstaff, 1993; Melbourne and Gilbert, 1994). Also, from tests to destruction on masonry arch bridges, it was discovered that the effect of the arch/fill interaction increases the carrying capacity by two and a half times that of the measured value without the contribution of the fill (Davey, 1953).

The limit analysis approach gives information about the ultimate load, the corresponding failure mechanism and force state at block interface (Begg and Fishwick, 1994) but is based on the assumption that the worst load is applied at quarter span and the assumed position of hinges may not be the most critical. The method has been computerised and calculations modified to include parameters such as material crushing at the hinge points and horizontal soil pressures (Harvey, 1988).

3.3.3 Finite element method

The use of FE in the elastic analysis of masonry arch bridges is a relatively new concept, which has been studied to some considerable depth in the past 10 years (Towler and Sawko, 1982; Towler, 1985; Crisfield, 1984). One dimensional straight and/or curved beam elements were used in early '80s to represent the arch barrel and no account was made of the inherent contribution of the fill which was only treated as a dead load. The work showed the potential of the finite element method for computing load-deflection curves and the collapse load and also for providing data on the extent of cracking under loading. Later in the same decade (Crisfield and Wills, 1986) one dimensional fill elements were introduced in an attempt to model the passive resistance of the soil with the Mohr-Coulomb criterion.

In more recent research (Choo *et al.*, 1990), the fill elements contribution to the equilibrium is taken in account when the barrel moves horizontally into the fill because of load applied elsewhere on the arch and consequent sway of tlie ring (see figure 3.2). The stress strain relationship of the fill element is linear elastic until the stress in the fill reaches the failure value. However the contribution of the fill element is neglected in the region of the crown due to sliding failure along the interface between fill and arch ring, as the sliding happens at much lower stress values.

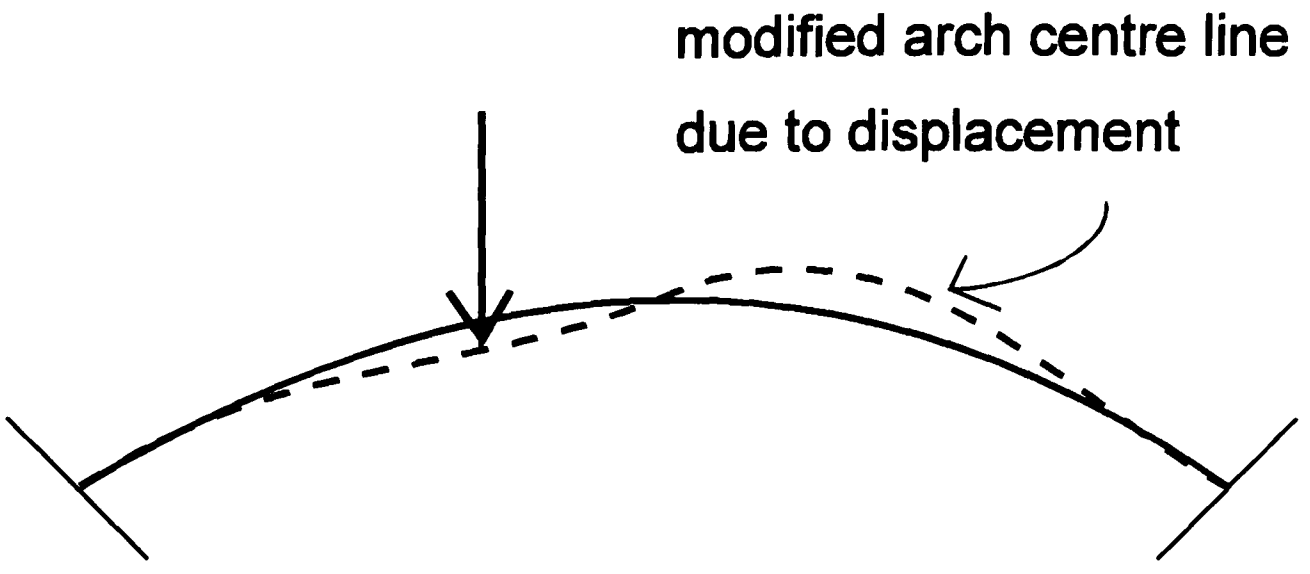

FIG. 3.2 Change of arch ring geometry (after Page, 1993)

This approach recognises that the curvature or shape of the ring and the roughness of the extrados have an influence on the value of failure in the fill, as it affects the friction action at the extrados-fill interface, but assumes that a smooth extrados surface represents the general case and therefore ignores the contribution of the fill in the crown area.

The review of construction typologies of historical bridges (chapter 2) showed that the shape of the extrados of the arch in masonry bridges can vary considerably and cases like the one represented in figure 3.3.b are not uncommon for the majority of short span masonry bridges. It is clear that in the case of an arch extrados as in figure 3.3.b, as compared with 3.3.a, the friction action at the interface arch-fill would be greater and even in the crown area the contribution of the fill is not negligible.

To be able to discriminate between the two situations would be of great help to the bridge assessing engineer. Thus a rapid, on site, non destructive method of investigating the structure, such as those at the centre of study in the work reported in this thesis, could give a valuable contribution in making this kind of information available for use as input parameters in analytical methods of analysis. The outcome of such an exercise would be a more realistic value of the load carrying capacity calculated for the bridge.

The imposed loading on the road level may be distributed on to the arch ring through the fill as shown in figure 3.4, using a dispersal angle θ which may vary from 0° to 45° or by assuming that the fill behaves as a semi-infinite elastic plane of unit thickness.

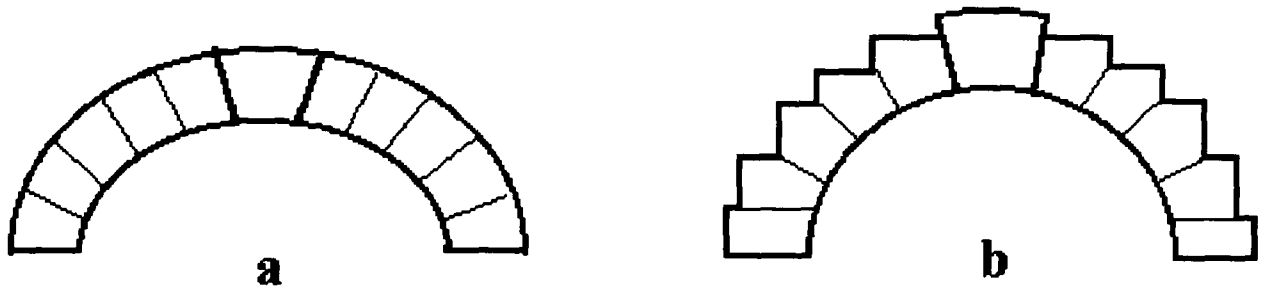

FIG. 3.3 - Different extrados shapes in segmental arch (a) and in semi-circular arch (b)

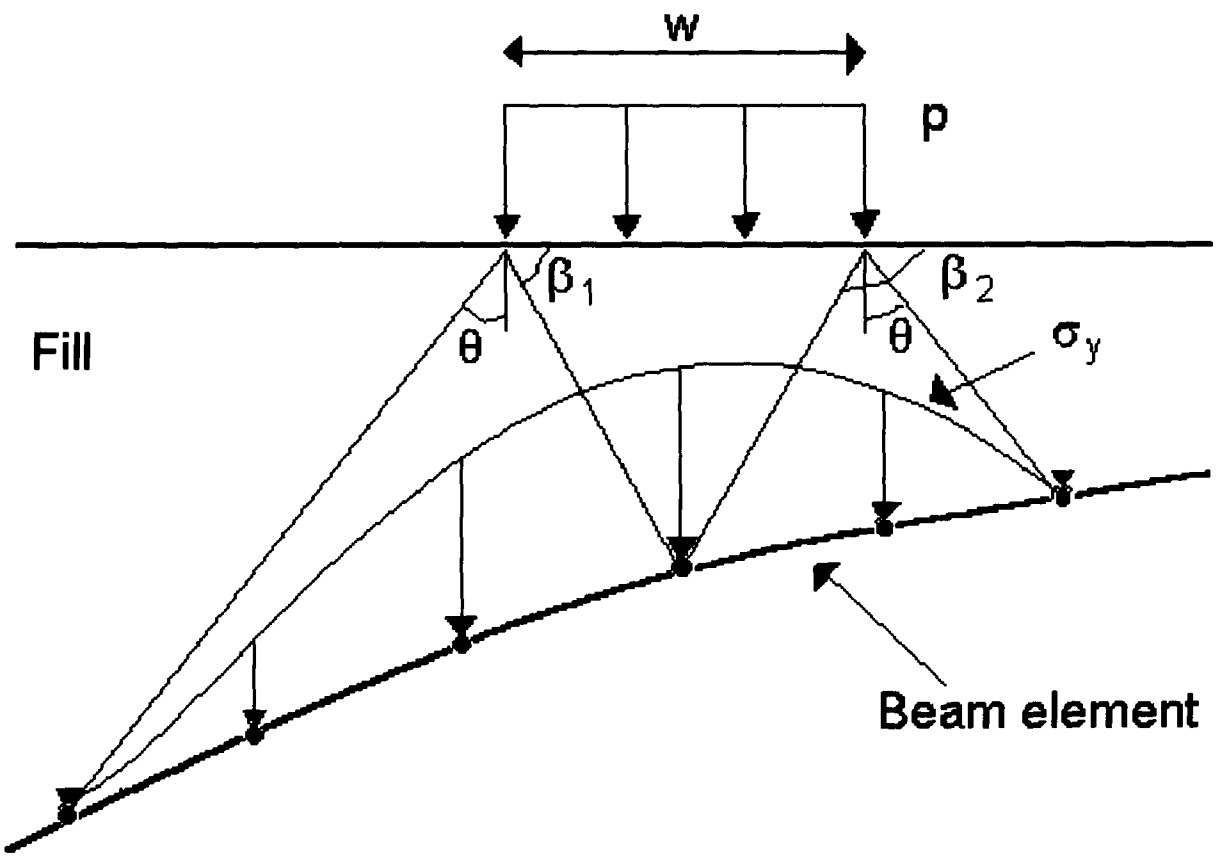

FIG. 3.4 - Distribution of the vertical fill pressure on the arch ring (after Page, 1993)

In the '90s, the finite element work developed further to allow for the effects of various defects to be included. These defects are important parameters such as missing bricks in the arches, cracking and separation of multi-ring barrels and the positions of defects. However three-dimensional effects, like the presence of spandrel walls, are still not taken into account (Choo *et al.*, 1991). Other work (Falconer, 1994) takes into consideration arch barrel and fill (lateral fill pressure). This work, based on the mechanism method and carried out on multi-span arches, also found that the failure

load was highly influenced by the pier height/thickness ratio. Complex pier sections, as described in chapter two, were not considered in the study.

More recently, effect of skew on the load carrying capacity of arch bridges has been examined using a shell finite element computer program (Choo and Gong, 1995). The relevance of this work is that a 3-dimensional study was adopted for skew arches but it could potentially be employed to model arch bridges where the internal geometry is varied by the addition of internal spandrels and/or structural backing.

In fact, shell theory is becoming more widely applied to masonry arches (Chandler and Chandler, 1995). This 3-dimensional analysis has the advantage to model more accurately the behaviour of an arch bridge and also the initial input time is considerably reduced when compared with 3D FE analysis. Some studies seem to conclude that when a shell is subjected to concentrated loads, like wheel loads, significant stresses are induced at a considerable distance from point of application and the structure is unlikely to collapse by the formation of plastic hinges at four locations as assumed in certain 2D analyses. (Romaya, 1995) This has repercussions on current assessment methods via use of packages based on the standard four hinge mechanism.

In terms of directing attention towards other spandrel typology than the soil filled one, recently, open spandrel masonry arch behaviour has been investigated (Melbourne and Tao, 1995). Open spandrel masonry arch bridges comprise a main arch which supports subsidiary arches spanning in the same direction. Using standard 2-dimensional, 6-noded triangular elements, a finite element technique has been proposed for studying 5 models with varying proportion of the main span thickness to piers thickness of the spandrel arches. The analytical study concluded that the stiffness of the main arch is dominant in the formation of a mechanism but influenced by the horizontal restraint capacity of the spandrel arches. Also, whilst the 'filled' spandrel arch bridge receives a contribution to stability of the arch barrel from soil/structure and spandrel/wing walls interaction, the open spandrel bridge tends to have brittle failure once the horizontal restraint capacity of the spandrel arches has been reached.

In the case of masonry arch bridges, the lack of knowledge regarding material properties, internal construction details and initial stress state indicate that the use of sensitive, computationally intensive FE methods may not be justified.

3.3.4 Computerised Assessment Programs

This section briefly describes a few of the analysis computer packages which have been developed from some of the techniques and methods dealt with above. These are relevant to the part of the work in this thesis which focuses on the importance of the construction materials and their properties. These analysis programs take account of the contribution of the fill and its strength in different ways. They are generally based or comply with the requirements of the Department of Transport (Department of Transport, 1993 a & b).

The computerised MEXE allows for arch shape, arch rib section and span to rise ratio to be changed (but not for extrados shape to be modelled); loading can be dispersed both transversely and longitudinally and applied anywhere; fill density does not need to be the same as masonry density; compressive strength value can be chosen.

One of the most widely used of these programs is ARCHIE, developed by Harvey (Harvey, 1988) and based on the mechanism method, like those developed by Davies (Davies, 1989 a), Falconer, Cascade Software Ltd and Crisfield (Crisfield and Packham, 1987). In ARCHIE the backfill is represented by a horizontal force simulating earth pressure, at relevant point on extrados. The value of horizontal force assumed is based on a coefficient of earth pressure between 'at rest' and the 'passive' coefficients. This horizontal force has the effect of altering the line of thrust and will maintain it within the barrel for higher loads than if the contribution of the fill had not been included.

Crisfield and Packham's approach was later refined by the Transport and Road Research Laboratory to account for inclusion of lateral resistance of fill.

In Davies' computer analysis method, MARCH, active and passive pressure from the fill are allowed for with four possible distributions of pressure. The "choice" of which case to use is left to the user. (Davies, 1989 b; Davies, 1985)

In the CTAP program, by Bridle and Hughes (1989 and 1990), soil pressure effects are taken into account in a similar manner to that described above by Harvey.

3.4 On site methods of assessment

3.4.1 Inspection

Inspection of bridges is usually divided into three types (Branco and de Brito 1996): (i) *current inspections* which are performed at a fixed time interval, e.g. 15 months, and are mainly visual inspections. (ii) *Detailed inspections* which are also periodical at a time interval which is a multiple of the current inspection time interval, e.g. 5 years. The detailed inspections are also visual inspections, but can include non destructive and in-situ tests and, if there are no construction drawings, a dimensional survey. (iii) *Structural assessments* are only performed when a current or detailed inspection shows some serious defects which require a more detailed investigation. Thus, structural assessments are not periodical and can include laboratory tests, in situ tests with non-portable equipment, static and dynamic load tests. These tests are usually very costly compared with the other two inspection types. A structural assessment will also be performed when changes in the use of the bridge are being performed.

3.4.1.1 Visual inspection

Visual inspection is probably the most widely used NDT method for the inspection of structures, for quality control and in the field. It is usually used to give an initial appraisal before a more detailed examination by another method.

Visual bridge assessment can be split up generally into considerations of structure, materials and foundations. Inspection data are recorded on prepared sketches and data sheets of the various structural elements, then elaborated and organised using a database system. Inspection reports form an important historical record of damage even if information is mainly visual.

In contrast to modern structures, historical or old bridges appear to present very little help to the inspecting engineers. Their designers and builders generally had not taken into consideration future inspection (whilst thoughts of possible maintenance works had been taken care of with attention to design and accuracy during construction).

Roped access is used more and more often to inspect 'difficult' structures because it allows access to confined or restricted spaced or when the dimensions of the structure are too great to permit access via use of mechanical arms. This method also allows a very close-up inspection but this can be time consuming. Furthermore, if during inspection loose pieces of stone are located, they can be lowered safely to the ground (Fewtrell and Walsh, 1994).

There are several limitations to the use of visual inspection as the only method of structural examination. Visual inspection is inherently subjective because it relies on the judgement of different individuals and one inspector may spot something that another does not or may classify the same fault differently. Furthermore as there is a limit to the resolution of the eye, there is an associated limit to the size of defects that can be detected (placing a restriction on how early it is possible to detect potentially critical damage) and there may also be a problem of poor accessibility in certain regions of the structure. Finally, in the majority of cases, visual inspection only gives direct information regarding the 'skin' of the structure, not its internal condition.

3.4.2 Static load testing

Full scale load tests to collapse or not to collapse are used in Britain to calibrate the computer models used to calculate the loads in the many structural elements of bridges. (Parker, 1997) or the bridge capacity (Page, 1995b; University of Edinburgh, 1984).

A series of tests on redundant masonry arch bridges have been undertaken for research purposes to provide calibration data for assessment methods (Page, 1993). Dead load (fill) strain were generally not measured and they would need to be estimated by

calculation. In the case of multi-span arch bridges, studies concluded that consideration should be given to introducing an abutment factor into the MEXE assessment procedure to enable it to assess multi span bridges. The abutment factor would cover the case where the abutments are piers and its value would be less than one in the case where the arch is supported on piers. It is proposed that this value be derived from finite elements calculations of the capacity of multi-span bridges or from geometric dimensions and evaluation of their state, possibly obtained with Non Destructive Test (Page, 1994).

Load testing has not been used for assessing the traffic load capacity of masonry arch bridges in the United Kingdom. Standard procedure is by inspection and calculation by the application of limit state principles. This procedure is applicable to masonry arch bridges but the Department of Transport recommends that the modified MEXE method should be tried first. Load testing is not generally considered for assessment because of the costs involved, the possibility of causing structural damage and the difficulty of interpreting the test results. However, when a bridge has failed assessment by calculation but it is believed that the calculation has underestimated the load capacity of the bridge, then it may be decided that a load test is worthwhile (ICE, 1997 b).

The live loading for assessment of arch bridges should be single, double or triple axles. It is necessary to apply the maximum load that can be safely applied and guidance can be provided by previous load tests to failure, extrapolating the response of the bridge to the ULS load. It should not be assumed that the response of the bridge will be symmetrical (a small number of gauges may therefore give misleading results). Also it should not be assumed that the bridge will behave elastically. Another very important consideration is that the response of the bridge may change if monitored over a number of months and the difference in the deflection of the arch may be due to the amount of water in the bridge; temperatures low enough to freeze the water may have a very significant effect (Page, 1995a). An NDT method capable of detecting moisture content in the infill of the bridge would thus be of help to the assessing engineer.

3.4.3 Dynamic load testing

Dynamic testing is a technique which uses the dynamic properties of the specimen or structure itself to test its condition. In-situ dynamic testing of bridges has become a practical proposition over the last 20 years and prediction of the dynamic behaviour of bridges has become increasingly important. In particular the growing use of active control techniques demands accurate quantification of the passive structure. The destructive potential of vibrations is well known although the sources of excitation are diverse and many analytical models are insufficiently sophisticated to predict response behaviour under service conditions. Once in service, periodic testing can indicate progressive changes in the properties of the structure. Once the structural properties are determined, the state of the structure and the effects of design modification can be estimated. (Brandon, 1994)

Dynamic testing is older than usually thought. Originally it involved striking a specimen with a hammer and listening to the sound produced. Today the potential scope of dynamic testing has considerably broadened owing to the availability of electronic instruments capable of generating and detecting vibrations in the sub-audible range. In principle it should be possible to detect a wide range of faults with dynamic testing. This is because any fault that affects the local properties, usually stiffness and damping, should affect the dynamic response. It can be applied to any structure that has resonance within the scope of experimental measurement (generally below 20 kHz), including bridges.

There are two main approaches to dynamic testing of structures: forced excitation tests and ambient excitation tests. Each has its advantages and faults.

Ambient excitation tests - Ambient excitation, due to wind loading, seismic action, wave action, traffic noise, internal machinery, etc. is used to excite the modes of vibration in some way and to measure the natural frequencies, damping and mode shapes. Changes in these properties during the life of the structure would be indicators of damage. Increased damping reduces the amplitude of the high frequencies; damaged material is usually less stiff and results in a lower frequency response locally.

Encouraging results have been reported for bridges including a railway bridge (Luz and Wallaschek, 1992).

There are three persuasive arguments for using excitation from the local environment of the structure under test. Firstly the possibility that artificial excitation may influence the properties of the system under test (non linearities) is excluded. Secondly the possibility that the positioning of the exciters or response transducers may cause structural properties to be overlooked is reduced. Thirdly the ambient excitation is representative of the service environment of the structure. An inherent limitation is that it is often impossible to measure the input excitation directly, making it very difficult to estimate the energy required to excite each mode (and any consequent remedial action).

Forced excitation tests - The second approach is to apply an impact and observe the response spectrum or the spectrum of the interacting force. Commonly a single force input is used with multiple response measurement points. If the input actuator or response transducer is placed at a node of a mode then the characteristics of the mode will not be measurable. Besides, two modes (symmetric and anti-symmetric) have near coincident natural frequencies. In this case a single point test would excite a combination of these modes making them extremely difficult to resolve (Lauffer *et al.*, 1987).

There are considerable analytical advantages to measurement of the forced response of the structure rather than its free response. In practice, however, there are significant difficulties in the application of sufficiently large loads to excite the structure without encountering significant local nonlinearities. The structure can be deflected locally and then the free response to the known initial force and deflection is measured. Alternatively, the disturbance from the equilibrium state is obtained by an impact on the structure, often using an instrumented hammer so that the force input can be measured and hence the energy of the impact can be estimated. In either cases there is a significant probability that the loads necessary to provide measurable responses may induce geometric nonlinearities at the point of application.

However there have been numerous efforts to improve the sensitivity of frequency response methods, as it has been found that the sensitivity of methods based on measuring the dynamic response to flaws is generally disappointing. The presence of damage is often characterised by reduction in some modal frequencies: a classic indicator of stiffness reduction or mass change. A common approach to damage localisation and detection is to measure the modal frequency shifts caused by damage on the real structure and compare those, or parameters computed from them, with those predicted by a finite element model (FEM) of the structure. The shifts in modal frequency which characterise structural damage are accompanied by a reduction in the modal amplitude of the response near the original modal frequency. But comparing these amplitudes before and after damage is not a very sensitive method. The mode shape can also be used to identify damage, comparing the curvature mode shape, which is proportional to its second derivative of the mode shape, for damaged and undamaged cases. This method has been used to determine damage location and size on two simple structures modelled on a computer (Pandey *et al.*, 1991). However in practice it is very difficult to measure mode shapes accurately, especially for more complex structures.

Any full scale test is fraught with difficulties and dynamic testing is particularly so: besides logistical problems of testing remote bridges, there are ambient environmental factors which create problems for instrumentation and accuracy of data. Studies on a reinforced concrete bridge showed that natural frequencies were repeatable to an accuracy below 1.5 % (Agardh and Palm, 1992). In an extreme case changes in natural frequency exceeding 5 % were registered within a single day, due to ambient effects (Aktan *et al.*, 1994).

Natural frequency Abnormal loss of stiffness could be inferred when measured natural frequencies are substantially lower than expected (Morgan and Oesterle, 1985). For damage to be detected with confidence, natural frequency have to change by about 5% (Creed, 1987). For a particular structure, a wide frequency range needs to be monitored in order that many natural frequencies are monitored. At an increased

severity of deterioration, corresponds continual reduction in natural frequencies (Sun and Hardy, 1992). Furthermore natural frequencies of some torsional modes or combinations with bending modes may not change regularly with increasing crack damage (Slastan and Pietrzko, 1993). As bridge structures age then gradual changes will occur in their dynamic properties (Kroggel, 1993). Other work in trying to detect damage have utilised Frequency Response Function (FRF) Measurements (Law *et al.*, 1992) and also phase components of FRF's (Law *et al.*, 1991). However it would appear that frequency measurements alone cannot provide an adequate method for damage or deterioration detection.

Mode shape methods Some studies have suggested that changes in mode shapes may be more sensitive to damage than are natural frequency measurements and also may be able to identify the location. The greatest changes occur in the vicinity of the defect and appear to be more pronounced in the higher modes. However mode shape data is often in error, for in any one particular point there can be differences of 20% with poor repeatability (Salawu and Williams, 1994). Also, some modes, at advanced stages of deterioration, may not be present. Even the fundamental mode, with high damping, is very difficult to measure (Prato, 1997) and a damaged soil filled bridge might be such a cases. The method has been applied to steel bridges subject to critical fracture with some problems: only certain defects were detectable due to environmental noise. The testing was accompanied by FE modelling. (Idriss, 1993).

Damping value With damage occurring in a structure it would be expected to lead to an increase in damping. Unusually high damping would suggest more energy dissipation mechanism than expected, indicating the possibility of cracks in a structure (Agardh, 1991) (Slastan and Pietrzko, 1993). Measurements of damping in full scale structures is often inconsistent with very poor repeatability of results. In the extraction of modal parameters it is usually the damping value which has the greatest degree of uncertainty. It is a small effect and may be ignored for quantitative interpretation of non-destructive tests (Wong and Topping, 1988).

Computational Model Methods Often updated with the use of full scale test data and have led to some damage detection and location methods. Often incompleteness of the data and measurement noise are the first problems in making location of damage difficult using Finite Element models (Friswell and Penny, 1992).

There are examples of modal testing and analysis techniques, based on the impulse excitation method, deployed in the integrity assessment of masonry arch bridges. Research has included the study of brickwork arch dynamic testing whilst dynamic finite element analysis was used to model the behaviour of the arch under impulse loading. The method needs to be further explored for the detection of defects in arch bridges. (Bensalem *et al.,* 1994) but modal analysis has been undertaken with some success on model arch bridges (Armstrong *et al.,* 95; Bensalem *et al.,* 1997).

In the use of vibration for the condition-monitoring of arch bridges it has become evident that the complex modal characteristics of these bridges lead to difficulties in the interpretation of field results. The theory for vibration of complete masonry arches is complicated by the presence of spandrel walls and fill. This makes these structures complex, both geometrically and due to uncertain mechanical properties of the materials from which they are made. Besides there is virtually no literature on vibrations of masonry arch bridges as opposed to other closely related subjects in mechanical engineering (e.g. vibration of rings, which have different proportions); neither is there much literature on the modes of vibration beyond the very lowest order ones (fundamental extensional, inextensional and torsional).

Laboratory experiments have been conducted again on arch rings without spandrel walls or fill, to accurately predict mode shapes and natural frequencies. Ten modes of vibration have been predicted using a finite element model. By varying the end conditions a match has been obtained between theory and experiment for tlie vibration modes (Ellick and Brown, 1994). There is a great deal of confidence in the finite element technique for prediction but the method needs to be extended to the analysis of single and multi-span arch rings with spandrel walls and fill and to the analysis of the effects of damage to the arch.

The way in which excitation and instrumentation systems have been developed for structural dynamic testing often assumes that the instrumentation will be deployed specifically by specialists to investigate particular structural properties.

The development of methods utilising ambient excitation enables a more long-term view to be taken. In particular it may be expected that passive transducer systems will be deployed routinely for continuous monitoring of the condition of large structures (Prentice, 1996). The techniques are far from complete and currently depend on the availability of skilled engineers to plan the tests and interpret the response signals. As a consequence the emphasis is likely to move towards detection of changes in patterns of response under operational loadings. Such methods are emerging at a rapid rate (Samman *et al.*, 1991) (Worden and Tomlinson, 1994).

3.5 Conclusions

Masonry arch bridges have complex structural behaviour and constructional variations occur from bridge to bridge. Their assessment is a complicated matter made more difficult by the lack of knowledge of traditional materials and construction techniques. Studies have highlighted the relevance of considering all bridge components equally important in the assessment process of the bridge. Arch, fill, abutment, spandrel and wing walls, all react to the load applied and interact with each other depending on their relative stiffness.

Current methods of analytical assessment ignore the contribution of some of the mentioned elements to the bridge behaviour, with the consequence that important parameters are not identified in any of the available assessment programs:

-hinges may occur remote from the barrel but in such a way as to allow the formation of a global mechanism and thus result in failure;

-spandrel walls apply a crucial role in the stability of the barrel. The wall acts as a very stiff geometric constraint on the failure mechanism and can cause the hinge to form in the arch barrel in a different position and for a higher load than in an arch without spandrel (and fill);

-the extent and stiffness of the wing walls and abutments interact with the bridge arches.

All these elements, affecting the structural flexibility, effect the failure mechanism and hence the failure loads and are therefore most important in the assessment of the load carrying capacity of the bridge. As a 3D consideration of the behaviour of the bridge is necessary to take into account the contribution of the above mentioned factors, analytical methods have not included them so far. All the assessment methods available at present analyse a two-dimensional longitudinal slice of the bridge. They cannot take into account transverse bending of the arch ring under a wheel load or the stiffening effect of the spandrel walls.

In the case of analytical methods of calculation, accurate input parameters are necessary and needed, and NDT can help obtain them. It is fundamental to know the geometrical dimensions of walls and arch, their shape, and the nature and condition of their material. In addition the possibility of any hidden strength within the structure must be considered and investigated.

It is well known that the load assessments derived from the application of the various methods, computerised or not, often result in large differences compared to the assessed load capacities. This is because of the different assumptions underlying the structural representation, loading applications, load and strength factors, formation of hinges and mechanisms, material properties, etc. No single method appears to perform significantly better than others in consistently predicting more accurate load capacity and all seem to give reasonably safe load estimates. Also the outcome is affected by lack of control on the 'assumptions' and 'workings' of these methods.

Moreover, analytical methods at present available are inadequate to use to compare with load test data. They all have limitations. The MEXE and mechanism methods provide no calculation of the stress and displacement for comparison with a load test. The elastic and finite element models available model a two dimensional slice of bridge and cannot take into account transverse bending of the arch ring or the stiffening effect

of spandrel walls. Material properties for the arch bridges are particularly difficult to estimate or measure because they are likely to be very variable.

When it comes to assessment of the load capacity through site tests, static load tests are not used because they are costly, time consuming and presenting the risk to damage the structure.

In relation to use of vibration techniques for condition assessment of bridges, there is a very wide range of views, concepts and data. There is a need to improve the understanding of the fundamentals of the dynamic behaviour of bridges. Monitoring of natural frequencies and mode shapes alone can be used to detect damage or deterioration in bridges provided the changes are large. Damping is not a suitable measurement due to inaccurate estimation of values. For any structure tested, there must be an estimation of the changes in parameters due to local environmental factors. Methods based on flexibility and computational models should continue to be explored.

CHAPTER 4

THREE NDT METHODS: RADAR, SONICS and CONDUCTIVITY

4.1 NDT techniques and their role in bridge investigation

In recent years, a number of non-destructive testing methods have been used, mainly on a trial basis to investigate a variety of structures, including bridges. Although such applications have sometimes been intended for use in the precise location of relatively small features, such as reinforcement bars and structural cracks, in general the results from these methods are expected to be qualitative. This is because most of these methods rely on reflected electro-magnetic or acoustic signals, or dynamic responses, which give a very complex but imprecise picture of the reality.

The Highways Agency has for some time been actively examining the various NDT methods for use in different aspects of the management of the network. Advice is already available on the use of ground penetrating radar (GPR) for road pavement assessment (HA 72/94, 1994) and guidelines have been drafted for supplementary load testing to assess the load carrying capacity of bridges (ICE, 1997). The present research work is intended eventually to contribute to provide similar guidance for bridge-related use of radar, sonics and conductivity.

The electromagnetic investigative techniques of impulse radar and conductivity may be applied to the assessment of bridges constructed of concrete, brick or stone masonry, and which include soil fill. The sonic method may be used for these materials and, in addition, metal structures, but bearing in mind that sonics will not cross an air boundary such as a full width crack or discontinuity.

Radar applications in masonry include identifying: wall thickness, voids, arch barrel shape and thickness, retaining wall thickness, bridge structure behind spandrel walls - fill or cellular structure- and capillary rise in masonry.

Applications of impulse sonic testing include: wall thickness in masonry, void identification and mapping, spandrel wall and arch thickness and structural integrity and deterioration.

Applications of non-contact conductivity testing include identifying: moisture movement over time, layering within masonry and inhomogeneities.

There are many types of bridges where conventional assessments are not likely to be conclusive and which are therefore amenable to the use of NDT methods in some form for added confidence. The following are some typical examples of such bridges and other situations where such methods could be useful:

(1) Masonry arch bridges are extremely difficult to analyse numerically and all methods are considered to be very approximate. As such, there is a strong case for using the "monitor" option for masonry bridges which fail assessment by a narrow margin.

(2) Jack Arch and Trough-Deck Bridges are also difficult to analyse because the structural details are not amenable to straight-forward idealisation. The assessment calculations can therefore be suspect.

(3) Older composite Bridges. In some of these bridges concrete or other types of fill were placed directly on steel plates of various configuration, with or without shear connections. Assessment calculations tend to underestimate the composite action in such cases.

(4) Bridge Deterioration. Physical deterioration of bridges in general, and that of problematic bridges, such as post-tensioned bridges, in particular.

(5) Monitoring Following Load Tests. In some forms of load-testing of bridges, substantial magnitudes of loads may be applied to a bridge. In such cases, there is a

risk of hidden damage being caused to the bridge during these tests, making a rigorous regime of subsequent monitoring essential.

In all these cases, the outcome of the research work contained in this dissertation may be of direct benefit. In the following sections, the three NDT techniques of radar, sonics, and conductivity, will be presented. By describing the various factors that control the electrical behaviour of the material investigated under typical in-situ conditions, this chapter attempts to provide the theoretical background within which these techniques operate and against which electromagnetic and sonic surveys are performed.

4.2 Radar

Detection of buried objects by use of radio waves was first reported at the beginning of the century (Daniels *et al.,* 1988) but it was in the early 1950s that the technique became more widely employed. In the 1970s, applications covered determination of the thickness and structure of glaciers (Bertram *et al.,* 1972), location of sewer lines and buried cables (Morey and Harrington, 1972), thickness of sea ice (Campbell and Orange, 1974), profiling the bottom of rivers and lakes (Morey, 1974), and detection of corpses (Alongi, 1973).

Within the geophysical community, ground penetrating radar (GPR) is seen as a technique which offers a way of viewing shallow soil and rock conditions. The areas of application for ground penetrating radar are diverse and include groundwater exploration, geotechnical and archaeological investigations (Vaughan, 1986; Goodman and Nishimura, 1992, 1993; Davis and Annan, 1989), as well as engineering examples (Ulriksen, 1982) related to bridge scour (Haeni and Trent, 1988; Davidson *et al.,* 1995, 1997; Millard *et al.,* 1997), post tensioned bridges (Cooke *et al.,* 1993), concrete pavements and decks (Clemena *et al.,* 1987; Holt and Eales, 1987; Washer, 1997), and structures (Henderson, 1990).

Some specific applications, like changes of rock type, soil strata and water table in coarse grained soils, detection of buried walls, pipes, tunnels (Daniels, 1988; Botros *et al.*, 1984; Fenning and Brown, 1995), and buried containers (Bowders and Koerner, 1982; Lord and Koerner, 1987) have generated an increasing demand for subsurface imaging with higher resolution than previously possible.

The use of radar for investigation of concrete structures (Hobbs *et al.*, 1993; Krause *et al.*, 1995), though relatively recent, is well known and generally successful but its capability in different conditions still needs to be validated. Numerical and laboratory approaches on simple models have investigated radar resolution on concrete of varying quality and moisture content (Padaratz, 1996). Similar work on concrete has also been carried out just via laboratory experiments (Bungey *et al.*, 1993; Buyukozturk and Rhim, 1995).

Radar investigation of masonry structures is much more recent and limited (Kahle and Hillich, 1992; Arndt *et al.*, 1994; Kahle *et al.*, 1994; Binda *et al.*, 1994; Riccioni and Rossi, 1995; Chidiac *et al.*, 1995; Paxton, 1996). Its use has been suggested on heritage buildings where the use of appropriate non-destructive inspection techniques is essential for the preservation of the original fabric of the structure, where the objective of the radar survey is to investigate multi-wythe stone masonry walls, identify thickness of materials, voids, discontinuities and anomalies, conditions of mortar and rubble fills, and moisture capillary rise. Results have been encouraging, suggesting that radar is a promising tool for masonry investigation, but the quality of the data depends on many factors, including the smoothness of the interface boundary in multiple leaf masonry, and on the ratio of the electrical properties of the materials crossed (Pitt, 1994; Kahle, 1993; Silman and Ennis, 1993). The evaluation of the structural integrity of masonry walls (i.e. continuity, connections, etc.) has proved difficult and does not lead to a satisfactory conclusion without supplementary borescope investigation. This is especially the case when extensive voiding renders the wall too complex.

Examples of radar application to masonry bridges are not known to the author. Therefore, from the above review, it is clear that there is great need for collecting data on a number of masonry structures and arch bridges, for assessing the performance and capabilities of the radar method.

4.2.1 Radar survey and waveform image display

Ground penetrating radar (GPR) uses short electromagnetic energy pulses of high centre frequency (50-2500 MHz) to detect buried objects in any non-metallic material. These waves are sent through antennas into the "ground" (any medium different from air) and when enough dielectric contrast exists between the boundaries of two consecutive layers, part of the transmitted energy is reflected back and picked up by the receiver in the antenna. The remainder of the energy is transmitted and refracted through the subsequent material and the propagation continues until the next interface, where the process is repeated.

Since the energy radiated by the antenna is a divergent beam, reflections from targets (any layer or anomaly) may be recorded even if the antenna is not positioned right above them, with the consequence that the true shape of the target appears modified and distorted on the radar plot. A computer records and merges the GPR data to create an image. Hyperbola (arches) displayed on this image indicate the placement and depth of objects in the survey area (Fig. 4.1). Measurements must be made at many points to ensure accurate representation of the area being examined.

In a digital radar system, such as the GSSI SIR 10 (see Appendix B) employed in this research work, the waveforms are digitally sampled and can be stored for post processing. To aid data interpretation, each waveform is analysed in terms of the magnitude of its deflection from the zero line. The minimum to maximum amplitude is generally split into 16 equal sections and each section is assigned a colour or a grey tone (Fig. 4.2). This is known as a linear transform but others may be used: fig. 4.3.a is an exponential transform which emphasises the small amplitude changes. Waveforms are then placed adjacent to each other and plotted as depth, or two-way

travel time, on the vertical axis, against horizontal distance moved by the antenna on the horizontal axis. The magnitude of deflection from the zero line is shown as a point of colour. Therefore, a horizontal layer of homogeneous material will show up as a band of colour on the radar system output. A complete profile is known as a line scan image.

Alternatively the data can be displayed as a time domain plot or wiggle plot, with a discrete number of waveforms sampled by the radar's built-in oscilloscope (Fig. 4.3.b).

Each waveform is generally called a "scan" and it is made up of "sample points": typical radar settings include sampling of the order of 512 samples per scan, approximately 40 scans per second and a linear gain increasing with depth. Settings vary depending on the site conditions, the goal of the survey, and the desired resolution.

Filtering is an option for enhancing the data resolution, but excessive filtering may deteriorate the data and be expensive in terms of analysis time. Two kinds of filter were occasionally used on the experimental data of chapters 5 and 6, when accurate calculations of velocity or dielectric constant were performed:

I) Averaging and stacking, which is used for high frequency noise reduction. The noise component will always be different owing to its random nature, so that by averaging a number of records the noise will tend to zero whereas the signal remains the same. On this basis the two components can be separated and the quality, or signal to noise ratio, can be improved.

II) Background removal, which is a form of high-pass filter applied to remove constant features along the scan plot, such as surface reflection. This was done through a simple differencing operation, subtracting adjacent waveforms.

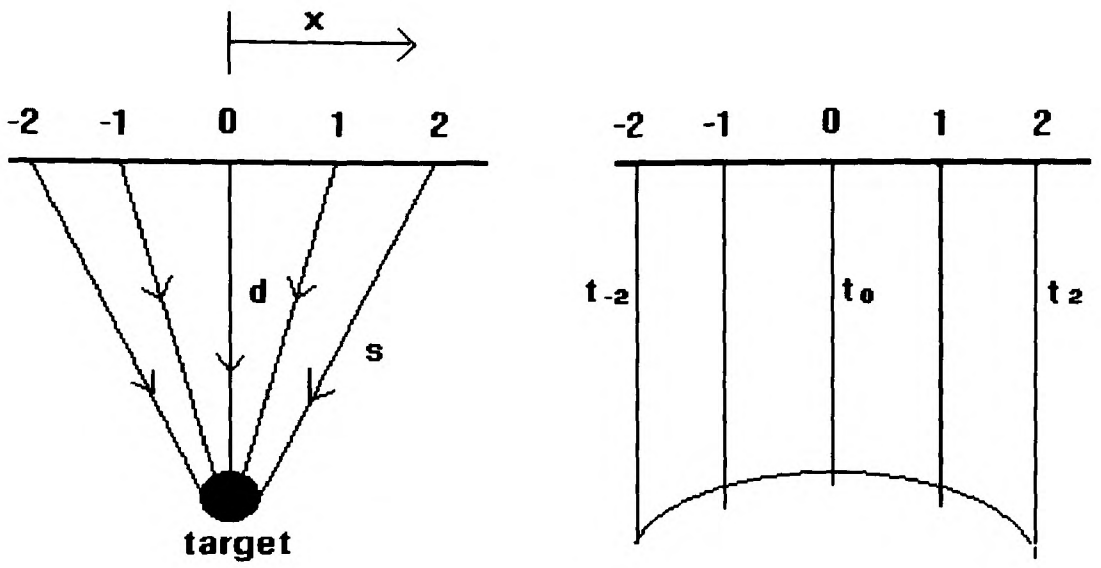

Fig. 4.1 - Representation of radar survey (left), time domain data display (right).

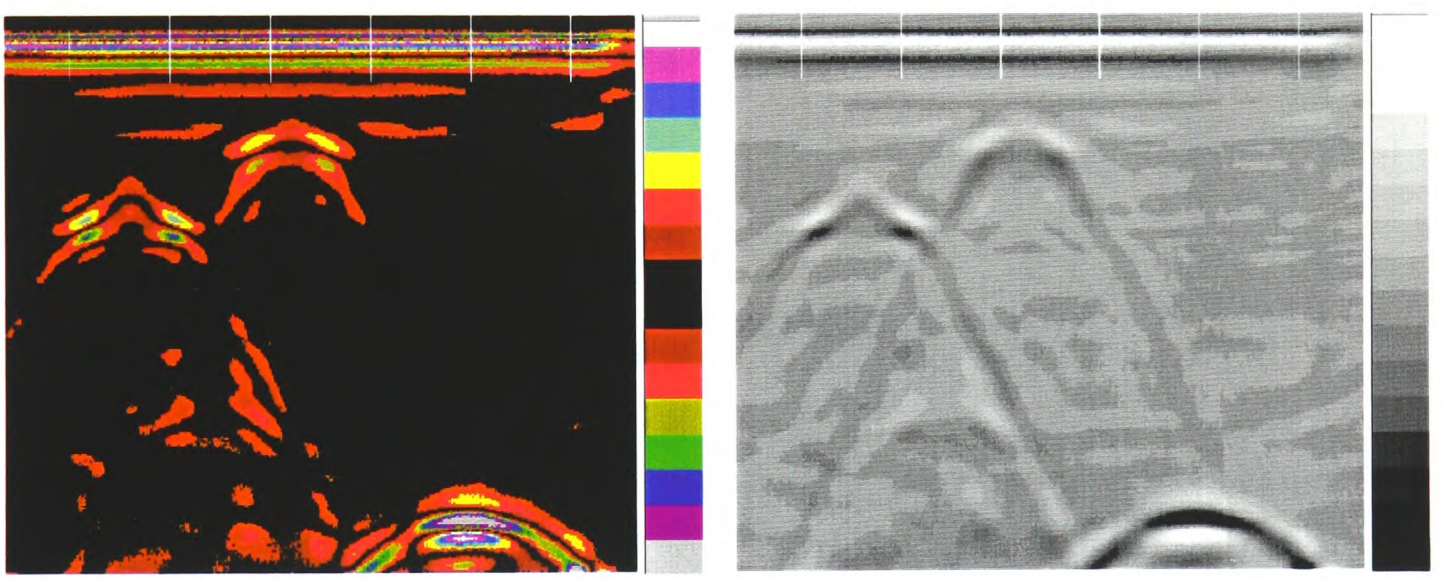

Fig. 4.2 - Radar line scan image: linear transform a) in colour; b) in grey tones.

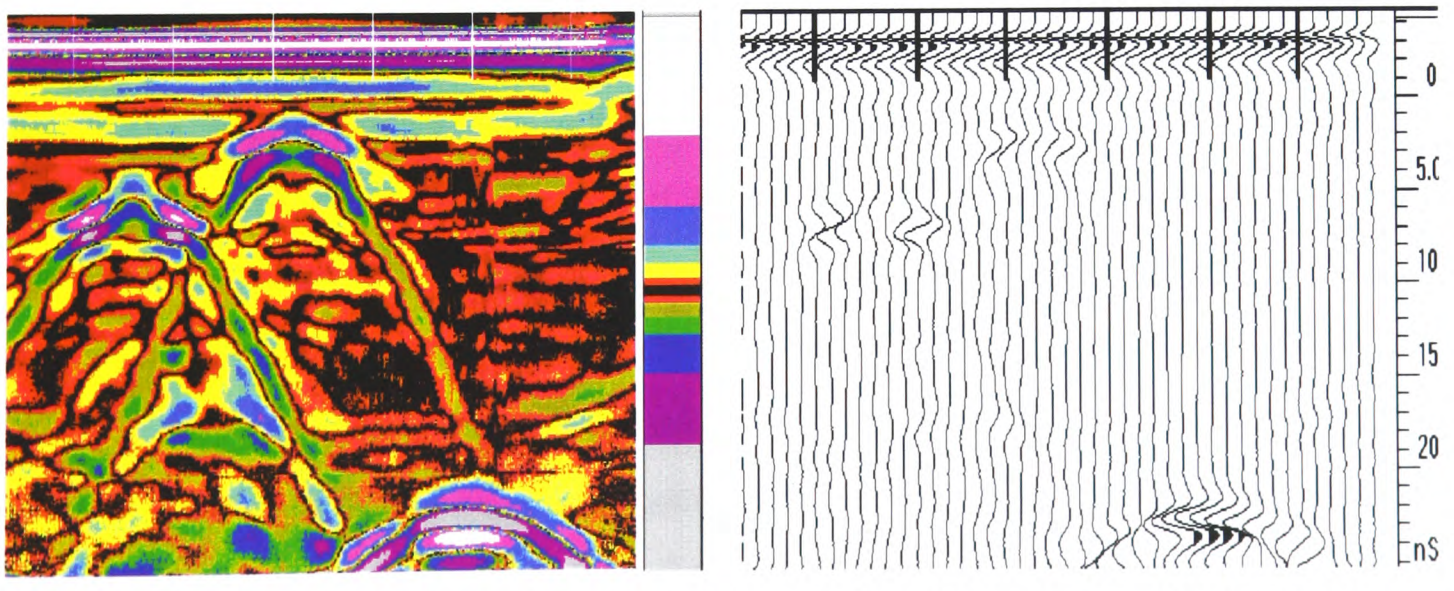

Fig. 4.3 - Radar data display: a) exponential transform line scan; b) wiggle plot.

4.2.2 Wave propagation and material electrical properties

The characteristics of wave propagation - velocity, attenuation, reflection and refraction - are determined by the dielectric properties of the materials involved and the antenna frequency used (Topp *et al.*, 1980; Greaves *et al.*, 1996).

Conductors and dielectrics. According to their electrical properties, materials are classified as conductors if they have high electrical conductivity (most metals), and insulators or dielectrics, if they have low conductivity (most geological and building materials).

If $\frac{\sigma}{\omega\varepsilon} >> 1$ the material is classified as a good conductor;

if $\frac{\sigma}{\omega\varepsilon} << 1$ the material is a good dielectric (or low loss material)

where σ = conductivity,

$\omega = 2\pi f$ angular frequency,

ε = dielectric constant or relative permittivity.

Conductivity. The conductivity, σ, is a measure of the response of free charges in the material to the flow of electric fields. It is frequency dependent and affected by the clay, water and salt content in the material. On site measurements are only done at low frequency, up to 100 MHz, using DC conductivity meters or resistivity methods, and both cases will underestimate the actual values of conductivity. Conductivity is of paramount importance for the attenuation of the wave and its propagation depth. Ground penetrating radar has demonstrated the capacity to sound to depths of tens of metres in low conductivity (less than 1 $mS.m^{-1}$) materials such as sand, gravel, rock and fresh water. The range decreases to a shallow depth in conductive materials such as clays, silts and soils with saline or contaminated pore water. An indication of the maximum depth of penetration as a function of conductivity is given by McDowell *et al.* (1988) and presented in Fig. 4.4. For a more extended treatment of conductivity see section 4.4.1.

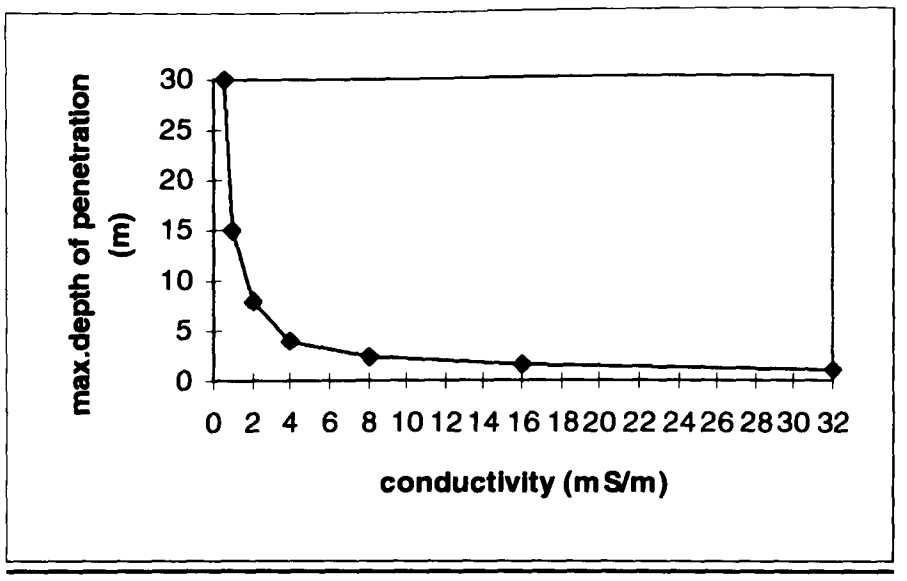

Fig. 4.4 - Effective depth of radar penetration against material conductivity (after McDowell *et al.*, 1988).

Relative permittivity. The permittivity measures the distortion of electric charge in the material when an electric field is applied. The Complex permittivity of a material is given by

$$\varepsilon_c = \varepsilon' - j\varepsilon'' \qquad (4.1)$$

where ε' = real part of the complex permittivity,

ε'' = imaginary part of the complex permittivity (loss factor),

$j = \sqrt{-1}$

The real part of equation (4.1) is called the dielectric constant or relative permittivity, ε_r , and it describes the high frequency electrical properties of the materials since, at these frequencies, the displacement (polarisation) properties dominate the conductive properties for many materials. As can be seen from equations (4.12) and (4.13), the dielectric constant of the material directly affects the wave velocity. Note that the dielectric constant of water is $\varepsilon_r = 80$ and that of most dry geological materials is in the range of 4-8. This large difference explains why the radar signal velocity is strongly dependent on the water content in materials. Table 4.1 shows values reported in the literature of dielectric constant, for most common materials.

Material	ε_r	σ (mS/m)	Material	ε_r	σ (mS/m)
Air	1	0	Clays	5-40	2 -1000
Metal (iron)	1	10^8	Dry clay	3	1-10
PVC	3		Saturated clay*	15	10^2-10^3
Fresh water	81	1	Rock	4-10	
Sea water	81	4 x 10^3	Dry Granite	5	10^{-5} - 1
Ice	3-4	0.01	Wet granite	7	1
Sand	4-25		Limestone	4-8	0.5 - 2
Dry sand	3	10^{-4} - 1	Wet sandstone	6	
Saturated sand*	25	10^{-1} - 10	Asphalt	3-6	
Soil (dry)	2-6		Dry concrete	6	1
Soil (wet)	5-15		Saturat. concrete	12	10^8

* Fresh water

Table 4.1 - Relative permittivity and conductivity of common materials.

Electromagnetic wave attenuation. When an electromagnetic signal passes through a dielectric medium (masonry is a low loss dielectric, with the exception of any metal which might be present) the amplitude of the signal will be attenuated. The attenuation is dependent on a variety of parameters: permeability, permittivity, angular frequency, and primarily conductivity. For conductive materials, the attenuation can be shown to be (Von Hippel, 1954):

$$\alpha = \omega\left[\frac{\mu\varepsilon'}{2}\left(\sqrt{1+tan^2\delta}-1\right)\right]^{1/2} \qquad (4.2)$$

where α = attenuation constant,

μ = magnetic permeability,

$$tan\delta = \frac{\varepsilon''}{\varepsilon'} \cong \frac{\sigma}{\omega\varepsilon'} \qquad \text{the loss tangent (or dissipator factor),} \qquad (4.3)$$

$$\text{where } tan\delta = 1.8x10^{10}\frac{\sigma}{f\varepsilon_r} \qquad (4.4)$$

with σ in S/m.

At radar frequencies, ε' can be assumed constant and independent of frequency (Hoekstra and Delaney, 1974). Dividing equation (4.1) by $\varepsilon_0 = 8.854 \times 10^{-12}$ F/m (permittivity of free space) and knowing that $\mu_0 = 4\pi \times 10^{-7}$ H/m and $\mu_r \cong 1$ for non-magnetic materials, from (4.2) can be derived:

$$\alpha = 1.482 x 10^{-8} f \sqrt{\varepsilon_r} \left[\sqrt{1 + tan^2 \delta} - 1 \right]^{1/2} \qquad (4.5)$$

where α = attenuation constant in nepers/m

f = centre frequency of the transmitted signal (Hz)

$\varepsilon_r = \varepsilon_r'$ = dielectric constant

or in decibels/m:

$$8.686\alpha = 12.9 x 10^{-8} f \sqrt{\varepsilon_r \left[\sqrt{1 + tan^2 \delta} - 1 \right]^{1/2}} \qquad (4.6)$$

For dielectric materials, (4.6) can be simplified to:

$$\alpha = 1.64 x 10^3 \frac{\sigma}{\sqrt{\varepsilon_r}} \qquad \text{(in dB/m)} \qquad (4.7)$$

where $\sigma = \sigma_{dc} + \omega \varepsilon'' \varepsilon_0$ combines both d.c. conductivity and dielectric losses.

High conductivity causes strong attenuation in the signal. The effect of signal scattering by small scale heterogeneities can also increase attenuation.

Skin depth: The attenuation of a signal gives rise to the concept of a skin depth (D). The definition of skin depth is that a signal will attenuate to a value of 1/e times its original strength when a depth of $1/\alpha$ has been reached. The skin depth is given by

$$D = \frac{1}{\alpha} \qquad (4.8)$$

where α = attenuation in nepers/m given by (4.5).

For dielectrics, the simplified equation of D is:

$$D = \frac{5.31 \text{ x } 10^{-3} \sqrt{\varepsilon_r}}{\sigma} \qquad (4.9)$$

with σ in S/m.

For good conductors, the simplified equation of D is (Cheng, 1989):

$$D \cong \frac{16}{\sqrt{f\sigma}} \qquad (4.10)$$

with f in MHz,

σ in mS/m.

If a signal of unit intensity passes through a depth, d (m), of a low loss dielectric with an attenuation of α, then the attenuation factor, A, is given by:

$$A = 1\text{-}d\alpha e^{-1} \qquad (A>0). \qquad (4.11)$$

The wave will be completely attenuated if $A \leq 0$ and therefore no propagation occurs.

Independent of the operational centre frequency, the skin depth is greatly affected by conductivity: in low loss materials for values of conductivity between 1 and 10 mS/m, the skin depth is reduced from a few tens of meters to 1-2 meters (Padaratz, 1996).

The skin depth gives an indication of how well GPR energy penetrates a medium, but does not define the absolute depth of propagation.

Electromagnetic wave velocity. The velocity is an important factor when the aim of the survey is to estimate the depth of the target. The general equation of velocity for conductive dielectric materials is :

$$v = \frac{c}{\left[\frac{\varepsilon_r}{2}\left(\sqrt{1 + tan^2\,\delta} + 1\right)\right]^{1/2}} \qquad (4.12)$$

For low loss materials ($\tan\delta << 1$), (4.12) can be simplified (to be independent of frequency and conductivity) to:

$$v = \frac{c}{\sqrt{\varepsilon_r}} \qquad (4.13)$$

where v = electromagnetic wave velocity,

c = velocity of wave propagation in free space (3×10^8 m/s).

Transmission and reflection of electromagnetic wave. When an electromagnetic wave propagates through one material to another, there is partial reflection and transmission at that interface. The amount of reflection and transmission is dependent on the respective impedance, Z_r, of the materials.

In the case of oblique incidence, it will be:

perpendicular polarisation

$$R = \frac{Z_2 \cos\theta_i - Z_1 \cos\theta_t}{Z_2 \cos\theta_i + Z_1 \cos\theta_t}$$

$$T = \frac{2Z_2 \cos\theta_i}{Z_2 \cos\theta_i + Z_1 \cos\theta_t}$$

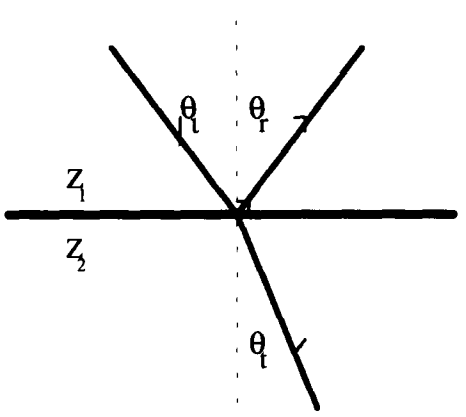

Fig. 4.5. Angles at wave incidence.

parallel polarisation

$$R = \frac{Z_2 \cos\theta_t - Z_1 \cos\theta_i}{Z_2 \cos\theta_t + Z_1 \cos\theta_i}$$

$$T = \frac{2Z_2 \cos\theta_i}{Z_2 \cos\theta_t + Z_1 \cos\theta_i}$$

where Z_1 is the impedance of the first material,

Z_2 is the impedance of the second material,

and $$Z = \sqrt{\frac{j\omega\mu}{\sigma + j\omega\varepsilon}} \qquad \text{(intrinsic impedance)} \qquad (4.14)$$

where $\mu = \mu_r \mu_0 = \mu_0 = 4\pi \times 10^{-7}$ is the material permeability,

$\varepsilon = \varepsilon_r \varepsilon_0 = \varepsilon_r \left[8.854 \times 10^{-12}\right]$ is the relative permittivity,

$\omega = 2\pi f$ (rad/s) is the angular frequency,

σ (S/m) is the conductivity.

If the dielectric constant of the second layer is substantially higher than that of the first layer there will be a marked phase change (a negative number will give a change in polarity of the reflected wave).

The angle of refraction of the transmitted wave is (Corson and Lorrain, 1962):

$$\theta_t = sin^{-1}\left(sin\theta_i \frac{Z_2}{Z_1} \right)$$

For a normal incidence plane wave: $\theta_i = 0$ and $\theta_t = 0$. Thus:

$$R = \frac{Z_2 - Z_1}{Z_2 + Z_1} \qquad \text{and} \qquad T = \frac{2Z_2}{Z_2 + Z_1}$$

Most geological and building materials may be classified as low loss materials (low conductivity) and non-magnetics with $\mu_r = 1$. For these materials, (4.14) may be reduced to:

$$Z = \sqrt{\frac{\mu_0}{\varepsilon_r \varepsilon_0}} \tag{4.15}$$

For normal incidence, reflection (R) and transmission (T) coefficients may be written only as functions of the respective real parts of the complex permittivity:

$$R = \frac{\sqrt{\varepsilon_{r1}} - \sqrt{\varepsilon_{r2}}}{\sqrt{\varepsilon_{r1}} + \sqrt{\varepsilon_{r2}}} \tag{4.16}$$

$$T = \frac{2\sqrt{\varepsilon_{r1}}}{\sqrt{\varepsilon_{r1}} + \sqrt{\varepsilon_{r2}}} \tag{4.17}$$

where ε_{r1} = dielectric constant of first material,

ε_{r2} = dielectric constant of second material.

In reality the interface between two materials is not perfect and surface roughness is present. Equations (4.16) and (4.17) thus give approximate maximum coefficients. For metals, considered to be perfect conductors, the reflection coefficient will be approximately -1 and no penetration occurs.

High water content gives rise to strong radar reflections at interfaces, causing part of the transmitted signal to be reflected.

Influence of frequency. The depth of exploration and image definition depend on the frequency used: the higher the frequency, the better the resolution, but the lower the penetration. Low frequencies are used for deep geological mapping because these frequencies do not attenuate as rapidly as high frequencies; however their resolution power is limited. High frequencies are necessary for high definition imaging, such as delineating reinforcing bars in concrete, but they attenuate quickly. Radar systems offer a wide range of antenna frequencies to accommodate numerous applications. For the civil engineering field, the antennas employed are normally in the range of 100 to 1500 MHz. Available radar antennas transmit pulses over a broad frequency spectrum, though the antennas are defined by their nominal centre frequency. Still, the user has to make a choice between resolution and penetration power and a compromise must be reached depending on the goal of the survey.

Electromagnetic wavelength (λ). This is the duration in space of a cycle of a travelling wave and can be calculated from:

$$v = \lambda \times f \tag{4.18}$$

From (4.13) it can be seen that the wavelength increases with decreasing frequency and/or dielectric constant.

Vertical resolution is the ability to recognise closely-spaced vertical reflectors and to distinguish their reflected signals in the time domain. The resolution is considered to be between 1/4 and 1/2 of the dominant wavelength of the pulse.

Horizontal resolution is the ability to identify and distinguish individual targets at the same depth. The reflected signal from each target will include contributions at depth "d" and from all parts of the surrounding circular area at distance "d + $\lambda/4$" from the antenna (Fig. 4.6). This area is called the Fresnel zone and its width is the limit for horizontal resolution: targets at spacing of less than "2r" will not be individually distinguishable. The radius, r, of the Fresnel zone is given by:

$$r^2 = \frac{\lambda d}{2} + \frac{\lambda^2}{16} \qquad (4.19)$$

from which it can be seen that the resolution improves with increasing frequency and decreasing depth.

4.3 Sonics

NDT methods based on the analysis of sonic wave propagation have been used for at least 30 years for the evaluation of engineering structures. These same methods are used to appraise the elastic characteristics, degree of homogeneity and possible state of decay of masonry.

Originally, sonic wave propagation methods were typically used in geophysical applications, an area for which they are still relevant. Direct and semidirect transmission measurements in geophysics have been reported for the investigation of the presence of voids such as tunnels. The rock mass between two boreholes can be investigated by careful cross-hole measurement of the travel times and/or amplitudes of seismic energy (McCann *et al.*, 1986). Most attention is also given to measuring the propagation velocity of compressional and shear waves in the frequencies 1-100 Hz and 10-30 kHz (Mooney, 1974). Field techniques involve sources of impulse either at the ground surface or in boreholes, with measurements being made at the

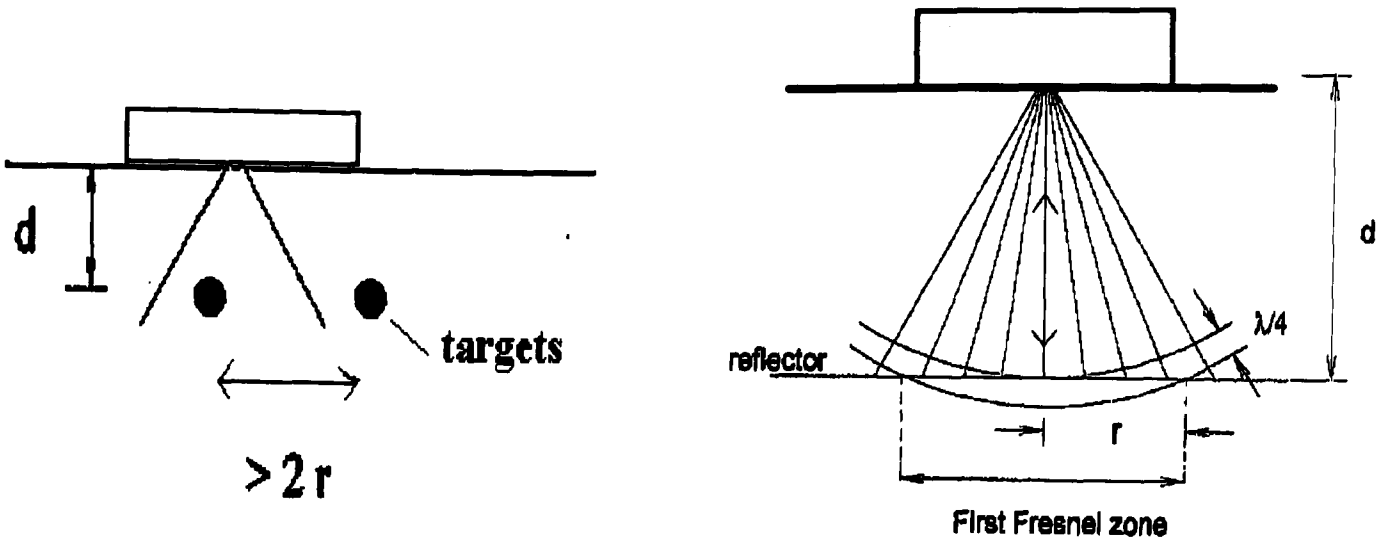

Fig. 4.6 - Horizontal resolution and Fresnel zone.

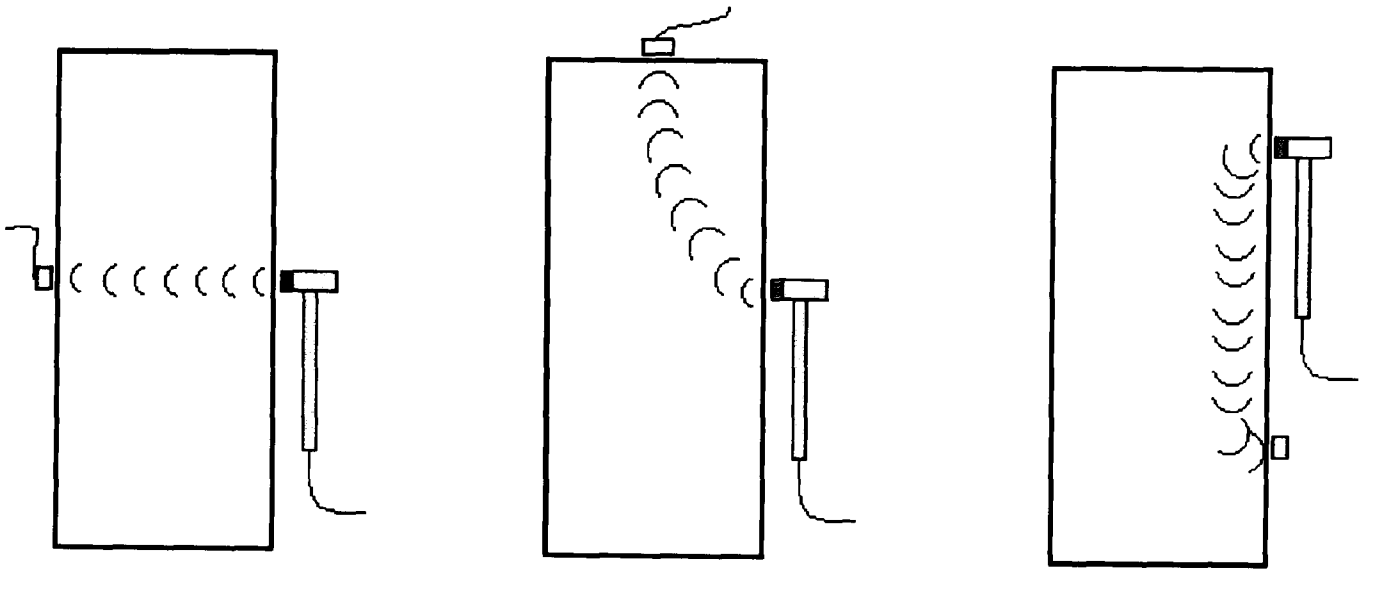

Fig. 4.7 - Transmission modes for sonic wave tests: a) direct, b) semidirect, c) indirect.

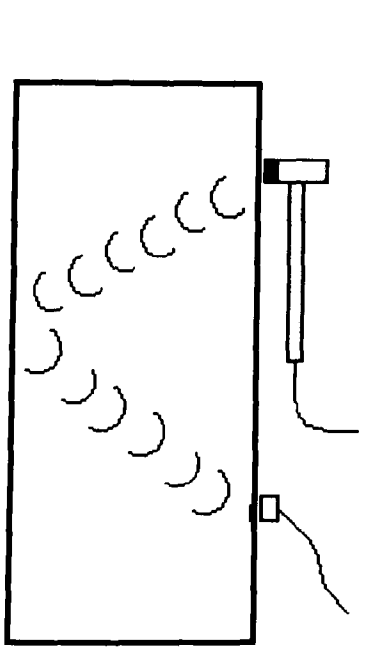

Fig. 4.8 - Sonic reflection mode.

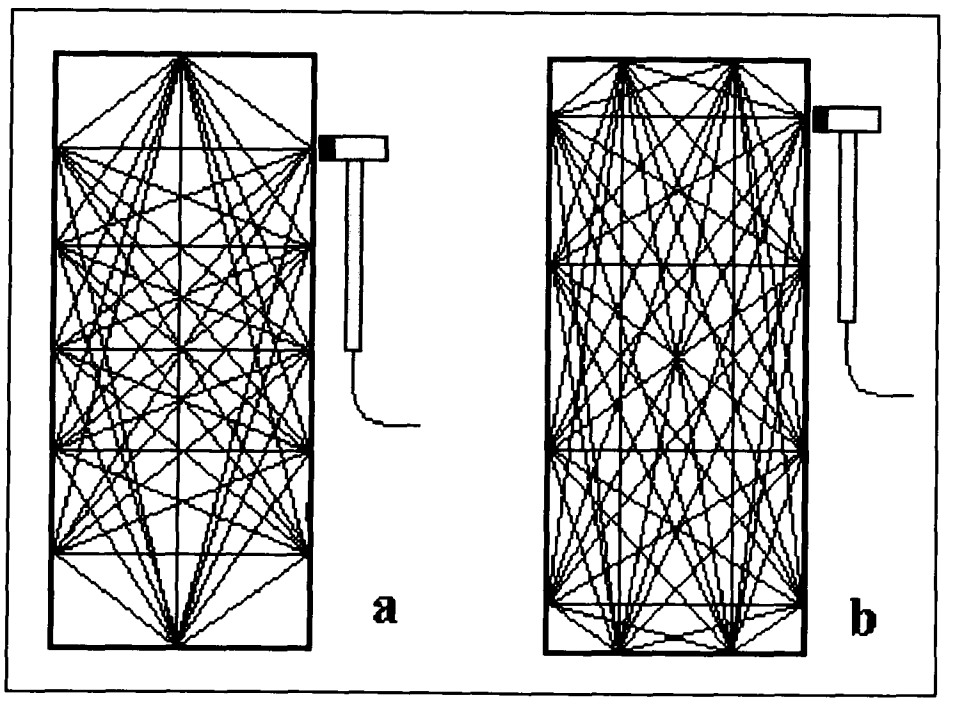

Fig. 4.9 - Sonic tomography.

ground surface or adjacent boreholes by clamped triaxial geophones (Hoar and Stokoe, 1978).

The analysis of materials and structures by mechanically induced sonic pulses has been used for various purposes. These range from assessing the dynamic properties of a structure (Maguire and Severn, 1987) to the detection of flaws in masonry (Abrams and Epperson, 1989; Kingsley *et al.*, 1987; Leaird, 1984). The method has been used in attempts to relate pulse velocity to the mechanical compressive strength of the masonry; studies on multi-wythe masonry prisms with this purpose are also reported (Anzani *et al.*, 1995). Furthermore the sonic technique has been employed to evaluate the efficacy of grouting technique for strengthening masonry (Berra *et al.*, 1991).

One difficult point to establish is the pulse velocity through an unflawed region of masonry. In addition, variations in masonry material components may have some effect on wave propagation. Direct comparison between two different material types are thus difficult to make. However, evaluation of the relative uniformity of a given material can be effectively performed.

Other application of sonic tests to masonry structures include the investigation of conditions behind tunnel linings (Fenning *et al.*, 1989) and the testing of masonry sewers (Sibbald, 1988).

Applications to masonry arch bridges include assessment for detection and location of voids in the fill and unconformities, via direct transmission tests through the spandrel walls (Komeyli-Birjandi, 1986; Armstrong, 1994). The reported values of sonic velocity, averaged through spandrel walls and soil fill, are generally of the order of 1500 m/s; echo tests in stone masonry retaining wall may give velocity values as low as 1350 m/s, depending on the type of wall and its state.

More recently tomographic elaborations of direct and semidirect sonic data have been used. The first tomographic applications of this kind were performed in the mining and geophysical fields where the use of acoustic tomography is reported for strata measurements and void mapping between adjacent boreholes (McCann *et al.*, 1986; Dines and Lytle, 1979). The technique is also extensively used for concrete dam investigation (Rhazi *et al.*, 1996).

Sonic tomography on masonry was first used on historical and monumental structures for investigation of the structural state (Ranieri *et al.*, 1988), then for control of masonry repair (Cote' *et al.*, 1992; Schuller *et al.*, 1994). Tomographic imaging has been extensively studied to evaluate the condition of masonry wall specimen following construction to characterise the initial masonry conditions, to identify damage following lateral load cycles and, after repairing the walls by grout injection, to quantify the effects of the repair (Schuller *et al.*, 1995).

4.3.1 Sonic test procedures and instrumentation

The sonic pulse velocity test is a low frequency (around 10 kHz) test generally induced by mechanical means via an instrumented hammer (see Appendix B). The vibrations in the structure resulting from the propagating wave are measured by an accelerometer mounted on the masonry wall surface with grease (it is important that good transducer coupling is achieved at the receiving station). A two dimensional grid is marked out on the wall and a series of pulse velocity tests are performed at each node point. The signals of both the hammer and the accelerometer are recorded by the acquisition system for each point. The time interval for the sonic wave to travel between the hammer and the accelerometer is defined as the transit time. The data collected from the test provide the transit time (or travel time) of the stress waves through each particular path connecting transmitter (hammer) and receiver (accelerometer) across the structure. Difficulties in calculating the exact travel time of the wave, are a real limitation in sonic tests, because of the slightly different characteristics of each recorded sonic pulse, even for the same test location. In some cases, the precise point of initiation and reception of the sonic wave is difficult to

define. Transit distances involved can be small and minor errors in the determination of the time can thus lead to more significant variations of the calculated velocity. The analysis required to determine the transit time for the many tests performed can therefore be very time consuming. Furthermore, in field measurements, high noise levels can be expected from both the physical measurement and the electronic instrumentation used for data capture and processing. Therefore averaging is generally a requirement before the transit time is calculated (see section 4.2.1).

To determine the pulse velocity, the transit distance is also required at each point. In most masonry walls or structures, the thickness is fairly consistent, varying only by one or two per cent. The exact thickness is difficult to establish at each test point. In this case average values from all accessible locations are used.

To analyse the results and evaluate the presence of flows, inhomogeneities and poor density areas, the pulse velocity of the wave can be easily calculated at each location by the equation

$$v = d/t \qquad (4.20)$$

where v = pulse velocity

d = length of path

t = transit time.

The sonic pulse velocity of the stress wave is affected by average material properties between the hammer impact point and the accelerometer: brick or stone, mortar joints, soil fill and air voids or other defects.

The frequency of the pulse affects the attenuation of the wave and the ability to detect the presence of inhomogeneities. The propagation of the wave can only be affected by flaws which are wider than the wavelengtlı of the pulse. The low frequency associated with the sonic tests results in a longer wavelength than for the ultrasonic case, and the minimum size of inhomogeneity which can affect the transmission of a sonic pulse is therefore increased. The attenuation of a stress wave is affected by the

number and size of flaws and interfaces present in the materials. The level of attenuation of the sonic pulse is less than that of higher frequency signals such as in the ultrasonic pulse test. Attenuation is also related to the number of damped cycles of the propagating wave. The low frequency of the sonic pulse results in fewer cycles over the same distance, resulting in an increase of effective distance over which the pulse velocity measurements can be performed (Epperson and Abrams, 1898).

Sonic waves are elastic deformation waves and their propagation characteristics (velocity and attenuation) depend on the elastic properties of the materials they cross and the anisotropic behaviour of the masonry. Anisotropic effects are studied by measuring sonic wave velocities along opposite directions of the structure.

4.3.2 Sonic transmission modes

Common application techniques are the direct, semidirect and indirect measurements, reflection measurements and sonic tomography:

- Direct transmission (Fig. 4.7.a): this involves the passing of a stress wave through the thickness of the wall (or the structure) under investigation. Transmission of the wave is initiated on one side of the structure by the impact of the force hammer, and reception on the opposite side is performed by an accelerometer. The force hammer is impacted at a location directly opposite the accelerometer (and this is a difference with the sonic tomography). The resulting wave velocity is an average of the local velocity along the path and it is not possible to establish the position and the extent of any possible inhomogeneity. The velocity magnitudes may be plotted in a contour map format, with the grid points as X and Y co-ordinates and the pulse velocity as the Z co-ordinate. This format allows a simple evaluation of the relative conditions of the masonry. It has generally been recognised that the direct transmission arrangement is preferable because it provides a better defined path length. Furthermore, since the arrival time of the first wave is of primary concern, no attempt to distinguish complex wave frequencies and reflections is required for the analysis (see below: reflection measurements). This method has been successfully used to evaluate material

uniformity, detect the presence of voids, estimate the depth of surface cracks and estimate compressive strength. The detection of flaws is possible due to the fact that sonic waves cannot transit through an air gap, which could be due to a crack, void or delamination at the interface between brick or stone and mortar, or at an interface between wythes. A propagating wave must find a path around the void, resulting in attenuation and an increase in the transit time of the signal. Typical values of direct transmission pulse velocity in masonry are reported in Table 4.2.

Type of structure or sample	**velocity (m/s)**
multi-wythe brickwall	1640- 2370 (Epperson & Abrams, 1989)
masonry piers	1050-1450 (Berra *et al.*, 1992)
multi-wythe masonry prisms	1165-2350 (Berra *et al.*, 1992)
multi-wythe masonry prisms	1240-2480 (Anzani *et al.*, 1995)

Table 4.2 - Direct transmission velocity in masonry

- Semidirect transmission (Fig. 4.7.b): it involves the reception of the wave on a wall at an angle with respect to the wall where the hammer is impacted.

- Indirect transmission (Fig. 4.7.c): in this mode both the initiation and reception of the sonic wave are performed on the same face of the masonry wall. The accelerometer is mounted at one location for each test series and transit time is altered by impacting the hammer at increasing distances from the accelerometer position. The stress wave recorded using this method generally passes only through the outer wythe of the wall and only provides a measure of material quality near the surface. To represent the results, a graph is made for each test series by plotting the transit time versus the surface distance. It has been found for concrete that the pulse velocity determined by the indirect method (V_i) will generally be lower than the velocity measured by direct method (V_d):

$$V_d = 1.05 \times V_i \qquad (4.21)$$

In brick masonry it was found that velocity in the horizontal direction is significantly higher than in the vertical direction (Epperson and Abram, 1989). This may be

explained by the lower number of mortar joints in the horizontal direction than in the vertical direction for equal path lengths.

- Reflection measurements (Fig. 4.8): in this mode again both the initiation and reception of the sonic wave are performed on the same face of the masonry as in the case of indirect transmission, but the stress wave recorded is the direct stress wave echoed by any internal flaw or rear face of the structure investigated. Due to the different velocity of V_d and V_i, and their different path lengths it is in fact possible to distinguish their respective travel times. The value of velocity is a measure of the local velocities along the path. This form of testing is used successfully for the evaluation of metal but it is much less practical in concrete and masonry because the numerous material boundaries in these materials result in scattering of both incident and reflected waves. Despite this fact, it has been successfully used for identifying and locating specific flaws in concrete.

- Sonic tomography (Fig. 4.9): this represents an improvement in the sonic test method not only because it combines direct and semidirect methods but because tests are performed in the direct mode also along paths which are not perpendicular to the wall surfaces. The masonry section is thus crossed by a dense net of raypaths and the tomographic elaboration of the data accounts for curved wave propagation paths. Sonic tomography gives a detailed map of wave velocity across the structure or sample section so that local values of velocity can be read across the section and the extent and location of flaws can be identified.

It is usual to assume a linear structural response in tomographic methods. This is because the response is measured with transducers which are normally mounted well away from the location of impact where non-linearities arise. Any variation from the expected travel time is therefore attributed to in-homogeneity in the structure or damage occurred. In order to obtain good statistical accuracy it is necessary to maximise the amount of experimental data included in any calculation used.

As the method has been used for site investigation work reported in chapter 5, a more extended discussion of tomography is contained in the next section.

4.3.3 Sonic tomography

The word "tomography" is derived from the Greek "tomos", meaning slice and involves reconstructing a section of an object using measurements taken from outside the object. The sonic tomographic imaging method uses pulse velocity information taken through a section to develop a three-dimensional reconstruction of the velocity distribution in that section (Kak and Slaney, 1988). The reconstructed image is used to locate features concealed beneath the material surface. Potential applications include the location of cracks, voids or deteriorated material, indication of density variations and qualification of repair and retrofit procedures, as discussed earlier. A number of inversion algorithms are available for tomographic reconstruction and a Simultaneous Iterative Reconstruction algorithm is used in the software package employed for elaboration of tomographic data collected during the research work reported in this thesis. The interested reader is referred to the program manual for mathematical concepts and operating strategies (Jackson and Tweeton, 1994).

Data acquired usually exhibits a good deal of velocity scatter, resulting from variations in the strength and nature of the hammer hit generating the input signal, the interpretation of acquired waveforms by the operator and coupling of the receiving transducer to the masonry surface (Williamson, 1991). Data scatter has the effect of increasing the residual error (Jackson and Tweeton, 1994) of tomographic velocity reconstruction and may lead to identification of false anomalies. The accuracy of the velocity reconstruction can be improved by a better understanding of the input signals, by a carefully planned choice of position and number of the reading stations and by simple data smoothing prior to analysis.

It is important that the ray paths are uniformly distributed across the section investigated and that the maximum possible area is crossed by the sonic paths. In this view, fig. 4.9.b represents an improved configuration over the section represented in

Fig. 4.9.a. Both cases have been obtained by locating 12 reading stations around the section, but the modified spacing of case (b) not only allows for a better coverage of the area but the number of ray paths also increases from 92 to 104 (or 208 if back readings are recorded, to account for anisotropy of the material).

There is a marked reduction in measured velocity as the angle between transmitter and receiver is increased. This effect is due to the anisotropic properties of the masonry materials (and concrete), which cause the wave not to propagate with a spherical migrating wavefront. This anisotropic material behaviour must be accounted for in the tomographic reconstruction by calculating the ratio between V_d and V_s:

$$V_d/V_s \qquad (4.22)$$

where V_d = direct path velocity

V_s = semidirect path velocity which decreases with increasing incidence angle. The minimum averaged value of semidirect velocity will be used in the ratio of (4.22).

Incidence angles approaching 90 degrees should be avoided, as should very short raypaths. It is advisable to increase the number of ray paths to increase data redundancy (Fig. 4.10). Spurious reading, those showing isolated high deviation from the average velocity in the area, should be eliminated prior inputting in the tomographic software.

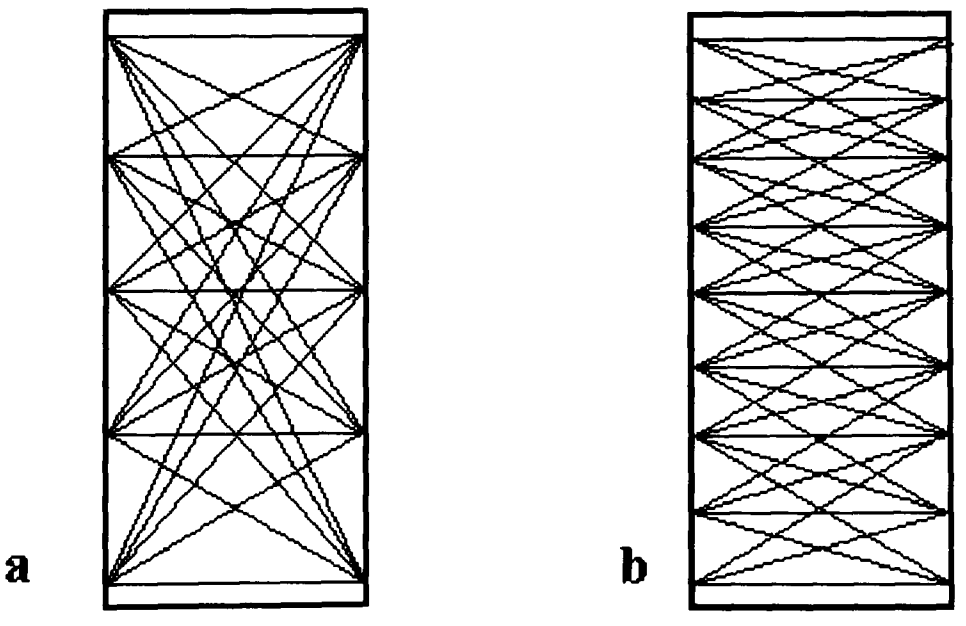

Fig. 4.10 - Variations in ray path configuration and number.

4.4 Conductivity measurements

Some geophysical methods, for example radar, have been previously used for structure investigation, whilst use of geophysical conductivity tools are new in civil engineering. It was near the beginning of this century that sub-surface geology was first investigated by injecting electrical currents into the ground and mapping the resulting field distribution. Since then measurement of terrain resistivity has been applied to a variety of geological problems including the determination of rock lithology and bedrock depth; the location and mapping of aggregate, clay deposit, groundwater extent, salinity and geothermal areas. Other applications include geophysical mapping, archaeological sites investigation, detection of pollution plumes in groundwater and agricultural applications. (Archie, 1942 a & b) .

In many instances resistivity mapping provides definite geological information, however there are cases where the results are uninterpretable since the "geological noise" is too high. The actual value of resistivity itself is seldom diagnostic and, as a result of this ambiguity, the variation of resistivity, either laterally or with depth, is often examined to outline the features of interest and indicate the transition from one soil or rock type to another.

But problems arise in that the area actually surveyed is often too small to fully ascertain the background against which the anomalous features are to be defined. Furthermore, resistivity inhomegeneities much smaller than the depth of exploration (determined by interelectrode spacing), yield large errors in the measurement if they are located near the electrodes, and thus a noisy profile may be recorded. The high number of recordings needed to generate an "image" of the soil profile together with the relatively large amount of manpower required for the positioning of the electrodes mean that the conventional resistivity survey is time-consuming to carry out. For these reasons, the use of this type of resistivity technique is not common for engineering problems.

Yet the potential of resistivity measurements has lead to the development of instrumentation employing electromagnetic techniques to measure terrain conductivity. A sinusoidally varying electromagnetic field induces currents in the ground in such a manner that their amplitude is linearly proportional to the conductivity. The magnitude of these currents is determined by measuring the magnetic field which they in turn will generate. The response fields of the ground at the receiving coil location differ both in phase and amplitude from the transmitted one. These differences reveal the presence of the conductor and provide information on its geometry and electrical properties. The induction of current flow results from the magnetic components of the EM field, consequently there is no need for physical contact with the surface.

4.4.1 Factors affecting the conductivity of soil and rocks

The reciprocal of the electrical resistivity is defined as the electrical conductivity, a measure of the ease with which an electrical current can be made to flow through a substance. In the MKS system the unit of conductivity is the mho per meter - or Siemen per meter - and a resistivity of one ohm-meter (1 Ωm) exhibits a conductivity of one mho per meter (1 ω/m) or one Siemen per meter (1 S/m), see table 4.3. For convenience, conductivity values are usually defined in milliSiemens per meter (mS/m).

Unconsolidated materials at temperate ambient temperatures usually display a range of conductivity between 1 and 1000 mS/m, whilst the conductivity of rocks lies between 0.01 mS/m and 100-200 mS/m. These values are usually recorded when direct current is employed for the measurements but it must be noted that the electrical properties of the sample vary with frequency and in soil and rocks complex mechanisms govern the mode of current flow (Olhoeft, 1975a & b; Ward and Fraser, 1967; Keller and Frischknecht, 1966). For materials with conductivity between 1 and 1000 mS/m the electrical properties which control the current flow are relatively independent of frequency and the DC or low frequency conductivity measured with

conventional resistivity equipment will essentially be the same as that measured using low frequency (up to 300 kHz) electromagnetic techniques (McNeill, 1980a).

Resistivity	Conductivity
1 Ωm	1 S/m
10 Ωm	0.1 S/m
100 Ωm	0.01 S/m
1000 Ωm	0.001 S/m or 1 mS/m

Table 4.3 - Unit conversion factors for resistivity/conductivity.

A complete set of measurements by Smith-Rose (Smith-Rose, 1934) on a variety of British soils from different depths, with different moisture contents, and measured at various frequencies, show that at the lower frequencies the conductivity of soils is essentially independent of frequency. At higher frequencies the conductivity rises and the increase in conductivity is generally greatest for the most poorly conducting samples. It must be noted that these frequencies are much lower than frequencies used in civil engineering radar applications (ranges from 100 MHz to 1 GHz), but conductivity figures for building materials, obtained at radar frequencies, are not available in the literature.

Most soil and rock minerals forming building materials are insulators and conduction through the rock matrix only takes place when certain clay materials, native metals and graphite are present. The minerals in the sand and silt fractions of the soil are electrically neutral and are generally excellent insulators. Completely dry clay is also an insulator but the introduction of moisture changes the situation radically as cation exchange on the surface of the particles can take place. The electrical conductivity of the material is thus primarily controlled by the particle size, the amount of water present in the pores and by the conductivity of the pore fluid. The general trend is that conductivity will increase with reducing particle size, increasing moisture content and increasing salt content.

Smith-Rose concludes that clays have the highest conductivities, greater than 10 mS/m, loams and chalks are of the order of 10 mS/m and sandy or gritty soils are appreciably less. Tables 4.4 and 4.5 give a broad indication of the conductivity of soil and rock materials but extreme caution must be exercised in employing these values for anything than a rough guide.

Rock Type	Conductivity range (mS/m)
Argillites	80 - 100
Conglomerates	0.1 - 2
Sandstones	6.4×10^{-5} - 1
Limestone	10^{-4} - 500
Unconsolidated wet clay	200
Clays	10 - 1000
Alluvium and sands	80 - 100

Table 4.4 - Typical values of conductivity for geological and building materials (Telford *et al.*, 1976).

Soil Type	Conductivity range (mS/m)
Clay and marl	10 - 1000
Loam	600 - 6000
Top soil	30 - 700
Clayey soils	10 - 60
Sandy soils	7 - 70
Loose sand	0.01 - 1
River sand and gravel	7 - 10
Limestones	5 - 700
Sandstones	0.1 - 300

Table 4.5 - Conductivity ranges for various terrain materials (Culley *et al.*, 1975).

Measurements made on a soil sample at 1.2 MHz as a function of the moisture content by weight, show a conductivity that increases approximately as the square of the moisture content (Smith-Rose, 1934).

In distilled water there are few ions and the conductivity is low, but the solutions of salts in pore water will substantially increase the material conductivity. For example the addition of only one part per million of sodium chloride by weight in water, produces the appreciable conductivity of 0.22 mS/m, but the concentration of dissolved salts in natural groundwater is substantially higher. The solution of ions and cations in natural water is normally derived by the rock and soil matrix, but particularly high salt content can be found in structures like bridges where salt is used for de-icing operations.

Precipitation water has conductivity of 1 to 30 mS/m; surface waters (lakes, rivers) from 0.3 mS/m for very pure water to 10,000 mS/m for salt lakes, but usually between 2 and 100 mS/m; normal groundwaters from 6 to 1000 mS/m (Heiland, 1968). These values are important when the conductivity (or radar) survey is conducted near the foundations of a structure, the base of a bridge pier, for river bed scour investigation, and similar.

The temperature dependence of the electrical conductivity of the electrolyte is almost entirely due to the temperature dependence of the viscosity of the liquid, which affects the ionic mobility. The conductivity for a temperature other than 25 °C is given by

$$\sigma(T) = \sigma(25°C)[1 + \beta(T - 25°C)] \qquad (4.23)$$

where $\beta = 2.2 \times 10^{-2}$ per °C

T = temperature (°C) at which conductivity is to be calculated.

A change in conductivity of 2.2 % per degree implies that for high seasonal changes of temperature, the conductivity over the normal range of ambient temperature may double.

4.4.2 Principles of instrumentation operation

A transmitter coil Tx energised with an alternating current at an audio frequency is placed on the material surface (assumed uniform) and a receiver coil Rx is located a short distance *s* away. The magnetic field arising from the alternating current in the transmitting coil induces very small currents in the material (earth or structure). These currents generate a secondary magnetic field H_s which is sensed, together with the primary magnetic field H_p, by the receiver coil (figures 4.11 and 4.12).

In general this secondary magnetic field is a complicated function of the intercoil spacing *s*, the operating frequency *f* and the conductivity σ. Under the constraints of "operation at low values of induction number" (incorporated in the instrumentation design and discussed below) the secondary magnetic field is a very simple function of these variables and is shown to be:

$$\frac{H_s}{H_p} \cong \frac{i\omega\mu_\circ\sigma s^2}{4} \qquad (4.24)$$

where H_s = secondary magnetic field at the receiver coil

H_p = primary magnetic field at the receiver coil

ω = $2\pi f$

f = frequency (Hz)

$\mu_\circ$ = permeability of free space

σ = ground conductivity (S/m)

s = intercoil spacing (m)

i = $\sqrt{-1}$

The ratio of the secondary to the primary magnetic field is therefore linearly proportional to the material conductivity, a fact that makes it possible to construct a

direct-reading conductivity meter by simply measuring this ratio. Given H_s/H_p the apparent conductivity indicated by the instrument is defined from equation (4.25) as

$$\sigma_a = \frac{4}{\omega\mu_o s^2}\left(\frac{H_s}{H_p}\right) \qquad (4.25)$$

The measured quantity is the ratio of the secondary magnetic field H_s at the receiver when both coils are lying on the surface of the homogeneous half space of conductivity σ, to the primary magnetic field H_p in the absence of the half space (i.e. as if the coils were in free space). H_p is measured during the calibration operation, with the instrument lifted in air at a height greater than its depth of penetration.

The field ratios for vertical and horizontal dipole configurations (see below) are given by equations 4.26 and 4.27 respectively.

$$\left(\frac{H_s}{H_p}\right)_V = \frac{2}{(\gamma s)^2}\left\{9 - \left[9 + 9\gamma s + 4(\gamma s)^2 + (\gamma s)^3\right]e^{-\gamma s}\right\} \qquad (4.26)$$

$$\left(\frac{H_s}{H_p}\right)_H = 2\left[1 - \frac{3}{(\gamma s)^2} + \left[3 + 3\gamma s + (\gamma s)^2\right]\frac{e^{-\gamma s}}{(\gamma s)^2}\right] \qquad (4.27)$$

where $\gamma = \sqrt{i\omega\mu_o\sigma}$

These expressions are functions of the variable γs which is a function of frequency and conductivity. However under certain circumstances they can be simplified.

A well known characteristic of a homogeneous half space is the electrical skin depth δ which is the distance that a propagating plane wave has travelled when its amplitude has been attenuated to 1/e of the amplitude at the surface. The skin depth is given by

$$\delta = \sqrt{\frac{2}{\omega \mu_{\circ} s}} = \frac{\sqrt{2i}}{\gamma} \tag{4.28}$$

and therefore

$$\gamma s = \sqrt{2i}\,\frac{s}{\delta} \tag{4.29}$$

The ratio s/δ is defined as the induction number B and if it is much less than unity then $\gamma s << 1$. It follows that

$$\left(\frac{H_s}{H_p}\right)_V \cong \left(\frac{H_s}{H_p}\right)_H \tag{4.30}$$

and equation (4.25) can be obtained.

The condition B<<1 is equivalent to stating that for all current loops that affect the receiver output, the operating frequency is so low that we can ignore any magnetic coupling between the loops (Fig. 4.11). Thus the current that flows in any loop is (a) completely independent of the current that flows in any other loop since they are not magnetically coupled and (b) is only a function of the primary magnetic flux linking that loop and of the local material conductivity.

If no current flow crosses an interface and if there is no magnetic coupling between the loops, changing the conductivity of any one of the layers of a horizontally stratified structure will not alter the geometry of the current flow. Varying the conductivity of any layer will proportionally vary only the magnitude of the current in that layer. To calculate the resultant magnetic field at the surface it is simply necessary to calculate the independent contribution from each layer, which is a function of its depth and conductivity, and to sum all the contributions.

Finally it should be noted that for a given frequency and intercoil spacing, as the conductivity increases, the approximation of equation (4.30) eventually breaks down and the instrumental output is no longer proportional to the conductivity. The calibration of the instrument would then need to be repeated (McNeill, 1980b).

The conductivity metre - Geonics EM38 - employed for the conductivity surveys described in the following chapter has intercoil spacing of 1 meter and provides a maximum depth of exploration of 1.5 m in Vertical Dipole Mode (0.75 m in Horizontal Mode) operating at a frequency of 14.6 kHz. The lateral extent of the volume whose conductivity is sensed by the meter is approximately the same as the vertical depth.

The depth of penetration depends upon "s" and the frequency used, but it is independent from the conductivity distribution of the subsurface. The lower the frequency, the deeper the penetration but the poorer the resolution - as amplitude decreases exponentially with depth (Kearey and Brooks, 1991; Milsom, 1989).

The instrument can be rolled over so that the vertical dipole transmitter/receiver geometry becomes a horizontal dipole transmitter/receiver geometry. This feature is useful in diagnosing and defining a layered media. In figure 4.13, the function $\phi_V(z)$ describes the relative contribution to the secondary magnetic field arising from any thin layer at any depth z (where z is the normalised depth i.e. the depth divided by the intercoil spacing s) when the instrument is operated in Vertical Dipole mode. We see from the figure that material located at a depth of approx. 0.4 s gives maximum contribution to the secondary field but material at a depth of 1.5 s still contributes significantly. At zero depth, the near surface material makes a very small contribution to the field and therefore this coil configuration is insensitive to changes in near surface conductivity (table 4.6).

Also in figure 4.13, the function $\phi_H(z)$ describes the case in which transmitter and receiver are in horizontal dipole mode. The contribution from material near the surface is large and the response falls off monotonically with depth. The figure also shows that for regions greater than one intercoil spacing in depth, the vertical dipole mode gives approximately twice the relative contribution of the horizontal mode.

Depth	Contribution to $\phi_V(z)$
<0.3 z	7 %
0.3-0.8 z	48 %
0.3-1.5 z	75 %
0.3-2.5 z	89 %
>2.5 z	4 %
>1.3 z	23 %

Table 4.6 - The % contribution to $\phi_V(z)$ of a range of depths in a homogeneous material.

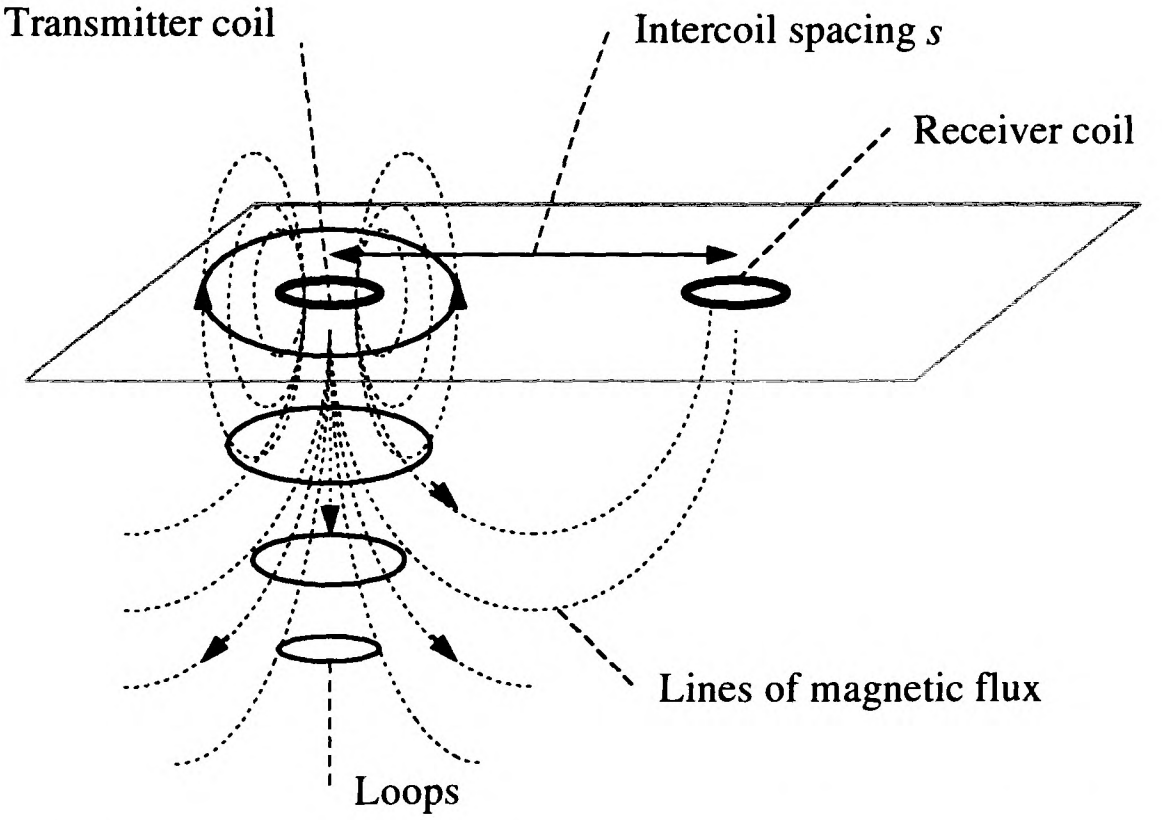

Fig. 4.11 - Induced current flow in a homogeneous halfspace with coils working in vertical dipole mode.

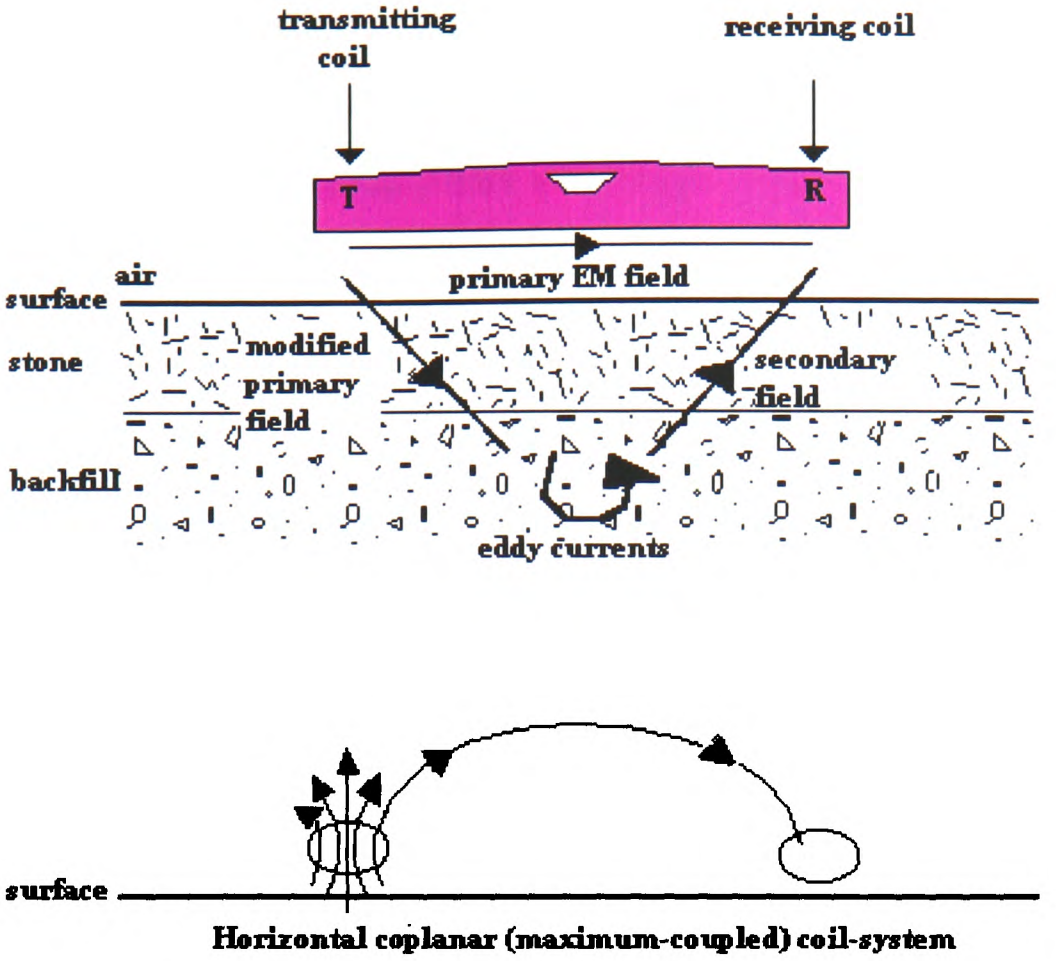

Fig. 4.12 - Conductivity instrument operating on the structure.

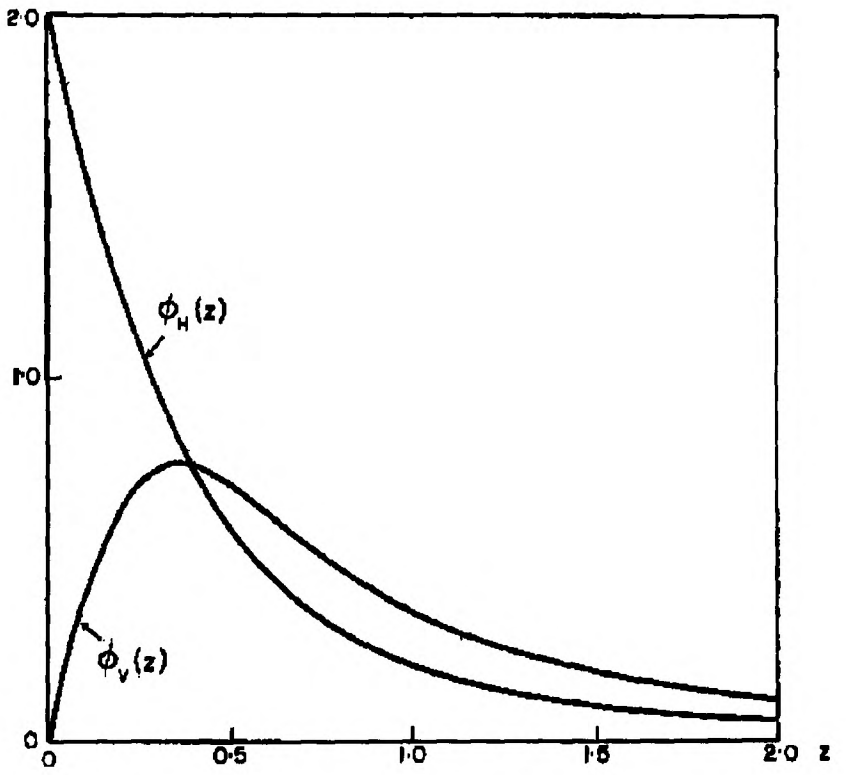

Fig. 4.13 - Comparison of relative responses for vertical and horizontal dipoles (McNeill, 1980b).

To analyse a layered section of earth it is possible to raise the instrument above the material surface, measuring the apparent conductivity as a function of instrument

height for both vertical and horizontal dipole configuration. This has the effect of shifting the response curve of fig. 4.13 upwards through the various regions of the structure and the variation of conductivity with height is therefore of diagnostic value in determining the nature (higher or lower conductivity and thickness) of any layering.

4.5 Discussion

The common characteristics of all these methods are:

(1) Most of the methods were originally developed for purposes other than structural testing.

(2) Highly sophisticated equipment is available commercially.

(3) The instruments come with a wide range of capabilities, a large part of which could be inappropriate for any particular application.

(4) Most equipment is portable, and the tests can be carried out quickly and conveniently without much disruption to traffic.

The general principles of the electromagnetic methods employed in this research work - radar, sonic and conductivity - are that:

(1) Radar will propagate through most materials, including air, but not metals; however it is rapidly attenuated in saline conditions and in clays.

(2) Sonics will propagate through most materials including metals, but not air.

(3) The conductivity technique is essentially a high powered metal detector and will identify changes in ground conductivity. Shallow metal would shield deeper penetration due to its high conductivity.

The crucial aspect of a radar survey is the interpretation of the data. The plots can appear very complex and their interpretation depends on many factors. Significant sub-surface features will appear as abstract forms on the output trace and their detection may be difficult. Objects such as pipes and ducts however are easily identified due to significant changes in dielectric constant. Frequently, sophisticated signal processing is required when the data present high noise levels or complex signatures. Yet signal processing does not always improve the results significantly and

is thus not always justifiable. Penetration depth with radar is conditioned by material conductivity and frequency used. Radar techniques have found a variety of applications within civil engineering and a few were reviewed.

Sonic testing has been proved to be a successful technique in a number of applications in different fields. While advantages over other (higher frequency) techniques are clear (primarily the reduced problems with attenuation typical of sonic waves allow for velocity to be measured over longer distances), limitations do exist: some specific to the method, other typical of applications to masonry structures. For example, repeatability of the test results at each point is dependent on variations in the amplitude and time duration of impact of the hammer, and higher variations in wave velocity are typical of shorter transit distances. Sonic wave velocity tests however show less scatter of measured data (due to their longer wavelength) than ultrasonic tests.

It is difficult to establish pulse velocity for unflawed sound masonry because variations in masonry material components have some effect on wave propagation. Direct comparison between two different masonry types is thus difficult to make and evaluation of the quality of the masonry can only be done in relative terms. Evaluation of the relative uniformity of a given masonry type can be effectively performed.

The biggest problem with traditional sonic testing is that the sensitivity needs to be improved so that the method is capable of detecting smaller defects or inhomogeneities. By measuring the local response, tomography overcomes this problem and although great care must be used in collecting and elaborating the data, results have been shown to be very encouraging for investigation of masonry elements. Therefore it was decided to investigate the possibility of applying the sonic tomography method to sections of masonry arch bridges which would include masonry walls and soil fill.

The concept of conductivity was discussed and some of the properties of soil and rocks that affect their conductivity were examined. Some values on typical terrain materials were reviewed. It was seen that a limitation of conductivity surveys is that the actual value of conductivity itself is seldom diagnostic: it does not reveal the specific type of soil or rock or pore water/salt content. It is the lateral or vertical variations which form the basis of any interpretation. Many parameters may affect the material conductivity, fortunately at any given location relatively few are usually dominant however the survey interpreter should be aware of the possible alternatives for a more accurate interpretation of the survey data.

4.6 Conclusions

The interpretation of the radar data is one of the most difficult tasks of this technique. The material conditions can strongly affect the success of the survey when they are characterised by high conductivity. The choice of antenna frequency is crucial and is often a compromise between penetration and resolution. The "right" antenna depends on the goals of the survey.

Radar is generally successful for the investigation of concrete structures and is believed to have potential in the investigation of masonry. Its application in this field is very recent and at an experimental stage. Therefore there is a great need for collecting data on masonry structures and verifying the efficacy of the technique on structures of this type.

Sonics are a consolidated method for the evaluation of civil structures and numerous applications have been successful in qualifying the state of masonry elements and structures, and in verifying intervents of repair. Tomographic applications combine the advantages of traditional sonic testing and offer the advantage that large areas can be evaluated easily. The internal condition of the structure is revealed by local information across the section.

Great care is required in performing the tests and collecting the data: factors like choice of the number and position of the reading stations, raypath coverage across the section, raypath incidence angle and length, number of ray paths and back readings can greatly affect the final result of the inversion. The same attention must be paid to choosing the transit times during processing of the data. Knowledge of factors which may affect the pulse velocity is required to smooth the data prior to data inversion.

Conductivity is usually determined by one of more of the following parameters: clay content, moisture content, moisture salinity, temperature. Of these the most complex is usually the moisture profile which is affected by the material type and its compaction/porosity, and seasonal variations.

The technique allows for lateral variations of conductivity to be accurately measured. Simple multi-layered conductivity surveys are also possible by raising the instrument above the material/ structure surface. The maximum depth of exploration is limited by the coil spacing. The values of conductivity, directly read on the instrument, are a function of the frequency used and coil spacing. Furthermore, the figures do not represent the conductivity at any particular depth, rather the value is a function of all the matter between the face of the instrument and the maximum depth of exploration.

A ground conductivity survey does not supply quantitative information, however the technique is quick and its cost efficiency is high. It is a technique which should be considered for providing non quantitative data prior to drilling or for providing additional information between boreholes.

CHAPTER 5

FIELD TESTING OF BRIDGES

5.1 Introduction

A large proportion of the bridge stock in the United Kingdom consists of masonry arch bridges of various forms. This will continue to be the case for a long time to come since, the vast majority of these bridges are still in perfectly serviceable condition. This means that periodic assessment of their load carrying capacity will remain an essential part of the bridge authorities' management activities for the foreseeable future. The outcome of these assessments can be very significant in terms of resulting financial and logistical burdens for the authorities. It is therefore in their interest to seek, wherever possible, improvements in the methods of assessment.

Under the sponsorship of the Department of Transport/Highways Agency and other bridge authorities, considerable efforts have been made in recent years to develop numerical methods for predicting the collapse strength of masonry arch bridges. A number of newly developed methods were then tested against the results obtained from full-scale tests. A comparative summary of the findings were given in BA 16/93 (Department of Transport, 1993b), and also by Das (Das, 1993). The overall lessons learnt from the developments so far can be summarised as follows.

5.2 Findings from large scale bridge research

In principle, the structural system of an arch bridge, composed of a number of elements (i.e. the foundations, the barrel and the surrounding fill) can be conveniently analysed using advanced numerical methods of analysis, such as the finite element method. However, in practice, the accuracy of the results becomes questionable due to a multitude of complexities inherent in an arch bridge. These are:-

(i) For the sake of computational practicality, the analyses are usually carried out with simplified methods, e.g. the two-dimensional analysis, or the mechanism method. These methods by necessity bring in added approximations which make the structural idealisation somewhat remote from reality.

(ii) Soil structure interaction is a major problem in analysing the behaviour of even new structures; for these old bridges involving surrounding materials of unknown properties, this becomes a major problem. For anything but the flattest arches, soil support characteristics significantly influence the load carrying capacity. For all sophisticated assessment methods, the soil resistance parameters have to be input, and the means of estimating these values are very approximate.

(iii) As most of the arch bridges do not usually have any reliable records of construction or repair details, it is difficult to determine the physical dimensions of the main structural elements, or the presence or otherwise of additional features such as the haunching at supports, saddling over the barrel or internal spandrel walls and ribs. Many unsuspected examples of such features, including voids that have been subsequently filled, have come to light following demolition - Fig. 5.1. Because of the difficulty in identifying these features, idealisation of old arch bridges can never be fully satisfactory.

(iv) In most cases, the quality of the structural materials and condition of the structural elements cannot be determined or idealised with any precision.

In the presence of the factors referred to above, the computational precision of the analytical assessment methods largely becomes uncertain. The results from these programs cannot be relied upon to give a definitive indication of the capacity of a bridge, since these analyses are dependent upon the dimensional input data and those relating to the soil parameters which cannot be determined with precision or consistency.

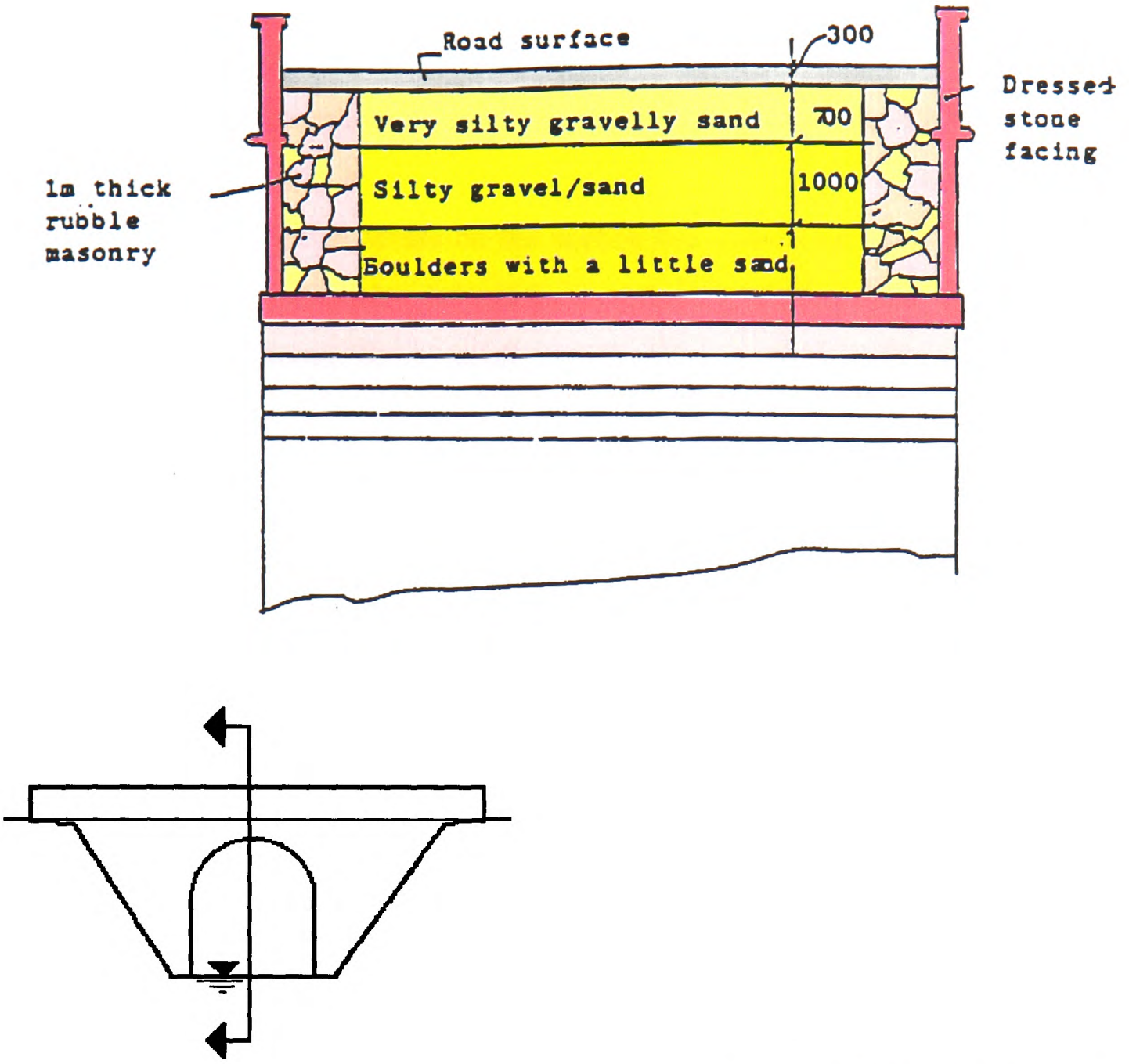

Fig. 5.1 - Sections of bridges revealed at demolition.

5.3 The way forward in Bridge Assessment

It is becoming increasingly clear that results from any calculation based arch assessment method may have to be viewed as giving only a qualitative assessment of capacity, and in order to decide on the appropriate action, one may have to rely on additional, perhaps qualitative, information obtained by other means. Thus, if an arch bridge fails assessment by a small margin, it is not showing any significant deterioration, and it is suspected that additional structural features such as internal ribs are present within the fill, then it may be reasonable to consider the bridge to be satisfactory for the time being. In such situations, NDT methods such as radar, sonic, vibration and/or conductivity techniques may provide a relatively quick and inexpensive means for making a qualitative judgement on the likelihood of a bridge having any additional reserves of strength. NDT methods can also be used for monitoring material deterioration or development of faults, either by directly identifying the faults, or by recording changes in the characteristics of the bridge.

5.4 Present needs for monitoring

In order for the bridge authorities to use the methods described in the previous chapter with confidence, the following aspects need to be addressed:

(1) Trials

The methods need to be applied, on a trial basis, to a variety of bridge types and situations in order to identify the scope for useful application.

(2) Specification of Equipment and Procedures

Based on the trial applications, specifications for use on particular bridges and problems, including the specification of equipment, the procedures to be followed for the testing, and the expertise required of the personnel to be involved should be established.

(3) Presentation of Results and Verification

Criteria should be developed so that the testing bodies can follow certain common standards for reporting the results. Also guidance should be provided so that non-specialist assessing engineers and clients can verify their accuracy.

(4) Testing of Full Scale Structures

Even though it may seem more convenient to reproduce in the laboratory the site situations and to test in ideal conditions, it is often difficult to scale experiments and this is particularly true for NDT because of the nature of the methods used. So whilst it is possible to scale load testing, it is nearly impossible to recreate in a laboratory the conditions which would make the use of 100 MHz antennae on site ideal. Initial attention was therefore focused on full scale structures.

5.5 Other purposes of site testing

Two structures were chosen for site investigation and selected on the basis of their accessibility and overall characteristics and dimensions: Middleton Bridge, in Lothian, and Kilbucho Bridge, in the Borders, both in Scotland.

Reasons for testing included:

1) verify previous NDT survey - in the case of Middleton Bridge -. Sonic tests had been performed on the East abutment/wing walls of the bridge (Forde & Batchelor, 1984; Forde *et al.,* 1985) and any new test would not only have provided a chance to monitor the structure after maintenance work but also permitted comparison of the outcome of the structural evaluation obtained through different NDT techniques and through sonic tests applied in different modes.

2) verify digital NDT techniques. A study of the performance of the NDT method used would consider the effectiveness of the testing method as a function of the site conditions in order to identify requirements for useful applications.

3) innovative NDT. The characteristic of a research driven project was the ideal environment for innovative applications of established testing methods (radar application on masonry bridges), novel engineering applications (conductivity survey) and new testing procedures (tomography).

4) data imaging. The imaging of the processed data and visualisation of the survey results was considered of primary importance in the use and spread of

the NDT techniques. A cross-sectional representation of the structure investigated was obtained through the application of tomographic techniques.

5.6 Field work

North Middleton Bridge and Kilbucho Bridge are both stone masonry arch bridges located in Scotland (fig. 5.2).

North Middleton Bridge is a twin span arch with each arch spanning 3.7m and the width of the bridge being just over 8 m (fig. 5.3). Non-destructive investigation surveys were undertaken on the East abutment and wing walls and consisted of radar sonic and conductivity tests.

Kilbucho Bridge is a single span low rise skew brick arch with stone spandrel walls (fig. 5.4). The overall width of the bridge is 5.1 m and the segmental arch spans 3.56 m with a span to rise ratio of 3. The stone parapets are 1.1 m high and 0.3 m thick. The multi-ring brick arch barrel is 0.36 m apparent thickness; and the fill is 0.3 m thick at the crown, including the black-top road surface, giving a total thickness of approximately 0.66 m from the road to the intrados of the arch at the crown. Radar tests were performed along the road and arch intrados, and on the upstream parapet and spandrel wall.

5.7 Middleton Bridge

5.7.1 Radar Survey

A wide range of antennae was available for investigation of the structure, from 100 MHz to 1 GHz frequency. They were used with different intentions and in different configurations to investigate the internal structure of the bridge: specifically the condition of the bridge backfill material, the thickness and condition of the stone spandrel walls.

a) Scotland

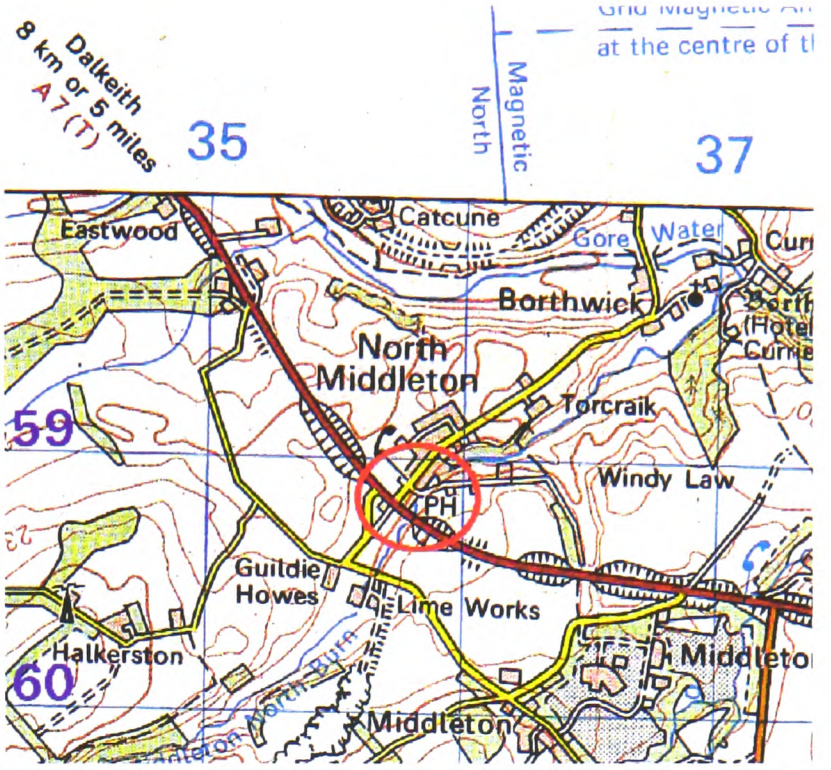

b) North Middleton Bridge (OS 73, 1993)

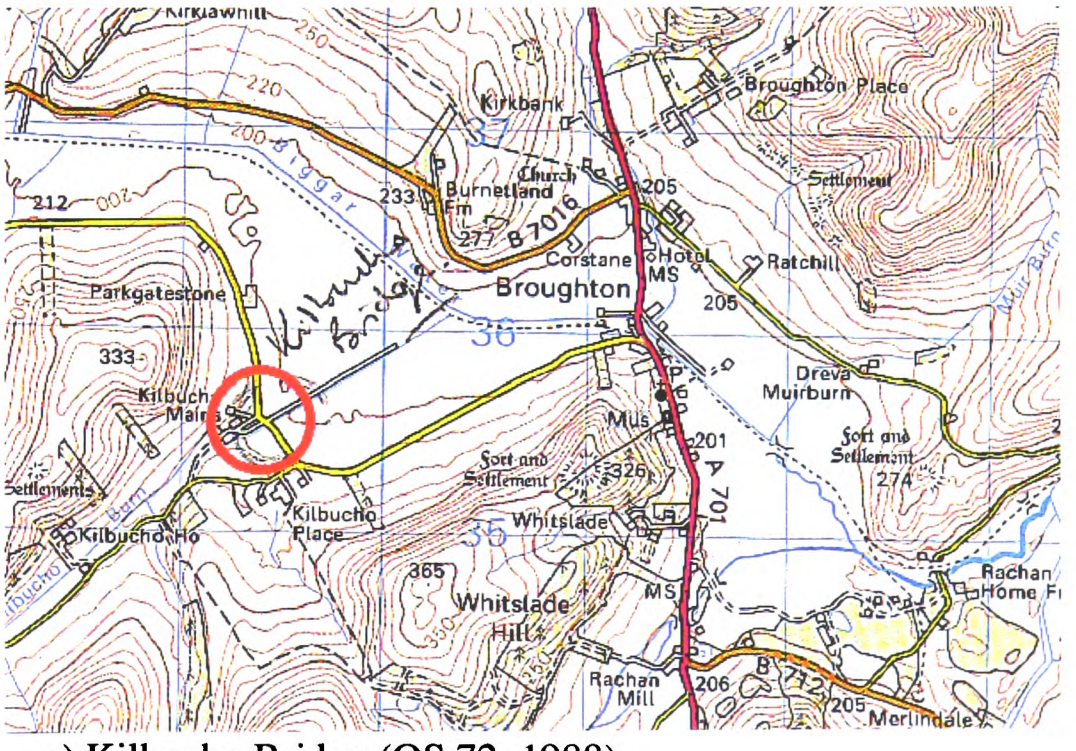

c) Kilbucho Bridge (OS 72, 1988)

Fig. 5.2 - Location of the bridges investigated (published by permission of the Ordnance Survey).

a) White line marks level of radar tomography as from figure 5.5.

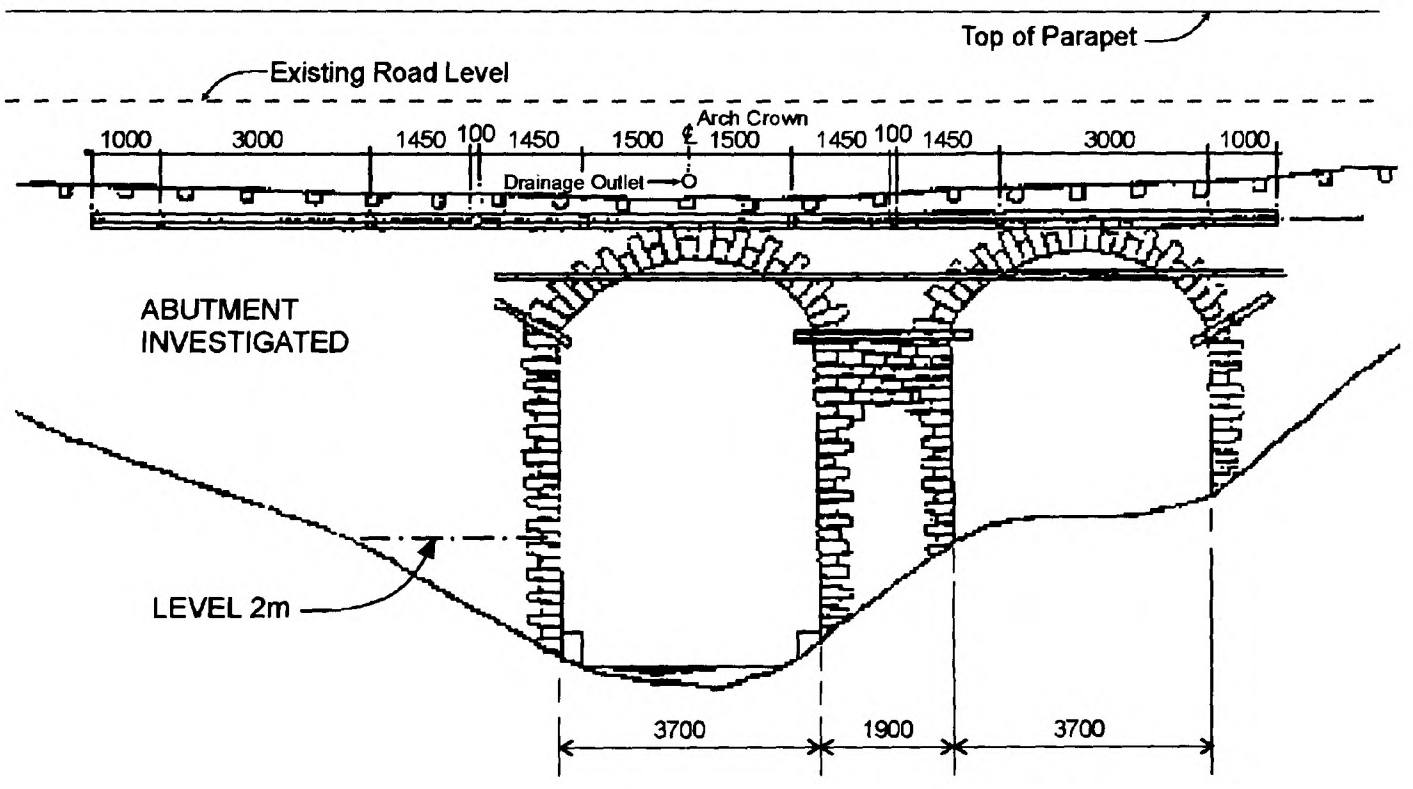

b) Main dimensions and wing wall where tests were performed.

Fig. 5.3 - North Middleton Bridge, downstream view.

a) Downstream view.

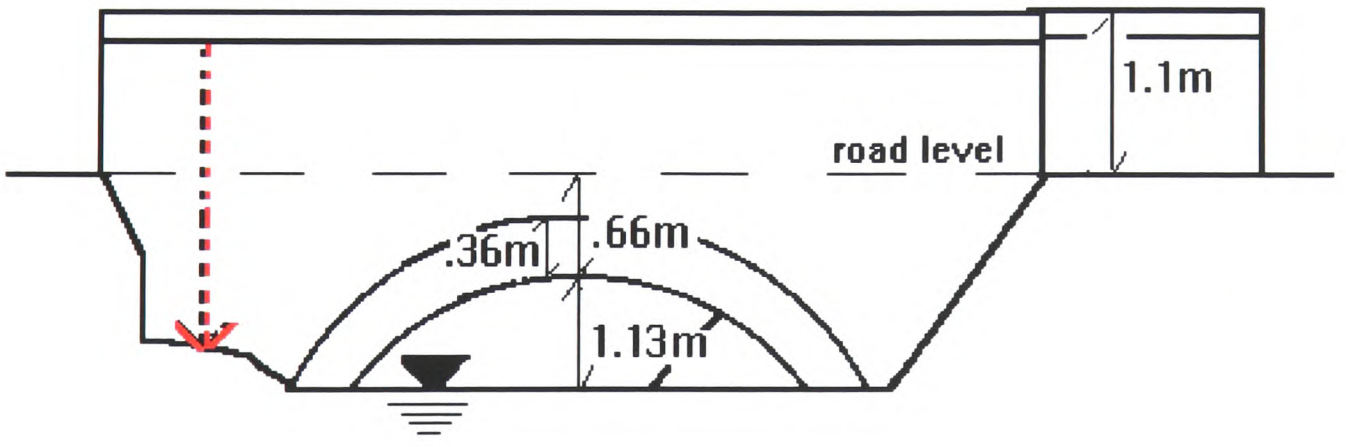

b) Upstream elevation (dotted vertical line marks position of radar test in fig. 5.22).

Fig. 5.4 - Kilbucho Bridge

In general high frequency antennae give good spatial resolution but give only shallow penetration as the signal becomes rapidly attenuated and may suffer from clutter (Padaratz & Forde, 1995a & 1995b). In this project, high frequency antennae were used for the identification of masonry wall thickness and near-surface voids /defects. Lower frequency antennae are better suited to penetrate deeper into the abutment as they emit more powerful signals, but their longer wave length is a detriment to spatial resolution. Also, targets of "small dimensions" or "small thicknesses" can be missed. Given equations (4.13) and (4.18) for velocity and wavelength respectively, and assuming the achievable resolution to be $\lambda/2$, then the resolution of the antennae used in this research project were:

Material	**Antenna Frequency (MHz)**					
	100	500	900	100	500	900
	Wavelength (m)			**Resolution (m)**		
Air ($\varepsilon = 1$)	3.00	0.60	0.33	1.50	0.30	0.16
Wet sandstone ($\varepsilon = 6$)	0.87	0.17	0.10	0.43	0.085	0.05
Wet clayey soil ($\varepsilon = 15$)	0.77	0.15	0.09	0.38	0.075	0.045

Table 5.1 - Antenna resolution

During the radar tests, the antennae were moved along vertical and horizontal survey lines on the vertical surfaces of the East abutment and wing walls. The survey had to overcome a few practical difficulties due to the construction of the bridge and the rough surface of the stone masonry work. Scaffolding was not available and the antennae were lowered vertically with ropes from the top of the parapet, or manually moved horizontally across both the upstream and downstream sides of the bridge. The problem encountered when the antenna is not constantly and completely in contact with the surface to be investigated is that the air gaps left between antenna and

structure (because of uneven surface) generates a strong interface and cause reflection in the signal. This reflection merges with the emitted pulse and the reflection from the real structure surface: therefore the recorded signal becomes difficult to interpret. Moreover, because of the reflection at the air gap, the power of the signal propagating through the structure is diminished. However this is not too problematic provided that the separation does not exceed $\lambda/10$ (Davidson and Forde, 1996).

In the case of this structure, it was not possible to scan through the bridge in the reflection mode, even when using a 100 MHz antenna. The reasons were: the significant width the radar signals had to travel through (over 8 metres) and the dielectric properties of the filling materials behind the stone walls. When the radar equipment is operated in reflection mode, the radar signal has to travel twice the distance from the antenna to the target. Signals are propagated into the structure and their reflections at different interfaces are picked up by a receiving device located - in the same or different antenna - on the same side of the structure.

In view of the above, radar tomography was undertaken in the transmission mode by using two 100 MHz antennae positioned on opposite sides of the bridge. The transmitter, on the downstream east wing wall was moved along the white dashed line shown in fig. 5.3a, in the direction shown by the arrow, while the receiver was stationary, at the same level, on the upstream wing wall. The survey was repeated a number of times with the same movement procedure for the transmitter, whilst the receiver moved along in 1m steps to obtain an adequate coverage of the bridge section (fig. 5.5). Due to the slope of the river bank on the upstream side, movement of the receiver was limited. The tomographic survey procedure enables one to record travel time maps of the section investigated and therefore localise defects and inhomogeneities in the structure.

This antennae configuration, maintaining one antenna stationary whilst the other is moved, offers the advantage that accurate readings can be recorded. In fact, only the movement of one antenna needs to be controlled and its position can be monitored

accurately by marking the radar plots at regular intervals of distance travelled by the transmitter or by attaching a survey wheel to the moving antenna. In the case of parallel tomography (see section 5.7.2) both antennae need to be dragged at exactly the same velocity to maintain them in a constant facing position so that accurate measurements of the travel time can be recorded. This can introduce a small timing errors if the survey is not carried out with precision.

5.7.1.1 Radar tomography

Tomography measurements aim to localise the presence of defects and inhomogeneities by indirectly mapping the variation of the velocity in the materials investigated or the signal attenuation due to the dielectric properties of the materials crossed and the number of interfaces encountered. This is obtained by plotting the distribution of EM velocity or the amplitude of the received signal.

The tomographic technique involves the use of a transmitter and a receiver positioned on opposite sides of the structure and moved in a series of possible combinations to obtain time domain maps of the same cross section of the structure. From the elaboration of these scans, local variations of dielectric constant may be identified and related to engineering features/defects of the structure.

Figure 5.6 shows the section coverage obtainable with a single tomographic scan of the structure. The situation depicted in (a) is the most widely used in radar tomography and the most recommendable since the angle of the paths connecting transmitter and receiver gives rise to better location and resolution of anomalies at the inversion imaging stage. Usually the survey with this antennae configuration is repeated a number of times with the receiver moving in discrete steps in the same direction of movement as the transmitter. The survey stops when a satisfactory coverage of the section area has been achieved. Ideally a combination of surveys (a) and (b) should be performed. Case (b) gives a complete cover of the section area,

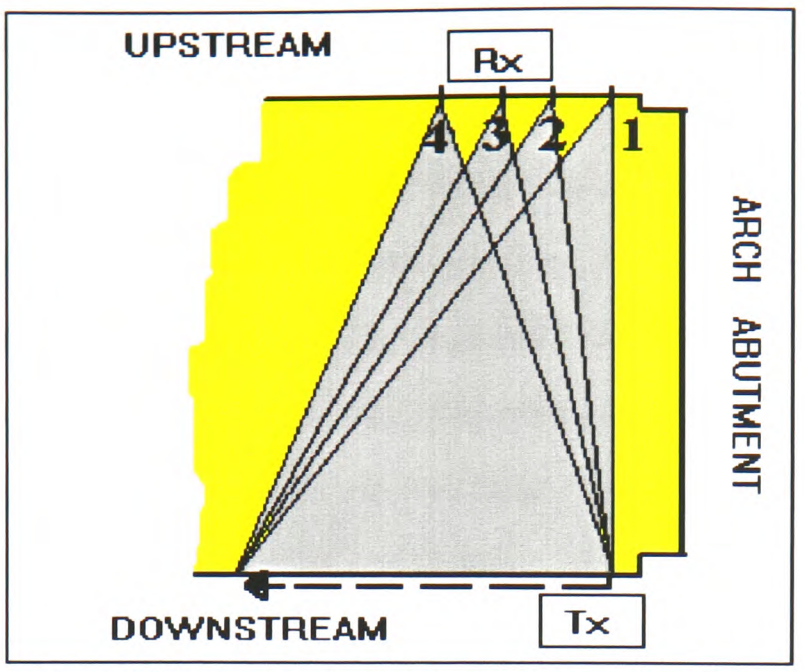

Fig. 5.5 - Middleton Bridge: horizontal section showing coverage of radar tomography (see also fig. 5.3).

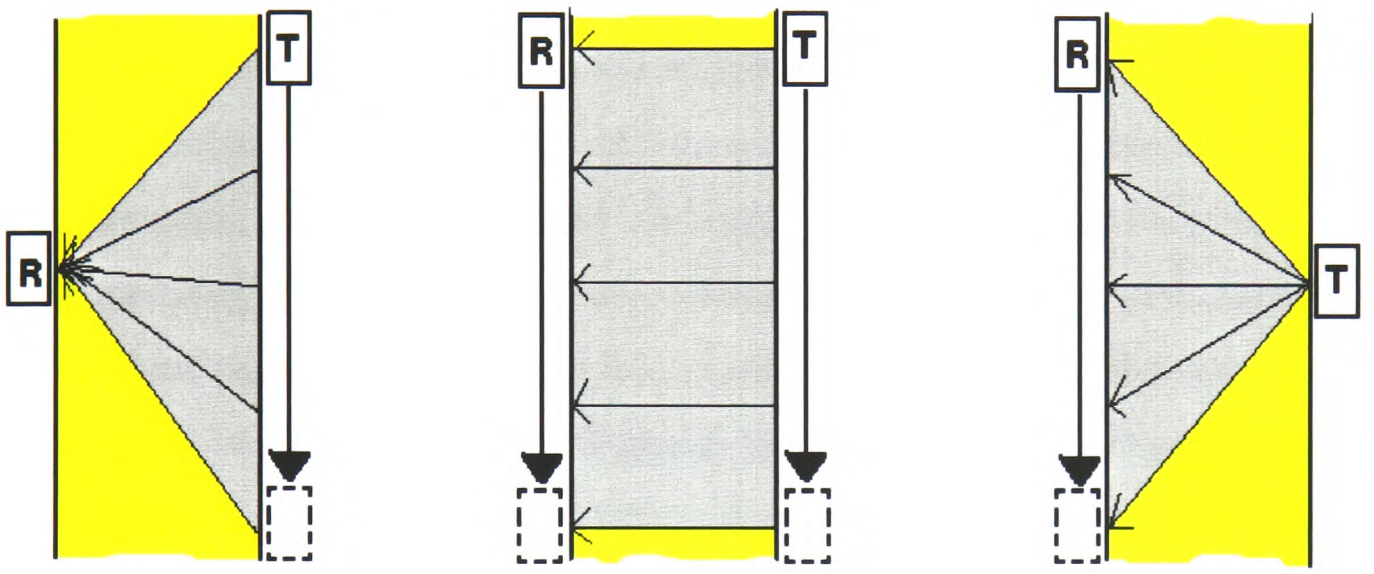

Fig. 5.6 - Section coverage obtainable with a single tomographic scanning of the structure: a) transmitting antenna (T) scans while receiver (R) is stationary; b) both antennae move in parallel; c) stationary transmitter and mobile receiver.

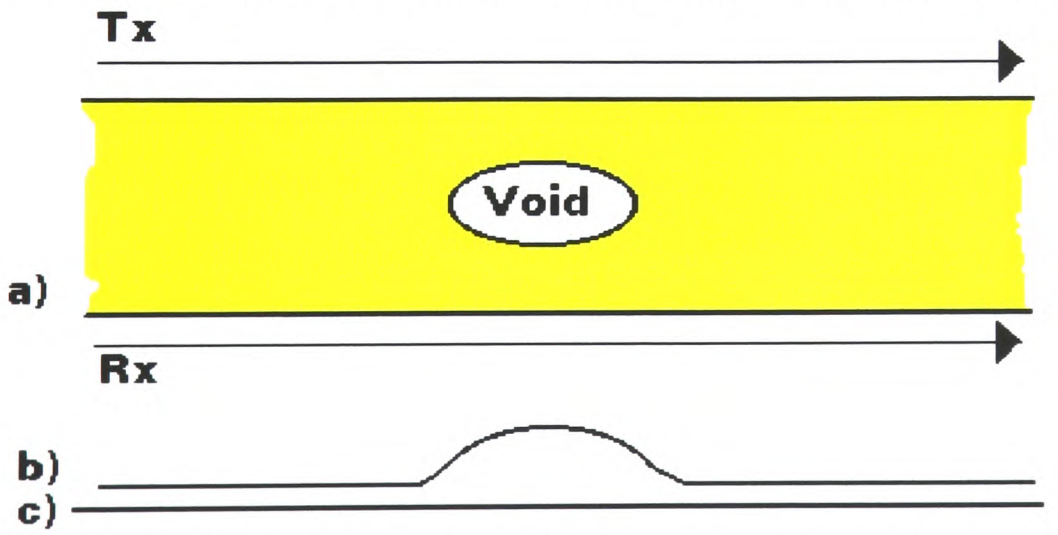

Fig. 5.7 - Representation of arrival time for the case of fig. 5.6b and the presence of an air void: a) plan view; b) shorter time in correspondence of the air void; c) arrival time in the case of homogeneous section.

however because of the direction of direct propagation of the 'first arriving' signal the data obtained will locate the presence of the anomaly but will not resolve its time/depth position. The consequence of this is poor vertical resolution. The problem is made more challenging by the shifting of the zero position of the radar signal along the time axis when the antenna is coupled to the material (and because of imperfect radar systems). This instability of the zero time will affect tomography readings in general and parallel readings as in situation (b) in particular. Better results are obtained when combinations of case (b) with (a) or (c) are used.

Just as in sonic tomography (Colla *et al.*, 1996), radar tomography is undertaken by measuring the time taken by an impulse to transmit through the structure. In contrast to the sonic waves which tend to travel through the denser material - via paths rarely straight because of the inhomogeneities present - the radar signal velocity will be higher when travelling across highly porous dry materials, with the highest velocity registered when travelling in air (0.3 m/ns). The radar plots will register shorter arrival times of the received signal when the wave has travelled at higher speed through an air filled void. Fig. 5.7b represent the arrival time at the receiver: if the section is homogeneous and constant in width, the arrival time will be constant, but if a void is present, a shorter time will be recorded at that location. Time variations associated with significant voids will be sudden but variations of the order of 10 or 20 % may indicate scattering (McCavitt & Forde, 1991) or clutter problems (Annan, 1995). At the same time, the dielectric properties of the materials in the structure will have affected the wave energy and the received signal amplitude will be modified. Both arrival times and signal amplitudes of the single ray paths can be used as input parameters in the tomographic inversion. An image is built up by an iterative process, where velocities through the various materials or signal magnitude are mapped in a cross-sectional representation related to material properties (primarily dielectric constant and conductivity). Voids, defects and other features may be located in this way. One of the advantages of using radar for tomography is the possibility of continuous data reading which makes the survey much faster than when performing conventional sonic tomography. For the same reason, continuous movement of the antenna is

recommended and preferably over stepped movements when conducting parallel tomography (fig. 5.6b).

5.7.1.2 Radar imaging

The primary finding from this radar survey were a generally low velocity of the EM signal which indicates the values of the dielectric constant within the bridge to be significantly different from the values expected for construction or fill materials. The average value for the dielectric constant (ε_r) for the composite bridge construction [masonry/soil fill/masonry] was computed through use of the simplified expression for E.M. velocity (equation 4.13) and found to be approximately 56. This value is well above reference values published in the literature and could be explained by a high moisture content in the fill, due to possible moisture-drainage problems in the bridge as highlighted by the conductivity survey carried out and discussed in section 5.7.3. The high water content in the bridge materials associated with salt in the water would increase both permittivity and conductivity (refer to section 4.4 for a more detailed interpretation of the conductivity phenomena) so explaining the low velocity measured and the high dielectric constant value calculated. However, equation (4.13), which is valid for low loss materials, does not take conductivity into account. At high values of conductivity and low frequency of the antenna, as might be the case of this structure, the material would behave as a conductor (see section 4.2.2) and therefore equation (4.12) would need to be used instead. Indeed, by calculating the loss factor from equation (4.4) with $\varepsilon = 56$, $\sigma = 150$ mS/m and $f = 100$ MHz,

$\tan \delta = 0.48$

is obtained. For values of $\tan\delta > 1$ the material behave as a conductor. This point will be returned upon later.

The time domain plots obtained from radar tomographic investigation, are of the kind shown in figures 5.8 and 5.9, which are raw data where the first arrival travel times are recorded at the receiver location (upstream). Consider in fig. 5.8 the position of the receiver Rx in relation to the transmitter on the downstream side. As the EM

waves travel in straight lines the shortest ray paths and corresponding shortest travel times are to be expected when the transmitter reaches the position just opposite the receiver Rx - assuming that the material within the bridge is homogeneous. Similarly the received signal would show the maximum amplitude (brightest colours) at this location - its attenuation being minimum there - whilst at longer transmitter/receiver distances the signal would show greater attenuation. In fig. 5.8 this is true for the received signals to the right of the Rx position, but not to its left hand side. In fig. 5.9 the situation is even more complex: at a transmitter position between 0 and 1 m on the downstream side and a receiver position of 3.5 m on the upstream wall - the longest distance travelled by the signal - actually corresponds to the shortest travel time registered on the scan. Also, the attenuation of the signal is greater, compared with the case of fig. 5.8. This indicates inhomogeneous signal propagation characteristics and consequently varying wave velocity. If one assumes that the simplified equation for velocity is valid, then it can be postulated that the phenomena can be attributed to uneven dielectric constant values across the bridge section, with materials characterised by lower dielectric constants between 0 and 2.5 m through the section, than between 2.5 and 5 m. Since the attenuation of the received signal seems to follow the same trend seen for the velocity and it is particularly noticeable when the receiver is at location 3.5 m, it can be deduced that materials on the right hand side of the section are characterised by higher dielectric constants and also by higher conductivity values. The above assumptions based upon the simplified equation for EM wave velocity can be considered in the light of the general equation for EM wave velocity (4.12). This relationship between velocity, frequency and conductivity at a given value of ε_r, was plotted graphically (Padaratz & Forde, 1995a). Fig 5.10 illustrates a parametric analysis of the above equation for a material with $\varepsilon_r = 56$, at the variation of antenna frequency and material conductivity. In this survey, two 100 MHz frequency antennae were used and fig. 5.10 shows that, at these low frequencies, the velocity will decrease significantly with any increase in conductivity, as will the amplitude of the signal due to increased attenuation. Thus, it is possible that the dielectric constant across the bridge section has not actually changed

significantly - rather the reduction in velocity may result from the increase in conductivity.

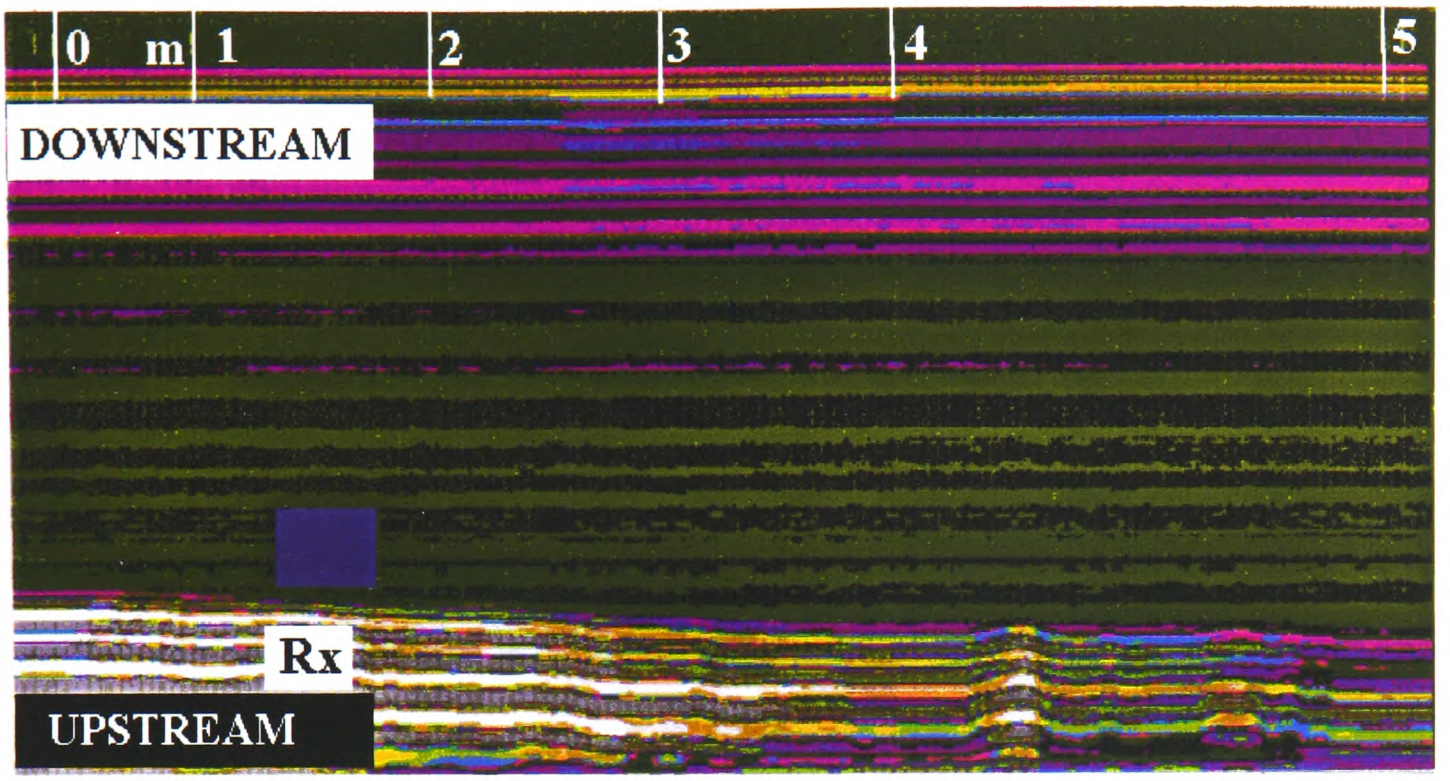

Fig 5.8 - Radar time section for tomographic survey: receiver at 1.5 m on upstream side (300 ns range).

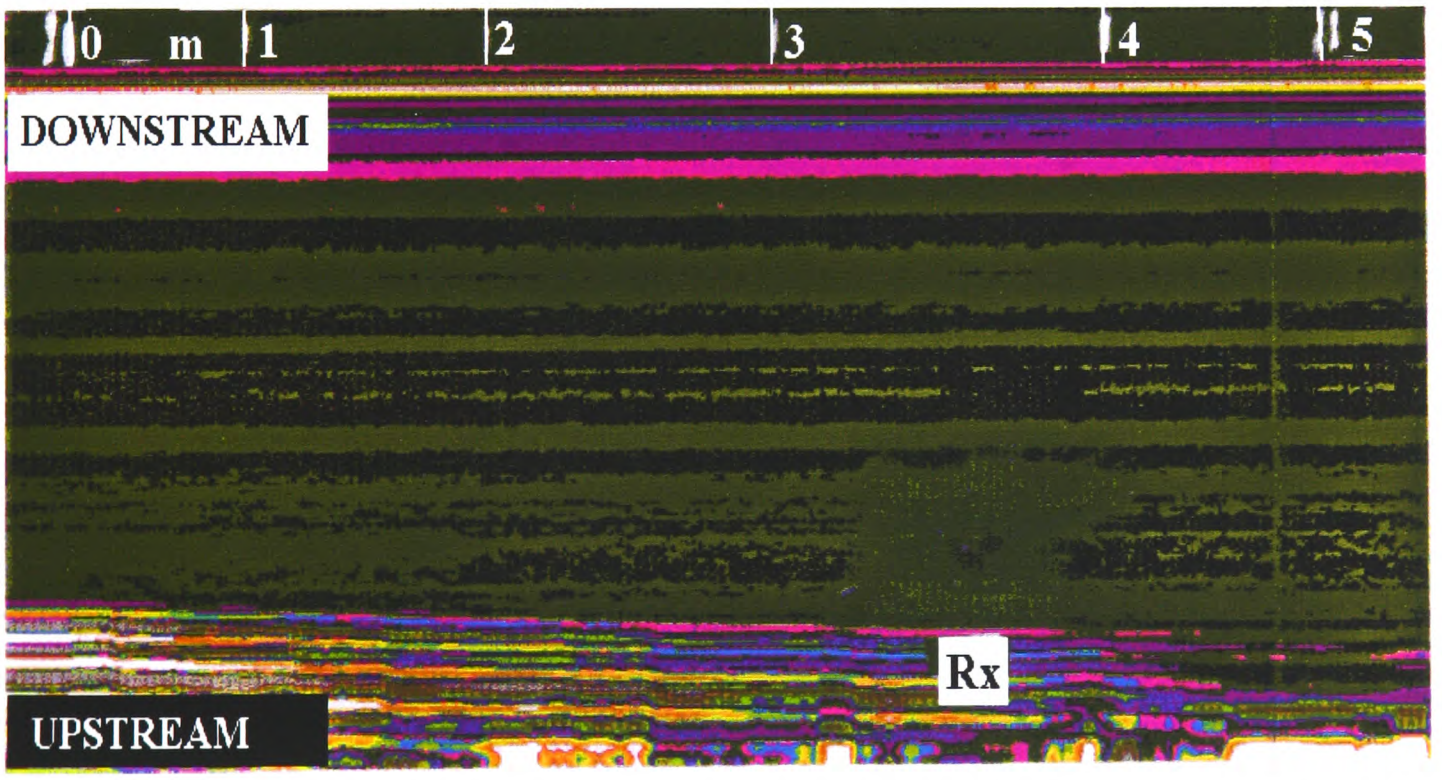

Fig 5.9 - Radar time section for tomographic survey: receiver at 3.5 m on upstream side (300 ns range).

Given the amount of data which can be recorded during tomographic radar surveys and which need to be processed to obtain tomographic maps of signal velocity and/or attenuation, data need handling through a network analyser for input in tomographic inversion and subsequent imaging of the structural composition and defect location.

5.7.2 Sonic Survey

Tests were carried out on the wing walls and abutment of the bridge - as from fig. 5.3b - using a modally tuned impact hammer, fitted with a force transducer, to excite the structure. An accelerometer was fixed to the wall to monitor the structure response waveforms. The hammer and accelerometer were connected to a multiple channel tape recorder, so that two simultaneous channels of data were recorded digitally on tape for post processing with dual channel signal analyser, B&K 2034 (see also Appendix B).

Readings were collected at a number of horizontal levels on the structure under investigation by marking a regular grid on the walls. At each level, measurement points were located on the three walls of abutment, downstream wing wall and upstream wingwall at 1 metre spacing. All points on the grid were alternatively used as transmitting and receiving stations, so to also allow collection of "back readings".

The waveforms obtained were analysed in the time domain. The time delay between the excitation given with the hammer and recorded on the first channel, and the reception of the hammer blow on the second channel, together with the distance between source and receiver, permitted calculation of the velocity of the sonic signal through the material. This value is dependant upon the quality of the material (in this case stone masonry and bridge soil fill) and can be used to rank the integrity of the structure.

5.7.2.1 Sonic tomography

At level 2 m of the grid (see fig. 5.3b), 15 stations were used for a total of 142 rays. Fig. 5.11 shows a cross section of the abutment with location of transmitters and

receivers (ray paths were assumed straight at the beginning of the tomographic reconstruction).

From the first data analysis outcome (Fig. 5.12) it is clear that high velocity areas are located along the walls corresponding with the stone masonry, while values of velocity between medium to low are situated towards the centre of the plot, indicating backfill materials.

Looking in more detail, along the upstream and especially downstream wall, very high velocity areas relate to a continuous homogeneous dense material which subsequent endoscopic investigations revealed to be cement grouted zones. By applying constraints to the model and re-iterating (Fig. 5.13), masonry thickness on the down stream side was calculated and found to be comparable with the one determined from the conductivity survey detailed below.

5.7.3 Conductivity Survey

The application of this digital conductivity meter is novel in the civil engineering field. The meter used - Geonics EM38 - has intercoil spacing of 1m and provides a maximum depth of exploration of 1.5 m in Vertical Dipole Mode (0.75 m in Horizontal Mode) operating at a frequency of 14.6 kHz. The lateral exploration of conductivity is approximately the same as the vertical depth.

The meter has been used on both the upstream and downstream sides of this 2-span bridge and on the wall beneath the main vault. The measurement stations followed a grid marked on the walls, in an area well clear of any evident metallic objects (drains, reinforcing beams). For maximum accuracy and good spatial resolution, measurements have been overlapped to have reading stations every half a meter. The lateral extent of the volume of structure whose conductivity is sensed, permits to accurately measure small changes in conductivity, for example of the order of 5% or 10%. Contacting and non-contacting - at 0.25, 0.5 and 0.75, 0.9 m distance from the wall -(Fig. 5.14a) conductivity measurements were taken, to obtain data at different depths inside the

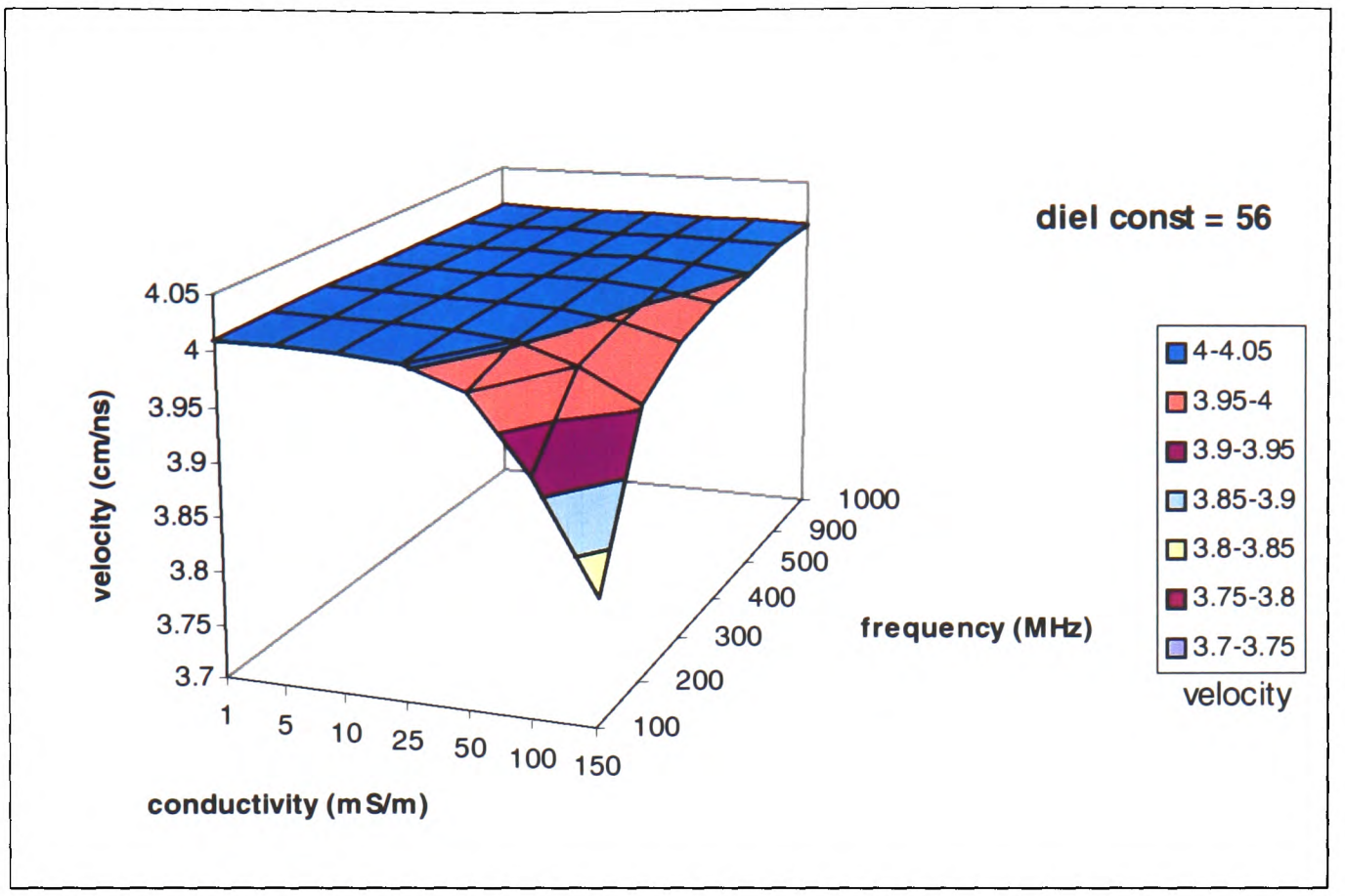

Fig. 5.10 - EM wave velocity for varying antenna frequency and increasing conductivity.

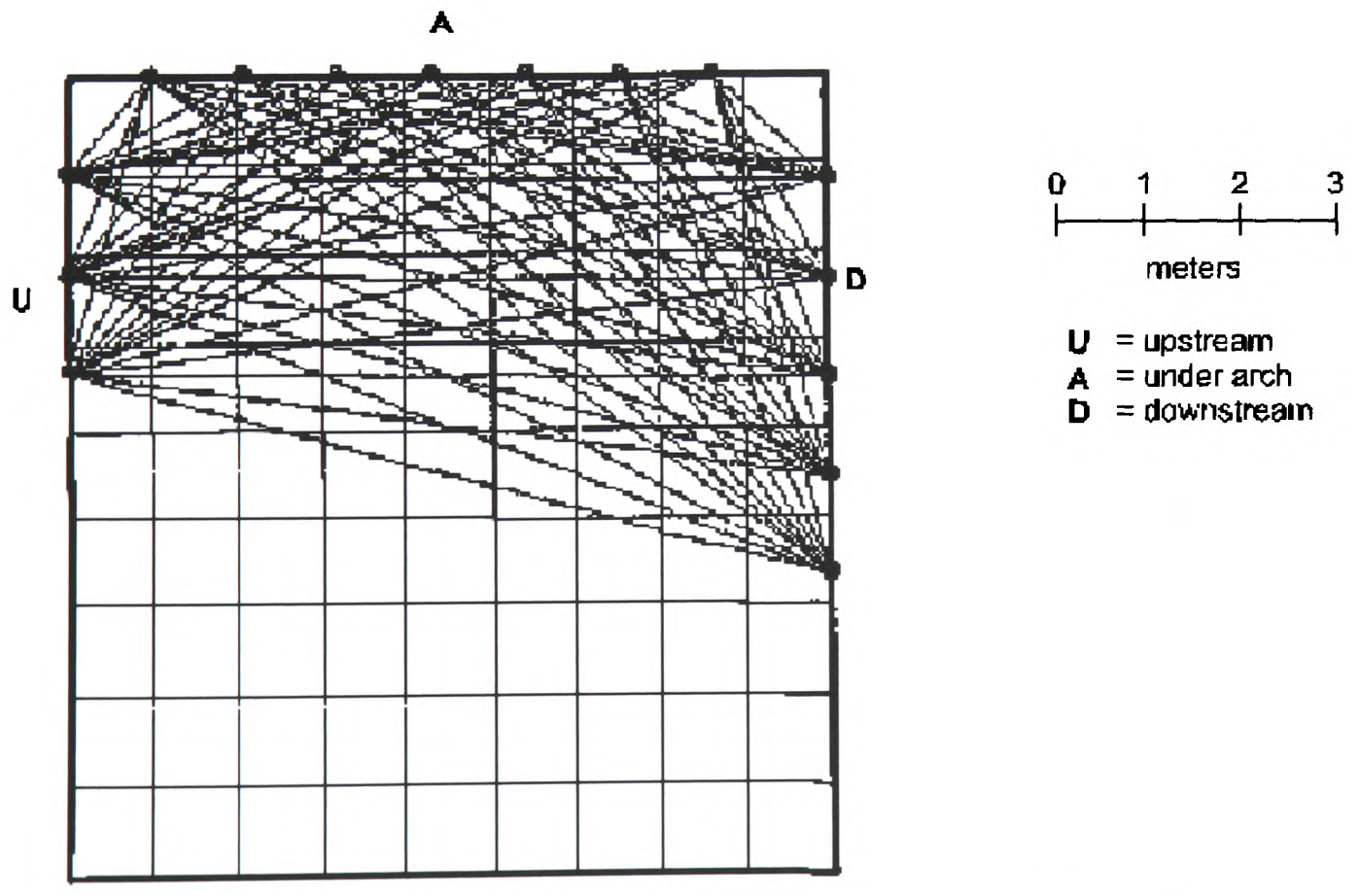

Fig. 5.11 - Middleton Bridge (2 m level): initial assumed density of sonic ray paths.

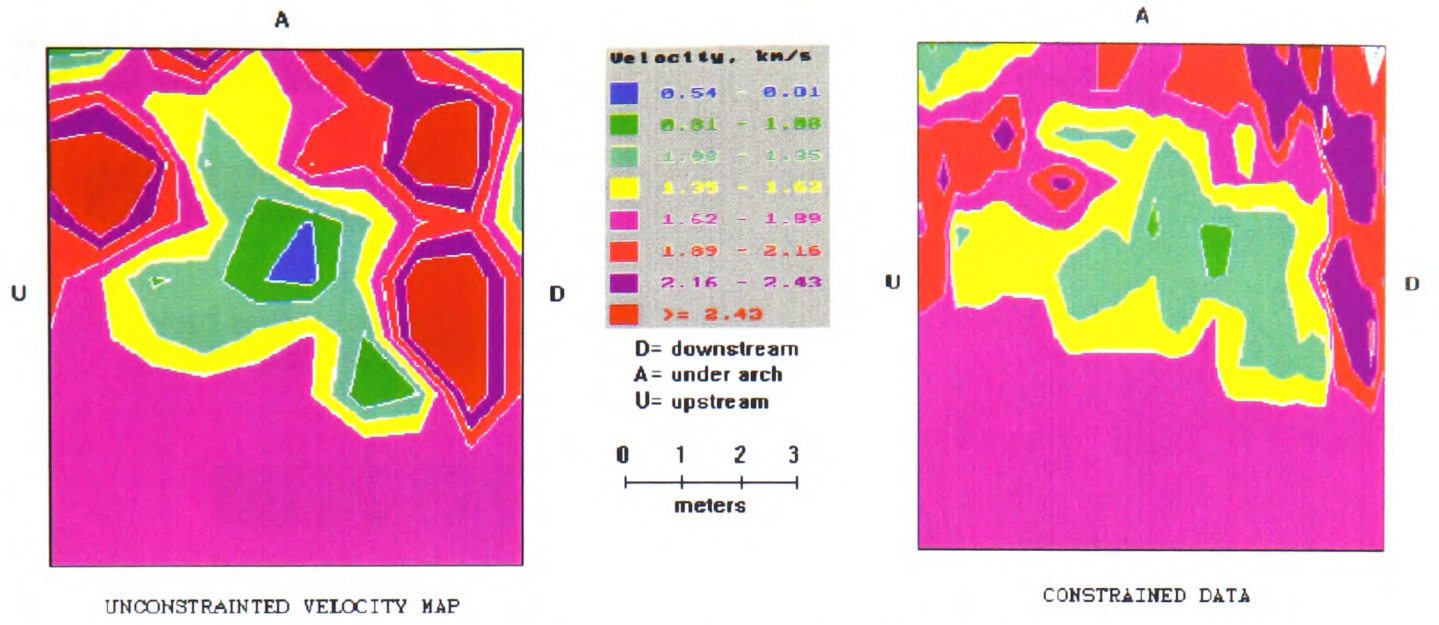

Sonic tomographic reconstruction

Fig. 5.12 - Sonic unconstrained data.

Fig. 5.13 - Sonic constrained data.

structure. Data were collected using a digital data recorder and later transferred to a PC (Fig. 5.14b).

The results have been plotted to produce contour maps of the conductivity distribution along horizontal and vertical planes within the structure. Fig. 5.15 is the plot of the conductivity data obtained on a vertical plane of the downstream side for depth up to 1.5 m from the wall surface. Figure. 5.17, instead, is a cross-sectional representation along a horizontal plane with the data iterated through tomographic software.

Data have been analysed with two different software packages and differences were noticed in the resolution of the resulting contour plots. In particular, the "geophysical" programme has given satisfactory results when mapping data collected along surfaces coplanar to the three abutment walls. The tomography programme has shown to be more accurate in the cross section elaborations, when data collected at different depths from the wall surface have been plotted together (see fig. 5.17 for comparison).

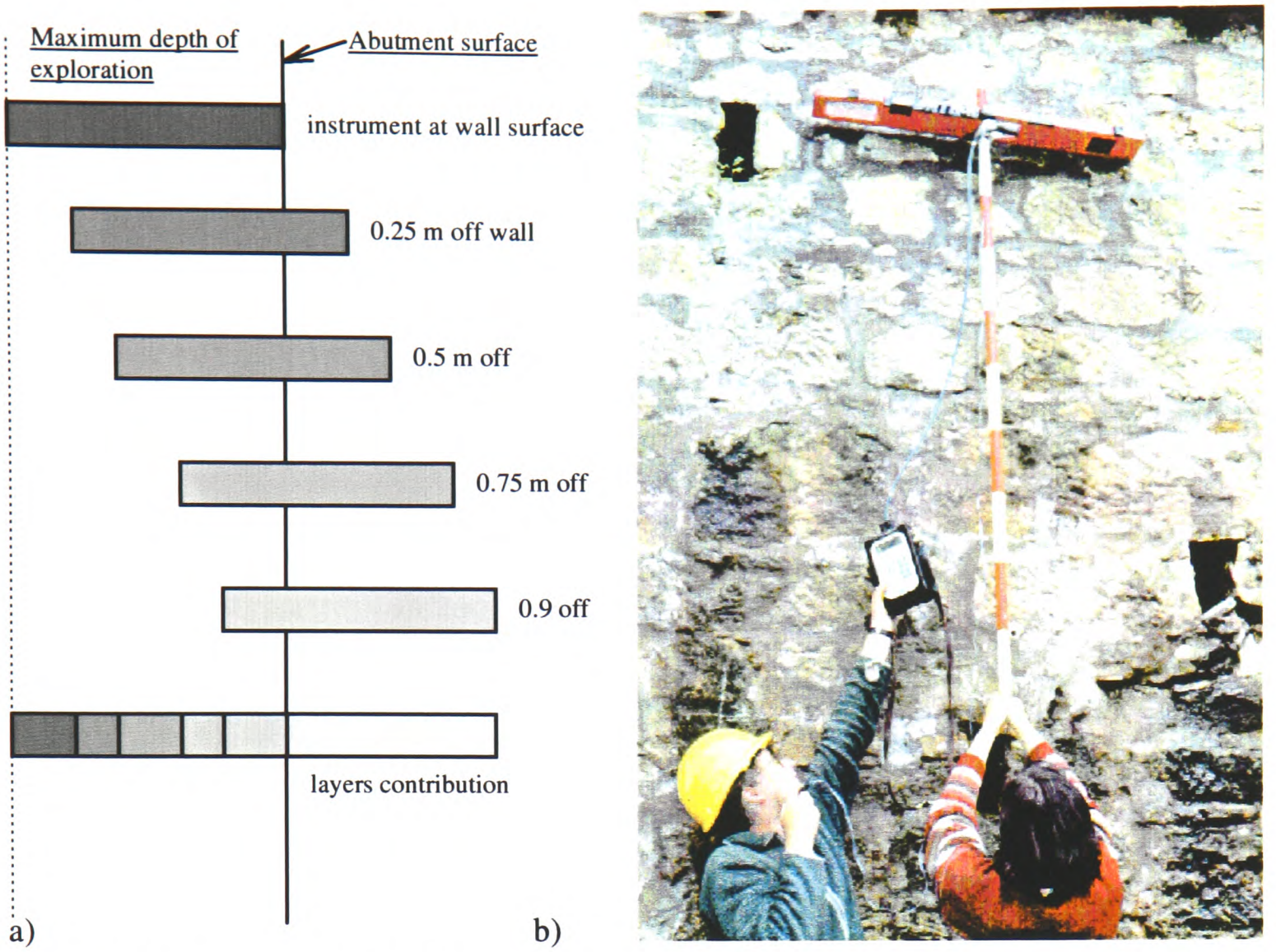

Fig. 5.14-In situ conductivity data collection: a)instrument lifting positions, b) in contact.

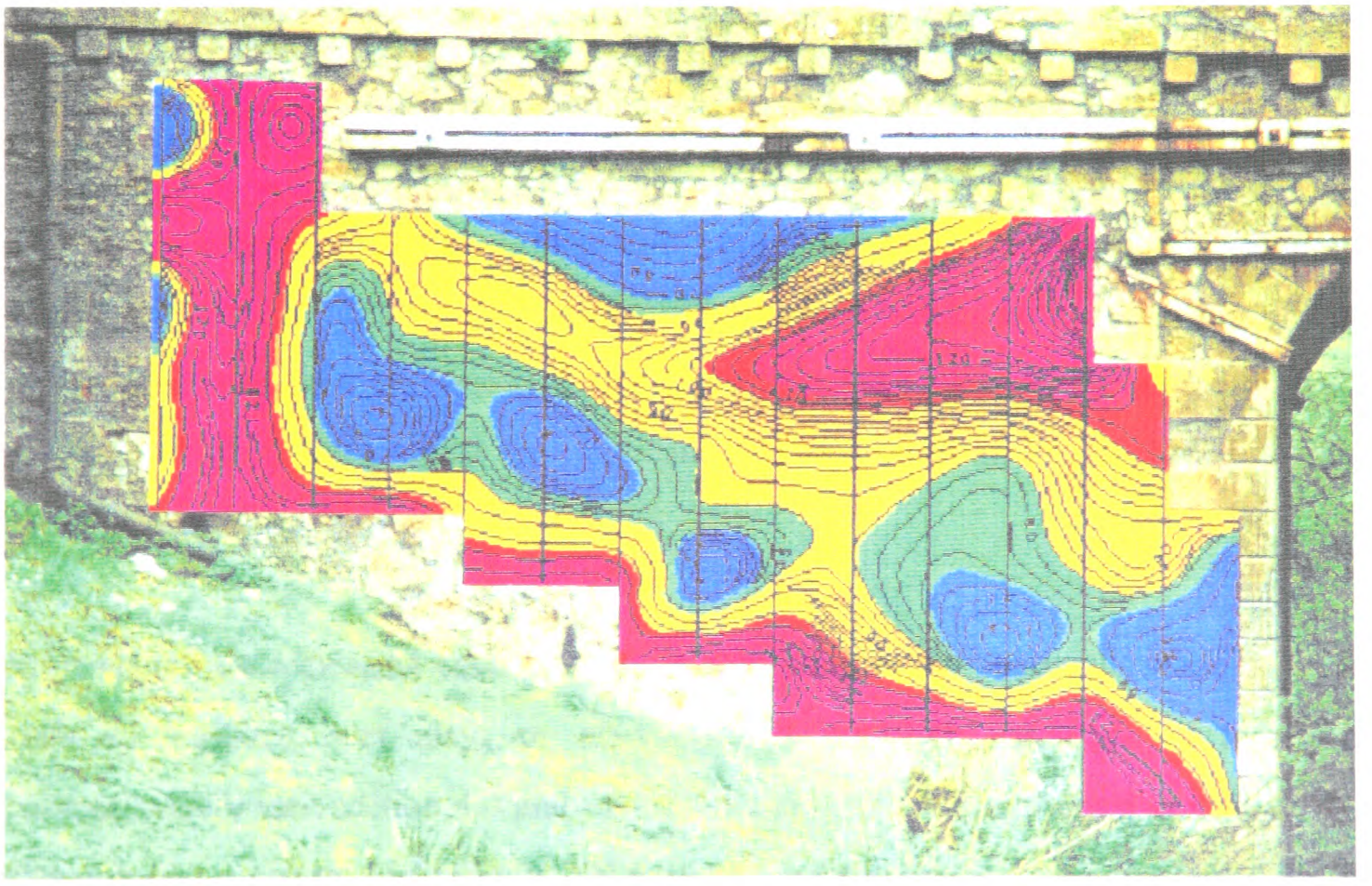

Fig. 5.15a - Conductivity distribution on downstream side up to 1.5 m depth

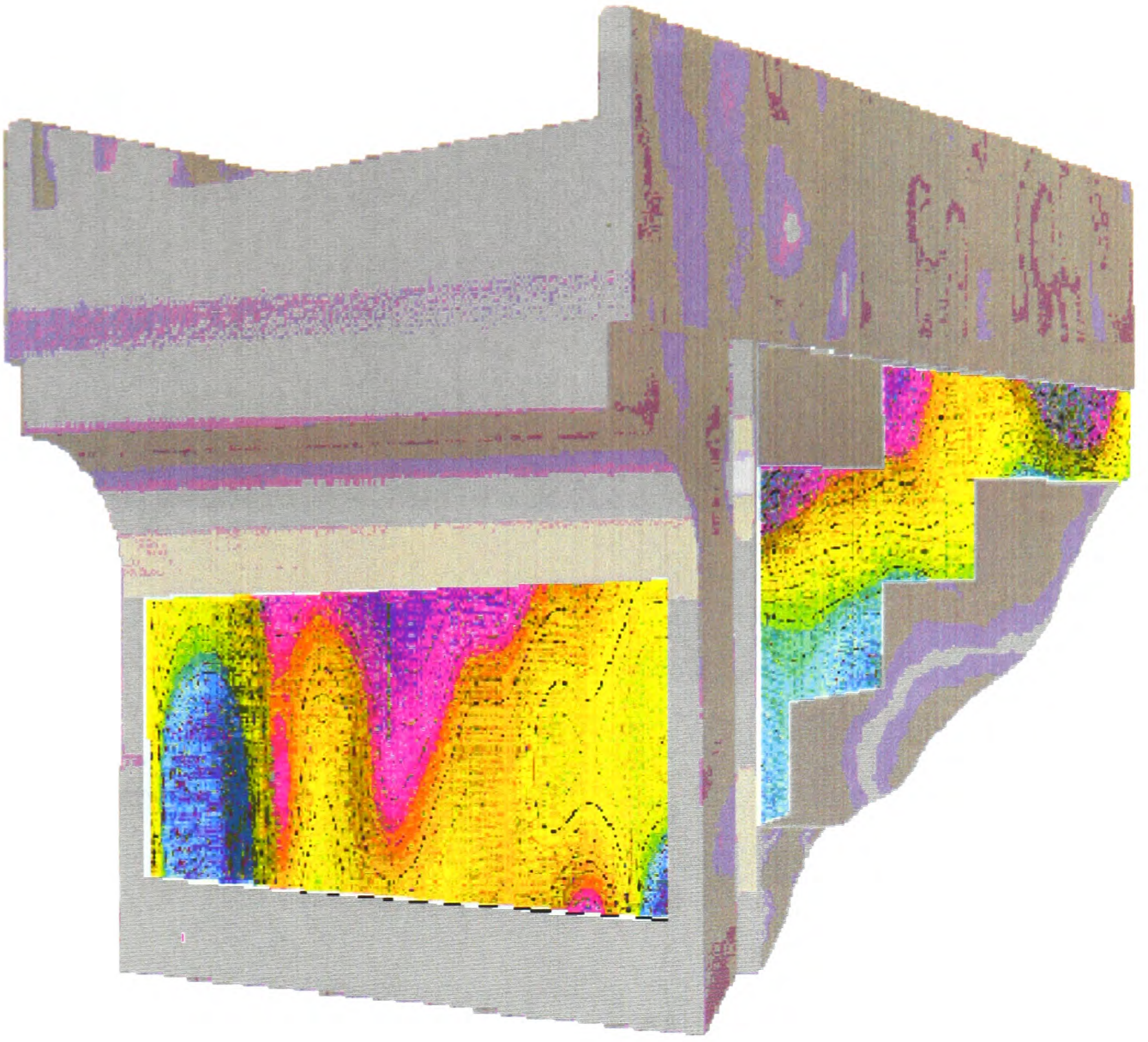

Fig. 5.15b - Conductivity distribution on upstream side and abutment wall

The values obtained are in a high and very wide range: conductivity readings registered were as high as 120 mS/m. The highest values were recorded on the downstream side with an average of 60 mS/m, and the lowest on the abutment wall (average of 38 mS/m), whilst the upstream side registered an average conductivity value of 40 mS/m.

Such values are indicating heterogeneity in soil filling in the abutment, made of rock such as argillites, wet clays or alluvium and sand; **or** variations in moisture content/salinity (see section 4.4 and tables 4.4 and 4.5). Conductivity is controlled by clay content, moisture and salinity. Of these the most complex is usually the moisture profile as it was seen in chapter 4.

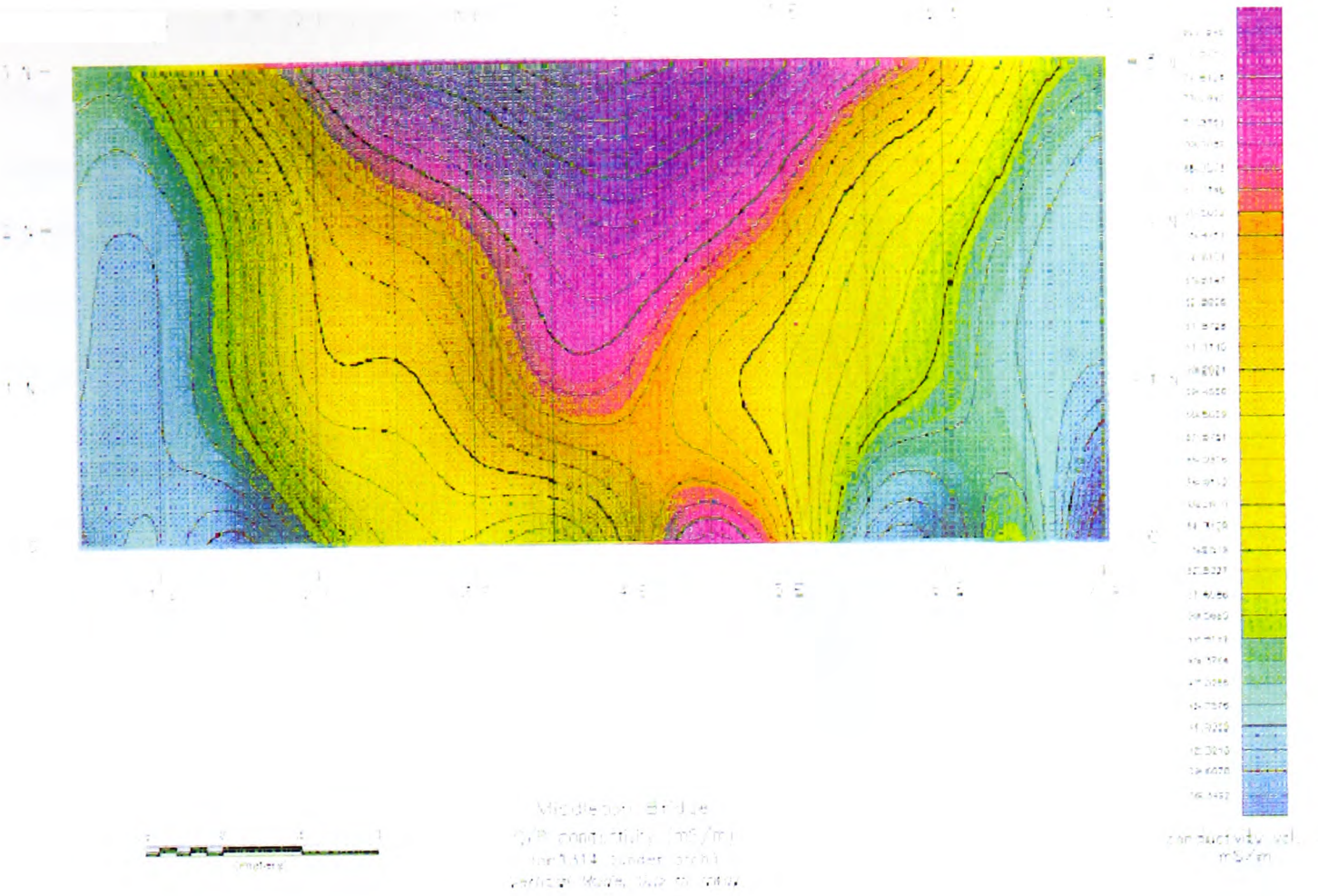

a) wall A: dry season

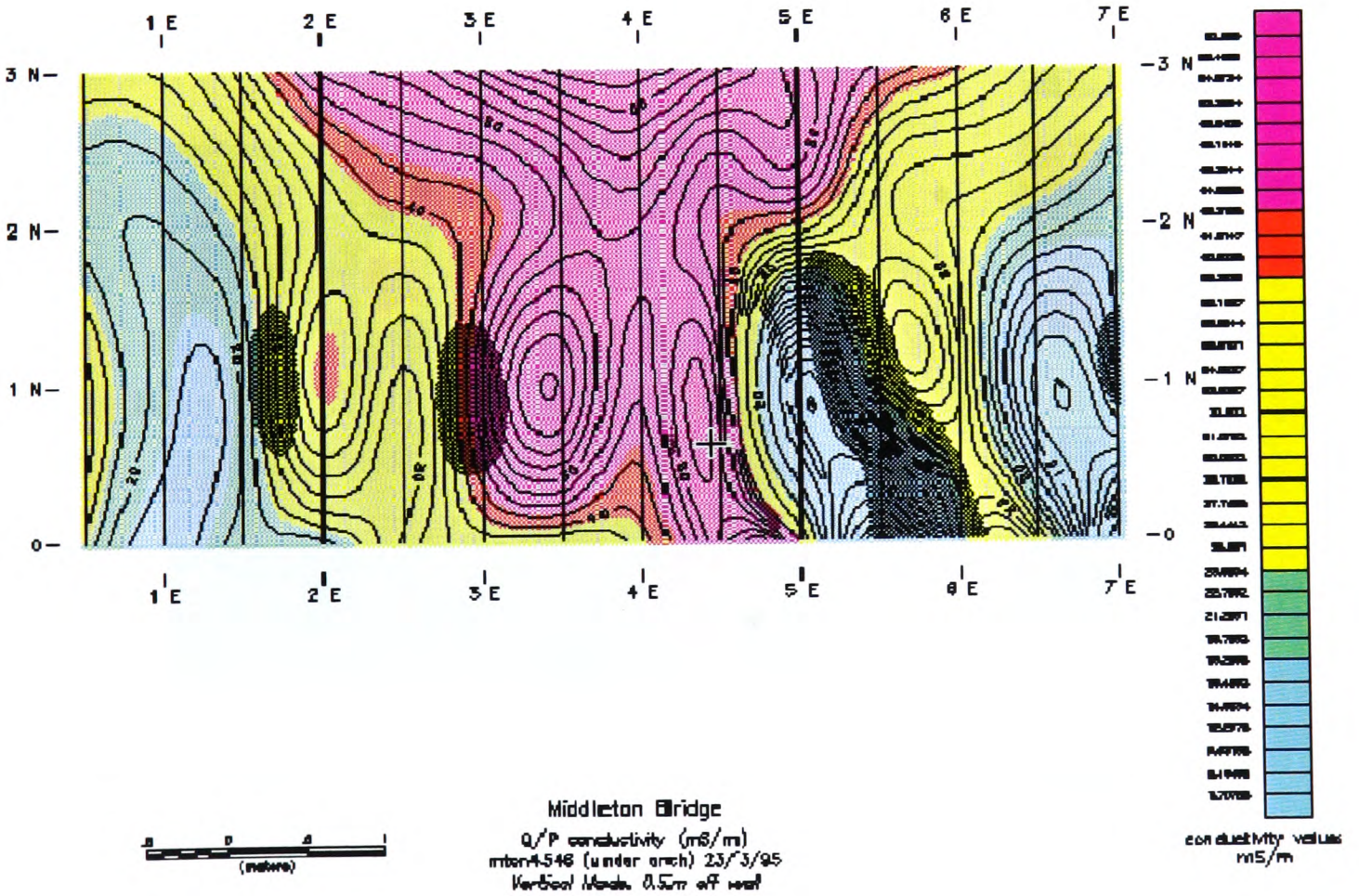

b) wall A: wet season

Fig. 5.16 - Conductivity distribution on abutment wall: comparison between dry and wet season.

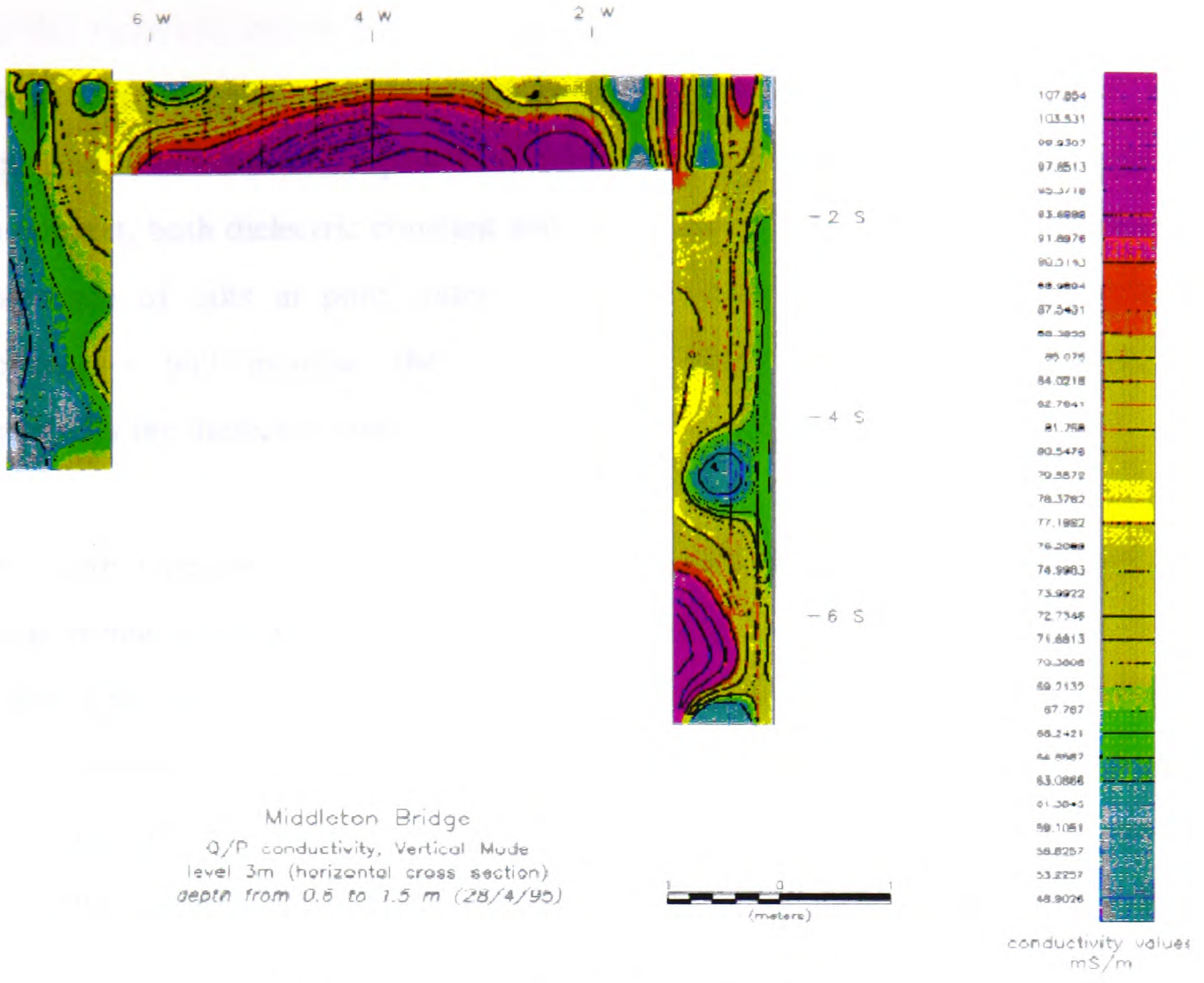

a) elaboration with "geophysical" software

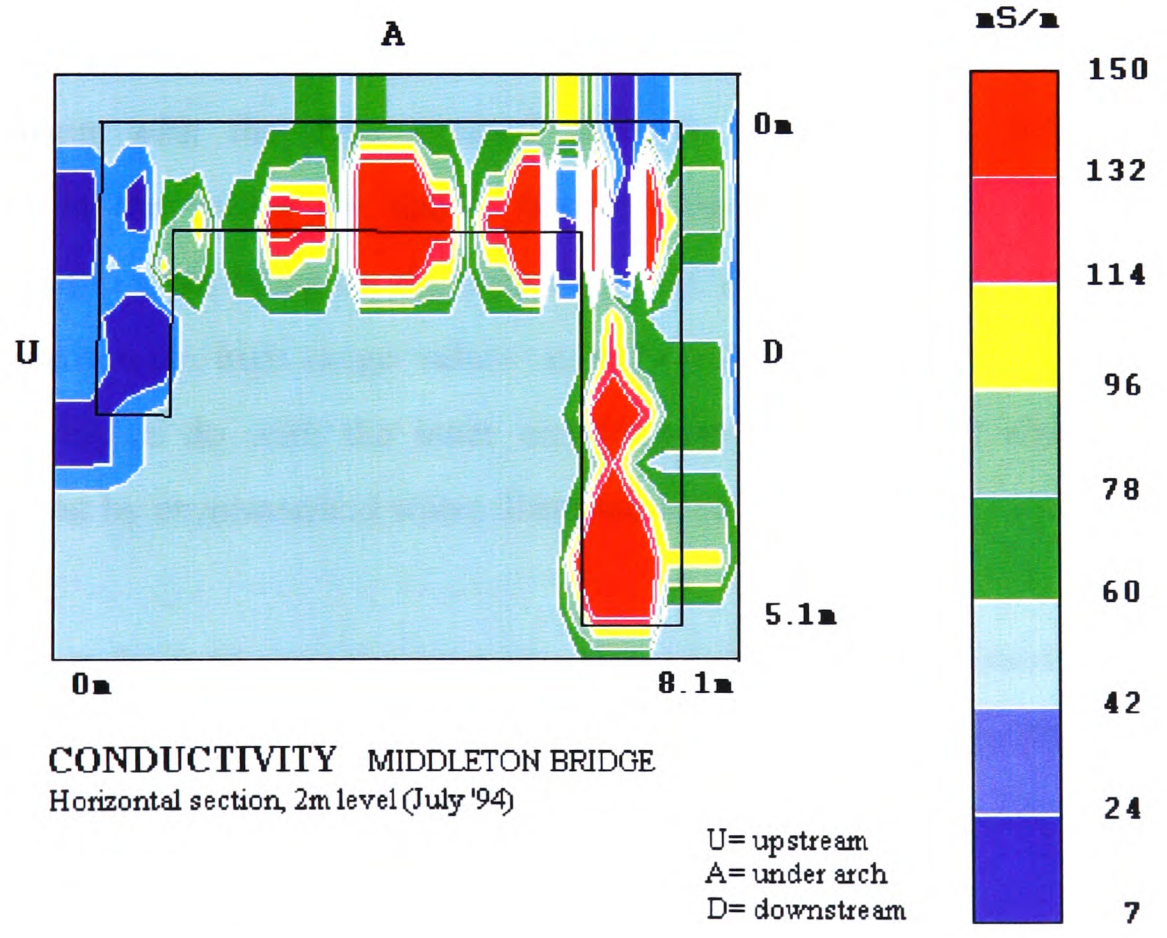

b) elaboration with tomographic programme

Fig. 5.17 - Conductivity distribution of cross section, at level 2m.

The bridge investigated was a structure with moisture-drainage problems and attempts had been made in the past to alleviate the problem but with limited success. In this context, both dielectric constant and conductivity increase with water content. The presence of salts in pore water - mainly coming from routine winter road maintenance - will increase the conductivity even further, without affecting proportionally the dielectric constant.

Surveys were repeated over a period of months and differences were noticed, in particular behind the wall under the vault - Fig. 5.16. Comparison of results from data taken with maximum depth of exploration (1.5 m) lead to the hypothesis that a significant moisture/water movement is taking place in an area at the rear face of that wall with concern about the possible loss of the fine part of the filling; this hypothesis was reinforced by the low velocity values obtained from sonic tomography in that same area.

Conductivity data collected at different depths (Fig. 5.14 a) have also been plotted to obtain a horizontal cross-section of the abutment. Figure 5.17 is a cross sectional representation with the data iterated through tomographic software. Clear differences in the values are visible between the upstream and downstream wall situation, with values being on the bottom end of the range in the upstream side and showing medium to high range values on the downstream side. This finding clearly had something to do with the inner construction of the bridge and could not be explained just by asymmetrical water distribution in the structure.

Subsequent endoscopic investigation into the structure has confirmed the hypothesis and revealed that hollow compartments were built into the bridge and that some of them have been partially or totally filled by grout injection during earlier strengthening and reinforcing operations.

Where the moisture moves from backfill to grouted zones, a clear difference in conductivity values is visible between the grouted material and the external wall. This enabled the thickness of the stone wall on the down stream side of the abutment to be calculated. A similar situation may pertain to the arch wall.

The upstream side is dry because the void behind the wall is not totally grout filled and this makes it difficult to calculate the thickness.

The conductivity distribution in localised areas near the exterior of the section yields the hypothesis that the wall is not solid stone masonry but may be layered within itself. This was also later confirmed by visual and endoscopic inspection and the wall has a compound structure: stone-rubble-stone. Depth of penetration of the conductivity meter used was equivalent to the masonry wall thickness.

5.8 Kilbucho Bridge

Radar surveys were carried out with 100, 500 and 900 MHz antennae, utilised in transmission and/or reflection mode to investigate the nature of the bridge backfill material, the thickness and condition of the stone spandrel walls and the thickness of the brick arch barrel.

5.8.1 Radar survey

A radar scan along the road centre line was first performed with a 100 MHz antenna in reflection mode (time window of 70 ns), to probe the depth of penetration of the signal and to establish a suitable time range that could include the features of interest. The presence of the arch was detected (marked by the arrow in fig. 5.18) but, as expected, the resolution of the antenna was not sufficient to determine the shape of the arch nor its thickness or time depth to the crown. Marks at the top of the radar plot mark the distance travelled along the road and are 1 metre spaced.

The use of the 500 MHz antenna (again in reflection mode) with its shorter wavelength and greater resolution, and a shorter time range of 40 ns, allowed

detection of the difference in the ground between the natural soil at the bridge approaches and the bridge fill. The latter ('2' in fig. 5.19) appear to be of homogeneous consistency in contrast with the layered original soil ('1'). The disturbance towards the bottom third of the plot is noise due to the linear gain applied to the signal for increasing its power and contrasting its attenuation. Furthermore, the intrados of the arch is visible (indicated by the arrow) and the overall velocity through fill plus arch barrel was estimated via the simplified formula to be 0.12 m/ns giving an overall average dielectric constant of the order of 5.7. The hyperbolic feature above the intrados was interpreted as the extrados of the arch at the crown and, assuming the thickness of the arch (0.3 m) to be unchanged through the width of the bridge, velocity and dielectric constant through the fill and the brick arch were calculated as reported in Table 5.2.

Mode	Frequency (MHz)	Material	Velocity (m/ns)	Diel. Const.
Reflection	500	Fill + Arch	0.12	5.7
"	500	Brick Arch	0.15	4
"	500	Fill	0.10	8

Table 5.2. Values of velocity and ε calculated via 500 MHz measurements in reflection mode.

A survey with 500 MHz frequency and use of two antennae on two channels was subsequently performed: on the first channel measurements were recorded from the first antenna moving again along the road surface and operating again in reflection mode. On the second channel the response at the transmission from the first antenna was recorded, with this antenna stationary at the crown intrados of the arch. Time range used was 20 ns on each channel.

Figure 5.20 shows the central part of the radar plot obtained, where on the horizontal axis the dotted lines mark 1 metre spacing along the road and the double mark corresponds to the arch crown and the position of the second antenna. It can be seen from the channel 2 record that there is no reception of the signal at the

second antenna until the transmitter is at about 1.5 m from the crown position. Even in this area the signal is very attenuated with a better signal only received when both the antennas are located at the crown. The two waveforms below the radar plot have been sampled at the crown position. Considering the relatively short distances the signal is travelling through (0.66 m at the crown), the cone of emission of the antenna and the fact that the E.M. signal travels in straight lines, the poor propagation of the signal may be explained more by the configuration of the antennas (when not facing each other) than by the dielectric properties of the bridge materials or the number of interfaces encountered. The one way travel time between the two antennas at the crown (Δt between the trigger on each channel) was not considered accurate enough to calculate the signal velocity through fill plus arch. In fact, the resolution of the signal is dependent on its wavelength (λ) and is generally estimated to be $\frac{1}{2}\lambda$. For a 500 MHz signal propagating in air, $\lambda_{air} = 60$ cm whilst, for that same signal travelling through any other material, the wavelength would decrease and the resolution increase with the increase of material dielectric property. However, in practice the frequency decreases due to antenna coupling effects and attenuation of the higher frequency components of the signal and the resolution suffers of these effects. Note the anomalous shape of the signal on channel 2 compared with the one obtained via 900 MHz antenna (fig. 5.21).

This survey was then repeated with 900 MHz frequency antennae and a time range of 12 ns on each channel. In reflection mode, on channel 1, the intrados of the arch is not resolved owing to the signal attenuation. In transmission mode, the reception of the signal on channel 2 only happens when the two antennas are opposite each other (Fig. 5.21) and even in this situation the signal is rather attenuated. This phenomenon is due to the lower energy of the 900 MHz signal and to its tendency to grater attenuation, compared with the 500 MHz signal. The signal velocity was calculated to be around 0.15 m/ns and the dielectric constant approximately 4. (Tab. 5.3).

These values differ from those reported in table 5.2 and obtained with 500 MHz antenna but the difference can be explained by the greater resolution accuracy of the higher frequency antenna employed for the measurements reported in table 5.3 and by the greater precision in the calculation due to the smaller time window used. Also it must not be forgotten that the equipment used were developed for geophysical and geological applications and suited to operate at much greater depths than those typical of civil engineering, and a margin of inaccuracy may be expected from the system.

Mode	Freq. (MHz)	Material	Velocity (m/ns)	Diel. Const.
Transmission	900	Fill + Arch	0.153	3.8

Table 5.3. Values of velocity and ε with 900 MHz in transmission mode.

Measurements were carried out with a 900 MHz frequency antenna in reflection mode to investigate the stone parapet and spandrel wall thickness. A vertical scan was performed on the upstream side of the bridge, starting from the parapet wall and moving downwards (Fig. 5.4b and Fig. 5.22). The "time thickness" of the stone parapet was first obtained, then data were analysed for identification of whether the spandrel wall had greater thickness and stepped rear face towards its base.

In the parapet wall, a 2-way travel time of 4.93 ns was measured (Fig. 5.23a). Due to the small thickness of the parapet wall (0.3 m) and consequent short time-distance of the rear face of it from the antenna, the transmitter/receiver separation (Fig. B.2 & 3) in the antenna was accounted for (Fig. 5.23b) and a velocity of 0.125 m/ns was calculated; the corresponding dielectric constant value is 5.69.

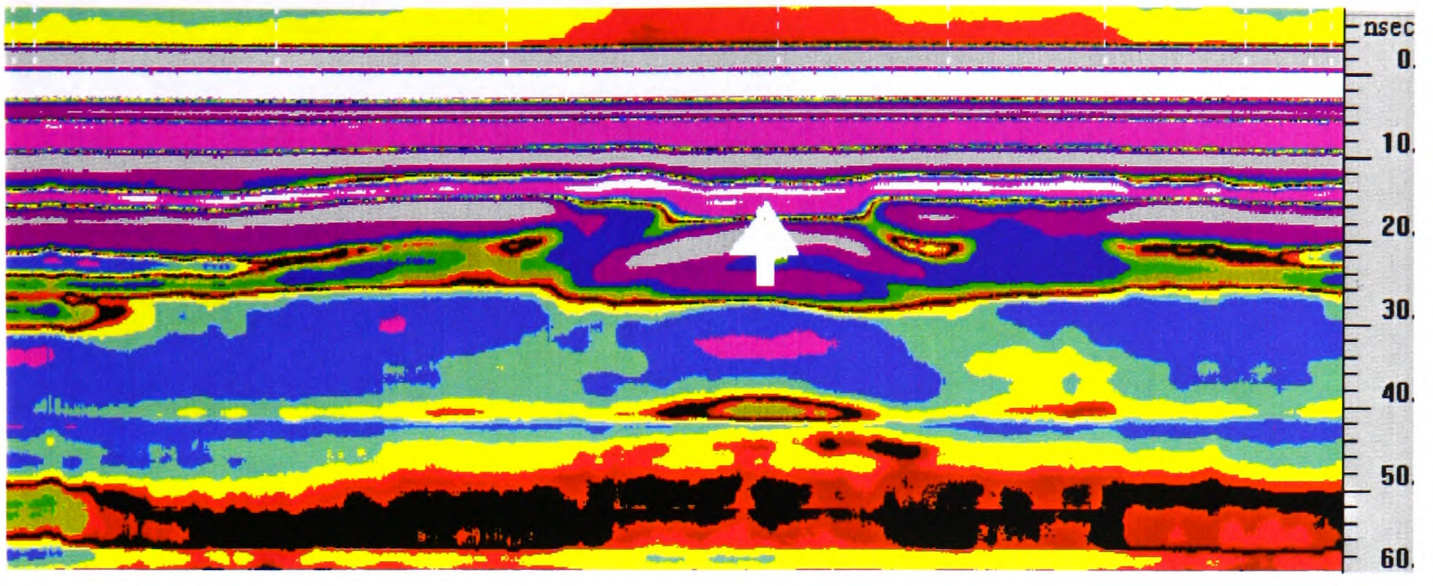

Fig. 5.18. Kilbucho Bridge: radar plot obtained with 100 MHz and 70 ns range (mark spacing: 1 m). Arrow marks arch crown.

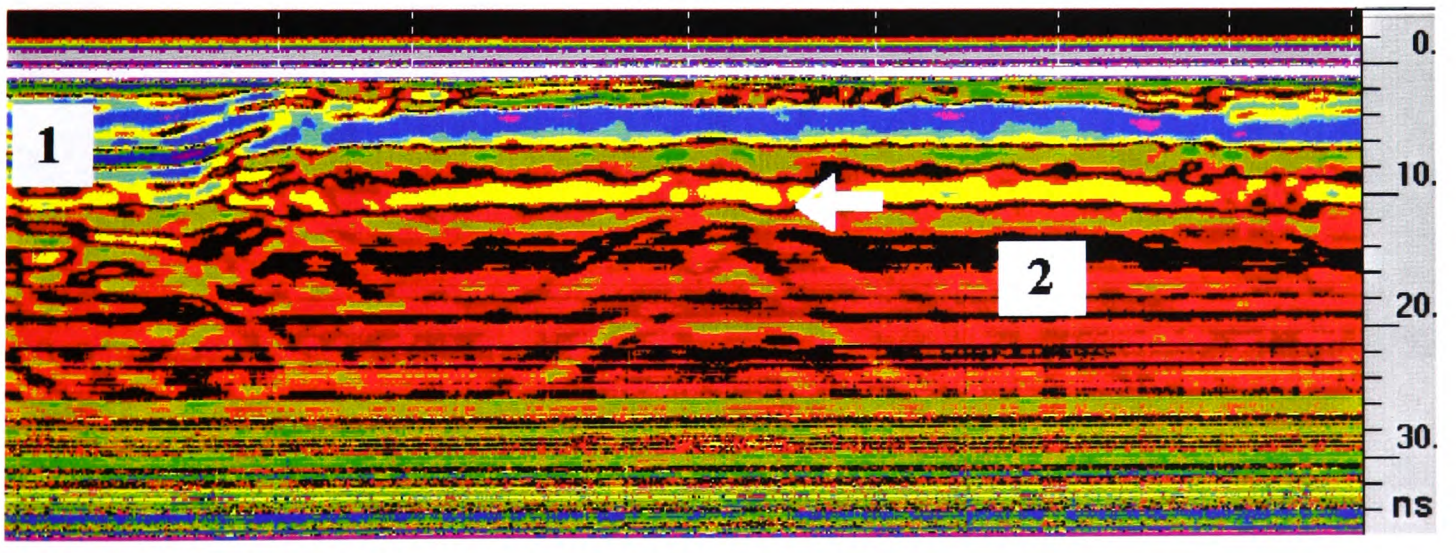

Figure 5.19. Kilbucho Bridge (500 MHz and 40 ns range), arrow marks the arch intrados. 1) original soil; 2) fill.

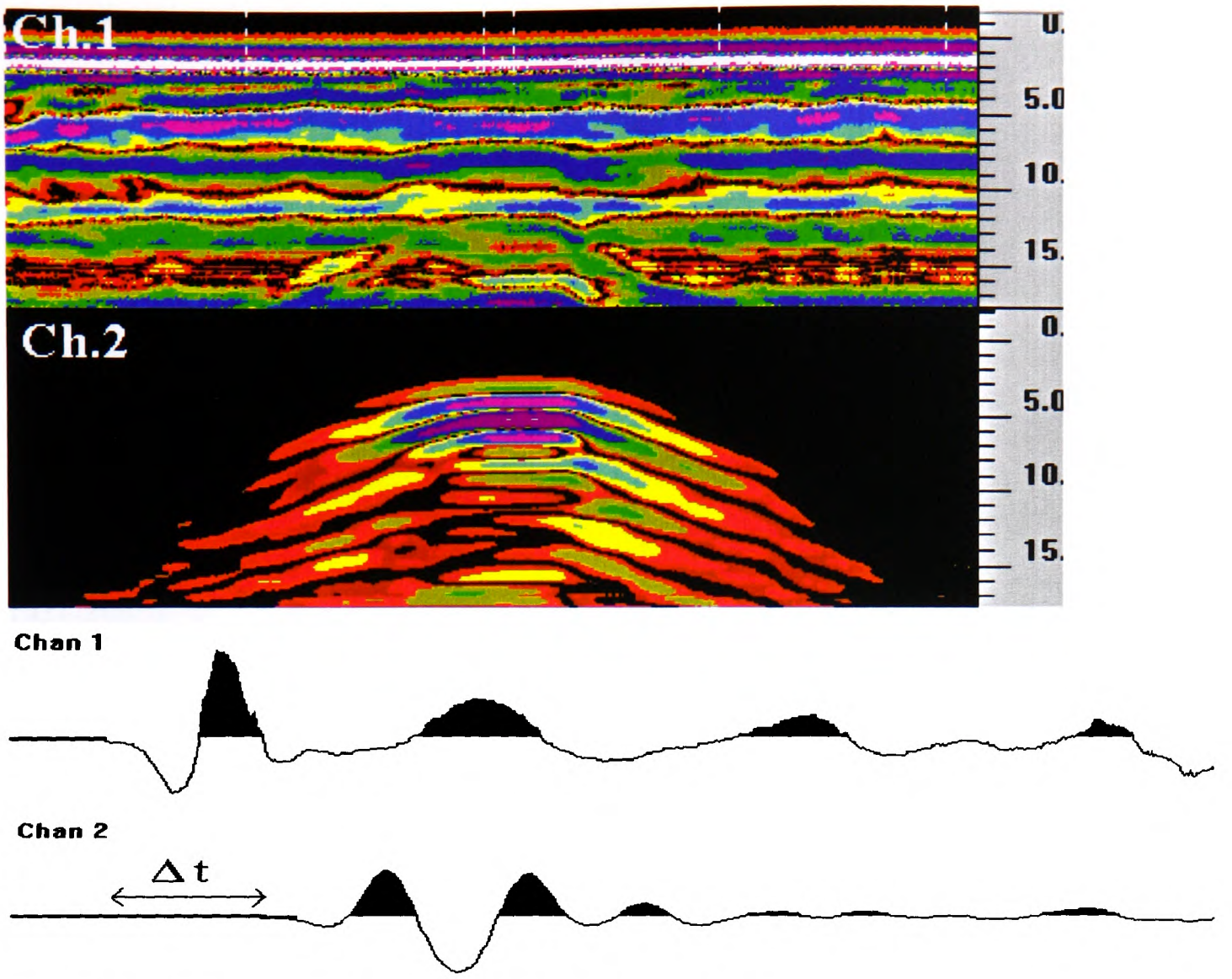

Fig. 5.20 - Kilbucho Bridge, 500 MHz, 2 channels, 20 ns range.

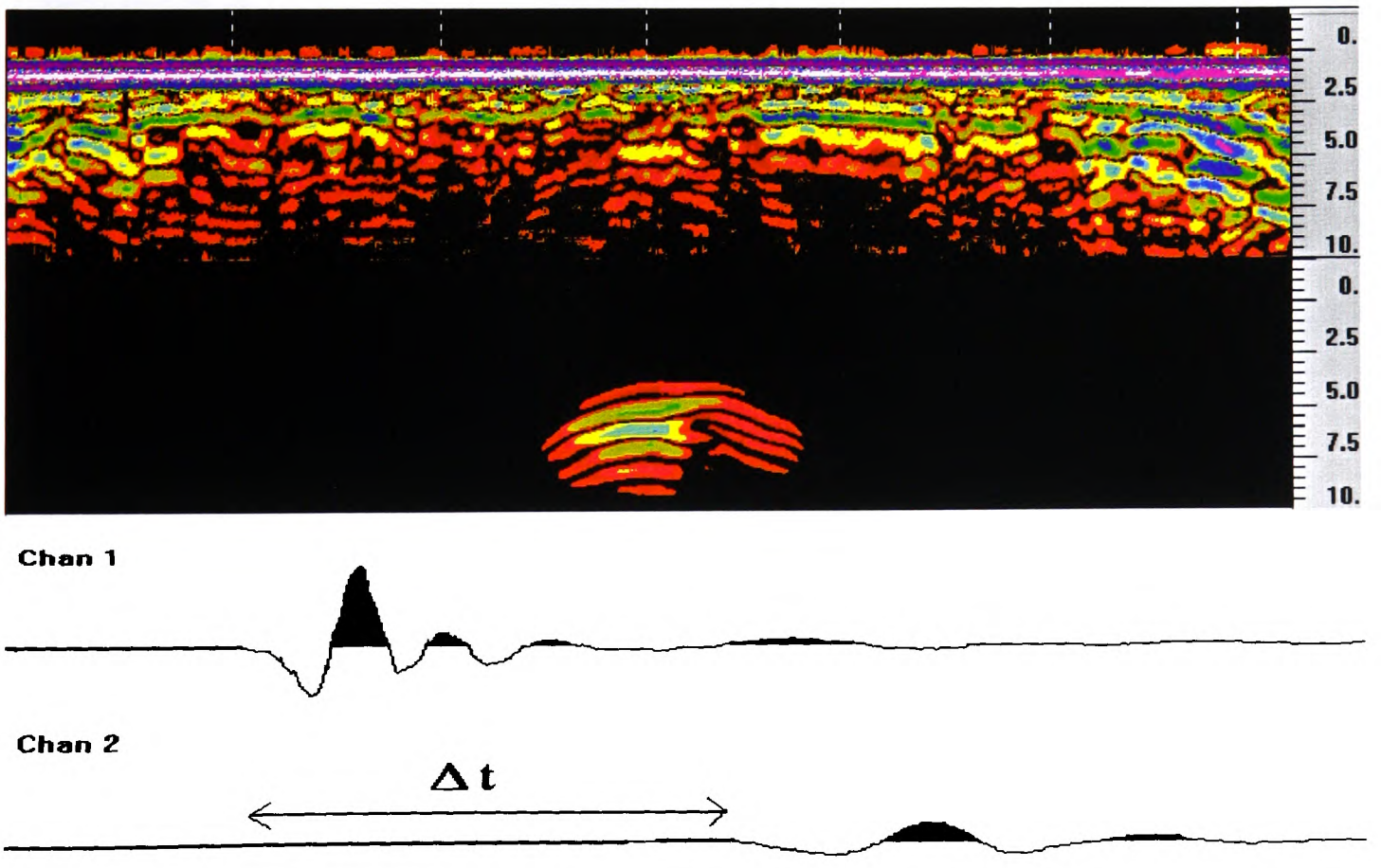

Fig. 5.21 - Kilbucho Bridge: 900 MHz, 2 channels, 12 ns range.

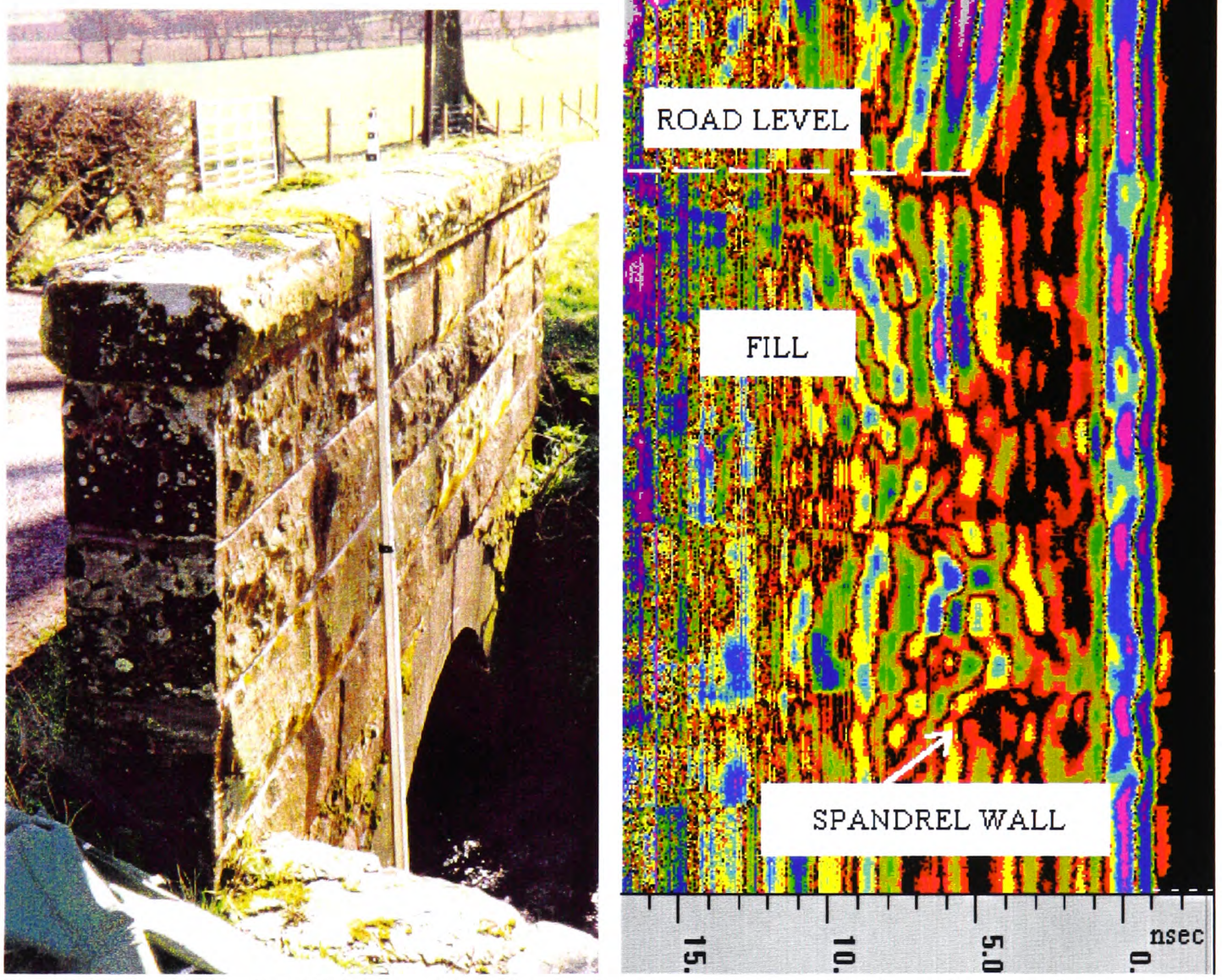

Fig 5.22 - Kilbucho Bridge: side view of stone parapet (left); radar vertical section through parapet and spandrel wall (right).

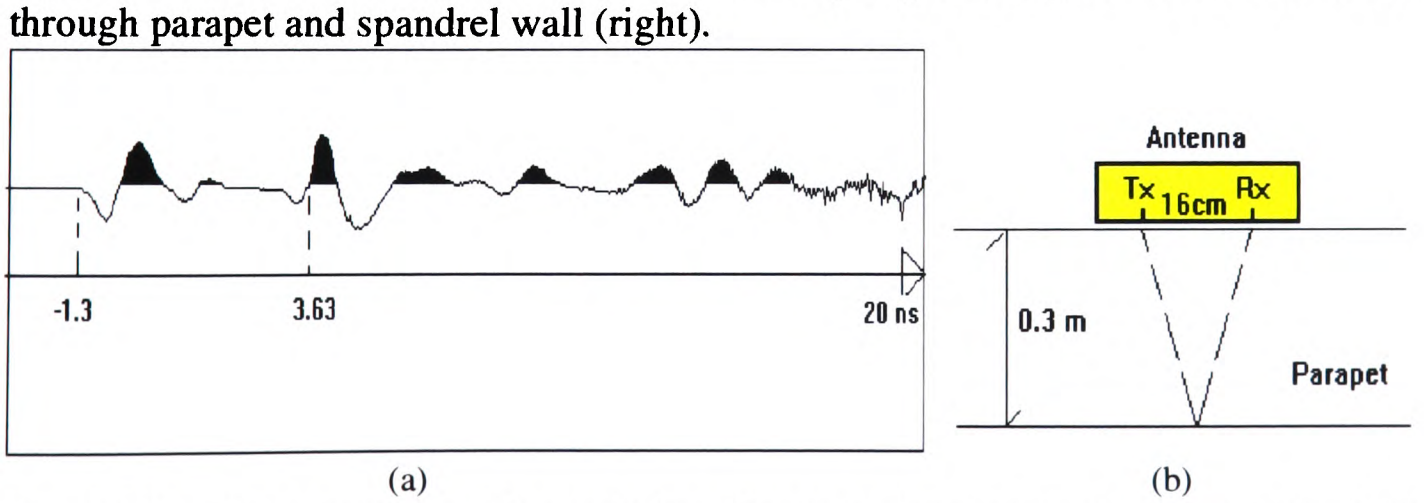

(a) (b)

Fig. 5.23 - Measurements of travel time through stone parapet: 2-way travel time record (a); transmitter-receiver separation in 900 MHz antenna (b)

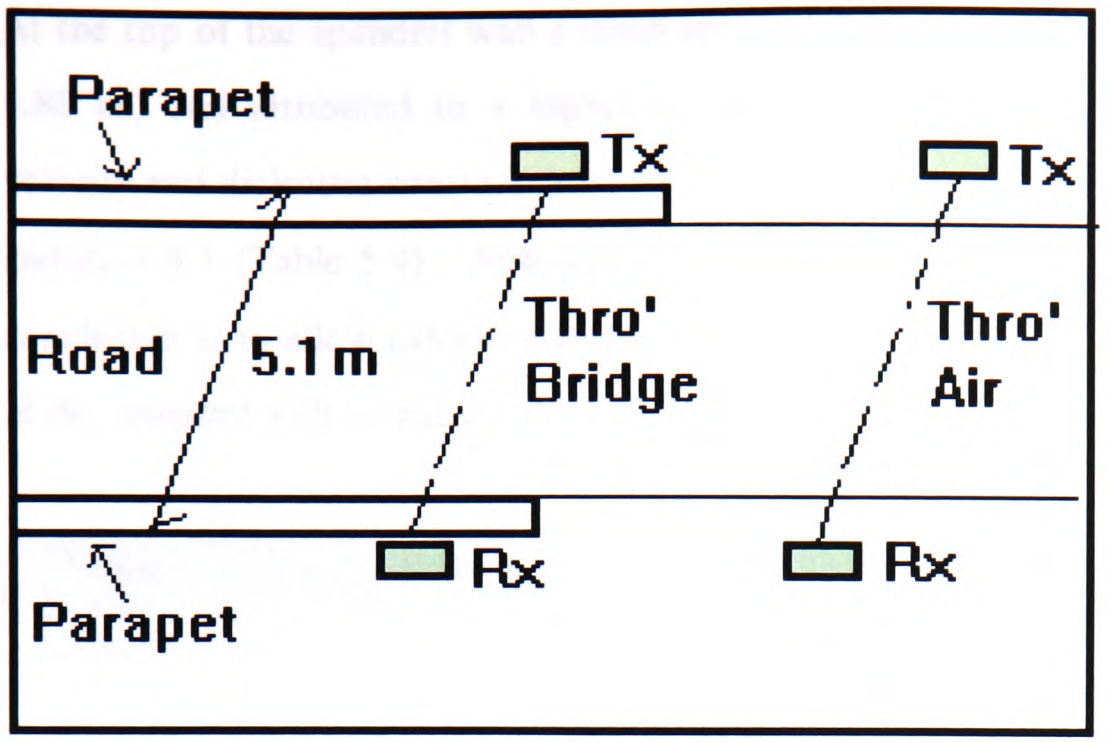

a)

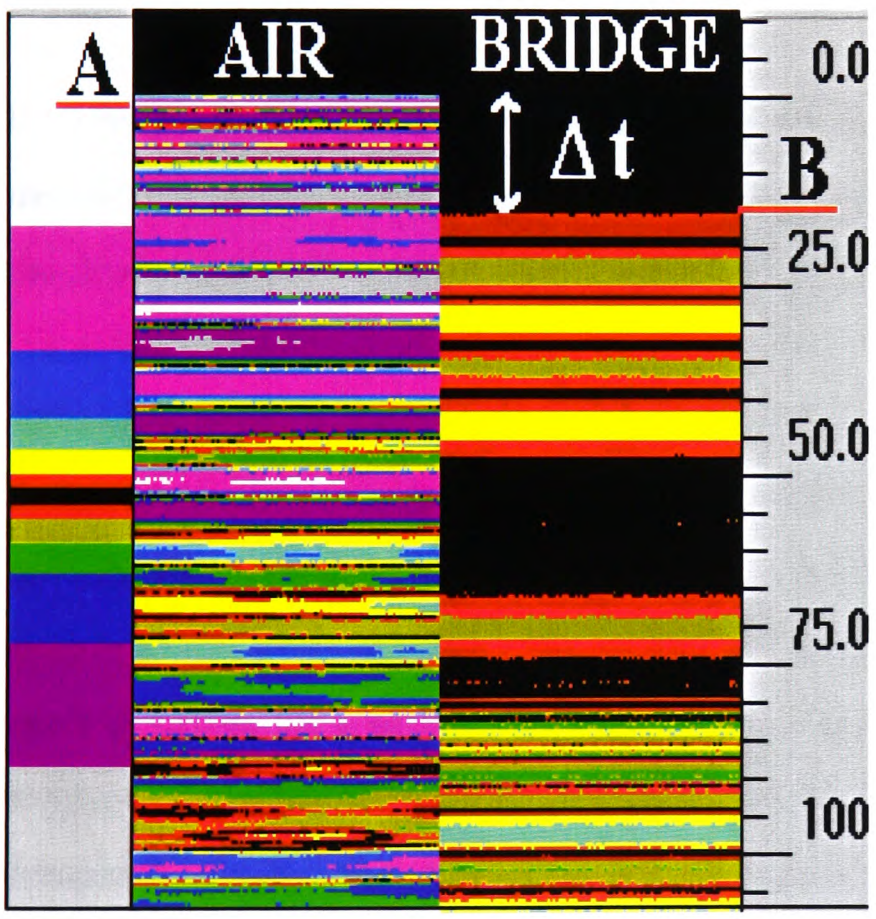

b)

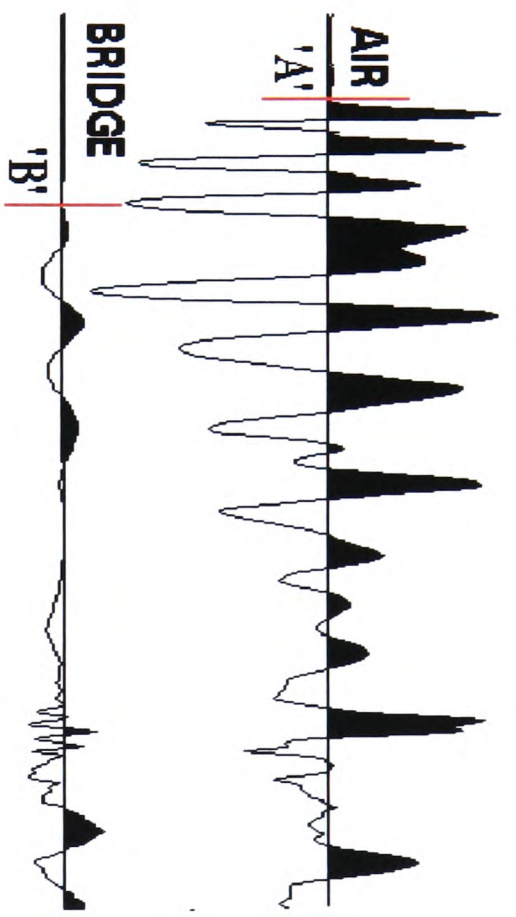

c)

Fig. 5.24 - Transmission measurements of travel time through bridge from spandrel to spandrel and reference reading through air: a) plan view of antennae configuration; b) time domain line-scan through air (A) and through bridge (B); c) corresponding waveforms in wiggle plot format through bridge ('B') and air ('A').

At the top of the spandrel wall a small increase in travel time was registered (t.t. = 5.88 ns) and attributed to a higher moisture content. Similarly to the parapet, velocity and dielectric constant were calculated for the spandrel wall: v = 0.105 m/ns and ε_r = 8.1 (Table 5.4). Although the interpretation of the radar plot was not as conclusive as to allow calculation of the thickness of the wall, an increased thickness of the spandrel wall is registered in its lower position.

Mode	Freq. (MHz)	Material	Vel. (m/ns)	Diel. Const.
Reflection	900	Stone Parapet	0.125	5.7
"	900	Stone Spandrel Wall	0.105	8.1

Table 5.4 - Values of velocity and ε calculated via 900 MHz measurements in reflection mode.

In order to determine the overall dielectric constant through the width of the bridge, measurements of the travel time of the electromagnetic wave from the upstream to the downstream spandrel walls were performed by use of two 100 MHz antennae in transmission mode. The received signal was first recorded between the transmitting antenna located at the upstream spandrel wall and the receiving antenna on the downstream spandrel wall, then the measurement was repeated transmitting in air with the same antenna spacing as before (Fig. 5.24a). In fig. 5.24 b&c the received signals at the receiving antenna position are recorded and the red marks sign the exact point in time of the reception of the signal. Note the attenuation of the received signal after travelling through the bridge and its delayed arrival time compared with the transmission in air. The measurement through air allows one to determine the zero point on the time axis of the signal transmission (signal trigger), given that the signal propagation velocity in air is known (0.3 m/ns) and the antenna separation is also known. By adding the difference in arrival time (Δt) between the signal in air and through the bridge, with the reference signal in air, the total time through the bridge fill and spandrel walls can be determined. The corresponding calculated velocity is 0.11 m/ns giving a total dielectric constant for fill + spandrels of ε_r = 6.5. From the above calculation of velocity through the stone spandrel walls

(see Table 5.4), by difference, as expressed in equation (5.1) below, the dielectric constant through the fill alone was estimated. The results are reported in Table 5.5. Note that, depending on the real thickness of the spandrel walls, the dielectric constant of the fill materials may oscillate between 4 and 5 or above.

$$v_{fill} = \frac{d_{tot} - (d_{sp} \times 2)}{t_{tot} - (t_{sp} \times 2)} \qquad (5.1)$$

where v_{fill} velocity through fill material,

d_{tot} total bridge width,

d_{sp} spandrel wall thickness,

t_{tot} travel time through total bridge width,

t_{sp} travel time through spandrel wall.

Mode	Freq. (MHz)	Material	Vel. (m/ns)	Diel. Const.
Transmission	100	Fill + Spandrels	0.11	6.5
"	100	Fill	0.14	4.4

Table 5.5 - Values of velocity and ε calculated via 100 MHz frequency.

A comparison between values of dielectric constant for the fill material, as measured with 500 and 100 MHz frequency, show discrepancy (see tables 5.2 and 5.5) but, again, the reduced resolution power of the lower frequency antenna - 100 MHz - associated with its longer wavelength (λ = 300 cm in air, longer through bridge materials), may account for a less accurate measurement and the low value of ε registered in the fill.

5.9 Discussion

In the evaluation of masonry arch bridges, impulse radar testing is starting to be used and has advantages over other techniques in certain circumstances, but problems can exist with regard to the interpretation of radar data.

A good example of this would be when the radar antenna is drawn along the surface of a masonry arch bridge with the objective of identifying hidden geometry and character of the soil fill with precision. Such investigation would have to proceed through the various layers of material and if the soil fill is heterogeneous the problem is compounded to the extent that the data is usually uninterpretable.

Tomographic maps have been used for plotting cross-sections of the structure situation. The use of three-sided tomography (i.e. upstream-wing-wall/abutment/downstream-wing-wall or upstream-spandrel-wall/arch-intrados/ downstream-spandrel-wall) when possible gives even better coverage of the sections investigated and a better reconstructed image resolution. Furthermore, it has been discussed how the greater angle of the ray paths connecting Tx and Rx antennae would improve the defect location by enhancing the "time-depth" of any anomaly present. Yet, variations in the composite fill of the arch bridge were discussed in relation to the general equation of electromagnetic wave velocity taking account of conductivity and frequency effects.

Through the sonic method little information is gained as to the condition and make up of the masonry but it confidently predicts anomalous zones of both weak and strong material in function of the calculated velocities. For example a high velocity area (denser material) was seen close to the under arch face towards the downstream end of the bridge. In the same area the conductivity maps show areas of low conductivity persistent throughout each survey. A possible explanation for the finding is that both techniques reveal an area of cement grouting in the bridge, the density of which is greater than that of the surrounding masonry of fill, thereby

explaining the high velocity but also the low conductivity (denser material will have a lower moisture content).

When it comes to correlate the results from each individual techniques, the comparison may sometimes not be straightforward, nevertheless corroboration of the findings is possible and the techniques are suited to complement one another, together providing information over the whole structure.

5.10 Conclusions

- It can be seen from the examples in the chapter that NDT methods can be employed for bridge assessment and monitoring purposes in a number of ways.
- The main difficulties envisaged are that the results of the tests are sometimes of a qualitative nature and require expert knowledge for their interpretation.
- Furthermore, the available ranges of equipment and testing methods are such that the scope and specification for each area of applications need to be drawn up carefully.
- All the techniques used have had considerable success in finding anomalies either in the masonry walls or in the fill material behind or both.
- With regard to radar, where multiple changes of interface between dielectric layers take place, the change of dielectric constant will be identified but the resolution of the final target layer may prove particularly elusive.
- On arch bridge fill with high attenuation properties, conventional reflection surveys proved ineffective for target resolution.
- Results from transmission measurement surveys have been more satisfactory.
- In one case, Middleton Bridge, significantly higher dielectric constants were calculated than might have been expected from published literature. This has been attributed to moisture/salinity factors in the structure.
- Tomographic imaging was used to gain greater insight into the structure and proved to be very useful.

- The antenna frequency plays a key role in the radar survey and a compromise must often been reached between resolution and penetration power of the antennae chosen.
- By using a range of antenna frequencies at Kilbucho Bridge it was possible to obtain information regarding the dielectric properties of bridge fill and masonry materials. Comparison of results extracted from measurements recorded with different frequencies and through varying antenna configurations and locations - some of these innovative.

The NDT methods used in this project have demonstrated the ability to be valid site techniques, rapid, low cost, contacting and non-contacting for bridge assessment and monitoring purposes. From radar, sonic and conductivity tomographic cross-sections, inhomogeneity identification, moisture movement detection over time and layering within the masonry have been detected.

Each method has proved to be effective and their parallel use in the investigation has drawn an organic picture of the state of the structure revealing both construction details and modification/problems which have arisen with time. Whilst some of the information gathered was common to more than one method, other knowledge has been obtained due to the special measurements of a particular technique.

Whilst the conductivity method has given detailed information up to a certain depth into the structure, no data could be collected at deeper locations. Its low cost particularly in terms of time in the data collection phase and post data-collection analysis, makes it convenient for repetitive surveys. Furthermore the techniques allows for high resolution in the conductivity variations detected, thereby improving the quality of the results interpretation. The instrumentation is compact and light which makes it suitable for bridge applications. The tomographic elaboration of the conductivity data has provided a clearer picture of any layered configuration in the structure section. The particular depth of penetration of the instrument used was a

limitation of the survey as detail from the fill material behind the masonry wall could not be revealed.

Sonics are a reliable method when great attention is spent in recording the data; a meticulous work is also necessary during the preparation and analysis of the data, but good results can be achieved when the optimal grid density is set in relation to the goal of the test.

Radar's advantages over the other two methods are rapidity and reproducibility in allowing continuous scan recording which makes it ideal for tomographic surveys. Improvements in the understanding and wider use of this technique on masonry structures is expected in the near future.

CHAPTER 6

LABORATORY MODELLING OF MASONRY STRUCTURES

6.1 Introduction

Research into the performance of non-destructive test methods was carried out by undertaking a calibration study in the laboratory and with the aim of developing guidelines for the selection and application of inspection methods, in order to achieve a reasonable level of confidence in the structural condition. The work aims to identify the limits of detection, noise in measurements, variation in performance for different levels of damage, and the influence of environmental factors.

For some inspection methods, such as radar and conductivity survey of masonry structures, performance focuses mainly on the ability of the methods to detect target geometry: size, location, and orientation. Other methods, such as sonic tomography, rely on a correlation of a physical quantity, density, with damage. Such methods are limited by the response of a physical quantity to damage, and are based on a change in physical measurement that can indicate damage.

6.2 Objectives

In order to undertake effective assessment of a structure, there must be a clear and unambiguous knowledge of the internal construction of the masonry arch bridge. One of the key factors is knowledge of whether the bridge is an arch backfilled with soil thus giving load dispersion (Fairfield & Ponniah, 1993), or whether the bridge has a cellular hollow construction (Fig. 5.1). If the bridge is soil filled, knowledge of the condition of the soil - wet or dry, compact or loose - is also relevant. These aspects, combined with an interpretation study of radar signatures on plots obtained from

surveying a series of engineering cases (arches, intersections of walls, cavities), were also a relevant part of the laboratory research work.

An extensive calibration of radar propagation through masonry structures such as bridges has been undertaken in a controlled environment in order to study the effect of variations of material dielectric properties on radar performance. The main objectives of the experiments were the resolution and penetration power of different radar frequencies and the influence of water and salt content on the electrical properties of building materials.

In the laboratory, radar tests have been performed on a multi-span masonry bridge model, both when empty and back filled. At the same time, a brick masonry box has been built and tested. It has been filled with water and brine in different concentrations, and sand in varying moisture, salinity and density conditions. Furthermore, voids and defects have been simulated: targets of different shape, size and orientation were located in the box fill at varying depths. Finally the test rig was modified to simulate a composite/ cellular masonry structure as may be encountered in historical bridges and tests were performed both on the hollow and sand filled model.

Thus the test rigs served two purposes: (1) to calibrate the radar technique in controlled conditions (2) to allow, on a scaled down version of the site case, the performance of these reflection mode measurements which the on-site conditions of the materials and dimensions of the structure did not permit. The aims of the work reported herein can be summarised as follows:

- to identify the effectiveness of radar penetration through conductive materials (saline solutions at increasing concentration). In the case of highways bridges in northern climates, where snow and ice are predominant, the influence of salt concentration on the effectiveness of NDE techniques is important.
- to evaluate the effectiveness of identifying targets within a soil fill and behind a masonry wall.

- to characterise effects due to signal propagation in composite and hollow structures.
- to improve the understanding of the response of heterogeneous civil engineering bridge materials to NDT techniques, through conducting large scale laboratory experiments and calibrating these measurements with field surveys.

6.3 Double arch bridge model

6.3.1 Test rig characteristics

A semi-circular double span arch model - originally constructed for experimental work related to soil fill-arch interaction studies on multi-span masonry arch bridges (Prentice, 1996) - was available in the laboratory at the time when the NDT tests on the masonry box (see section 6.4) were being carried out. Given that the dimensions of the test rig were suitable for laboratory NDT testing and its materials were consistent with those of the other test rig, the bridge model was considered appropriate for radar tests. These were intended for the purpose of calibrating the reflection mode technique over masonry arches in controlled conditions. The test rig materials and dimensions are shown in figures 6.1 & 6.2, where all units are in metres.

The arch barrels were laid in English bond using a single ring of class B engineering concrete bricks - set on their side - to give an arch thickness of 102 mm. A total of 41 bricks were used for each arch with a nominal 10 mm mortar bond between each. A mortar mix of 1:¼:3 of cement, lime, sand was specified for the barrels and a Ferrocrete quick-drying cement was used which enabled the mortar to reach full strength within seven days and thus allow testing to proceed.

As the double-span model was to represent in the above mentioned study a 2-dimensional "slice" through an arch barrel, structural spandrel walls were not used in the construction of the bridge but instead the fill was contained using 15 mm thick timber sheets pre-cut to the shape of the arch barrels. Stiffening in the form of 50x50x6 mm steel angles were applied along the length of each wooden "spandrel wall" to decrease the overall flexibility, as shown in figure 6.3. In addition, six tension

bars (∅15 mm) were threaded through the bridge to ensure no induced lateral deflections could take place from the applied surface loads once the sand was in place. Location of all these tension bars can be seen in figures 6.3 and 6.5.

Timber end walls were used to contain the sand at each end of the bridge and were securely connected to the side walls. They were positioned at a distance from the springing of the arches to ensure that no secondary effects of load dispersal onto the extrados of the arches could take place. This distance also served the purpose of the radar survey as substantial support to the end walls was provided by an arrangement of heavy duty steel beams which were bolted to the strong concrete floor. Figure 6.3 details one end of the rig and shows the position of the steel beams.

For the purpose of the above mentioned experiment (Prentice, 1996), thick polythene sheets were used to line the inside of the timber spandrel walls and laid approx. 40 cm over the extradoses, to minimise the friction between fill and spandrels. These sheets acted to close any possible gap between timber wall and barrels and to contain the sand fill and are believed not to have any effect on the radar survey.

While the fill was poured and compacted in the test rig, stress cells were placed in pockets pre-cut into the bricks of the barrels, while total pressure cells were placed in the fill. A total of 18 cells were positioned in the rig at a depth which varied in a range between 150 and 500 mm below the sand surface. The cables were drawn through the sand to one side for connection with the data acquisition system. Figure 6.5 shows the line of placement of the cells in the sand fill and embedded in the extrados of the arches. Due to the small dimensions of the cells and their position, their effect on the radar tests is minimal. Cells of different make and dimensions were used as can be seen in table 6.1.

Cell prefix	Area of active face (mm)	Thickness (mm)
Cam	45x25	30
Glm	35x30	35
N	50 ∅	10
Kul	55 ∅	12

Table 6.1 - Cells dimensions.

The sand fill was chosen to be consistent with previous work carried out at the University of Edinburgh on single-span arch bridges (Fairfield, 1994). It is a sand fill whose properties are discussed below and which was placed from a zero drop height and hand compacted with a tamping rod in layers of approx. 100 mm to achieve a consistent density throughout the arch. The fill was laid to a height of 150 mm above the crown - as seen in figures 6.1 & 6.2 - and levelled off to obtain a smooth surface and ensure an even distribution of applied load during the load tests. No road paving surface or material of any kind was present on the top of the sand.

The fill can be described as a medium, uniformly graded dry silica sand with rounded particles. The particle size distribution is shown in figure 6.4 where it can be seen that 26.5 % of the particles has diameter between 1.18 and 1.7 mm, and 68.7 % of the sand has diameter between 1.18 and 0.6 mm. The remaining 4.8 % has $\varnothing < 0.6$ mm. The in-situ density was calculated from the total weight of the sand placed in the bridge (from the number of 25 kg bags necessary to fill it and the average weight per bag calculated from a representative sample) and the internal volume of the bridge. The sand density calculated from the relationship shown in equation (6.1) below, had a value of 1517 Kg/m^3.

$$\sigma = \frac{m}{v} \qquad (6.1)$$

where σ is the density of the sand in Kg/ m^3 ; m is the mass in Kg and v is the volume in m^3 .

Shear box tests were carried out in accordance with British Standard (BS 1377, 1990) to establish the angle of shearing resistance in the sand at the density used in the rig. The value was calculated to be $\phi = 34°$. Although not directly influencing the radar data and their interpretation, the angle of shearing resistance is important since it produces a change in the coefficient of earth pressure, K_o, through the relationship $K_o = (1 - \sin\phi)$. K_o is used as input parameter in analytical assessment methods and its changes affect the distribution of stress throughout the fill.

6.3.2 Radar survey procedures

The test rig, described in the previous section, presents metal reinforcement bars as an integral parts of its construction. Any metal parts in the test rig which were close enough to the position of the antenna or of such orientation and size in relation to the wavelength of the frequency used, to be picked up during the radar survey, would show up on the radar plots and possibly mask other information. Fortunately, the distances and the dimensions of supports, reinforcements, cells and other instrumentation also served to facilitate the radar survey as it was possible to select a scanning area relatively clear of any such metal.

The radar surveys were conducted along a longitudinal scanning line, midway between the cell line and the opposite timber spandrel wall. The antenna was attached to a timber beam running along the bridge and transversely sliding on the top of the timber spandrel walls. This beam was dragged manually by two persons, one on each side of the test rig, so as to maintain the antenna in a straight line and allow repeatability of readings. This configuration also served to maintain the antenna at a fixed height above the ground, which was especially important during the first phase of the survey, when the rig was still empty and the antenna was suspended and in airborne mode. In the second series of tests, surveys were repeated with the antenna resting on the sand fill surface. Fig. 6.6 is a view of the test rig, still without backfill, as used for the first set of radar survey of which figure 6.7 is an example.

Reflection data at a single antenna (transmitting and receiving) were collected through use of 900 and 500 MHz antennae, scanning downward through the (fill and) masonry arches. When the fill was not present, reflectors were positioned on extrados and intrados of one of the arches and their effect investigated. Example records from the 900 MHz antenna are shown in the next section.

6.3.3 Radar data analysis

Figures 6.7 and 6.8 are the radar plots obtained from scanning the test rig with a 900 MHz frequency antenna in reflection mode.

The top picture (Fig. 6.7) represents the data from the empty model: the features representing the two arches are clearly recognisable even though their shapes do not reproduce the semicircles of the original concrete arches. The crown of the arches, at the extrados, appears at about 1 nanosecond on the time scale, which is the time taken for the signal to travel from the antenna to the arch crown and return, given that the antenna is suspended at 15 cm above the arch crown and the E.M. signal travels in air at 0.3 m/ns. The reflection from the crown, though, is still merged with the emitted pulse from the antenna. This is represented by the horizontal continuous lines at the top of the picture, starting from about -0.5 ns and decaying away as the signal propagates in the vertical direction. The arches appear to be "multi-ring": these curves, representing the reflection from the arches, are an effect due to the change in signal phase when the signal reaches the interfaces air-concrete (at the extrados) and concrete-air (at the intrados). Immediately below the arch curves, the other curves are given by the attenuation in the reflection and the pulse decaying away (or ringing down).

The arches seem to meet at about 4.5 ns and continue down. In fact, this is an effect due to the "field of view" of the antenna and its cone of emission (see figure 4.1). The antenna starts to "see" and register a signal component reflected from the second adjacent arch when it is still above the first one. For the same reason, reflections from that arch are still recorded when the antenna is now above the second arch. It has

therefore to be noted that the springing of the arches is not represented by the "meeting" of the 2 arches at 4.5 ns. Below the arches, at about 8.5 ns, the horizontal line of the concrete floor can be identified. This 2-way time again concurs with the distance between antenna and floor, and signal velocity in air.

Fig. 6.8 is the plot obtained by repeating the survey on the sand filled test rig. The presence of the compact sand, with its lower velocity, produces the modified shape of the arches which now appear more rounded. In fact, along the horizontal direction of the plot, the signal travels through varying depths of sand (from 15 cm at the crown to approx. 110 cm at the springings. The shift of the arches and floor at increased time positions (crown extrados at approx. 2 ns, and floor at approximately 10 ns) is also due to the presence of the sand.

In fig. 6.9 portions from two files recorded over the empty rig are compared: in (a) a thin reflector is placed on an area of the arch extrados whilst in (b) the reflector follows the curvature of the arch at the intrados. Note the change in phase and amplitude in the reflected signal from the arch: this is shown by the changes in shades of colours on the plot. Through careful waveform analysis, the exact location of the reflector would reveal the position of the arch interfaces and allow the calculation of velocity through the thin concrete arch ring with higher accuracy than from a plot of the type in figure 6.7.

In figure 6.10 a reflector is placed on the intrados of the arch when the rig is sand filled. Note the higher amplitude of the reflection obtained, if compared with figure 6.9b, and its restricted area on the plot. In this case the signal travels through construction material until it reaches the reflector. There is no air gap between the antenna and the target.

6.4 Masonry box model

6.4.1 Test rig characteristics

A 2.4 m long x 1 m wide x 1.5 m high experimental test rig was built in the laboratory. Its dimensions and materials were decided in relation to the purposes of the experiments to be carried out: the geometrical dimensions take account of the antenna frequencies to be used in the laboratory and edge effects, typical of the radar technique, arising from too small a test rig. The latter effects needed to be kept to a minimum, compatible with the availability of space in the laboratory and the economic and temporal resources available, by building a test rig of optimum size. The primary materials used, namely clay solid bricks, sand and water were selected to simulate in the laboratory environment some of the engineering features and material characteristics and properties that the engineer would encounter on site. The specific sand used was chosen for compatibility with the 2-span model previously described.

Besides constituting a container for soil material to be tested in varying density and moisture conditions for the purpose of collecting data related to the dielectric properties of materials, the test rig permits to simulate a composite masonry structure with soil backfill and to resemble the kind of configuration typical of the abutment of a bridge or of other historical masonry structures. Its main part consists of a 3-sided masonry box with the fourth side equipped with a timber gate to gain easy access to the inside of the test rig and to facilitate any loading and unloading of fill material (fig. 6.12). In a later phase of the experimental work, the masonry box was modified by adding a longitudinal partition wall in the middle, and so obtaining a 2-cell masonry structure (fig. 6.13).

The masonry brick wall is built of Class A Engineering solid clay bricks and mortar in the proportion 1:¼:3 of cement, lime, sand by volume. The wall, in English bond, is one header thick and rests on a plywood base laid on the concrete floor. The floor where this rig is built is a simple concrete floor, as opposed to the strong concrete floor where the double-span arch model (section 6.3) was built.

Care was taken in the design phase of the rig to avoid using any metal part which could later interfere with the radar survey during collection of data, leaving unwanted signatures on the radar plots. For the same reason the gate on one of the short sides of the rig is constructed of timber. It was designed so that it could slot into place between the two ends of the brick wall and a slot cut in the plywood base (Fig. 6.11), with no need for a metal locking device.

During the phase when the water constituted the fill material, the masonry rig was lined with a PVC sheet to create a watertight container to maintain the brickwall (and the operative premises) in dry conditions and the rig was filled with water up to 1.3 m level. Later, sodium chloride was dissolved into the water to create brine solution in different concentrations: 0.05 %, 0.1 %, 0.25 % and 0.5% by weight of salt to the water.

The other fill material used in the test rig during subsequent phases of the experimental work was silica sand. This is exactly the same sand used also for the double arch bridge model previously described and its grading curve can be seen in section 6.3.1. Experimental set-ups included: (a) dry sand compacted (see previous description); (b) dry loose sand; (c) moist compact sand (10% moisture content); (d) moist salty compact sand (10% moisture content and 0.5% of salt content in the water). The fill was laid to a height of 1.3 m. Example data will be shown of cases (a) and (c) with variable size and shape of targets buried in the fill.

For the last phase of the experimental work, a partition wall was added longitudinally in the middle of the rig to simulate a composite masonry structure. The cellular structure so obtained presents 2 identical cells, each of width 0.35 m, and separated by a brickwall of the same characteristics as the perimetral brickwall. Tests were conducted both with no fill material present and with fill material in one half of the structure, having filled one of the two cells with dry sand in loose conditions (Fig. 6.15).

Voids, defects and engineering "targets" in the fill were simulated through the use of re-bars and plastic containers (jerry can). Three rebars of Ø = 3.5 cm were immersed in the water or buried in the sand fill (depending on the set-up) and maintained vertical by suspending them from a timber frame which was also built around the rig (fig. 6.11). When in water, the metal rods were located at 10, 40 and 70 cm away from the brickwall along which the radar antenna was dragged for data collection (Fig. 6.14).

The containers allowed the simulation of voids and water inclusions in the fill; set-ups of its content included: (i) air; (ii) fresh water; (iii) salt water (at varying salinity); (iv) dry sand; (v) saturated sand. The container, whose size (dimensions 43x35x19 cm) was also chosen bearing in mind the frequency of the radar antennae to be used, was suspended in water or buried in the fill at a known fixed depth from the surface of the fill, so to be fully "visible" to the antenna without being masked by wall reflection effects. For the purpose of studying the resolution of the antenna, during the experiments with water as fill material of the masonry box, the tests were repeated with the container occupying fixed positions and orientations. These were: (a) the container standing at the back of the wall where the radar antenna was located; (b) in the middle of the masonry box; (c) against the opposite wall; (d) (e) (f) the previous positions but with the container orientated at 90°, i.e. with its smaller side facing the antenna.

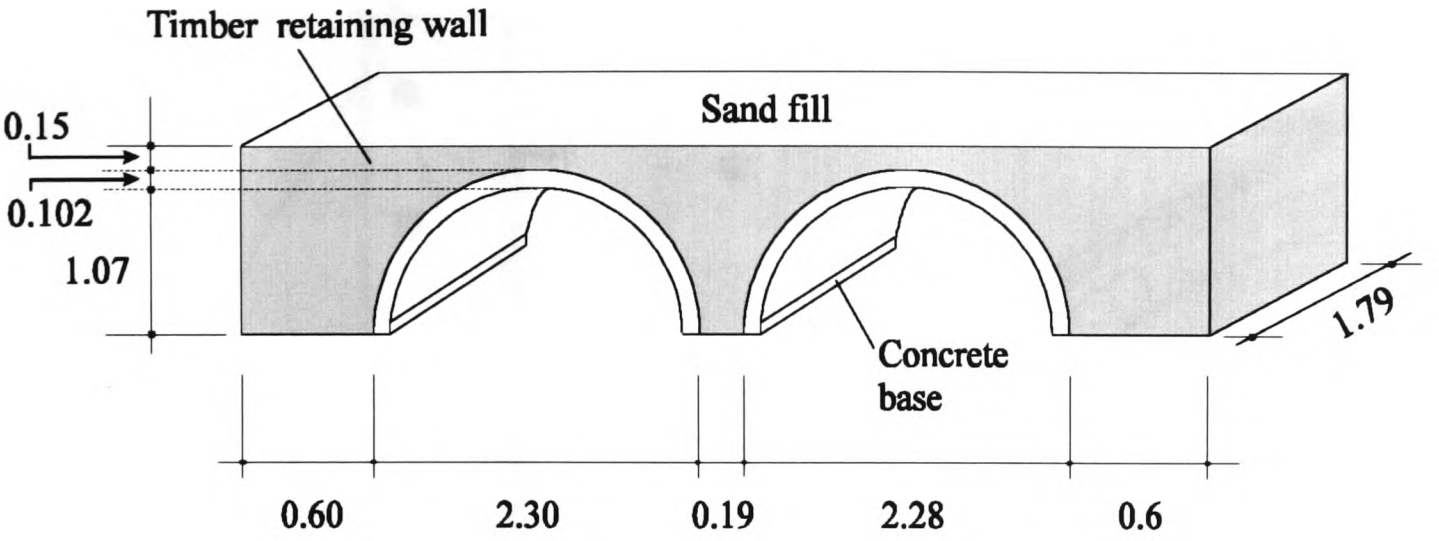

Fig. 6.1 - Dimensions of double-span arch model (in metres).

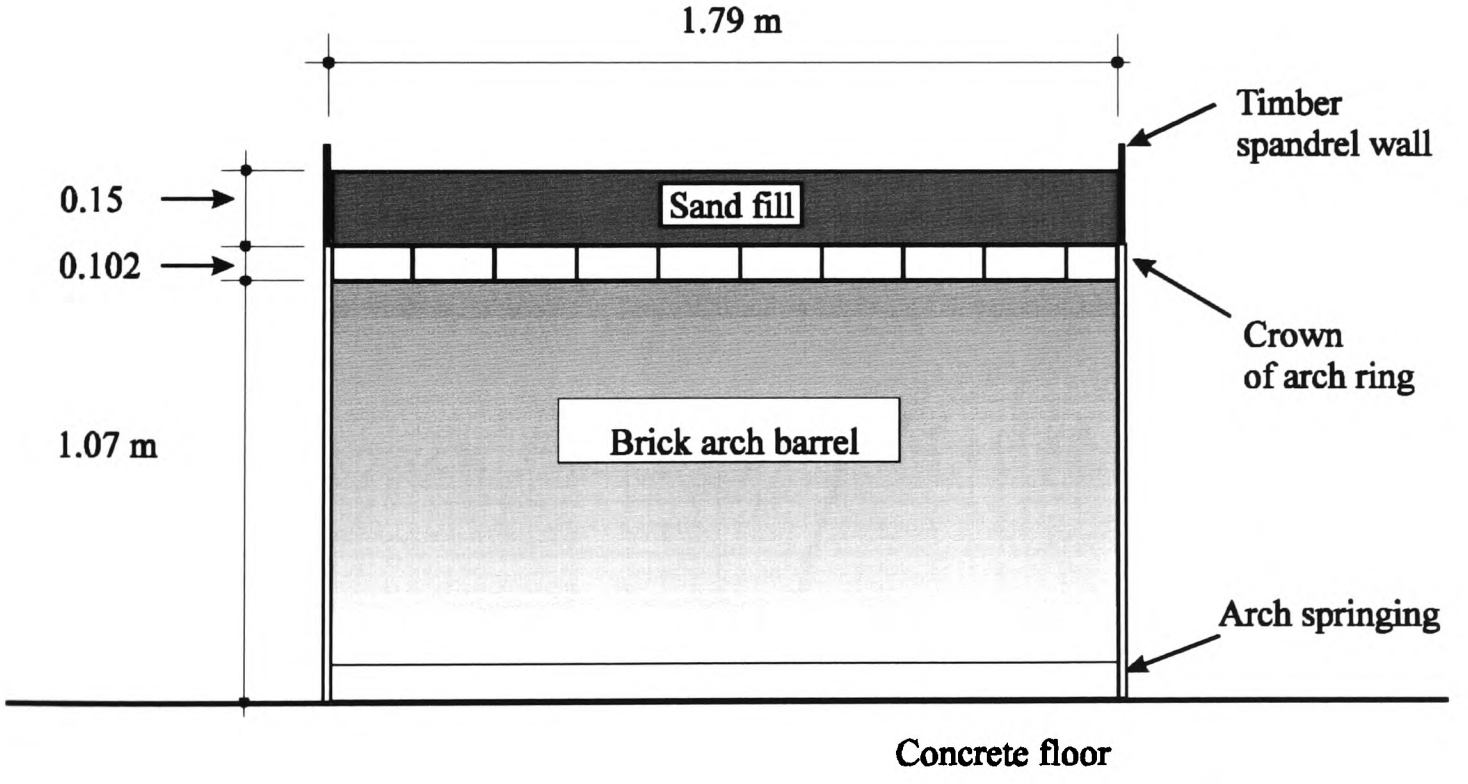

Fig. 6.2 - Vertical section, at the crown, through one of the arches (dimensions in metres).

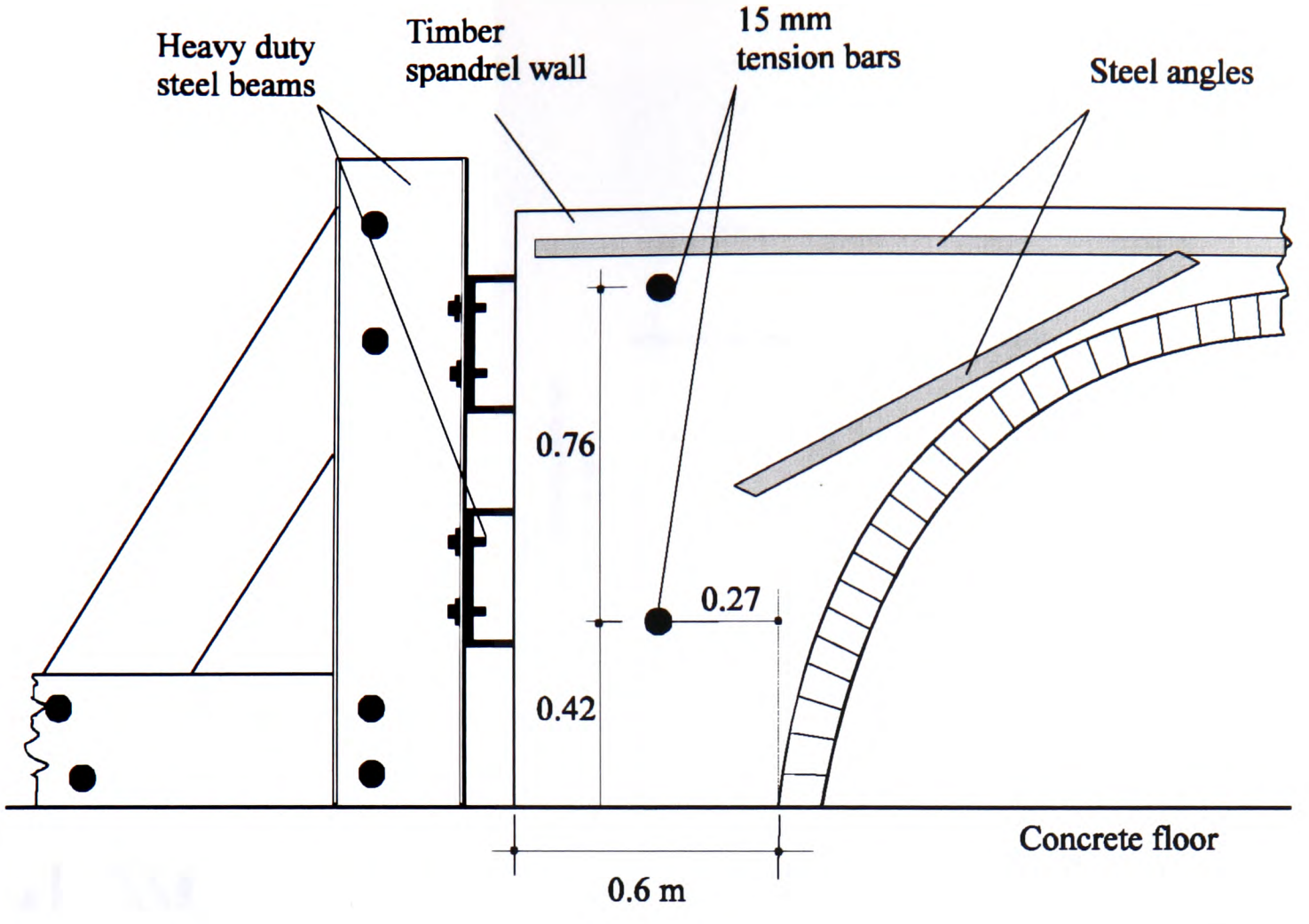

Fig. 6.3 - Detail of left end of the rig, with position of the steel beams and tendons.

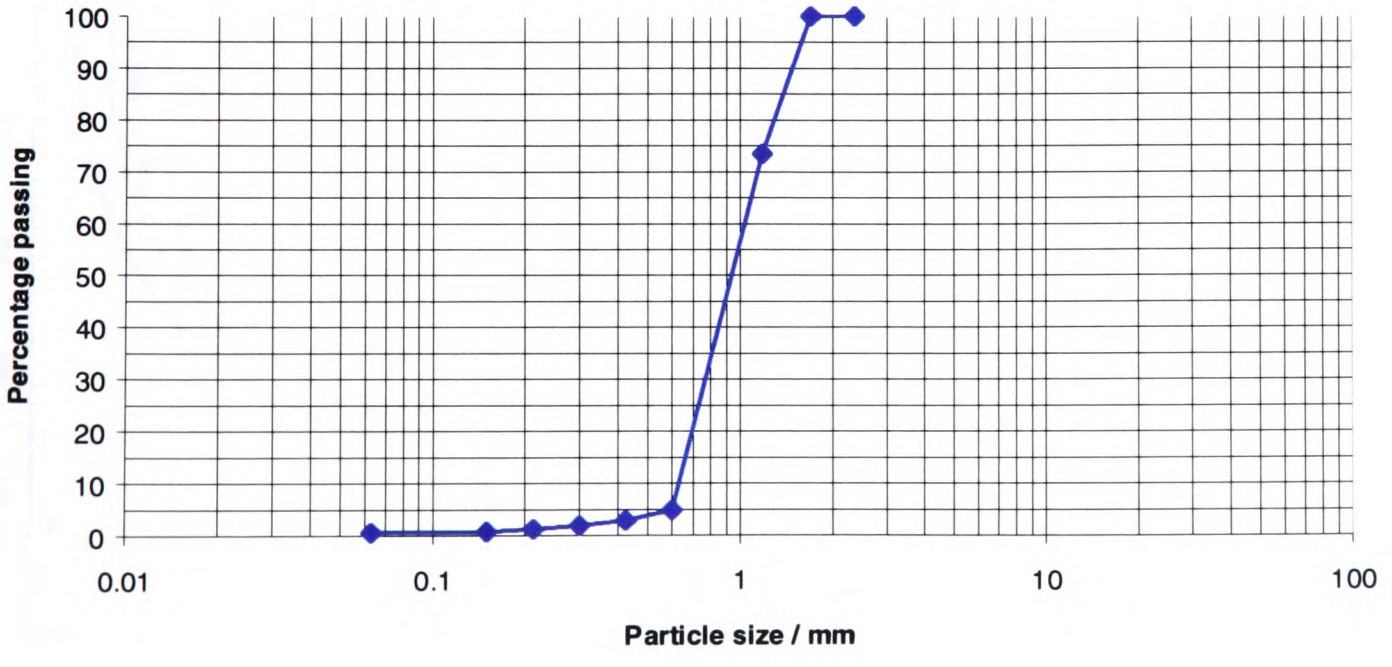

Fig. 6.4 - Particle size distribution for the sand used.

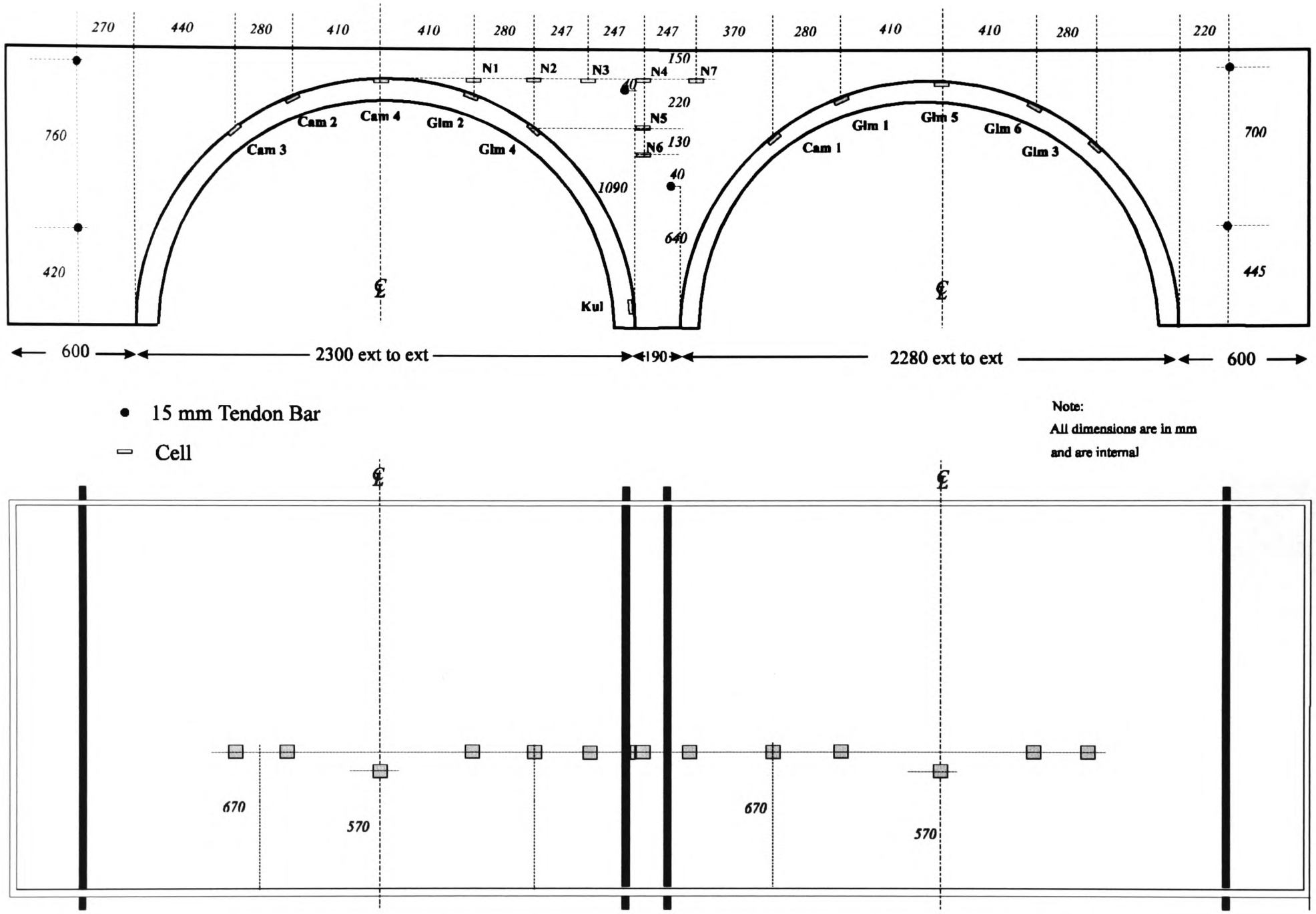

Fig. 6.5 - Position of instrumentation and other metal objects: vertical section (top) and horizontal section looking down (bottom).

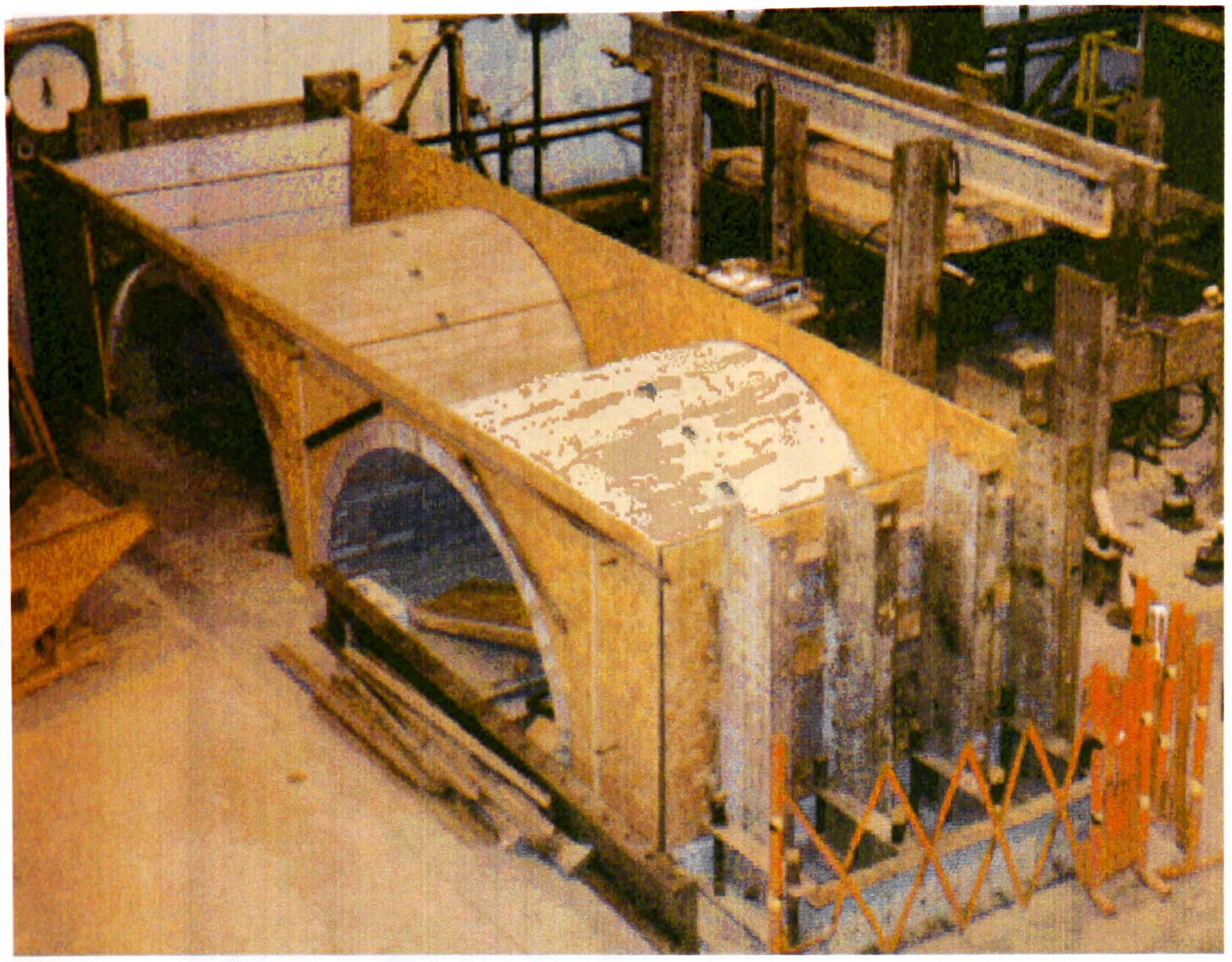

Fig. 6.6 Bird view of the empty double span bridge model.

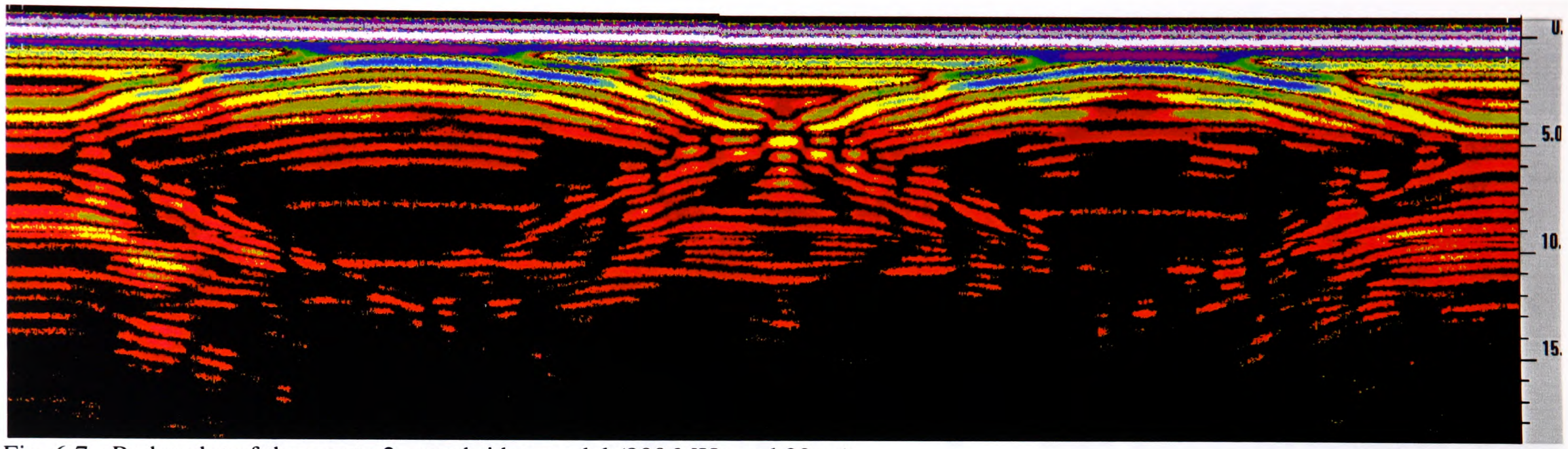

Fig. 6.7 - Radar plot of the empty 2-span bridge model (900 MHz and 20 ns).

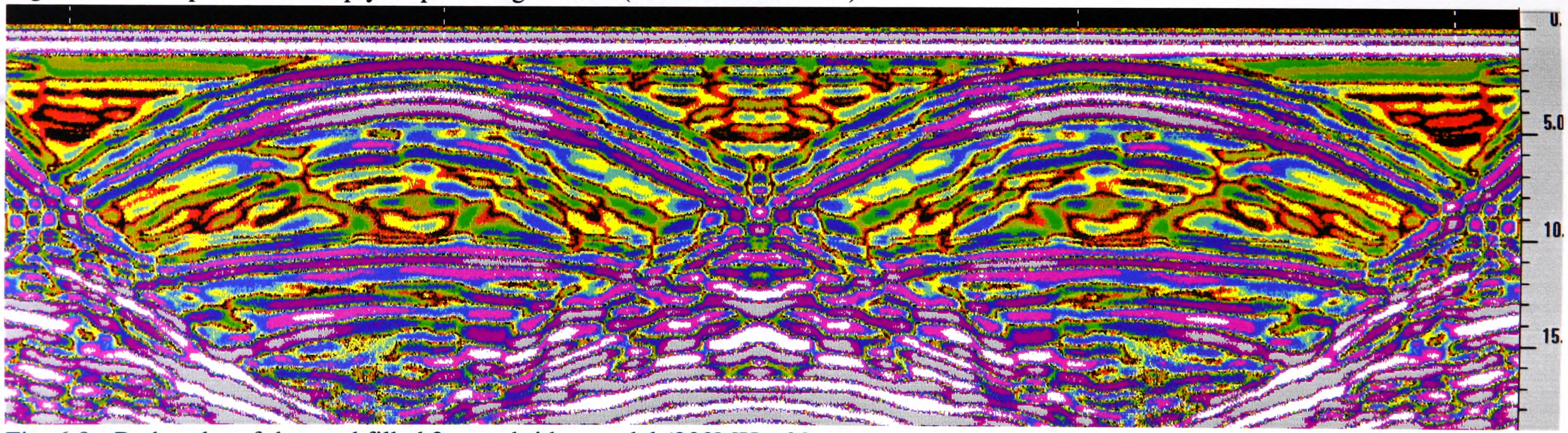

Fig. 6.8 - Radar plot of the sand filled 2-span bridge model (900MHz, 20nsec).

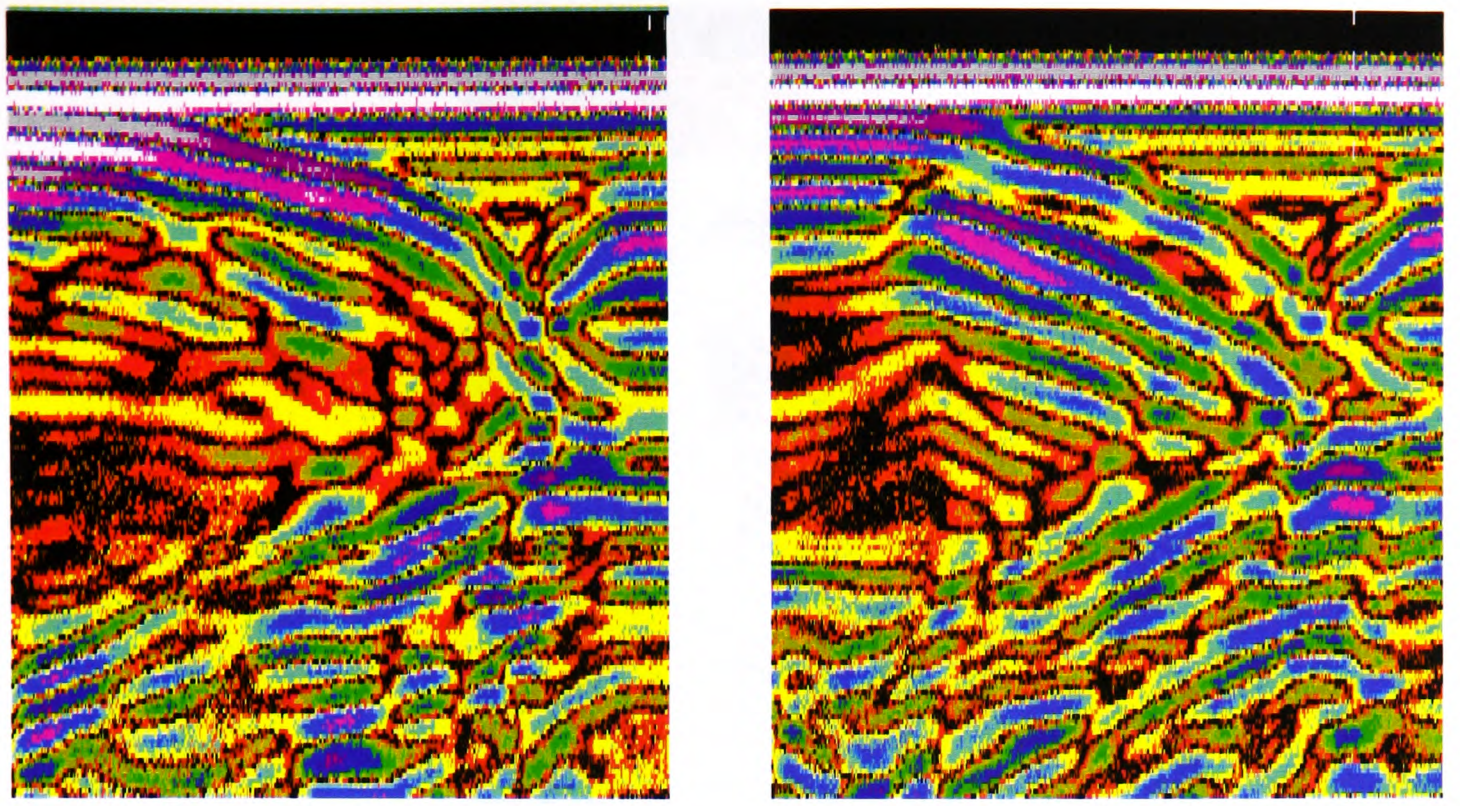

a) reflector placed on extrados

b) reflector on intrados of arch

Fig. 6.9 - Edited details of one of the arches from the empty test rig (900 MHz antenna and 15 ns time range).

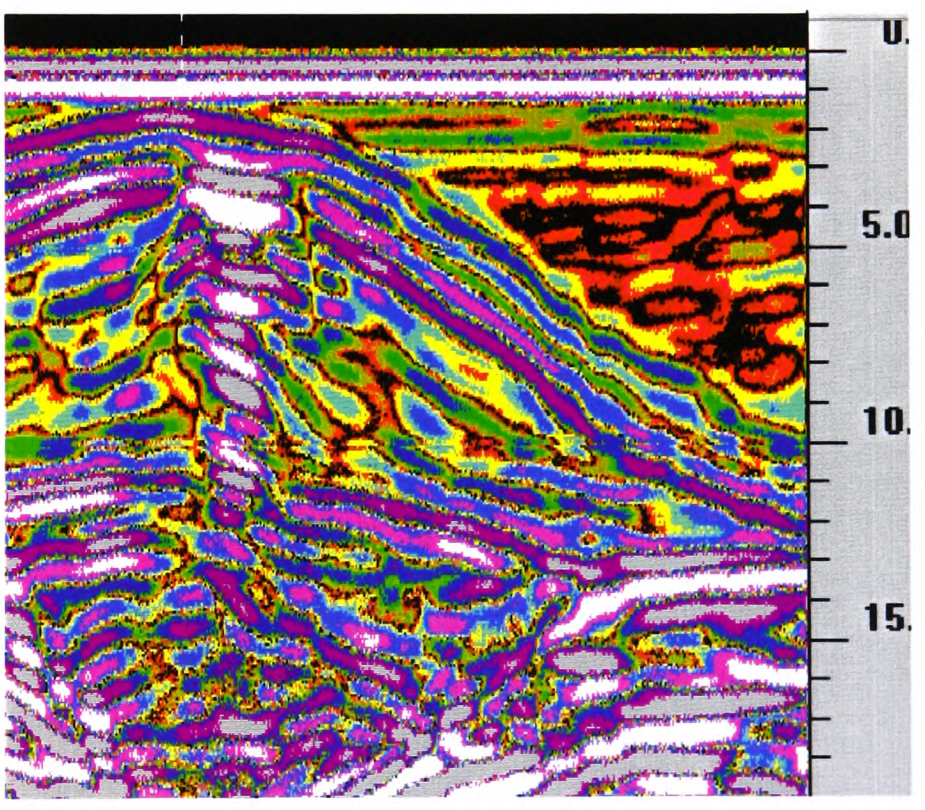

Fig. 6.10 - Edited detail of one of the arches from the sand filled test rig (900 MHz antenna and 20 ns time range).

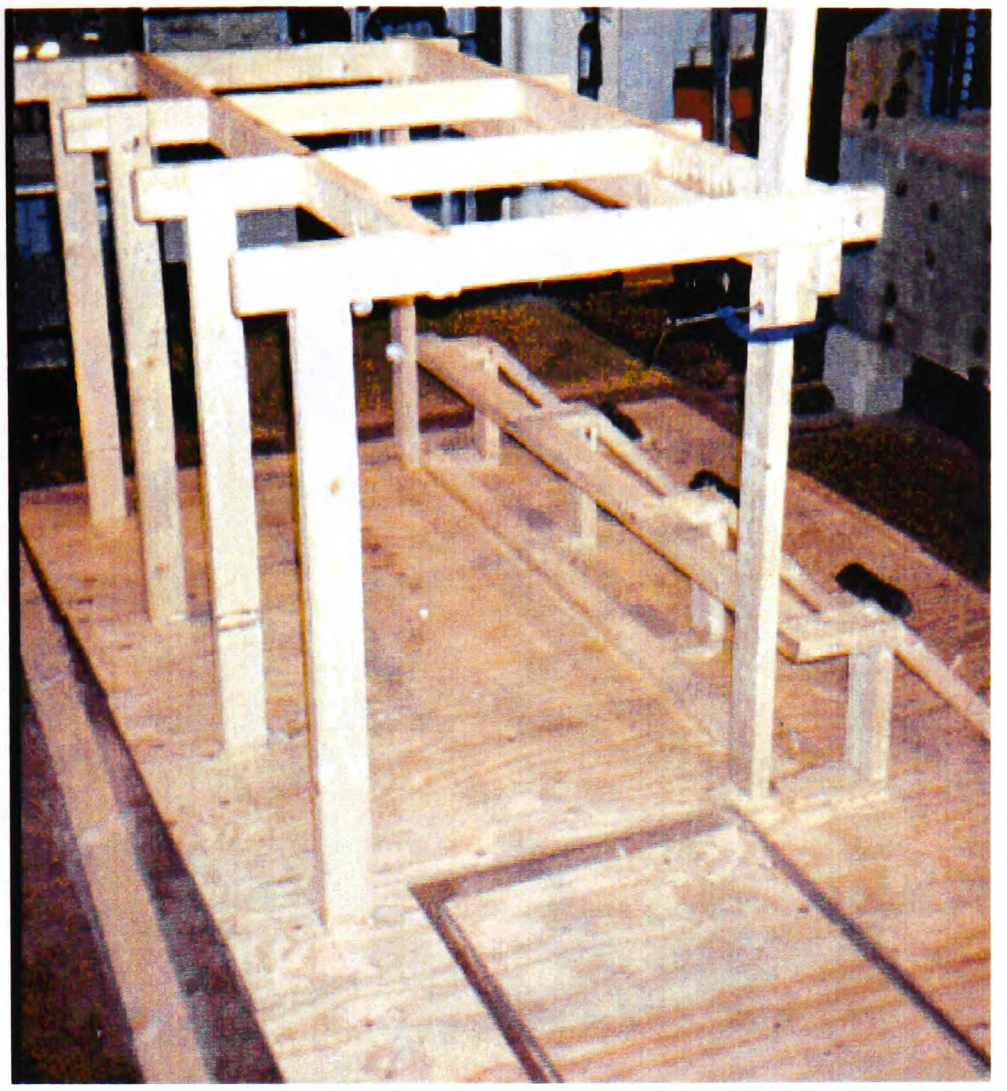

Fig. 6.11 - Plywood base and timber framework.

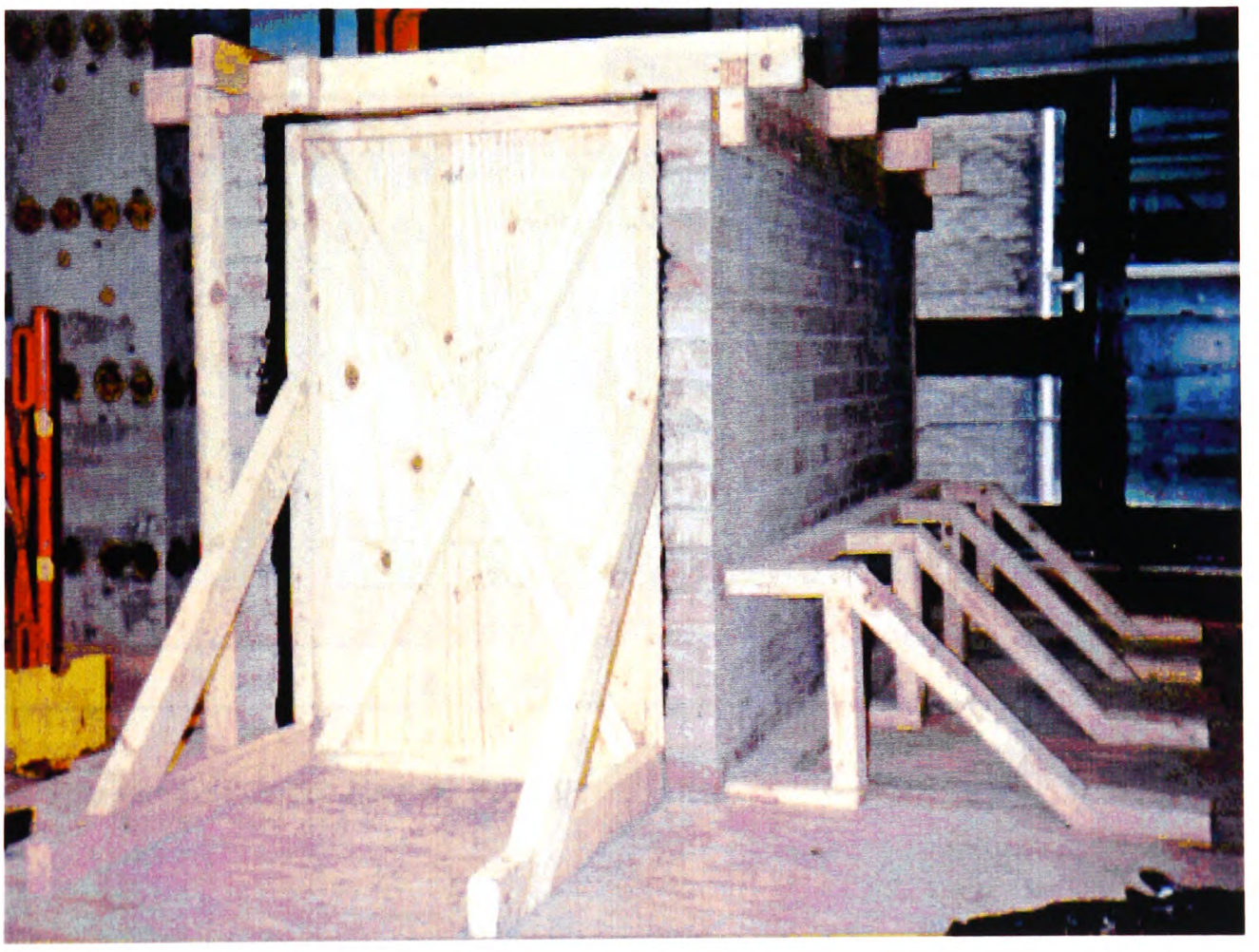

Fig. 6.12 - View of the completed test rig from the timber gate side.

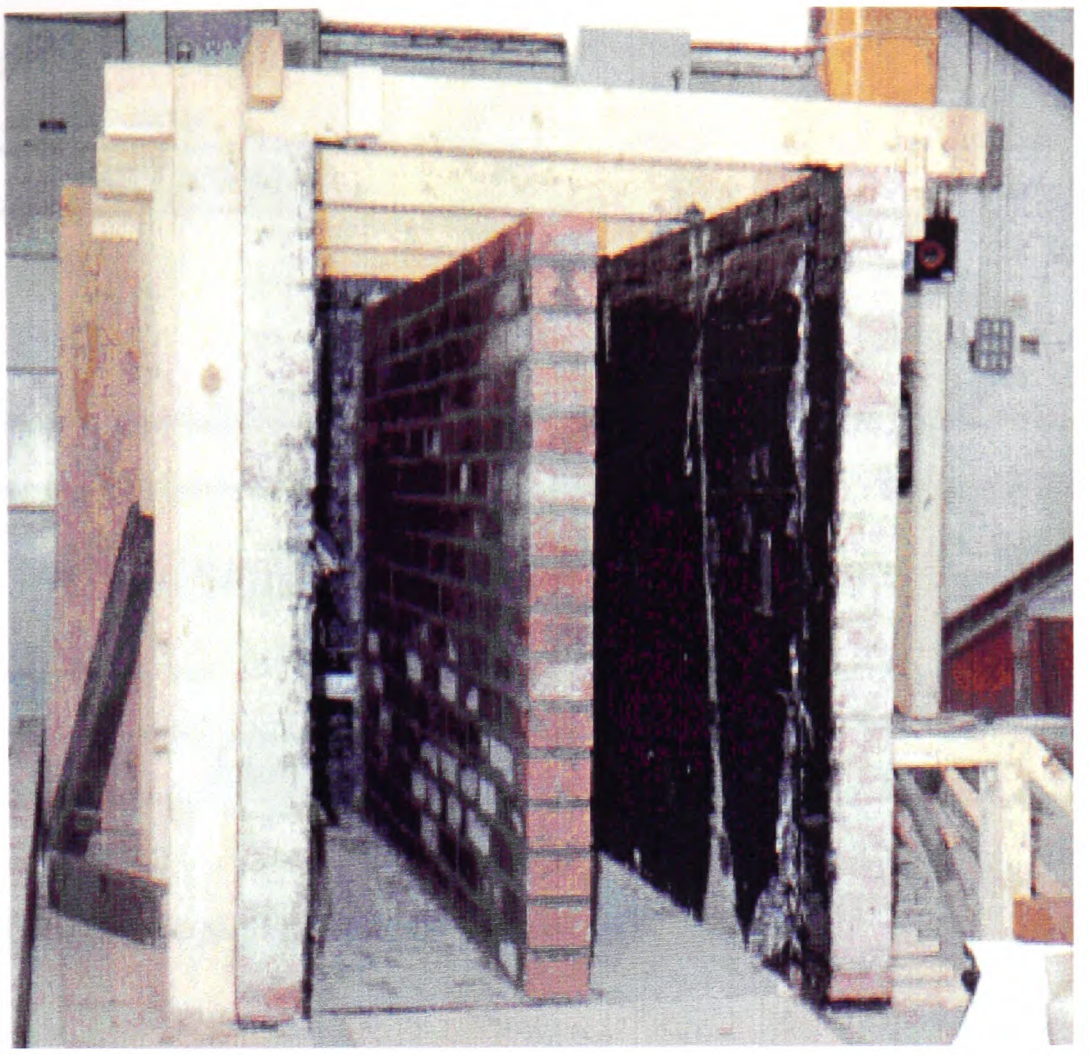

Fig. 6.13 - Modified test rig with partition wall.

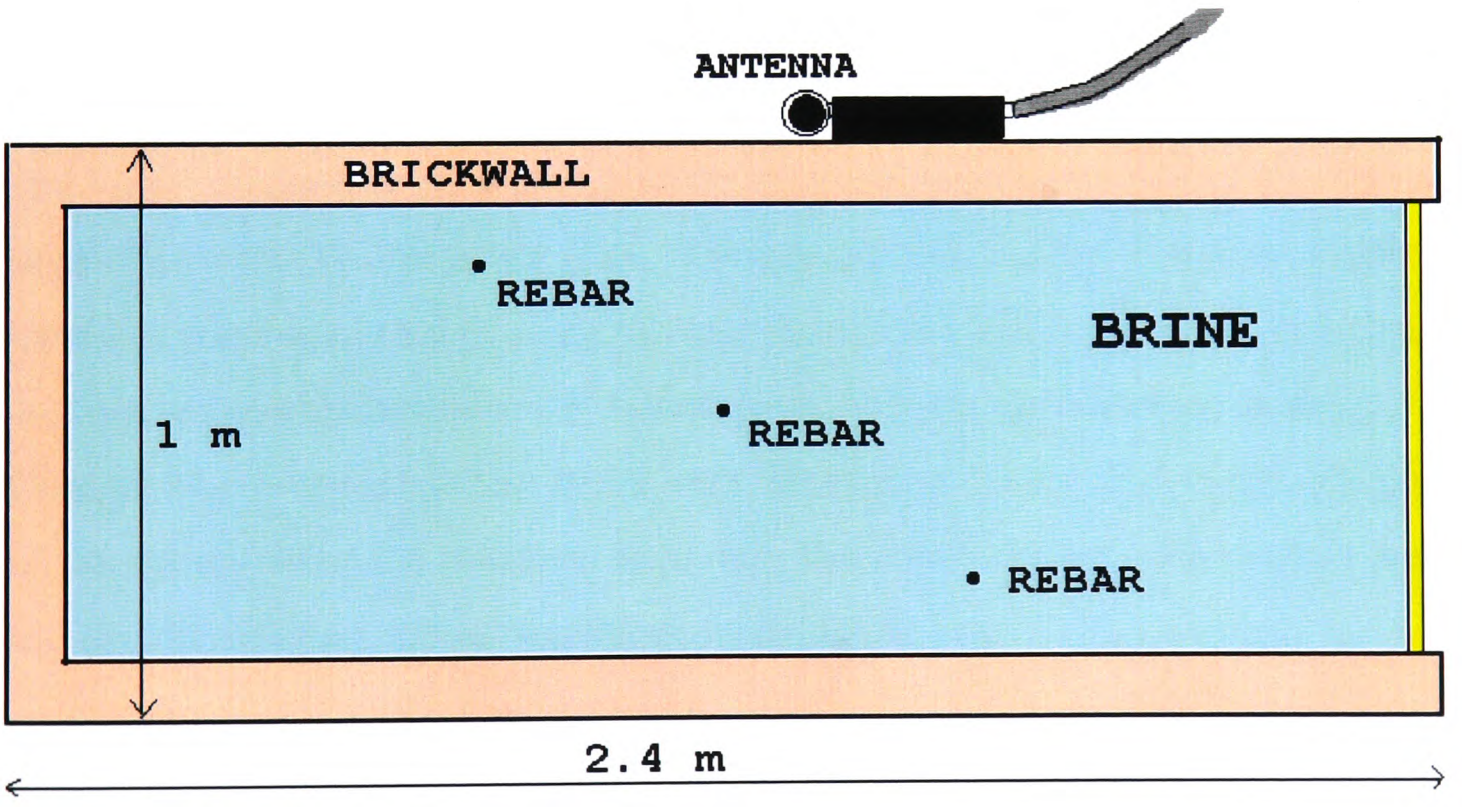

Fig. 6.14 - Top view of experimental test rig.

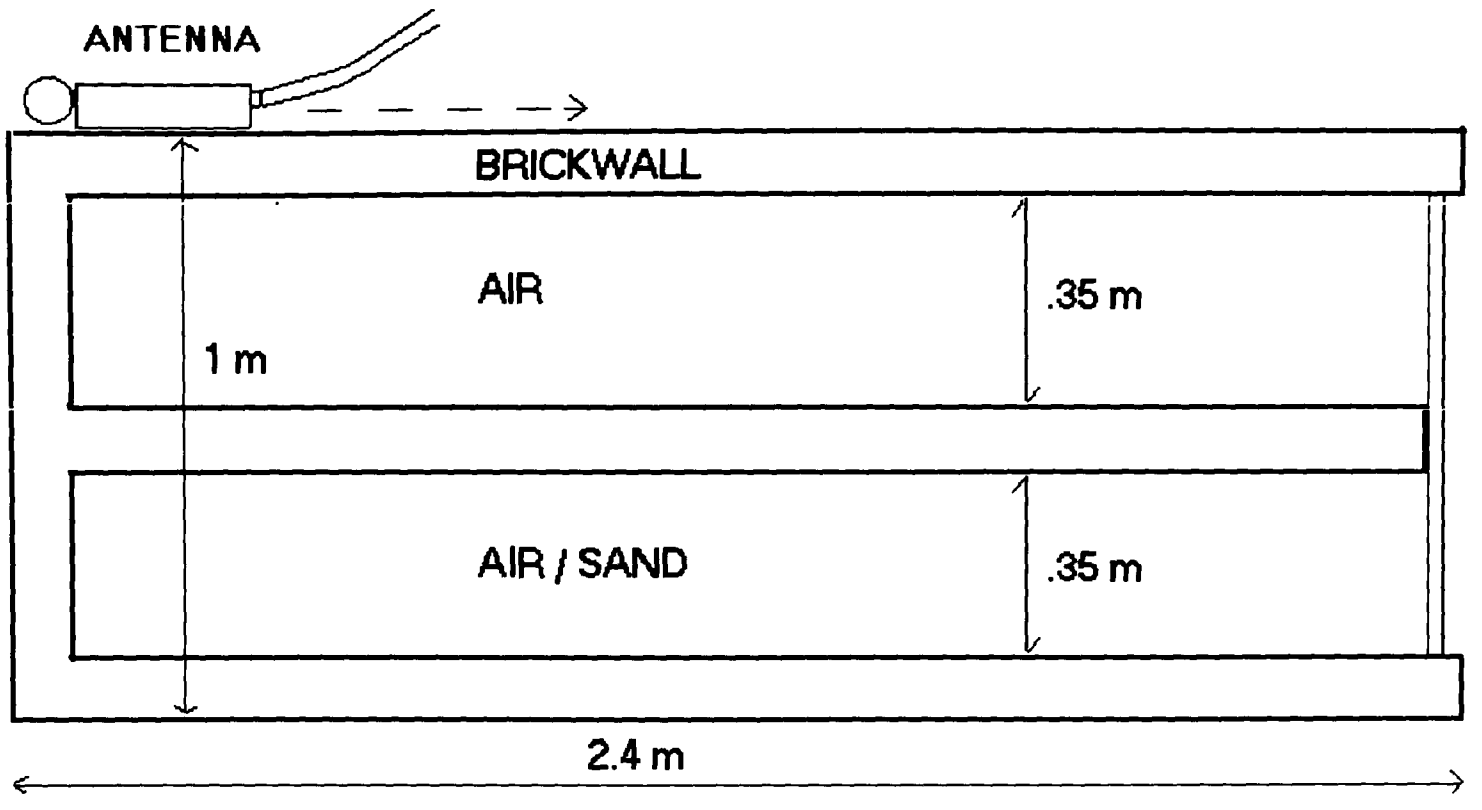

Fig. 6.15 - Top view of test rig modelling a composite masonry structure.

6.4.2 Radar survey procedures

In the initial experiments, the rig was tested empty and a series of radar measurements were collected for rig calibration purposes. This gave an indication of the data obtainable and the time ranges and gains to be used, together with the changes that would have occurred when fill was present in the rig, so that plots from different rig set-ups but with similar signal gains and time ranges could be compared.

Radar antennae with nominal centre frequencies of 500, 900 and 1000 MHz were used to collect transmission and reflection data on 1 and 2 channels, within time ranges of 15 to 120 ns. Data presented and analysed in the following sections were collected with a single 500, 900 or 1000 MHz bow-tie antenna in reflection mode and time ranges between 15 and 60 ns. The antenna was moved horizontally along one side of the masonry rig, scanning in the horizontal direction, to plot horizontal cross sections of the model structure. The timber framework was also used as a guidance for the position of scanning of the antenna, guaranteeing repeatability of the readings.

For the case where the set up included brine and re-bars, the radar plots presented here were collected with a shielded 900 MHz antenna moved along the 2.4 m brickwall, as can be seen in Fig 6.14. The antenna had a survey wheel attached to record a constant number of scans per unit distance travelled and to obtain a more accurate and smooth picture of the radar targets. Twenty centimetre marks along the direction of movement of the antenna were recorded at the top of the plots. Targets of the survey were the masonry walls and the metal re-bars. The survey was repeated for different salt concentrations in the water.

In the simulation of the composite cellular structure, the radargrams show data collected with 500 and 900 MHz antennae along the 2.4 m wall. Data collected with 1000 MHz antenna on the 1 m long head-wall are also presented and the position of the middle wall is marked at the top of the radar images. Reflection effects from the

masonry walls were investigated. Tests were repeated for comparison with the situation where sand was present.

6.4.3 Radar data analysis

6.4.3.1 Experiment with brine and re-bars

To study the effect of material conductivity on the radar survey and data, it was thought that a simple way of proceeding was to vary the conductivity of the chosen material by adding fixed quantities of conductive substance. Water and salt were considered the obvious materials to operate with, given that these are readily available and economic and are generally found in structural materials of bridges because of environmental site conditions (rain, snow, de-icing salt, etc.).

The saturation of water with sodium chloride (NaCl) is reached at approximately 26% of salt content to the water, depending on the temperature (see table 6.2). It was therefore planned to increase the salinity by adding sodium to the fresh water in 0.5 % concentration steps and to continue until the conductivity of the solution would yield such signal attenuation that the rebars (which would constitute the survey targets) could not be detected in the solution. Temperature and DC conductivity of the saline solution would be recorded at each step and related to the attenuation.

Solubility Wt. %	temperature (°C)	Solubility Wt. %	temperature (°C)
23	-21.1	26.83	50
24.25	-15	27.04	60
25	-10	27.27	70
25.6	-5	27.54	80
26.28	0	27.8	90
26.29	10	28.12	100
26.37	20	28.46	118
26.43	25	29.63	140
26.49	30	30.37	160
26.65	40	30.98	180

Table 6.2 - Solubility of sodium chloride in water (Seidell, 1940)

At the first stage of the experiment (0.5% salt concentration by weight) it was evident that the conductivity was already so high that, at that antenna frequency -900 MHz -, none of the re-bars was detected. The salt concentration had then to be decreased by deluting the solution. Data were recorded at 0.25, 0.1 and 0.05 % concentrations. Brine temperature and conductivity were monitored throughout the different stages of the experiment and values are recorded in table 6.3.

Brine temperature	Salt concentration	Conductivity
18 °C	0.05 %	735 µS
16.5 °C	0.1 %	1147 µS
17 °C	0.25 %	Out of range
19 °C	*0.5 %*	*Out of range*

Table 6.3 - Values of brine temperature, concentration and conductivity measured during the experiment.

The radargrams from set-ups with water at 0.05, 0.1 and 0.25 % chloride content were compared (Fig. 6.16, 6.17 & 6.18). The GPR method transmits and receives signals recorded over a spatial window - the antenna aperture. Because of the wide field of view of the radar antenna, objects off to the side of the antenna can be recorded, resulting in hyperbolic reflection patterns - as in the case of the metal rods. These patterns may vary slightly with the frequency used and the electromagnetic properties of the materials under study. In all the cases presented here, the hyperbolas from the rebars have relatively low amplitude and show short and flat branches which indicates a decrease of the energy power in the radar waves, probably with loss of the high frequency components of the signal. The phenomenon of the flat hyperbolas is explainable with the fact that the signal reaches the rebars following the propagation through the masonry wall. The wall has the effect of spreading the signal beyond the cone of emission of the antenna so that at the wall-water interface, the signal source is not focused at a point but is spread and weakened. Compare for example the shape of the hyperbolas in figures 6.16 and 6.33 which are both radargrams of rebars in brine at 0.05% salt content, but in the

test rig of figure 6.33, the masonry wall is replaced by a thin polyethylene plastic tank.

In figure 6.16, the brine has a sodium chloride concentration of 0.05 % by weight. The radar waves travel through the front brick masonry wall and 80 cm depth of water to reach the back wall, and encounter the three rebars along the way. Reflections from the three rebars are all visible, as is the reflection from the back wall. It is worth noting the great difference between the amplitude of the signature of the front wall and that of the back wall. The dissimilarity shows up in the amplitude of the signal and is due to various factors - primarily the attenuation of the wave. Causes of this attenuation are the variation in electrical properties of the materials at the interface between brick masonry and water. This strong interface causes a large part of the signal to be reflected back, with only a small part of the wave energy capable of travelling through the water and reaching the back wall, the signature of which is very much attenuated compared to that from the front wall.

A similar comparison can be made between the hyperbolas of the three re-bars. The deeper the signal travels through the conductive material that is salt water, the more it is attenuated. In fact, another factor that distinguishes microwave radiation is its dispersive nature. As a result of the high permittivity of water (typical values of dielectric constant for water are of the order of ε = 80-81) and high conductivity of brine, the signal attenuates quickly; and whilst the reflection from the first re-bar is fully visible, the reflection from the third re-bar is only just noticeable (radar plots are shown in logarithmic grey scale transform which greatly emphasises the low amplitudes).

Fig. 6.17 shows the case of brine concentration of 0.1% and fig. 6.18 shows the experiment with 0.25% chloride concentration. In Fig. 6.17, the reflection from the back wall has completely disappeared and so has the reflection from the third re-bar. Branches of the hyperbola from the first re-bar are shorter and less pronounced than in the previous case. Reflection from the second re-bar is almost reduced to a flat thin

line. In the case of Fig. 6.18, reflection from the first re-bar is almost reduced to a point: no branches are visible. None of the patterns from other features of the experimental set-up, except for the front wall, are evident.

Following this comparison work, signal waveforms were analysed in the time domain to quantify the reduction of signal power due to the increasing conductivity values with increasing salt concentrations, as from table 6.3. The impulse response to the propagation in water with increasing conductivity was estimated from the reflections obtained from the immerse metal rods. The decrease in energy was calculated in relative terms, measuring the amplitude of the peaks generated by the first re-bar.

For each salt concentration, the waveforms chosen in correspondence of the apex of the hyperbola from the re-bar - here the amplitude is maximum - were first averaged (a function included in the radar software, RADAN ©, allows "stacking" of the chosen number of scans)(Fig 6.19). Then, the linear gain (applied at the time of recording the data as a mean of contrasting the signal attenuation at increasing scan depth) was removed and the amplitudes of the waveforms were normalised so that they can be directly compared (Fig. 6.20). These operations were performed with software (Excel © and Matlab ©) which allowed more sophisticated signal processing and data handling.

Fig. 6.21 shows edited unfiltered portions of the three waveforms shown in figure 6.20, zooming on the main reflection peaks generated from the re-bar, in the form of a sinusoid between 7 and 10 ns on the time axis. It is this peak which has been used for the calculations of the relative decrease of signal amplitude with increased conductivity.

From Fig. 6.22 and Table 6.3 it is evident how an increase in conductivity of only 0.4 $mS.m^{-1}$, causes a reduction of 34% in the amplitude of the signal, when passing from 0.05% to 0.1 % salt content in the water: one third of the power of the signal is lost. When the salt content increases to 0.25%, the signal amplitude decreases a further

17%, reaching only 50% of the power of the signal registered at 0.05% salt content. Note that even though the sodium chloride content doubles from 0.05 to 0.1%, and increases five times to reach 0.25%, the salt concentrations considered in the experiment are low values compared to sea water (3 - 3.5% on average) or to localised high concentrations of salt as could be encountered in masonry arch bridges and other historical and modern structures due to de-icing salt, capillary suction from ground through foundations and other environmental factors (Baronio *et al.*, 1995; Baronio and Binda, 1989).

The outcome from the amplitude analysis study is an exponential reduction in signal amplitude as the conductivity of the material increases due, in this case, to increasing sodium chloride content. From the above discussion and equation (4.3) it follows that conductivity affects the attenuation of the signal, which in turn governs the penetration capability of the signal.

To verify and confirm whether the phenomena observed were to be attributed primarily to a variation of the real part of the dielectric constant or to the increased conductivity of the material, a calculation of the dielectric constant of salt water was conducted. First, the velocity of the electromagnetic wave through brine was calculated for the three chloride concentrations considered. From the known geometrical position of the reflectors in brine (10, 40, 60 cm), and the 2-way travel times from each reflector measured from the radargrams, the pulse velocity was calculated by time domain analysis and found to be constant throughout (see Fig. 6.23). From the velocity values obtained and equation (4.2), the dielectric constant of brine at the salt concentrations used in the experiment was calculated and found to be in the narrow range between 80 and 81 which covers the dielectric constant values of sea water and fresh water. The calculation, whilst agreeing with values published in literature regarding the dielectric constant of salt water (Kraus, 1988; Von Hippel, 1954; Nat. Bureau of Standards, 1958), confirms the initial hypothesis of constant dielectric constant at the increase of salt content. That is, at this frequency, the permittivity controls the speed of the E.M. pulse, whilst increasing conductivity

reduces the depth of penetration. For more experimental data regarding wave velocity in salt water and calculation of dielectric constant, see also section 6.5.

6.4.3.2 Experiment with sand and air/water inclusions

Figures 6.24 & 6.25 refer to experiments in which a re-bar and a void, or alternatively a water pocket, were embedded in sand fill. The sand was in a dry compact condition in the case of fig. 6.24, and with a 10% moisture content and still compact conditions in fig. 6.25. The target's dimensions and positions are represented by a circle and a rectangle which have been drawn above the radar signatures of the targets for ease of identification.

From comparison of 6.24 (a) and (b), it can be seen how in (b), the fresh water inclusions offers a greater reflection signature (in width of the "hyperbola" and magnitude of the reflected signal) than in the case of air void. The rear brickwall of the test rig, which is partially visible in (a), has almost disappeared in (b), because it is masked by the water pocket. When the fresh water is replaced by salt water (0.5% salt content) such as in case (c), only a trace of the rear brick wall is visible. The "length in time" of the air void signature is much shorter than in the case of water pocket and this is due to the higher velocity of the wave in air.

In case of wet fill (fig. 6.25), the higher dielectric property of the sand, due to water content, causes the signal to have a smaller depth of penetration and greater attenuation than in the case of dry fill. The rear brickwall is not identifiable in any of cases (a), (b) or (c) and reflections from all types of targets are weaker than when embedded in dry sand. The reflection from the inclusion is more visible in (a) than (b) or (c), because of the higher reflection coefficient between air and wet sand in (a), than between water and wet sand in (b) or (c).

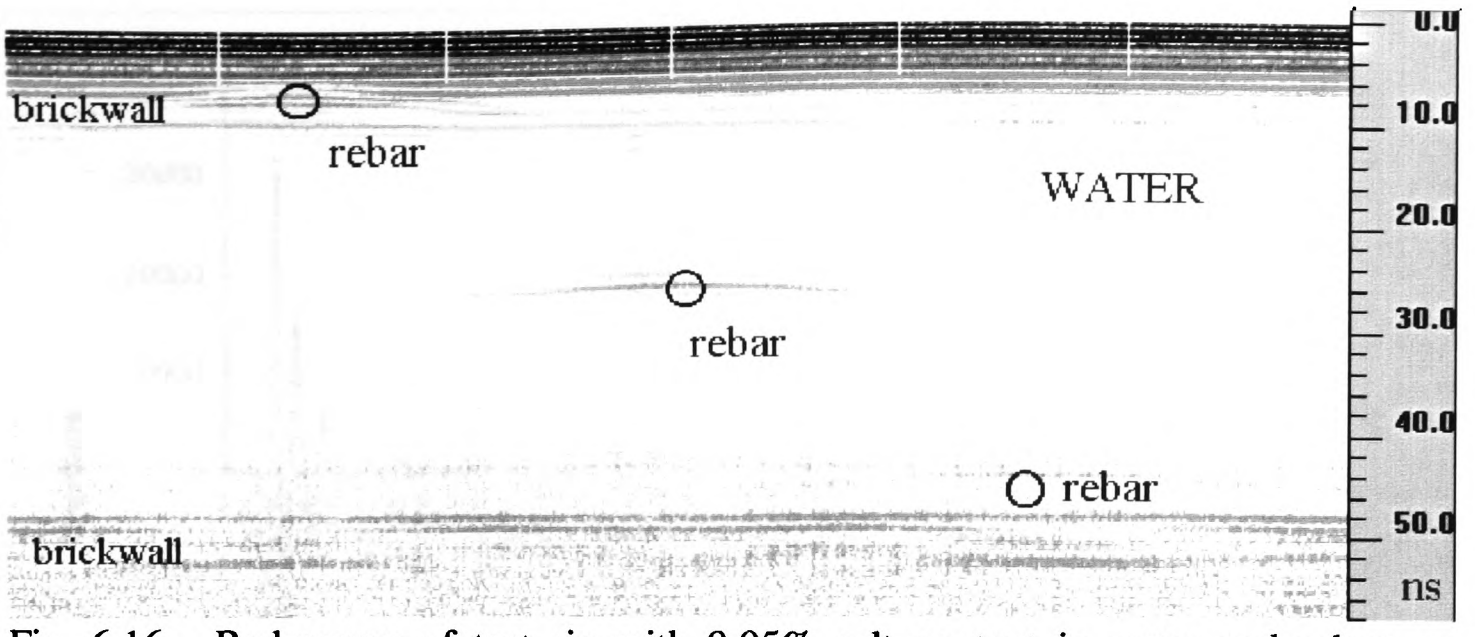

Fig. 6.16 - Radargram of test rig with 0.05% salt content in water and rebars at increasing depth.

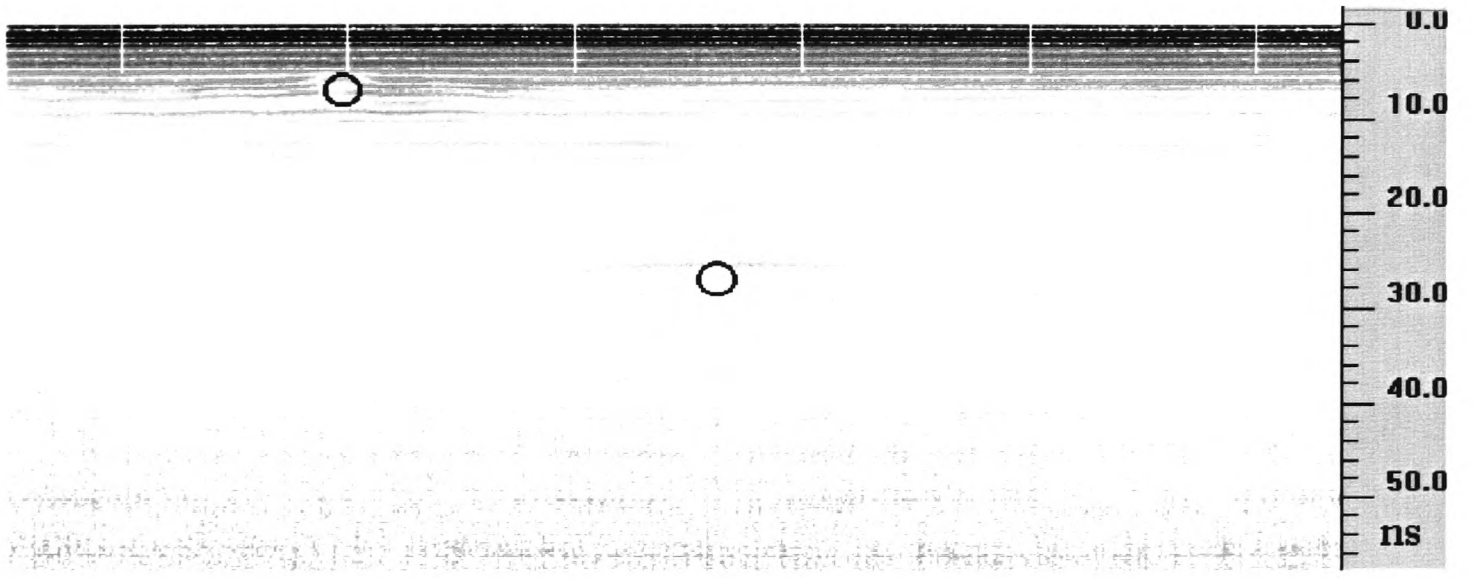

Fig. 6.17 - Radargram of test rig with 0.1% salt content in water and only two re-bars visible.

Fig. 6.18 - Radar plot of test rig with 0.25% salt content and reflection from first re-bar visible.

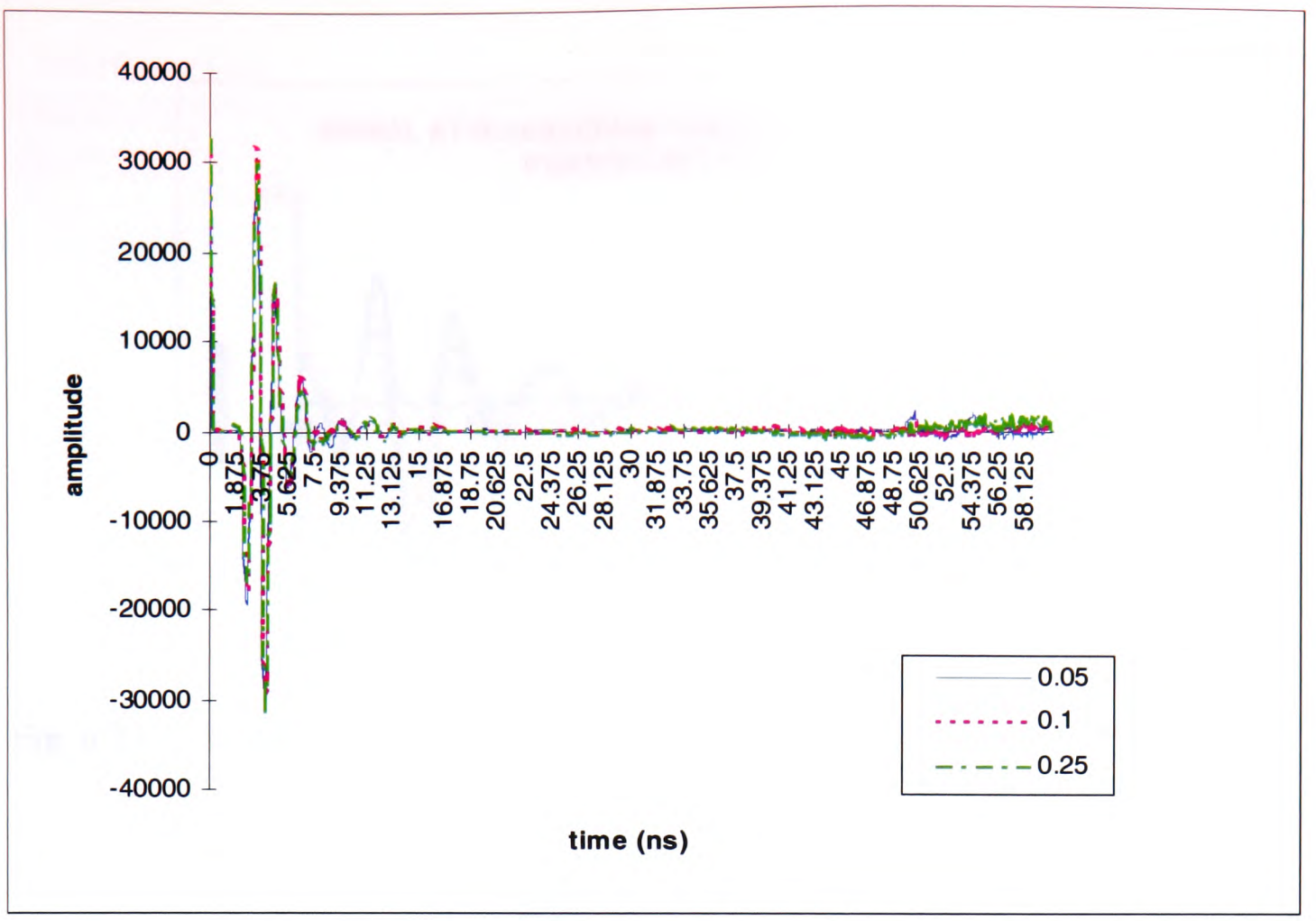

Fig. 6.19 - The averaged waveforms obtained for each brine concentration.

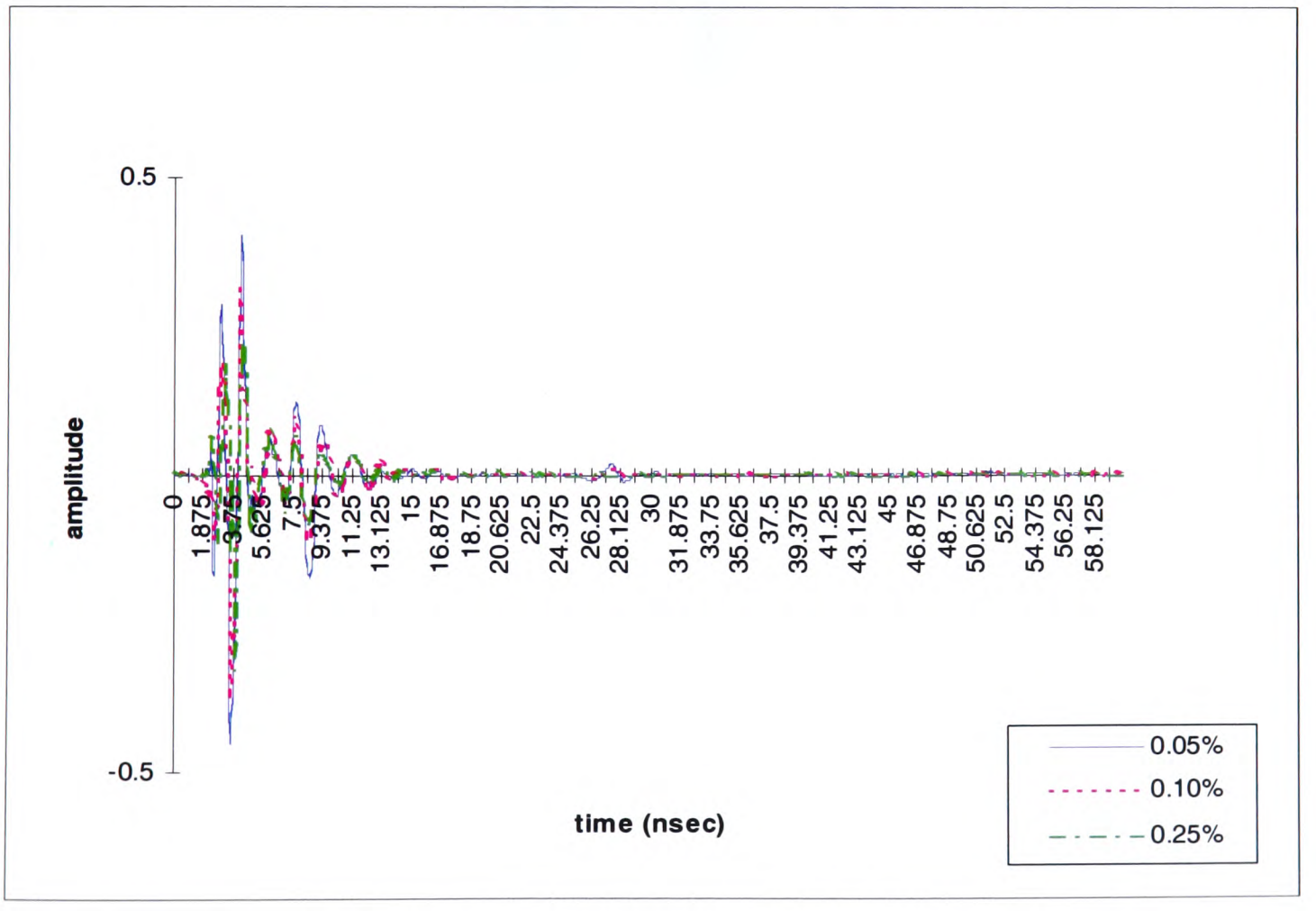

Fig. 6.20 - The normalised amplitude of the waveforms after removing the linear gain.

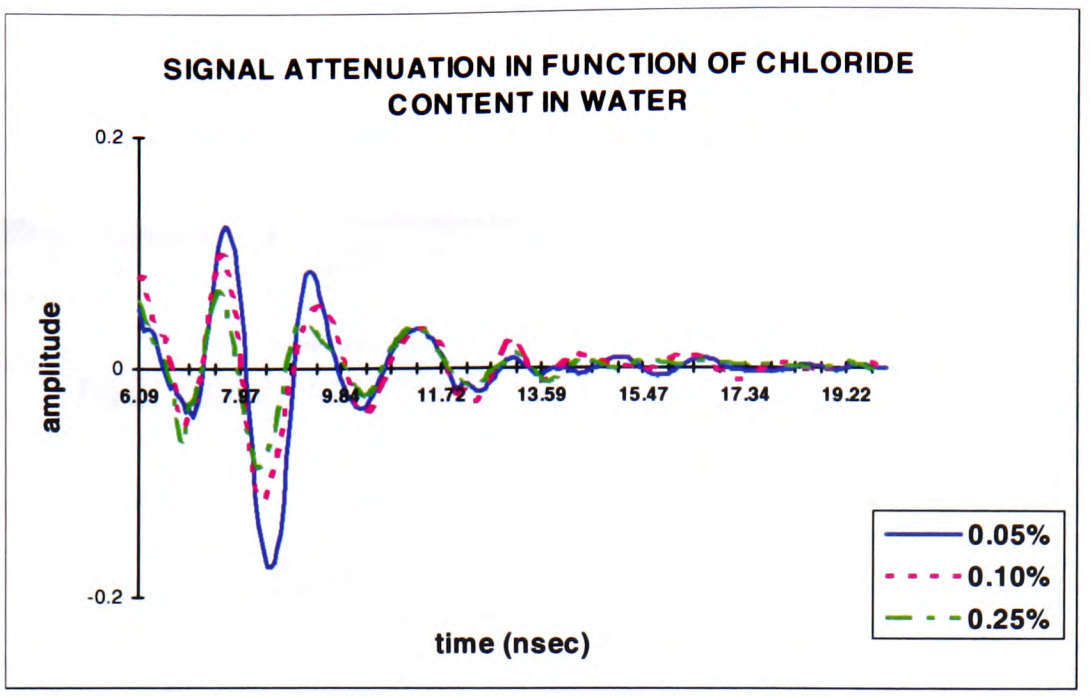

Fig. 6.21 - The reflection from the first re-bar at the increase of salt content in water.

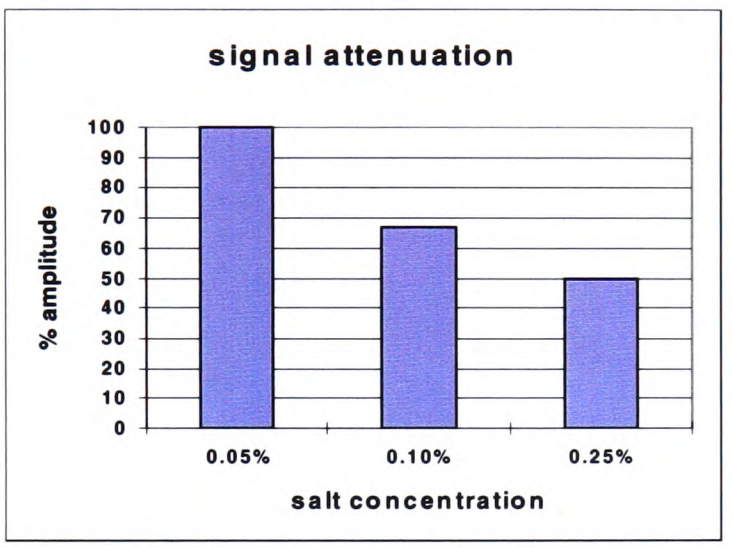

Fig. 6.22 - The relation between salt concentration in water and the relative decreased amplitude of the signal, calculated from the experimental data.

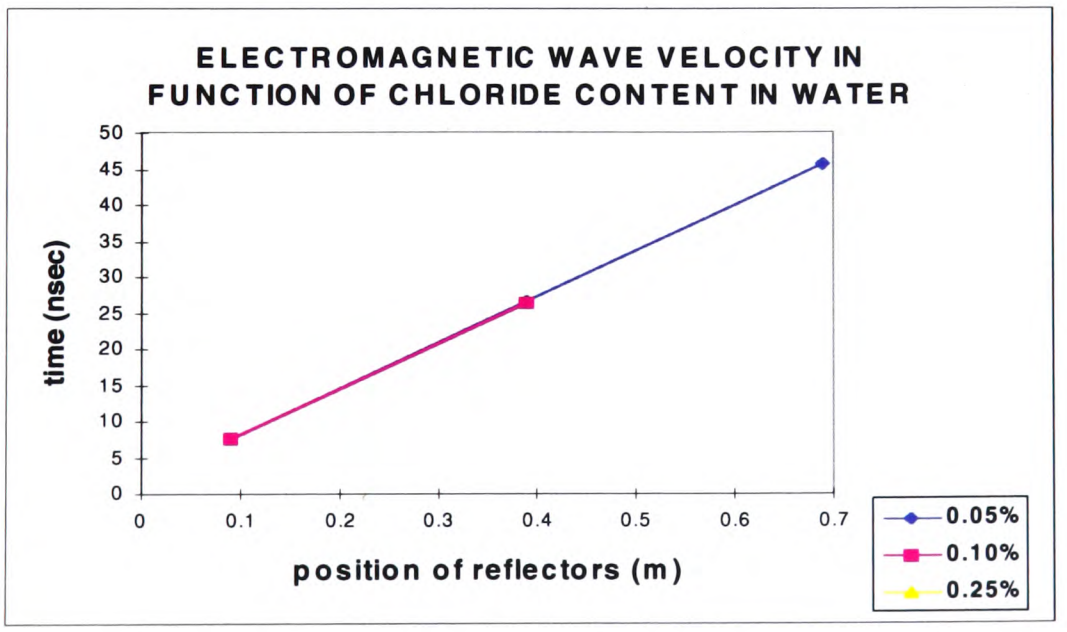

Fig. 6.23 - Representation of the electromagnetic wave velocity measurements calculated by time domain analysis.

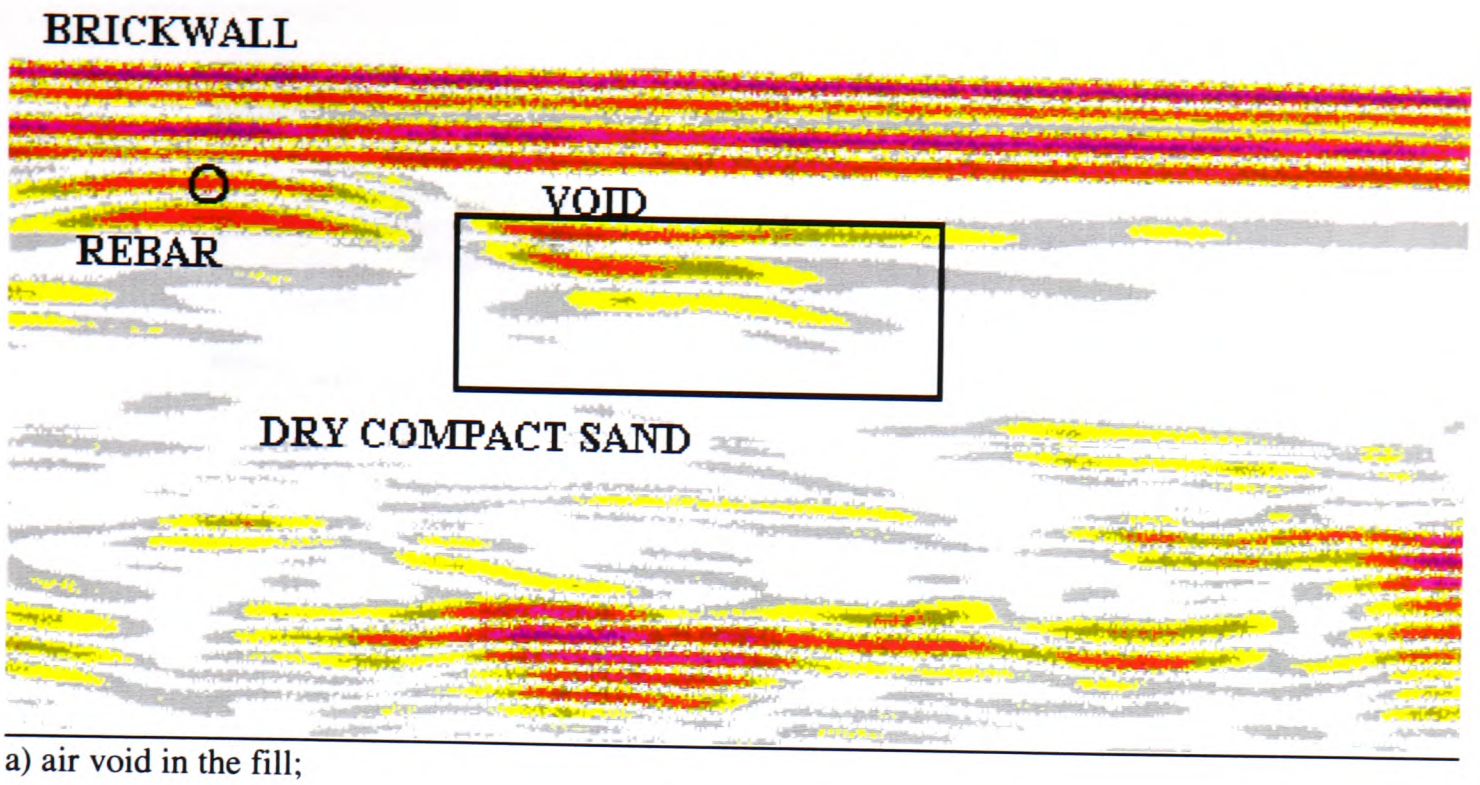

a) air void in the fill;

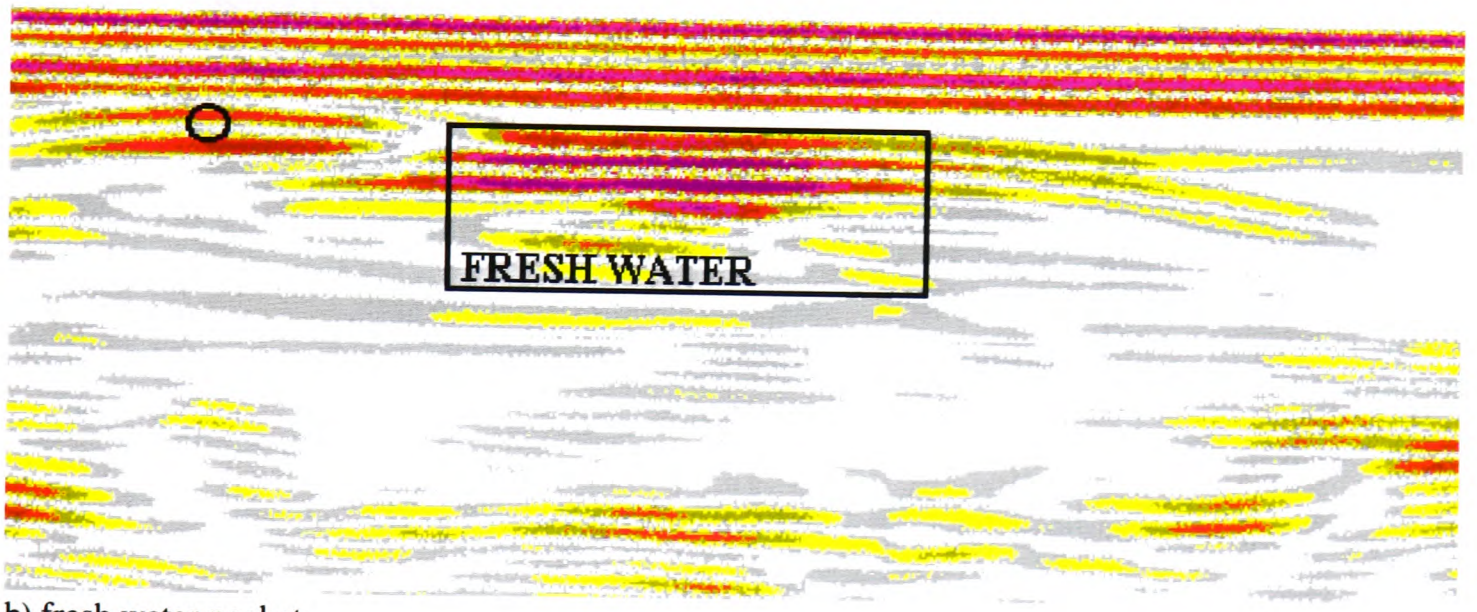

b) fresh water pocket;

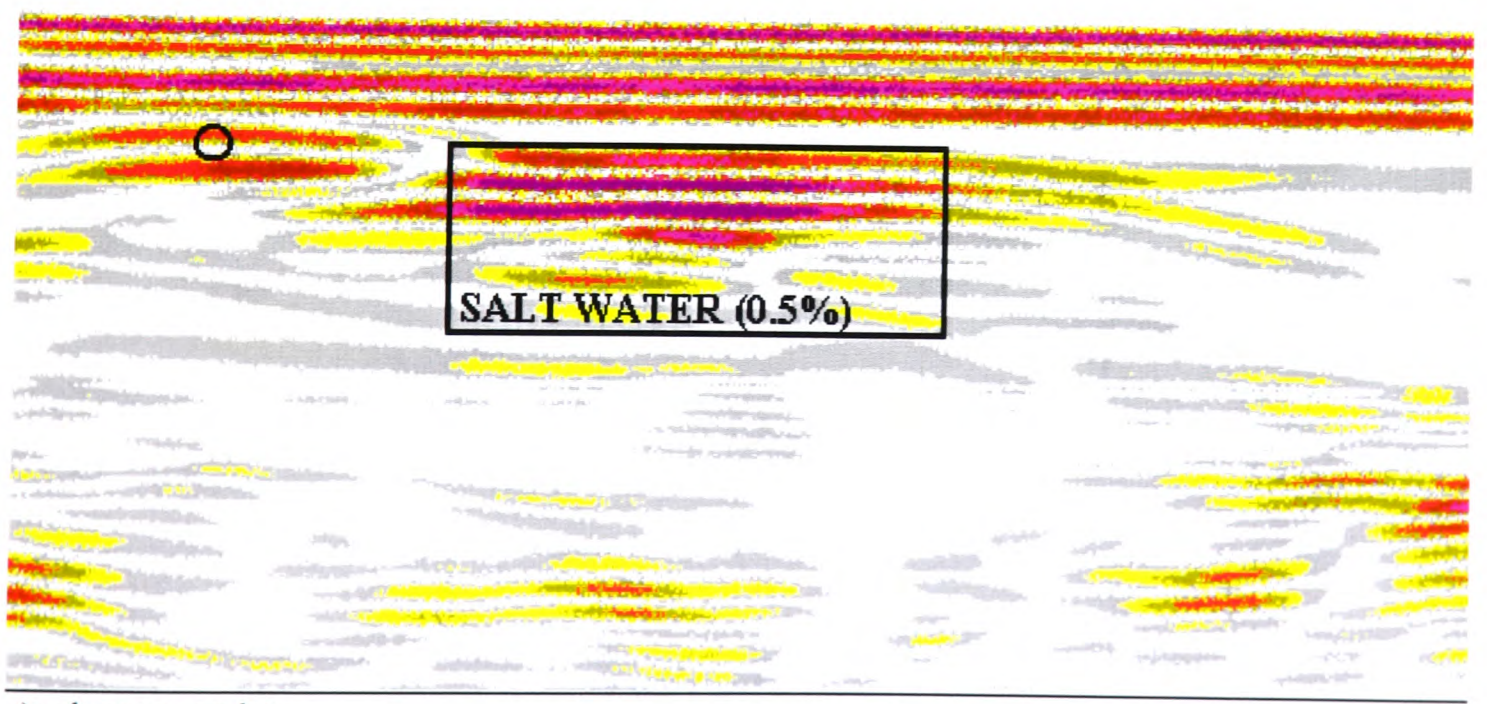

c) salt water pocket;

Fig. 6.24 - Radar plots of test rig with dry compact sand as backfill material.

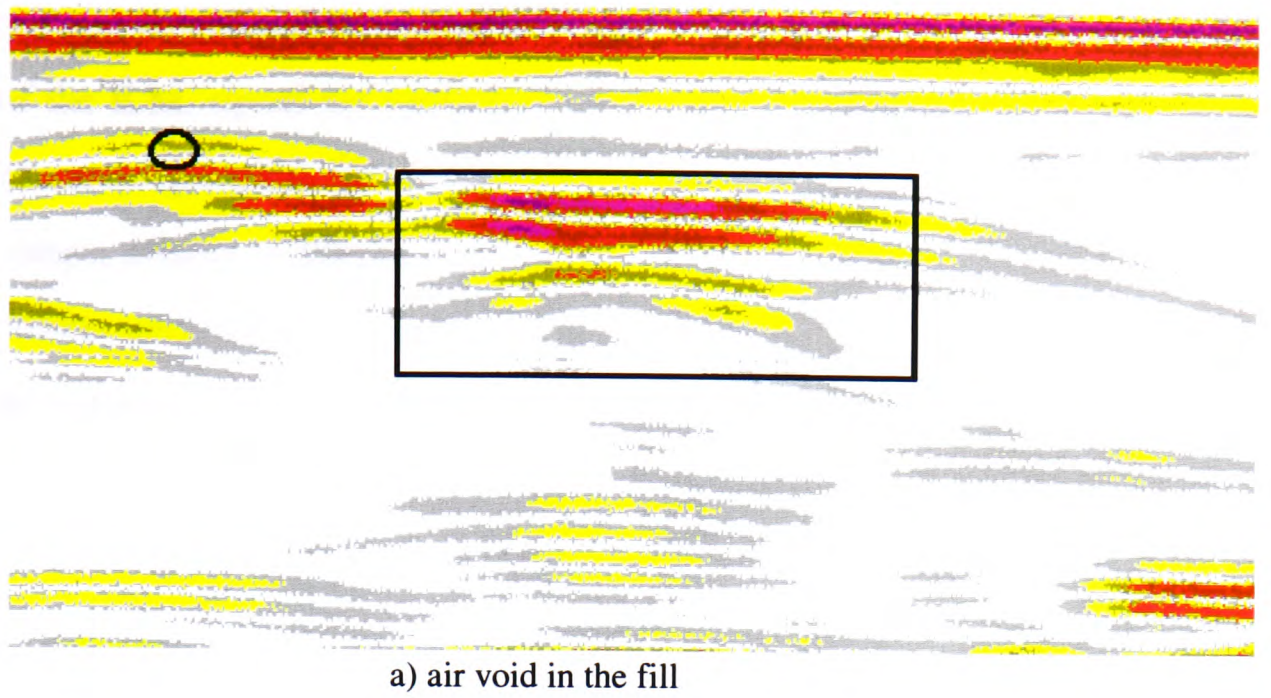

a) air void in the fill

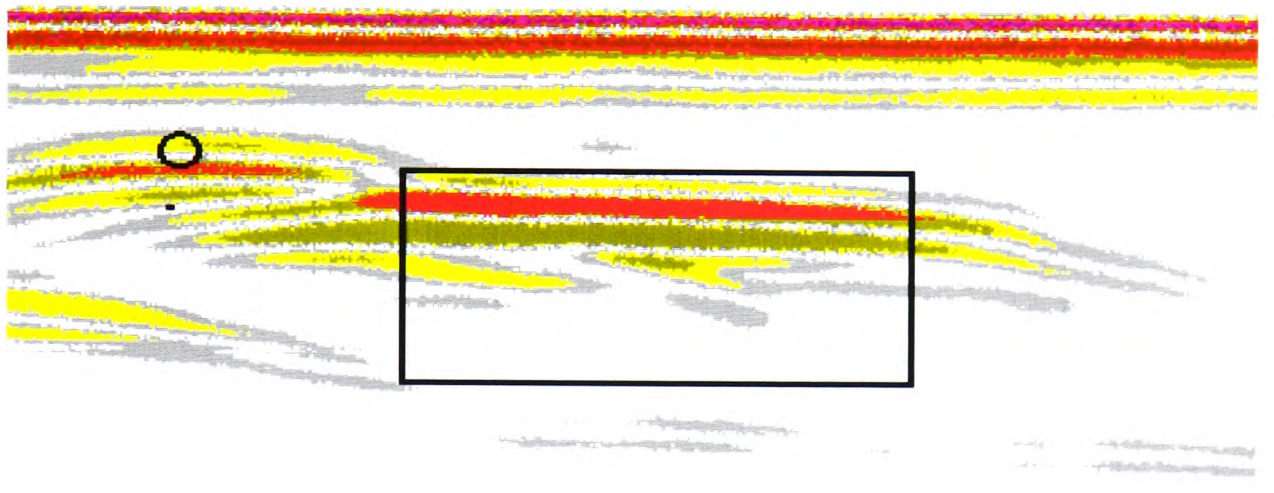

b) fresh water pocket;

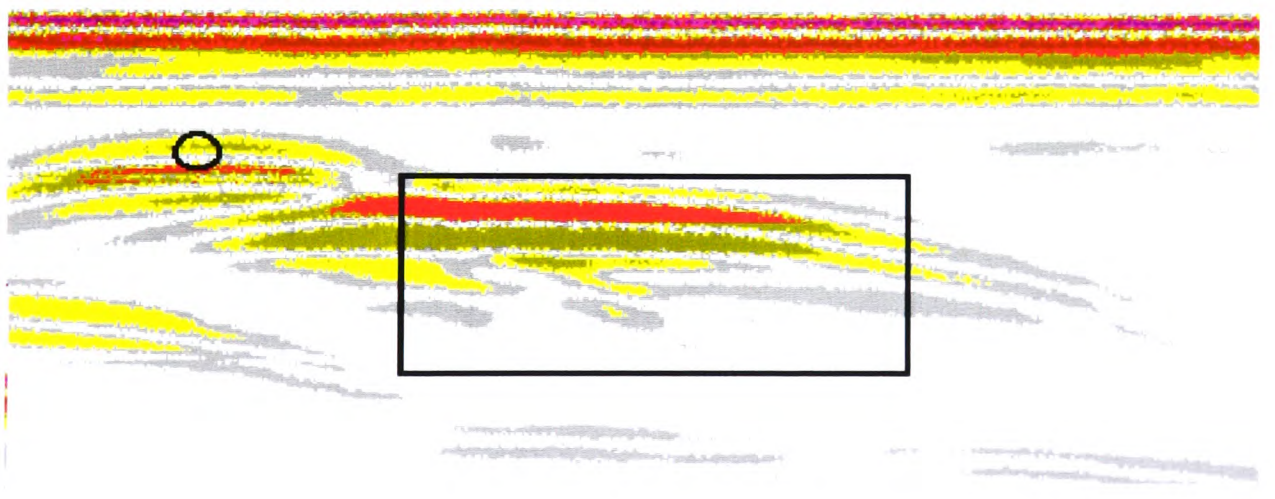

c) salt water pocket;

Fig. 6.25 - Radar plots of test rig with wet (10% m.c.) compact sand as backfill material.

6.4.3.3 Experiment with cellular structure

In the case of composite masonry structures, when no fill is present, phenomena of defraction of the E.M. signal are more evident. Fig. 6.26 is the radar plot obtained from the structure depicted in Fig. 6.15, with a 500 MHz frequency antenna. Over a 60 ns time range, effects of symmetrical refraction of the signal from the side walls are clearly visible and manifested primarily in the two "St. Andrew's crosses" with centre at approximately 16 and 28 ns time-depth. Multiple reflections from the longitudinal walls are also noticeable. The phenomenon is accentuated by the propagation of the signal through air which causes the antenna field pattern to modify and the beam of propagation of the signal to spread over a wider angle when travelling in air than when transmitting through soil or other material.

The plot in Fig. 6.27 is obtained from the same structure, with the use of 900 MHz antenna and a 15 ns time window. The three longitudinal walls are identified and their position has been indicated on the plot at approximately 2, 5 and 8 ns. As a result of the relatively large change of dielectric constant at each wall/air interface, the value of the reflection coefficient between brickwall and air, calculated from equation (4.4), is high. This permits a small portion of the signal to reach the 3rd wall, which is resolved, but whose reflection is highly attenuated compared with that from wall 2.

In Fig. 6.28 the time shift of wall 3 is visible and due to the presence of dry loose sand in the bottom half of the section of the structure. The sand in the 2nd cell, with its associated lower E.M. velocity, causes the reflection from the 3rd wall to appear in a lower position (approximately 9.5 ns), corresponding to an increased 2-way travel time if compared with Fig. 6.27. The velocity through the sand was estimated to be 0.205 $m.ns^{-1}$ (Fig. 6.29) and a dielectric constant of 2.1 was consequently calculated. This value is relatively low and at the bottom end of the range of dielectric constant expected for sand, confirming that the physical properties of the material (moisture content near 0% and porosity high) affect its electromagnetic behaviour and dielectric constant.

In order to investigate the radar signature obtained from a wall constructed perpendicular to the direction of scan of the antenna and the effect of the presence of fill at the back of a wall, data were collected with a 1000 MHz antenna scanning on the 1m long head-wall (Figs 6.30 & 6.31). In the radar plot of Fig. 6.30 the presence of the perpendicular wall is clearly resolved and the position marked with a dashed white line. Effects of the refractions of the E.M. waves from the side walls are similar to the signatures noticed in fig. 6.26 but made more complicated by the presence of the intermediate wall. On the left hand side of the radar plot (Fig. 6.31) the presence of sand at the back of the wall causes the reflection at the interface wall/sand to have a reduced amplitude compared with the wall/air situation and refraction effects due to the side walls are also attenuated.

6.5 Polyethylene box model

6.5.1 Test rig characteristics

A 450 litres capacity tapered rectangular polyethylene tank of 1500x585x740 mm dimensions (fig. 7.1), was used to reproduce similar testing set-ups to those reported in section 6.4.3.1. Identical re-bars to those described earlier, were suspended in water at the salinity concentrations reported in table 6.4; the corresponding conductivity values were also measured and are reported in tab. 6.4 and fig. 6.32. The same 900 MHz antenna as in 6.4.3.1 was moved on the external rig surface.

6.5.2 Experiment with re-bars in fresh and salt water for calculation of velocity and ε.

The experiments were aimed for comparison with those reported in 6.4.3.1, where the test rig was built in brick masonry. Therefore the position of the rebars replicated that of those experiments. For the tests carried out in this case, an example of the plots obtained is shown in figure 6.33 for re-bars in water with 0.05% salt content.

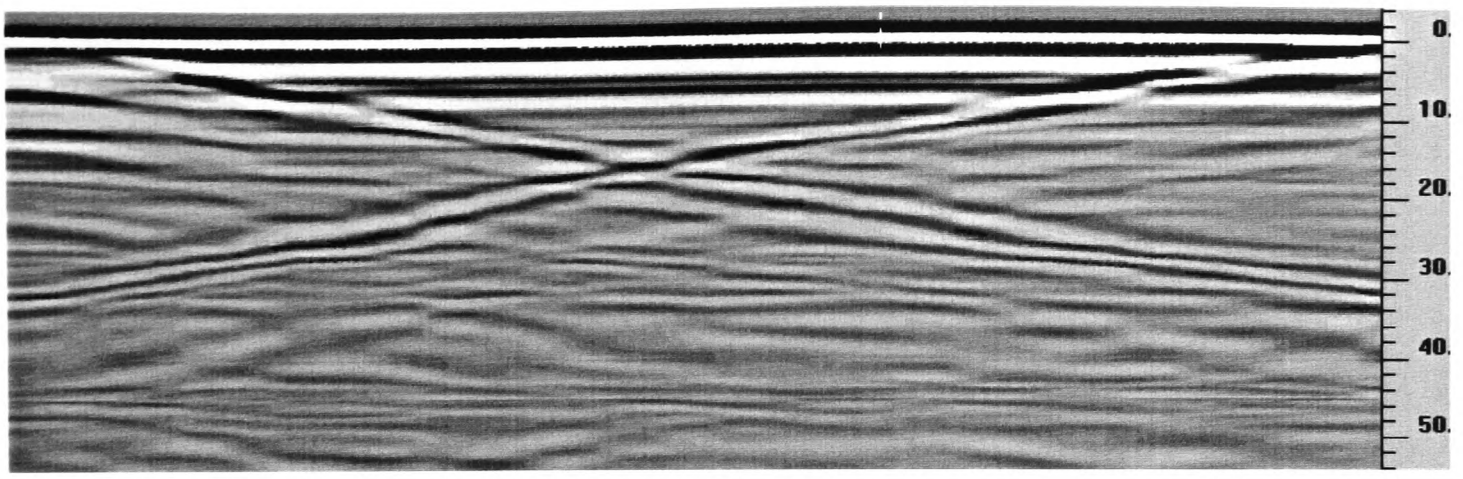

Figure 6.26 - Reflection and refraction pattern obtained over empty cellular structure with 500 MHz frequency antenna (60 ns).

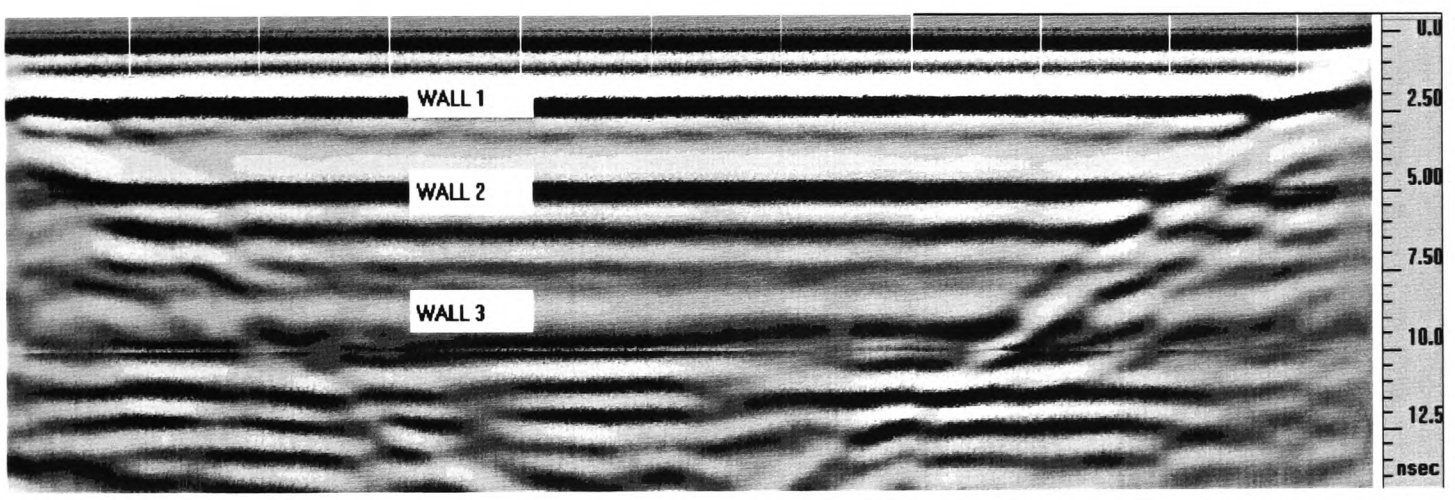

Figure 6.27 - Plot obtained from empty structure with 900 MHz antenna and 15 ns range.

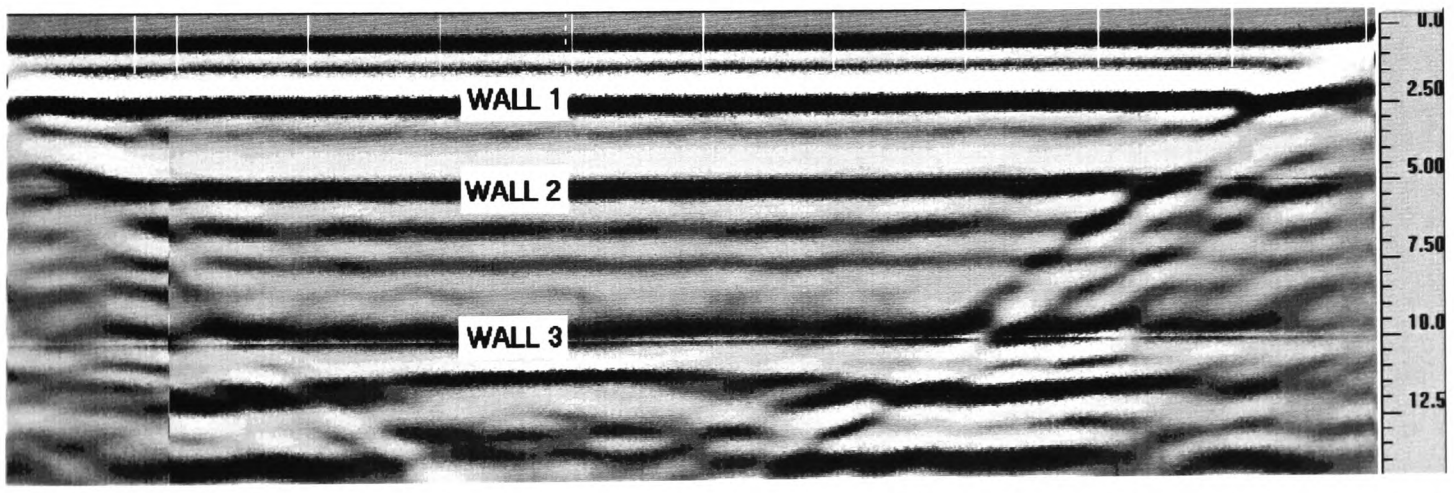

Figure 6.28. Radar plot obtained when loose dry sand is present in second cell (900 MHz antenna and 15 ns range).

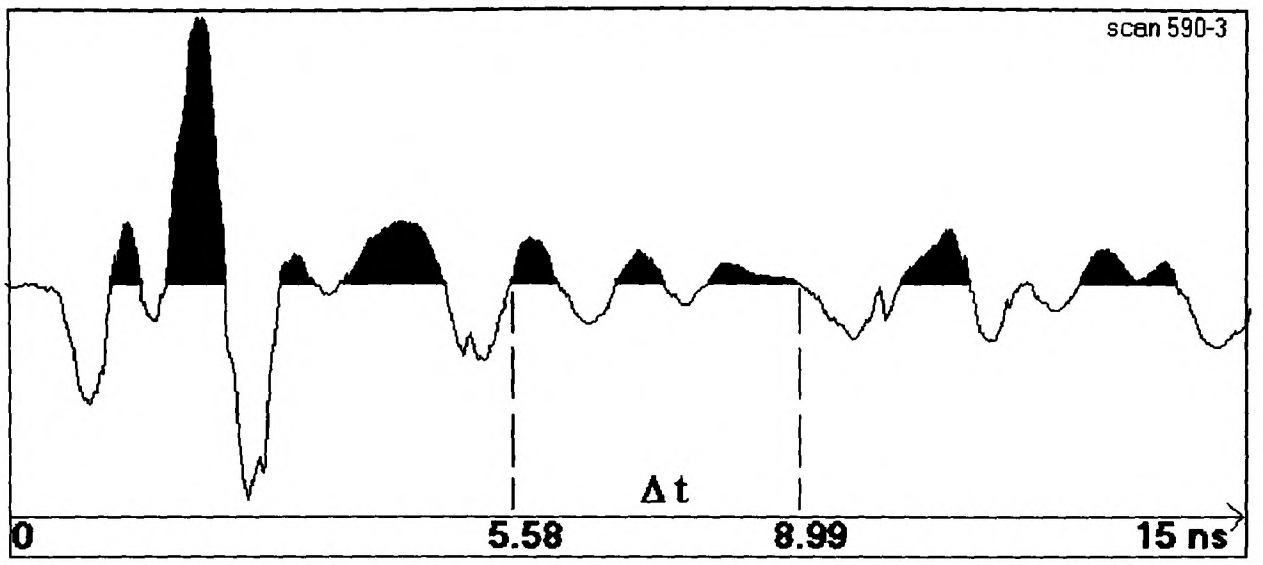

Figure 6.29- Measurement of 2-way travel time through dry loose sand.

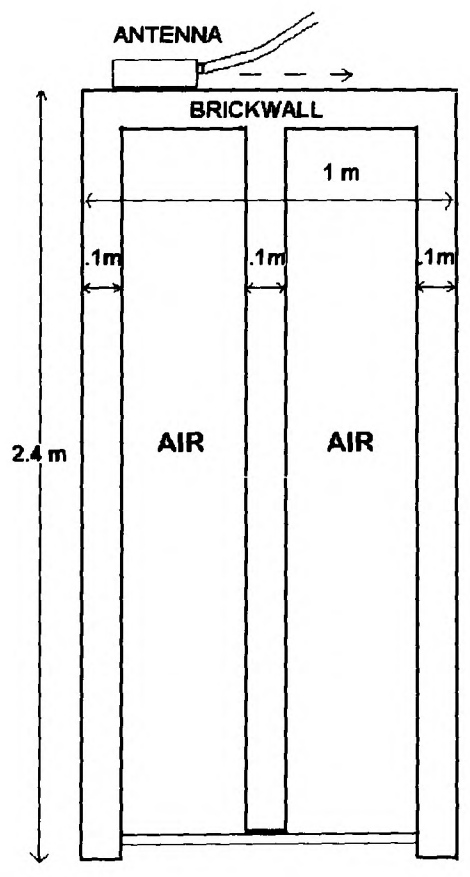

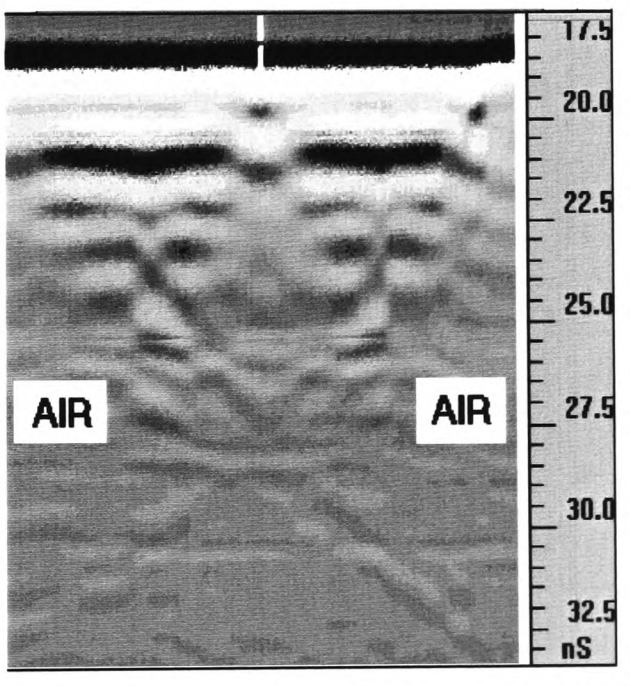

Figure 6.30. Composite structure with empty cells: drawing showing position of antenna and direction of movement during scanning (left); radar plot obtained with 1000 MHz, and 15 ns time window (right).

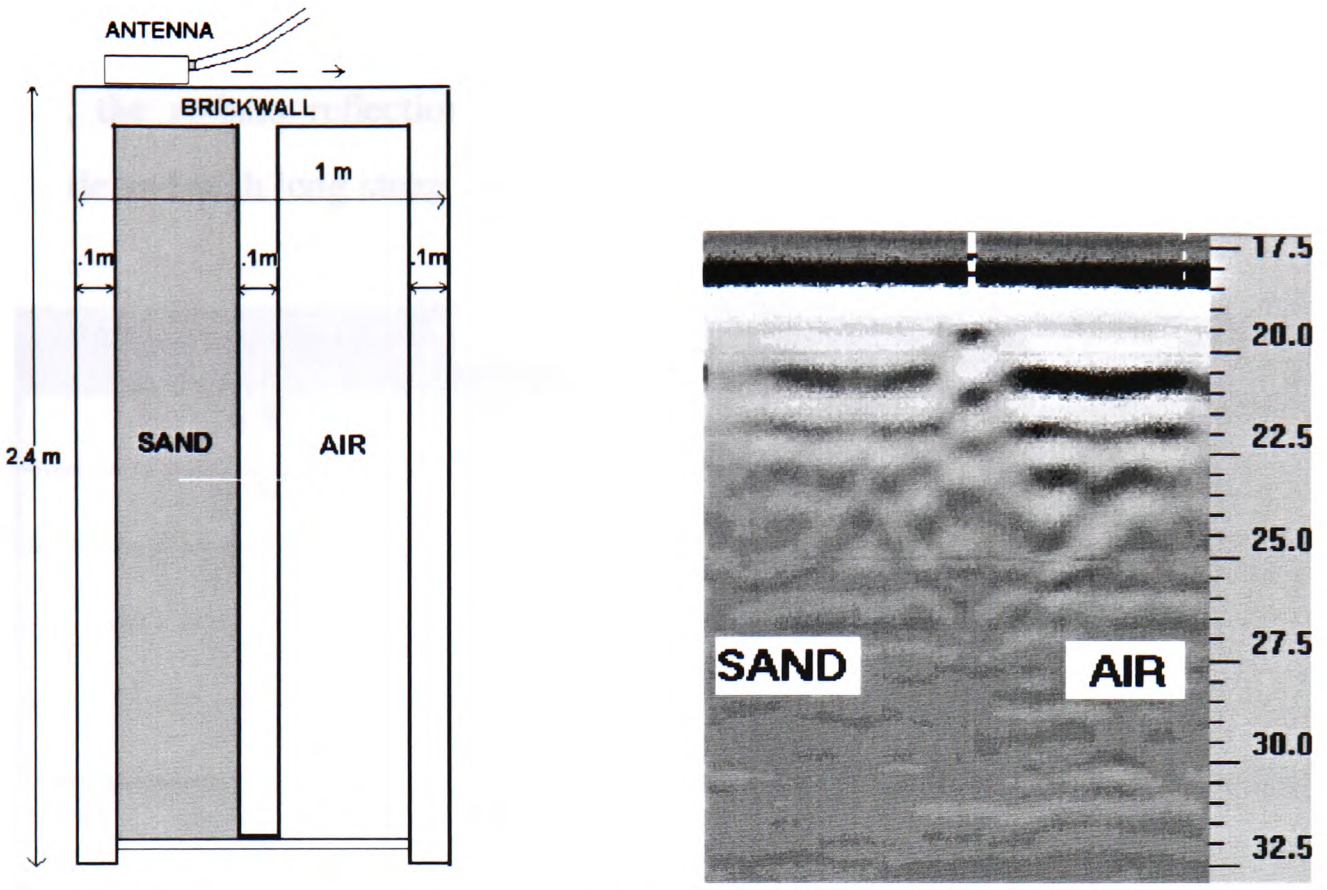

Figure 6.31 - Composite structure partially filled: drawing shows left hand side cell filled with sand, position of antenna and direction of movement during scanning (left); radar plot obtained with 1000 MHz, and 15 ns time window (right).

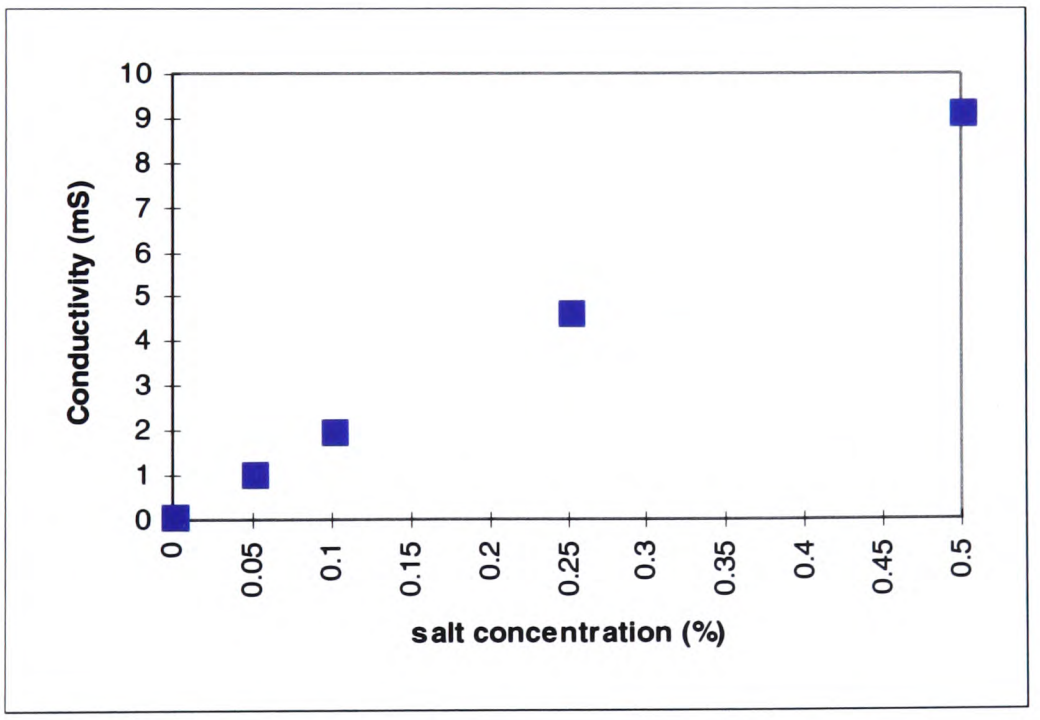

Fig. 6.32 - Relation between salt concentration in water and conductivity.

From comparison with fig. 6.16, it is clear how, in this case where no brick wall is present, the re-bars reflections are properly shaped hyperbolas, of greater signal amplitude and with long steep branches.

Water temperature	Salt concentration	Conductivity
14 °C	0 %	0.098 mS
14 °C	0.05 %	1.08 mS
14 °C	0.1 %	2.01 mS
14 °C	0.25 %	4.7 mS
14 °C	*0.5 %*	*9.15 mS*

Table 6.4 - Values of brine temperature, concentration and conductivity measured during the experiment.

With these conductivities and use of 900 MHz antenna, the material is not a conductor. In fact from equation (4.4), $\tan \delta = 0.002$ (values of $\varepsilon_r = 81$, $\sigma = 10$ mS/m, f = 900 MHz). In this case of low loss material, the simplified equation for velocity (4.13) was employed for measurements of velocity and calculation of dielectric constant in a similar way to that reported in section 6.4.3.1. For the case of 0.05% salt content, typical results are shown in fig. 6.34: the calculated velocity was v = 0.0333 m/ns, and corresponding dielectric constant of $\varepsilon = 81.3347$. The values of velocity and dielectric constant for the other salt concentrations are reported in table 6.5. These values coincide with those reported in literature for these materials.

Salt concentration (%)	Velocity (m/ns)	ε
0	0.0333	81.3998
0.05	0.0333	81.3347
0.1	0.0330	82.5334
0.25	0.0313	92.1192

Table 6.5 - Values of velocity and dielectric constant.

Therefore, these results confirm that the method for calculating signal velocity and material dielectric constant through time-domain analysis and use of the simplified formula, is reliable and can be extended to similar calculations for other building materials. These measurements were valid because a high frequency antenna was used (900 MHz) on low loss materials. Under these conditions the velocity value does not change significantly with increasing conductivity.

6.5.3 Experiments with rebars for evaluating horizontal resolution

Experiments were conducted to investigate the horizontal resolution of 900 MHz antenna in water, by varying spacing and depth of re-bars as from figures 6.35 to 6.39. The data results are commented in section 6.5.3.2. where they are compared with the outcome of a numerical analysis, which is reported in the next section.

6.5.3.1 Numerical analysis of horizontal resolution

A numerical analysis was conducted to plot theoretical values of horizontal resolution in water as a function of the antenna frequency used. The analysis was carried out using the concept of Fresnel zone, which represent the limit to distinguish two separate targets; equation 4.19 was therefore used. The antennae centre frequencies used were those specified by the manufacturer for transmission in air but corrected to take into account changes in frequency due to coupling to a medium different from air (Rashkovskij, 1981). For values of dielectric constant above 15, this formula tends to lower the centre frequency by approximately 75%. For a nominal centre frequency in air of 900 MHz, a frequency of 640 MHz would result for the antenna coupled in water.

Table 6.6 plots the results obtained for antennae frequency from 100 MHz to 1 GHz and depths up to 10 metres. It can be seen that the resolution improves for higher values of antenna frequency used and for shallower depths. In fact, as the wave propagates at increasing depths, the centre frequency is expected to lower and the pulse to become larger, reducing the resolution.

To evaluate the influence of the material dielectric constant on the horizontal resolution of the antenna, similar tables to that seen for horizontal resolution in water are plotted for transmission in dry and saturated sand (Tables 6.7 and 6.8). The electrical properties for the materials are chosen according to the figures reported in literature. The centre frequency for a 900 MHz antenna would shift to 734 and 649 MHz respectively for the case of dry and saturated sand. It can be seen from the tables, that the horizontal resolution improves with increasing dielectric constant. A higher material dielectric constant seems to modify the signal beam by focusing it. Thus, the dielectric properties affect the beam spread and in case of very low dielectric constant, for example with $\varepsilon_r = 1$ (air), it can be expected that the width of the emitted beam will be maximum (this hypothesis is reinforced by the outcome and discussion of the radar tests on a hollow structure as seen in section 6.4.3.3.), and the horizontal resolution minimum. The numerical analysis for horizontal resolution in air confirms this hypothesis (see table 6.9).

DIELECTRIC CONSTANT = 81 (water)						
DEPTH	**FREQUENCY (MHz)**					
D (m)	**100**	**200**	**300**	**500**	**900**	**1000**
0.05	0.42	0.25	0.18	0.13	0.09	0.09
0.1	0.49	0.30	0.24	0.18	0.13	0.12
0.2	0.61	0.40	0.32	0.24	0.17	0.17
0.25	0.66	0.44	0.35	0.26	0.19	0.18
0.40	0.80	0.54	0.43	0.33	0.24	0.23
0.50	0.88	0.60	0.48	0.37	0.27	0.26
0.75	1.05	0.72	0.58	0.45	0.33	0.32
1.00	1.19	0.83	0.67	0.52	0.38	0.36
1.50	1.44	1.01	0.82	0.63	0.47	0.45
2.00	1.66	1.16	0.94	0.73	0.54	0.51
2.50	1.84	1.29	1.05	0.81	0.61	0.57
3.00	2.01	1.42	1.15	0.89	0.66	0.63
4.00	2.32	1.63	1.33	1.03	0.77	0.73
5.00	2.59	1.82	1.49	1.15	0.86	0.81
10.00	3.64	2.57	2.10	1.62	1.21	1.15

Table 6.6 - Minimum horizontal spacing (in m) between reflectors for resolution in water.

DIELECTRIC CONSTANT =	3 (dry sand)					
	FREQUENCY (MHz)					
DEPTH D (m)	100	200	300	500	900	1000
0.05	1.40	0.74	0.52	0.35	0.22	0.21
0.1	1.49	0.83	0.60	0.41	0.28	0.26
0.2	1.65	0.97	0.73	0.52	0.37	0.35
0.25	1.73	1.04	0.79	0.57	0.41	0.38
0.40	1.94	1.21	0.94	0.70	0.50	0.47
0.50	2.07	1.31	1.03	0.77	0.56	0.53
0.75	2.36	1.54	1.22	0.92	0.67	0.64
1.00	2.62	1.74	1.39	1.05	0.77	0.73
1.50	3.08	2.08	1.67	1.28	0.94	0.89
2.00	3.48	2.37	1.91	1.46	1.08	1.03
2.50	3.83	2.63	2.13	1.63	1.21	1.15
3.00	4.16	2.87	2.32	1.78	1.32	1.26
4.00	4.74	3.29	2.67	2.06	1.53	1.45
5.00	5.26	3.66	2.97	2.29	1.71	1.62
10.00	7.32	5.14	4.18	3.23	2.41	2.28

Table 6.7 - Minimum horizontal spacing (in m) between reflectors for resolution in dry sand.

DIELECTRIC CONSTANT = 25 (saturated sand)						
	FREQUENCY (MHz)					
DEPTH D (m)	100	200	300	500	900	1000
0.05	0.67	0.38	0.27	0.19	0.13	0.12
0.1	0.75	0.45	0.34	0.24	0.17	0.16
0.2	0.89	0.56	0.44	0.32	0.24	0.22
0.25	0.95	0.61	0.48	0.36	0.26	0.25
0.40	1.12	0.74	0.59	0.44	0.33	0.31
0.50	1.22	0.81	0.65	0.49	0.36	0.34
0.75	1.44	0.97	0.78	0.60	0.44	0.42
1.00	1.62	1.11	0.90	0.69	0.51	0.48
1.50	1.95	1.35	1.09	0.84	0.62	0.59
2.00	2.22	1.55	1.26	0.97	0.72	0.68
2.50	2.47	1.72	1.40	1.08	0.80	0.76
3.00	2.69	1.88	1.53	1.18	0.88	0.83
4.00	3.09	2.17	1.76	1.36	1.01	0.96
5.00	3.45	2.42	1.97	1.52	1.13	1.08
10.00	4.84	3.41	2.78	2.15	1.60	1.52

Table 6.8 - Minimum horizontal spacing (in m) between reflectors for resolution in saturated sand.

DIELECTRIC CONSTANT =			1 (air)			
DEPTH	**FREQUENCY (MHz)**					
D (m)	**100**	**200**	**300**	**500**	**900**	**1000**
0.05	1.60	0.84	0.59	0.39	0.25	0.23
0.1	1.69	0.93	0.67	0.46	0.31	0.29
0.2	1.86	1.08	0.81	0.57	0.40	0.38
0.25	1.94	1.15	0.87	0.62	0.44	0.42
0.40	2.16	1.33	1.02	0.75	0.54	0.51
0.50	2.29	1.44	1.12	0.83	0.60	0.57
0.75	2.60	1.68	1.32	0.99	0.73	0.69
1.00	2.87	1.89	1.50	1.14	0.83	0.79
1.50	3.35	2.25	1.80	1.37	1.01	0.96
2.00	3.77	2.56	2.06	1.58	1.17	1.11
2.50	4.15	2.84	2.29	1.76	1.30	1.23
3.00	4.50	3.09	2.50	1.92	1.42	1.35
4.00	5.12	3.54	2.87	2.21	1.64	1.56
5.00	5.68	3.94	3.20	2.47	1.83	1.74
10.00	7.89	5.53	4.50	3.48	2.59	2.45

Table 6.9 - Minimum horizontal spacing (in m) between reflectors for resolution in air.

6.5.3.2 Comparison of experimental and numerical findings

Experimental data were compared with figures from the table which plotted theoretical values of horizontal resolution in water.

The results obtained from the experimental data show that the target resolution is better than predicted by the numerical analysis and this is especially true for increasing distances from the antenna. Recommendations are (Petroy, 1994) that the size of the target be at least 50% of the Fresnel zone to expect to identify it on unprocessed radar records. Considering that the Fresnel zone increases its area with depth while in the experiment the same size of target was used throughout, it can be deduced that the outcome of the numerical analysis is conservative. Two possible explanations come to mind: either the Rashkovskij formula is too drastic and the frequency of the coupled antenna does not actually decreases of approximately 25%; or there is a reduction in the signal beam width due to attenuation with depth. Both the mentioned

factors, frequency and beam width, would improve the resolution. Experiments on concrete (Padaratz, 1996) exclude the former hypothesis and confirm the latter. This phenomenon is caused by the earlier attenuation of the outer rays of the emitted signal cone, as the antenna does not radiate energy with the same intensity in all directions.

It must be remembered though, that the targets used in this experiments were metal rods, and in this case total reflection occurs. Therefore it may be expected that metal targets can be spaced less than the values given in table 6.5 and still be distinguishable. However, the table also represents the minimum horizontal spacing between reflectors for any vertical penetration to happen, and, because of the targets' high conductivity, masking effects result from the intense reflections from metal targets, with the consequence that detection of any features located deeper may prove very difficult.

Given that the table becomes less accurate with increasing depth and that the thicknesses generally considered in the majority of civil engineering applications vary in a range from a few centimetres to 1-2 metre, probably up to a maximum of 5 metres in the case of historical structures, it may be concluded that the table may need amending for depths greater than the skin depth. Therefore it is recommended that values given in table 6.5 be considered only as a guidance for practical applications.

6.6 Discussion

It has been seen from the work presented in the previous chapter, that a certain amount of valuable information on site investigation with radar was assembled. However for advanced analytical purposes it is often desirable to obtain more quantitative results, such as measurements of dielectric properties of materials and hidden geometrical dimensions of masonry elements in arch bridges. The study presented in this chapter therefore, attempts to overcome the gap of data available -

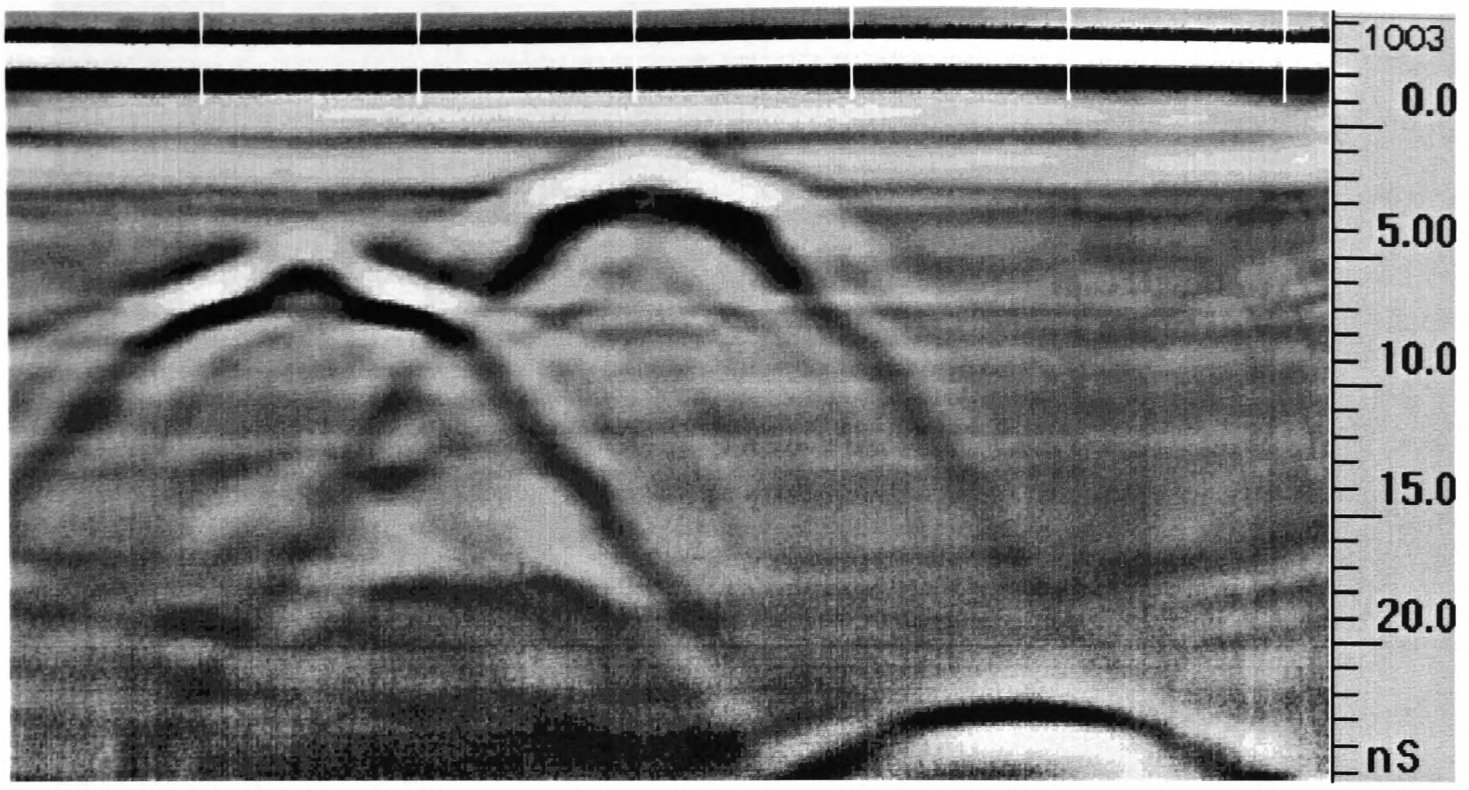

Fig. 6.33 - Radargram of rebars (at 5, 10, 40 cm away from antenna position) within water with 0.05% salt content.(30 ns range, exponential transform).

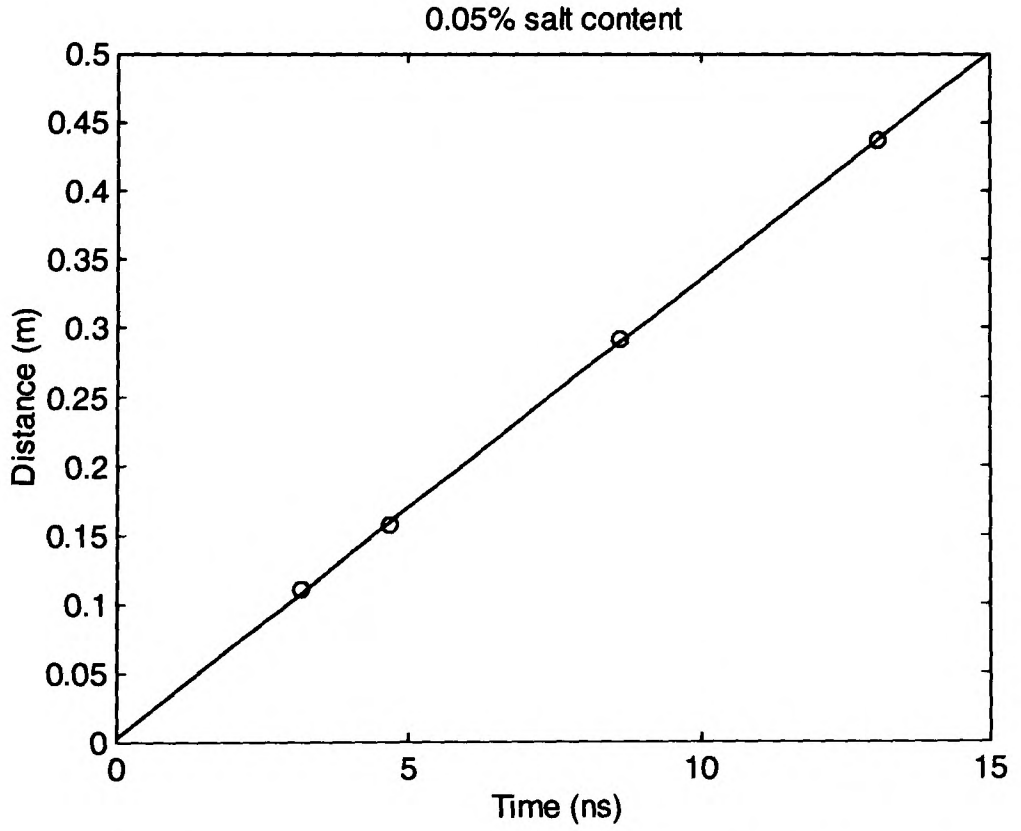

Fig. 6.34 - Calculation of velocity in brine with 0.05% salt content, and re-bars at 5, 10, 25 and 40 cm.

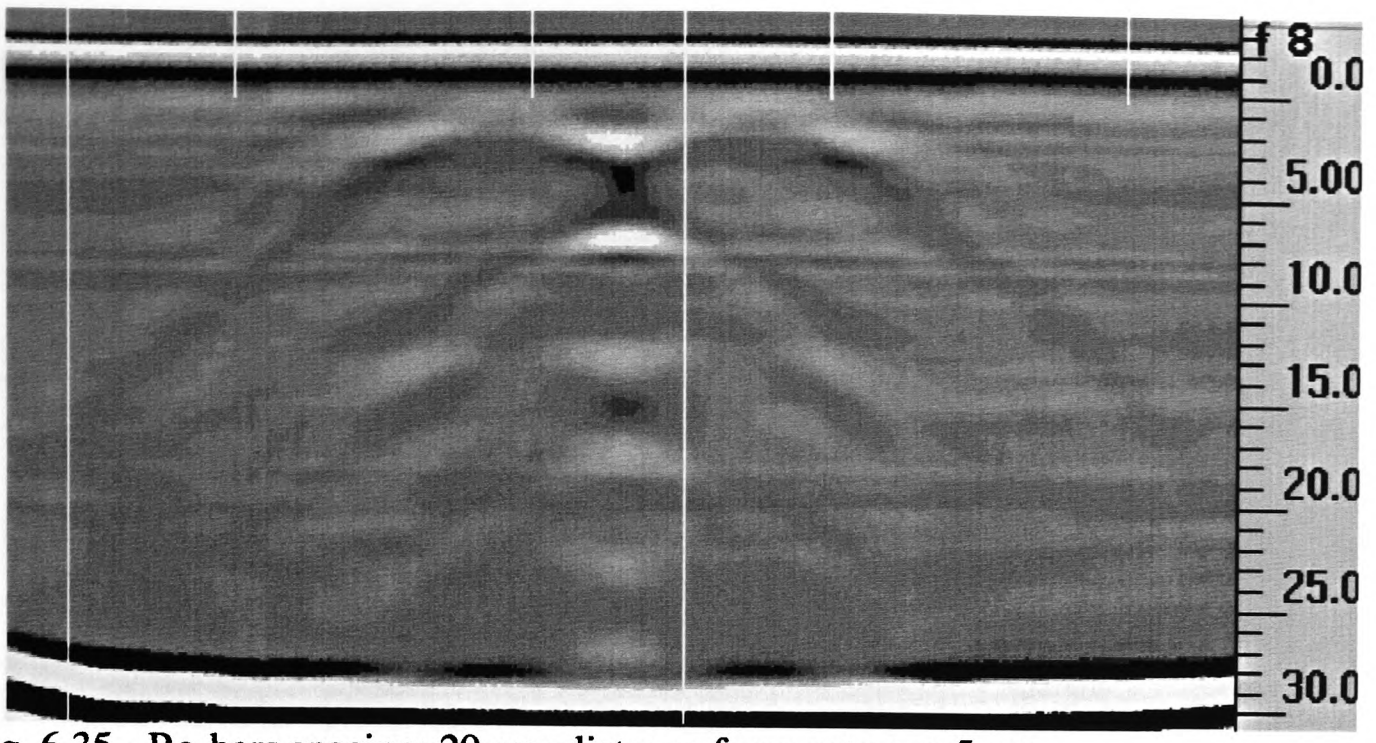

Fig. 6.35 - Re-bars spacing: 20 cm; distance from antenna: 5 cm.

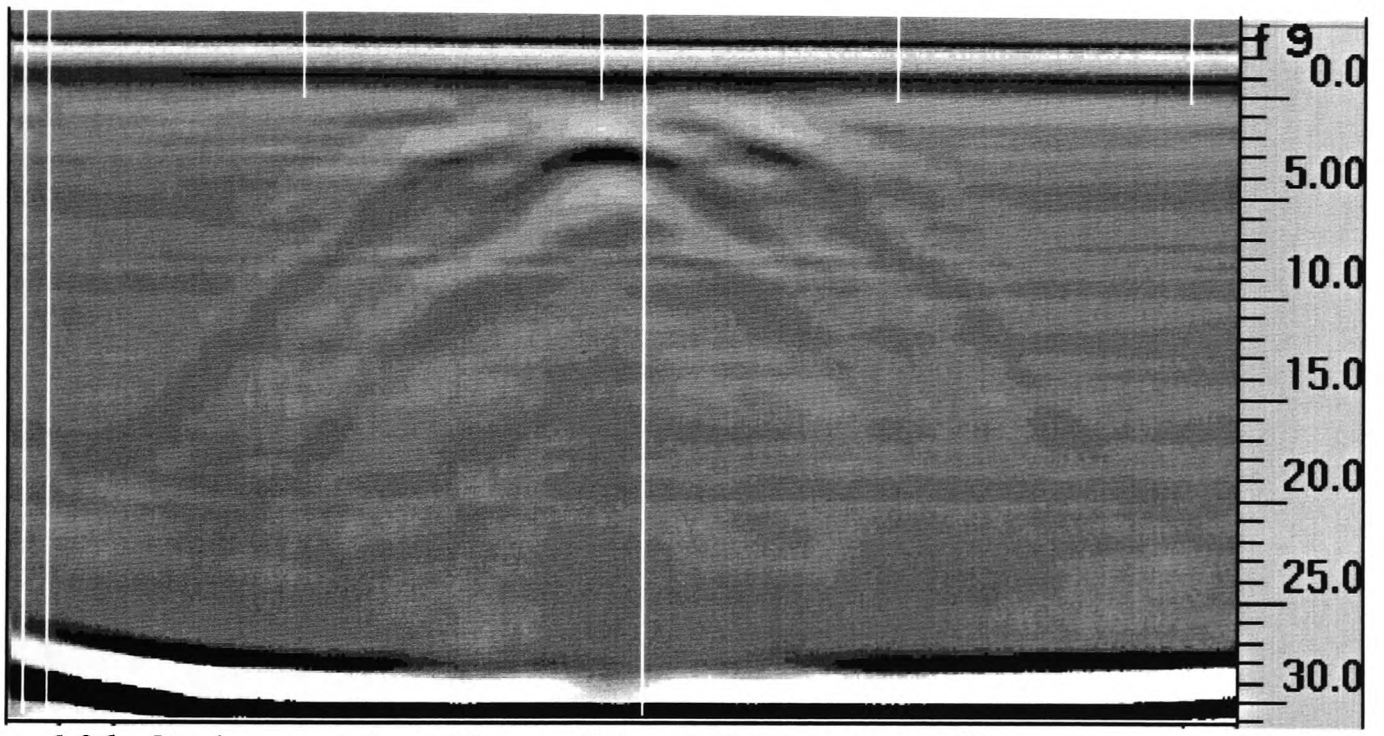

Fig. 6.36 - Re-bars spacing: 10 cm; distance from antenna: 5 cm.

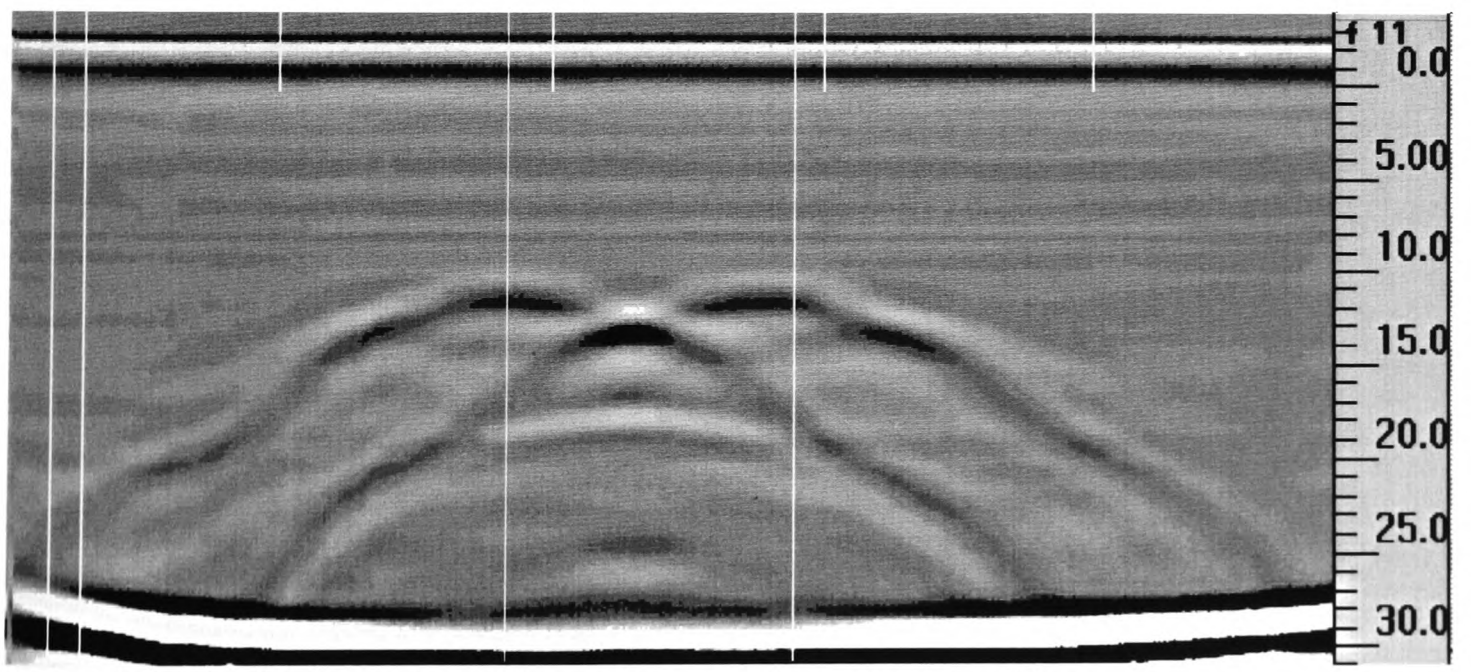

Fig. 6.37 - Re-bars spacing: 20 cm; distance from antenna: 20 cm.

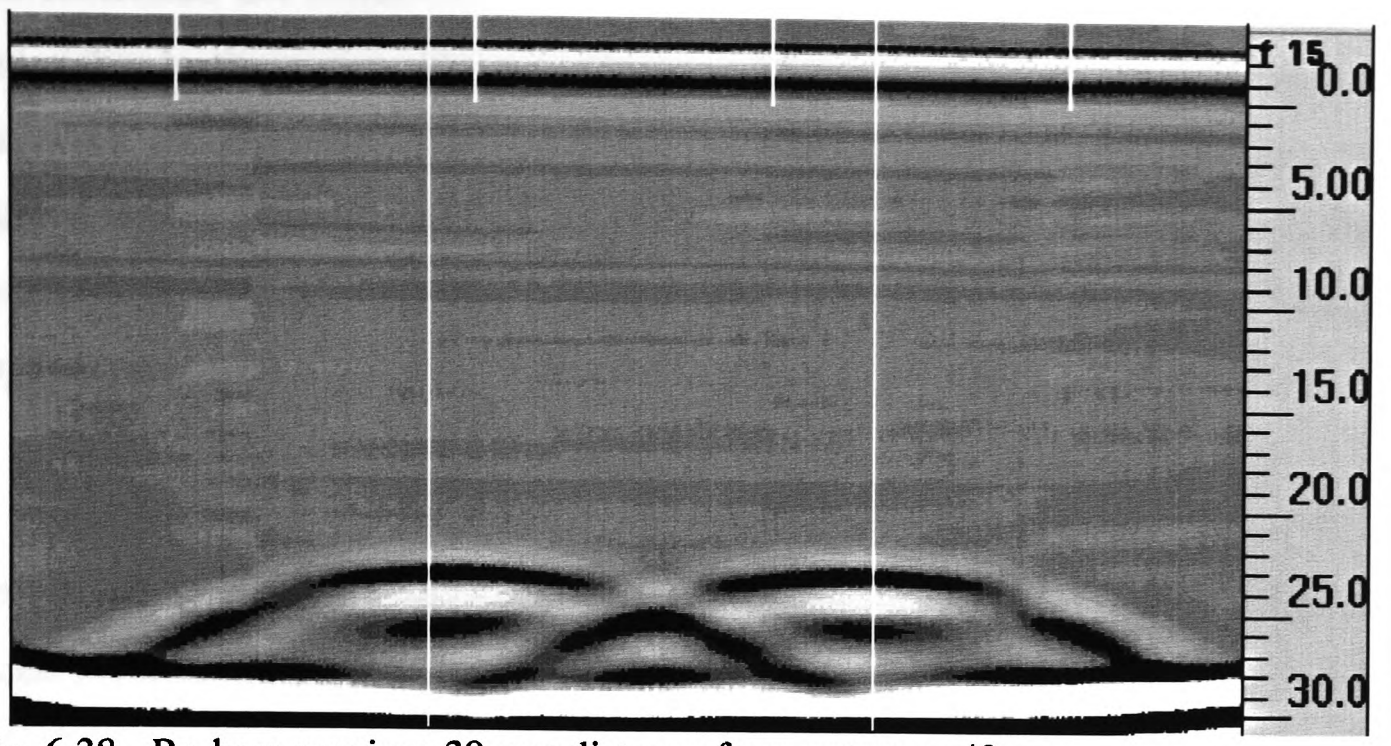

Fig. 6.38 - Re-bars spacing: 30 cm; distance from antenna: 40 cm.

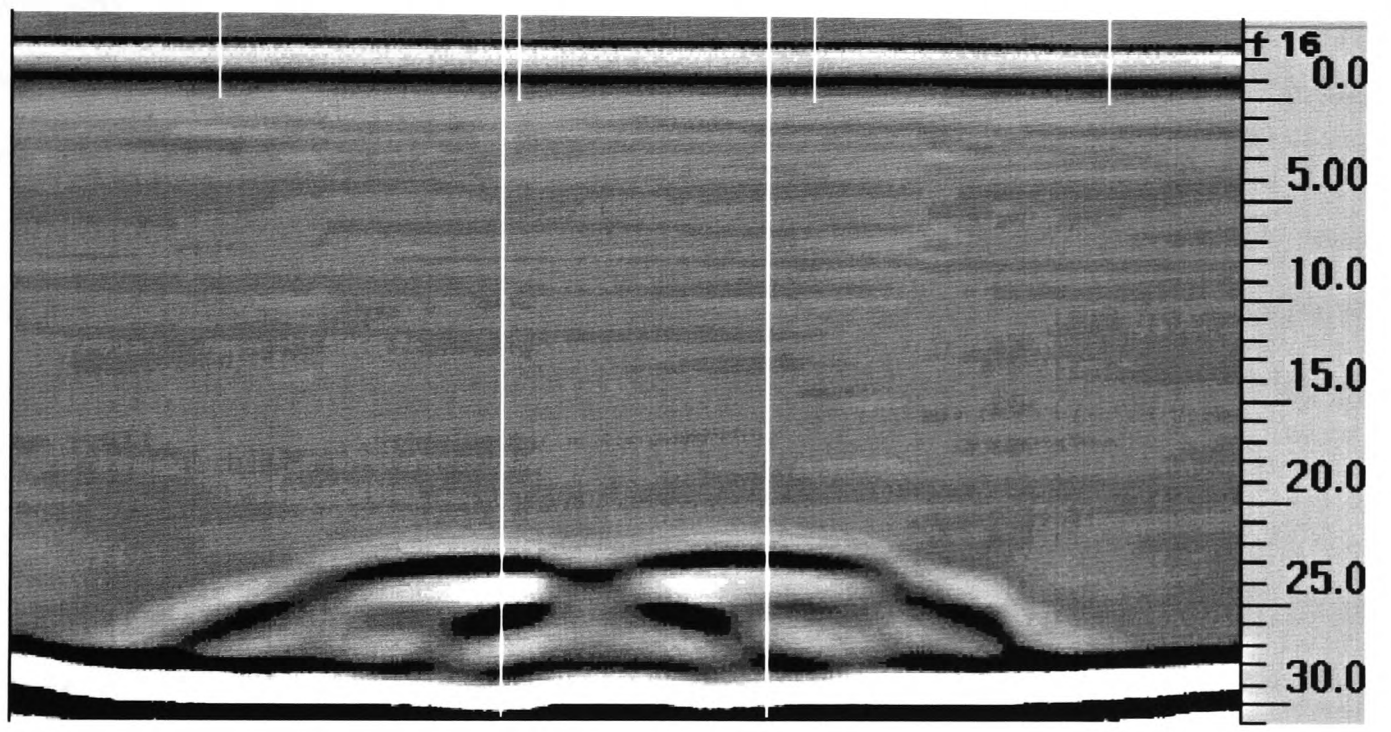

Fig. 6.39 - Re-bars spacing: 20 cm; distance from antenna: 40 cm.

and sometimes not obtainable on site - on full scale testing of structures. This is undertaken by the construction and testing of two masonry models. The results from this work are reported herein indicating the reliability and ease of identifying the various targets through GPR. The technique offers a rapid, contacting and non-contact high resolution method for detecting and mapping features in engineering applications.

The double span arch model was successfully used for calibration of the reflection technique above masonry arches in controlled conditions. Effects of the signal velocity, as affected by the material density, on the shape of the arches were discussed. Although a direct relationship between the exact value of material density and electromagnetic properties is not known, nevertheless density affects the radar data and the signal propagation. Limitations in the use of the technique for the localisation of the arch springings were identified in relation to the specific case of two semicircular arches in close proximity. The phenomena of the cone of emission of the antenna and "merging" effects in the signatures of two such arches were also discussed.

In relation to the experiment with brine and rebars, the statement is frequently made that radar will not work through saline water. This simplistic statement is only partially accurate: the radar signal is rapidly attenuated as the conductivity of the background medium increases. However at relatively low saline contents (0.05%) and therefore relatively low conductivity the radar will have limited penetration as seen from the above experimental data. This is substantially less than the saline content of sea water (3.5%). It would therefore seem most unlikely that any significant penetration would be achieved through sea water using bow tie antennae of the type used in this experiment at the frequencies used in this experiment. As part of this same experiment, velocity values were calculated by time domain analysis for salt water and values of dielectric constant derived. Furthermore it was seen that radar signals are very sensitive to changes in material conductivity and the

relationship between conductivity and signal attenuation is exponential. For this reason the radar technique cannot be used for high resolution soundings in great depth ranges, in environments with high electrical conductivity. The range and resolution of GPR decreases with the presence of conductive materials such as brine or conductive pore water and at saline contents of 0.05% by weight, 900 MHz bow tie antenna signals were significantly attenuated.

In the context of the experiments using dry sand and wet sand in the box it can be seen that the best radar penetration and resolution was obtained using the dry sand. Significant signal attenuation occurred when the soil was wet. It was seen from the experimental data that radar can be used for detection of localised areas with high salt content or contaminant.

When investigating hollow structures by means of GPR the effects of reflections of the E.M. signals on walls and cavities were identified and discussed. It was found that multiple reflections may mask the target of the survey. Also, because of the high value of the coefficient of reflection when in the presence of air, the signal propagation can be severely affected if multiple interfaces are present. Propagation of the signal through air causes the signal cone to propagate with a wider angle than through soil. When the masonry structure investigated is backfilled with soil, reflection effects are attenuated and the presence of targets may be better resolved.

6.7 Conclusions

1. Soil density affects radar signal propagation.

2. The 30^0 cone of emission from the radar antenna resulted in interference when scanning over the pier of a two-span masonry arch bridge.

3. Radar signals through brine are highly attenuated in salt contents of 0.05%, by weight - significantly less than the 3.5% concentration of sea water.

4. Radar signals through wet sand were significantly attenuated in comparison with the same target configurations in dry sand.

5. Radar signals through voided cellular structures will be distorted due to multiple reflections.

6. When the masonry structure investigated is backfilled with soil, reflection effects are attenuated and the presence of targets may be better resolved.

CHAPTER 7

SIMULATION OF RADAR DATA FOR IMAGE INTERPRETATION

7.1 Introduction

Ground penetrating radar has been used for over 30 years for resolving shallow subsurfaces in geophysical applications and more recently in engineering. The development of the method, especially in civil engineering for the investigation of structures, has been restricted due to the complexity of the systems and the need for specialist interpretation of the data (Forde & McCavitt, 1993).

The user of a radar system is required to have knowledge of the concepts of physics (electromagnetic properties of materials, wave propagation and response of the structure) and electronics (pulse emitted, operating antennae), together with an engineering understanding of the problem being investigated. Depending on the complexity of the structural element under investigation, the nature of the problem, the conditions of the environment where the survey is carried out, the antennae configuration used during data acquisition, the radar user may be able to interpret the raw data or depending upon his interpretative experience s/he may need to use sophisticated signal processing software (short pass, long pass, horizontal or vertical filtering; plus signal amplification) (Olhoeft, 1993). In addition the user must be aware of the limitations of the technique and have realistic expectations. Radar cannot penetrate good electrical conductors, such as saltwater (Colla *et al.*, 1997), metal or fine reinforcing mesh (Padaratz & Forde, 1995a) or wet clays. Features may appear on the plots and, whilst some of the more common ones are recognisable and interpretable by the practised engineer, others are generated by complex effects of multiple reflections and/or refractions. Not only can their interpretation prove difficult, but they can mask valuable information generated by true anomalies. Other

data interferences include periodic radio frequency noise introduced by site conditions, distortion at data acquisition, antenna ringing, poor antenna coupling and effects introduced by the structure itself because of its complexity or material grading such as clutter (Padaratz & Forde 1995b). Each of the above requires special digital signal processing with the risk of degrading the data if manipulation is improperly applied.

In complex cases it may be more convenient, in terms of time and effectiveness, to model the site situation and predict the radar performance and structure response. Therefore there is a need for a method of simulation which aids the interpretation of GPR surveys by allowing rapid simulation of varying geometries and materials. The combination of digital GPR system along with simulation software will help a better engineering assessment to be made.

In order to aid the analysis of site data in terms of engineering assessment, a simulation of relatively simple geometries and material electromagnetic properties was undertaken and compared with laboratory experimental data from rebar detection in homogeneous media. It is expected that, in a second phase, more complex engineering structures can be simulated, including single-span masonry arch bridges.

7.2 Radar simulation

Building on the experience of previous in-house simulation software for masonry arch bridge investigation (McCavitt & Forde, 1991), a programme was developed with the purpose of including features proper to the radar system which were not previously accounted for. The existing simulation program assumed that the antenna sends the pulse at a particular location and receives the time domain signal at the same point. In order to simplify the simulation, the bridge model was assumed at each specific location to have parallel interfaces. Furthermore the antenna was idealised to pulse vertically with no divergence, or cone of emission.

The modelling software developed uses a conventional ray-tracing process to model sinusoidal input pulse and trace propagation along angles that cover the emitting field of commercially available radar antennas, and to recursively detect interfaces between various sub-surface features (strata and anomalies) and determine their boundaries. The algorithm reproduces the paths of individual radar wavelets from radar emitter to receiver through the various interfaces. At each interface, because of the different electromagnetic characteristics of the two materials present, the wavelet splits into different components and is partially transmitted through the second material and partially reflected in the receiver direction. The response from all the traces sent out at different angles from the transmitter are then combined according to the Principle of Superposition (Lynn and Fuerst, 1989) to produce a complete 1-D simulated image for each sample point constituting the received signal waveform and these in turn are combined to obtain a complete 2-D scan over the simulated area.

Image processing software provides the ability to produce colour line scan images.

In order to prevent excessive computational overheads, various termination conditions have been included and the signal propagation arrests if :

- the chosen two-way-time limit has been reached;
- the chosen number of simulated transmissions and reflections has been exceeded;
- the signal has entered a "convoluted" interface and, as a result of the wavelet defraction resulting from the difference in material properties, it has become trapped below the interface.

Input to the modelling program takes the form of a text file where geometrical dimensions, location and electromagnetic properties of embedded target objects and material strata are expressed in terms of their co-ordinates, permittivity and conductivity. The radar antenna characteristics are expressed in the form of centre frequency. Other information specific to the simulation process is also entered,

including the maximum 2-way travel time in ns, the aperture of the receiver, and the distance to be covered by the antenna during the survey (see Appendix C).

Antenna and Signal Characteristics

The emitter frequency is set as the centre frequency for the range being considered. Frequencies considered ranged from 200 to 900 MHz. The source wavelet is assumed to be 3-phase sinusoidal in format (or 3 half wavelength). Absolute signal strength is calculated in relation to the angle from the normal to the radar emitter. The directional response function is used as described in (Goodman and Nishimura, 1992).

Target Specifications

Embedded object geometrical shapes included circles and polygons - triangles and rectangles - and were described in terms of their equations and main electromagnetic properties (dielectric constant and conductivity).

Simulation Specifications

Other information specific to the simulation process and entered in the modelling input file included:

- the step size in angle degrees between each ray trace: - Although a full beam with more than 20 ray traces per degree would be required for complete accuracy, scans with 1 to 5 trace/degree would provide the user with a reasonable target image;
- the number of scans per metre. - Scan number at the density used by digital radar systems (1024 scans/metre or less) could be employed, but fewer scans/metre may be convenient to obtain faster results. Too low a number of scans/metre may cause poor image resolution;
- the number of reflection patterns to be recorded. - This allows signal and image decomposition, so that it becomes possible to recognise the effects of primary/secondary reflection.

The output of the analysis is given in the same format as the digital radar system data files, so that it can be viewed with the same image processing software.

7.3 Laboratory and simulation set-ups

The experimental tests were conducted in the laboratory on a rig which allowed the position and spacing of two reflectors (3.5 cm in ∅) to be varied, as per the plan layout in Fig. 7.1. The distance of the reflectors from the antenna varied from 0.05 to 0.4 m, and the relative spacing between the two targets varied from 0.1 to 0.4 m. The background medium during the tests was fresh water. The antenna used was a 900 MHz bow tie, with survey wheel, drawn along one long side of the container to produce horizontal cross sections of the rig. Simulated models presented herein reproduced these same conditions.

7.4 Comparison of simulated and experimental results

Output images obtained from the simulation program are shown and compared with the radargram obtained from the corresponding set-up in the laboratory. Both sets of outputs are shown in line scan format. At the top of any simulated image, the input pulse can be seen to interfere with the material surface and produce a continuous horizontal line. Below this, the reflections from the fill/target interfaces take the shape of hyperbolic patterns. Similarly, in the experimental data plots, the continuous horizontal line at the top of the radargrams shows the surface reflection and container edge. Equally, the black feature at the bottom of the plots, indicates the container opposite side.

Consider figures 7.2a and 7.2b: the first is the laboratory plot obtained with 20 cm reflector spacing, at 20 cm depth from the surface (antenna position); the second is the output of the corresponding simulation. The apparent depth of the targets ties well in the two cases, as does the pattern of the hyperbolic reflections from the targets.

In figures 7.3a and 7.3b it is shown the case of 10 cm separation of the reflectors and 20 cm depth: good comparison is possible between the two situations. Note the modified pattern, compared with fig. 7.2, due to the reduced spacing between the targets.

Figures 7.4a and 7.4b compare 40 cm separation of reflectors and 40 cm depth: the primary reflection pattern from the rebars is shown. The hyperbolas also present a flatter shape due to the increase target distance from the antenna.

7.5 Signal decomposition

One of the special features of the simulation is signal decomposition: this allows signal propagation to be interrupted after one or more reflections, avoiding unwanted effects such as multiples and keeping the output plot simpler.

Consider figures 7.3a and 7.5a which compare laboratory experimental data with the simulated image of two rebars at 0.2 m depth and 0.1 m spacing. In fig 7.5a, b, and c a longer time window has been used than in 7.3a and 7.3b, for the purpose of showing multiple reflection. If in the case of figure 7.5a signal propagation were stopped at the first reflection, then figure 7.5c would have been obtained, and if continued after 7.5c - then figure 7.5b would have resulted.

7.6 Antenna evaluation

Specifications of radar antennae state that the signal will be emitted at certain angles (depending on the type of antenna, the cone of emission width may be approximately 60 degrees or up to 90 degrees angle).

Figures 7.6a and 7.6b simulate two rebars at 0.05 m depth and 0.1 m spacing. Figure 7.6a simulates an emitted beam angle of 60 degrees whilst in Fig. 7.6b the angle is 89 degrees. Figure 7.6c is the corresponding laboratory experimental image obtained. It is therefore deduced that the beam angle of the commercial antenna may be greater than 60 degrees.

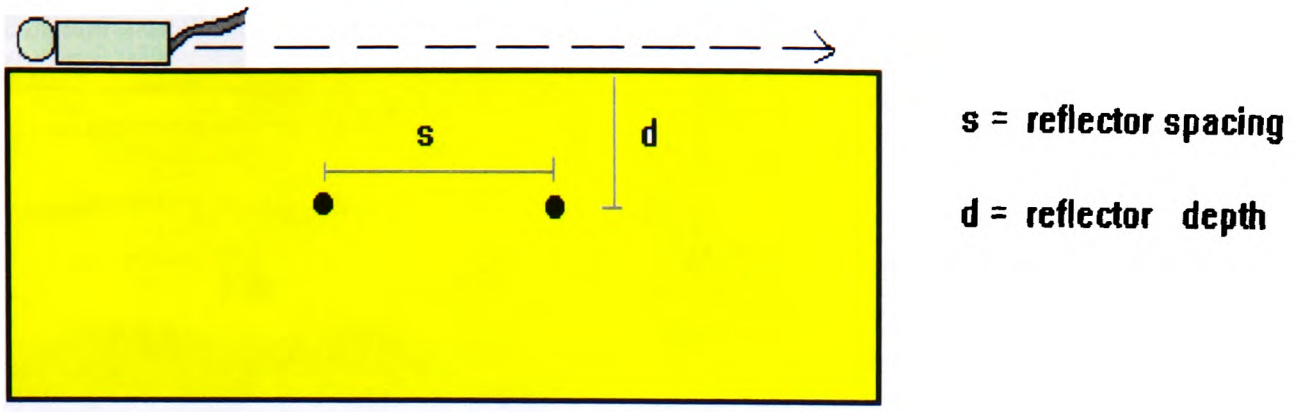

Figure 7.1. Plan view of rig used for experimental tests.

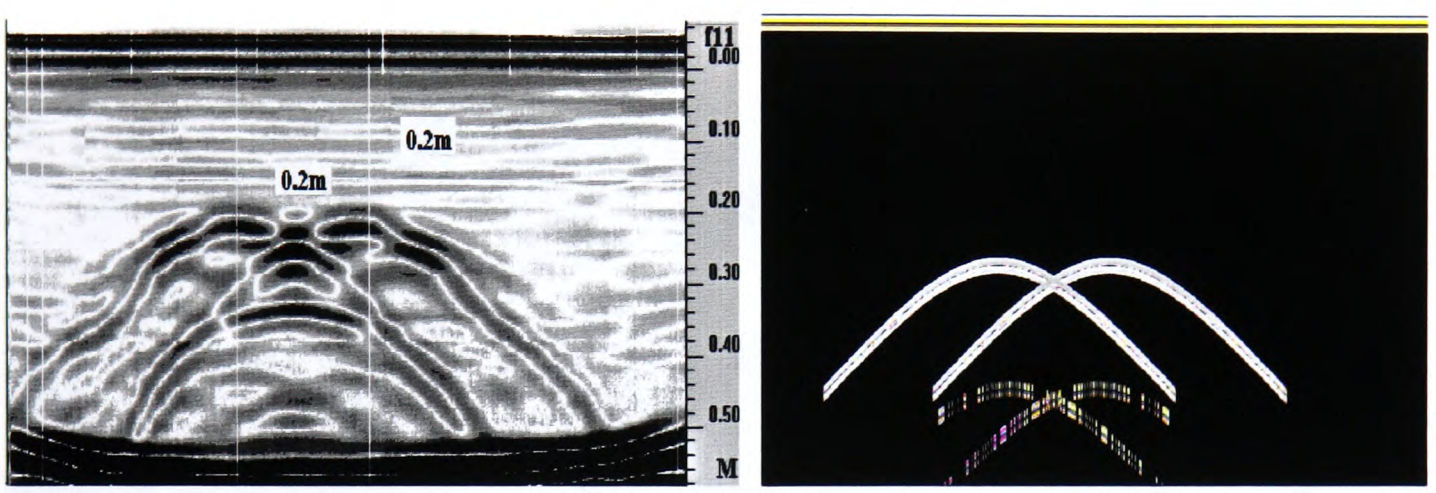

a) b)

Figure 7.2 - Reflectors spacing 20 cm, depth 20 cm: (a) laboratory; (b) simulation.

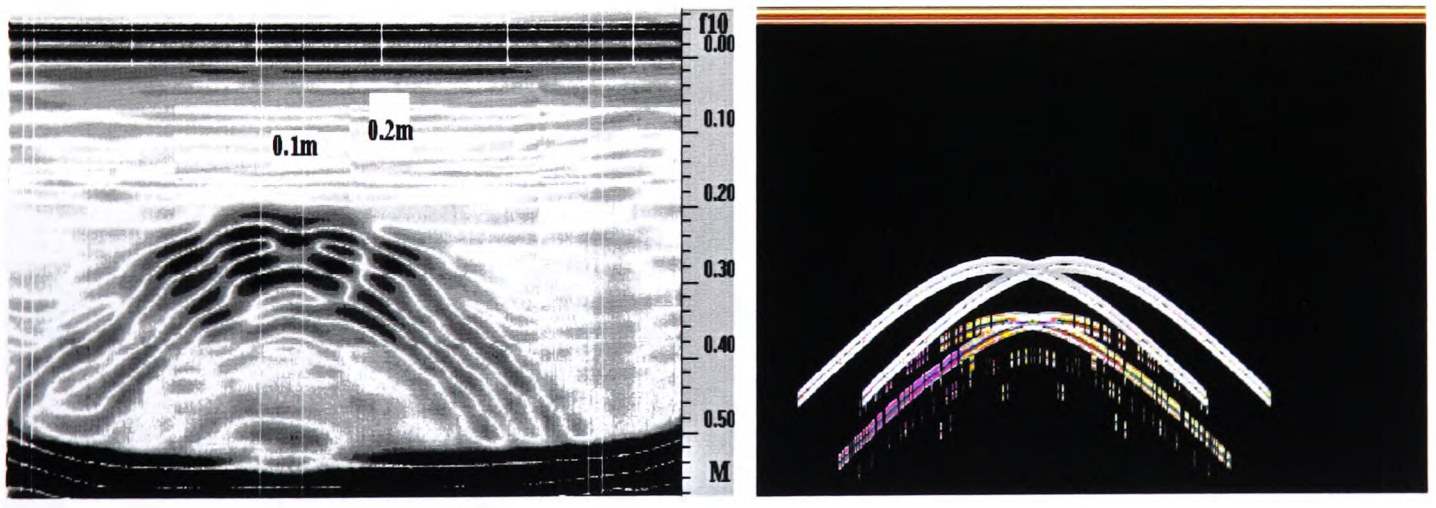

a) b)

Figure 7.3 - Reflectors spacing 10 cm, at 20 cm depth: (a) laboratory; (b) simulation.

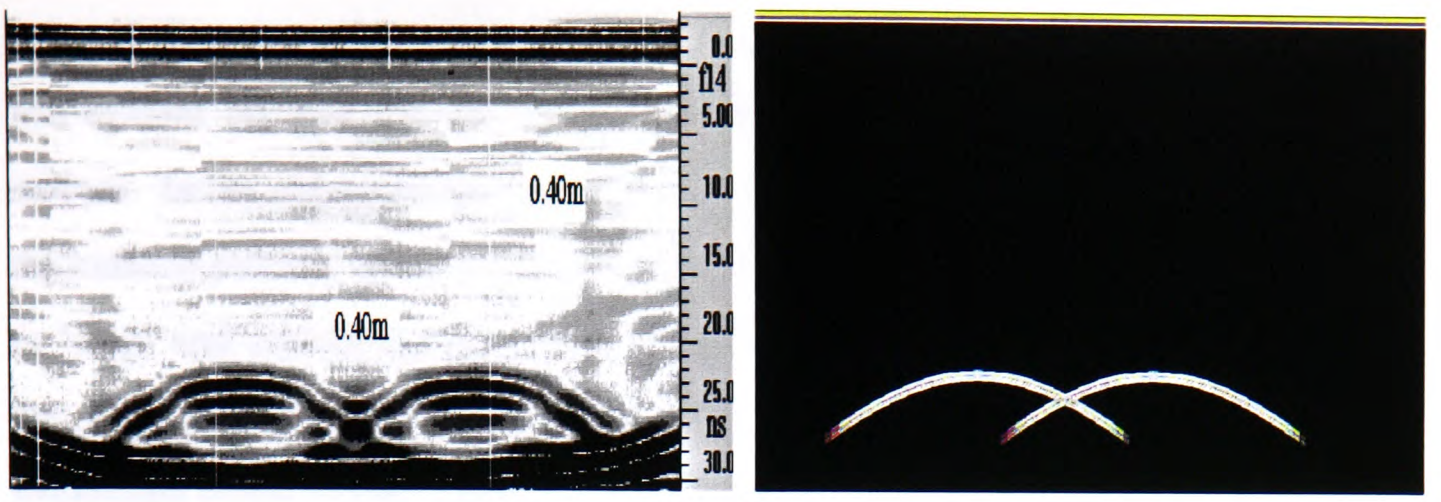

a) b)

Figure 7.4 - Reflectors spacing 40 cm, depth 40 cm: (a) laboratory; (b) simulation.

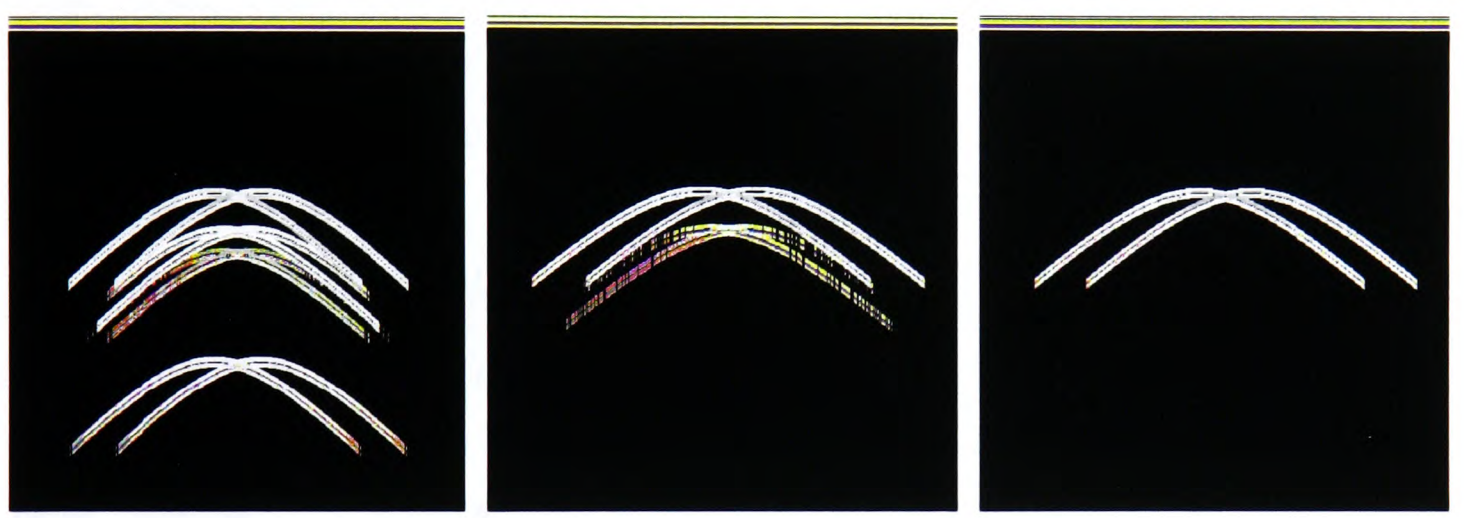

a) b) c)

Figure 7.5 - Decomposition of the received signal.

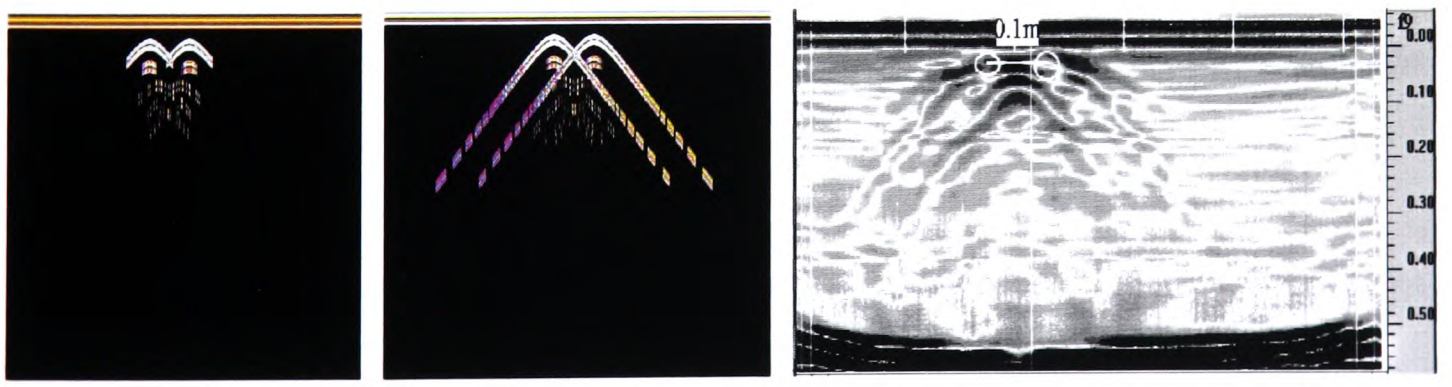

a) b) c)

Figure 7.6. Variations in the beam width of the emitted signal.

Note that the simulated hyperbolas present, in this case, a sharper apex due to the reduced distance antenna/target. In the experimental data plot, this phenomenon is less evident because the top of the hyperbolas merges with the reflection from the surface. In the experimental case, in fact, we deal with a not strictly theoretical pulse: the emitted pulse is never the ideal 3-phase sinusoidal wave. Instead the signal tends to "ring" and creates the grey-shaded horizontal lines below the surface reflection in the experimental data plots. The merging with the hyperbolas appears as a smoothing effect on their apex.

7.7 Discussion

The research work on the simulation of radar response presented herein is part of a wider study focused on the investigation of composite masonry structures and masonry arch bridges conducted at the University of Edinburgh, where the radar technique is one of the Non-Destructive methods being researched for the investigation of structures. It is expected that simulation will allow the interpretation of actual surveys to be more readily understood, which will in turn allow a better engineering assessment to be made of a structure under investigation. The output from in-house ray tracing simulation software provides a mean by which the impulse radar response of a structural system can be readily simulated. Radar simulations were undertaken of re-bar targets in a tank, with 900 MHz antenna.

The simulations undertaken have shown the effects which target spacing and depth have on the radar signature shapes and the results compare well with real case survey plots. Simulation data has also been used to assess the output specification from a commercial antenna.

The main advantage of ray tracing is mathematical accuracy - each ray from the source is modelled with considerable precision, allowing for more accurate placement than compatible FE or FD processes. The weakness normally attributed to the process is its slowness and computational power required for complex situations. In the case of the radar simulation, another limitation of ray tracing is the inability to

model with accuracy the defraction effect of the E.M. wavelet being transmitted through "convoluted" interfaces which may trap the wave.

The simulated radar survey has a number of practical advantages including its use as a training tool, a pre-survey forecast, post-data collection analysis aid, and system tester for digital equipment performance.

Training: ray-tracing is a more intuitive approach than alternative processes such as Finite Difference Time Domain (FTFD) (Nelson, 1994). The variables listed above for input in the programme, are easily derived and apply in practice just as readily as to the simulation. Thus the simulation approach could be used for the training of new users and for didactic purposes. Since the simulation produces more homogeneous (less complicated) images than digital radar systems produce on site, simulated radar plots offer the advantage of being more easily understood and interpreted.

Moreover one of the special features of the simulation is signal decomposition: this allows signal propagation to be interrupted after one or more reflections, avoiding effects such as multiples and keeping the output plot simpler. This is potentially of great help for improved interpretation of site data.

Expert systems: an accurate simulation can be used to provide an interpretation of the radar image obtained from site surveys. Although this work is still some way from an iterative process where radar images can be back-analysed to produce the real site image, it is possible to compare site data with simulated models to try a 'best comparison' interpretation. Similarly the simulation may be used as part of the preparation before or during a site visit to give an understanding of the results obtained. The simulation program developed is PC based and can be run, and results plotted, in a very short time - making it suitable for site use. With the further usage of image analysis tools, a simulated survey plot could be used to provide a template for a scan from the field to allow the engineer to observe key differences and spot any anomaly not yet accounted for.

Equipment evaluation: if an idealised radar image can be derived from a simulation, then simulations could produce 'ideal' images of real case surveys to be used as benchmarks for the testing of radar equipment, thus making it possible to require more standard equipment systems and antennae.

For example, it is possible to compare experimental data with simulated data for an evaluation of the beam angle of commercially available antennas.

7.8 Conclusions

1. A ray tracing program was developed which gave good correlation with laboratory experiments.

2. Successful simulations were focused on the detection of re-bars at various spacings and compared favourably with experiments of identical dimension.

3. The facility of decomposition incorporated into the program enabled a clearer insight to be gained into radar propagation through media and target identification.

4. The claimed calibration of a 900 MHz commercial antenna was evaluated using the simulation program.

CHAPTER 8

DISCUSSION OF FINDINGS

8.1 Introduction

From the discussion of bridge management problems and strategies it has been identified that a key input parameter in the assessment of masonry arch bridges is NDT. Conventional methods of assessment of arch bridges, both numerical methods and other global NDT techniques such as load testing, are critically appraised. The expectations from Non-destructive Testing by the "bridge community" are, at the moment, the provision of qualitative condition information. It has been underlined that in critical bridge assessment situations - when the bridge fails assessment by small margins - even such information would be worth knowing. Meanwhile the "NDT community" is eagerly working at promoting some of these techniques from a qualitative stage to one where quantitative information can be provided. Therefore, the primary objectives of this project were to develop NDT techniques which would aid in assessing the integrity condition of masonry arch bridges by revealing information related to bridge materials and bridge construction details. The techniques would have to be capable of obtaining information relating to the bridge elements and materials in situation where other assessment methods have failed because they are unreliable, expensive or time consuming. Thus, the structure evaluation operation performed via NDT would assess whether the structure is capable of coping with new loads and, albeit indirectly, would extend the life of the bridge. Finally, the testing would provide input information to mathematical methods of assessment. These are all objectives of the investigation.

8.2 Desk Study of Bridges

The way forward for a rational bridge assessment is to begin by collecting the information available related to the structure, and thus by doing a desk study prior any

site testing. This procedure is similar to site investigation practice. By knowing the type of masonry bridge which is to undergo investigation, its component materials, and possible modifications it has been subjected to, the Engineer can start sketching a picture of the behaviour of the load and of the material conditions of the bridge. Unfortunately, the puzzle is often incomplete because the Engineer is unaware of historical methods of construction, and archive information related to strengthening or widening operations is often lost.

To help the Engineer in this task, the research has first reviewed historical bridge types and then tried to suggest how to recognise the different forms of inner spandrel construction, materials employed and arch shapes, in function of the area, the age and the designer of the bridge. If it is possible for the Engineer to have concepts about whether the bridge is soil filled, composite or it presents a hollow cellular structure, then this knowledge is not only valuable but precious, when it is the only information available. This a-priori knowledge related to the materials and the complexity of the structure under investigation is useful both when a NDT survey has to be carried out and for the purpose of load capacity assessment. In particular cases it is not excluded that, from the historical review, it might also be possible to discern whether the structure has undergone modifications. Not last, the surveyor would be facilitated in identifying decay and defects and could advice for early repair or preventive action.

An additional fact emerged from the review of historical bridges: the interaction between the different parts of the structure is often difficult to quantify but the ancient builders were well aware that structural interaction takes place between elements. Examples such as Pontypridd and North Bridge are self explanatory. Structures like Perth Bridge would instead provide improved stiffening. Dean Bridge is nowadays still a remarkably sound structure. The majority of these bridges were built when there was no theory, and mistakes and experience were the way of learning for masons, carpenters, architects and engineers. Intuition was the guide for the project and this led to a multitude of bridge designs. Limitations of materials and difficulties in construction were gradually overcome by experience and, in relatively recent times,

an increased knowledge of theory of structures and material strength. It is ironic that, although today sophisticated numerical methods and testing procedures are available for bridge assessment, the Engineer still needs to exercise his/her own judgement on the outcome of such methods and on the state of the structure.

Furthermore, from the outcome of the review and the site and laboratory testing, it was pointed out that some of the materials present in masonry bridges (specifically clay materials in wet conditions) and some types of bridges (hollow cellular bridges) may affect the performance of the NDT techniques and even compromise the survey results. For example, the presence of a heavily reinforced concrete saddle above the extrados of the bridge arch, would prevent a radar survey from being carried out from the road level, because the metal mesh would obstruct the EM wave propagation to the arch.

8.3 NDT Techniques

A number of techniques are available for bridge testing, however Radar, Sonics and Conductivity have been selected because they are completely non invasive and reversible, unlike some local techniques such as coring material samples, or global ones such as load testing. Furthermore some of these NDT techniques, such as conductivity measurements, are non contacting; others, like sonics and radar, have shown confident results on concrete structures and promising results on masonry structures. All, except perhaps sonic tomography, allow for a rapid survey time, with minimum disruption to the traffic activity. Another benefit they share is that data obtained through these techniques are suitable for elaboration through tomographic software, so that results can be presented in the form of cross-sections of the structure - in which indirect information related to materials and defects can be read.

A number of applications of these techniques is contained in this dissertation: testing on two masonry bridges has been followed and complemented by testing of two laboratory masonry test rigs. Valuable information has been collected on site, where, for the purpose of identifying the situation in which radar is "working", the cases of

unsuccessful applications of radar with high frequency antenna in highly conducting environment, have been considered as valuable as the more positive results obtained. In more favourable material conditions, examples have been shown of how to calculate average values of material properties through the bridge, by performing transmission mode measurement in two possible ways. Other applications of reflection mode measurements demonstrated how to calculate values of velocity through the single elements; how to measure thickness of walls; how to identify defects embedded and locate their position. Laboratory work aimed at the appraisal of electromagnetic wave propagation characteristics in relation to varying bridge type (hollow or filled composite masonry structure), bridge filling and material properties.

Properties of the materials, and conductive behaviour in particular, have been at the centre of the attention throughout the comments on the data collected - especially the radar results which occupy a key position in this thesis. Differences in radar performance have been compared for the case of dry and wet granular fill, for saline materials, for wave propagation through cellular structures either hollow or soil filled (the type of composite structure that the Engineer can come across on site). Target signature shapes have been analysed both for structural elements (segmental and semicircular arches, and solid brickwalls either parallel or perpendicular to the direction of movement of the antenna) and for defects (air and water pockets, metal rebars). Results have also been related, both for the site and laboratory case, to the antenna frequency and the shape of the signal beam emitted by the antenna. All the results cannot be reviewed here and the reader is referred to the various sections throughout chapters 5 and 6. Some of the findings are nevertheless reported herein.

Laboratory radar experiments were undertaken to investigate the effects of radar beam propagation beyond a solid masonry wall as opposed to the case when the wall is not present (for example in concrete structures):

- When a wall is present, the continuous interface at the wall/air or wall/fill boundary causes reflection of part of the wave, before the signal can reach the

target, with the consequence that a weaker signal travels through the fill than if the wall was not there. A reduced depth of penetration can be expected.

- Multiple reflections inside the masonry wall will also cause changes of the beam angle with spreading of the signal beam portion that eventually passes into the fill, thus modifying the signature shape of the resolved target.

- From the comparison of radar plots showing metal bars in fill, contained or not by a masonry wall, the target shape analysis clearly showed that, when the wall is present, the reflection hyperbolas from the targets in the fill appear weaker, flatter and with shorter branches.

Laboratory radar experiments were undertaken to investigate the effects of beam propagation beyond a solid masonry wall when either air or fill are present at the wall interface opposite that where the antenna is located:

- Comparison of data recorded when either no fill was present or a dry sand fill was in place, showed that a stronger reflection appears at the interface in the former case. Brickwall/air boundary thus constitutes a stronger interface than brickwall/fill, and the calculation of the reflection coefficient confirmed this observation.

- The above has great importance when hollow masonry structures are investigated by means of radar.

For measurements of material velocity it was observed, both from site and laboratory data, that:

- Small variations in the measured travel time may be noted when changing the antenna frequency used.
- The use of the simplified formula for low loss material velocity is valid, unless low frequency antennae are employed on materials with high conductivity. In

such case the material will behave as a conductor and the simplified formula for conductors can be used.

Radar experiments were undertaken to investigate the effects of material conductivity on wave velocity and attenuation. In particular, the case of fill (water) material with increasing conductivity (salt content) was examined:

- At the range of conductivity considered, it was seen from the time domain analysis that the variation in conductivity leaves the value of dielectric constant virtually unchanged.

- From a detailed analysis of reflected signal magnitude it was seen that the conductivity greatly affects the attenuation of the signal; in particular that material conductivity increase, exponentially affects the reduction in signal amplitude.

Factors affecting the target signature shape:

- from comparison of data from tests conducted to investigate the effect of a wall presence on target resolution and other data from tests conducted on rebars at varying depth for horizontal resolution purposes, it was seen that targets may appear to have varying hyperbola curvature caused by varying view angle of the signal beam.

- For constant velocities of antenna survey (or constant number of scans recorded per unit distance travelled) the phenomenon is due to spreading of the signal caused either, at an "early" travel time, by the passage through the wall/fill interface, or, with increasing target depth, by the change in view point with which the antenna "sees" the target. The effect in both cases is flatter hyperbola shape.

- From the interpretation of horizontal resolution tables obtained by parametric study, it was noted that, all other parameters being equal, an increase in

material dielectric constant would increase the resolution power. This was attributed to focusing of the signal beam caused by earlier attenuation of the external beam rays. This would also have an effect on target signature shape and the hypothesis was formed that hyperbolas may appear more curved and shorter with increasing dielectric constant.

Experiments were conducted to investigate the horizontal resolution of 900 MHz antenna in water:

- Data were compared with figures from a table which plotted theoretical values of horizontal resolution in water as a function of the antenna frequency used. The numerical analysis was carried out using the concept of Fresnel zone, which represents the limit to distinguish two separate targets, whilst the antenna centre frequencies used were those specified by the manufacturer for transmission in air but corrected to take into account changes in frequency due to coupling to a medium different from air. Figures were also plotted for the case of dry and saturated sand. It was seen that the resolution improves for higher values of antenna frequency used and for shallower depths. In fact, as the wave propagates, its centre frequency is expected to lower and the pulse to become larger, reducing the resolution. Furthermore it was seen from the tables and discussed how the horizontal resolution improves with increasing dielectric constant. A higher material dielectric constant seems to modify the signal beam by focusing it and in case of air the beam width will be maximum and the horizontal resolution a minimum. Results from radar tests conducted on a hollow masonry structure in the laboratory confirmed this hypothesis. The results obtained from the experimental data show that the target resolution is better than predicted by the numerical analysis and this is especially true for increasing distances from the antenna. Two possible explanations come to mind: either the frequency of the coupled antenna is higher than predicted or there is a reduction in the signal beam width due to attenuation with depth. Both these factors would improve the resolution.

8.4 Conclusions

From the above discussion it can be concluded that, whilst not providing the answers to all structural survey problems, radar has demonstrated to be very promising for the investigation of bridges. Problems can exist with regard to the interpretation of radar data in complex situations but this limitation was addressed by simulation work. Furthermore, in such cases, radar may be used in conjunction with other NDT methods to provide additional information before expediting the necessary repair or demolition work. Material conductivity can be monitored before applying radar, by low frequency conductivity measurements. When high moisture conditions or saline material are present, resulting in high attenuation of the radar signal, then sonic tomography can be performed instead. This is a powerful technique which is successful based upon the assumption that the measurement density is proportional to the size of target to be identified. The comparative use of these methods and complementation of the results is recommended for a complete diagnosis of the structural condition.

CHAPTER 9

CONCLUSIONS

9.1 General Conclusions:

- The NDT methods in this project: digital impulse radar (often referred to as ground probing radar - GPR), conductivity and sonics, have demonstrated the ability to be rapid, low cost, contacting and non-contacting techniques to aid bridge assessment and monitoring purposes. The results of the laboratory experiments and field surveys aid the transition from a qualitative procedure to quantitative techniques
- The analysis procedure involving the construction of tomographic cross-sections has enabled: inhomogeneity identification, moisture movement detection over time and identification of layering within the masonry.
- Each investigation and analysis method has proved to be effective and their parallel use in this investigation has drawn an organic picture of the state of the structure revealing both construction details and modification/problems which have arisen with time.
- Whilst some of the information gathered was common to more than one method, other knowledge has been obtained due to the special measurements of a particular technique.

9.2 Conclusions relating to bridge preliminary surveys:

- The review of masonry arch bridge construction forms has highlighted an array of possible combinations of materials and shapes, some not at all apparent from the outside of the structure.
- The Engineer who is fully aware of this scenario will be facilitated in the tasks of 1) recognising the type of structure under investigation with regard to the arch

extrados profile and spandrel internal solution, 2) applying correctly any NDT technique he may choose, 3) interpreting the data collected and evaluating the structure, 4) reaching a judgement of the outcome of the analytical programs for bridge assessment.

- Geometrical and material information has been summarised in tabular form for thirteen bridges: Table 2.1.
- Medieval bridges are heavy constructions with round or more often pointed arches and massive piers and abutments. Made of local stone, they are often of irregular shape and have uneven spans.
- In Scotland, and the Highlands especially, between 1724 and 1829, bridges have spans between 3 and 6 m and, in the forms and materials, they continue the pre-1724 tradition: the masonry of the arch is irregular schistose stone with voussoirs not radial to the curve of the soffit. The shapes are segments of no more than 90° or 100°. All the spandrels were made of the local rubble stone, either granite or schist, and filled with gravel or earth; they continued without break into the wingwalls (a difference with later bridges).
- In the 18th Century Wales, the materials were hard stone and hydraulic mortar. Spandrels are of neater masonry, almost hewn work. The arches, segmental or semicircles, have strictly radial joints and the thickness may be less in the inner of the barrel than on the ring faces. At the same time in England, county bridges are very narrow (3 to 4.2 m), still ribbed or pointed (semicircular arches are not common) with max. segments of 90° - 120°.
- The construction of Westminster Bridge, from 1734, introduced a number of innovations which will be rapidly spread over the Country: 1)higher span/pier ratios (about 4.5); 2) semicircular arch shape; 3) arch backed with a tapering secondary arch; 4) spandrel space divided into 9 compartments by 4 perpendicular walls of dry stone and filled with gravel; 5) hollow segmental arches resting on the thinner semicircular arches of a sunken pier (1748).
- In 1756, Pontypridd Bridge introduces the concept of a lighter fill above a thin arch, with voids through each rubble masonry spandrel and charcoal infilling. The

innovative features were extensively copied after 1760 in South Wales and adjacent counties of England, with examples in North England and Scotland.

- Blackfriars Bridge (1759) introduced thin elliptical arches with counter arches in between, filled with rubble work and topped by a horizontal course of stone from haunch to haunch - the middle portion of the arch acts as a segment of arch supported by stiff piers filled with rubble. Each arch course was built of stones alternatively the full thickness of the arch and half the thickness. All other bridges by the same designer, Robert Mylne, have segmental arches, between 85° and 120° and present a taper (thicker sections at the haunches and springings), and thinner sections in the inside of the barrel.
- John Smeaton's large bridges present segmental arches (about 120°) with triple keystones and ornaments on the spandrels (masonry rings with keystones at the end of vertical and horizontal diameters). Scrabbled masonry is used for piers and spandrels, and rubble masonry infill for 1.8 m above the springings and gravel - of poor quality - from there to the road. These features were copied on most large Scottish bridges, whilst small bridges show variety of design. Instead, Perth Bridge (1769) presents a full design for the method of hollowing: longitudinal voids covered by pointed vaults of good rubble masonry and tied by iron chain-bars.
- From 1768-69, there were two ways of building large bridges:

  a) longitudinal voids between walls- running back to back of adjacent arches;

  b) large cylindrical voids running from spandrel to spandrel hidden on the outside.
- By 1828 this was the accepted way of building spandrels between large arches both in Scotland and England.
- From 1760, bridge presenting the "Adam style" are recognisable because of their very ornate, of classical form, with spandrel of radial courses and masonry rings on them, and elliptical arches. There is no information about internal construction. Bridges by Alexander Stevens are very ornate, following the Adam style, with tapered arches and hollow spandrels with 2 longitudinal walls supporting the road. They are built of red and yellow sandstone.

- Between 1790 and 1800, John Rennie introduces more elliptical arches and inverted arches of hewn stone between spans, and longitudinal voids above them. In place of rubble masonry, he used ashlar masonry. Telford, instead, seldom uses elliptical arches. His bridges have solid piers up to a certain height and hollow above (for inspection): a feature which became copied by others.
- With the 19th Century, 1) spans lengthen, 2) cutwaters are pointed with round shoulders and extend up above the springings, 3) arches, either segments of circles or ellipses, have very low profile, 4) piers are narrow (span to pier ratios up to 9), 5) edges of arches may present "cornes de vache" profile. Bridges by Rennie have tapered arches of large thickness and spandrels hollowed by longitudinal voids. Inner spandrels may be built of brick masonry. In contrast, bridges by Telford in the Highlands are rubble stone, as the previous in the area, but with longer single spans, wider roadways, but buttered form of wingwalls. They have no ornaments, no inverted arches over the piers and no radiated courses in the abutments; always solid pilasters of considerable bulk. His large bridges have slim projecting piers with subsidiary arches springing from the piers; hollow interiors with inner walls 0.6 m thick, covered with flat stones, and outer walls 0.9 m thick of excellent sandstone masonry; the walls are connected with crosswalls and tie-stones; the road material utilises clay seal and hydraulic concrete.
- By mid-1800 masonry bridges are obsolete but still hundreds were built following the traditional methods. In the 20th Century many such bridges were widened and strengthened by laying concrete over arches and spandrel voids; many of these operations are unrecorded.

9.3 Conclusions relating to radar testing:

- GPR offers a rapid, non-contact high resolution method for detecting and mapping features in engineering applications.
- The advantages of digital radar over conductivity and sonic methods are: rapidity and reproducibility in allowing continuous scan recording.

- Radar signals are very sensitive to changes in material conductivity and the relationship between conductivity and signal attenuation is exponential.
- Radar can be used for the detection of localised areas with high salt content or contaminant.
- The radar technique cannot be used for high resolution soundings at great depth ranges, in environments with high electrical conductivity.
- The range and resolution of GPR decreases with the presence of conductive materials such as brine or conductive pore water: significant signal attenuation occurred when the soil was wet. At saline contents of 0.05% by weight, 900 MHz bow tie antenna signals were significantly attenuated.
- In the case of a hollow composite structure, propagation of the radar signal through air causes the signal beam to propagate with a wider angle than through soil.
- In hollow masonry structures, refraction effects can be dominant over reflection from targets, with the risk of masking relevant data.
- The high value of reflection coefficient in air may affect the signal propagation if multiple interfaces are present.
- When a structure investigated is filled with soil, refraction effects are attenuated and the presence of targets may be better resolved.
- When testing through soil, the best results were obtained when using radar through dry soil.
- Where multiple changes of interface between dielectric layers take place, the change of dielectric constant will be identified but the resolution of the final target layer may prove particularly elusive.
- When a wall is present, the continuous interface at the wall/air or wall/fill boundary causes reflection of part of the wave, before the signal can reach the target, with the consequence that a weaker signal travels through the fill than if the wall was not there. A reduced depth of penetration can be expected.

- Multiple reflections inside the masonry wall will also cause changes of the beam angle with spreading of the signal beam portion that eventually passes into the fill, thus modifying the signature shape of the resolved target.
- From the comparison of radar plots showing metal bars in fill, contained or not by a masonry wall, the target shape analysis clearly showed that, when the wall is present, the reflection hyperbolas from the targets in the fill appear weaker, flatter and with shorter branches.
- Comparison of data recorded when either no fill was present or a dry sand fill was in place, showed that a stronger reflection appears at the interface in the former case. Brickwall/air boundary thus constitutes a stronger interface than brickwall/fill, and the calculation of the reflection coefficient confirmed this observation.
- The above has great importance when hollow masonry structures are investigated by means of radar.
- The antenna frequency plays a key role in the radar survey and a compromise must often be reached between resolution and penetration power of the antennae chosen. The "correct" antenna depends on the goals of the survey.
- From comparison of data from tests conducted to investigate the effect of a wall presence on target resolution and other data from tests conducted on rebars at varying depth for horizontal resolution purposes, it was seen that target's hyperbola curvature may vary due to varying view angle of the signal beam.
- Hyperbola curvature of the target may appear to change, depending on the velocity of movement of the antenna.
- For constant velocities of antenna survey (or constant number of scans recorded per unit distance travelled) the phenomenon is due to spreading of the signal caused either, at an "early" travel time, by the passage through the wall/fill interface, or, with increasing target depth, by the change in view point with which the antenna "sees" the target. The effect in both cases is flatter hyperbola shape.
- From the interpretation of horizontal resolution tables obtained by parametric study, it was noted that, all other parameters being equal, an increase in material dielectric constant would increase the resolution power. This was attributed to

focusing of the signal beam caused by earlier attenuation of the external beam rays. This would also have an effect on target signature shape and the hypothesis was formed that hyperbolas may appear more curved and shorter with increasing dielectric constant.

- A higher material dielectric constant seems to modify the signal beam by focusing it and in case of air the beam width will be maximum and the horizontal resolution a minimum. Results from radar tests conducted on a hollow masonry structure in the laboratory confirmed this hypothesis.
- Small variations in the measured travel time may be noted when changing the antenna frequency used.
- The use of the simplified formula for low loss material velocity is valid, unless low frequency antennae are employed on materials with high conductivity. In such case the material will behave as a conductor and the simplified formula for conductors can be used.
- Digital impulse radar surveys were undertaken on two stone masonry arch bridges: Middleton Bridge and Kilbucho Bridge, both in the Scottish Borders.
- Tomographic imaging was used to gain greater insight into the structure.
- Variations in the composite fill of arch bridges were discussed in relation to the general equation of electromagnetic wave velocity taking account of conductivity and frequency effects.
- On arch bridge fill with high attenuation properties, conventional reflection surveys proved ineffective for target resolution.
- Results from transmission measurement surveys have been more satisfactory.
- In one case, Middleton Bridge, significantly higher dielectric constants were calculated than might have been expected from published literature. This has been attributed to moisture/salinity factors in the structure.
- By using a range of antenna frequencies at Kilbucho Bridge it was possible to obtain information regarding the dielectric properties of bridge fill and masonry materials. Comparison was made of results extracted from measurements recorded with different frequencies and through varying antenna configurations and locations.

- In the laboratory a double span arch model was successfully used for calibration of the reflection technique above masonry arches in controlled conditions.
- Effects on the signal velocity, due to the material density, in relation to the shape of the arches was discussed.
- Limitations of radar for the localisation of the arch springings were identified in relation to the specific case of two semicircular arches in close proximity. The phenomena of the cone of emission of the antenna and "merging" effects in the signatures of two such arches were also discussed.

9.4 Conclusions relating to conductivity testing:

- The low cost, in terms of time in the data collection phase and post data-collection analysis, makes conductivity surveying convenient for repetitive surveys.
- Furthermore the techniques allows for high resolution in the conductivity variations detected, thereby improving the quality of the results interpretation.
- The instrumentation is compact and light which makes it suitable for bridge applications.
- Conductivity is usually determined by one or more of the following parameters: clay content, moisture content, moisture salinity, temperature - the most complex is usually the moisture profile which is affected by the material type and its compaction/porosity, and seasonal variations.
- The technique allows for lateral variations of conductivity to be accurately measured.
- Simple multi layered conductivity surveys are also possible by raising the instrument above the material/ structure surface.
- The maximum depth of exploration is limited by the coil spacing.
- The values of conductivity, directly read on the instrument, are a function of the frequency used and coil spacing - the figures do not represent the conductivity at any particular depth, rather the value is a function of all the matter between the face of the instrument and the maximum depth of exploration.

- Whilst the conductivity method has given detailed information up to a certain depth into the structure, no data could be collected at deeper locations.

9.5 Conclusions relating to sonic testing:

- Sonics are an established method for the evaluation of civil structures and numerous applications have been successful in qualifying the state of masonry elements and structures, and in verifying the integrity of repair.
- Sonics are a reliable method when great attention is spent in recording the data; meticulous work is necessary during the collection and analysis of the data.
- Good results can be achieved when the optimal grid density is set in relation to the goal of the test: size of inhomogeneities and/or possible voids, thickness of walls, thickness of arch and other structural elements.

9.6 Conclusions relating to tomographic analysis:

- Tomographic imaging was used to gain greater insight into the structure and proved to be very useful.
- In this project tomographic modelling was undertaken using sonics, conductivity and impulse radar.
- Tomographic applications combine the advantages of traditional sonic testing and offer the advantage that large areas can be evaluated easily. The internal condition of the structure is revealed by local information across the section.
- Great care is required in performing the tests and collecting the data: factors like choice of the number and position of the reading stations, raypath coverage across the section, raypath incidence angle and length, number of ray paths and back readings can greatly affect the final result of the inversion. The same attention must be paid to choosing the transit times during processing of the data. Knowledge of factors which may affect the pulse velocity is required to smooth the data prior to data inversion.

- The tomographic elaboration of the conductivity data has provided a clearer picture of any layered configuration in the structure section. The particular depth of penetration of the instrument used was a limitation of the survey, as details from the fill material behind the masonry wall could not be revealed.
- Digital impulse radar surveys for tomographic inversion were undertaken on a stone masonry arch bridge Middleton Bridge and Kilbucho Bridge, both in the Scottish Borders.
- Radar tomographic imaging was aimed at gaining greater insight into the structure.
- Three-sided tomography (i.e. upstream-wing-wall/abutment/downstream-wing-wall or upstream-spandrel-wall/arch-intrados/downstream-spandrel-wall) would give better coverage of the sections investigated and a better reconstructed image resolution.
- The greater the angle of the ray paths connecting Tx and Rx would improve the defect location by enhancing the "time-depth" of any anomaly present.

9.7 Conclusions from ray tracing simulation experiments:

- It has been shown that the ray tracing simulation method provides a mean by which the impulse radar response of a structural system can be readily simulated.
- The simulations undertaken have shown the effects which target spacing and depth have on the radar signature shapes.
- Simulation results well compare with the real case survey plots.
- Simulation data has been used to assess the output specification from a commercial antenna.
- It is expected that simulation will allow the interpretation of actual surveys to be more readily understood, which will in turn allow a better engineering assessment to be made of a structure under investigation.

9.8 Recommendations for further work:

This broad ranging project on the non-destructive testing of masonry arch bridges has identified many areas where further work is required, including:

- The compilation of an archive of bibliographic information pertinent to individual historical bridges. The library of data on bridges could be collected when the arch ring is exposed. This would facilitate the work of the assessment engineer.
- A data base of electromagnetic wave velocity, conductivity and dielectric constant values for engineering materials in different physical conditions (moisture content and density) would be valuable since values are available in the literature for geophysical materials and concrete but very little information is readily available for masonry materials typical of historical composite structures such as stone masonry bridges with soil fill.
- More radar site data needs to be collected on masonry structures and masonry bridges: information regarding dimensions and shape of the main structural elements (arch and walls), nature of the materials and condition of the fill (wet or dry, loose or compact) are considered extremely important in order to assess the strength and condition of the structure. The availability of comparative data would increase the confidence of the assessing engineer. At present, little or no comparative data are available, because the applications of radar to masonry structures is still at an experimental stage.
- A database of surveys carried out with NDT tests on masonry bridges be initiated, containing print-outs of the results obtained and clear description of the methodologies of collection of the data. Not only the exact location of the reading positions need to be registered but also the precise settings used on the instrumentation as the systems have great capabilities and data can be recorded in a number of ways. In published papers regarding radar applications, not only in the civil engineering field, data plots are sometimes not shown either because of difficult interpretation to the non-expert reader or because of lack of confidence in the interpretation by the radar user. When radar plots are presented, basic information is sometimes missing, such as indications of the time range used or even the antenna frequency employed and surface distance surveyed. Data

information regarding radar applications should include the antenna frequency employed, the number of operating antennas and mode of operation, the time range, the rate of data recording (number of scans per second, number of samples per scan), whether filtering and gain are applied and which kind, use of survey wheel on the antenna, antenna orientation in relation to the direction of scanning, and any other useful site information. If complete data and survey information is available, comparison with new data - either for repair outcome control or for monitoring purposes, will be possible.

- Guidelines on use of these NDT techniques on masonry structures and bridges should be made available for guidance with the survey procedures and result presentation. The effect on the user, of increased confidence in the method would eventually make the techniques more widely employed and accepted.
- Improved radar signal processing software is required for profiling continuous reflections on the radar plot and automatically calculating the depth and velocity through the layer (given the input of appropriate dielectric constant value).
- Additional work is required on the horizontal resolution of radar taking into account the Fresnel Zone.
- Additional work is required on the frequency components of the transmitted frequency of the radar signal through masonry and composite structures.
- The amount of data processing and analysis required on data for sonic, conductivity and radar tomographic inversion means that the data will need to be elaborated through a network analyser because the individual manual picking of the wave travel times (or signal magnitude) from individual scans and their input in tomographic software is unrealistic in terms of time and energy, requiring incredible patience and precision..
- Material conductivity figures used in civil engineering practice are either extracted from geophysical literature publications or directly obtained from site/sample measurements. In both cases, conductivity values are read with the use of DC or low frequency (10 - 300 kHz) instrumentation; these frequencies are much lower than frequencies used in civil engineering radar applications (ranges from 100 MHz to 1 GHz). The conductivity values are known to increase with increasing

frequency, therefore correction factors should be derived for higher frequencies prior inputting of these conductivity values in the radar equations for calculation of other dielectric parameters.

- Custom equipment for determining conductivity at variable depth is to be developed and the enhancement of interpretation software and 3-D modelling is being carried out. Full scale field and laboratory calibrations would be required.

REFERENCES

Abrams, D.P., Epperson, G.S., (1989 a), Evaluation of shear strength of unreinforced brick walls based on non-destructive measurements, *Proc. 5th Canadian Masonry Symposium*, Vancouver, B.C., June '89.

Abrams, D.P., Epperson, G.S., (1989 b), *Nondestructive evaluation of masonry buildings*, Res. Rep. No. 89-26-03 sponsored by Army Research Office, 208 pp., Advanced Construction Technology Center, University of Illinois at Urbana-Champaign, Illinois, USA.

Agardh, L., (1991), "Modal Analysis of two concrete bridges", *Structural Engineering International*, vol. 1 (4), pp. 35-39.

Agardh, L., Palm, J., (1992), "Modal analysis of a highway concrete bridge excited with impact", *American Concrete Institution Spring Convention*, Washington.

Aktan, A.E., Lee, K.L., et al., (1994), "Modal testing for structural identification and condition assessment of constructed facilities", *12th Int. Modal Analysis Conference*, Honolulu, Hawaii, vol. 1, pp. 462-468.

Alexander, D., (1990), Failing the stress test, *New Civil Engineer*, ICE, Thomas Telford, London, 1 Feb. '90, p. 22-23.

Alongi, A.V., (1973), A short-pulse high-resolution radar for cadaver detection, *Proc. 1st Int. Electronic Crime Countermeasures Conf.*, p. 79-87.

Annan, A.P., (1995), "Personal communication", Sensors & Software Inc, 5 June 1995.

Anon, (1976), "*Bridge inspection*", Organisation for Economic Co-operation, Paris.

Anon, (1994), Arched back, *New Civil Engineer,* ICE, Thomas Telford, London, 17 Feb '94, p. 6.

Anzani, A., Binda, L., Melchiorri, G., (1995), Time dependent damage of rubble masonry walls, *4th Int. Masonry Conf.,* London.

Archie, G.E., (1942 a), The electrical resistivity log as an aid in determining some reservoir characteristics, *Petroleum Tech.*, **5**:1-8.

Archie, G.E., (1942 b), The electrical resistivity log as an aid in determining some reservoir characteristics, *Transactions of the Mining and Metallurgical Engineers*, 146, 54-62.

Armstrong, D.M., Sibbald, A., Forde, M.C., (1993), Integrity assessment of masonry arches using the dynamic stiffness technique, *Proc. 5th SFR-'93*, Edinburgh, 29 June - 1 July, vol. 3, p. 297-302.

Arndt, D., Borchardt, K., Croy, P., Geyer, E., Henschen, J., Maierhofer, Ch., Niedack-Nad, M., Rudolph, M., Schaurich, D., Weise, F., Wiggenhauser, H., (1994), "Anwendung und Kombination zerstorungsfreier Prufverfahren zur Bestimmung der Mauerwerksfeuchte im Deutschen Dom", *Forschungsbericht 200 der BAM*, Berlin, Bremerhaven: Wirtschaftsverlag NW Verlag fur neue Wissenschaft, 75 pp.

BA 16/93. (1993), *The assessment of highway bridges and structures*, HMSO, London.

Baronio, G., Binda, L., (1989), Studio sull'alterazione delle murature in laterizio, *L' edilizia e l'industrializzazione*, No. 6, p. 313-320 (1st part) and No. 7/8, p. 366-373

(2nd part). First presented at the seminar *Problemi di intervento sulle strutture dell'edilizia storica*, Turin, Italy, 1985.

Baronio, G., Binda, L., et al., (1995), Degrado dei monumenti milanesi e interventi di conservazione delle superfici esterne, *Conf. Milano restaura il monumento e il suo doppio,* J. A-LETHEIA, **6**: 48-50

Barr, B., (1978), "Bridge building in Wales", *The Highway Engineer*, p. 2-9.

Barr, B., (1994), "Bridge building in Wales - Yesterday and today", *Bridge Assessment Management and Design*, (B.I.G. Barr et al. eds.), Elsevier, Amsterdam, pp. 5-10.

Barr, B.I.G., Evans, H.R., Harding, J.E. (Eds.), (1994), Bridge Assessment Management and Design, *Proc. Centenary Year Bridge Conference*, Cardiff, U.K., 26-30 Sept 1994, Elsevier, Amsterdam, 508 pp.

Begg, D.W., Fishwick, R.J., (1994), "Limit analysis of masonry arch bridges", *Bridge assessment management and design*, (eds.) B.I.G. Barr et al., Elsevier, Amsterdam, pp. 175-180.

Bensalem, A., Fairfield, C.A., Sibbald, A., (1994), "Application of the impact excitation method to an arch bridge", *Bridge Assessment Management and Design*, (eds.) B.I.G. Barr et al., Elsevier, Amsterdam, pp. 157-162.

Bensalem, A., Fairfield, C.A., Sibbald, A., (1997), "Non-destructive evaluation of the dynamic response of a brickwork arch", *Proc. ICE Structs & Bldgs,* **122,** Feb., 69-82.

Berra, M., Binda, L., Anti., Fatticcioni, A., (1991), Non destructive evaluation of the efficacy of masonry strengthening by grouting techniques, *9th Int. Brick/Block Masonry Conf.*, Berlin, vol. 3, p. 1457-1464.

Berra, M., Binda, L., Anti., Fatticcioni, A., (1992), Utilisation of sonic tests to evaluate damaged and repaired masonries, *Conf. Nondestructive Evaluation of Civil Structures and Materials*, Boulder, Colorado, p. 329-338.

Bertram, C.L., Campbell, K.J., Sandler, S.S., (1972), Locating large masses of ground ice with an impulse radar system, *Proc. 8th Int. Symp. Remote Sensing*, Willow Run Laboratory, Michigan University.

Binda, L., Colla, C., Forde, M.C., (1994), "Identification of moisture capillarity in masonry using digital impulse radar", *J. Construction & Building Materials*, **8**(2), p. 101-107.

Binet, C., (1996), Condition and repair cost estimate of the French road bridge assets, *Proc. of US-Europe Bridge Engineering Workshop*, Barcelona, Spain, 15-17 July 1996, in *Recent advances in bridge engineering: evaluation, management and repair*, (eds. Casas, J.R., et al.), CIMNE, Barcelona, 66-75.

Botros, A.Z., Olver, A.D., Cuthbert, L.G., Farmer, G., (1984), Microwave detection of hidden objects in walls, *Electron Lett.*, **20**, p. 379-380.

Bowders, J.J., Koerner, R.M., (1982), Buried container detection using ground probing radar, *J. Hazard. Mater.*, **7**, p. 1-17.

Branco, F.A., deBrito, J., (1996), Bridge management: from design to maintenance, *Proc. of US-Europe Bridge Engineering Workshop*, Barcelona, Spain, 15-17 July 1996, in *Recent advances in bridge engineering: evaluation, management and repair*, (ed. Casas, J.R., et al.), CIMNE, Barcelona, 76-98.

Brandon, J.A., (1994), "Dynamic testing of bridges: current practice and future prospects", *Bridge Assessment Management and Design*, (eds. B.I.G. Barr et al.), Elsevier, Amsterdam, p. 73-78.

Brangwyn, F., (1915), *A book of bridges*, J.Lane, London, 415 pp.

BS 1377, (1990), "Methods of test for soil for civil engineering purposes", BSI, London.

BS 5390, (1976), *Code of practice for stone masonry,* British Standard Institution, London, HMSO.

BS 5628, (1992), *Use of masonry, Structural use of unreinforced masonry*, Part 1, British Standard Institution, London, HMSO.

BS 6100, (1985), *Glossary of building and civil engineering terms,* Section 5.1, British Standard Institution, London, HMSO.

Bungey, J.H., (1997), The future of NDT in Civil Engineering, *Proc. IV Int. Conf. NDT-CE '97*, 8-11 April '97, Liverpool, UK, British Inst. of Non-Destructive Testing, vol. 1, p. 69-76.

Bungey, J.H., Millard, S.G., Shaw, M.R., (1993), "A simulation tank to aid interpretation of radar results on concrete", *Magazine of Concrete Research*, **45**(164), p. 187-195.

Buyukozturk, O., Rhim, H.C., (1995), "Radar using imaging of concrete specimens for non-destructive testing", *Proc. 6th. Int. Conf. Structural Faults & Repair-95,* London, July 1995, Engineering Technics Press, Vol. 2, 307-310.

Campbell, K.J., Orange, A.S., (1974), A continuous profile of sea ice and freshwater ice thickness by impulse radar, *Polar Rec.*, 17.31.

Chandler, H.W., Chandler, C.M., (1995), "The analysis of skew arches using shell theory", *Proc. 1st Int. Conf. Arch Bridges*, (ed.) C. Melbourne, Bolton, UK, 3-6 Sept. '95, p. 195-204.

Cheng, D.K., (1989), *Field and wave electromagnetics*, Addison-Wesley Publishing Company, USA, 703 pp.

Chidiac, J., Rainer, J. Davis, L., Johnson, B., (1995), "Use of impulse radar for investigating the integrity of stone masonry walls", *Proc. Int. Symp. Non-Destructive Testing in Civil Engineering (NDT-CE)*, Berlin, DGZfP, vol. 1, p. 487-494.

Choo, B.S., Coutie, M.G., Gong, N.G., (1990), "Analysis of masonry arch bridges by a finite element method", *Int. Conf. Forth Rail Bridge Centenary,* Edinburgh, UK.

Choo, B.S., Coutie, M.G., Gong, N.G., (1991), "The effects of cracks on the behaviour of masonry arches", *9th Int. Brick/Block Masonry Conference*, DGfM, Berlin, Germany, 13-16 Oct. '91, vol. 2, pp. 948-955.

Choo, B.S., Gong, N.G., (1995), "Effect of skew on the strength of masonry arch bridges", *Proc. 1st Int. Conf. Arch Bridges*, (ed.) C. Melbourne, Bolton, UK, 3-6 Sept. '95, pp. 205-214.

Clemena, G.G., Sprinkle, M.M., Long, R.R., (1987), Use of ground penetrating radar for detecting voids under concrete pavement, *Rep. No. 1109*, Transportation Research Board.

Colla, C., Das, P.C., McCann, D.M. & Forde, M.C., (1995), "Investigation of stone masonry bridges using sonics, electromagnetics and impulse radar", *Proc. 3rd Int.*

Symp. Non-Destructive Testing in Civil Engineering (NDT-CE), Berlin, Germany, 26-28 Sept. '95, vol. 1, 629-636.

Colla, C., Forde, M.C., McCann, D.M., Das, P.C., (1997) "Laboratory modelling of radar propagation through masonry", *Proc. IV Int. Conf. Non-Destructive Testing in Civil Engineering (NDT-CE '97)*, 8-11 April 1997, Liverpool, UK, vol. 1, 303-316.

Colla, C., Donati, M.C., et al., (1993), *Cascina Rosa: le indagini per la diagnostica e il progetto di conservazione,* Undergraduate Thesis, Faculty of Architecture, Politecnico di Milano, Milan, Italy, 4 vol., 1444 p.

Colla, C., McCann, D.C., Das, P.G., Forde, M.C., (1996), "Non contact NDE of masonry structures and bridges", Proc. *3rd Conf. Nondestructive Evaluation of Civil Structures and Materials*, Boulder, Colorado, USA, 9-11 September 96, vol. 1, 441-454.

Cooke, R.S., Ashurst, D.M., McCavitt, N. & Forde, M.C. (1993) Digital radar assessment of Besses o' th' Barn post-tensioned precast segmental rail bridge, *Proc. Int. Conf. Structural Faults & Repair-93,* University of Edinburgh, June 1993, Vol. 1, Engineering Technics Press, 305-314.

Corson, D., Lorrain, P., (1962), *Introduction to electromagnetic fields and waves.* W.H. Freeman and Company, London.

Cote', P., Gautier, V., Perez, A., Vanhoove, J.P, (1992), Mise en oeuvre d'auscultations tomographiques sur ouvrages d'art, *Bull. Liaison Labo. P. et Ch.*, **178**, mars-avr '92.

Creed, S.G., (1987), "Assessment of large engineering structures using data collected during in service loading", *Structural Assessment*, (eds.) F.K. Garas et al., Butterworths, London, pp. 55-62.

Crisfield, M.A., (1984), "*A finite element computer program for the analysis of masonry arches*", TRL Report No. 1115, Crowthorne, UK.

Crisfield, M.A., Packham, A.J., (1987), "*A mechanism program for computing the strength of masonry arch bridges*", TRRL Research Report No. 124, Crowthorne, UK.

Crisfield, M.A., Wills, J., (1986), "Nonlinear analysis of concrete and masonry structures", *Finite elements methods for nonlinear problems*, (eds.) Gergan et al., Springer-Verlag, Berlin, Germany.

Culley, R.W., Jagodits, F.L., Middleton, R.S., (1975), E-phase system for detection of buried granular deposits, *Symposium on Modern Innovations in Subsurface Explorations*, 54th Annual Meeting of Transportation Research Board.

Daniels, D.J., Gunton, D.J., Scott, H.F., (1988), "Introduction to sub-surface radar", *Proc. IEE*, **135-F**(4), p. 278-320.

Daniels, J., (1988), Locating caves, tunnels and mines. *The leading edge*, vol. 7, No. 3, p. 32-37.

Das, P.C., (1993), Examination of masonry arch assessment methods. *Symp. Structural preservation of the architectural heritage*, IABSE, Rome, 385-392.

Das, P.C., (1994), Reliability analysis of bridges: past and potential applications, *Proc. of the Centenary Year Bridge Conference*, Cardiff, U.K., 26-30 Sept 1994, in Bridge Assessment Management and Design, (ed. Barr, B.I.G., et al.), Elsevier, Amsterdam, p. 133-138.

Das, P.C., (1996), Bridge management methodologies, in *Recent advances in bridge engineering: evaluation, management and repair*, (ed. Casas, J.R., et al.), CIMNE, Barcelona, *Proc. of US-Europe Bridge Engineering Workshop*, Barcelona, Spain, 15-17 July, p. 56-65.

Das, P.C., Davidson, N.C., Colla, C., (1995), Potential applications of non-destructive testing methods for bridge assessment and monitoring, *1-day seminar Analysis & Testing of Bridges*, I.Struct.E. H.Q., London, 26 April, 26 p.

Davey, N., (1953), "*Tests on road bridges*", Research Paper No. 16, National Building Studies Research Station, HMSO, London.

Davidson, N.C., Forde, M.C., Hardy, M.S.A., McCann, D.M., Colla, C., Clark, M., Broughton, K.J., Das, P.C., (1997) "Field trials to establish accuracy of radar for scour detection", *Proc. VII Int. Conf. Structural Faults and Repair -'97*, Edinburgh, 8-10 July 1997, Engineering Technics Press, vol. 1, 171-178.

Davidson, N.C., Forde, M.C., (1996), A laboratory appraisal of ground-penetrating radar over water, *Journal of NDE International,* vol. 12. no. 4. p. 219-242.

Davidson, N.C., Padaratz, I.J., Forde, M.C., (1995), "Quantification of bridge scour using impulse radar", *Proc. Int. Symp. Non-Destructive Testing in Civil Engineering (NDT-CE)*, Berlin, DGZfP, vol. 1, p. 61-68.

Davies, S.R., (1985), The assessment of load carrying capacity of masonry arch bridges, *Proc. 2nd Int. Conf. on Civil Structures and Engineering Computing*, Civil-Comp. Press, Edinburgh, vol. 2, p. 203-206.

Davies, S.R., (1989 a), "MARCH - a computer program for the assessment of masonry arches", *Proc. Int. Conf. Structural Faults and Repair '89*, M.C. Forde (ed.), London, June '89, vol. 1, pp. 277-287.

Davies, S.R., (1989 b), Some difficulties in the assessment of masonry arches, *Proc. Int. Conf. Structural Faults and Repair '89*, M.C. Forde (ed.), London, June '89, vol. 1, p. 289-295.

Davis, J.L. & Annan, A.P., (1989), Ground- penetrating radar for high-resolution mapping of soil and rock stratigraphy. *Geophysical Prospecting*, **37** (5): 531-551.

De Mare, E., (1975), *The bridges of Britain*, Batsford, London, 136 pp.

Department of Transport, (1993a), "*The Assessment of Highway Bridges and Structures*", Departmental Standard BD 21/93, HMSO, London, UK.

Department of Transport, (1993b), "*The Assessment of Highway Bridges and Structures*", Advice Note BA 16/93, HMSO, London, UK.

Department of Transport, (1994), *Inspection of highway structures; design manual for roads and bridges*, Departmental Standard BA 63/94, HMSO, London, UK, vol.3.

Dines, K.A., Lytle, R.J., (1979), Computerised geophysical tomography, *Proc. IEEE*, **67**, 1065-1073.

Ellick, J.C.A., Brown, G., (1994), "Vibration of masonry arch rings", *Bridge assessment management and design*, B.I.G. Barr et al., (eds.), Elsevier, Amsterdam, pp. 163-168.

Fairfield, C.A. & Ponniah, D.A., (1993), Geotechnical considerations in arch bridge assessment, *J. Instn Highways & Transportation*, **40** (7), 11-15.

Fairfield, C.A., (1994), "*Soil-structure interaction in arch bridges*", PhD thesis, University of Edinburgh, Civil Engineering Dept., Edinburgh, UK, vol 1.

Falconer, R.E., (1994), "Assessment of multi-span arch bridges", *3rd Int. Conf. Inspection, appraisal, repair and maintenance of buildings and structures*, Bangkok.

Fenning, P.J., Brown, A.J., (1995), Ground probing radar investigation within pipes and tunnels, *Proc. 6th Int. Conf. Structural Faults and Repair*, London, vol. 3, p. 101-105.

Fenning, P.J., Thompson, P.M., Veness, K.J., (1989), Geophysical investigation of tunnels, *Proc. 2nd Int. Conf. Foundations and Tunnels*, Edinburgh, vol. 2, p. 341-352.

Fewtrell, A., Walsh, B., (1994), "Inspecting the Giants of Wales", *Bridge Assessment Management and Design*, B.I.G. Barr et al., (eds.), Elsevier, Amsterdam, pp. 25-30.

Forde, M.C., McCavitt, N., (1993 a), Impulse radar testing of structures, *Proc. Instn Civ Engrs Structs & Bldgs*, 1993, **99**, Feb., 96-99.

Forde, M.C., McCavitt, N., (1993 b), Modal testing of reinforced concrete pavements, *Proc. Int. Conf. Structural Faults & Repair-93,* University of Edinburgh, June 1993, Vol. 2, Engineering Technics Press, 95-104.

Forde, M.C. (Ed.), (1993), *Structural Faults & Repair-93*, Engineering Technics Press, Edinburgh, 3 vols.

Forde, M.C. (Ed.), (1995), *Structural Faults & Repair-95*, Engineering Technics Press, London, 3 vols.

Forde, M.C. (Ed.), (1997), *Structural Faults & Repair-97*, Engineering Technics Press, Edinburgh, 3 vols.

Forde, M.C., Batchelor, A.J., (1984), "Low Frequency NDT testing of historic structures", *Proc. 3rd European Conf. on NDT*, Florence, Oct 1984, Vol 3, 316-324.

Forde, M.C., Komeyli-Birjandi, F., Batchelor, A.J., (1985), "Fault detection in stone masonry bridges by non-destructive testing", *Proc. 2nd Int. Conf. Structural Faults & Repair-85*, April 1985, London, Engineering Technics Press, 373-378.

Frangopol, D.M., Hearn. G., (1996), Managing the life cycle safety of deteriorating bridges, *Proc. of US-Europe Bridge Engineering Workshop*, Barcelona, Spain, 15-17 July 1996, in *Recent advances in bridge engineering: evaluation, management and repair*, (ed. Casas, J.R.), CIMNE, Barcelona, 38-55.

Friswell, M.I., Penny, J.E.T., (1992), "The use of vibration data and model updating to detect damage", *Structural integrity assessment*, Elsevier Applied Science, London.

Gilbert, D.J., (1997), *NDT yearbook 97*, The British Institute of Non-Destructive Testing, Northampton, 280 p.

Goodman, D. & Nishimura, Y., (1992), 2-D synthetic radargrams for archaeological investigation, *4th Int. Conf. Ground Penetrating Radar*, Finland Geol. Sur.

Goodman, D. & Nishimura, Y., (1993), A ground-radar view of Japanese burial mounds. *Antiquity*, 1993. **255** (67): 349-354.

Goodman, D., (1994), Ground penetrating radar simulation in engineering and archaeology. *Geophysics*, **59** (2): 224-232.

Greaves, J.G., Lesmes, D.P., Jung, M.L. & Toksoz, M.N., (1996), Velocity variations and water content estimated from multi-offset, ground-penetrating radar. *Geophysics*, 1996. **61**(3): 683-695.

HA 72/94, (1994), *Design Manual For Roads and Bridges*, The Highways Agency.

Haeni, F.P., Trent, R.E., (1988), Measuring scour with ground penetrating radar, sonar and seismic geographical methods, *Proc. 67th Annual Meet. Transportation research Board*, Washington D.C.

Hannah, I.C., (1934), *Story of Scotland in stone*, Oliver and Boyd, Edinburgh, 332 pp.

Harris, J., Lever, J., (1993), *Illustrated glossary of architecture 830-1830*, Faber, London, 218 pp.

Harvey, W.J., (1988), "Application of the mechanism analysis to masonry arches", *The structural engineer*, vol. 66 (5/1), pp. 77-84.

Harvey, W.J., (1995), Bridge testing, *1-day seminar Analysis & Testing of Bridges*, I.Struct.E. H.Q., London, 26 April, 6 p.

Harvey, W.J., (1997), "Personal communication", The University of Exeter, 10 Sept. '97, E-mail exchange.

Harvey, W.J., Maxwell, J.W.S., Smith, F.W., (1988), Arch bridges are economic, *8th Int. Brick/Block Masonry Conf.*, Trinity College, Dublin, Rep. of Ireland, 19-21 Sept., vol. 3, p. 1302-1310.

Heiland, C.A., (1968), *Geophysical exploration*, Hafner Publishing Co., New York, Ch.10.

Henderson, D., (1990), "The Use of Radar for the Investigation of Hidden Features and Defects in Structures", *The British Journal of Non-Destructive Testing*, **32**(8).

Hendry, A.W., Davies, S.R., Royles, R. & Ponniah, D.A., (1986), Load test to collapse on a masonry arch at Bargower, Strathclyde, *TRRL Contractor Report No. 26.*

Heyman, J., (1980), "The estimation of the strength of masonry arches", *Proc. ICE*, vol. 69.

Heyman, J., (1982), *The masonry arch*, EllisHorwood Ltd., Chichester, England, 117

Highways Agency, (1996), *The appearance of bridges and other highway structures*, London, HMSO, 192 p.

Hoar, R.J., Stokoe, K.H., (1978), Generation and measurement of shear wave in situ, *in Dynamic geotechnical testing*, American Society for Testing and Materials, Special Teclinical Pubblication 654, Philadelphia, Pa., p. 3-29.

Hobbs, C.B., Temple, J.A.G., Hillier, M.J., Silk, M.G., (1993), Radar inspection of civil engineering structures, *Proc. Int. Conf. Non-Destructive Testing in Civil Engineering*, Northampton, Brit, Inst of NDT, p. 79-86.

Hodge, A.T., (1992), *The Roman aqueducts and water supply*, Duckworth, London, 504 pp.

Hoekstra, P., Delaney, A., (1974), "Dielectric properties of soils at UHF and microwave frequencies", *J. Geophys. Res.*, **79**, p. 1699-1708.

Holt, F.B., Eales, J.W., (1987), Non-destructive evaluation of pavements, *Concrete International*, 9(6), p. 41-45.

Howe, M.A., (1897), *A treatise on arches*, John Wiley & Sons, Newyork, .

Hume, I.J., (1989), "Assessment, monitoring and temporary support of historically important structures", *Conservation of engineering structures*, ICE, Thomas Telford, London, pp. 63-72.

Hutton, C., (1772), *The principles of bridges: containing the mathematical demonstrations of the properties of the arches, the thickness of the piers, the force of the water against them*, T. Saint, Newcastle, 102 pp.

ICE (1989), Conservation of engineering structures, *Proc. of Conf. organised by ICE*, London, 13 March 1989, Thomas Telford, 156 p.

ICE, (1975?), *Our engineering heritage: three notable examples*, Edinburgh.

ICE, (1993), *Bridge investigation and repair*, 1-day seminar, Edinburgh and East of Scotland Association, University of Edinburgh, Edinburgh, 25 Nov. '93.

ICE, (1997 a), *The appearance of bridges and other highways structures*, 1-day seminar, Thomas Telford Conferences, ICE & Highways Agency, London, UK, 24th Feb. '97.

ICE, (1997 b), *Bridge testing, guidelines for supplementary load testing*, 1-day seminar, Thomas Telford Conferences, ICE & National Steering Committee, London, ICE HQ, 18 Sept. '97.

Idriss, R.L., White, K.R., Woodword, C.B., et al., (1993), Evaluation and testing of a fracture critical bridge: the 1-40 bridge over the Rio Grande, *Proc. 5th SFR-'93*, Edinburgh, 29 June -1 July, vol. 1, p. 47-52.

Jackson, M.J., Tweeton, D.R., (1994), MIGRATOM, Geophysical tomography using wavefront migration and fuzzy constraints, *R.I. 9497*, Bureau of Mines, United States Department of Interior, 35 pp.

Jervoise, E., (1931), *Ancient bridges in the North of England*, .

Jervoise, E., (1936), *The ancient bridges of Wales and Western England*, The Architectural Press, .

Joby, R.S., (1983), *The railway builders: lives and works of the Victorian railway contract*, David & Charles, Newton Abbot, 200 pp.

Jones, M., (1996), *NDT definition*, Non-destructive Testing newsgroup, e-mail 27 Dec. '96.

Kahle, M., Hillich, B., (1992), Einsatz des Radarverfahrens zur Erkundung von Struktur und Zustand historischen Mauerwerks, *Bautechnik* vol. 69, p. 342-354.

Kahle, M., (1993), "Investigation of historic masonry by means of radar", Proc. Structural Preservation of the Architectural Heritage", *IABSE Symposium*, Rome, p. 205-212.

Kahle, M., Fichtner, Neuwald-Burg, C., (1994), "Investigation of masonry in a medieval castle ruin", *Proc 10th Int Brick and Block Masonry Conf.*, Calgary, Alberta, Canada, 5-7 July, vol.3, p. 1551-1560.

Kak, A.C., Slaney, M., (1988), *Principles of computerised tomographic imaging*, The Institute of Electrical and electronic Engineers Press, New York.

Kearey, P., Brooks, M., (1991), *An Introduction to Geophysical Exploration*, Oxford.

Keller, G.V., Frischknecht, F.C., (1966), *Electrical methods in geophysical prospecting*, Ch. 1. Pergamon Press, N.Y.

Kingsley, G.R., Noland, J.L., Atkinson, R.H., (1987), Nondestructive Evaluation of masonry structures using sonic, and ultrasonic puls evelocity technique, *Proc. 4th North American Masonry Conference*, Los Angeles, CA, Aug. 87.

Komeyli-Birjandi, F., (1986), *Sonic investigation of masonry structures*, PhD thesis, Univ. of Edinburgh.

Kraus, J.D., (1988), *Antennas*, McGraw-Hill Book Company, New York, 2nd ed., 892 pp.

Krause, M., Maierhofer, Ch., Wiggenhauser, H., (1995), Thickness measurement of concrete elements using radar and ultrasonic impulse echo technique, *Proc. 6th Int. Conf. Structural Faults and Repair*, Edinburgh, vol. 2, p. 17-24.

Kroggel, O., (1993), "Non-destructive testing of the integrity of bridges; an EC project", *Bridge Management 2*, (eds.) J. E. Harding et al., Thomas Telford, London, pp. 727-737.

Lauffer, J.P., Tucker, M.D., Smallwood, D.O., (1987), "Multi-point transient modal testing", *5th Int. Modal Analysis Conference*, London, pp. 394-398.

Law, S.S., Wldron, P., Taylor, C., (1991), "Phase components of the FRF as a tool in structural fault diagnosis", *Asia-Pacific Vibration Conference*, Melbourne, Australia.

Law, S.S., Wldron, P., Taylor, C., (1992), "Damage detection of a reinforced concrete bridge deck using the frequency response function", *10th Int Modal Analysis Conference*, San Diego, California, vol. 2, pp. 772-778.

Leaird, J.D., (1984), A report on the pulsed acoustic emission technique applied to masonry, *J. Acoustic Emission*, vol. 3, No. 4.

Lord, A.E., Koerner, R.M., (1987), Nondestructive testing techniques to detect contained subsurface hazardous, *Rep. EPA/600/2-87/078*, Drexel University, Philadelphia.

Luz, E., Wallaschek, J., (1992), *Int. J. Analytical and Experimental Modal Analysis*, vol. 7 (1), 29-39.

Lynn, P.A., Fuerst, W., (1989), *Introductory Digital Signal Processing with computer applications,* Chichester, UK, John Wiley & Sons Ltd.

Maguire, J.R., Severn, R.T., (1987), Assessing the dynamic properties of prototype structures by hammer testing, *Proc. ICE*, vol. 83, Pt. 2, Dec. 87.

Mair, A.J., (1994), *A new UK design standard for unreinforced arch bridges,* unpublished report, 10 p.

Mancino, E., Pardi, L., (1994), A probabilistic approach to the prediction of the behaviour of the Italian Highways bridges, *Proc. Centenary Year Bridge Conference*, Cardiff, UK, 26-30 Sept. 1994, in *Bridge Assessment Management and Design*, (ed. Barr, B.I.G., et al.), Elsevier, Amsterdam, 127-132.

McCann, D.M., Baria, R., Jackson, P.D., Green, A.S.P., (1986), Applications of cross-hole seismic measurements in site investigation, *Geophysics*, **51**, p. 914-925.

McCavitt, N & Forde, MC, (1991), The application of the method of convolution to the simulation of the response of masonry arch bridges to ground probing radar, *J. Non-Destructive Testing & Evaluation*, vol. 6, 3: 179-194.

McDowell, P.W., Hooper, J.W., Barker, R.D., Darracott, B.W., Jackson, P.D., McCann, D.M., Skipp, B.O., (1988), Engineering geophysiscs, Report by the Geological Society Engineering Group Working Party, *The Quaterly Journal of Engineering Geology*, Vol. 21, No. 3, p. 207-271.

McMillan, A.A. (Ed.), (1987), *Building stones of Edinburgh*, Edinburgh Geological Society, 196 pp.

McNeill, J.D. (1980) "*Electrical Conductivity of Soils and Rocks*", Technical Note TN-5,, Geonics Ltd., October 1980.

McNeill, J.D., (1980a), *Electrical conductivity of soils and rocks*, Technical Note TN-5, Geonics Limited, Ontario, 22 pp.

McNeill, J.D., (1980b), *Electromagnetic terrain conductivity measurement at low induction numbers*, Technical Note TN-6, Geonics Limited, Ontario, 15 pp.

Melbourne, C. (Ed.), (1995), *Arch bridges*, Thomas Telford, London, UK., 693 pp.

Melbourne, C., (1990), *The behaviour of semi-circular brickwork masonry arch bridge models*, Bolton Institute of Higher Education, Contract No. TRR 842/543, Final Report, 45 p.

Melbourne, C., Colla, C., Ruddock, E., (1997), "Personal communication", London, ICE H.Q., 24 Feb 1997, informal discussion.

Melbourne, C., Gilbert, M., (1994), "The application of limit analysis techniques to masonry arch bridges", *Bridge assessment, management and design*, B. I. G. Barr et al. (eds.), Elsevier, Amsterdam, p. 193-198.

Melbourne, C., Tao, H., (1995), "The behaviour of open spandrel masonry arch bridges", *Proc. 1st Int. Conf. Arch Bridges*, C. Melbourne (ed.), Bolton, UK, 3-6 Sept. '95, p. 239-244.

Melbourne, C., Wagstaff, M., (1993), "Load tests to collapse of three large-scale multi-span brickwork arch bridges", *Bridge management 2*, (ed.) J.E. Harding et al., Thomas Telford, London, p. 227-235.

MEXE, (1963), "*Military load classification of civil bridges by reconaissance and correlation methods*", SOLOG study B38, Technical Memorandum (Bridges) No. BE4, Military Engineering Experimental Establishment, Christchurch, May '63.

Millard, S.G., Bungey, J.H., Thomas, C., Soutsos, M.N., (1997), Assessing bridge pier scour by radar, *Proc. IV Int. Conf. Non-Destructive Testing in Civil Engineering (NDT-CE '97)*, 8-11 April 1997, Liverpool, UK, vol. 1, 303-316.

Mills, R.L., (1989), Assessment of viaducts and bridges (listed structures and ancient monuments), *Conservation of engineering structures*. London, ICE, Thomas Telford, 5-18.

Milsom, J., (1989), *Field Geophysics*, Geological Society of London Handbook, 182 p.

Ministry of Transport, (1967), *"The assessment of highway bridges for construction and user vehicles"*, Report No. Technical Memorandum (Bridges) No. BE4, Ministry of Transport, London, UK, Jan. 1967, technical memorandum, .

Mitchell, C.G., Chettoe, C.S., (1925), "Strengthening and widening of bridges", *Public Works, Roads and Transport Congress*, London, 24th Nov. 25, 300-320.

Mitchell, G.R., (1954), "*Dynamic stresses in cast iron girder bridges*", Report No. Research Paper No. 19, HMSO, National Building Studies Research Station, London, research paper, .

Mooney, H.M., (1974), Seismic shear waves in engineering, *American Society of Civil Engineers, Journal of Geotechnical Engineering*, **100**, p. 905-923.

Morey, R.M, (1974), Application of downward looking impulse radar, *Proc. 13th Annual Canadian Hydrographic Conf.*, Canada Centre for Inland Waters, Burlington, Ontario, Canada.

Morey, R.M., Harringon, W.S., (1972), Feseability of electromagnetic subsurface profiling, *Rep. EPA-R2-72-082*, U.S. Environmental Protection Agency, Washington D.C.

Morgan, B.J., Oesterle, R.G., (1985), "On-site modal analysis - a new powerful inspection technique", *2nd Int. Bridge Conference*, Pittsburg, Pennsylvania, June 1985, 108-114.

Murray, P., Stevens, M.A. (Eds.), (1996), *Living Bridges - The Inhabited Bridge: Past, Present and Future.*, Prestel-Verlag, London, UK., 160 pp.

National Bureau of Standards, (1958), *Dielectric dispersion data for pure liquids and dilute solutions*, Circular No. 589.

Nelson, G., (1990), *Highland bridges*, Aberdeen University Press, Aberdeen, 223 pp.

Nelson, SD, (1994), "Electromagnetic modelling for ground-penetrating imaging radar (GPIR) using 3-D finite difference time-domain (FDTD) modelling codes", *SPIE-The Int Soc for Optical Engng Advanced Microwave and Millimeter-Wave Detectors*, San Diego, CA, USA, 25-26 July 94, vol. 2275, 186-195.

Northwestern University Infrastructure Technology Institute, (1996), *NDT*, http://iti.acns.nwu.edu/clear/bridge/ndt.html

O'Neill, H., (1965), *Stone for building*, Heinemann, London, 198 pp.

Olhoeft, G.R., (1975), Electrical properties of rocks, *The physics and chemistry of rocks and minerals*, J.Wiley and Sons, N.Y., p. 261-278.

Olhoeft, G.R., (1977), Electrical properties of natural clay permafrost, *Can J. Earth Science*, vol. 15, p. 16-24.

Olhoeft, G.R., (1993), "Processing, modelling and presentation of ground penetrating radar data", *2nd Government Workshop GPR - Advanced Ground Penetrating Radar: Technologies and Applications*, Ohio, 26-28 Oct 93, p. 23.

Ordnance Survey © Map 72, (1988), "Upper Clyde Valley", 1:50000

Ordnance Survey © Map 73, (1993), "Peebles and Galashiels", 1:50000

Padaratz, I.J. & Forde, M.C. (1995a) A theoretical evaluation of impulse radar wave propagation through concrete, *J. Non-destructive Testing & Evaluation*, **12**, 9-32

Padaratz, I.J., Forde, M.C., (1995b), Influence of antenna frequency on impulse radar surveys of concrete structures, *Proc. 6th Int. Conf. Structural Faults & Repair-95,* London, July 1995, Vol. 2, Engineering Technics Press, 331-336.

Padaratz, I.J., (1996), *A numerical and experimental investigation of radar coupling and propagation through concrete*, PhD thesis, Civil and Environmental Engineering Dept., The University of Edinburgh, 219 pp.

Padaratz, I.J., Hardy, M.S.A., Forde, M.C., (1997), "Coupling effects of radar antennae on concrete", *Proc 4th Int Conf: NDT-CE,* University of Liverpool, 8-11 April 1997, Vol 1, 237-245.

Page, J. (Ed.), (1993), *Masonry arch bridges*, HMSO, London, 118 pp.

Page, J., (1989), Discussion, *Conservation of engineering structures*, ICE, Thomas Telford, London, p. 147-148.

Page, J., (1994), "*Load test to collapse on the three span brick masonry arch Rotherham Road Railway bridge*", Report No. Project Report PR/CE/49/94 E508A/BL, TRL, unpublished report, 15+appendix+fig.

Page, J., (1995a), "Load tests for assessment of in-service arch bridges", *Proceedings of the 1st International Conference on Arch Bridges*, C. Melbourne Ed., Bolton, UK, 3-6 Sept. 95, in 'Arch bridges', p. 299-308.

Page, J., (1995b), "Load tests to collapse on masonry arch bridges", *Proceedings of the 1st International Conference on Arch Bridges*, C. Melbourne Ed., Bolton, UK, 3-6 Sept. 95, in 'Arch bridges', p. 289-298.

Pandey, A.K., Biswas, M., Samman, M.M., (1991), "Damage detection from changes in curvature mode shapes", *Journal of Sound and Vibration*, vol. 145(2), 321-333.

Parker, D., (1997), "Closure looms for repair starved Hammersmith bridge", *New Civil Engineer,* Issue, 23 Jan. '97, No. 3.

Paterson, A.C., (1989), Opening address, *Conservation of engineering structures,* Thomas Telford, London,1-4.

Paxton, R., (?), "Dean Bridge, Edinburgh", *Our engineering heritage, Three notable examples in the Edinburgh area: Dean Bridge, Leith Docks, Forth Rail Bridge,* Dryden Printing Co., Edinburgh, pp. 5-13.

Paxton, R., (1996 a), The Chairman's column, *PHEW Newsletter,* ICE, Thomas Telford, London, March '96, **69**.

Paxton, R., (1996 b), Conservation of the 1811 Railway viaduct at Laigh Milton, Scotland, *Historical Studies of Civil Engineering (Japanese journal),* No.16, June,1-16.

Paxton, R., Ruddock, E.C., (1979), *A heritage of bridges between Edinburgh, Kelso and Berwick,* I.C.E., Edinburgh and East of Scotland Ass., Dryden Printing Co., Edinburgh.

Petroy, D.E., (1994), Assessment of ground penetrating radar applicability to specific site investigations: simple methods for pre-survey estimation of likely dielectric constants, target resolution and reflection strengths, *Proc. Symp. Application of Geophysics to Engineering and Environmental Problems (SAGEEP),* Boston, Massachusetts, 27-31 March 1994, p 21.

Pippard, A.J., Chitty, L., (1951), "*A study of the Fussier arch*", National Building Research Station, HMSO, Research paper No. 11, .

Pippard, A.J.S., (1948), "The approximate estimation of safe loads on masonry bridges", *Civil engineer in war*, vol. 1, p. 365.

Pitt, J.B., (1994), "The use of impulse radar in the investigation, restoration and change of use of old buildings", *Construction Papers*, No. 30, p. 2-8.

Prato, C.A., (1997), *Dynamic testing of full-scale structures*, Civil Engineering Dept, National University of Cordoba, Argentina, talk given at University of Edinburgh, Civil Eng. Dept., 5 Sept. '97.

Prentice, D.J., (1996), *An appraisal of the geotechnical aspects of multi-span masonry arch bridges*, PhD Thesis, The University of Edinburgh, Edinburgh, 1 vol., 344 pp.

Prentice, D.J., Ponniah, D.A., (1994), "Testing of multi-span model masonry arch bridges", *Bridge assessment management and design*, (B.I.G. Barr et al. eds.), Elsevier, Amsterdam, pp. 169-174.

Pride, G., (1975), *Glossary of Scottish buildings*, Scottish Civic Trust.

Ranieri, G., Giani, G.P., Ferrero, D., (1988), Tomografie sismiche del Duomo di Orvieto, *Proc. Nat. Congress AIPnD*, Bologna, Italy.

Rankine, W.J.M., (1900), *A manual of Civil Engineering*, 21st ed., revised by W.J. Millar, C. Griffin, London, 820pp.

Rashkovskij, S.L., (1981), Linear vibrator characteristics near the boundary of two media, *Radiophysics (in Russian)*, vol. 24, n. 4.

Rhazi, J., Kharrat, Y., Ballivy, G., Khayat, K., (1996), Acoustical imaging for condition assessment of civil structures, *Proc. 3rd Conf. Nondestructive Evaluation of Civil Structures and Materials*, Boulder, Colorado, p. 211- 224.

Riccioni, R., Rossi, P.P., (1995), "*Restauro edilizio e monumentale, diagnosi e consolidamento*", ISMES Spa, Bergamo, Italy, 179 pp.

Robins, F.W., (1948), *The story of the bridge*, Cornish Bros., Birmingham, 278 pp.

Robinson, J.R., (1964), *Piers, abutments and formwork for bridges*, C. Lockwook, London, 286 pp.

Romaya, R.M., (1995), "The application of cylindrical shell theory to masonry arch bridges", *Proceedings of the 1st International Conference on Arch Bridges*, C. Melbourne Ed., Bolton, UK, 3-6 Sept. 95, in 'Arch bridges', p. 181-194.

Ruddock, E.C., (1974), "Hollow spandrels in arch bridges: a historical study", *Structural Engineer*, **52,** 281-293.

Ruddock, E.C., (1979), *Arch bridges and their builders 1735-1835*, Cambridge University Press, Cambridge, 254 pp.

Ruddock, E.C., (1996), "Personal communication", visit to Nasmyth Bridge conservation works, Edinburgh, Dec. 96, informal discussion.

Salawu, O.S., Williams, C., (1994), "Damage location using vibration mode shapes", *12th Int Modal Analysis Conference*, Honolulu, Hawaii, vol. 1, p. 933-939.

Samman, M.M., Biswas, M., Pandey, A.K., (1991), *International Journal of Analytical and Experimental Modal Analysis*, vol. 6(1), 35-44.

Schuller, M., Berra., M., Atkinson, R., Binda, L., (1995), Acoustic tomography for evaluation of unreinforced masonry, Proc. 6th Int. Conf. Structural Faults and Repair 95, vol. 3, p. 195-200.

Schuller, M., Berra., M., Fatticcioni, A., Atkinson, R., Binda, L., (1994), Use of tomography for diagnosis and control of masonry repairs, *Proc. 10th Int. Brick/Block Masonry Conf.*, Calgary, vol. 3.

Sibbald, A., (1988), *Impact hammer testing of masonry sewers*, PhD thesis, The University of Edinburgh, Edinburgh, 2 vol.

Siedell, A., (1940), *Solubility of inorganic, metalorganic and organic compounds,* New York, 3rd ed.

Silman, R., Ennis, M., (1993), "Non-Destructive Evaluation to document historic structures", Proc. Structural Preservation of the Architectural Heritage, *IABSE Symposium*, Rome, p. 195-203.

Slastan, J., Pietrzko, S., (1993), "Changes of RC-beam modal parameters due to cracks", *11th International Modal Analysis Conference*, Kissimmee, Florida, vol. 1, p. 70-76.

Smith-Rose, R.L., (1934), Electrical measurements on soil with alternating currents, *Proc. IEE*, **75**, p. 221-237.

Southwest Research Institute, (1996 a), *NDT definition,* http://www.nde.swri.edu: 8080/charter.html, NDE Science and Technology Division, San Antonio, Texas.

Southwest Research Institute, (1996 b), *NDE Research and Materials Characterisation,* http://www.swri.org/3pubs/brochure/d17/nderes/nderes.htm, NDE Science and Technology Division, San Antonio, Texas.

Sowden, A.M., (1990), *The maintenance of brick and stone masonry structures*, E & F N Spon., London, .

Steinman, D., (1957), *Bridges and their builders*, Dover Publications, New York, 401 pp.

Stewart, D., (1939), *Influence lines: their practical use in bridge calculation*, Constable & Company Ltd., London, 215 pp.

Sun, X., Hardy, H.R., (1992), "An investigation on applicability of modal analysis as non-destructive evaluation method in geotechnical engineering", *10th Int Modal Analysis Conference*, San Diego, California, vol. 1, p. 9-19.

Telford, T., (1838), "*Life of bridge*", J. Rickmann, ed., pp. 201-202.

Telford, W.M., Geldart, L.P., Sheriff, R.E., Keys, D.A., (1976), *Applyed Geophysics*, Ch. 5, Cambridge University Press, N.Y.

Thoft-Christensen, P., (1996), Bridge management systems. Present and future, *Proc. of US-Europe Bridge Engineering Workshop*, Barcelona, Spain, 15-17 July 1996, in *Recent advances in bridge engineering: evaluation, management and repair*, (ed. Casas, J. R., et al.), CIMNE, Barcelona, 13-37.

Topp, G.C., Davis, J.L., & Annan, A.P., (1980), Electromagnetic determination of soil water content: measurements in coaxial transmission lines, *Water Resources Research*, **16**(3): 574-582.

Towler, K., Sawko, F., (1982), "Limit state behaviour of brickwork arches", *6th International Brick Masonry Conference*, Rome, Italy.

Towler, K.D.S., (1985), "The non-linear finite element analyses of Bridgemill masonry arch bridge", *Masonry International*, vol. 5.

Ulriksen, P., (1982), *Application of impulse radar to civil engineering*, PhD thesis, Dept. of Engineering Geology, 1982, Lund University of Technology: Lund. p. 175.

University of Edinburgh, (1984), "*Bridgemill: test on a masonry arch bridge*", Dept. Civ. Eng., VHS, test to failure record.

Vaughan, C.J., (1986), Ground Penetrating Radar Surveys used in Archeological Investigations, *Geophysics*, **51**(3), pp. 595-604.

Von Hippel, A.R. (Ed.), (1954), *Dielectric materials and applications*, Chapman and Hall Ltd., London, 438 pp.

Walker, R.B.J., (1979), *Old Westminster bridge. The bridge of fools*, David and Charles, New Abbot, 319 pp.

Ward, S.H., Fraser, D.C., (1967), Conduction of electricity in rocks, *Ch. 2. Mining Geophysics*, Soc. of Exploration Geophysicists, Tulsa, Oklahoma, vol. 2.

Washer, G.A., (1997), Developments for the Non-Destructive Evaluation of Highways Bridges in the United States, *Proc. IV Int. Conf. Non-Destructive Testing in Civil Engineering (NDT-CE '97)*, 8-11 April '97, Liverpool, UK, vol. 2, 543-552.

Watson, W.J., (1927), *Bridge architecture*, W. Helburn, New York, 288 pp.

Weale, J., (1843), *The theory, practice and architecture of bridges of stone, iron, timber and wire*, Architectural Library, London .

Williamson, P.R., (1991), A giude to limits of resolution imposed by scattering in ray tomography, *Geophysics,* **56**, pp. 202-207.

Wong, F.L., Topping, B.H.V., (1988), "Finite element studies for non-destructive vibration tests", *Computer and Structures*, vol. 30(3), p. 653-699.

Wood, J.G.M., (1995), Testing to enhance structural analysis and appraisal. An overview, *1-day seminar Analysis & Testing of Bridges*, I.Struct.E. H.Q., London, 26 April, 4 p.

Worden, K., Tomlinson, G.R., (1994), "Damage location and quantification using neural networks", *2nd Int Conf on Structural integrity assessment*, p. 11-31.

Yanez, M.A., Alonso, A.J., (1996), The actual state of bridge management system in the state national highway network of Spain, *Proc. of US-Europe Bridge Engineering Workshop*, Barcelona, Spain, 15-17 July, in *Recent advances in bridge engineering: evaluation, management and repair*, (ed. Casas, J.R., et al.), CIMNE, Barcelona, 99-115.

APPENDIX A

Appendix A

Glossary of terms associated with arch bridges

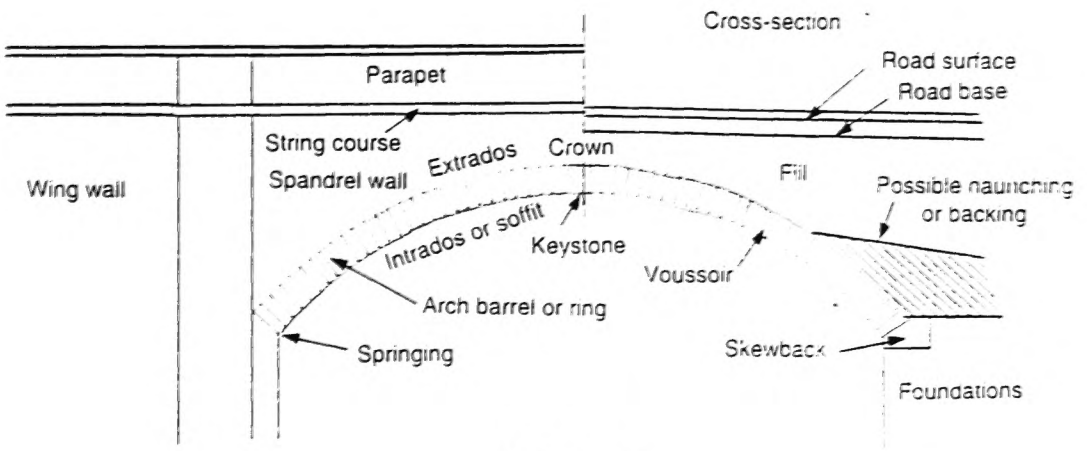

(a) Elevation

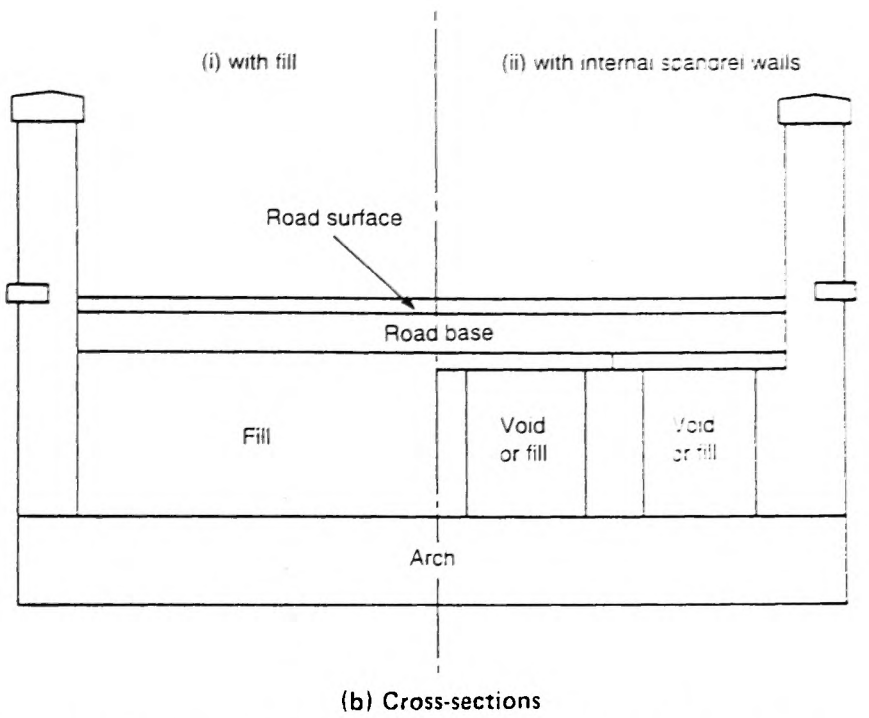

(b) Cross-sections

FIG. A.1 Typical masonry arch bridge elevation and sections (Page, 1993)

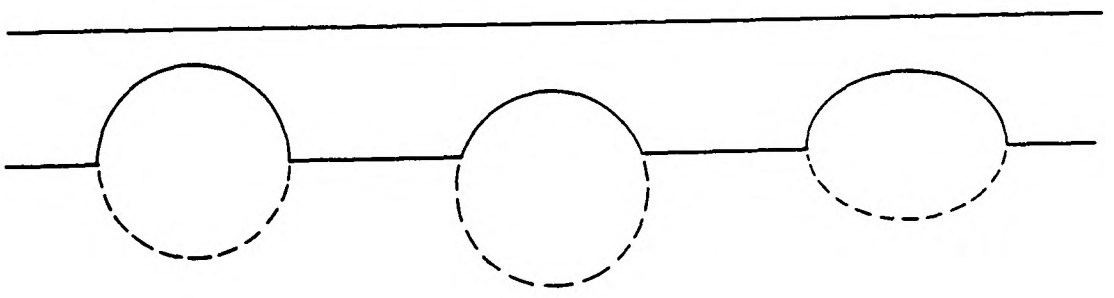

FIG. A2 Arch shapes: semicircular (left), segmental (centre) and elliptical (right). (Nelson, 1990)

Abutment	The wall or body, usually of masonry, which provides the resistance to the thrust of the arch.
Arch	A curved structural member, generally carrying a distributed load transverse to a line drawn between its ends, or springing, producing mostly internal compression. *Relieving arch* or *counter-arch* is a concealed arch springing approximately from the haunches of two main arches and designed to relieve the weight in the spandrels and/or receive the thrust from those arches.
Archivolt	A projecting moulding which follows the curve of an arch above the extrados. Sometimes the arch ring on the facade, or the shape of the arch curve.
Arch ring	The load bearing part of an arch. Also, barrel.
Ashlar	Masonry consisting of square-hewn dressed blocks of stone, giving a uniform pattern of vertical and horizontal joints.
Backing	Material used to fill in or give support at the haunches of an arch. It consists usually of lower quality material, but other times of block-in-course, coursed rubble or random rubble, and sometime of concrete.
Barrel	Masonry roof of tunnel constructions. See also "arch ring" or "vault".
Bond stone	A stone, generally long, which extends from one course or other division of masonry into another, thus bonding the two together.
Buttress	A pier at right angles to a wall, built to help the wall resist lateral, overturning forces, like earth or arch thrust or water pressure.
Catenary	The form assumed by a hanging chain under the action of gravity. Catenary forms are usually close to parabolic.
Centering	Temporary shoring, usually constructed of timber, to support arches or vaulting during construction.
Clam	A single span bridge formed of flag stone.
Clapper	A clam bridge with several spans and low, drystone piers. Often called a 'flag bridge' in Scotland.
Coping	The top of a parapet, often projecting or decorated.
Crosswall	A wall running across the full width of the bridge.
Crown	The highest part in an arch.
Cutwater	The base of a bridge pier, at water level, protruding beyond the face of the spandrels and shaped to divide the water flow. Often it has triangular shape.
Dead weight	Or dead load: the self weight of a structure
Dressing	Surface finish to a stone produced by working.
Dry wall	Wall constructed without mortar.
Extrados	The outer (convex) curve of an arch.
Fill (or Infill)	Material (like rubble or 'rubbish') or soil of different nature (mostly clay but also sand, gravel, coal, etc.) packed in layers between the spandrel walls to constitute support for the road and distribute the load.
Flush	To pour liquid mortar onto completed masonry (e.g. on the extrados

	of an arch) to fill the joints.
Footing	The projecting base of a pier or wall that distributes loadings to the subsoil and improves stability. See also 'cutwater'.
Grout	A fluid or semi-fluid cement slurry or a slurry made with other materials for pouring into the joints of brickwork or masonry or other cavities in order to fill them.
Haunch	The lower section of the arch ring towards the springing. Also called *rein.*
Header	A masonry unit laid with its longer dimension normal to the face of a wall.
Hearting	Infilling of broken stone.
Hewn stone	Stone worked to smooth joint surfaces to give fine mortar joints. The external surfaces are also worked but may be smooth (ashlar), rusticated, etc.
Impost	The upper stone course of an abutment or pier which supports an arch springing line or other superstructure.
Intrados	The inner (concave) curve of an arch.
Joggled arch	Arch in which adjacent voussoir are interlocked by means of visible rebates or steps.
Keystone	The central voussoir of a masonry arch, in the crown position. Sometimes larger than the other stones or projecting/decorated.
Modelling	Techniques used in engineering to solve for structural behaviour. Physical modelling involves taking measurements, usually from a small scale model, which are scaled to give the response of a prototype full-scale structure. In numerical modelling, the abstracted material properties, geometry and loading of the prototype are programmed into a computer. In finite-element (numerical) modelling, the prototype form is represented by a series of co-ordinates taken at finite intervals on its surface.
Oculus	A circular or oval ornament (like a wreath or an eye) in the spandrel, sometimes hollow, always with a moulded rim.
Parapet	Upward extension of a spandrel wall above road surface level. It can be a low wall or railing.
Pile	Foundation timber piles were used to consolidate the river bed or reach for firm ground. Driven into the river bed, usually of elm, oak or fir, and shod with an iron point.
Pier	An upright structure of masonry acting mainly to support vertical loads. In multi-span arch bridges, support between adjoining bridge spans.
Platform	The horizontal frame or floor of wood on which the masonry of a pier is built. Consists of a grating covered by boards.
Pointing	The finishing of joints in mortar as the work proceeds or the filling with mortar of the joints in a wall from which the bedding or jointing mortar has been raked out.
Puddle	Clay worked with water (and sometimes sand) until it is uniformly plastic and impermeable. Can be used to protect masonry against the penetration of water from behind. Often used to waterproof the extrados of the arch.

	Clay is freed of all large stones, roots of plants and the like, and containing as much sand and fine gravel as is consistent with its holding water; if there is too little sand, the puddle is liable to crack in dry weather. It is made by working the clay in layers about 9 inches (23 cm) thick, with enough water to reduce it to a pasty condition, by means of a tool with a poaching action until it becomes a uniform and compact mass. The labour is about five times that of shovelling the same quantity of material.
Refuge	Alcove in the parapet for the safety of pedestrian, usually formed by a half-pillar being built above a pier or abutment.
Revetment	A protective covering to a surface to prevent scour by water or weather.
Rib	In a vault, one of the projecting arches from below the vault's surface with function of true structural support. The webbing is the stone surface of a vault seen as infilling between the ribs. *Rib wall* is an interior wall along the piers.
Rip-rap	Relatively heavy stones used to provide a revetment.
Rise (of arch)	Vertical height from springing level to the crown of the intrados.
Rubble	Masonry constructed of stones largely unworked, used as they come. Sometimes very rough, but in Scotland frequently finished with great neatness. The term describes many different types of masonry, including random rubble (stones as they come from the quarry) either coursed or uncoursed, and squared rubble (either coursed or uncoursed).
Saddle	A concrete slab cast over an arch to strengthen it or distribute loads upon it.
Segmental	Arch curve part of a semicircle. See fig. A2.
Shoulder (of a pier)	The vertical line at which the angled or curved face of the cutwater meets one of the parallel sides of the pier.
Skew arch	Arch whose longitudinal and transverse axes are not at right angles.
Skewback	Surface of an inclined springing.
Soffit	The underside of an arch. Also 'vault'.
Span	Distance between two abutments or between abutment and pier.
Spandrel	Triangular shaped masonry wall between the outer edge of an arch and the wing wall or between two arches. It extends up to the parapet and out to the abutment.
Springing	Plane from which an arch springs. It is the lowest point of the arch, where the curve begins on the abutment or pier.
Starling	An underwater guard made of stone or piles round the cutwater to form extra-protection for the pier against floating objects and scour.
Stayed	Of a bridge that is held together with iron ties because the spandrels give way under lateral pressure.
Stretcher	A masonry unit laid with its longer dimension parallel to the face of the wall
Tie wall	An internal transverse wall at right angles to the spandrel walls.
Vault	A ceiling or roof structure of arched section. A barrel vault is a continuous vault of semicircular section.
Voussoirs	Wedge-shaped stones composing a masonry arch or vault.

Wing wall Continuation of the abutment side walls which extend beyond the bridge to retain the earth behind the abutment, often providing an embankment for the approach road.

Wythe A continuous vertical section of masonry, one unit in thickness.

Sources: (BS 5390, 1976; BS 5628, 1992; BS 6100, 1985; Hannah, 1934; Harris, 1993; Nelson, 1990; Page, 1993; Pride, 1975; Rankine, 1900; Ruddock, 1979; Sowden, 1990; Walker, 1979).

APPENDIX B

APPENDIX B - EQUIPMENT USED

B.1 RADAR SYSTEM

The system used on this project was a GSSI SIR System 10 digital radar set (Fig. B.2). The system comprises a pulse generator producing an electromagnetic pulse to be emitted by an antenna of appropriate centre frequency. In this study antennae of 100, 500, 900 and 1000 MHz centre frequency were used. The data from the GSSI SIR 10 radar system were stored on a 2.3 Gb digital tape drive for subsequent view (data may also be stored digitally on hard disk) and transfer to a PC for analysis. The system is portable and battery operated (Fig. B.1).

Analysis and digital signal processing of the radar data can be done through purpose written software (RADAN ®) or through more flexible packages (MATLAB © and Microsoft EXCEL©).

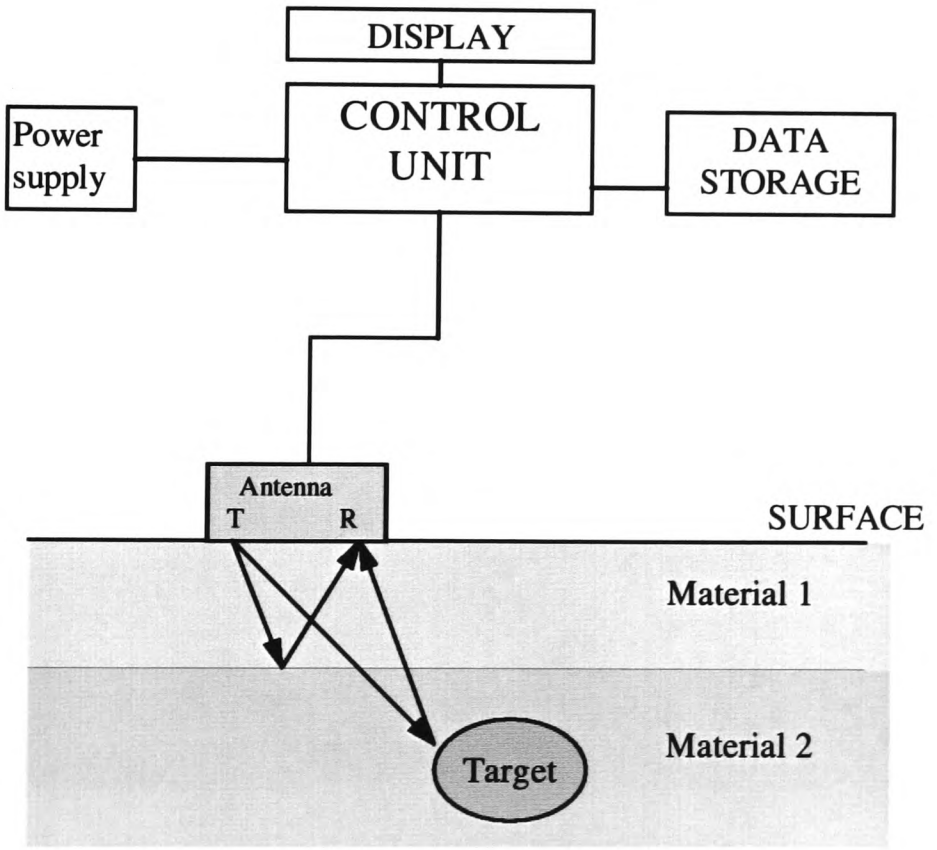

Fig. B.1 - Components of digital radar system operating with monostatic antenna.

FIG. B.2 GSSI Digital Radar System SIR 10: control unit and display.

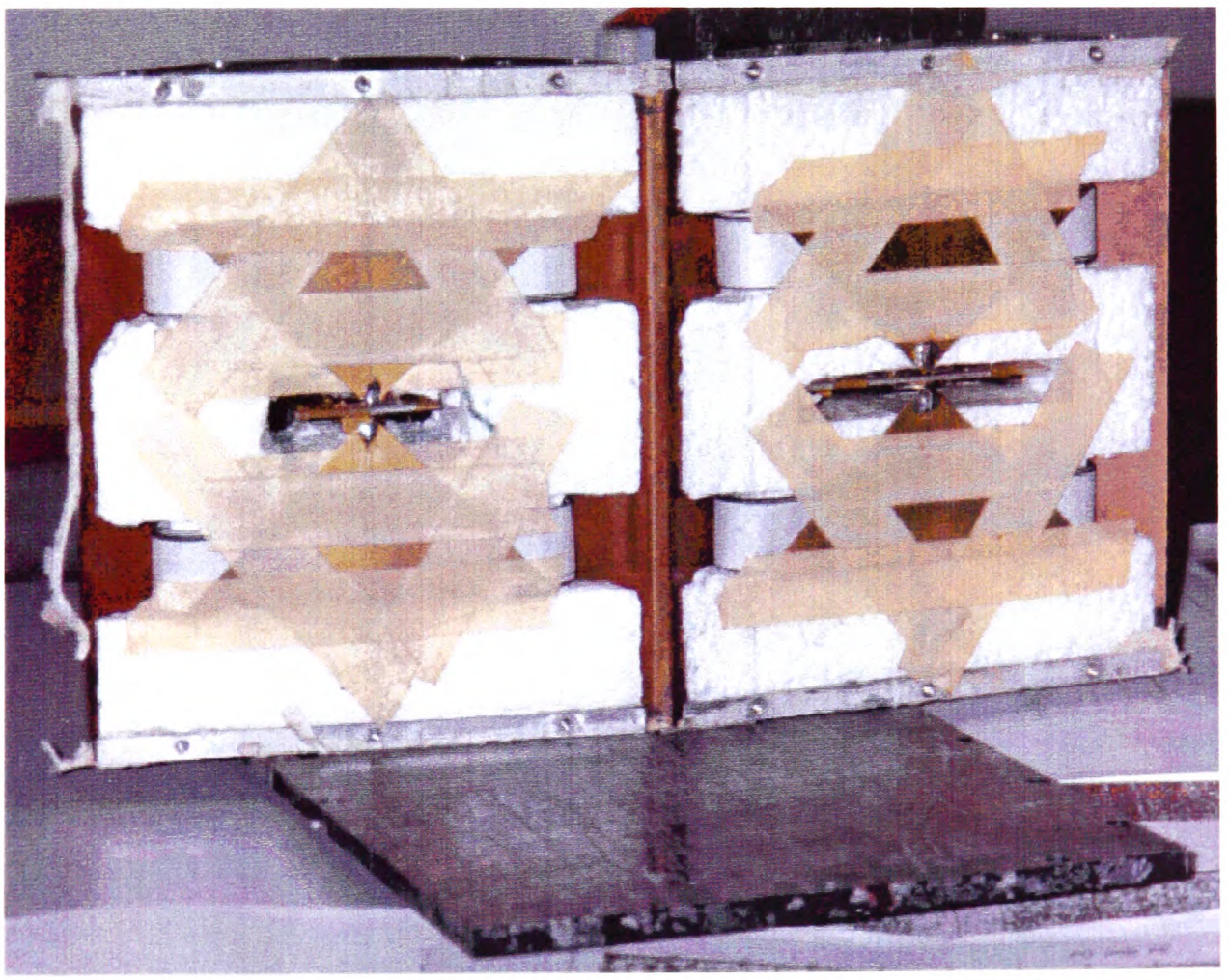

FIG. B.3 - Front of bow-tie antennae in 900 MHz commercial antenna showing transmitter/receiver separation.

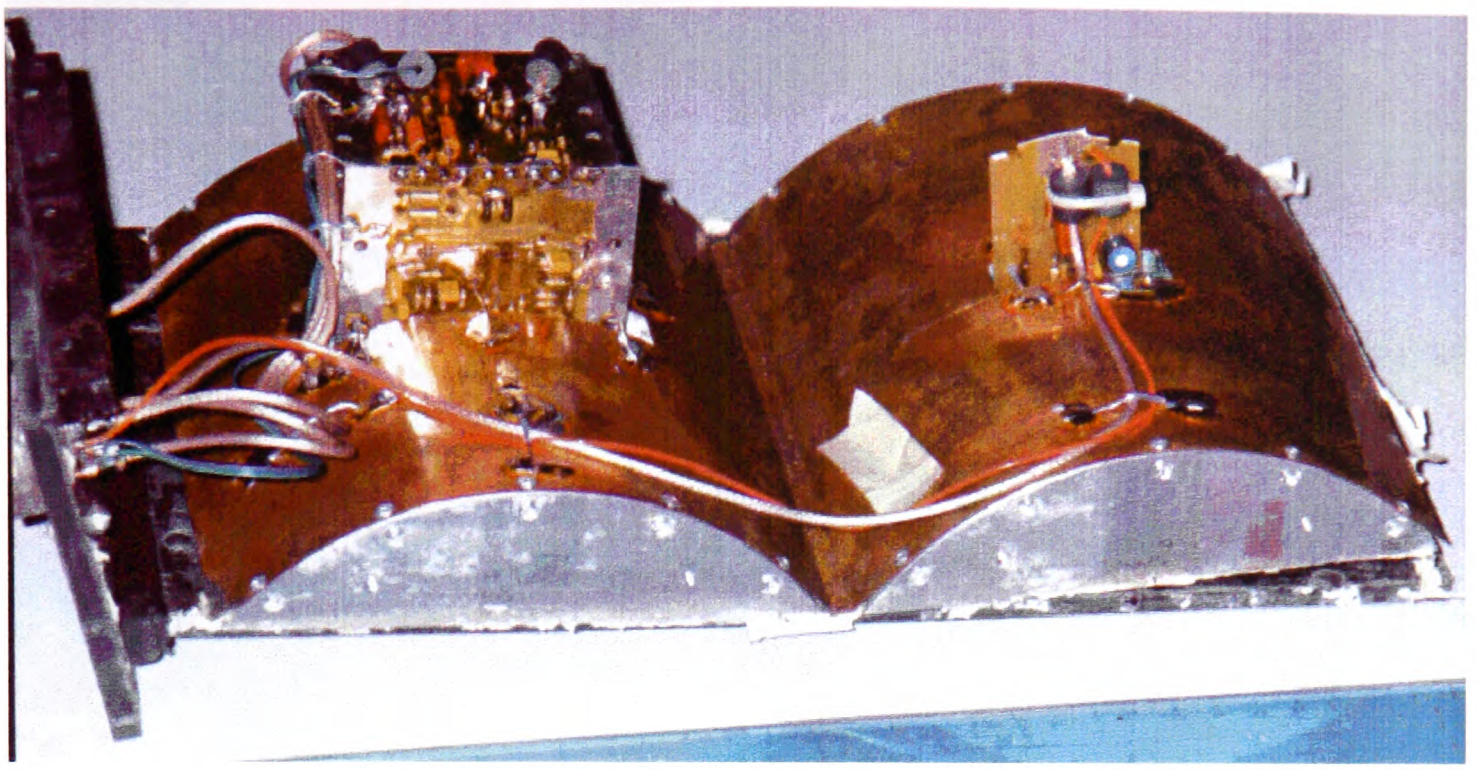

FIG. B.4 The shields and electronics on the back of the bow-ties.

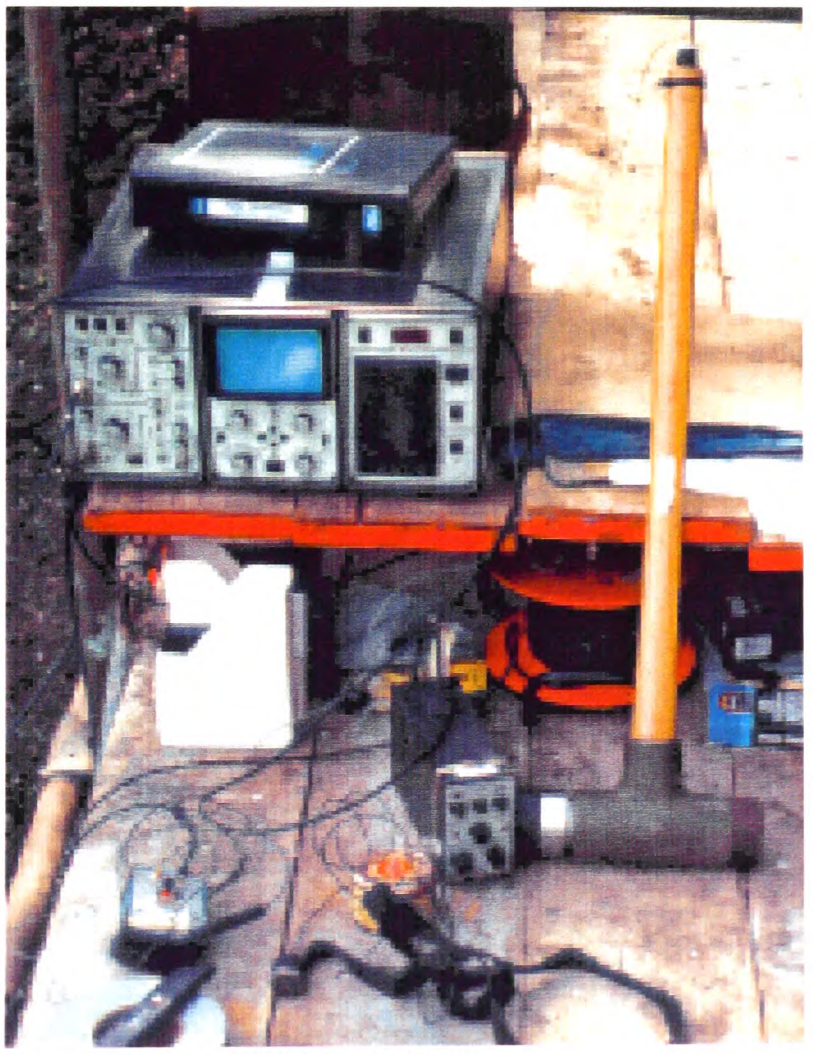

Fig. B. 5 - Sonic system used at Middleton Bridge.

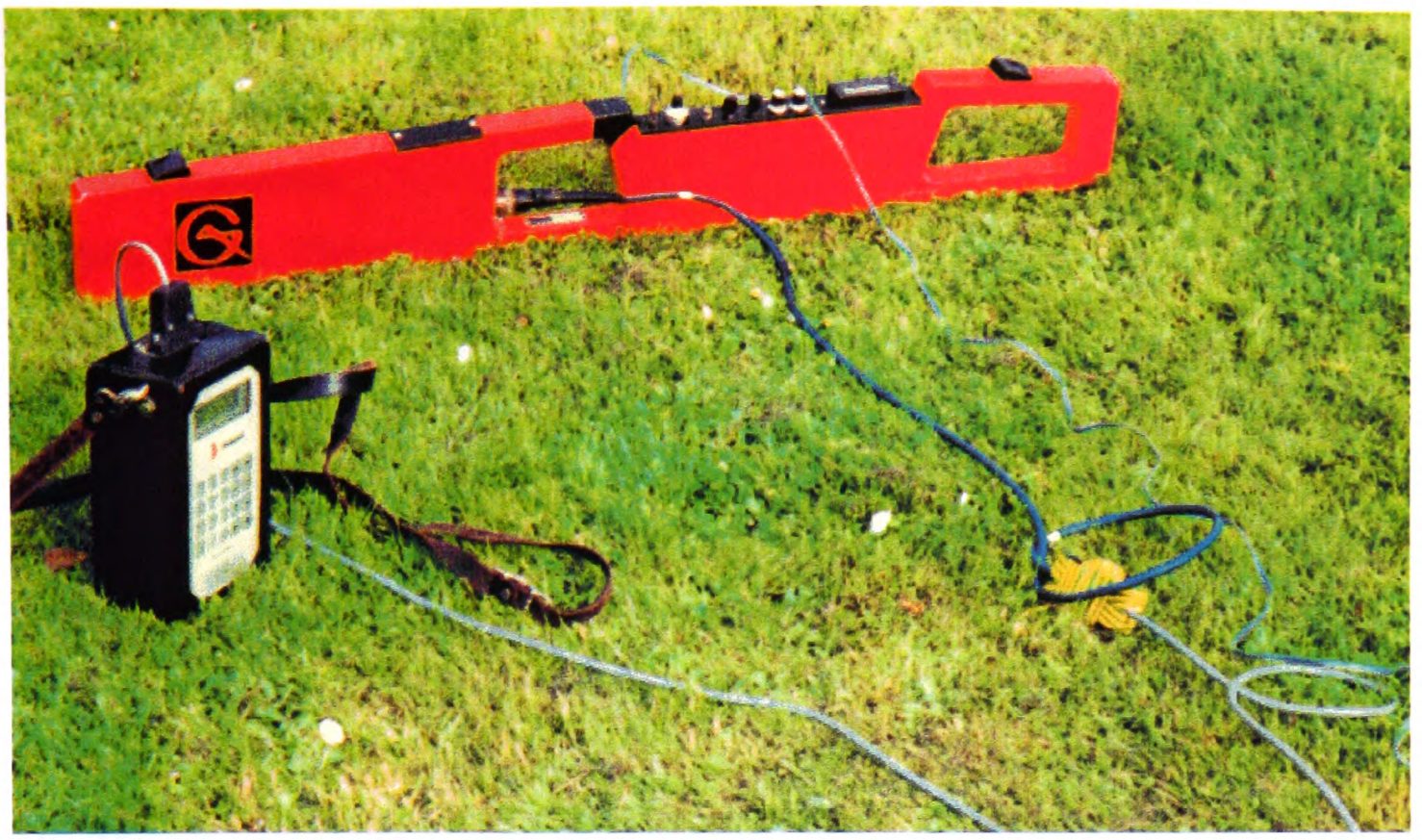

Fig. B.6 - EM 38 Geonics conductivity meter and data logger.

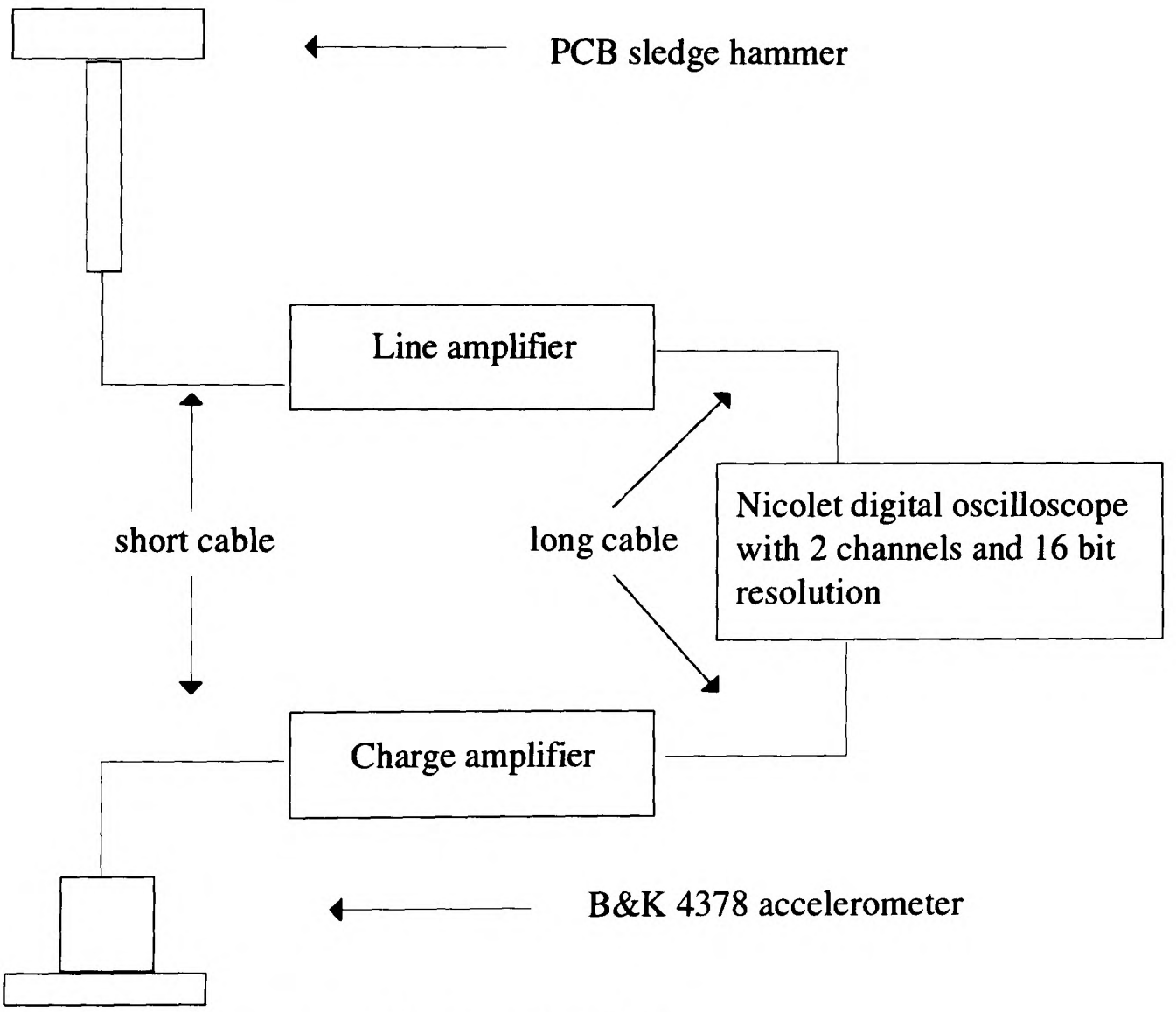

Fig. B.7 - The equipment used in the sonic testing

The antennae, which are connected through cables to the control unit, present inside separated transmitting and receiving shielded bow-tie antennae (Fig. B.3 and B.4) (Rogers, 1997). The system is operated in monostatic mode when the same antenna works as transmitter and receiver; bistatic mode when two separate transmitting and receiving antennas are used. Antennas are usually manually dragged or vehicle towed along the surface to be scanned. A device (survey wheel) can be attached to the antenna to mark the radar plots at regular intervals of distance travelled or to record a constant number of scans per unit distance travelled.

B.2 Sonic instrumentation

The equipment required for the sonic tests consists of several components (Fig. B.7). An impulse force hammer manufactured by PCB Piezotronics was used to initiate the stress waves. This impact hammer weights 5.4 kg, with a head diameter of 7.6 cm, it is instrumented with a load cell which produces an analogue voltage signal proportional to the impulse force transferred into the structure. Various density strike tips allow for limited modification of the frequency content of the impulse force.

The vibrations of the structure resulting from the propagating wave are measured by an accelerometer. A B&K Model 4378 accelerometer was used, mounted on the wall surface with water pump grease. Where, because of the damp surface of the wall, the accelerometer would not stick, a combination of paraffin grease, talcum powder and candle wax was used.

The electronic signals of both the impact hammer and the accelerometer are recorded by a fast scanning data acquisition system. The equipment used is a Nicolet 4094 two channel digital oscilloscope.

The data was stored on the Nicolet's 5&1/4 inch floppy drive which allowed analysis of the sonic waveforms to be performed after an entire set of tests had been completed. A view of the equipment used is shown in fig. B.5.

To optimise the damage detection in non-tomographic sonic tests two governing factors are taken into consideration, velocity of impact and the hammer specifications, particularly tip stiffness and head mass.

Load cell of hammer: the measured force on impact is mainly due to deceleration of the mass behind the load cell in the direction of impact. Therefore the load cell is mounted at the front of the hammer head so that the force delivered to the structure is close to the measured force.

Hammer impact: an attempt should be made to repeat the force of hammer impact for all test locations. In manual impact, random variations are likely to be the largest source of experimental error and will therefore determine the sensitivity of the traditional sonic method (not tomographic method) to detect damage as different impact force, introduces different frequencies and this is affecting the velocity of travel of the wave and its attenuation characteristics - equation 4.18. It is therefore important to use an instrumented hammer so that the force input can always be measured and related to the recorded output at the receiver. A well experienced testing engineer will, however, tend to input the same amount of force and, for velocity calculations, the contribution of the input force can be ignored. For calculation that would consider the attenuation of the signal, however, a normalisation transform between output and input (hammer blow) would be necessary as the attenuation in more sensitive to the amount of force input or frequency components, as higher frequencies tend to attenuate more quickly than lower frequencies thus affecting the amplitude of the peaks. The maximum amplitude is the parameter which is generally used to measure the occurrence of the attenuation.

Impact tips are originally of a spherical shape so that a force acting normal to the surface and at a small off-axis angle, is conducted to the tip's screw thread which is coaxial. Another advantage of the spherical tip is that the contact area of the impact is very small and this reduces spurious effects. Changes in local stiffness give rise to

characteristic alterations in the wave form of the input force and an improvement in sensitivity can be achieved by introducing an impulse characterised by shorter wavelength. This can be obtained by increasing the contact stiffness using stiffer hammer tips: this has the effect of introducing a higher frequency bandwidth and a shorter impulse width.

Hammer mass: in time domain an increase in hammer mass is accompanied by an increase in both the impulse duration and the peak force. A heavier hammer generates an impulse with a longer duration therefore there are a larger number of data points and the statistical accuracy is increased. In the frequency domain an increase in hammer mass is accompanied by an increase in the amplitude at zero frequencies.

Surface condition: the surface of the structure to be tested has less effect on the sonic velocity test than it would have in the case of ultrasonic test, thus less attention to surface condition is required.

APPENDIX C

APPENDIX C

TYPICAL INPUT FILES FOR RADAR SIMULATION PROGRAMME

Example 1: two targets embedded in homogeneous material

900.000000[a] 75.000000[b]

25.000000[c] 0.300000[d]

2.000000[e]

2[f]

1[g] 2[h] 0.50000[i] -0.20000[j] 0.10000[k]

1 2 0.90000 -0.20000 0.10000

1[l] 0[m]

2[u]

80.00000[v] 0.500000[w] water[x]

1.000000[y] 11000000[z] metal[aa]

0.100000[ab] 1.000000[ac] 200[ad] 255[ae] 512[af] 1[ag]

E:\circ_12N.dat[ah]

Example 2: strata in the material

900.000000 75.000000

25.000000 0.300000

2.000000

0

1 1

1[n] 1[o] 2[p] 0.00000[q] 0.10000[r] 2.00000[s] 0.15000[t]

2

80.00000 0.500000water

1.000000 11000000metal

0.100000 1.000000 200 255 512 1

E:\str_2.dat[ah]

Input File Data

Radar data

a) Frequency of the Radar (MHz)

b) Maximum scan angle from the vertical (degrees).

c) Maximum two-way time (ns)

d) Aperture of receiver (m)

e) Length of ground covered by the antenna (m)

Object information

f) Number of objects in scan area

g) Form of object (1= circle, 2= rectangle, 3= triangle, 4= polygon)

h) Material number of the object

Position of target

I) Distance along x-axis (m)

j) Distance along y-axis (m)

k) Radius of circle (m)

Strata details

l) Material in the top left hand corner

m) Number of strata used

n) Form of strata in the material (1 = straight layer)

Type of material

o) Material above interface

p) Material below interface

Co-ordinates of the left-hand end of the Strata

q) X co-ordinate

r) Y co-ordinate

Co-ordinates of the right-hand end of the material strata

s) X co-ordinate

t) Y co-ordinate

Material details

u) Number of Materials

v) Dielectric Constant of material 1

w) Conductivity of material 1

x) Name of material 1

y) Dielectric Constant of material 2

z) Conductivity of material 2

aa) Name of material 2

Details for the computer program

ab) Incremental increase of the scan angle (degrees)

ac) Colour transform code

ad) Number of scans over the length of the ground covered

ae) Transmission/reflection code

af) Number of samples per scan

ag) Determines the form that the output file takes (1= Radan, 2= Syn-view)

ah) File name for the output file

APPENDIX D

Appendix D.

LIST OF PUBLICATIONS

Journal Publications

1. Binda, L., Colla, C. & Forde, M.C. "Identification of moisture capillarity in masonry using digital impulse radar", *J. Construction & Building Materials*, 1994, 8, No. 2, 101-107.

2. Colla, C., Das, P.C., McCann, D., Forde, M.C., "Sonic, electromagnetic & impulse radar investigation of stone masonry bridges", *J. Non-destructive testing and evaluation International*, 1997, vol. 30, No. 4, pp. 249-254.

3. Colla, C., Burnside, C.B., Clark, M.R., Forde, M.C., "Comparison of laboratory and simulated data for radar image interpretation", J. *Non-destructive testing and evaluation International*, submitted (1997).

4. Colla, C., Forde, M.C., McCann, D., "Influence of soil, moisture and salt content on radar detection of buried targets", *J. ASCE*, in preparation (1997).

Sections in books

5. Colla, C., McCann, D., Das, P., Forde, M.C., "Investigation of a stone masonry bridge using electromagnetics", in *Evaluation and strengthening of existing masonry structures*, ed. Binda, L., Modena, C., 1997, RILEM, p. 163-172.

Conferences and Seminars

6. Forde, M.C., McCavitt, N., Binda, L., Colla, C. "Identification of moisture capillarity in masonry using digital impulse radar", *Proc. 5th Int. Conf. Structural Faults and Repair-93*, University of Edinburgh, 29 June-1 July 1993, Engineering Technics Press, vol. 2, 397-403.

7. Das, P.C., Davidson. N.C., Colla, C. "Potential applications of NDT methods for bridge assessment and monitoring", *1-day seminar "Analysis & testing of bridges",* I.Struct.E., London, 26 April 1995.

8. Colla, C., McCann, D., Das, P., Forde, M.C., "Investigation of a stone masonry bridge using electromagnetics", *RILEM TC127MS - CIBW23 WALL STRUCTURES Joint Int. Workshop "Evaluation and strengthening of existing masonry structures",* June 28-29, 1995, University of Padua, Italy.

9. Colla, C., Forde M.C., McCann, D., Das, P.C., "Investigation of masonry arch bridges using non-contacting NDT", *Proc. VI Int. Conf. Structural Faults and Repair-'95,* Westminster Central Hall, London, 3-5 July 1995, Engineering Technics Press, vol. 1, p. 235-239.

10. Colla, C., Das, P.C., McCann, D., Forde, M.C., "Investigation of stone masonry bridges using sonics, electromagnetics & impulse radar", *Proc. III Int. Symp. Non-Destructive testing in Civil Engineering (NDT-CE),* 26-28 September 1995, Berlin, Germany, vol. 1, p. 629-636.

11. Colla, C., McCann, D., Das, P., Forde, M.C., "Non contact NDE of masonry structures and bridges", *Proc. III Conf. Non-destructive Evaluation of Civil Structures and Materials*, 9-11 September 1996, Regal Harvest House, Boulder, Colorado, p. 441-454.

12. Colla, C., Forde, M.C., McCann, D.M., Das, P.C., "Laboratory modelling of radar propagation through masonry", *Proc. IV Int. Conf. Non-Destructive Testing in Civil Engineering (NDT-CE '97),* 8-11 April 1997, Liverpool, UK, vol. 1, p. 303-316.

13. Colla, C., McCann, D.M., Forde, M.C., Das, P.C., Batchelor, A.J., "Radar tomography of masonry arch bridges", *Proc. VII Int. Conf. Structural Faults and*

Repair -'97, Assembly Room, Edinburgh, 8-10 July 1997, Engineering Technics Press, vol. 1, 143-153.

14. Davidson, N.C., Forde, M.C., Hardy, M.S.A., McCann, D.M., Colla, C., Clark, M., Broughton, K.J., Das, P.C., "Field trials to establish accuracy of radar for scour detection", *Proc. VII Int. Conf. Structural Faults and Repair -'97,* Assembly Room, Edinburgh, 8-10 July 1997, Engineering Technics Press, vol. 1, 171-178.

15. Colla, C., Forde, M.C., Das, P., McCann, D., "Radar imaging in composite masonry structures", *Proc. VII Int. Conf. Structural Faults and Repair -'97,* Assembly Room, Edinburgh, 8-10 July 1997, Engineering Technics Press, vol. 3, 493-504.

16. Colla, C., Burnside, C.B., Clark, M.R., Forde, M.C., "Comparison of laboratory and simulated data for radar image interpretation", *Proc. VII Int. Conf. Structural Faults and Repair -'97,* Assembly Room, Edinburgh, 8-10 July 1997, Engineering Technics Press, vol. 3, 523-528.

STRUCTURAL FAULTS + REPAIR - 95

Proceedings of the Sixth International Conference on Structural Faults and Repair 1995

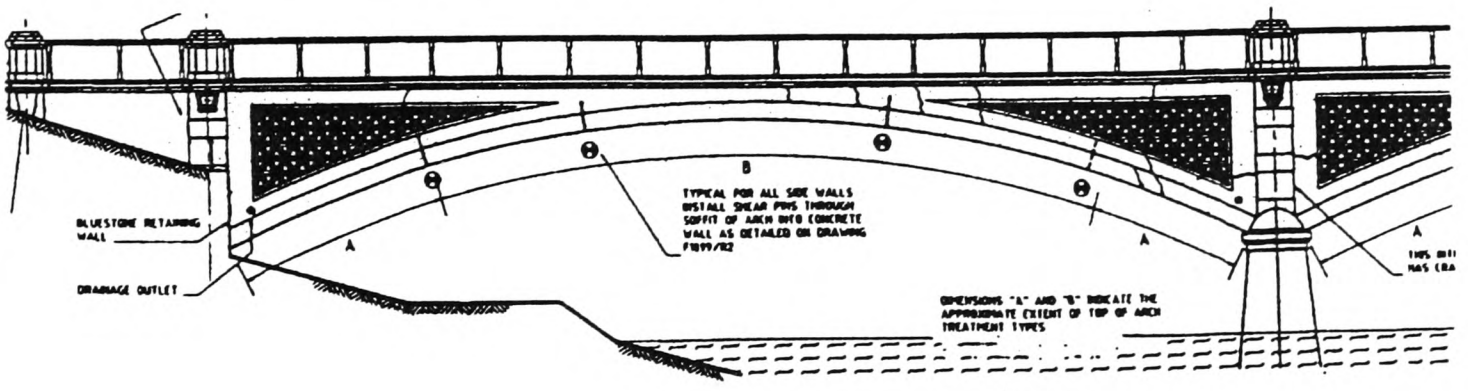

"EXTENDING THE LIFE OF BRIDGES"

Volume 1

INVESTIGATION OF MASONRY ARCH BRIDGES USING NON-CONTACTING NDT

C Colla & Professor M C Forde, Univesity Edinburgh,
Dr D M McCann, British Geological Survey, Keyworth and
Dr P C Das, Highways Agency, London, UK

A strategic overview of the assessment of masonry arch bridges is given. It is proposed that where a bridge fails the load carrying capacity assessment by a small margin, and it looks to be in good condition, that further investigation be undertaken using NDT techniques.

Radar and conductivity methods are reviewed and the results from a non-contact conductivity NDT survey are discussed. It was concluded that the conductivity technique has demonstrated the ability to be a rapid, low cost, non-contacting technique from which tomographic cross-sections, inhomogeneity identification, moisture movement detection over time and layering within the masonry can be achieved.

1. INTRODUCTION

A large proportion of the bridge stock in the United Kingdom consists of masonry arch bridges of various forms. This will continue to be the case for a long time to come since, the vast majority of these bridges are still in perfectly serviceable condition. This means that periodic assessment of their load carrying capacity will remain an essential part of the bridge authorities' management activities for the foreseeable future. The outcome of these assessments can be very significant in terms of resulting financial and logistical burdens for the authorities. It is therefore in their interest to seek, wherever possible, improvements in the methods of assessment.

Under the sponsorship of the Department of Transport/Highways Agency and other bridge authorities, considerable efforts have been made in recent years to develop numerical methods for predicting the collapse strength of masonry arch bridges. A number of newly developed methods were then tested against the results obtained from full-scale tests. A comparative summary of the findings were given in BA 16/93 [1], and also by Das [2]. The overall lessons learnt from the developments so far can be summarised as follows.

2. FINDINGS FROM LARGE SCALE BRIDGE RESEARCH

In principle, the structural system of an arch bridge, composed of a number of elements: i.e. the foundations, the barrel and the surrounding fill, can be conveniently analysed using advanced numerical methods of analysis, such as the finite element method. However, in practice, the accuracy of the results becomes questionable due to a multitude of complexities inherent in an arch bridge. These are:-

(i) For the sake of computational practicality, the analyses are usually carried out with simplified methods, e.g. the two-dimensional analysis, or the mechanism method. These methods by necessity bring in added approximations which make the structural idealisation somewhat remote from reality.

(ii) Soil structure interaction is a major problem in analysing the behaviour of even new structures; for these old bridges involving surrounding materials of unknown properties, this becomes a major problem. For anything but the flattest arches, soil support characteristics significantly influence the load carrying capacity. For all sophisticated assessment methods, the soil resistance parameters have to be input, and the means of estimating these values are very approximate.

(iii) As most of the arch bridges do not usually have any reliable records of construction or repair details, it is difficult to determine the physical dimensions of the main structural elements, or the presence or otherwise of additional features such as the haunching at supports, saddling over the barrel or internal spandrel walls and ribs. Many unsuspected examples of such features, including voids that have been subsequently filled, have come to light following demolition - Fig.1. Because of the difficulty in identifying these features, idealisation of old arch bridges can never be fully satisfactory.

(iv) In most cases, the quality of the structural materials and condition of the structural elements cannot be determined or idealised with any precision.

In the presence of the factors referred to above, the computational precision of the analytical assessment methods largely becomes immaterial. The results from these programs cannot be relied upon to give a black and white indication of the capacity of a bridge, since these analyses are dependent upon the input data such as those relating to the soil parameters which cannot be determined with any precision or consistency.

3. THE WAY FORWARD IN BRIDGE ASSESSMENT

It is becoming increasingly obvious that results from any calculation based arch assessment method may have to be viewed as giving only a qualitative assessment of capacity, and in order to decide on the appropriate action, one may have to

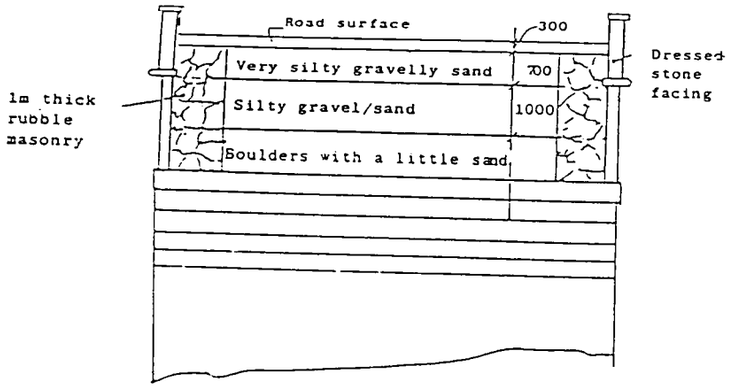

Fig. 1 Section of bridge revealed on demolition

rely on additional, perhaps qualitative, information obtained by other means. Thus, if an arch bridge fails assessment by a small margin, and it is not showing any significant deterioration, and it is suspected that additional structural features such as internal ribs are present within the fill, it may be reasonable to consider the bridge to be satisfactory for the time being. In such situations, NDT methods such as radar, sonic, vibration and/or conductivity techniques may provide a relatively quick and inexpensive means for making a qualitative judgement on the likelihood of a bridge having any additional reserves of strength.

4. NDT METHODS

Two NDT methods were investigated during the work reported in this paper - radar and conductivity. The experimental work was undertaken using the latter technique.

4.1 Impulse radar

In the evaluation of masonry arch bridges, impulse radar testing is starting to be used and has advantages over other techniques in certain circumstances, but very real problems can exist with regard to the interpretation of radar data. Where multiple changes in interface between dielectric layers take place, the change of dielectric constant will be identified but the resolution of the final target layer may prove particularly elusive. An example would be when the objective of a radar survey on a stone masonry arch bridge is to identify hidden geometry and characteristics of the soil fill with precision. Such an investigation would have to proceed through the various layers of material and if the soil fill is heterogeneous the problem is compounded to the extent that the data may be uninterpretable.

Furthermore the phenomenon may be accentuated if the dielectric constants of the materials present on site are calculated to be significantly higher than might be expected from published literature [3]. The investigation of these factors, still being researched, has produced very interesting data - as explained later in the discussion.

4.2 Conductivity Surveys

Originally developed for geophysical mapping, then for archaeological and agricultural applications, conductivity is a novel application in the civil engineering field.

Conductivity is an electromagnetic method which makes use of the response of the ground to the propagation of electromagnetic fields generated through the transmitting coil. The response fields differ both in phase and amplitude from the transmitted one. These differences reveal the presence of the conductor and provide information on its geometry and electrical properties. The induction of current flow results from the magnetic components of the EM field, consequently there is no need for physical contact with the surface.

The measured field is generally a complex function of the coil spacing "s", of the conductivity meter, the operating frequency "f" and the conductivity distribution of the subsurface "σ". The depth of penetration depends upon "s" and the frequency used, but it is independent from the conductivity distribution of the subsurface. [3][4]. The depth of penetration also depends on the frequency used. The lower the frequency, the deeper the penetration but the poorer the resolution - as amplitude decreases exponentially with depth [3][5].

5. FIELD WORK

Conductivity surveys were undertaken on one abutment of an historical stone masonry structure which was known to present the problems described above [6] - Fig. 2.

In the case of the structure investigated and presented here, the digital conductivity meter used has intercoil spacing of 1m and provides a maximum depth of exploration of 1.5m in vertical dipole mode operating at a frequency of 14.6 kHz. The meter was used on both the upstream and downstream sides of this 2-span bridge and on the wall beneath the main vault. The measurement stations followed a grid marked on the walls, in an area well clear of any evident metallic objects (drains, reinforcing beams). For maximum accuracy and good spatial resolution, measurements were overlapped to have readings

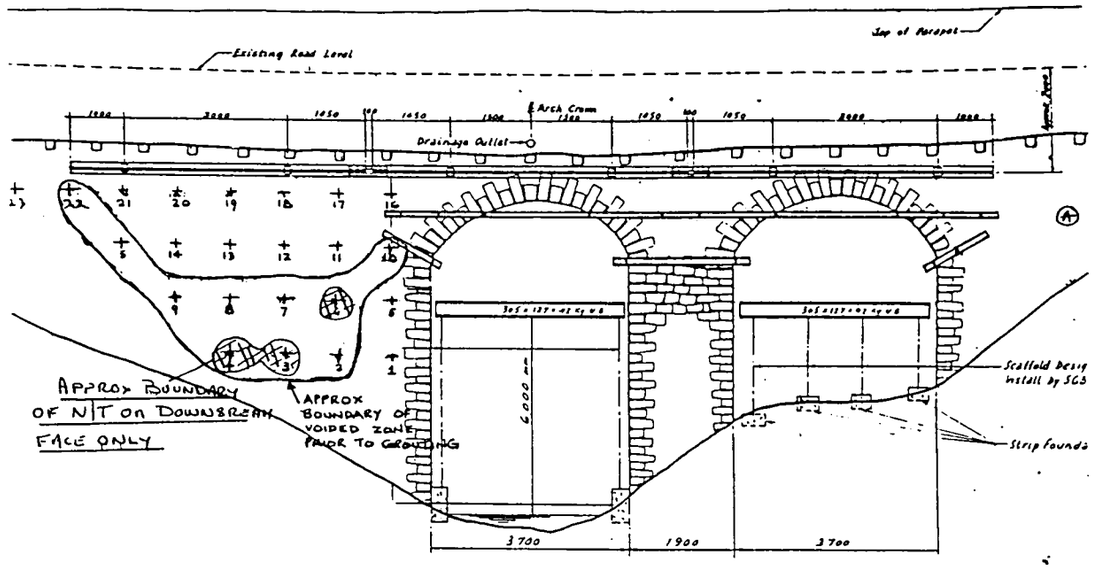

Fig. 2 Elevation of North Middleton Bridge

every half a metre. Contacting and non-contacting conductivity measurements were taken, to obtain data at different depths. Data were collected using a digital data recorder and later transferred to a P.C. The results were plotted to produce contour maps of the conductivity distribution Figs 3 and 4.

The values obtained are in a high and very wide range indicating heterogeneity in soil filling in the abutment, made of rock such as argillites, wet clays or alluvium and sand; or variations in moisture content/salinity [8].

Rock Type	Conductivity (mS/m)
Argillites	1-80
Conglomerates	0.2-2
Sandstones	$1 - 6.4 \times 10^{-5}$
Unconsolidated wet clay	200
Clays	10-1000
Alluvium and sands	80-100

Conductivity is usually controlled by one or more of the following parameters: (1) clay content, (2) moisture, (3) salinity.

Of these, the most complex is usually the moisture profile. Measurements on a soil sample [9] as a function of moisture content, showed that conductivity increases approximately as the square of the moisture content.

The bridge investigated was a structure with moisture-drainage problems and attempts had been made in the past to alleviate the problem but with limited success. In this context, both dielectric constant and conductivity increase with water content. The presence of salts in pore water - mainly coming from routine winter road maintenance - will increase the conductivity even further, without affecting proportionally the dielectric constant.

The surveys were repeated over a period of months and differences were noticed, in particular behind the wall under the vault. Comparison of results from data taken at 1m depth lead to the hypothesis that a significant moisture/water movement is taking place at the rear face of that wall with concern about the possible loss of the fine part of the filling; this hypothesis was reinforced by the low velocity values obtained from sonic tomography cross-sections.

Conductivity data have also been plotted to obtain a horizontal cross-section of the abutment. Clear differences in the values are visible between the upstream and downstream wall situation, with values being on the bottom end of the range in the upstream side and showing medium to high range values on the downstream side. This finding clearly had something to do with the inner construction of the bridge and could not be explained just by asymmetrical water distribution in the structure.

Subsequent endoscopic investigation into the structure has confirmed the hypothesis and revealed that hollow compartments were built into the bridge and that some of them have been partially or totally filled by grout injection during earlier strengthening and reinforcing operations, which the bridge has been subjected to.

The findings from the survey were:

- Depth of penetration of the conductivity meter used was equivalent to the masonry wall thickness
- The upstream side is dry because the void behind the wall is not filled with grout
- On the downstream side, water moves from backfill to grout to external wall and leaks outside
- A similar situation may pertain on the abutment

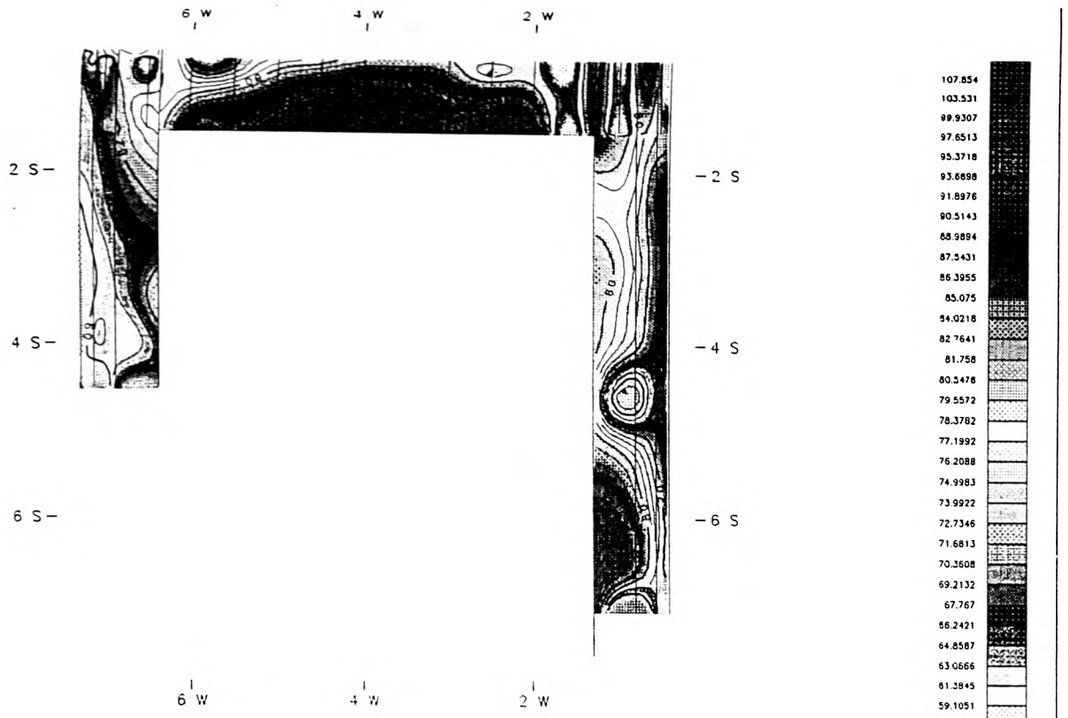

Fig. 3 Conductivity Survey Contours

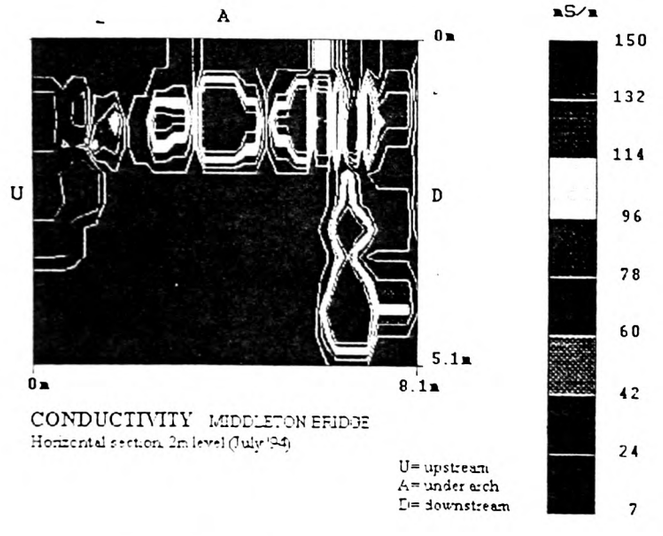

Fig. 4 Conductivity Survey Contours

Furthermore, looking at details of the downstream wall conductivity distribution, gives rise to the hypothesis that the wall is not solid stone masonry but may be layered within itself. This has been confirmed by visual and endoscopic inspection: the wall appears to be made of stone-rubble-stone.

6. FUTURE WORK

- Coring is planned to be carried out in the next few months, to verify the internal construction.
- Custom equipment for determining conductivity at variable depth is to be developed and the enhancement of interpretation software and 3-D modelling is being carried out.
- Full scale field and laboratory calibrations will be undertaken

7. CONCLUSIONS

The conductivity technique has demonstrated the ability to be a rapid, low cost, non-contacting technique from which tomographic cross-sections, inhomogeneity identification, moisture movement detection over time and layering within the masonry can be achieved.

8. ACKNOWLEDGEMENTS

The first author gratefully acknowledges the financial support of the EPSRC and the Highways Agency, London. The authors acknowledge the facilities made available by the University of Edinburgh and access to Middleton Bridge by Lothian Regional Council. Scaffolding was generously provided by Mr A.J. Batchelor of Holequest Ltd.

9. REFERENCES

[1] BA 16/93. (1993) The assessment of highway bridges and structures. HMSO, London 1993.

[2] Das, P.C. (1993) Examination of masonry arch assessment methods. *Symposium on Structural preservation of the architectural heritage*. IABSE, Rome, 1993.

[3] Kearey, P. & Brooks, M. (1991) "*An Introduction to Geophysical Exploration*", Oxford, 1991.

[4] Das, P.C., Davidson N.C. & Colla, C. (1995) "Potential applications of NDT Methods for Bridge Assessment and Monitoring", *I.Struct.E. Seminar*, April '95, London.

[5] Wilson, J. (1989) "*Field Geophysics*", Geological Society of London Handbook, 1989.

[6] Forde, M.C., Birjandi, F.K. & Batchelor, A.J. (1985) Fault detection in stone masonry bridges by non-destructive testing, *Proceedings of 2nd International Conference: Structural Faults and Repair-85*, Engineering Technics Press, Edinburgh, 373-379.

[7] McNeill, J.D. (1980) "*Electrical Conductivity of Soils and Rocks*", Technical Note TN-5,, Geonics Ltd., October 1980.

[8] Telford W.M. et al, (1976) "*Applied Geophysics*", Ch. 5, Cambridge University Press, N.Y.

[9] Smith-Rose, R.L. (1934) "Electrical Measurements on Soil with Alternating Currents", *Proc. IEE* No. 75, 221-237.

BAM

BUNDESANSTALT FÜR
MATERIALFORSCHUNG
UND -PRÜFUNG

INTERNATIONAL UNION OF TESTING
AND RESEARCH LABORATORIES FOR
MATERIALS AND STRUCTURES

THE BRITISH INSTITUTE
OF NON-DESTRUCTIVE
TESTING

INTERNATIONAL COUNCIL
FOR BUILDING STUDIES
AND DOCUMENTATION

TECHNISCHE
UNIVERSITÄT
BERLIN

DEUTSCHE
GESELLSCHAFT FÜR
ZERSTÖRUNGSFREIE
PRÜFUNG E.V.

Edited by
G. Schickert, H. Wiggenhauser

International Symposium

Non-Destructive Testing in Civil Engineering (NDT-CE)

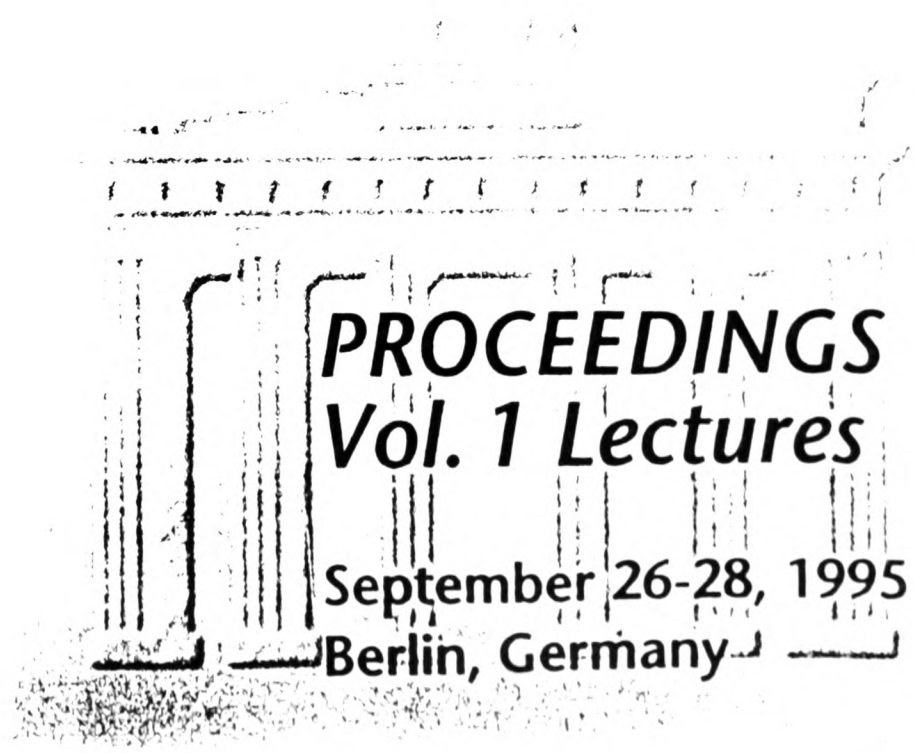

PROCEEDINGS
Vol. 1 Lectures

September 26-28, 1995
Berlin, Germany

International Symposium Non-Destructive Testing in Civil Engineering (NDT-CE) 26.-28.09.1995

Investigation of stone masonry bridges using sonics, electromagnetics and impulse radar

C. Colla, P. Das, D. McCann**, M. Forde*
University of Edinburgh, Edinburgh (GB)
**Highways Agency, London (GB)*
***British Geological Survey, Nottingham (GB)*

Keywords: *Bridge, Electromagnetics, Masonry, Radar, Scour*

Masonry arch bridge assessment is overviewed strategically. It is proposed that where a bridge fails the load carrying capacity assessment by a small margin, and it looks to be in good condition, that further investigation be undertaken using NDT techniques.

NDT techniques: radar, sonic and conductivity methods are reviewed and the results from sonic and conductivity NDT surveys are discussed. It was concluded that these techniques are effective and that tomographic plots aid interpretation of data. The conductivity technique has demonstrated the ability to be a rapid, low cost, non-contacting technique from which tomographic cross-sections, inhomogeneity identification, moisture movement detection over time and layering within the masonry can be achieved.

1. INTRODUCTION

Masonry arch bridges form a large proportion of the bridge stock in the United Kingdom and this will continue to be the case for a long time to come, since the vast majority of these bridges are still in perfectly serviceable condition. This means that periodic assessment of their load carrying capacity will remain an essential part of the bridge authorities' management activities for the foreseeable future. The outcome of these assessments can be very significant in terms of resulting financial and logistical burdens for the authorities. It is therefore in their interest to seek, wherever possible, improvements in the methods of assessment.

The UK Department of Transport/Highways Agency and other bridge authorities have sponsored major research projects in recent years to develop numerical methods for predicting the collapse strength of masonry arch bridges. A number of newly developed methods were then tested against the results obtained from full-scale tests. A comparative summary of the findings were given in BA 16/93 [1], and also by Das [2]. The overall lessons learnt from the developments so far can be summarised as follows.

2. UK LARGE SCALE MASONRY ARCH BRIDGE RESEARCH PROGRAMME

Idealistically, the structural system of an arch bridge, composed of a number of elements: i.e. the foundations, the barrel and the surrounding fill, can be conveniently analysed using advanced numerical methods of analysis, such as

the finite element method. However, in practice, the accuracy of the results becomes questionable due to a multitude of complexities:-

(i) Computational expediency often means that the analyses are carried out with simplified methods, e.g. the 2-D analysis, or the mechanism method. These methods by necessity bring in added approximations which make the structural idealisation somewhat remote from reality.

(ii) Soil structure interaction is a major problem in analysing the behaviour of even new structures; for these old bridges involving surrounding materials of unknown properties, this becomes a major problem. For anything but the flattest masonry arches, soil arching and support characteristics significantly influence the load carrying capacity. For all sophisticated assessment methods, the soil resistance parameters have to be input, and the estimation of these values is very approximate.

(iii) Since most of the arch bridges do not usually have any reliable records of construction or repair details, it is difficult to determine the physical dimensions of the main structural elements, or the presence or otherwise of additional features such as the haunching at supports, saddling over the barrel or internal spandrel walls and ribs. Many unsuspected examples of such features, including voids that have been subsequently filled, have come to light following demolition - Fig. 1. Because of the difficulty in identifying these features, idealisation of old arch bridges can never be fully satisfactory.

(iv) Generally, the quality of the structural materials and condition of the structural elements cannot be determined or idealised with any precision.

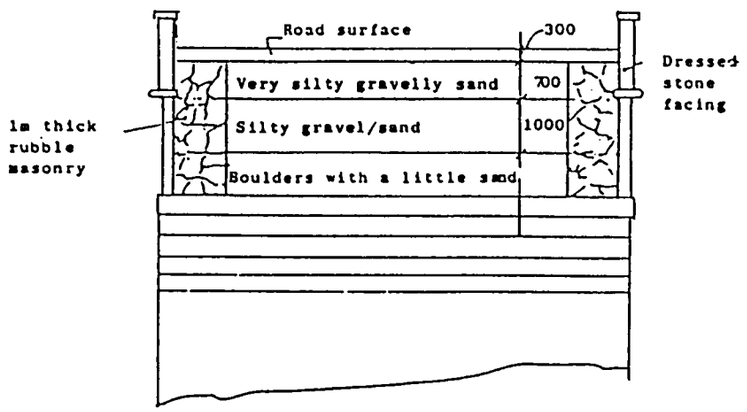

Fig. 1 Section of bridge revealed on demolition

In the presence of the factors referred to above, the computational precision of the analytical assessment methods largely becomes immaterial. The results from these programs cannot be relied upon to give a black and white indication of the capacity of a bridge, since these analyses are dependent upon the input data such as those relating to the soil parameters which cannot be determined with any precision or consistency, .

3. FUTURE RATIONAL BRIDGE ASSESSMENT

Experience is showing that results from any calculation based arch assessment method may have to be viewed as giving only a qualitative assessment of capacity, and in order to decide on the appropriate action, one may have to rely on additional, perhaps qualitative, information obtained by other means. Thus, if an arch bridge fails assessment by a small margin, and it is not showing any significant deterioration, and it is suspected that additional structural features such as internal ribs are present within the fill, it may be reasonable to consider the bridge to be satisfactory for the time being. In such situations, NDT methods such as radar, sonic, vibration and/or conductivity techniques may provide a relatively quick and inexpensive means for making a qualitative judgement on the likelihood of a bridge having any additional reserves of strength.

4. NDT METHODS FOR MASONRY ARCH BRIDGES

Three NDT methods were investigated during the work reported in this paper - radar, sonic and conductivity.

4.1 Impulse radar

Impulse radar testing is starting to be used in the evaluation of masonry arch bridges and has advantages over other techniques in certain circumstances, but very real problems can exist with regard to the interpretation of radar data. Where multiple changes in interface between dielectric layers take place, the change of dielectric constant will be identified but the resolution of the final target layer may prove particularly elusive. An example would be when the objective of a radar survey on a stone masonry arch bridge is to identify hidden geometry and characteristics of the soil fill with precision. Such an investigation would have to proceed through the various layers of material and if the soil fill is heterogeneous the problem is compounded to the extent that the data may be uninterpretable.

The phenomenon may be accentuated if the dielectric constants of the materials present on site are calculated to be significantly higher than might be expected from published literature [3]. Preliminary investigation of these factors has produced very interesting data - as explained below.

4.2 Impulse Sonics

Time domain impulse sonics were undertaken by measuring the time taken by an impulse from a modally tuned instrumented hammer to transmit through the structure. The data was recorded on a 100 kHz digital oscilloscope. Sonic tomographic plots were constructed using the first arriving wave energy transmitted through the abutment, from a number of sources and picked up by the receivers - Fig 2. An image is built up by interpreting the travel time of single ray paths. By an iterative process, sonic velocities through the various materials are mapped in a cross-sectional representation. The sonic velocities are related to material densities. The cross-sectional representation is an over-simplification as the ray paths will not be in straight lines in reality.

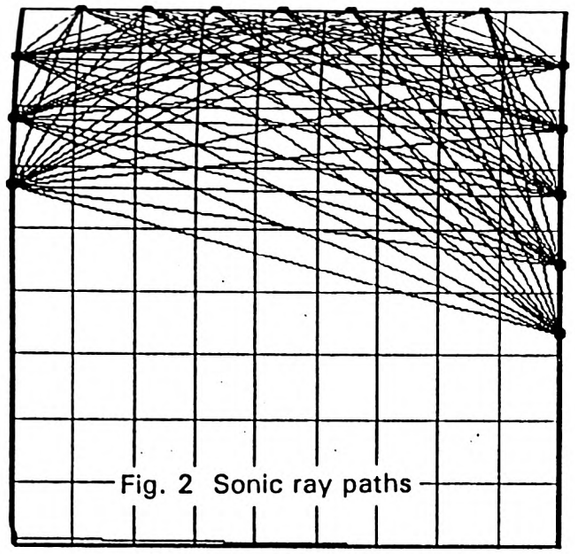

Fig. 2 Sonic ray paths

RAY PATHS: MIDDLETON BRIDGE
Level 2 meters (April '95)

4.3 Conductivity Surveys

Originally developed for geophysical mapping, then for archaeology and agricultural, conductivity is a novel application in the civil engineering field. Conductivity is a technique which makes use of the response of the ground to the propagation of electromagnetic fields generated through the transmitting coil. The response fields differ both in phase and amplitude from the transmitted one. These differences reveal the presence of the conductor and provide information on its geometry and electrical properties. The induction of current flow results from the magnetic components of the EM field, consequently there is no need for physical contact with the surface.

The measured field is generally a complex function of the coil spacing "s", of the conductivity meter, the operating frequency "f" and the conductivity distribution of the subsurface "σ". Penetration depth depends upon "s" and the frequency used, but is independent from the conductivity distribution of the subsurface. [3][4]. Penetration also depends on the frequency used. The lower the frequency, the deeper the penetration but the poorer the resolution - as amplitude decreases exponentially with depth [3][5].

5. FIELD WORK

Non-destructive investigation surveys were undertaken on one abutment of an historical stone masonry structure which was known to present the problems described above [6] - Fig. 3.

5.1 Radar Survey

The preliminary findings from the radar survey indicate values of the di-electric

constant within the bridge which are significantly different from published data. The average value for the di-electric constant (ε) for the composite bridge construction [masonry/soil fill/masonry] was computed to be ε = 56.

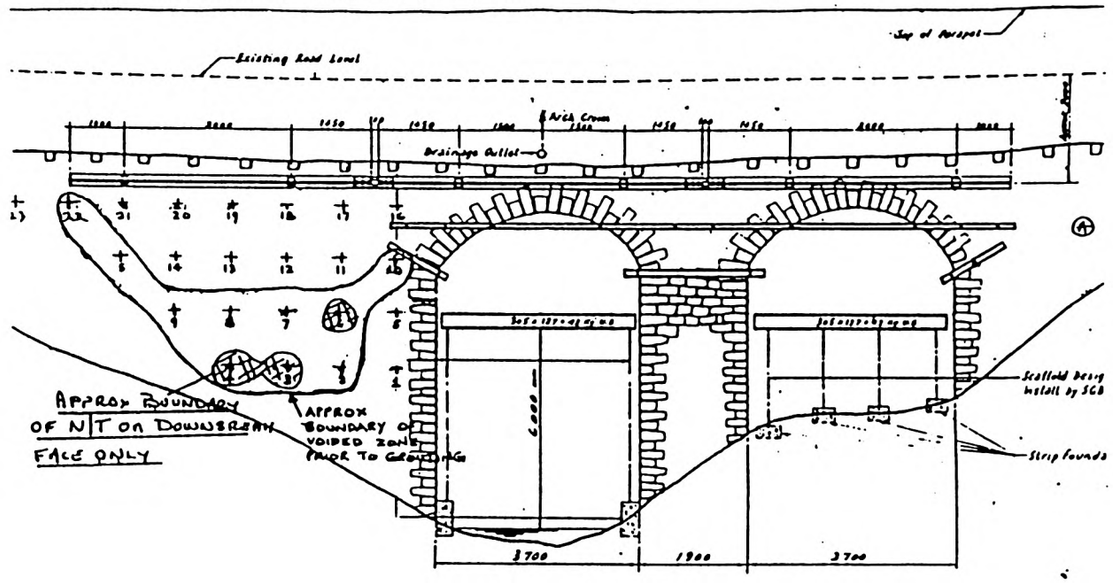

Fig. 3 Elevation of North Middleton Bridge

5.2 Sonic Tomographic Survey

A sonic tomographic model was constructed, using the simplifying assumption of straight ray paths - Fig. 4. Values between medium to low are located towards the centre of the plot, indicating backfill materials. High velocity areas relate to grouted zones. By applying constraints to the model and re-iterating, masonry thickness on the down stream side was comparable with the one determined from the conductivity survey detailed below.

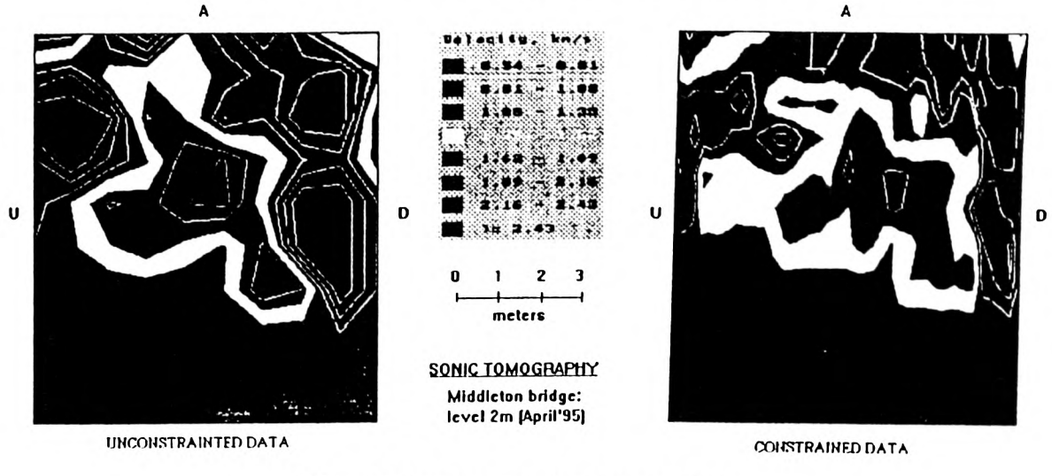

Fig. 4 Sonic tomographic model

5.3 *Conductivity Survey*

In the structure investigated here, the digital conductivity meter had intercoil spacing of 1m and provides a maximum depth of exploration of 1.5m in vertical dipole mode operating at a frequency of 14.6 kHz. The meter was used on both the upstream and downstream sides of this 2-span bridge and on the wall beneath the main vault. The measurement stations followed a grid marked on the walls, in an area well clear of any evident metallic objects (drains, reinforcing beams). For maximum accuracy and good spatial resolution, measurements were overlapped to have readings every half a metre. Contacting and non-contacting conductivity measurements were taken, to obtain data at different depths. Data were collected using a digital data recorder and later transferred to a P.C. The results were plotted to produce contour maps of the conductivity distribution. Figure. 5 is a cross-sectional representation with the data iterated through tomographic software.

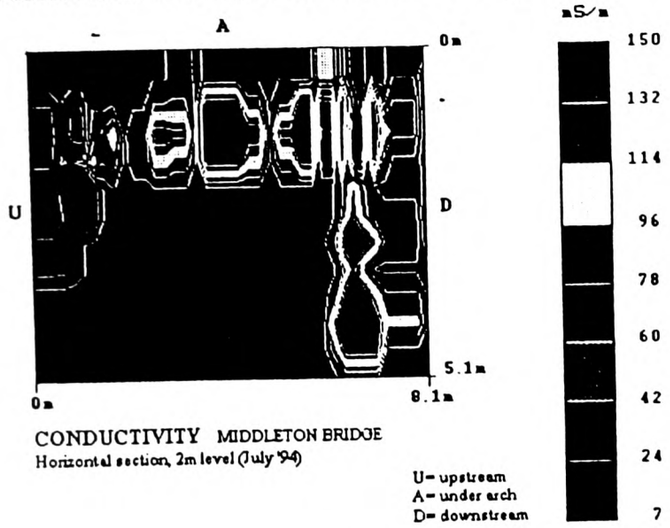

Fig. 5 Conductivity tomographic model

The values obtained are in a high and very wide range indicating heterogeneity in soil filling in the abutment, made of rock such as argillites, wet clays or alluvium and sand; or variations in moisture content/salinity [8].

Rock Type	Conductivity (mS/m)
Argillites	1-80
Conglomerates	0.2-2
Sandstones	$1 - 6.4 \times 10^{-5}$
Unconsolidated wet clay	200
Clays	10-1000
Alluvium and sands	80-100

Conductivity is controlled by one or more of the following: (1) clay content, (2) moisture, (3) salinity - the most complex is usually the moisture profile.

Measurements on a soil sample [9] as a function of moisture content, showed that conductivity increases approximately as the square of moisture content.

The bridge investigated was a structure with moisture-drainage problems and attempts had been made in the past to alleviate the problem but with limited success. In this context, both dielectric constant and conductivity increase with water content. The presence of salts in pore water - mainly coming from routine winter road maintenance - will increase the conductivity even further, without affecting proportionally the dielectric constant.

Surveys were repeated over a period of months and differences were noticed, in particular behind the wall under the vault. Comparison of results from data taken at 1m depth lead to the hypothesis that a significant moisture/water movement is taking place at the rear face of that wall with concern about the possible loss of the fine part of the filling; this hypothesis was reinforced by the low velocity values obtained from sonic tomography.

Conductivity data have also been plotted to obtain a horizontal cross-section of the abutment. Clear differences in the values are visible between the upstream and downstream wall situation, with values being on the bottom end of the range in the upstream side and showing medium to high range values on the downstream side. This finding clearly had something to do with the inner construction of the bridge and could not be explained just by asymmetrical water distribution in the structure.

Subsequent endoscopic investigation into the structure has confirmed the hypothesis and revealed that hollow compartments were built into the bridge and that some of them have been partially or totally filled by grout injection during earlier strengthening and reinforcing operations. The findings from the survey were:

- Depth of penetration of the conductivity meter used was equivalent to the masonry wall thickness
- Upstream side is dry because the void behind the wall is not grour filled.
- Downstream, water moves from backfill to grout to external wall.
- A similar situation may pertain on the abutment.

The conductivity distribution, yields the hypothesis that the downstream wall is not solid stone masonry but may be layered within itself. Later confirmed by visual and endoscopic inspection, the wall is stone-rubble-stone.

6. FUTURE WORK

- Coring is planned to be carried out in the next few months, to verify the internal construction.
- Custom equipment for determining conductivity at variable depth is to be developed.
- Full scale field and laboratory calibrations will be undertaken

7. CONCLUSIONS

The NDT methods used in this project have demonstrated the ability to be rapid, low cost, techniques from which tomographic cross-sections, inhomogeneity identification, moisture movement detection over time and layering within the masonry can be detected.

8. ACKNOWLEDGEMENTS

The first author gratefully acknowledges the financial support of the EPSRC and the Highways Agency, London. The authors acknowledge the facilities of the University of Edinburgh; access to Middleton Bridge by Lothian Regional Council and scaffolding provided by A.J. Batchelor of Holequest Ltd.

9. REFERENCES

[1] BA 16/93. (1993) The assessment of highway bridges and structures. HMSO, London 1993.

[2] Das, P.C. (1993) Examination of masonry arch assessment methods. *Symp on Structural preservation of the architectural heritage*. IABSE, Rome, 1993.

[3] Kearey, P. & Brooks, M. (1991) "*An Introduction to Geophysical Exploration*", Oxford, 1991.

[4] Das, P.C., Davidson N.C. & Colla, C. (1995) "Potential applications of NDT Methods for Bridge Assessment and Monitoring", *I.Struct.E. Seminar*, April 1995, London.

[5] Wilson, J. (1989) "*Field Geophysics*", Geological Society of London Handbook, 1989.

[6] Forde, MC., Birjandi, F.K. & Batchelor, A.J. (1985) Fault detection in stone masonry bridges by non-destructive testing, *Proc. 2nd Int. Conf. Structural Faults & Repair-85*, Engineering Technics Press, Edinburgh, 373-379.

[7] McNeill, J.D. (1980) "*Electrical Conductivity of Soils and Rocks*", Technical Note TN-5,, Geonics Ltd., October 1980.

[8] Telford W.M. et al, (1976) "*Applied Geophysics*", Ch. 5, Cambridge University Press, N.Y.

[9] Smith-Rose, R.L. (1934) "Electrical Measurements on Soil with Alternating Currents", *Proc. IEE* No. 75, 221-237.

PROCEEDINGS

3RD CONFERENCE

NONDESTRUCTIVE EVALUATION OF CIVIL STRUCTURES AND MATERIALS

September 9, 10, 11, 1996
Regal Harvest House
Boulder, Colorado

SPONSORED IN PART BY
THE NATIONAL SCIENCE FOUNDATION

NON CONTACT NDE OF MASONRY STRUCTURES AND BRIDGES

C. Colla[1]
D. M. McCann [2]
P. C. Das[3]
M. C. Forde [4] (*)

SUMMARY

Masonry arch bridge assessment is overviewed strategically. It is proposed that where a bridge fails the load carrying capacity assessment by a small margin, and it looks to be in good condition, that further investigation be undertaken using NDT techniques.

NDT techniques: radar, sonic and conductivity methods are reviewed and the results from sonic and conductivity NDT surveys are discussed. It was concluded that these techniques are effective and that tomographic plots aid interpretation of data. The conductivity technique has demonstrated the ability to be a rapid, low cost, non-contacting technique from which tomographic cross-sections, inhomogeneity identification, moisture movement detection over time and layering within the masonry can be achieved.

Key Words: stone, masonry, bridge, tomography, radar, sonics, conductivity.

1. INTRODUCTION

Masonry arch bridges form a large proportion of the bridge stock in the United Kingdom and this will continue to be the case for a long time to come, since the vast majority of these bridges are still in perfectly serviceable condition. This means that periodic assessment of their load carrying capacity will remain an essential part of the bridge authorities' management activities for the foreseeable future. The outcome of these assessments can be very significant in terms of resulting financial and logistical burdens for the authorities. It is therefore in their interest to seek, wherever possible, improvements in the methods of assessment.

The UK Department of Transport/Highways Agency and other bridge authorities have sponsored major research projects in recent years to develop numerical methods for predicting the collapse strength of masonry arch bridges. A number of newly developed methods were then tested against the results obtained from full-scale tests. A comparative summary of the findings were given in BA 16/93 [1], and also by Das [2]. The overall lessons learnt from the developments so far can be summarised as follows.

(*) 1 Dept of Civil Engineering, University of Edinburgh, The Kings Buildings, Edinburgh EH9 3JN, UK
2 British Geological Survey, Keyworth, UK
3 Highways Agency, St Christopher House, Southwark Street, London SE1 0TE, UK
4 Tarmac Chair of Civil Engineering, University of Edinburgh, Edinburgh EH9 3JN, UK

2. UK LARGE SCALE MASONRY ARCH BRIDGE RESEARCH PROGRAMME

Idealistically, the structural system of an arch bridge, composed of a number of elements: i.e. the foundations, the barrel and the surrounding fill, can be conveniently analysed using advanced numerical methods of analysis, such as the finite element method. However, in practice, the accuracy of the results becomes questionable due to a multitude of complexities:-

(i) Computational expediency often means that the analyses are carried out with simplified methods, e.g. a 2-D analysis, or the mechanism method. These methods by necessity bring in added approximations which make the structural idealisation somewhat remote from reality.

(ii) Soil structure interaction is a major problem in analysing the behaviour of even new structures; for these old bridges involving surrounding materials of unknown properties, this becomes a major problem. For anything but the flattest masonry arches, soil arching and support characteristics significantly influence the load carrying capacity. For all sophisticated assessment methods, the soil resistance parameters have to be input, and the estimation of these values is very approximate.

(iii) Since most of the arch bridges do not usually have any reliable records of construction or repair details, it is difficult to determine the physical dimensions of the main structural elements, or the presence or otherwise of additional features such as the haunching at supports, saddling over the barrel or internal spandrel walls and ribs. Many unsuspected examples of such features, including voids that have been subsequently filled, have come to light following demolition - Fig. 1. Because of the difficulty in identifying these features, idealisation of old arch bridges can never be fully satisfactory.

(iv) Generally, the quality of the structural materials and condition of the structural elements cannot be determined or idealised with any precision.

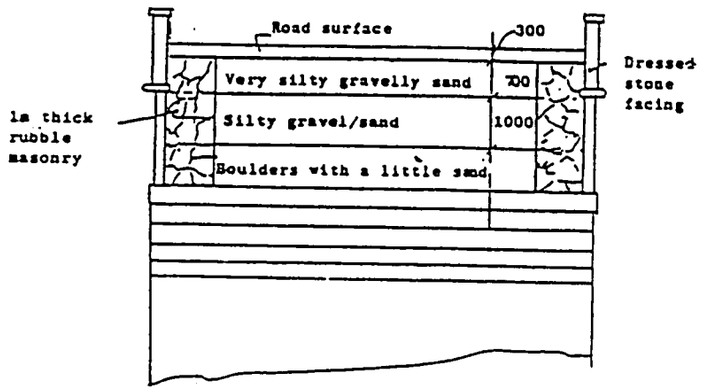

Fig. 1 - Section of bridge revealed on demolition

In the presence of the factors referred to above, the computational precision of the analytical assessment methods largely becomes immaterial. The results from these programs cannot be relied upon to give a black and white indication of the capacity of a bridge, since these analyses are dependent upon the input data such as those relating to the soil parameters which cannot be determined with any precision or consistency.

3. FUTURE RATIONAL BRIDGE ASSESSMENT

Experience is showing that results from any calculation based on the arch assessment method may have to be viewed as giving only a qualitative assessment of capacity. In order to decide on any appropriate action, one may have to rely on additional, perhaps qualitative, information obtained by other means. Thus, if an arch bridge fails assessment by a small margin, and:

- it is not showing any significant deterioration
- it is suspected that additional structural features such as internal ribs are present within the fill,

then it may be reasonable to consider the bridge to be satisfactory for the time being. In such situations, NDT methods such as radar, sonic, vibration and/or conductivity techniques may provide a relatively quick and inexpensive means for making a qualitative judgement on the likelihood of a bridge having any additional reserves of strength in the form of unknown structural traits.

4. NDT METHODS FOR MASONRY ARCH BRIDGES

Three NDT methods were investigated during the work reported in this paper - radar, sonic and conductivity.

4.1 Impulse radar

Impulse radar testing is starting to be used in the evaluation of masonry arch bridges and has advantages over other techniques in certain circumstances, but very real problems can exist with regard to the interpretation of radar data.

In radar applications to masonry the survey is very much dependent on the complexity of the structure and especially on the dielectric properties of the materials involved.

The success of a radar investigation is a function of a number of factors, including the number of interface changes, the values of dielectric constant for materials involved, their conductivity, the width of the structure to be investigated, the thickness of single layers and the choice of a suitable frequency.

In the case of complex or critical conditions, valuable data may be difficult to obtain and their interpretation requires expert knowledge.

Where multiple changes in interface between dielectric layers take place, the change of dielectric constant will be identified but the resolution of the final target layer may prove

particularly elusive. An example would be when the objective of a radar survey on a stone masonry arch bridge is to identify hidden geometry and characteristics of the soil fill with precision. Such an investigation would have to proceed through the various layers of material and if the soil fill is heterogeneous the problem is compounded to the extent that the data may be uninterpretable.

The phenomenon may be accentuated if the dielectric constants of the materials present on site are calculated to be significantly higher than might be expected from published literature [3, 10]. Preliminary investigation of these factors has produced very interesting data - as explained below.

4.2 Impulse Sonics

Time domain impulse sonics were undertaken by measuring the time taken by an impulse from a modally tuned instrumented hammer to transmit through the structure. The data was recorded on a 100 kHz digital oscilloscope. Sonic tomographic plots were constructed using the first arriving wave energy transmitted through the abutment from a number of sources and picked up by the receivers. An image is built up by interpreting the travel time of single ray paths. By an iterative process, sonic velocities through the various materials are mapped in a cross-sectional representation where the sonic velocities are related to material densities.

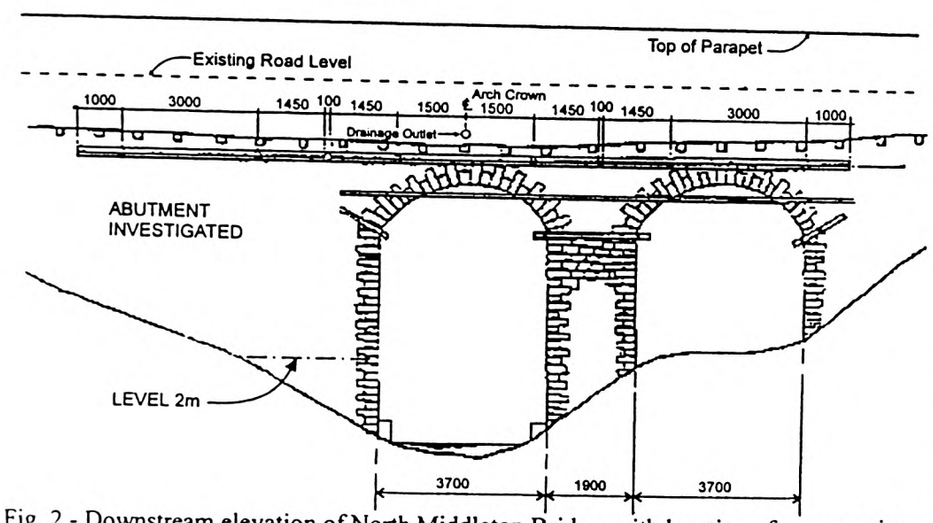

Fig. 2 - Downstream elevation of North Middleton Bridge, with location of cross section fig. 3, 4 and 5 refer to.

4.3 Conductivity Surveys

Originally developed for geophysical mapping, then for archaeology and agriculture, conductivity is a novel application in the civil engineering field.

Conductivity is a technique which makes use of the response of the ground to the

propagation of electromagnetic fields generated through the transmitting coil. The response fields differ both in phase and amplitude from the transmitted one. These differences reveal the presence of the conductor and provide information on its geometry and electrical properties. The induction of current flow results from the magnetic components of the E-M field, consequently there is no need for physical contact with the surface.

The measured field is generally a complex function of the coil spacing "s" of the conductivity meter, the operating frequency "f" and the conductivity distribution of the subsurface "σ". Penetration depth depends upon "s" and the frequency used, but is independent from the conductivity distribution of the subsurface [3][4]. Penetration dependence on frequency implies that the lower the frequency used, the deeper the penetration but the poorer the resolution - as amplitude decreases exponentially with depth [3][5].

5. FIELD WORK

Non-destructive investigation surveys were undertaken on one abutment of an historic stone masonry structure which was known to present the problems described above [6] - Fig. 2.

5.1 Radar Survey

A wide range of antennae was available for investigation of the structure, from 100 MHz to 1 GHz frequency, and they were used with different intent and in different configurations.

High frequency antennae give good spatial resolution but give only shallow penetration as the signal becomes rapidly attenuated. These antennae were used for the identification of masonry wall thickness and near-surface voids /defects.

Low frequency antennae are better suited to penetrate deeper into the abutment as they emit more powerful signals, but their long wave length is a detriment to spatial resolution. Also, targets of "small dimensions" or "small thicknesses" can be missed.

In the case of this structure, its significant width (over 8 metres) and the dielectric properties of the filling materials did not permit the use of even the lowest frequency antenna in a reflection mode, to scan the whole section of the abutment. (Operating the equipment in this mode, the radar signal has to travel twice the distance from the antenna to the target. Signals are propagated into the structure and their reflections at different interfaces are picked up by a receiving device located - in the same or different antenna - on the same side of the structure.)

In view of the above, radar tomography was carried out. This technique involves the use of a transmitter and a receiver positioned on different sides of the abutment and moved in a series of combinations to obtain time domain maps of the same cross section of the structure. From the elaboration of these scans, local variations of dielectric constant may

be identified and related to engineering features/defects of the structure.

The preliminary findings from this radar survey indicate values of the di-electric constant within the bridge which are significantly different from published data for construction materials. The average value for the di-electric constant (ε) for the composite bridge construction [masonry/soil fill/masonry] was computed to be ε = 56.

5.2 Sonic Tomographic Survey

Readings were collected at different levels of the structure under investigation. At each level, measurement points were located on the three walls of the abutment: downstream, upstream and under the arch. All points of the grid were alternatively used as transmitting and receiving stations, so to also allow collection of "back readings".

At level 2 m of the grid (see fig. 2), 15 stations were used for a total of 142 rays. Fig. 3 shows a cross section of the abutment with location of transmitters and receivers (ray paths were assumed straight at the beginning of the tomographic reconstruction).

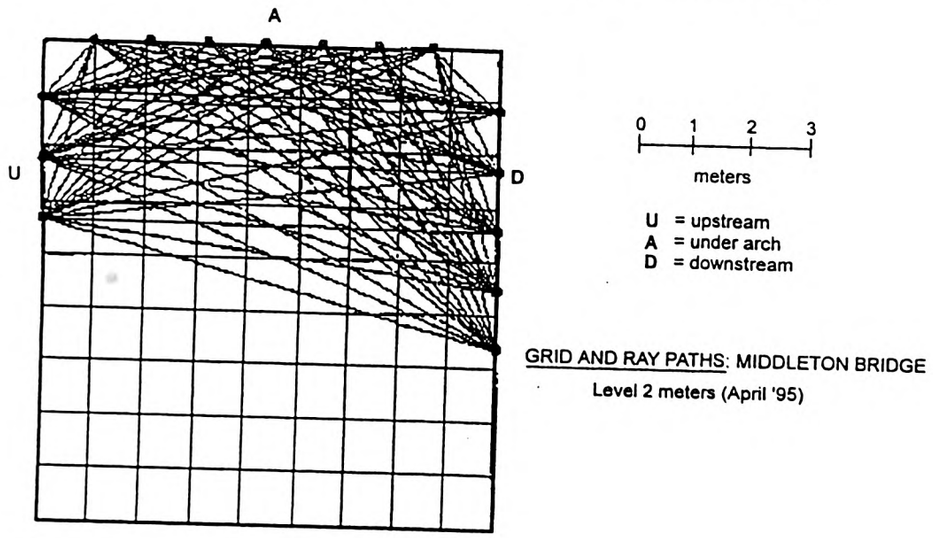

Fig. 3 - Initial assumed density of sonic ray paths.

Consider Fig. 4: from the first data analysis outcome it is clear that high velocity areas are located along the walls corresponding with the stone masonry, while values of velocity between medium to low are situated towards the centre of the plot, indicating backfill materials.

Looking in more detail, along the upstream and especially downstream wall, very high velocity areas relate to a continuous homogeneous dense material which subsequent

endoscopic investigations revealed to be cement grouted zones. By applying constraints

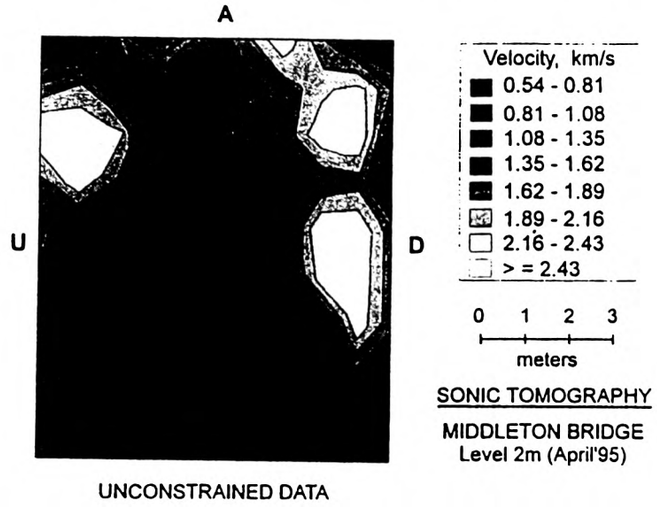

Fig. 4 - Sonic tomographic reconstruction

to the model and re-iterating, masonry thickness on the down stream side was calculated and found to be comparable with the one determined from the conductivity survey detailed below.

5.3 Conductivity Survey

In the structure investigated here, the digital conductivity meter had intercoil spacing of 1m and provides a maximum depth of exploration of 1.5m in vertical dipole mode operating at a frequency of 14.6 kHz. The meter was used on both the upstream and downstream sides of this 2-span bridge and on the wall beneath the main vault. The measurement stations followed a grid marked on the walls, in an area well clear of any evident metallic objects (drains, reinforcing beams). For maximum accuracy and good spatial resolution, measurements were overlapped to have readings every half metre. Contacting and non-contacting conductivity measurements were taken, to obtain data at different depths. Data were collected using a digital data recorder and later transferred to a P.C. The results were plotted to produce contour maps of the conductivity distribution along horizontal and vertical planes within the structure.

Data have been analysed with two different software packages and differences were noticed in the resolution of the resulting contour plots. In particular, the "geophysical" programme has given satisfactory results when mapping data collected along surfaces coplanar to the three abutment walls..The tomography programme has shown to be more accurate in the cross section elaborations, when data collected at different depths have been plotted together (see fig. 7 for comparison).

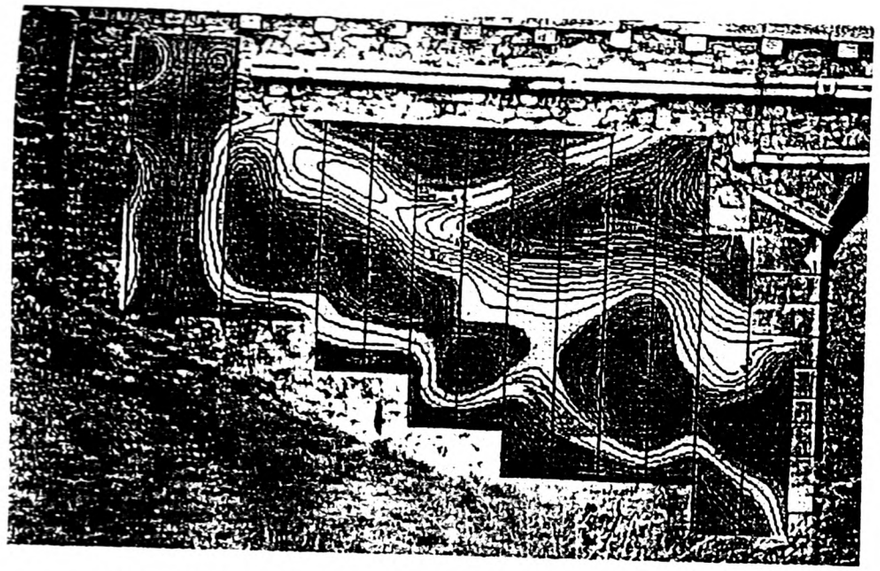

Fig. 5 - Conductivity distribution on downstream side at 1.5 m depth

Consider now Fig. 5 - the values obtained are in a high and very wide range - indicating heterogeneity in soil filling in the abutment, made of rock such as argillites, wet clays or alluvium and sand; or variations in moisture content/salinity [8].

Rock Type	Conductivity (mS/m)
Argillites	1-80
Conglomerates	0.2-2
Sandstones	$1 - 6.4 \times 10^{-5}$
Unconsolidated wet clay	200
Clays	10-1000
Alluvium and sands	80-100

Conductivity is controlled by one or more of the following: (1) clay content, (2) moisture, (3) salinity - the most complex is usually the moisture profile. Measurements on a soil sample [9] as a function of moisture content, showed that conductivity increases approximately as the square of moisture content.

The bridge investigated was a structure with moisture-drainage problems and attempts had been made in the past to alleviate the problem but with limited success. In this context, both dielectric constant and conductivity increase with water content. The presence of salts in pore water - mainly coming from routine winter road maintenance - will increase the conductivity even further, without affecting proportionally the dielectric

constant.

Surveys were repeated over a period of months and differences were noticed, in particular behind the wall under the vault - Fig. 6. Comparison of results from data taken at 1m

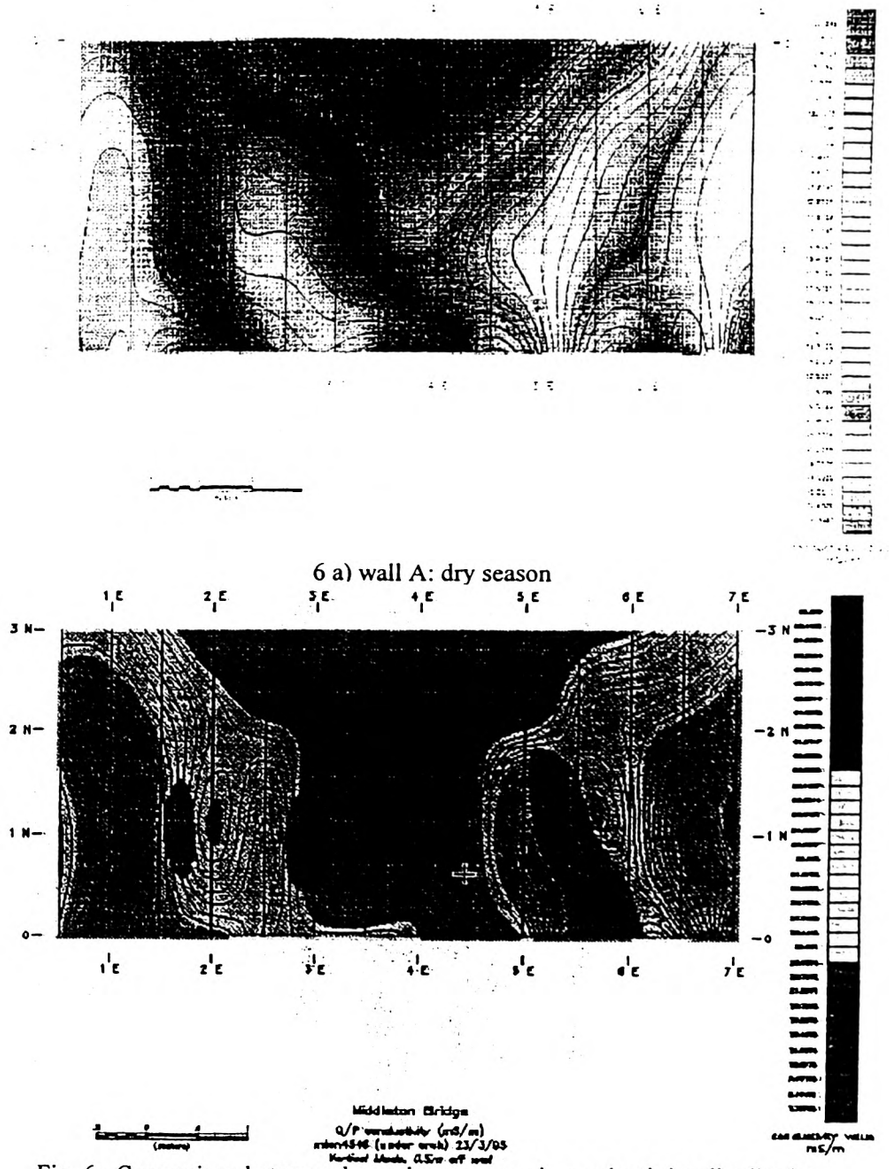

6 a) wall A: dry season

Fig. 6 - Comparison between dry and wet season in conductivity distribution

depth lead to the hypothesis that a significant moisture/water movement is taking place in an area at the rear face of that wall with concern about the possible loss of the fine part of the filling; this hypothesis was reinforced by the low velocity values obtained from sonic tomography in that same area.

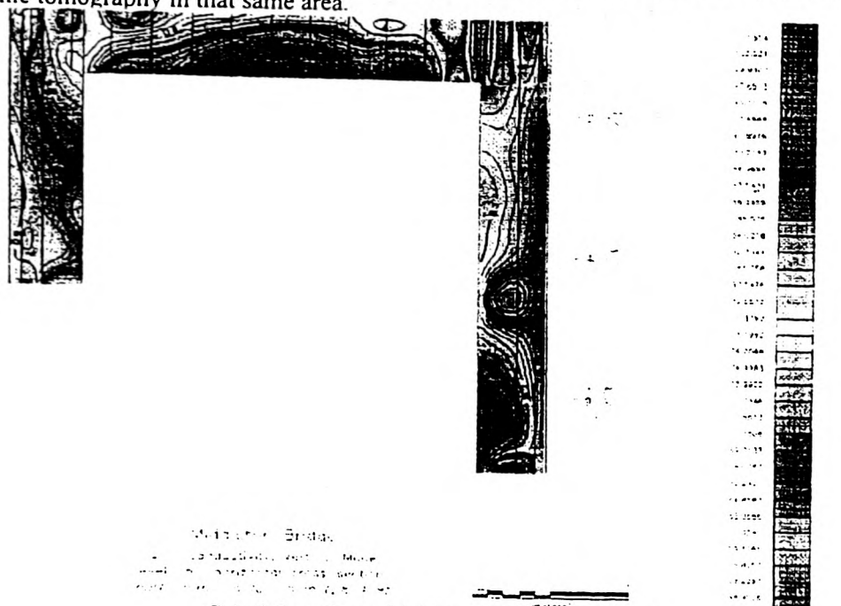

7a) elaboration with "geophysical" software

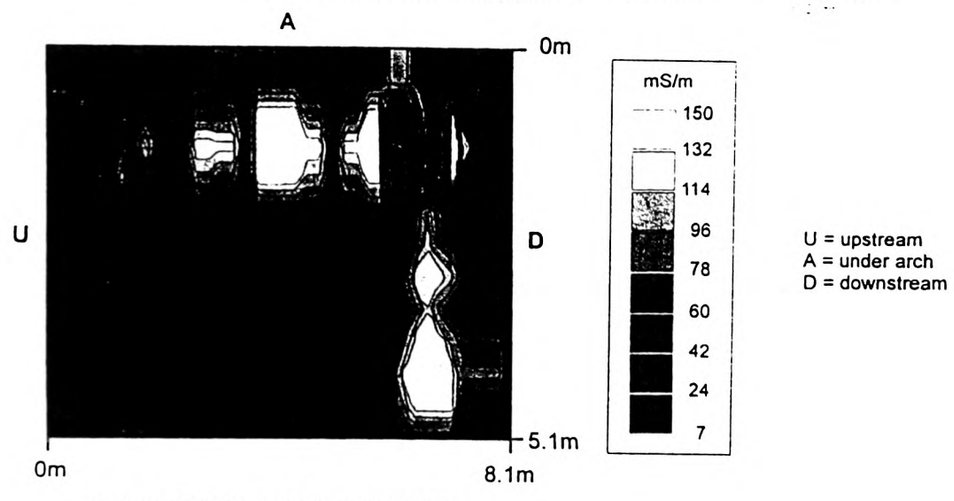

7b) elaboration with tomographyc programme

Fig. 7 - Conductivity distribution of cross section, at level 2m.

Conductivity data have also been plotted to obtain a horizontal cross-section of the abutment. Figure 7 is a cross sectional representation with the data iterated through tomographic software. Clear differences in the values are visible between the upstream and downstream wall situation, with values being on the bottom end of the range in the upstream side and showing medium to high range values on the downstream side. This finding clearly had something to do with the inner construction of the bridge and could not be explained just by asymmetrical water distribution in the structure.

Subsequent endoscopic investigation into the structure has confirmed the hypothesis and revealed that hollow compartments were built into the bridge and that some of them have been partially or totally filled by grout injection during earlier strengthening and reinforcing operations.

Where the moisture moves from backfill to grouted zones, a clear difference in conductivity values is visible between the grouted material and the external wall. This enabled the thickness of the stone wall on the down stream side of the abutment to be calculated. A similar situation may pertain to the arch wall.

The upstream side is dry because the void behind the wall is not totally grout filled and this makes it difficult to calculate the thickness.

The conductivity distribution in localised areas near the exterior of the section yields the hypothesis that the wall is not solid stone masonry but may be layered within itself. This was also later confirmed by visual and endoscopic inspection and the wall has a compound structure: stone-rubble-stone.

6. LABORATORY WORK

Extensive laboratory calibration is being undertaken in order to study, in a controlled environment, the effect of variations of dielectric properties and conductivity on radar performance. In particular the resolution and penetration power of different radar frequencies and the influence of water content on the electrical properties of building materials are the main objectives of these experiments. Sonics and conductivity are also applied and compared where possible.

A brick masonry test rig has been built at the University of Edinburgh, in the form of a U- shaped wall, whose open end is closed by a wooden gate. The main dimensions of this masonry box are 1m width × 2.4 m length × 1.3 m height - Fig. 8.

Material has been compacted in the rig and experimental set ups included: sand in different compaction states, with different moisture and salt contents. Furthermore, voids and defects have been simulated. Size, depth and orientation of targets buried in the background material have also been studied.

Mainly 900 MHz and 500 MHz frequency antennae have been used during the radar test.

The effect of the orientation of the antenna on the target resolution has also been investigated.

Sonic data have been collected giving emphasis to 3D tomography.

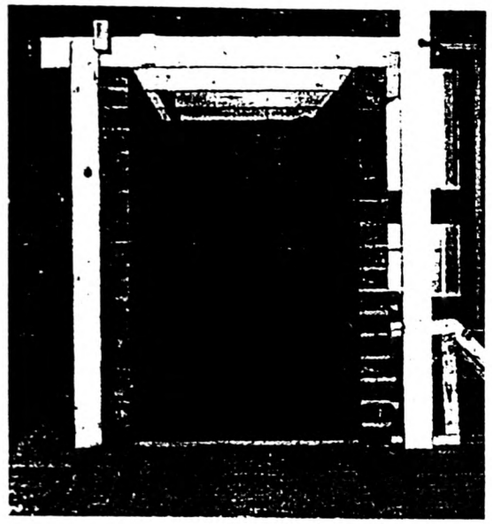

Fig. 8 - Test rig after completion, while still empty.

The rig set-up configuration shown in Fig. 8 has now been modified to simulate cellular structures as can be encountered in historical bridges - a wall has been built in the middle of the rig along its length.

7. FUTURE WORK

The near surface actual structure composition of the abutment of North Middleton Bridge has already been checked through visual and endoscopic investigation. To verify the inner construction of the bridge, coring is planned to be carried out.

As depth of penetration of the conductivity meter used on site was equivalent to masonry wall plus grouting thickness, no conductivity information was obtained from the core of the structure. Custom equipment for determining conductivity at variable depth is to be developed.

8. CONCLUSIONS

1. The NDT methods used in this project have demonstrated the ability to be rapid, low cost, contacting and non-contacting techniques for bridge assessment and monitoring purposes.
2. From tomographic cross-sections, inhomogeneity identification, moisture movement detection over time and layering within the masonry can be detected.
3. Each method has proved to be effective and their parallel use in this investigation has drawn an organic picture of the state of the structure revealing both construction details and modification/problems which have arisen with time.
4. Whilst some of the information gathered was common to more than one method, other knowledge has been obtained due to the special measurements of a particular technique.
5. Whilst the conductivity method has given detailed information up to a certain depth into the structure, no data could be collected at deeper locations. Its low cost particularly in terms of time in the post data-collection phase, makes it convenient for repetitive surveys.
6. Sonics are a reliable method when great attention is spent in recording the data; a meticulous work is also necessary during the preparation and analysis of the data, but good results can be achieved when the optimal grid density is set in relation to the goal of the test.
7. Radar's advantages over the other two methods are rapidity and reproducibility in allowing continuous scan recording. When the structure to be investigated presents a complex situation in terms of construction and dielectric characteristics, a compromise may need to be reached between resolution and penetration power of the antennae chosen. Improvements in the understanding and use of this technique on masonry structures is expected in the near future.

9. ACKNOWLEDGEMENTS

The first author gratefully acknowledges the financial support of the EPSRC and the Highways Agency, London. The authors acknowledge the facilities of the University of Edinburgh; access to Middleton Bridge granted by Lothian Regional Council and scaffolding provided by A.J. Batchelor of Holequest Ltd, Galashiels. Figure 5 was prepared by undergraduate student Geoffrey Denton.

10. REFERENCES

[1] BA 16/93. (1993) The assessment of highway bridges and structures. HMSO, London 1993.

[2] Das, P.C. (1993) Examination of masonry arch assessment methods. *Symp on Structural preservation of the architectural heritage*, IABSE, Rome, 1993.

[3] Kearey, P. & Brooks, M. (1991) "*An Introduction to Geophysical Exploration*", Oxford, 1991.

[4] Das, P.C., Davidson N.C. & Colla, C. (1995) "Potential applications of NDT Methods for Bridge Assessment and Monitoring", *I.Struct.E. Seminar*, April 1995, London.

[5] Wilson, J. (1989) "*Field Geophysics*", Geological Society of London Handbook, 1989.

[6] Forde, MC., Birjandi, F.K. & Batchelor, A.J. (1985) Fault detection in stone masonry bridges by non-destructive testing, *Proc. 2nd Int. Conf. Structural Faults & Repair-85*, Engineering Technics Press, Edinburgh, 373-379.

[7] McNeill, J.D. (1980) "*Electrical Conductivity of Soils and Rocks*", Technical Note TN-5, Geonics Ltd., October 1980.

[8] Telford W.M. et al, (1976) "*Applied Geophysics*", Ch. 5, Cambridge University Press, N.Y.

[9] Smith-Rose, R.L. (1934) "Electrical Measurements on Soil with Alternating Currents", *Proc. IEE*, No. 75, 221-237.

[10] Petroy, D.E., (1994) Assessment of Ground Penetrating Radar applicability to specific site investigation: simple methods for pre-survey estimation of likely dielectric constants, target resolution & reflection strength, *Proc. SAGEEP March '94*, Boston, Massachusetts.

Non-Destructive Testing
in
Civil Engineering

NDT-CE '97

Editor: Professor J H Bungey

Volume 1

An International Conference
organised by
The British Institute of Non-Destructive Testing

LABORATORY MODELLING OF RADAR PROPAGATION THROUGH MASONRY MODELS

C Colla & Prof M.C. Forde
University of Edinburgh
Dept of Civil & Env Engng
Crew Building
The Kings Buildings
Edinburgh EH9 3JL
Scotland

Prof D.M. McCann
British Geological Survey
Keyworth
Nottingham NG12 5GG
England

Dr P.C. Das
The Highways Agency
Bridges Engineering Division
St. Christopher House
Southwark Street
London SE1 0TE
England

ABSTRACT

Masonry arch bridges represent a significant proportion of the UK bridge stock on both the roads and the railways. There are some 40,000 UK masonry arch road bridges and some 30,000 masonry arch rail bridges. If these bridges were taken out of service then both the UK road and rail networks would be completely inoperable.

In order to aid the load carrying capacity analysis of these bridges, a series of NDT techniques have been developed at the University of Edinburgh, primarily focused upon masonry structures. As part of this ongoing programme a laboratory study of radar propagation through masonry has been undertaken. A 2.4 m long x 1 m wide x 1.5 m high experimental test rig was built in the laboratory with brick walls on three sides and a wooden gate on the fourth narrow side.

Radar tests were undertaken using a 900 MHz bow-tie antenna with the box filled with fresh water and then saline water with different concentrations of sodium chloride. Further test were undertaken with the box filled with dry sand and wet sand. The results from this work are reported herein indicating the reliability and ease of identifying various targets.

It was found that radar signals were severely attenuated when the saline concentration exceeded 0.05%. Better results were obtained when the box was filled with dry sand rather than wet sand.

INTRODUCTION

Masonry arch bridges represent a significant proportion of the UK bridge stock on both the roads and the railways. There are some 40,000 UK road bridges and some 30,000 rail bridges. If these bridges were taken out of service then both the UK road and rail networks would be completely inoperable.

There has been considerable work undertaken in order to assess the load carrying capacity of masonry arch bridges [1,2,3]. The general conclusions from this work are that the existing methods of assessment for the masonry arch bridges may at times be too conservative. The work on dynamic load testing of masonry arch bridges at the University of Nottingham has indicated that the dynamic load capacity may be some 70% of the ultimate static load capacity of a masonry arch bridge. In order to undertake effective finite element work, which is being correlated with scale model work undertaken at Edinburgh and Nottingham Universities and also at Bolton Institute of Higher Education, there must be a clear and unambiguous knowledge of the internal construction of the masonry arch bridge. For example the size and shape of the arch is a critical factor as is the size and shape of the springers for the arch. Other key factors include knowledge of whether the bridge is an arch backfilled with soil thus giving load dispersion [4], or whether the bridge has a cellular hollow construction.

Recent work on bridge reliability by the UK Highways Agency [5], who are pioneering work within the international community on reliability strategies, clearly indicates that there is an ongoing need to understand the deterioration mechanism of masonry arch bridges. Whilst this work is being addressed the strategy of the bridge community is to assess a structure. If the structure fails the assessment but looks in good order, then the recommendation should not be simply pass/fail - but that of a new category of "monitor".

It is against the above background that the research reported herein was commenced.

The key areas to be identified in the sections below are target identification in masonry structures such as bridges. In the case of highway bridges, in the northern climates where snow and ice are predominant, the influence of salt concentration on the effectiveness of NDE

techniques is important. The specific non-destructive testing method discussed in this paper is impulse radar.

OBJECTIVES OF RESEARCH

The objectives of the work reported herein are:

- To identify the effectiveness of radar penetration through saline solutions.
- To identify the effectiveness of identifying targets within a soil fill.

GROUND PENETRATING RADAR

Within the geotechnical community, ground penetrating radar (GPR) is seen as a technique which offers a way of viewing shallow soil and rock conditions. The areas of application for ground penetrating radar are diverse and include groundwater exploration, geotechnical and archaeological investigations, [6-8], as well as engineering examples [9-10]. Some specific applications, like changes of rock type, soil strata and water table in coarse grained soils, detection of buried walls, pipes, tunnels [11], have generated an increasing demand for subsurface imaging with higher resolution than previously possible. The effective application of the radar for the high-resolution definition of features (stratigraphy, voids, defects) is a function of the antenna frequency used. The propagation of the radar signal depends on the electromagnetic response of the materials investigated.

GPR offers the possibility of a high resolution sounding capability with detection of features of the order of a few millimetres thickness at ranges of several metres. Ground penetrating radars have demonstrated the capacity to sound to depths of tens of metres in low conductivity (less than 1mS/m) materials such as sand, gravel, rock and fresh water. The range decreases to a shallow depth in conductive materials such as clays, silts and soils with saline or contaminated pore water. A numerical experiment on concrete clearly illustrated these points [12]

RADAR PRINCIPLES

Ground-penetrating radar produces short pulses of high frequency (10-1000 MHz) electromagnetic energy which are transmitted into the ground or the structure, depending on the case. The propagation of the radar signal depends on the electrical properties of the materials encountered. The velocity and the attenuation are the factors that describe the propagation of high frequency waves into the materials. These factors depend on the dielectric and conductivity properties of the materials, which also determine the signal power that is reflected at boundaries where the electrical properties vary [13-15].

The dielectric constant or relative permittivity describes the high frequency electrical properties of the materials since, at these frequencies, the displacement (polarisation) properties dominate the conductive properties for many materials. The complex dielectric constant is given by:

$$\varepsilon^* = \varepsilon' + i\left[\varepsilon'' + \frac{\sigma_{dc}}{\omega\varepsilon_o}\right] \qquad (1)$$

where ε' is the real part of the dielectric constant and the term in bracket is the imaginary or loss part of the dielectric constant. This is separated into high frequency and d.c. conductivity components of the loss, as follows:

ε" is the frequency-dependent loss associated with the relaxation response phenomena;

σ_{dc} is the d.c. conductivity (S/m);

ω is the angular frequency, 2πf;

ε_0 is the free space permittivity (8.854×10^{-12} F/m).

Radar signal velocities in low-loss materials are related to the real part of the dielectric constant by:

$$v = \frac{c}{\sqrt{\varepsilon'}} \qquad (2)$$

where $c = 3 \times 10^8$ m/s, the propagation velocity of electromagnetic waves in free space.

Note that dielectric constant in water is 80 and that of most dry geological materials is in the range of 4-8. This large difference explains why the radar signal velocity is strongly dependent on the water content in soils. High water content gives rise to strong radar reflections at interfaces, causing part of the transmitted signal to be reflected. High conductivity causes strong attenuation in the signal. Also the effect of signal scattering by small scale heterogeneities can increase attenuation.

In a low-loss medium, the attenuation is expressed as:

$$\alpha = \frac{1.69x10^3\sigma}{\sqrt{\varepsilon'}} dB/m \qquad (3)$$

where $\sigma = \sigma_{dc} + \omega\,\varepsilon''\,\varepsilon_0$ combines both d.c. conductivity and dielectric losses.

Expressions (2) and (3) are approximate and require that $\sigma/\omega\varepsilon'\varepsilon_0$ is much less than 1.

EXPERIMENTAL TEST RIG

A 2.4 m long x 1 m wide x 1.5 m high experimental test rig was built in the laboratory. Its main part consists of a 3-sided masonry box with the fourth side equipped with a timber gate to gain easy access to the inside of the test rig and to facilitate any loading and unloading of fill material (fig. 1).

The masonry brick wall was built of Class A Engineering solid bricks and mortar in the proportion 1:¼:3 of cement, lime, sand. The wall is one header thick and the foundations are secured into a slot cut out of a plywood base which also constitutes the base of the rig.

Care was taken in the design phase of the rig to avoid using any metal part which could later interfere with the radar survey during collection of data, leaving unwanted signatures on the radar plots. For the same reason the gate on one of the short sides of the rig is timber. It was designed so that it could slot into place between the two ends of the brick wall and a slot cut in the plywood base, with no need for a metal locking device.

The masonry rig was then lined with a PVC sheet to create a watertight container for the water which constituted the fill material and to maintain the brickwall in a dry condition. The rig was filled with water up to 1.3 m level and sodium chloride was dissolved into the water to create brine solution in different concentrations. Three different set ups were investigated, with brine in concentrations of 0.05 %, 0.1 % and 0.25 % by weight of salt to the water. Three rebars (Ø 3.5 cm) were immersed in the water and maintained vertical by suspending them from a timber frame which was also built around the rig. The metal rods were located at 20, 40 and 70 cm away from the brickwall where the radar antenna was located.

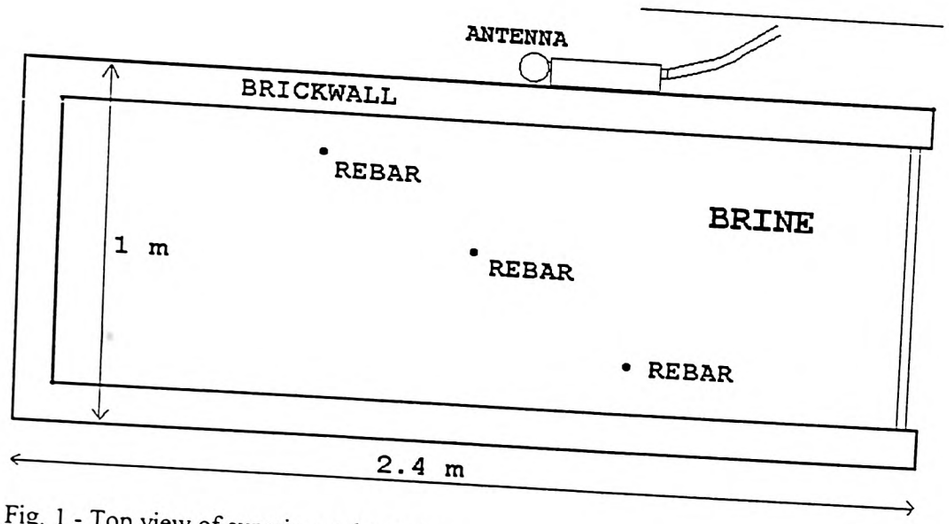

Fig. 1 - Top view of experimental test rig.

RADAR SURVEY

A shielded 900 MHz frequency antenna was used to collect radar reflection data within a 60 ns time window over the test rig. The antenna was moved along one side of the masonry rig, scanning in the horizontal direction, to plot horizontal cross sections on the rig. Reflections from the masonry walls and the metal re-barswere picked up. The survey was repeated for the different salt concentrations in the water.

The antenna had a survey wheel attached to record a constant number of scans per unit distance travelled and to obtain a more accurate and smooth picture of the radar targets. Twenty centimetre marks along the direction of movement of the antenna were marked at the top of the plots.

DATA ANALYSIS

Brine temperature and conductivity were monitored throughout the different stages of the experiment and values are recorded in table 1.

Brine temperature	Salt concentration	Conductivity
18 °C	0.05%	735 µS
16.5 °C	0.1%	1147 µS
17 °C	0.25%	Out of range

Table 1 - Values of brine temperature, concentration and conductivity measured during the experiment.

The measured radargrams from set-ups with water at different chloride content were compared.

The GPR method transmits and receives signals recorded over a spatial window - the antenna aperture. Because of the wide field of view of the radar antenna, objects off to the side of the antenna can be recorded, resulting in hyperbolic reflection patterns - as in the case of the metal rods. These patterns vary with the frequency used and the electromagnetic properties of the materials under study. In all the cases presented here, the hyperbolas from the rebars show short and flat branches which indicates a decrease of the energy power in the radar waves, probably with loss of the high frequency components of the signal.

In fig. 2, the brine has a sodium chloride concentration of 0.05 % by weight. The radar waves travelled through a brick masonry wall and 80 cm depth of water to reach the back wall, and encountered three rebars along the way. Reflections from the three rebars are all visible, as is

the reflection from the back wall. It is worth noting the great difference between the amplitude of the signature of the front wall and that of the back wall. The dissimilarity shows up in the amplitude of the signal and is due to various factors - primarily the attenuation of the wave. Causes of this attenuation are the variation in electrical properties of the materials at the interface between brick masonry and water. This strong interface causes a large part of the signal to be reflected back, with only a small part of the wave energy capable of travelling through the water and reaching the back wall, the signature of which is very much attenuated compared to that from the front wall. A similar comparison can be made between the hyperbolas of the three rebars.

Another factor that distinguishes microwave radiation is the dispersive nature of the microwave. As a result of the high permittivity of water (typical values of dielectric constant for water are of the order of ε = 80-81) and high conductivity of brine, the signal attenuates quickly; and whilst the reflection from the first re-bar is fully visible, reflection from the third re-bar is only just noticeable (radar plots of fig. 1, 2 and 3 are shown in logarithmic grey scale transform which greatly emphasise the low amplitudes).

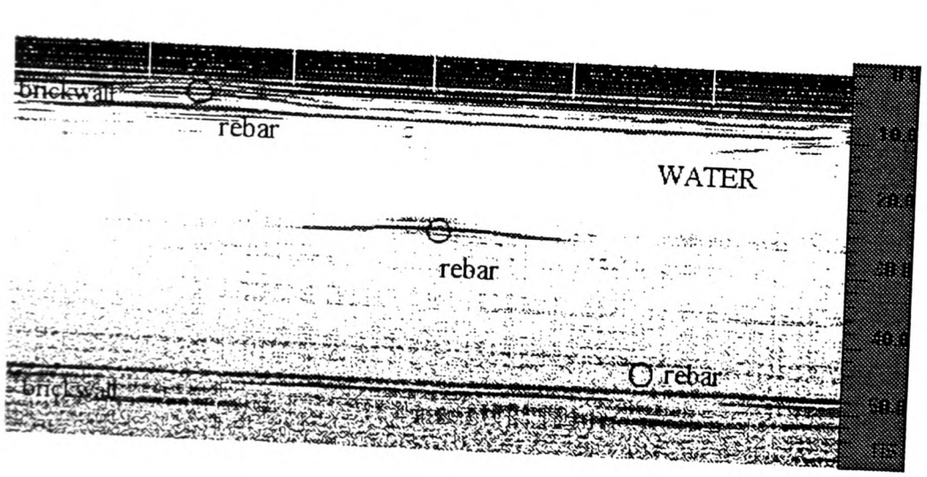

Fig. 2 - Radargram of test rig with 0.05% salt content in water and rebars at increasing depth.

Fig.3 shows the case of brine concentration of 0.1% and fig. 4 shows the experiment with 0.25% chloride concentration. In fig 3, the reflection from the back wall has completely disappeared and so has the reflection from the third re-bar. Branches of the hyperbola from the

first re-bar are shorter and less pronounced than in the previous case. Reflection from the second re-bar is almost reduced to a flat thin line. In the case of fig. 4, reflection from the first re-bar is almost reduced to a point: no branches are visible. None of the patterns from other features of the experimental set-up, except for the front wall, are evident.

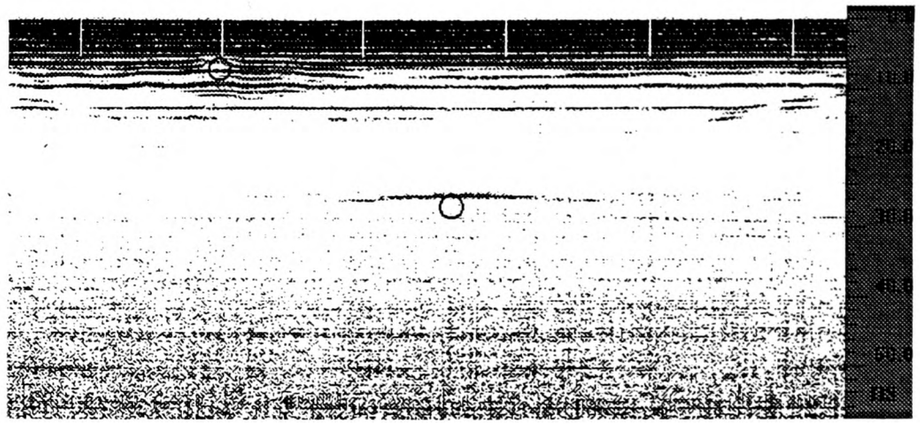

Fig. 3 - Radargram of test rig with 0.1% salt content in water and only two rebars visible.

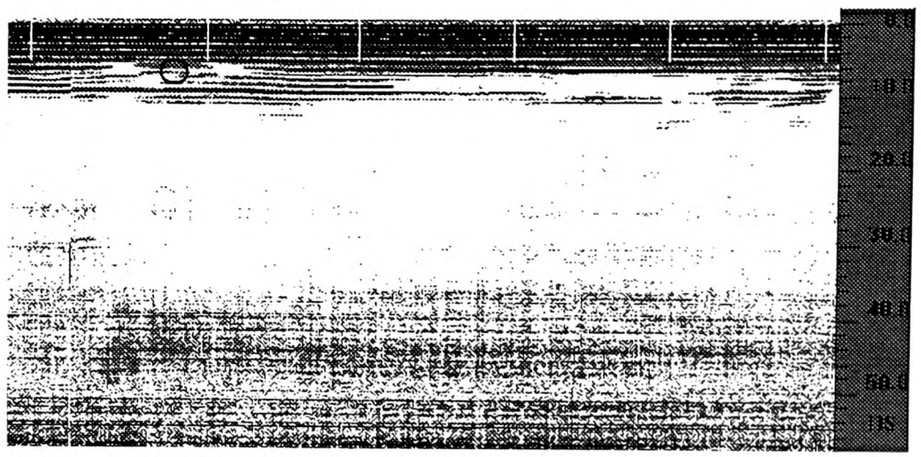

Fig. 4 - Radar plot of test rig with 0.25% salt content and reflection from first re-bar visible.

Following this comparison work, signal waveforms were analysed in the time domain to quantify the reduction of signal power due to the increasing conductivity values with increasing salt concentrations, as from table 1. The impulse response to the propagation in water with

salt concentrations, as from table 1. The impulse response to the propagation in water with increasing conductivity was estimated from the reflections obtained from the immerse metal rods. The decrease in energy was calculated in relative terms, measuring the amplitude of the waveforms corresponding with the peaks generated at the location of the first re-bar.

Fig. 5 shows edited unfiltered portions of the three waveforms corresponding to the centre of the hyperbolas from the first re-bar. The signal waveforms show the main reflection peaks generated from the re-bar, in the form of a sinusoid between 7 and 10 ns on the time axis. It is this peak which has been used for the calculations of the relative decrease of amplitude. From fig. 6 and table 1 is evident how an increase in conductivity of only 0.4 mS/m, causes a reduction of 34% in the amplitude of the signal, when passing from 0.05% to 0.1 % salt content in the water. One third of the power of the signal is lost. When the salt content increases to 0.25%, the signal amplitude decreases a further 17%, reaching only 50% of the power of the signal registered at 0.05% salt content. Note that even though the sodium chloride content doubles from 0.05 to 0.1%, and increases five times to reach 0.25%, the salt concentrations considered in the experiment are low values compared to sea water (3.5% on average) or to localised high concentrations of salt as could be encountered in masonry arch bridges due to de-icing salt [16].

The impulse response was estimated from reflections measured from the immersed metal rods.

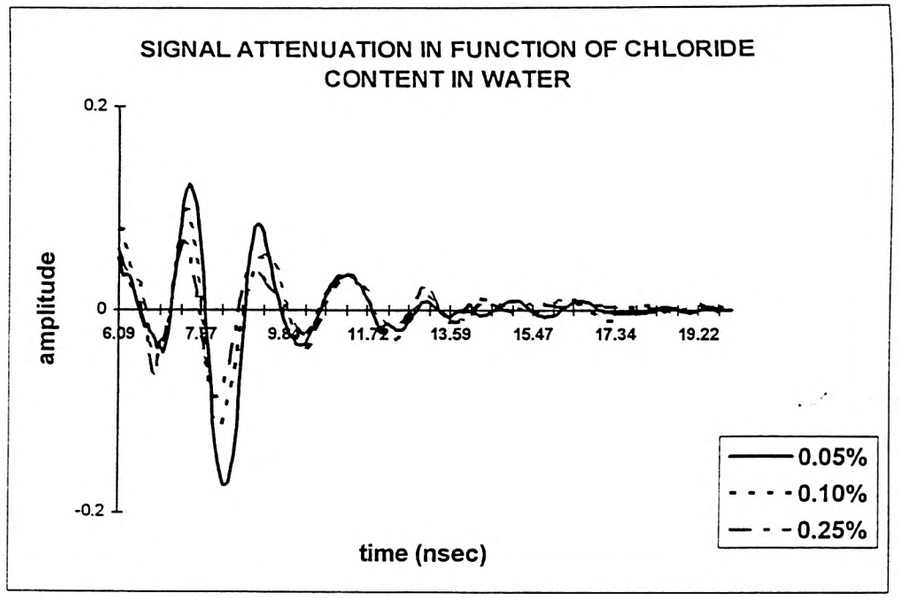

Fig. 5 - The relation between salt content at three different concentrations in water, and amplitude of the reflected signal from the first re-bar.

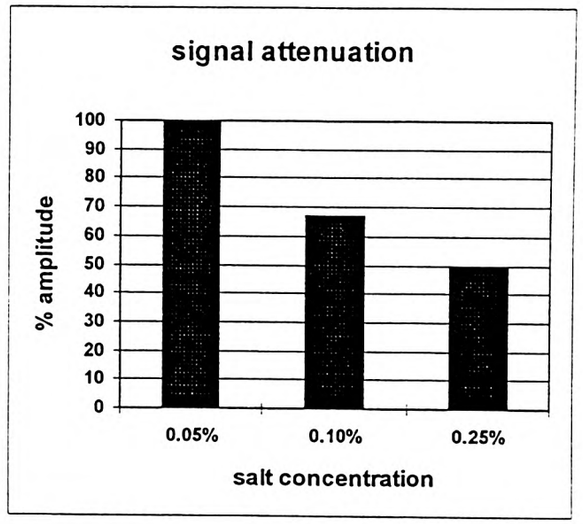

Fig. 6 - The relation between salt concentration in water and the relative decreased amplitude of the signal, calculated from the experimental data.

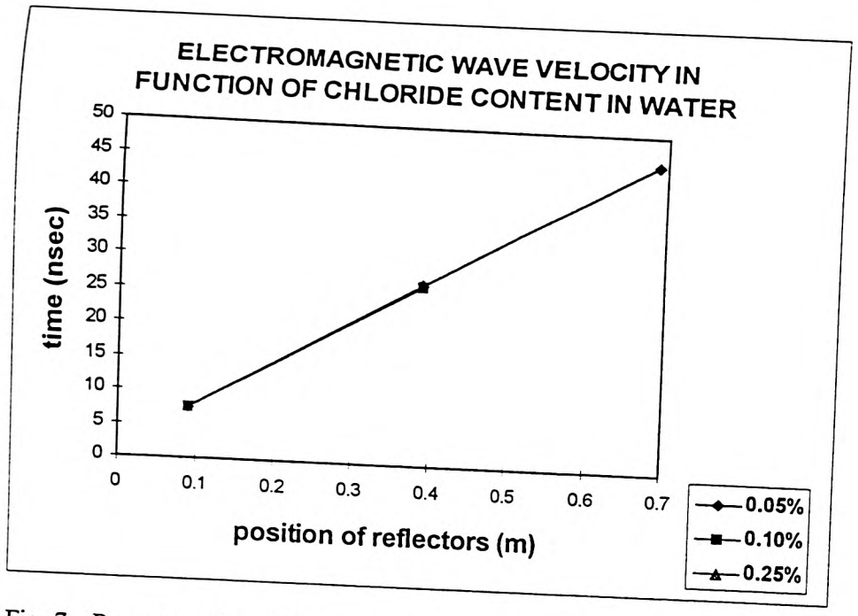

Fig. 7 - Representation of the electromagnetic wave velocity measurements calculated by time domain technique.

PRACTICAL IMPLICATIONS OF THE RESULTS

The statement is frequently made that radar will not work through saline water, but this simplistic statement is only partially accurate. The radar signal is rapidly attenuated as the conductivity of the background medium increases [12]. However at relatively low saline contents (0.05%) and therefore relatively low conductivity the radar will have limited penetration as seen from the above experimental data. This is substantially less than the saline content of sea water (3.5%). It would therefore seem most unlikely that any significant penetration would be achieved through sea water using 900 Mhz bow tie antennae of the type used in this experiment at the frequencies used in this experiment.

In the context of the experiments using dry sand and wet sand in the box it can be seen that the best radar penetration and resolution was obtained using the dry sand box. Significant signal attenuation occured when the soil was wet

CONCLUSIONS

1. GPR offers a rapid, no-contact high resolution method for detecting and mapping features in engineering applications.
2. The radar technique cannot be used for high resolution soundings in great depth ranges, in environments with high electrical conductivity.
3. The range and resolution of GPR decreases with the presence of conductive materials like brine or conductive pore water.
4. At saline contents of 0.05% by weight 900 MHz bow tie antenna were rapidly attenuated.
5. When testing through soil, the best results were obtained when using radar through dry soil.

ACKNOWLEDGEMENTS

The authors gratefully acknowledge the facilities of the University of Edinburgh and the financial support of the Highways Agency, London. The first author also gratefully acknowledges the financial support of the EPSRC. The technical help of Mr Kevin Broughton during data collection at the University of Edinburgh is also acknowledged.

REFERENCES

1. BA 16/93. (1993) The assessment of highway bridges and structures. HMSO, London 1993.
2. Das, P.C. (1993) Examination of masonry arch assessment methods. *Symposium on Structural preservation of the architectural heritage*. IABSE, Rome, 1993.
3. Hendry, A.W., Davies, S.R., Royles, R. & Ponniah, Load test to collapse on a masonry arch at Bargower, Strathclyde, *TRRL Contractor Report No. 26*, Crowthorne, 1986.
4. Fairfield, C.A. & Ponniah, D.A. Geotechnical considerations in arch bridge assessment, *J. Instn Highways & Transportation*, 40, No. 7, 1993, 11-15.
5. Das, P.C., Davidson N.C. & Colla, C. (1995) "Potential applications of NDT Methods for Bridge Assessment and Monitoring", *I.Struct.E. Seminar*, April '95, London.

6. Goodman, D. and Nishimura, Y. (1992) 2-D synthetic radargrams for archaeological investigation. in *4th International Conference on Ground Penetrating Radar*. 1992: Finland Geol. Sur.
7. Goodman, D. and Nishimura, Y., (1993) A ground-radar view of Japanese burial mounds. *Antiquity*, 1993. **255** (67): 349-354.
8. Davis, J. L. and Annan, A. P., Ground- penetrating radar for high-resolution mapping of soil and rock stratigraphy. *Geophysical Prospecting*, 1989. **37** (5): 531-551.
9. Goodman, D., Ground penetrating radar simulation in engineering and archaeology. *Geophysics*, 1994. **59** (2): 224-232.
10. Ulriksen, P.(1982) *Application of impulse radar to civil engineering*, PhD thesis, Department of Engineering Geology, 1982, Lund University of Technology: Lund. p. 175.
11. Daniels, J.(1988) Locating caves, tunnels and mines. *The leading edge*, 1988. 7(3): 32-37.
12. Padaratz, I.J. & Forde, M.C. (1995) A theoretical evaluation of impulse radar wave propagation through concrete, *J. Non-destructive Testing & Evaluation*, **12**, 9-32.
13. Topp, G. C., Davis, J. L., and Annan, A. P.(1980) Electromagnetic determination of soil water content: measurements in coaxial transmission lines. *Water Resources Research*, 1980. **16**(3): 574-582.
14. Smith-Rose, R. L.(1934) Electrical measurements on soil with alternating currents. Proc. IEE, 1934. **75**: p. 221-237.
15. Greaves, J. G., *et al.* (1996) Velocity variations and water content estimated from multi-offset, ground-penetrating radar. *Geophysics*, 1996. **61**(3): p. 683-695.
16. Baronio, G., Binda, L., et al., (1995). Degrado dei monumenti milanesi e interventi di conservazione delle superfici esterne. in *Conf. Milano restaura il monumento e il suo doppio*. 1995.

Proceedings

Evaluation and Strengthening of Existing Masonry Structures

Proceedings of the Joint International Workshop proposed by RILEM TC 127-MS and CIB W23

12 INVESTIGATION OF A STONE MASONRY BRIDGE USING ELECTROMAGNETICS

C. COLLA*, D. McCANN**, P. DAS***, M. C. FORDE*
* University of Edinburgh, Edinburgh, United Kingdom
** British Geological Survey, Nottingham, United Kingdom
*** Highways Agency, London, United Kingdom

Keywords: *Bridge, Electromagnetics, Masonry, Radar, Sonics, Tomography*

Masonry arch bridge assessment is overviewed strategically. It is proposed that where a bridge fails the load carrying capacity assessment by a small margin, and it looks to be in good condition, that further investigation be undertaken using NDT techniques.

NDT techniques: radar, sonic and conductivity methods are reviewed and the results from sonic and conductivity NDT surveys are discussed. It was concluded that these techniques are effective and that tomographic plots aid interpretation of data. The conductivity technique has demonstrated the ability to be a rapid, low cost, non-contacting technique from which tomographic cross-sections, inhomogeneity identification, moisture movement detection over time and layering within the masonry can be achieved.

1. INTRODUCTION

Masonry arch bridges form a large proportion of the bridge stock in the United Kingdom and this will continue to be the case for a long time to come, since the vast majority of these bridges are still in perfectly serviceable condition. This means that periodic assessment of their load carrying capacity will remain an essential part of the bridge authorities' management activities for the foreseeable future. The outcome of these assessments can be very significant in terms of resulting financial and logistical burdens for the authorities. It is therefore in their interest to seek, wherever possible, improvements in the methods of assessment.

The UK Department of Transport/Highways Agency and other bridge authorities have sponsored major research projects in recent years to develop numerical methods for predicting the collapse strength of masonry arch bridges. A number of newly developed methods were then tested against the results obtained from full-scale tests. A comparative summary of the findings were given in BA 16/93 [1], and also by Das [2]. The overall lessons learnt from the developments so far can be summarised as follows.

2. UK LARGE SCALE MASONRY ARCH BRIDGE RESEARCH PROGRAMME

Idealistically, the structural system of an arch bridge, composed of a number of elements: i.e. the foundations, the barrel and the surrounding fill, can be conveniently analysed using advanced numerical methods of analysis, such as the finite element method. However, in practice, the accuracy of the results becomes questionable due to a multitude of complexities:-

(i) Computational expediency often means that the analyses are carried out with simplified methods, e.g. the 2-D analysis, or the mechanism method. These methods by necessity bring in added approximations which make the structural idealisation somewhat remote from reality.

(ii) Soil structure interaction is a major problem in analysing the behaviour of even new structures; for these old bridges involving surrounding materials of unknown properties, this becomes a major problem. For anything but the flattest masonry arches, soil arching and support characteristics significantly influence the load carrying capacity. For all sophisticated assessment methods, the soil resistance parameters have to be input, and the estimation of these values is very approximate.

(iii) Since most of the arch bridges do not usually have any reliable records of construction or repair details, it is difficult to determine the physical dimensions of the main structural elements, or the presence or otherwise of additional features such as the haunching at supports, saddling over the barrel or internal spandrel walls and ribs. Many unsuspected examples of such features, including voids that have been subsequently filled, have come to light following demolition - Fig. 1. Because of the difficulty in identifying these features, idealisation of old arch bridges can never be fully satisfactory.

(iv) Generally, the quality of the structural materials and condition of the structural elements cannot be determined or idealised with any precision.

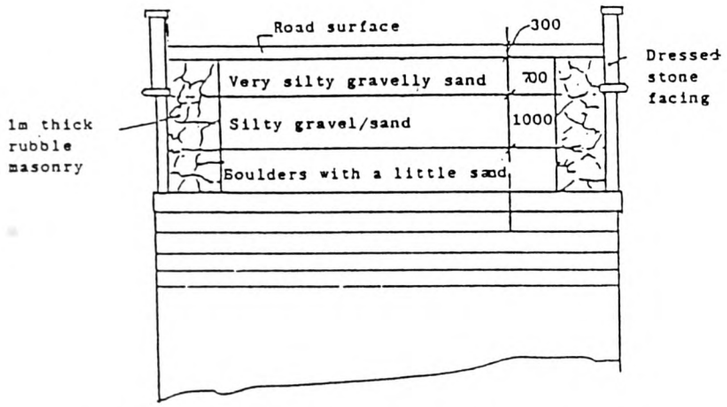

Fig. 1 Section of bridge revealed on demolition

In the presence of the factors referred to above, the computational precision of the analytical assessment methods largely becomes immaterial. The results from these programs cannot be relied upon to give a black and white indication of the capacity of a bridge, since these analyses are dependent upon the input data such as those relating to the soil parameters which cannot be determined with any precision or consistency.

3. FUTURE RATIONAL BRIDGE ASSESSMENT

Experience is showing that results from any calculation based arch assessment method may have to be viewed as giving only a qualitative assessment of capacity, and in order to decide on the appropriate action, one may have to rely on additional, perhaps qualitative,

information obtained by other means. Thus, if an arch bridge fails assessment by a small margin, and it is not showing any significant deterioration, and it is suspected that additional structural features such as internal ribs are present within the fill, it may be reasonable to consider the bridge to be satisfactory for the time being. In such situations, NDT methods such as radar, sonic, vibration and/or conductivity techniques may provide a relatively quick and inexpensive means for making a qualitative judgement on the likelihood of a bridge having any additional reserves of strength.

4. NDT METHODS FOR MASONRY ARCH BRIDGES

Three NDT methods were investigated during the work reported in this paper - radar, sonic and conductivity.

4.1 Impulse radar

Impulse radar testing is starting to be used in the evaluation of masonry arch bridges and has advantages over other techniques in certain circumstances, but very real problems can exist with regard to the interpretation of radar data. Where multiple changes in interface between dielectric layers take place, the change of dielectric constant will be identified but the resolution of the final target layer may prove particularly elusive. An example would be when the objective of a radar survey on a stone masonry arch bridge is to identify hidden geometry and characteristics of the soil fill with precision. Such an investigation would have to proceed through the various layers of material and if the soil fill is heterogeneous the problem is compounded to the extent that the data may be uninterpretable.

The phenomenon may be accentuated if the dielectric constants of the materials present on site are calculated to be significantly higher than might be expected from published literature [3]. Preliminary investigation of these factors has produced very interesting data - as explained below.

4.2 Impulse Sonics

Time domain impulse sonics were undertaken by measuring the time taken by an impulse from a modally tuned instrumented hammer to transmit through the structure. The data was recorded on a 100 kHz digital oscilloscope. Sonic tomographic plots were constructed using the first arriving wave energy transmitted through the abutment, from a number of sources and picked up by the receivers (in Fig 2 an over-simplification is shown as the ray paths will not be in straight lines in reality as the waves tend to travel through high velocity areas). An image is built up by interpolating the travel time of single ray paths by an iterative process. Sonic velocities through the various materials encountered are mapped in a cross-sectional representation where the velocities are related to material densities so revealing indication of location of structural defects and boundaries between different media.

4.3 Conductivity Surveys

Originally developed for geophysical mapping, then for archaeological and agricultural surveys, conductivity is a novel application in the civil engineering field.

Conductivity is a technique which makes use of the response of the ground to the propagation of electromagnetic fields generated through the transmitting coil. The response

fields, picked up by a receiving coil, differ both in phase and amplitude from the transmitted ones. These differences reveal the presence of the conductor and provide information on its geometry and electrical properties. The induction of current flow results from the magnetic components of the EM field, consequently there is no need for physical contact with the surface.

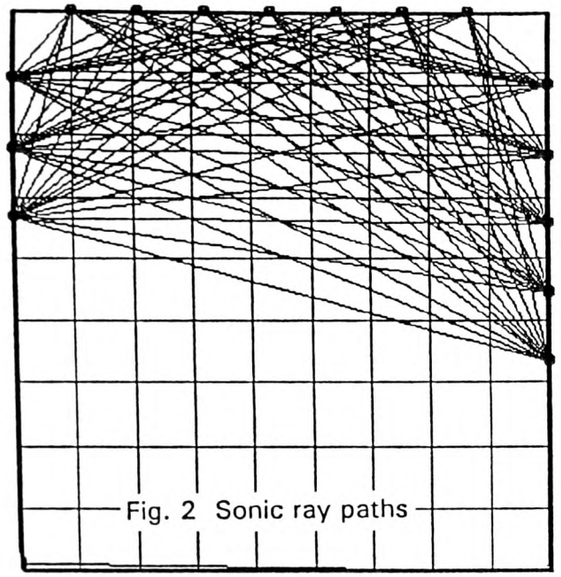

Fig. 2 Sonic ray paths

RAY PATHS: MIDDLETON BRIDGE

Level 2 meters (April '95)

The measured field is generally a complex function of the coil spacing "s" of the conductivity meter, the operating frequency "f" and the conductivity distribution of the subsurface "σ". Penetration depth depends upon "s" but is independent from the conductivity distribution of the subsurface. [3][4]. Penetration also depends on the frequency used and the lower the frequency, the deeper the penetration but the poorer the resolution - as amplitude decreases exponentially with depth [3][5].

5. FIELD WORK

Non-destructive investigation surveys were undertaken on one abutment of an historical stone masonry structure which was known to present the problems described above [6] - Fig. 3. North Middleton Bridge is located in Lothian, Scotland, and the thickness of the abutment investigated is just over 8 m.

5.1 Radar Survey

The preliminary findings from the radar survey indicate values of the di-electric constant within the bridge which are significantly different from published data. The average value for the di-electric constant (ε) for the composite bridge construction [masonry/soil fill/masonry] was computed to be

$\varepsilon = 56$.

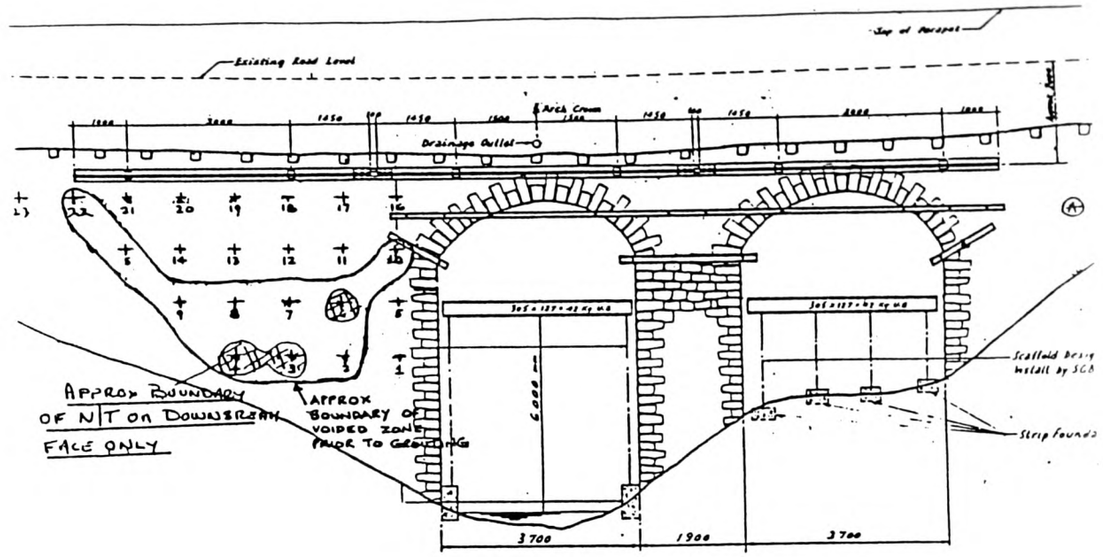

Fig. 3 Elevation of North Middleton Bridge

5.2 Sonic Tomographic Survey

A sonic tomographic model was constructed, using the simplifying assumption of straight ray paths. Then, starting from a uniform average velocity distribution and subsequently refining the image by inputting known properties and conditions of the structure, a cross sectional image is obtained - Fig. 4. Values between medium to low range are located towards the centre of the plot, indicating backfill materials. High velocity areas are distributed along the three sides of the abutment and relate
to the position of the masonry walls; within this region, a further delimitation of zones with the highest velocities corresponds to grouted zones. By applying constraints to the model and re-

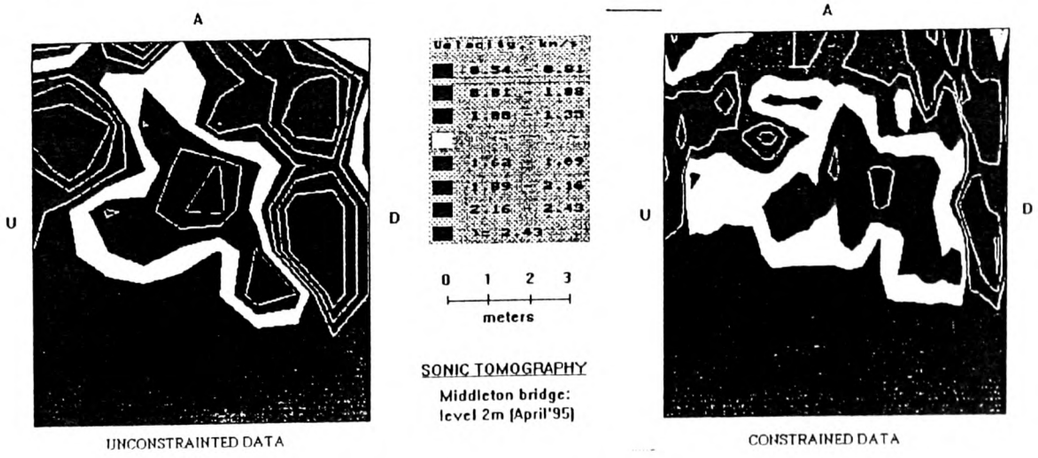

Fig. 4 Sonic tomographic model

iterating, masonry thickness on the down stream side was comparable with the one determined from the conductivity survey detailed below.

5.3 Conductivity Survey

In the structure investigated here, the digital conductivity meter has intercoil spacing of 1m and provides a maximum depth of exploration of 1.5 m in vertical dipole mode operating at a frequency of 14.6 kHz. The meter was used on both the upstream and downstream sides of this 2-span bridge and on the wall beneath the main vault. The measurement stations followed a grid marked on the walls, in an area well clear of any evident metallic objects (drains, reinforcing beams). For maximum accuracy and good spatial resolution, measurements were overlapped to have readings every half a metre. Contacting and non-contacting conductivity measurements were taken, to obtain data at different depths. Data were collected using a digital data recorder and later transferred to a P.C. The results were plotted to produce contour maps of the conductivity distribution. Figure. 5 is a cross-sectional representation with the data iterated through tomographic software.

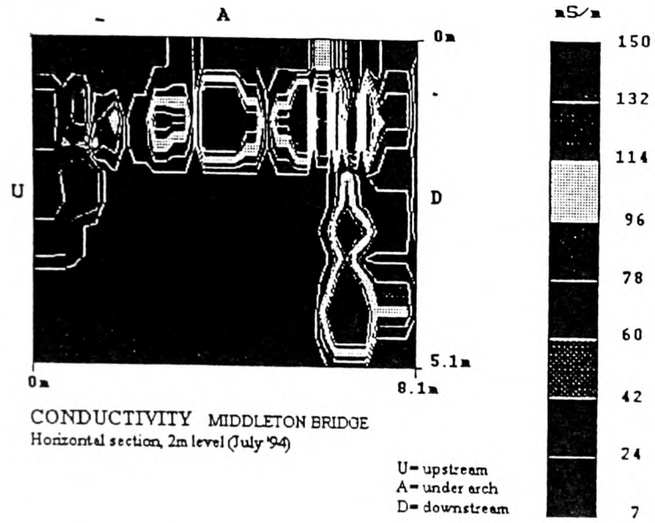

Fig. 5 Conductivity tomographic model

The values obtained are in a high and very wide range indicating heterogeneity in soil filling in the abutment, made of rock such as argillites, wet clays or alluvium and sand; or variations in moisture content/salinity [8].

Rock Type	Conductivity (mS/m)
Argillites	1-80
Conglomerates	0.2-2
Sandstones	1 - 6.4 x 10^{-5}
Unconsolidated wet clay	200
Clays	10-1000
Alluvium and sands	80-100

Conductivity is controlled by one or more of the following parameters: (1) clay content, (2) moisture, (3) salinity - the most complex is usually the moisture profile. Measurements on a soil sample [9] as a function of moisture content, showed that conductivity increases approximately as the square of moisture content.

The bridge investigated was a structure with moisture-drainage problems and attempts had been made in the past to alleviate the problem but with limited success. In this context, both dielectric constant and conductivity increase with water content. The presence of salts in pore water - mainly coming from routine winter road maintenance - will increase the conductivity even further, without affecting proportionally the dielectric constant.

Surveys were repeated over a period of months and differences were noticed, in particular behind the wall under the vault. Comparison of results from data taken at 1m depth lead to the hypothesis that a significant moisture/water movement is taking place at the rear face of that wall with concern about the possible loss of the fine part of the filling; this hypothesis was reinforced by the low velocity values obtained from sonic tomography.

Conductivity data have also been plotted to obtain a horizontal cross-section of the abutment. Clear differences in the values are visible between the upstream and downstream wall situation, with values being on the bottom end of the range in the upstream side and showing medium to high range values on the downstream side. This finding clearly had something to do with the inner construction of the bridge and could not be explained just by asymmetrical water distribution in the structure.

Subsequent endoscopic investigation into the structure has confirmed the hypothesis and revealed that hollow compartments were built into the bridge and that some of them have been partially or totally filled by grout injection during earlier strengthening and reinforcing operations.
Findings from the survey have shown that the upstream side is dry because the void behind the wall is not grout filled, while in the downstream case, water moves from backfill to grout to external wall.
A similar situation may pertain on the abutment.

The downstream conductivity distribution, yields the hypothesis that the wall is not solid stone masonry but may be layered within itself. Later confirmed by visual and endoscopic inspection, the wall is stone-rubble-stone.

6. FUTURE WORK

- Coring is planned to be carried out in the next few months, to verify the internal construction.
- Custom equipment for determining conductivity at variable depth is to be developed.
- Full scale field and laboratory calibrations will be undertaken

7. CONCLUSIONS

The NDT methods used in this project have demonstrated the ability to be rapid, low cost,

techniques from which tomographic cross-sections, inhomogeneity identification, moisture movement detection over time and layering within the masonry can be detected.

8. ACKNOWLEDGEMENTS

The first author gratefully acknowledges the financial support of the EPSRC and the Highways Agency, London. The authors acknowledge the facilities of the University of Edinburgh; access to Middleton Bridge by Lothian Regional Council and scaffolding provided by A. J. Batchelor of Holequest Ltd.

9. REFERENCES

[1] BA 16/93. (1993) The assessment of highway bridges and structures. HMSO, London 1993.

[2] Das, P.C. (1993) Examination of masonry arch assessment methods. *Symp on Structural preservation of the architectural heritage*. IABSE, Rome, 1993.

[3] Kearey, P. & Brooks, M. (1991) "*An Introduction to Geophysical Exploration*", Oxford, 1991.

[4] Das, P.C., Davidson N.C. & Colla, C. (1995) "Potential applications of NDT Methods for Bridge Assessment and Monitoring", presented at "Analysis and testing of bridges" *I.Struct.E. Seminar*, 26 April 1995, London.

[5] Milsom, J. (1989) "*Field Geophysics*", Geological Society of London Handbook, 1989.

[6] Forde, MC., Birjandi, F.K. & Batchelor, A.J. (1985) Fault detection in stone masonry bridges by non-destructive testing, *Proc. 2nd Int. Conf. Structural Faults & Repair-85*, Engineering Technics Press, Edinburgh, 373-379.

[7] McNeill, J.D. (1980) "*Electrical Conductivity of Soils and Rocks*", Technical Note TN-5,, Geonics Ltd., October 1980.

[8] Telford W.M. et al, (1976) "*Applied Geophysics*", Ch. 5, Cambridge University Press, N.Y.

[9] Smith-Rose, R.L. (1934) "Electrical Measurements on Soil with Alternating Currents", *Proc. IEE* No. 75, 221-237.

Fig. 1 Section of bridge revealed on demolition

Fig. 2 Sonic ray paths

Fig. 3 Elevation of North Middleton Bridge

Fig. 4 Sonic tomographic model

Fig. 5 Conductivity tomographic model

C.C.

STRUCTURAL FAULTS + REPAIR – 97

Proceedings of the Seventh International Conference on Structural Faults and Repair 1997

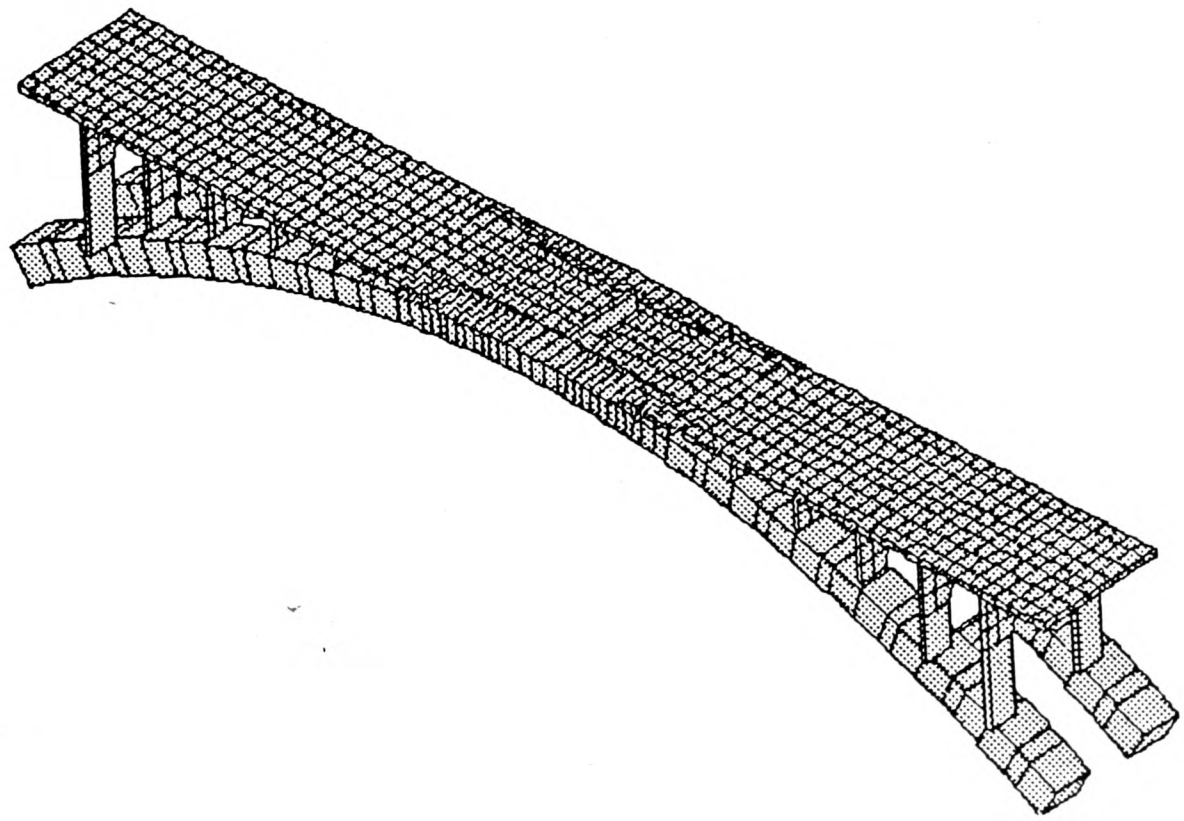

'EXTENDING THE LIFE OF BRIDGES'

Volume 1

RADAR TOMOGRAPHY OF MASONRY ARCH BRIDGES

C Colla, Prof DM McCann & Prof MC Forde
University of Edinburgh
Dept of Civil & Environmental Engineering
The Kings Buildings
Edinburgh EH9 3JL
Scotland, UK

Dr PC Das
The Highways Agency
Bridges Engineering Division
St. Christopher House
Southwark Street
London SE1 0TE, UK

AJ Batchelor
Holequest Ltd
Winston Road
Galashiels
Selkirkshire
Scotland, UK

KEYWORDS: Masonry, bridge, radar, tomography, transmission, reflection, velocity, dielectric constant, stone, fill, brick

ABSTRACT

Digital impulse radar surveys were undertaken on two stone masonry arch bridges: a single span low rise arch and a twin span arch. It was found that on highly attenuated arch bridge fill, conventional impulse radar reflection surveys proved ineffective. In the cases examined transmission radar surveys proved more effective. The second aspect of the work involved using tomographic imaging based on fuzzy logic to gain greater insight into the structure. It was found that three-sided tomography (i.e. upstream-wing-wall/abutment/downstream-wing-wall or upstream-spandrel-wall/arch-intrados/downstream-spandrel-wall) would give better coverage of the sections investigated and better reconstructed image resolution. The greater the angle of the ray paths connecting the radar transmitting antenna and the receiving antenna improved the defect location by enhancing the "time-depth" of any anomaly present. Variations in the composite fill of arch bridges were discussed in relation to the general equation of electromagnetic wave velocity taking account of conductivity and frequency effects.

RADAR TOMOGRAPHY

Tomography measurements aim to localise the presence of defects and inhomogeneities by indirectly mapping the variation of the dielectric constant in the materials investigated or the signal attenuation due to the dielectric properties of the materials crossed and the number of interfaces encountered. This is obtained by plotting the distribution of EM velocity or the amplitude of the received signal.

The tomographic technique involves the use of a transmitter and a receiver positioned on opposite sides of the structure and moved in a series of possible combinations to obtain time domain maps of the same cross section of the structure. From the elaboration of these scans, local variations of dielectric constant may be identified and related to engineering features/defects of the structure.

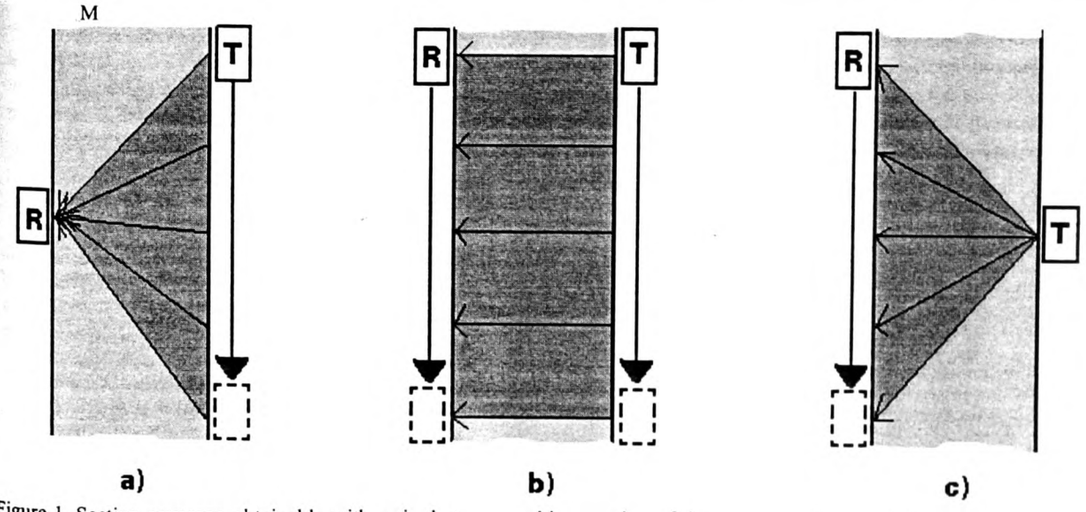

Figure 1. Section coverage obtainable with a single tomographic scanning of the structure: a) transmitting antenna (T) scans while receiver (R) is stationary; b) both antennae move in parallel; c) stationary transmitter and mobile receiver.

Fig. 1 shows the section coverage obtainable with a single tomographic scan of the structure. The situation depicted in (a) is the most widely used in radar tomography and the most recommendable since the angle of the paths connecting transmitter and receiver gives rise to better location and resolution of anomalies at the inversion imaging stage. Usually the survey with this antennae configuration is repeated a number of times with the receiver moving in discrete steps along the same direction

of movement as the transmitter. The survey stops when a satisfactory coverage of the section area has been achieved. Ideally a combination of surveys (a) and (b) should be performed. Case (b) gives a complete cover of the section area, however because of the direction of direct propagation of the 'first arriving' signal the data obtained will locate the presence of the anomaly but will not resolve its time/depth position. The consequence of this is poor vertical resolution. The problem is made more challenging by the shifting of the zero position of the radar signal along the time axis when the antenna is coupled to the material (and because of imperfect radar systems). This instability of the zero time will affect tomography readings especially and parallel readings as in situation (b) in particular. Better results are obtained when combinations of case (b) with (a) or (c) are used.

Just as in sonic tomography (Colla, McCann, Das & Forde, 1996), radar tomography is undertaken by measuring the time taken by an impulse to transmit through the structure. However sonic waves will tend to travel through the denser material - although the path is rarely straight because of the inhomogeneities present. In contrast the electro-magnetic (EM) radar signal travels through straight lines and its velocity will be higher when travelling across highly porous dry materials, with the highest velocity registered when travelling in air (0.3 m/ns). The radar plots will register shorter arrival times of the received signal when the wave has travelled at higher speed through an air filled void (Fig.2). Time variations associated with significant voids will be sudden but variations of the order of 10 or 20 % may indicate scattering (McCavitt & Forde, 1991) or clutter problems (Annan, 1995). At the same time, the dielectric properties of the materials in the structure will have affected the wave energy and the received signal amplitude will be modified. Both arrival times and signal amplitudes of the single ray paths can be used as input parameters in the tomographic inversion. An image is built up by an iterative process, where velocities through the various materials or signal magnitude are mapped in a cross-sectional representation related to material properties (primarily dielectric constant and conductivity). Voids, defects and other features may be located in this way. One of the advantages of using radar for tomography is the possibility of continuous data reading which makes the survey much faster than when performing conventional sonic tomography. For the same reason, continuous movement of the antenna is recommended and preferably over stepped movements when conducting parallel tomography (Fig. 1b).

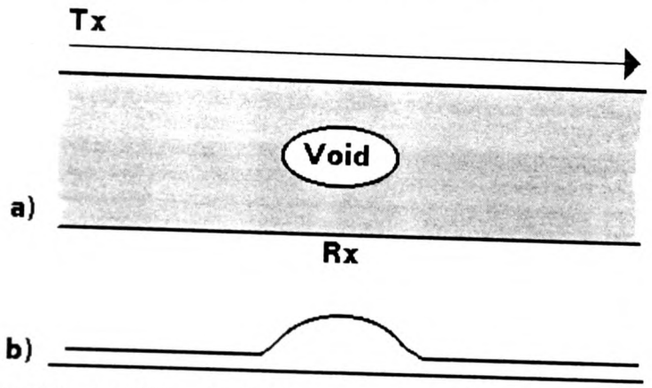

Figure 2. Representation of arrival time: shorter time in correspondence of the air void.

MIDDLETON BRIDGE

North Middleton Bridge, Lothian, Scotland is a twin arch stone masonry bridge (Fig. 3). Each arch spans 3.7m and the width of the bridge is just over 8 m. This particular structure has been investigated over nearly fifteen years by the University of Edinburgh using various NDT techniques (Forde & Batchelor, 1984; Forde, Komeyli-Birjandi & Batchelor, 1985). Radar antennae in the range from 100 MHz to 1 GHz centre frequency were used for the investigation of this structure, and they were used with different objectives and in different configurations.

In general high frequency antennae give good spatial resolution but give only shallow penetration as the signal becomes rapidly attenuated and may suffer from clutter (Padaratz & Forde, 1995a & 1995b). In this project, higher frequency antennae were used for the identification of masonry wall thickness and near-surface voids /defects. Lower frequency antennae are better suited to penetrate deeper into the abutment as they emit more powerful signals, but their long wave length is a detriment to spatial resolution. Also, targets of "small dimensions" or "small thicknesses" can be missed.

In the case of this structure, its significant width (over 8 metres) and the dielectric properties of the filling materials did not permit the use of even the lowest frequency antenna in a reflection mode, to scan the whole bridge section from upstream to downstream side. Operating the equipment in this mode, the radar signal has to travel twice the distance from the antenna to the target. Signals are propagated into the structure and their reflections at different interfaces are picked up by a receiving device located - in the same or different antenna - on the same side of the structure.

In view of the above, radar tomography was carried out by using two 100 MHz antennae positioned on opposite sides of the bridge. The transmitter, on the downstream east wing wall was moved along the white dashed line shown in Fig. 3a, whilst the receiver was stationary, at the same level, on the upstream wing wall. The survey was repeated a number of times with the same movement procedure for the transmitter, whilst the receiver moved along in 1m steps to obtain an adequate coverage of the bridge section. Due to the slope of the river bank on the upstream side, movement of the receiver was limited.

This antennae configuration, maintaining one antenna stationary whilst the other is moved, offers the advantage that more accurate readings can be recorded. In fact, only the movement of one antenna needs to be controlled and its position can be monitored accurately by marking the radar plots at regular intervals of distance travelled by the transmitter or by attaching a survey wheel to the moving antenna. In the case of Fig. 1b, both antennae need to be dragged at exactly the same velocity to maintain them in a constant facing position so that accurate measurements of the travel time can be recorded.

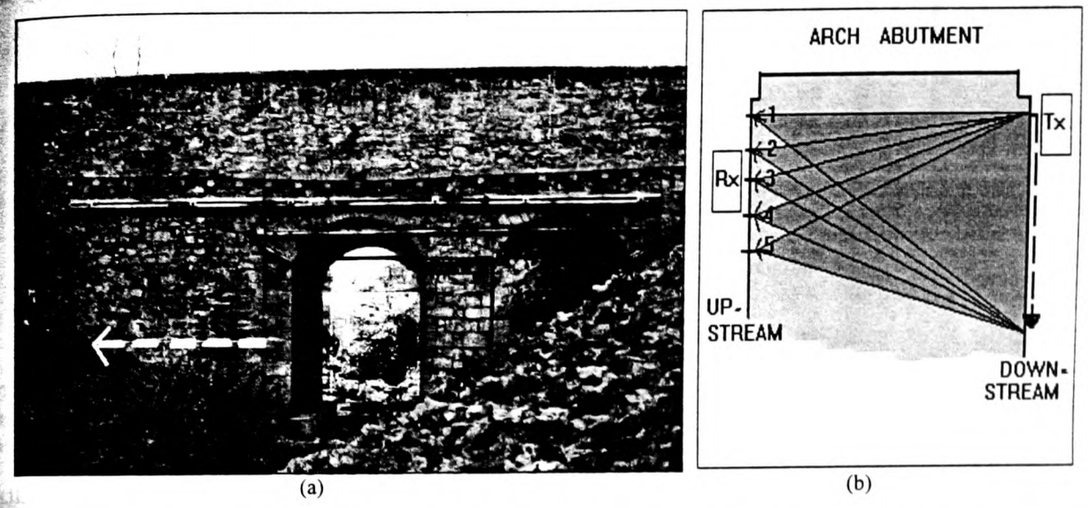

(a) (b)

Figure 3. Middleton North Bridge: downstream view. White dashed line marks position of transmitting antenna and direction of scan (a); horizontal section showing coverage of radar tomography (b).

The radar plots obtained are of the kind shown in Figures 4 & 5, where the first arrival travel times are recorded at the receiver location (upstream). The first finding from this radar survey is a generally low velocity of the EM signal which indicates the values of dielectric constant within the bridge to be significantly different from the values expected for construction or fill materials. The average value for the dielectric constant ε_r for the composite bridge construction [masonry/soil fill/masonry] was computed to be approximately 56. This value is well above reference values published in literature and could be explained by a high moisture content in the fill, due to possible moisture-drainage problems in the bridge.

Previous studies of the same structure and in particular a conductivity survey conducted on the abutment and wing walls (Colla, Das, McCann & Forde, 1995), highlighted such problems as high water content in the bridge materials. Conductivity values obtained were in a very high range indicating soil filling behind the abutment and wing walls comprising materials with high conductivity (argillites, wet clays or alluvium and sand), or high moisture content/salinity. Conductivity is controlled by clay content, moisture and salinity, alone or in combination, but the most complex parameter is usually the moisture profile - with conductivity increasing in the soil approximately as the square of moisture content (Smith-Rose, 1934). In this context, both dielectric constant and conductivity increase with increasing water content. The presence of salts in pore water - from routine winter road maintenance - will increase the conductivity even further, without affecting proportionally the dielectric constant.

Consider now Fig. 4 and the position of the receiver Rx in relation to the transmitter on the downstream side. As the EM waves travel in straight lines the shortest ray paths and corresponding shortest travel times are to be expected when the transmitter reaches the position just opposite the receiver Rx - assuming that the material within the bridge is homogeneous. Similarly the received signal would show the maximum amplitude at this location (its attenuation being minimum there) whilst at longer transmitter/receiver distances the signal would show greater attenuation. In Fig. 4 this is true for the received signals to the right of the Rx position, but not to its left hand side. In Fig. 5 the situation is even more complex: at a transmitter position between 0 and 1 m on the downstream side and a receiver position of 3.5 m on the upstream wall, the shortest travel

with the case of Fig. 4.

If one assumes that the simplified equation for velocity is valid:

$$v = \frac{c}{\sqrt{\varepsilon_r}} \qquad \text{.....(1)}$$

then it can be postulated that the phenomena can be attributed to uneven dielectric constant values cross the bridge section, with materials characterised by lower dielectric constants between 0 and 2.5 m on the wingwall than between 2.5 and 5 m. The attenuation of the received signal seems to follow the same trend seen for the velocity. Since it is particularly noticeable when the receiver is at location 3.5 m, it can be deduced that materials on the right hand side of the wingwall are characterised by higher dielectric constants and also by higher conductivity values.

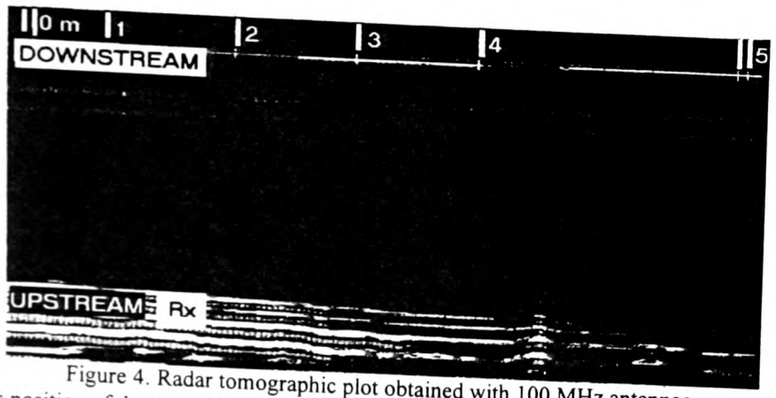

Figure 4. Radar tomographic plot obtained with 100 MHz antennae.
'Rx' marks position of the receiver on upstream side, whilst transmitter moves along downstream side.

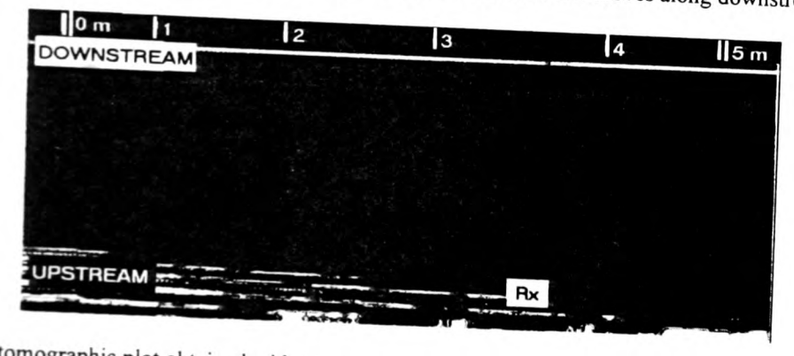

Figure 5. Radar tomographic plot obtained with 100 MHz antennae. 'Rx' moved further along on upstream wing wall.

The above assumptions based upon the simplified equation for EM wave velocity need to be reconsidered if the general equation for EM wave velocity is used:

$$v = \frac{c}{\left[\frac{\varepsilon_r}{2}\left(\sqrt{1+\tan^2\delta}+1\right)\right]^{1/2}} \qquad \text{.....(2)}$$

where c = speed of light
ε_r = dielectric constant (real)
tanδ = loss tangent

The above relationship was plotted graphically by Padaratz & Forde, 1995a. Fig 6 illustrates a parametric analysis of the above equation for a material with ε_r = 56

In this project a 100 MHz antenna was used thus Fig 6 shows that velocity will decrease significantly with any increase in conductivity, as will the amplitude of the signal due to increased attenuation. Thus it is possible that the dielectric constant has not actually changed - rather the reduction in velocity results from the increase in conductivity.

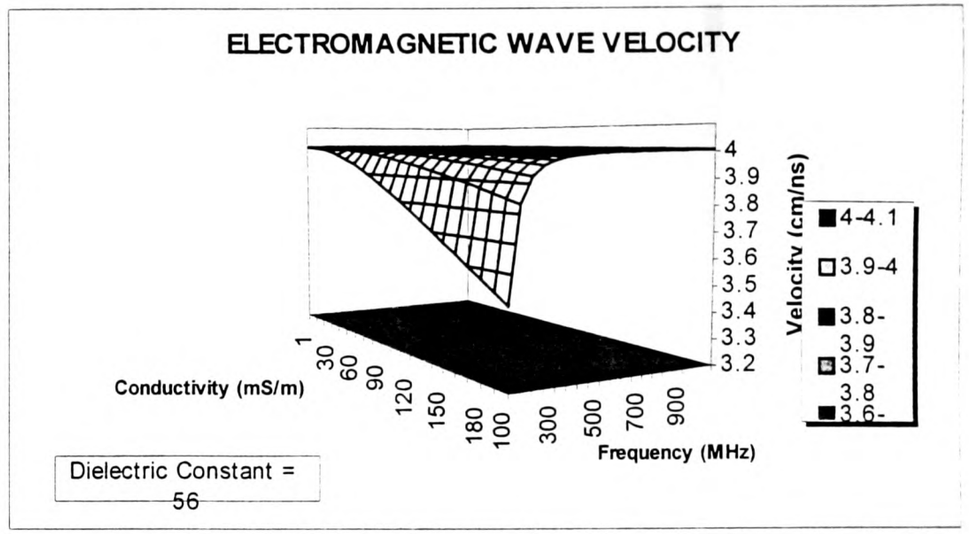

Fig. 6 - EM wave velocity for varying antenna frequency an increasing conductivity.

Given the amount of data which can be recorded during tomographic radar surveys and which need to be processed to obtain tomographic maps of signal velocity and/or attenuation, data are currently handled through a network analyser for input in tomographic inversion and subsequent imaging of the structural composition and defect location.

KILBUCHO BRIDGE

Kilbucho Mill Bridge, near Broughton in the Scottish Borders Region, is a skew stone masonry bridge with a brick arch (Fig. 7). The overall width of the bridge is 5.1 m and the segmental arch spans 3.56 m with a span to rise ratio of 3. The stone parapets are 1.1 m high and 0.3 m thick. The multi-ring brick arch barrel is 0.36 m apparent thickness; and the fill is 0.3 m thick at the crown, including the black-top road surface, giving a total thickness of approx. 0.66 m from the road to the intrados of the arch at the crown.

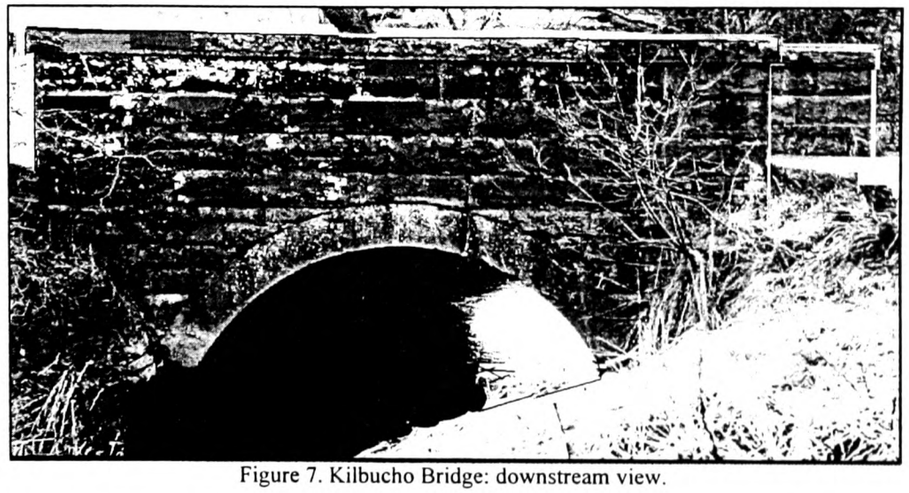

Figure 7. Kilbucho Bridge: downstream view.

Radar surveys were carried out with 100, 500 and 900 MHz antennae, utilised in transmission and/or reflection mode to investigate the nature of the bridge backfill material, the thickness and condition of the stone spandrel walls and the thickness of the brick arch barrel.

A radar scan along the road centre line was first performed with a 100 MHz antenna in reflection mode, to probe the depth of penetration of the signal and to establish a suitable time range that could include the features of interest. The presence of the arch was detected but, as expected, the resolution was not sufficient to determine the shape of the arch nor its thickness or the time-depth to the crown (Fig. 8).

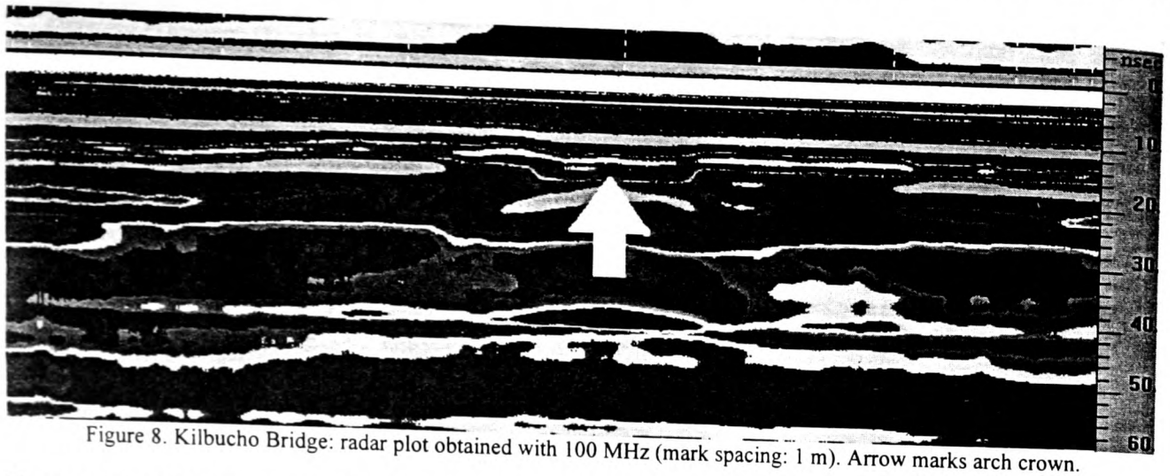

Figure 8. Kilbucho Bridge: radar plot obtained with 100 MHz (mark spacing: 1 m). Arrow marks arch crown.

The use of the 500 MHz antenna (Fig. 9) allowed detection of the difference in the ground between the natural soil at the bridge approaches, and the bridge fill. The latter appear to be of homogeneous consistency in contrast with the layered original soil. Furthermore, the intrados of the arch is visible and the overall velocity through fill plus arch barrel was calculated to be 0.12 m/ns giving a total dielectric constant of the order of 5.9. Multiple reflections from the arch are also visible. The hyperbolic feature above the intrados was interpreted as the extrados of the arch at the crown and, assuming the thickness of the arch to be unchanged through the width of the bridge, velocity and dielectric constant through the fill and the brick arch were calculated as reported in Table 1.

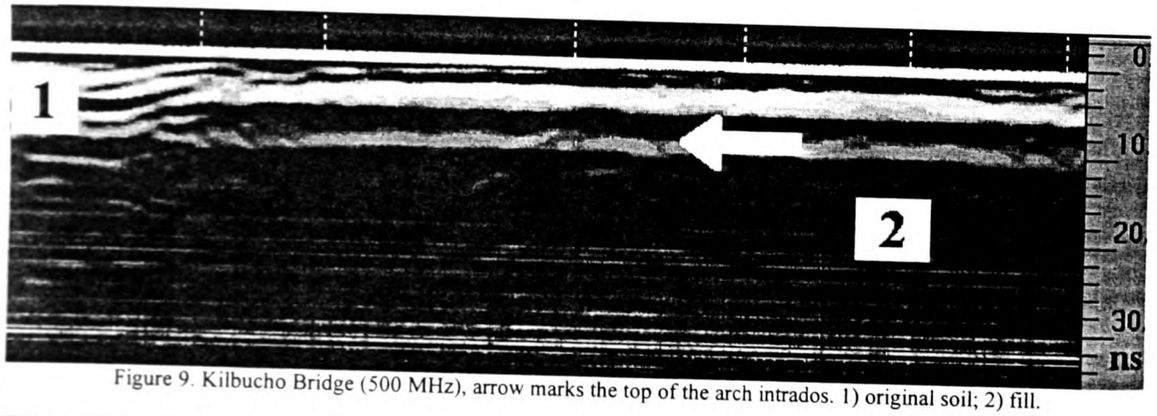

Figure 9. Kilbucho Bridge (500 MHz), arrow marks the top of the arch intrados. 1) original soil; 2) fill.

Frequency (MHz)	Material	Velocity (m/ns)	Dielectric Constant
500	Fill + Arch	0.12	5.9
500	Brick Arch	0.14	4.6
500	Fill	0.09	11

Table 1. Values of velocity and ε calculated via 500 MHz measurements in reflection mode.

Measurements of the stone spandrel wall thickness were obtained with a 900 MHz antenna in reflection mode. A vertical scan was performed on the upstream side of the bridge, starting from the parapet wall and moving downwards (Fig. 10a). The "time thickness" of the stone parapet was first investigated, then data from Fig. 10b were analysed for identification of whether the spandrel wall had increased in thickness.

In the parapet wall, a 2-way travel time of 4.93 ns was measured (Fig. 11a). Due to the small thickness of the parapet wall (0.3 m) and consequent short time distance of the rear face of it from the antenna, the transmitter/receiver separation in the antenna (Padaratz, Hardy & Forde, 1997) was accounted for (Fig. 11b) and a velocity of 0.125 m/ns was calculated. The corresponding dielectric constant value is 5.69. In the spandrel wall a small increase in travel time was registered (t.t. = 5.88 ns) and attributed to a higher moister content. Similarly to the parapet, velocity and dielectric constant were calculated for the spandrel wall: v = 0.105 m/ns and ε_r = 8.1 (Table 2).

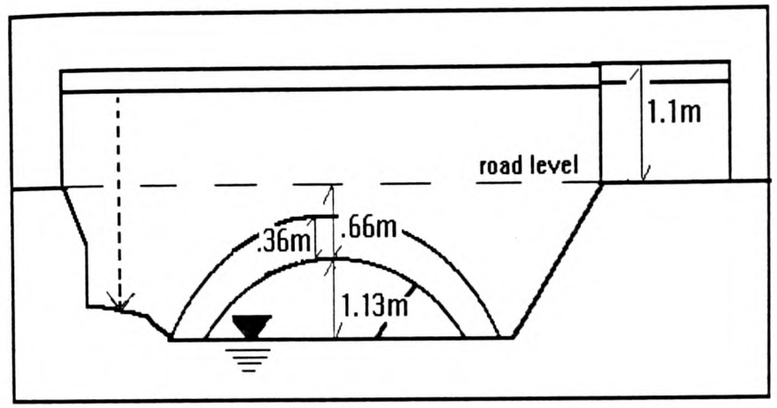

(a)

(b)

Figure 10. Kilbucho Bridge: a) upstream elevation (dotted vertical line marks position and direction of scanning); b) radar vertical section through parapet and spandrel wall.

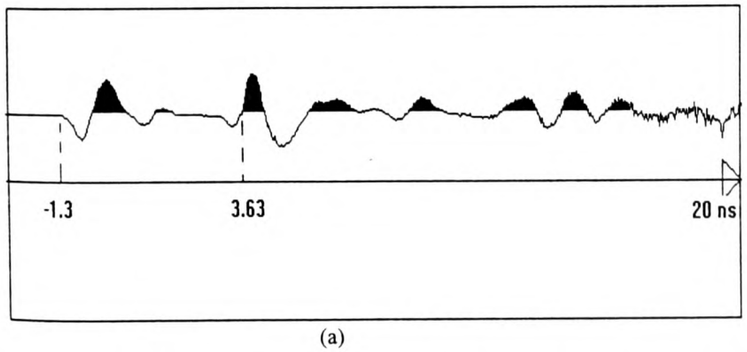

(a)

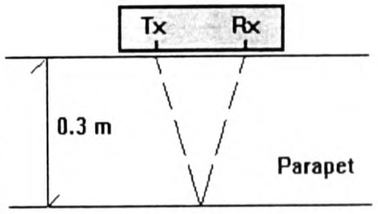

(b)

Figure 11. Measurements of travel time: 2-way travel time in parapet (a); transmitter-receiver separation (b).

Frequency (MHz)	Material	Velocity (m/ns)	Dielectric Constant
900	Stone Parapet	0.125	5.69
900	Stone Spandrel Wall	0.105	8.1

Table 2. Values of velocity and ε calculated via 900 MHz measurements in reflection mode.

In order to determine the overall dielectric constant through the width of the bridge, measurements of the travel time of the electromagnetic wave from the upstream to the downstream spandrel walls were performed by use of two 100 MHz antennae in transmission mode. The received signal was first recorded between the transmitting antenna located at the upstream spandrel wall and the receiving antenna on the downstream spandrel wall, then the measurement was repeated transmitting in

air with the same antenna spacing as before (Fig. 12a). Notice the attenuation of the received signal after travelling through the bridge (Fig. 12b&c) and its delayed arrival time compared with the transmission in air. The measurement through air allows one to determine the zero point on the time axis and by adding the difference in arrival time between the signal in air and through the bridge, with reference to the signal in air, the total time through the bridge fill and spandrel walls can be determined. The corresponding calculated velocity is 0.11 m/ns giving a total dielectric constant for fill + spandrels of ε_r = 6.5. From the above calculation of the dielectric constant through the stone spandrel walls (see Table 2), by difference, as expressed in equation (3) below, the dielectric constant through the fill alone was calculated. The results are reported in Table 3.

$$v_{fill} = \frac{d_{tot} - (d_{sp} \times 2)}{t_{tot} - (t_{sp} \times 2)} \qquad \text{.....(3)}$$

where v_{fill} velocity through fill material, d_{tot} total bridge width,
d_{sp} spandrel wall thickness, t_{tot} travel time through total bridge width,
t_{sp} travel time through spandrel wall.

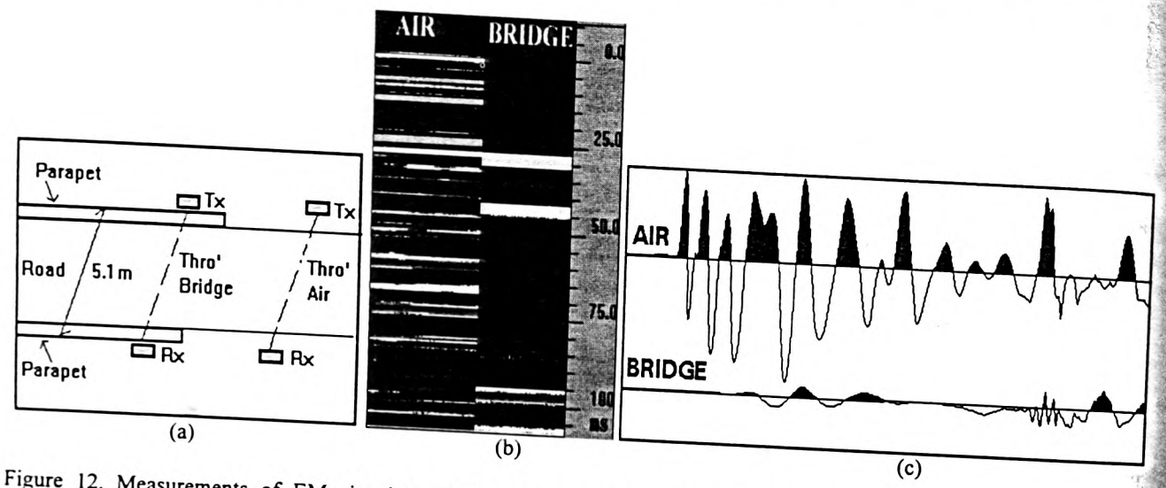

Figure 12. Measurements of EM signal travel time through bridge from spandrel to spandrel: a) sketch of antennae configuration; b) radar plot of received signal in air and through the bridge; c)corresponding signal waveforms.

Frequency (MHz)	Material	Velocity (m/ns)	Dielectric Constant
100	Fill + Spandrels	0.11	6.5
100	Fill	0.14	4.4

Table 3. Values of velocity and ε calculated via 100 MHz antennae operated in transmission mode.

CONCLUSIONS

1. Digital impulse radar surveys were undertaken on two stone masonry arch bridges.
2. On highly attenuated arch bridge fill, conventional reflection surveys proved ineffective.
3. Transmission radar surveys proved more effective on the highly attenuating masonry arch bridges reported herein.
4. Tomographic imaging was used to gain greater insight into the structure.
5. Three-sided tomography (i.e. upstream-wing-wall/abutment/downstream-wing-wall or upstream-spandrel-wall/arch-intrados/downstream-spandrel-wall) would give better coverage of the sections investigated and a better reconstructed image resolution.
6. The greater the angle of the ray paths connecting Tx and Rx would improve the defect location by enhancing the "time-depth" of any anomaly present.
7. Variations in the composite fill of arch bridges were discussed in relation to the general equation of electromagnetic wave velocity taking account of conductivity and frequency effects.

ACKNOWLEDGEMENTS

The authors wish to acknowledge: the financial support of EPSRC and the Highways Agency, London; the facilities made available by the University of Edinburgh; the invaluable technical assistance of K. Broughton; the valuable help of Dr NC Davidson during data collection at Kilbucho Bridge; the provision of scaffolding at Middleton Bridge by Holequest Ltd; permission to take readings at Middleton Bridge granted by Dr G McL Hazel of the City of Edinburgh Council; and permission to take readings at Kilbucho Bridge granted by Mr M Westwater of Scottish Borders Council.

REFERENCES

Annan, AP, (1995), "Personal communication", Sensors & Software Inc, 5 June 1995.

Forde, MC & Batchelor, AJ (1984) Low Frequency NDT testing of historic structures", *Proc. 3rd European Conf on NDT*, Florence, Oct 1984, Vol 3, 316-324.

Forde, MC, Komeyli-Birjandi, F & Batchelor, AJ (1985) Fault detection in stone masonry bridges by non-destructive testing, *Proc. 2nd Int. Conf. Structural Faults & Repair-85*, April 1985, London, Engineering Technics Press, 373-378.

Colla, C, Das, PC, McCann, DM & Forde, MC, (1995), "Investigation of stone masonry bridges using sonics, electromagnetics and impulse radar", *3rd International Symposium on Non-Destructive Testing in Civil Engineering (NDT-CE)*, Berlin, Germany, 26-28 Sept 95, vol. 1, 629-636.

Colla, C, McCann, DC, Das, P, Forde, MC, (1996), "Non contact NDE of masonry structures and bridges", Proc. *3rd Conf Nondestructive Evaluation of Civil Structures and Materials*, Boulder, Colorado, USA, 9-11 September 96, vol. 1, 441-454.

McCavitt, N & Forde, MC (1991) "The application of the method of convolution to the simulation of the response of masonry arch bridges to ground probing radar", *J. Non-destructive Testing & Evaluation*, **6**, No. 3, 1991, 179-194.

Padaratz, IJ & Forde, MC (1995a) A theoretical evaluation of impulse radar wave propagation through concrete, *J. Non-destructive Testing & Evaluation*, **12**, 9-32

Padaratz, IJ & Forde, MC (1995b) Influence of antenna frequency on impulse radar surveys of concrete structures, *Proc. 6th Int. Conf. Structural Faults & Repair-95,* London, July 1995, Vol. 2, Engineering Technics Press, 331-336.

Padaratz, IJ., Hardy, MSA & Forde, MC (1997) Coupling effects of radar antennae on concrete, *Proc 4th Int Conf: NDT-CE*, University of Liverpool, 8-11 April 1997, Vol 1, 237-245

Smith-Rose, RL, (1934), "Electrical measurements on soil with alternating currents", *Proc. IEE* **75**, 221-237.

STRUCTURAL FAULTS & REPAIR – 97

Proceedings of the Seventh International Conference on Structural Faults and Repair 1997

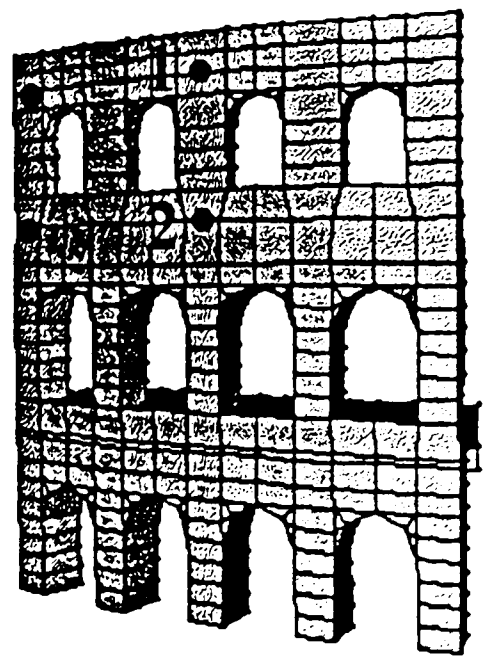

"EXTENDING THE LIFE OF BUILDINGS AND CIVIL STRUCTURES"

Volume 3

RADAR IMAGING IN COMPOSITE MASONRY STRUCTURES

C. Colla, Prof D.M. McCann & Prof M.C. Forde
University of Edinburgh
Dept of Civil & Environmental Engineering
The Kings Buildings
Edinburgh EH9 3JL
Scotland, UK

Dr PC Das
The Highways Agency
Bridges Engineering Division
St. Christopher House
Southwark Street
London SE1 0TE, UK

KEYWORDS: NDE, Radar, Conductivity, Attenuation, Masonry, Bridges, Structures, Composite

ABSTRACT
Masonry arch bridges represent a significant proportion of the UK bridge stock on both the roads and the railways. There are some 40,000 UK masonry arch road bridges and some 30,000 masonry arch rail bridges. If these bridges were taken out of service then both the UK road and rail networks would be completely inoperable.

In order to aid the load carrying capacity analysis of these bridges, a series of NDT techniques have been developed at the University of Edinburgh, primarily focused upon masonry structures. As part of this ongoing programme a laboratory study of radar propagation through masonry has been undertaken. A 2.4 m long x 1 m wide x 1.5 m high experimental test rig was built in the laboratory with brick walls on three sides and a wooden gate on the fourth narrow side.

Radar tests were undertaken using 500, 900 and 1000 MHz bow-tie antennae with the box filled with fresh water and then saline water with different concentrations of sodium chloride. Further test were undertaken with the box filled with dry sand and wet sand. Finally the test rig was modified to simulate a composite masonry structure and tests were performed both on the hollow and sand filled model. The results from this work are reported herein indicating the reliability and ease of identifying various targets.

It was found that radar signals were severely attenuated when the saline concentration exceeded 0.05%. Better results were obtained when the box was filled with dry sand rather than wet sand. In the case of the hollow cellular structure, refraction effects were more evident.

INTRODUCTION

Masonry arch bridges represent a significant proportion of the UK bridge stock on both the roads and the railways. There are some 40,000 UK road bridges and some 30,000 rail bridges. If these bridges were taken out of service then both the UK road and rail networks would be completely inoperable.

There has been considerable work undertaken in order to assess the load carrying capacity of masonry arch bridges (BA 16/93, 1993), (Das, 1993), (Hendry, Davies, Royles & Ponniah, 1986). The general conclusions from this work are that the existing methods of assessment for the masonry arch bridges may at times be too conservative. The work on dynamic load testing of masonry arch bridges at the University of Nottingham has indicated that the dynamic load capacity may be some 70% of the ultimate static load capacity of a masonry arch bridge. In order to undertake effective finite element work, which is being correlated with scale model work undertaken at Edinburgh and Nottingham Universities and also at Bolton Institute of Higher Education, there must be a clear and unambiguous knowledge of the internal construction of the masonry arch bridge. For example the size and shape of the arch is a critical factor as is the size and shape of the springers for the arch. Other key factors include knowledge of whether the bridge is an arch backfilled with soil thus giving load dispersion (Fairfield & Ponniah, 1993), or whether the bridge has a cellular hollow construction (Fig. 1). If the bridge is soil filled, knowledge of the condition of the soil - wet or dry, compact or loose - is also relevant.

Recent work on bridge reliability by the Highways Agency, London, UK (Das, Davidson & Colla, 1995), who are pioneering work within the international community on reliability strategies, clearly indicates that there is an ongoing need to understand the deterioration mechanism of masonry arch bridges. Whilst this work is being addressed the strategy of the bridge community is to assess a structure. If the structure fails the assessment but looks in good order, then the recommendation should not be simply pass/fail - but that of a new category of "monitor".

It is against the above background that the research reported herein was commenced.

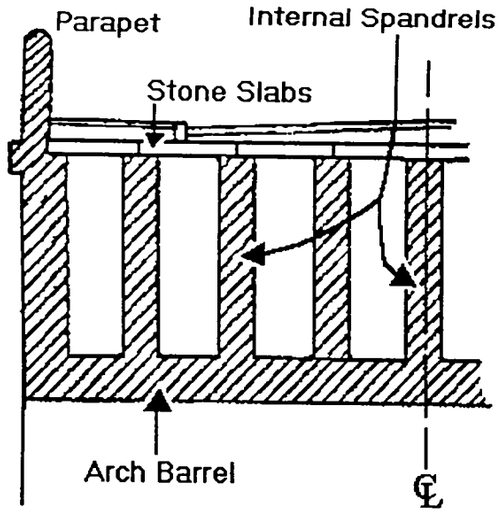

Figure 1. Vertical Section Through Masonry Arch Bridge With Internal Spandrel Walls.

The key areas to be addressed in the sections below are target identification in masonry structures such as bridges. In the case of highway bridges, in the northern climates where snow and ice are predominant, the influence of salt concentration on the effectiveness of NDE techniques is important. The specific non-destructive testing method discussed in this paper is impulse radar.

OBJECTIVES OF RESEARCH

The objectives of the work reported herein are:

- To identify the effectiveness of radar penetration through conductive materials (saline solutions).
- To identify the effectiveness of target localisation and resolution within a soil fill.
- To compare the propagation of radar signals through hollow and backfilled composite structures.

GROUND PENETRATING RADAR

Within the geotechnical community, ground penetrating radar (GPR) is seen as a technique which offers a way of viewing shallow soil and rock conditions. The areas of application for ground penetrating radar are diverse and include groundwater exploration, geotechnical and archaeological investigations, (Goodman & Nishimura, 1992 & 1993), (Davis & Annan, 1989), as well as engineering examples (Forde & McCavitt, 1993), (Cooke, Ashurst, McCavitt & Forde, 1993), (Ulriksen, 1982). Some specific applications, like changes of rock type, soil strata and water table in coarse grained soils, detection of buried walls, pipes, tunnels (Daniels, 1988), have generated an increasing demand for subsurface imaging with higher resolution than previously possible. The effective application of the radar for the high-resolution definition of features (stratigraphy, voids, defects) is a function of the antenna frequency used. The propagation of the radar signal depends on the electromagnetic response of the materials investigated.

GPR offers the possibility of a high resolution sounding capability with detection of features of the order of a few millimetres thickness at ranges of several metres. Ground penetrating radar has demonstrated the capacity to sound to depths of tens of metres in low conductivity (less than 1 $mS.m^{-1}$) materials such as sand, gravel, rock and fresh water. The range decreases to a shallow depth in conductive materials such as clays, silts and soils with saline or contaminated pore water. A numerical experiment on concrete clearly illustrated these points (Padaratz & Forde, 1995).

RADAR PRINCIPLES

Ground-penetrating radar produces short pulses of high frequency (10-1000 MHz) electromagnetic energy which are transmitted into the ground or the structure, depending on the case. The propagation of the radar signal depends on the electrical properties of the materials encountered. The velocity and the attenuation are the factors that describe the propagation of high frequency waves into the materials. These factors depend on the dielectric and conductivity properties of the materials, which also determine the signal power that is reflected at boundaries where the electrical properties vary (Topp et al, 1980), (Smith-Rose, 1934), (Greaves et al, 1996).

The dielectric constant or relative permittivity describes the high frequency electrical properties of the materials since, at these frequencies, the displacement (polarisation) properties dominate the conductive properties for many materials. The complex dielectric constant is given by:

$$\varepsilon^* = \varepsilon' + i\left[\varepsilon'' + \frac{\sigma_{dc}}{\omega\varepsilon_o}\right] \qquad (1)$$

where ε' is the real part of the dielectric constant and the term in bracket is the imaginary or loss part of the dielectric constant. This is separated into high frequency and d.c. conductivity components of the loss, as follows:

ε'' is the frequency-dependent loss associated with the relaxation response phenomena;
σ_{dc} is the d.c. conductivity (S/m);
ω is the angular frequency, $2\pi f$;
ε_0 is the free space permittivity (8.854×10^{-12} F/m).

Radar signal velocities at higher frequencies in low-loss materials may be related to the real part of the dielectric constant by the simplified equation (Padaratz & Forde, 1995):

$$v = \frac{c}{\sqrt{\varepsilon'}} \qquad (2)$$

where $c = 3 \times 10^8$ m/s, the propagation velocity of electromagnetic waves in free space.

Note that dielectric constant in water is 80 and that of most dry geological materials is in the range of 4-8. This large difference explains why the radar signal velocity is strongly dependent on the water content in soils. High water content gives rise to strong radar reflections at interfaces, causing part of the transmitted signal to be reflected. High conductivity causes strong attenuation in the signal. Also the effect of signal scattering by small scale heterogeneities can increase attenuation.

In a low-loss medium, the attenuation is expressed as:

$$\alpha = \frac{1.69x10^3\sigma}{\sqrt{\varepsilon'}} dB/m \qquad (3)$$

where $\sigma = \sigma_{dc} + \omega\,\varepsilon''\,\varepsilon_0$ combines both d.c. conductivity and dielectric losses.

Expressions (2) and (3) are approximate and require that $\sigma/\omega\varepsilon'\varepsilon_0$ is much less than 1.

The reflection and transmission coefficients for GPR signals may be written:

$$R = \frac{\sqrt{\varepsilon'_1} - \sqrt{\varepsilon'_2}}{\sqrt{\varepsilon'_1} + \sqrt{\varepsilon'_2}} \qquad (4)$$

$$T = \frac{2\sqrt{\varepsilon'_1}}{\sqrt{\varepsilon'_1} + \sqrt{\varepsilon'_2}} \qquad (5)$$

where: ε'_1 = dielectric constant of first material,
ε'_2 = dielectric constant of second material.

EXPERIMENTAL TEST RIG

A 2.4 m long x 1 m wide x 1.5 m high experimental test rig was built in the laboratory. Its main part consists of a 3-sided masonry box with the fourth side equipped with a wooden gate to gain easy access to the inside of the test rig and to facilitate any loading and unloading of fill material (Fig. 2). In a later phase of the experimental work, the masonry box was modified by adding a longitudinal partition wall in the middle, and so obtaining a 2-cell masonry structure.

The masonry brickwall was built of Class A Engineering solid bricks and mortar in the proportion 1:¼:3 of cement, lime, sand. The wall is one header thick and its foundations are secured into a slot cut out of a plywood base which also constitutes the base of the rig.

Care was taken in the design phase of the rig to avoid using any metal part which could later interfere with the radar survey during collection of data, leaving unwanted signatures on the radar plots. For the same reason the gate on one of the short

sides of the rig is timber. It was designed so that it could slot into place between the ends of the brick wall and a slot cut in the plywood base, with no need for a metal locking device.

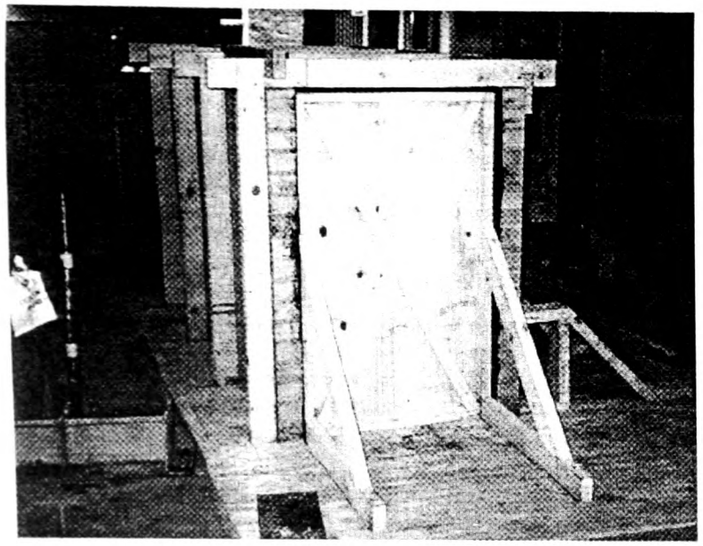

Figure 2. Side view of masonry test rig with wooden gate in the foreground.

In the initial experimental work, the masonry rig was lined with a PVC sheet to create a watertight container for the water which constituted the fill material and to maintain the brickwall in a dry condition. The rig was filled with water up to 1.3 m level and sodium chloride was dissolved into the water to create brine solution in different concentrations. Three different set ups were investigated, with brine in concentrations of 0.05 %, 0.1 % and 0.25 % by weight of salt to the water. Three rebars (Ø 3.5 cm) were immersed in the water and maintained vertical by suspending them from a timber frame which was also built around the rig. The metal rods were located at 10, 40 and 70 cm away from the brickwall along which the radar antenna was dragged for data collection (Fig. 3).

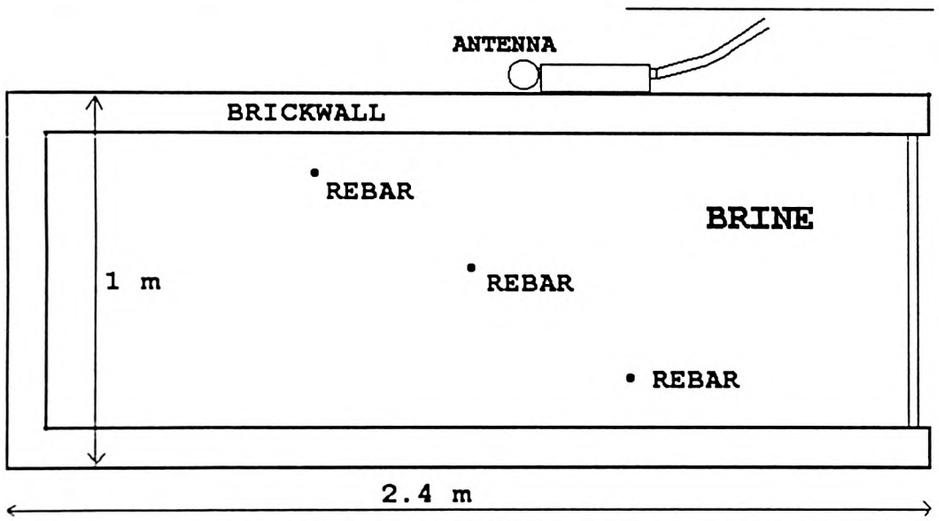

Figure 3. Plan view of experimental rig during initial tests.

For the second phase of the experiment, a partition wall was built longitudinally in the middle of the rig to simulate a composite masonry structure. The cellular structure so obtained presents 2 identical cells, each of width 0.35 m, and separated by a brickwall of the same characteristics as the perimetral brickwall. Tests were conducted both with no fill material present and with fill material in one half of the structure, having filled one of the two cells with dry sand in loose conditions (Fig. 4).

The sand can be described as a medium, uniformly graded silica sand with rounded particles. The particle size distribution (PSD) of the sand indicated that 26.5 % of the particles had a diameter between 1.18 and 1.7 mm, and 68.7 % of the sand has diameter between 1.18 and 0.6 mm. The remaining 4.8 % has Ø < 0.6 mm.

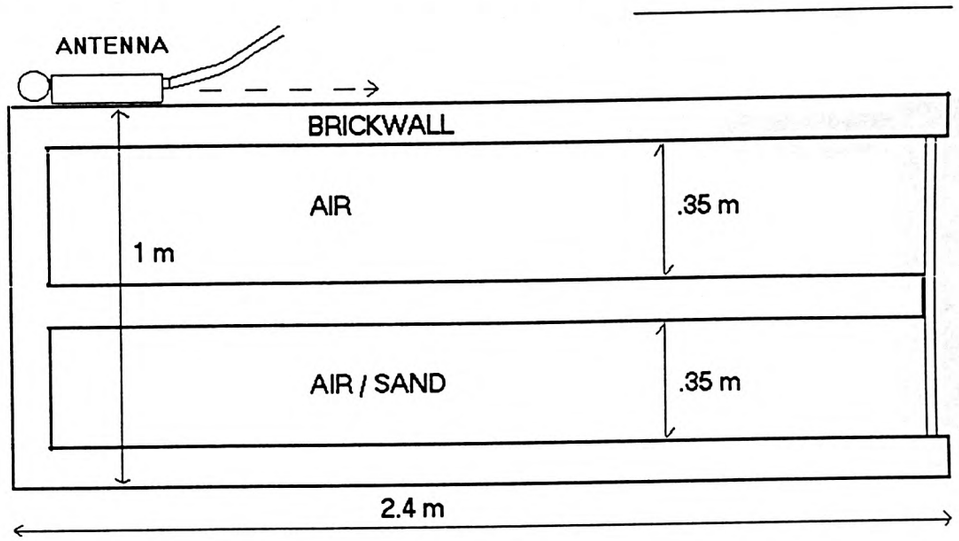

Figure 4. Top view of test rig modelling a composite masonry structure.

RADAR SURVEY

Radar antennae with nominal centre frequency of 500, 900 and 1000 MHz were used to collect reflection data within time ranges of 15 to 60 ns. The antenna was moved along one side of the masonry rig, scanning in the horizontal direction, to plot horizontal cross sections of the structure.

For the case where the set up included brine and re-bars, the radar plots presented here were collected with 900 MHz antenna moved along the 2.4 m brickwall, as can be seen in Fig 2. The antenna had a survey wheel attached to record a constant number of scans per unit distance travelled and to obtain a more accurate and smooth picture of the radar targets. Twenty centimetre marks along the direction of movement of the antenna were recorded at the top of the plots. Reflections from the masonry walls and the metal re-bars were picked up. The survey was repeated for the different salt concentrations in the water.

In the simulation of the composite cellular structure, the radargrams show data collected with 500 and 900 MHz antennae along the 2.4 m wall. Data collected with 1000 MHz antenna on the 1 m long head-wall are also presented and the position of the middle wall was marked at the top of the radar images. Reflections from the masonry walls and effects of side reflections and refractions from the same walls appear on the plots. Tests were repeated for comparison with the situation where sand was present.

DATA ANALYSIS

First Experiment - Brine temperature and conductivity were monitored throughout the different stages of the experiment and values are recorded in Table 1.

Brine temperature	Salt concentration	Conductivity
18 °C	0.05%	735 µS
16.5 °C	0.1%	1147 µS
17 °C	0.25%	Out of range

Table 1. Values of brine temperature, concentration and conductivity measured during the experiment.

The measured radargrams from set-ups with water at different chloride content were compared. The GPR method transmits and receives signals recorded over a spatial window - the antenna aperture. Because of the wide field of view of the radar

antenna, objects off to the side of the antenna can be recorded, resulting in hyperbolic reflection patterns - as in the case of the metal rods. These patterns vary with the frequency used and the electromagnetic properties of the materials under study. In all the cases presented here, the hyperbolas from the rebars show short and flat branches which indicates a decrease of the energy power in the radar waves, probably with loss of the high frequency components of the signal.

In Fig. 5, the brine has a sodium chloride concentration of 0.05 % by weight. The radar waves travelled through a brick masonry wall and 80 cm depth of water to reach the back wall, and encountered three rebars along the way. Reflections from the three rebars are all visible, as is the reflection from the back wall. It is worth noting the great difference between the amplitude of the signature of the front wall and that of the back wall. The dissimilarity shows up in the amplitude of the signal and is due to various factors - primarily the attenuation of the wave. Causes of this attenuation are the variation in electrical properties of the materials at the interface between brick masonry and water. This strong interface causes a large part of the signal to be reflected back, with only a small part of the wave energy capable of travelling through the water and reaching the back wall, the signature of which is very much attenuated compared to that from the front wall. A similar comparison can be made between the hyperbolas of the three rebars.

Another factor that distinguishes microwave radiation is the dispersive nature of the microwave. As a result of the high permittivity of water (typical values of dielectric constant for water are of the order of ε = 80-81) and high conductivity of brine, the signal attenuates quickly; and whilst the reflection from the first re-bar is fully visible, the reflection from the third re-bar is only just noticeable (radar plots are shown in logarithmic grey scale transform which greatly emphasises the low amplitudes).

Fig. 6 shows the case of brine concentration of 0.1% and Fig. 7 shows the experiment with 0.25% chloride concentration. In Fig. 6, the reflection from the back wall has completely disappeared and so has the reflection from the third re-bar. Branches of the hyperbola from the first re-bar are shorter and less pronounced than in the previous case. Reflection from the second re-bar is almost reduced to a flat thin line. In the case of Fig. 7, reflection from the first re-bar is almost reduced to a point: no branches are visible. None of the patterns from other features of the experimental set-up, except for the front wall, are evident.

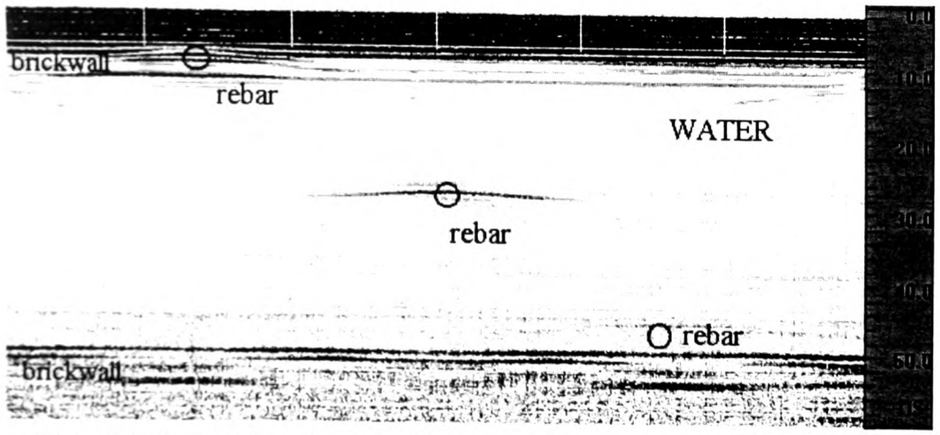

Figure 5. Radargram of test rig with 0.05% salt content in water and rebars at increasing depth.

Following this comparison work, signal waveforms were analysed in the time domain to quantify the reduction of signal power due to the increasing conductivity values with increasing salt concentrations, as per Table 1. The impulse response to the propagation in water with increasing conductivity was estimated from the reflections obtained from the immersed metal rods. The decrease in energy was calculated in relative terms, measuring the amplitude of the corresponding peaks generated at the location of the first re-bar.

Fig. 8 shows edited unfiltered portions of the three waveforms corresponding to the three salt concentration used during the experiment and chosen at the centre of the hyperbolas from the first re-bar. The signal waveforms show the main reflection peaks generated from the re-bar, in the form of a sinusoid between 7 and 10 ns on the time axis. It is this peak which has been used for the calculations of the relative decrease of amplitude. From Fig. 9 and Table 1 it is evident how an increase in conductivity of only 0.4 $mS.m^{-1}$, causes a reduction of 34% in the amplitude of the signal, when passing from 0.05% to 0.1 % salt content in the water. One third of the power of the signal is lost. When the salt content increases to 0.25%, the signal amplitude decreases a further 17%, reaching only 50% of the power of the signal registered at 0.05% salt content. Note that

even though the sodium chloride content doubles from 0.05 to 0.1%, and increases five times to reach 0.25%, the salt concentrations considered in the experiment are low values compared to sea water (3.5% on average) or to localised high concentrations of salt as could be encountered in masonry arch bridges due to de-icing salt (Baronio, Binda et al 1995). The outcome from the amplitude analysis study is an exponential reduction in signal amplitude as the conductivity of the material increases due, in this case, to increasing sodium chloride content From the above discussion and equation (3) it follows that conductivity affects the attenuation of the signal, which in turn governs the penetration capability of the signal.

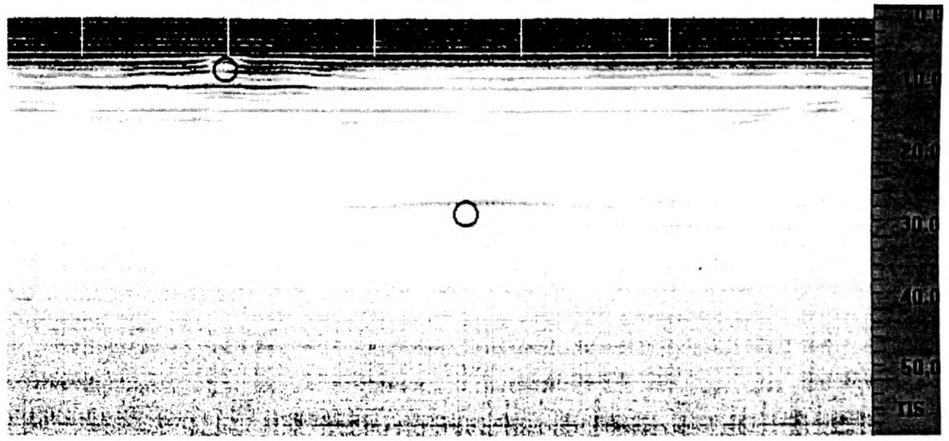

Figure 6. Radargram of test rig with 0.1% salt content in water and only two rebars visible.

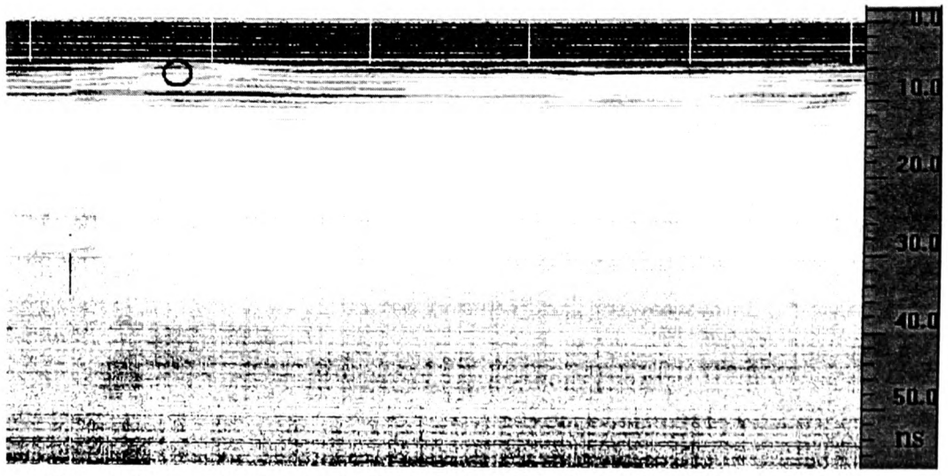

Figure 7. Radar plot of test rig with 0.25% salt content and reflection from first re-bar visible.

To verify and confirm whether the phenomena observed were to be attributed primarily to a variation of the real part of the dielectric constant or to the increased conductivity of the material, a calculation of the dielectric constant of salt water was conducted. First, the velocity of the electromagnetic wave through brine was calculated for the three chloride concentrations. From the known geometrical position of the reflectors in brine (10, 40, 60 cm), and the 2-way travel times from each reflector measured from the radargrams, the pulse velocity was calculated by time domain analysis and found to be constant throughout (see Fig. 10). From the velocity values obtained and equation (2), the dielectric constant of brine at the salt concentrations used in the experiment was calculated and found to be in the narrow range between 80 and 81 which covers the dielectric constant values of sea water and fresh water. The calculation, while agreeing with values published in literature regarding the dielectric constant of salt water (Kraus, 1988), (Von Hippel, 1954), (Nat. Bureau of Standards, 1958), confirms the initial hypothesis of constant dielectric constant at the increase of salt content. In other words, the permittivity controls the speed of the E.M. pulse, whilst increasing conductivity reduces the depth of penetration.

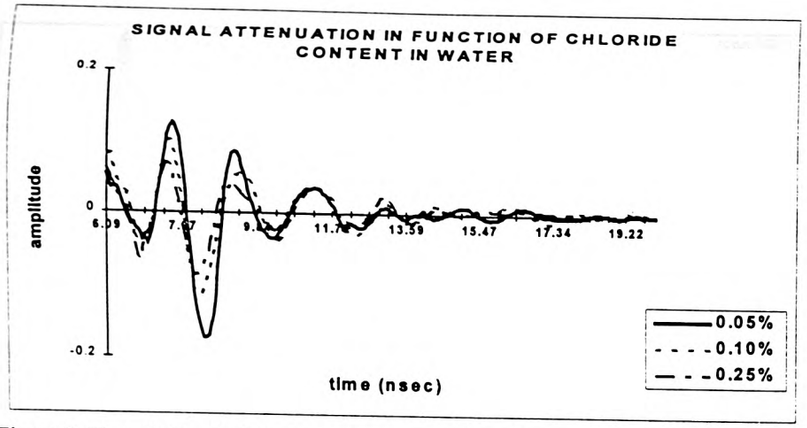

Figure 8. The relationship between salt content at three different concentrations in water, and amplitude of the reflected signal from the first re-bar.

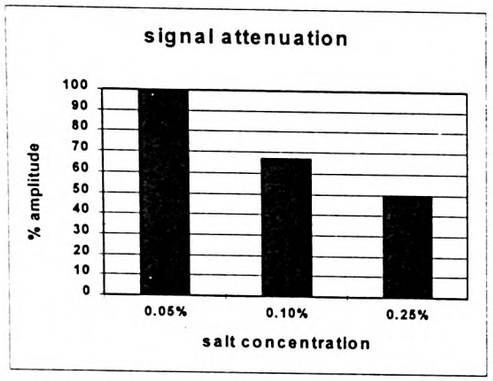

Figure 9. The relationship between salt concentration in water and the relative decreased amplitude of the signal, calculated from the experimental data.

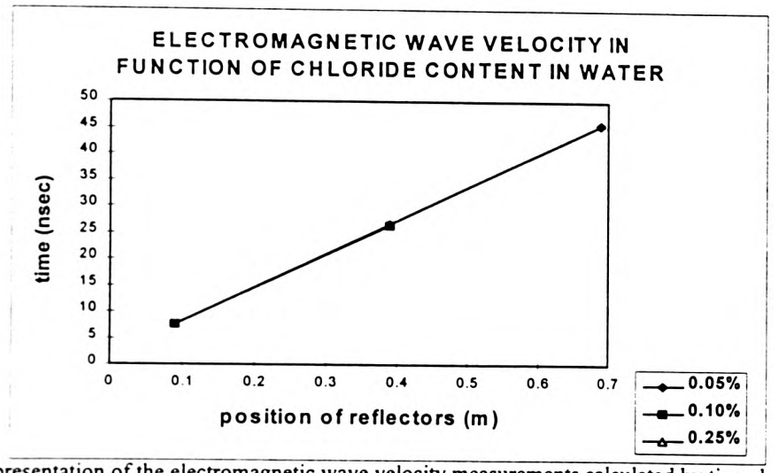

Figure 10. Representation of the electromagnetic wave velocity measurements calculated by time domain analysis.

Second Experiment - In the case of composite masonry structures, when no fill is present, phenomena of refraction of the E.M. signal are more evident. Fig. 11 is the radar plot obtained from the structure depicted in Fig. 4, with a 500 MHz frequency antenna. Over a 60 ns time range, effects of symmetrical refraction of the signal from the side walls are clearly visible and manifested primarily in the two "St. Andrew's crosses" with centre at approximately 16 and 28 ns time-depth. Multiple reflections from the longitudinal walls are also noticeable. The phenomenon is accentuated by the propagation of the signal through air which causes the antenna field pattern to modify and the beam of propagation of the signal to spread over a wider angle when travelling in air than when transmitting through soil or other material.

The plot in Fig. 12 is obtained from the same structure, with the use of 900 MHz antenna and a 15 ns time window. The three longitudinal walls are identified and their position has been indicated on the plot at approximately 2, 5 and 8 ns. As a result of the relatively large change of dielectric constant at each wall/air interface, the value of the reflection coefficient between brickwall and air, calculated from equation (4), is high. This permits a small portion of the signal to reach the 3rd wall, which is resolved, but whose reflection is highly attenuated compared with that from wall 2.

In Fig. 13 the time shift of wall 3 is visible and due to the presence of dry loose sand in the bottom half of the section of the structure. The sand in the 2nd cell, with its associated lower E.M. velocity, causes the reflection from the 3rd wall to appear in a lower position (approximately 9.5 ns), corresponding to an increased 2-way travel time if compared with Fig. 12. The velocity through the sand was estimated to be 0.205 $m.ns^{-1}$ (Fig. 14) and a dielectric constant of 2.1 was consequently calculated. This value is relatively low and at the bottom end of the range of dielectric constant expected for sand, confirming that the physical properties of the material (moisture content near 0% and porosity high) affect its electromagnetic behaviour and dielectric constant.

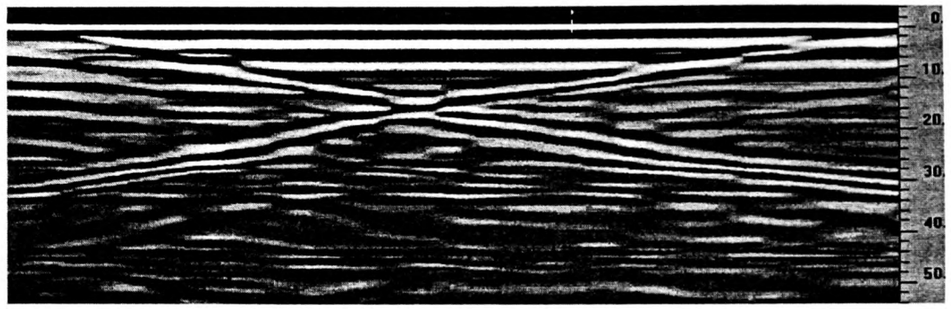

Figure 11. Reflection and refraction pattern obtained over empty cellular structure with 500 MHz frequency antenna (60 ns).

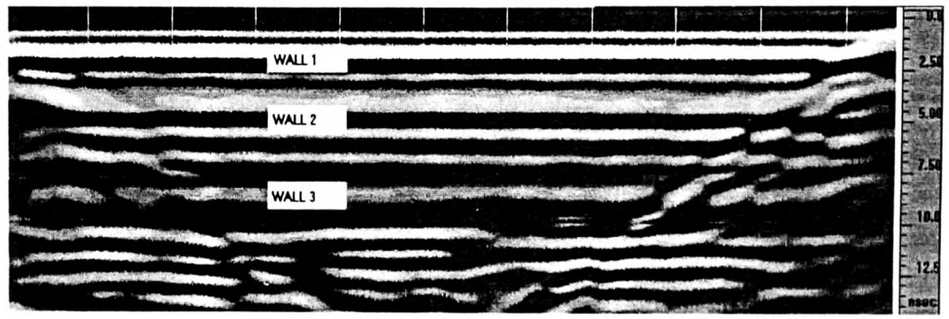

Figure 12. Plot obtained from empty structure with 900 MHz antenna and 15 ns range.

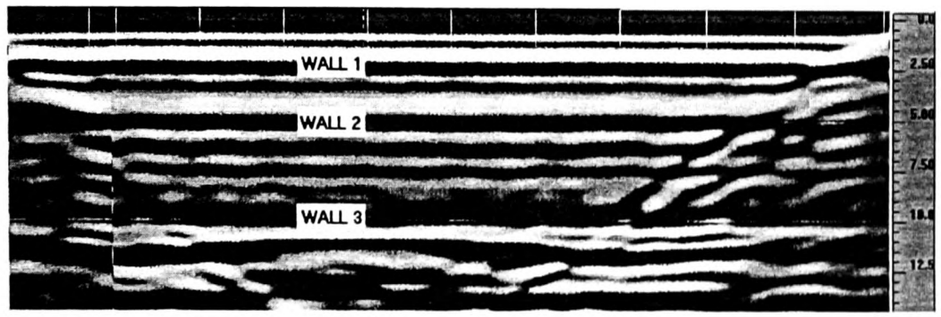

Figure 13. Radar plot obtained when loose dry sand is present in second cell (900 MHz antenna and 15 ns range).

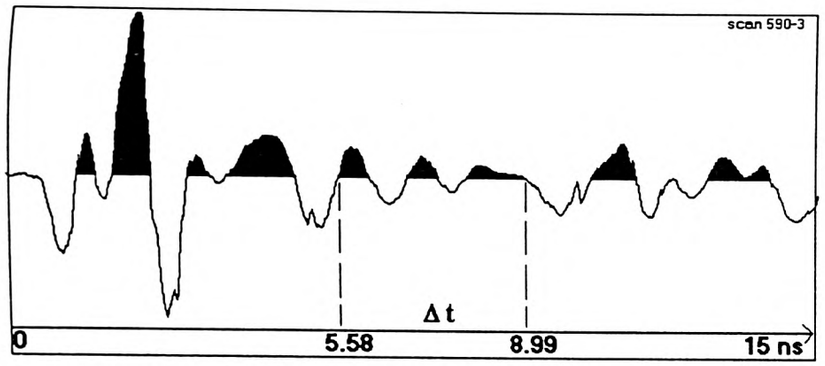

Figure 14. Measurement of 2-way travel time through dry loose sand.

In order to investigate the radar signature obtained from a wall constructed perpendicular to the direction of scan of the antenna and the effect of the presence of fill at the back of a wall, data were collected with a 1000 MHz antenna scanning on the 1m long head-wall (Figs 15 & 16). In the radar plot of Fig. 15 the presence of the perpendicular wall is clearly resolved and the position marked with a dashed white line. Effects of the refractions of the E.M. waves from the side walls are similar to the signatures noticed in Fig. 11 but made more complicated by the presence of the intermediate wall. On the left hand side of the radar plot of Fig. 16 the presence of sand at the back of the wall causes the reflection at the interface wall/sand to have a reduced amplitude compared with the wall/air situation and refractions effects due to the side walls are also attenuated.

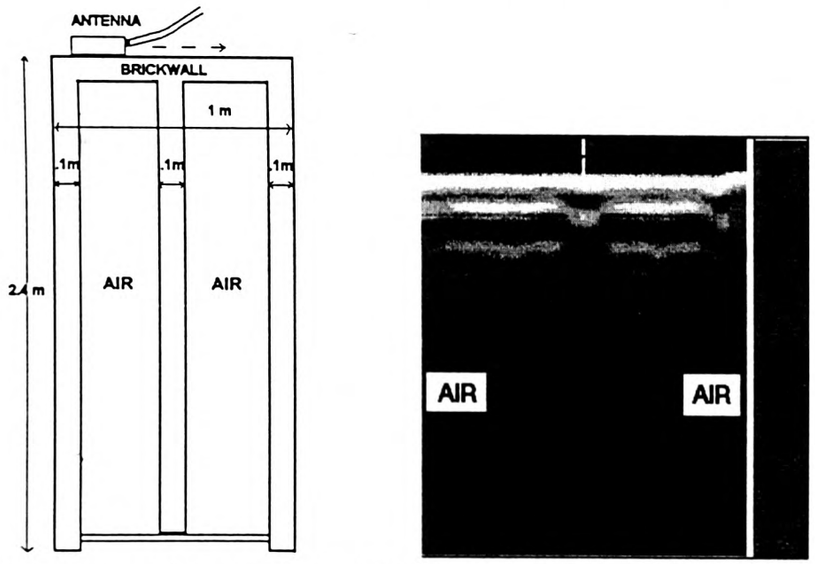

Figure 15. Composite structure with empty cells: drawing showing position of antenna and direction of movement during scanning (left); radar plot obtained with 1000 MHz, and 15 ns time window (right).

PRACTICAL IMPLICATIONS OF THE RESULTS

The statement is frequently made that radar will not work through saline water, but this simplistic statement is only partially accurate. The radar signal is rapidly attenuated as the conductivity of the background medium increases. However at relatively low saline contents (0.05%) and therefore relatively low conductivity the radar will have limited penetration as seen from the above experimental data. This is substantially less than the saline content of sea water (3.5%). It would therefore seem most unlikely that any significant penetration would be achieved through sea water using bow tie antennae of the type used in this experiment at the frequencies used in this experiment.

When investigating hollow structures by means of GPR the effects of refractions of the E.M. signal and multiple reflections may mask the target of the survey. Also, because of the high value of the coefficient of reflection when in the presence of air, the signal propagation can be severely affected if multiple interfaces are present.

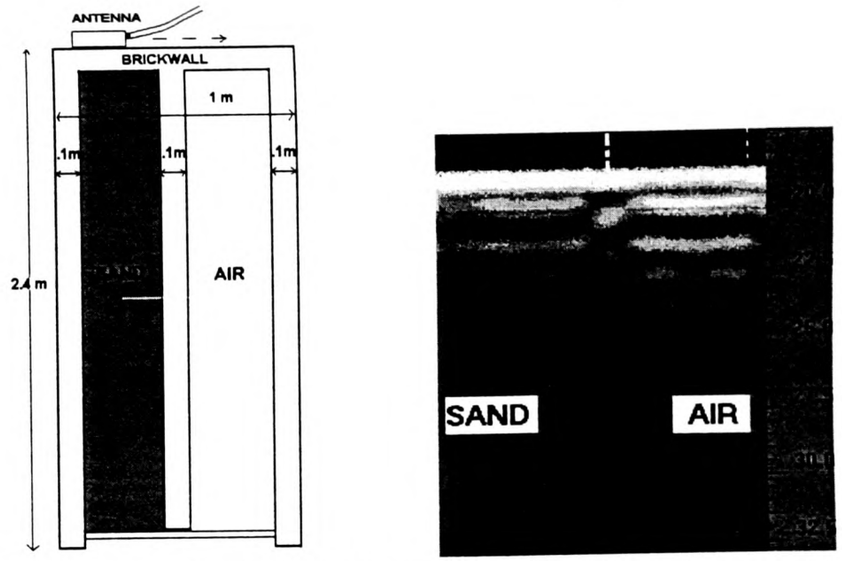

Figure 16. Composite structure partially filled: drawing shows left hand side cell filled with sand, position of antenna and direction of movement during scanning (left); radar plot obtained with 1000 MHz, and 15 ns time window (right).

CONCLUSIONS

1. GPR offers a rapid, non-contact high resolution method for detecting and mapping features in engineering applications.
2. Radar signals are very sensitive to changes in material conductivity and the relationship between conductivity and signal attenuation is exponential.
3. Radar can be used for detection of localised areas with high salt content or contaminant.
4. The radar technique cannot be used for high resolution soundings in great depth ranges, in environments with high electrical conductivity.
5. The range and resolution of GPR decreases with the presence of conductive materials such as brine or conductive pore water.
6. At saline contents of 0.05% by weight, 900 MHz bow tie antenna signals were significantly attenuated.
7. In the case of a hollow composite structure, propagation of the signal through air causes the signal beam to propagate with a wider angle than through soil.
8. In hollow masonry structures, refraction effects can be dominant over reflection from targets with the risk of masking relevant data.
9. The high value of reflection coefficient in air may affect the signal propagation if multiple interfaces are present.
10. When a structure investigated is filled with soil, refraction effects are attenuated and the presence of targets may be better resolved.

ACKNOWLEDGEMENTS

The authors gratefully acknowledge the facilities of the University of Edinburgh and the financial support of the Highways Agency, London. The first author also gratefully acknowledges the financial support of the EPSRC and wishes to thank Mr K. Broughton for technical help. Messrs C. Freeland and D. Pascal are acknowledged for labour provided.

REFERENCES

BA 16/93. (1993), *The assessment of highway bridges and structures*, HMSO, London.

Baronio, G., Binda, L., et al., (1995), Degrado dei monumenti milanesi e interventi di conservazione delle superfici esterne, *Conf. Milano restaura il monumento e il suo doppio,* J. A-LETHEIA, **6**: 48-50

Cooke, R.S., Ashurst, D.M., McCavitt, N. & Forde, M.C. (1993) Digital radar assessment of Besses o' th' Barn post-tensioned precast segmental rail bridge, *Proc. Int. Conf. Structural Faults & Repair-93,* University of Edinburgh, June 1993, Vol. 1, Engineering Technics Press, 305-314.

Daniels, J., (1988), Locating caves, tunnels and mines. *The leading edge*, 7(3): 32-37.

Das, P.C., (1993), Examination of masonry arch assessment methods. *Symp. Structural preservation of the architectural heritage*, IABSE, Rome, 385-392.

Das, P.C., Davidson, N.C. & Colla, C., (1995), "Potential applications of NDT methods for bridge assessment and monitoring", *Analysis & Testing of Bridges Seminar,* Instn. Struct. E. HQ, London, 26 April '95, 26 p.

Davis, J.L. & Annan, A.P., (1989), Ground- penetrating radar for high-resolution mapping of soil and rock stratigraphy. *Geophysical Prospecting*, **37** (5): 531-551.
Fairfield, C.A. & Ponniah, D.A., (1993), Geotechnical considerations in arch bridge assessment, *J. Instn Highways & Transportation*, **40** (7), 11-15.
Forde, M.C. & McCavitt, N. (1993) Modal testing of reinforced concrete pavements, *Proc. Int. Conf. Structural Faults & Repair-93*, University of Edinburgh, June 1993, Vol. 2, Engineering Technics Press, 95-104.
Goodman, D., (1994), Ground penetrating radar simulation in engineering and archaeology. *Geophysics*, **59** (2): 224-232.
Goodman, D. & Nishimura, Y., (1992), 2-D synthetic radargrams for archaeological investigation, *4th Int. Conf. Ground Penetrating Radar*, Finland Geol. Sur.
Goodman, D. & Nishimura, Y., (1993), A ground-radar view of Japanese burial mounds. *Antiquity*, 1993. **255** (67): 349-354.
Greaves, J.G., Lesmes, D.P., Jung, M.L. & Toksoz, M.N., (1996), Velocity variations and water content estimated from multi-offset, ground-penetrating radar. *Geophysics*, 1996. **61**(3): 683-695.
Hendry, A.W., Davies, S.R., Royles, R. & Ponniah, D.A., (1986), Load test to collapse on a masonry arch at Bargower, Strathclyde, *TRRL Contractor Report No. 26*.
Kraus, J.D., (1988), *Antennas*, McGraw-Hill Book Company, New York, 2nd ed., 892 pp.
National Bureau of Standards, (1958), *Dielectric dispersion data for pure liquids and dilute solutions*, Circular No. 589.
Padaratz, I.J. & Forde, M.C., (1995), A theoretical evaluation of impulse radar wave propagation through concrete, *J. Non-destructive Testing & Evaluation*, **12**, 9-32.
Smith-Rose, R.L.,(1934), Electrical measurements on soil with alternating currents. *Proc. IEE*, **75**: 221-237.
Topp, G.C., Davis, J.L., & Annan, A.P., (1980), Electromagnetic determination of soil water content: measurements in coaxial transmission lines, *Water Resources Research*, **16**(3): 574-582.
Ulriksen, P., (1982), *Application of impulse radar to civil engineering*, PhD thesis, Dept. of Engineering Geology, 1982, Lund University of Technology: Lund. p. 175.
Von Hippel, A.R. (Ed.), (1954), *Dielectric materials and applications*, Chapman and Hall Ltd., London, 438 pp.

COMPARISON OF LABORATORY AND SIMULATED DATA FOR RADAR IMAGE INTERPRETATION

C. Colla, C.B. Burnside, M.R. Clark & Professor M.C. Forde
University of Edinburgh
Dept of Civil & Environmental Engineering
Kings Buildings
Edinburgh EH9 3JN
Scotland

KEYWORDS: Radar, Simulation, Electromagnetic, NDT.

ABSTRACT
It has been shown that the output from in-house ray tracing simulation software provides a mean by which the impulse radar response of a structural system can be readily simulated. Radar simulations were undertaken of re-bar targets in a tank. A 900 Mhz commercial antenna was simulated. The simulations undertaken have shown the effects which target spacing and depth have on the radar signature shapes and the results compare well with real case survey plots. Simulation data has been used to assess the output specification from a commercial antenna, with interesting findings. It is expected that simulation will allow the interpretation of actual surveys to be more readily understood, which will in turn allow a better engineering assessment to be made of a structure under investigation.

INTRODUCTION

The research work on the simulation of radar response presented herein is part of a wider study focused on the investigation of composite masonry structures and masonry arch bridges conducted at the University of Edinburgh, where the radar technique is one of the Non-Destructive methods being researched for the investigation of structures.

Ground penetrating radar has been used for over 30 years for resolving shallow subsurfaces in geophysical applications and more recently in engineering. The development of the method, especially in civil engineering for the investigation of structures, has been restricted due to the complexity of the systems and the need for specialist interpretation of the data (Forde & McCavitt, 1993).

The user of a radar system is required to have knowledge of the concepts of physics (electromagnetic properties of materials, wave propagation and response of the structure) and electronics (pulse emitted, operating antennae), together with an engineering understanding of the problem being investigated. Depending on the complexity of the structural element under investigation, the nature of the problem, the conditions of the environment where the survey is carried out, the antennae configuration used during data acquisition, the radar user may be able to interpret the raw data or depending upon his interpretative experience he may need to use sophisticated signal processing software (short pass, longpass, horizontal or vertical filtering; plus signal amplification) (Olhoeft, 1993). In addition the user must be aware of the limitations of the technique and have realistic expectations. Radar cannot penetrate good electrical conductors, such as saltwater (Colla, Forde, et al., 1997), metal or fine reinforcing mesh (Padaratz & Forde, 1995a) or wet clays. Features may appear on the plots and, whilst some of the more common ones are recognisable and interpretable by the practised engineer, others are generated by complex effects of multiple reflections and/or refractions. Not only can their interpretation prove difficult, but they can mask valuable information generated by true anomalies. Other data interferences include periodic radio frequency noise introduced by site conditions, distortion at data acquisition, antenna ringing, poor antenna coupling and effects introduced by the structure itself because of its complexity or material grading such as clutter (Padaratz & Forde 1995b). Each of the above requires special digital signal processing with the risk of degrading the data if manipulation is improperly applied.

In complex cases it may be more convenient, in terms of time and effectiveness, to model the site situation and predict the radar performance and structure response. Therefore there is a need for a method of simulation which aids the interpretation of GPR surveys by allowing rapid simulation of varying geometries and materials. The combination of digital GPR system along with simulation software will help a better engineering assessment to be made (McCavitt & Forde, 1991).

RADAR PRINCIPLES AND THEORETICAL BACKGROUND

The radar technique involves the pulsing of radar waves into soil and/or construction materials. The propagation of the signal is affected by the dielectric properties of the materials so that its attenuation and reflected components vary accordingly. An examination of the reflected radar waveforms enables an interpretation of the material and/or structure under investigation.

The signal attenuation is given by:

$$e^{-\left(\sqrt{\sqrt{1+\left(\frac{1.8\times10^{4}\,.m}{f.e}\right)^{2}}-1.1.481\times10^{-2}\,.f.\sqrt{m}-d\right)}}$$

The amplitude reflection and transmission coefficients for the electromagnetic waves are:

$$R = \frac{Z_2 - Z_1}{Z_2 + Z_1} \qquad \text{and} \qquad T = \frac{2Z_2}{Z_2 + Z_1}$$

where Z_1 is the impedance of the first material,
Z_2 is the impedance of the second material

and $Z = \sqrt{\dfrac{j\omega\mu}{\sigma + j\omega\varepsilon}}$ is the value of intrinsic impedance.

$\mu = \mu_r\mu_0 = \mu_0 = 4\pi \times 10^{-7}$ is the material permeability,
$\varepsilon = \varepsilon_r\varepsilon_0 = \varepsilon_r\left[8.854 \times 10^{-12}\right]$ is the relative permittivity,
$\omega = 2\pi f$ (rad/s) is the angular frequency,
σ (S/m) is the conductivity.

In the case of oblique incidence it will be:

perpendicular polarisation

$$R = \frac{Z_2 \cos\theta_i - Z_1 \cos\theta_t}{Z_2 \cos\theta_i + Z_1 \cos\theta_t}$$

$$T = \frac{2Z_2 \cos\theta_i}{Z_2 \cos\theta_i + Z_1 \cos\theta_t}$$

parallel polarisation

$$R = \frac{Z_2 \cos\theta_t - Z_1 \cos\theta_i}{Z_2 \cos\theta_t + Z_1 \cos\theta_i}$$

$$T = \frac{2Z_2 \cos\theta_i}{Z_2 \cos\theta_t + Z_1 \cos\theta_i}$$

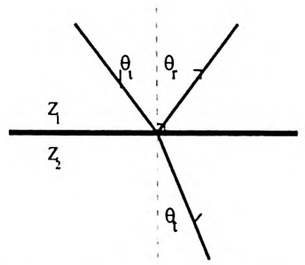

Fig. 1. Angles at wave incidence.

RADAR SIMULATION

In order to aid the analysis of site data in terms of engineering assessment, a simulation of relatively simple geometries and material electromagnetic properties was undertaken first. In a second phase, more complex engineering structures were simulated, including single-span masonry arch bridges. Results are presented herein for rebar detection in homogeneous media and compared with experimental data from the laboratory.

The modelling software uses a conventional ray-tracing process to model sinusoidal trace propagation along angles that cover the emitting field of commercially available antennas, and to recursively detect interfaces between various sub-surface features (strata and anomalies) and determine their boundaries. The algorithm reproduces the paths of individual radar wavelets from radar emitter to receiver through the various interfaces. At each interface, because of the different electromagnetic characteristics of the two materials present, the wavelet splits into different components and is partially transmitted through the second material and partially reflected in the receiver direction (Fig. 1). The response from all the traces sent out at different angles from the transmitter are then combined according to the Principle of Superposition to produce a complete 1-D simulated image for each sample point constituting the received signal waveform and these in turn are combined to obtain a complete 2-D scan over the simulated area.

In order to prevent excessive computational overheads, various termination conditions have been included and the signal propagation arrests if :

- the chosen two-way-time limit has been reached;
- the chosen number of simulated transmissions and reflections has been exceeded;
- the signal has entered a "convoluted" interface and, as a result of the wavelet defraction resulting from the difference in material properties, it has become trapped below the interface.

Input to the modelling program takes the form of a text file where geometrical dimensions, location and electromagnetic properties of embedded target objects and material strata are expressed in terms of their co-ordinates, permittivity and conductivity. The radar antenna characteristics are expressed in the form of centre frequency. Other information specific to the simulation process is also entered, including the maximum 2-way travel time in ns, the aperture of the receiver, and the distance to be covered by the antenna during the survey.

The main advantage of ray tracing is mathematical accuracy - each ray from the source is modelled with considerable precision, allowing for more accurate placement than compatible FE processes. The weakness normally attributed to the process - the inability to model with accuracy the defraction effect of the wavelet being transmitted through interfaces - has been dealt with in this model by the use of the equations listed in the theory section.

Antenna and Signal Characteristics

The emitter frequency is set as the centre frequency for the range being considered. Frequencies considered ranged from 200 to 900 MHz. The source wavelet is assumed to be 3-phase sinusoidal in format. Absolute signal strength is calculated in relation to the angle from the normal to the radar emitter. The directional response function is used as described in (Goodman and Nishimura, 1992).

Target Specifications

Embedded object geometrical shapes included circles and polygons - triangles and rectangles - and were described in terms of their equations and main electromagnetic properties (dielectric constant and conductivity).

Simulation Specifications

Other information specific to the simulation process and entered in the modelling input file included:

- the step size in angle degrees between each ray trace: - Although a full beam with more than 20 ray traces per degree would be required for complete accuracy, scans with 1 to 5 trace/degree would provide the user with a reasonable target image for training purposes.
- The number of scans per metre. - Scan number at the density used by digital radar systems (1024 scans/metre or less) could be employed, but fewer scans/metre may be convenient to obtain faster results. Too low a number of scans/metre may cause image deformation.
- The number of reflection patterns to be recorded. - This allows signal and image decomposition, so that it becomes possible to recognise the effects of primary/secondary reflection.

The output of the analysis is given in the same format as the digital radar system data files, so that it can be viewed with the same image processing software.

LABORATORY AND SIMULATION SET-UPS

The experimental tests were conducted in the laboratory on a rig which allowed the position and spacing of two reflectors (3.5 cm in ∅) to be varied, as per the plan layout in Fig. 2. The distance of the reflectors from the antenna varied from 0.05 to 0.4 m, and the relative spacing between the two targets varied from 0.1 to 0.4 m. The background medium during the tests was water and the antenna used was a 900 MHz bow tie with a survey wheel. Simulated models reproduced these same conditions.

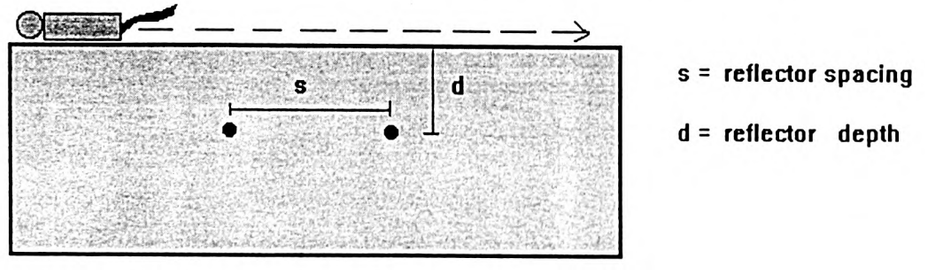

Figure 2. Plan view of rig used for experimental tests.

COMPARISON OF SIMULATED AND EXPERIMENTAL RESULTS

Consider figures 3a and 3b: the first is the laboratory plot obtained with 20 cm reflector spacing and 20 cm depth; the second is the output of the corresponding simulation.

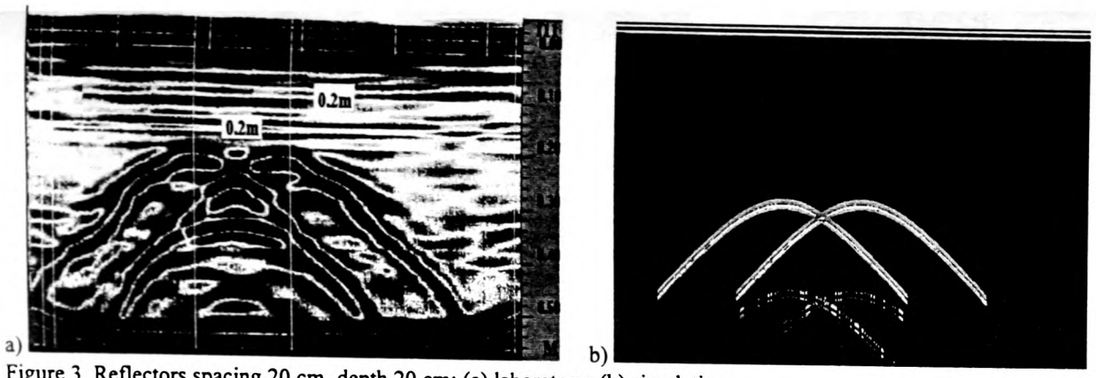

a) b)

Figure 3. Reflectors spacing 20 cm, depth 20 cm: (a) laboratory; (b) simulation.

In figures 4a and 4b comparison is shown for 10 cm separation of reflectors and 20 cm depth: laboratory data (left) and simulation (right).

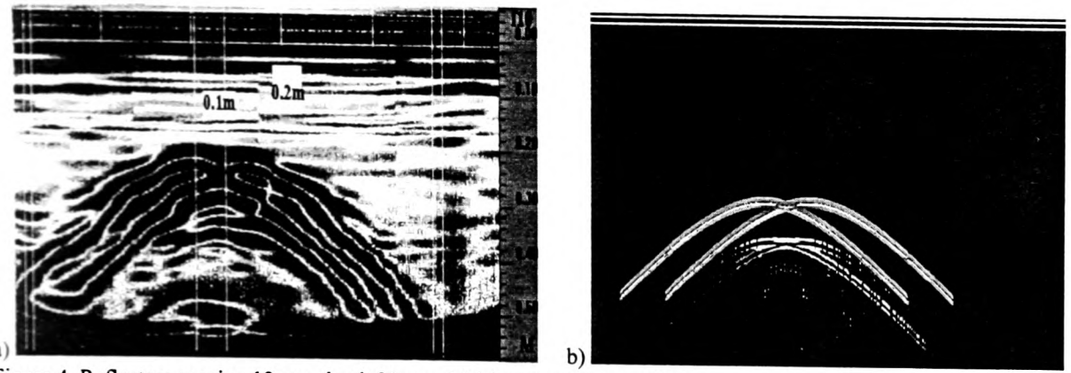

a) b)

Figure 4. Reflectors spacing 10 cm, depth 20 cm: (a) laboratory; (b) simulation.

In figures 5a and 5b comparison is shown for 40 cm separation of reflectors and 40 cm depth: laboratory data (left) and simulation (right).

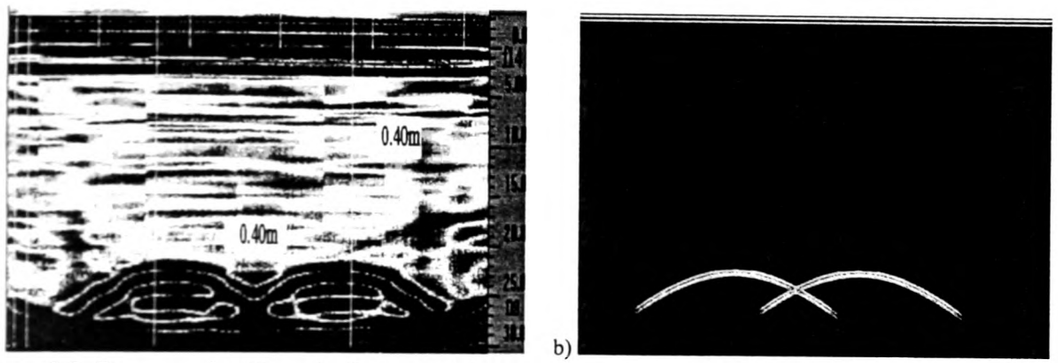

a) b)

Figure 5. Reflectors spacing 40 cm, depth 40 cm: (a) laboratory; (b) simulation.

PRACTICAL APPLICATIONS OF SIMULATION

The applications of a simulated radar survey can be listed as: a training tool, a pre-survey forecast, post-data collection analysis aid, and system tester for digital equipment performance.

Training

Ray-tracing is a more intuitive approach than alternative processes such as FTFD (Nelson, 1994). The variables listed above are easily derived and apply in practice just as readily as to the simulation. Thus the simulation approach could be used for the training of new users and for didactic purposes. Since the simulation produces more homogeneous (less complicated) images than digital radar systems produce on site, simulated radar plots offer the advantage of being more easily understood and interpreted. Moreover one of the special features of the simulation is signal decomposition: this allows signal propagation to be interrupted after one or more reflections, avoiding effects such as multiples and keeping the output plot simpler.

Consider figures 4a and 6a which compare laboratory experimental data with the simulated image of two rebars at 0.2 m depth and 0.1 m spacing. In fig 6a, b, and c a longer time window has been used than in 4a and 4b, for the purpose of showing multiple reflection. If in the case 6a signal propagation were stopped at the first reflection, then figure 6c would have been obtained, and if continued after 6c - then figure 6b would have resulted.

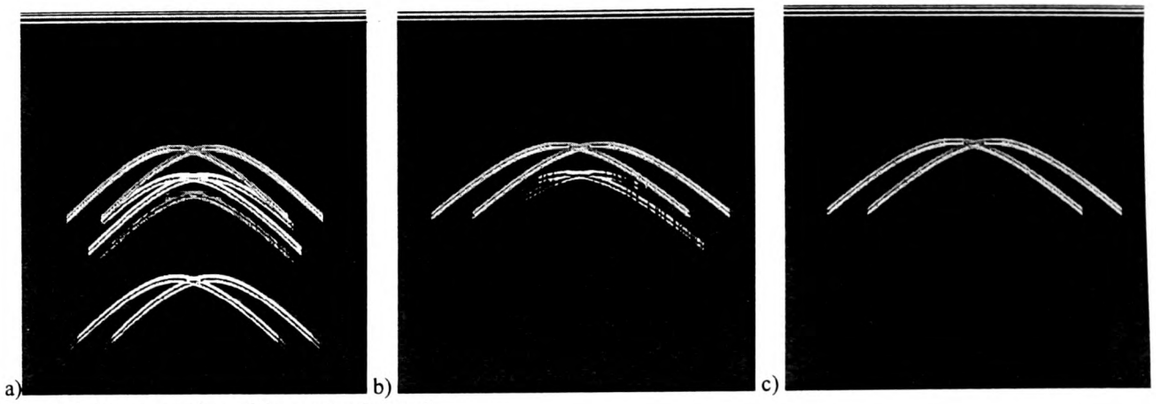

a) b) c)

Figure 6. Decomposition of the received signal.

Expert systems

An accurate simulation can be used to provide an interpretation of the radar image obtained from site surveys. Although this work is still some way from an iterative process where radar images can be back-analysed to produce the real site image, it is possible to compare site data with simulated models to try a 'best comparison' interpretation. Similarly the simulation may be used as part of the preparation before or during a site visit to give an understanding of the results obtained. The simulation program developed at the University of Edinburgh is PC based, and can be run and results plotted in a very short time - making it suitable for site use. With the further usage of image analysis tools, a simulated survey plot could be used to provide a template for a scan from the field to allow the engineer to observe key differences and spot any anomaly not yet accounted for.

Equipment Evaluation

If an idealised radar image can be derived from a simulation, then simulations could produce 'ideal' images of real case surveys to be used as benchmarks for the testing of radar equipment, thus making it possible to require more standard equipment and antennae.

For example, specifications of radar antennae may state that the signal will be emitted at certain angles (depending on the type of antenna, the signal beam width may be approximately 60 degrees or up to 90 degrees angle). It is possible to compare experimental data with simulated data for an evaluation of the beam angle of commercially available antennas.

Figures 7a and 7b simulate two rebars at 0.05 m depth and 0.1 m spacing. Figure 7a simulates an emitted beam angle of 60 degrees whilst in Fig. 7b the angle is 89 degrees. Figure 7c is the corresponding laboratory experimental image obtained. It is therefore deduced that the beam angle of the commercial antenna may be greater than 60 degrees.

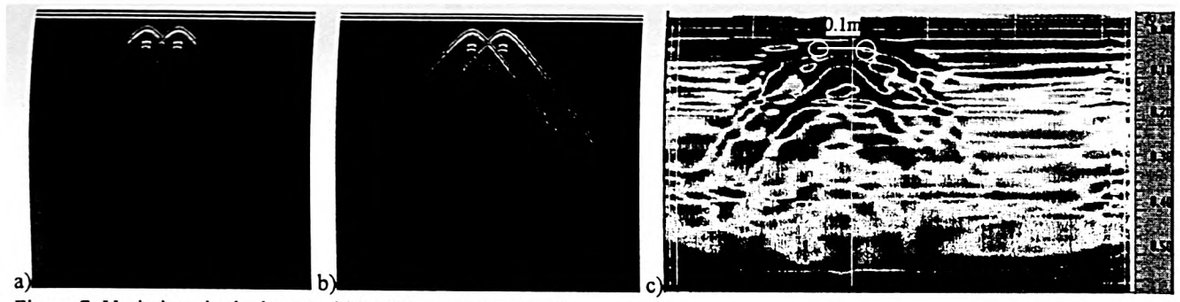

Figure 7. Variations in the beam width of the emitted signal.

CONCLUSIONS

1. It has been shown that the ray tracing simulation method provides a mean by which the impulse radar response of a structural system can be readily simulated.
2. The simulations undertaken have shown the effects which target spacing and depth have on the radar signature shapes.
3. Simulation results well compare with the real case survey plots.
4. Simulation data has been used to assess the output specification from a commercial antenna.
5. It is expected that simulation will allow the interpretation of actual surveys to be more readily understood, which will in turn allow a better engineering assessment to be made of a structure under investigation.

ACKNOWLEDGEMENTS

The authors wish to acknowledge the facilities made available by the University of Edinburgh and the work of Dr IJ Padaratz who was involved in the initial phase of the computer simulation. The authors gratefully acknowledge financial support provided by the Highways Agency, London.

REFERENCES

Colla, C, Forde, MC, McCann, DM, Das, PC, (1997) "Laboratory modelling of radar propagation through masonry", Proc. IV Int. Conf. Non-Destructive Testing in Civil Engineering (NDT-CE '97), 8-11 April 1997, Liverpool, UK, vol. 1, 303-316.

Forde, M.C. & McCavitt, N. (1993) Impulse radar testing of structures, *Proc. Instn Civ Engrs Structs & Bldgs*, 1993, **99**, Feb., 96-99

Goodman, D & Nishimura, Y, (1992), 2-D synthetic radargrams for archaeological investigation, *4th Int. Conf. Ground Penetrating Radar*, Finland Geol. Sur.

McCavitt, N & Forde, MC, (1991), The application of the method of convolution to the simulation of the response of masonry arch bridges to ground probing radar, *J. Non-Destructive Testing & Evaluation*, vol. 6, 3: 179-194.

Nelson, SD, (1994), "Electromagnetic modelling for ground-penetrating imaging radar (GPIR) using 3-D finite difference time-domain (FDTD) modelling codes", *SPIE-The Int Soc for Optical Engng Advanced Microwave and Millimeter-Wave Detectors*, San Diego, CA, USA, 25-26 July 94, vol. 2275, 186-195.

Olhoeft, GR, (1993), "Processing, modelling and presentation of ground penetrating radar data", *2nd Government Workshop GPR - Advanced Ground Penetrating Radar: Technologies and Applications*, Ohio, 26-28 Oct 93, p. 23.

Padaratz, I.J. & Forde, M.C. (1995a) A theoretical evaluation of impulse radar wave propagation through concrete, *J. Non-destructive Testing & Evaluation*, **12**, 9-32

Padaratz, I.J. & Forde, M.C. (1995b) Influence of antenna frequency on impulse radar surveys of concrete structures, *Proc. Int. Conf. Structural Faults & Repair-95,* London, July 1995, Vol. 2, Engineering Technics Press, 331-336.